

University of Warwick institutional repository: <http://go.warwick.ac.uk/wrap>

**A Thesis Submitted for the Degree of PhD at the University of Warwick**

<http://go.warwick.ac.uk/wrap/3372>

This thesis is made available online and is protected by original copyright.

Please scroll down to view the document itself.

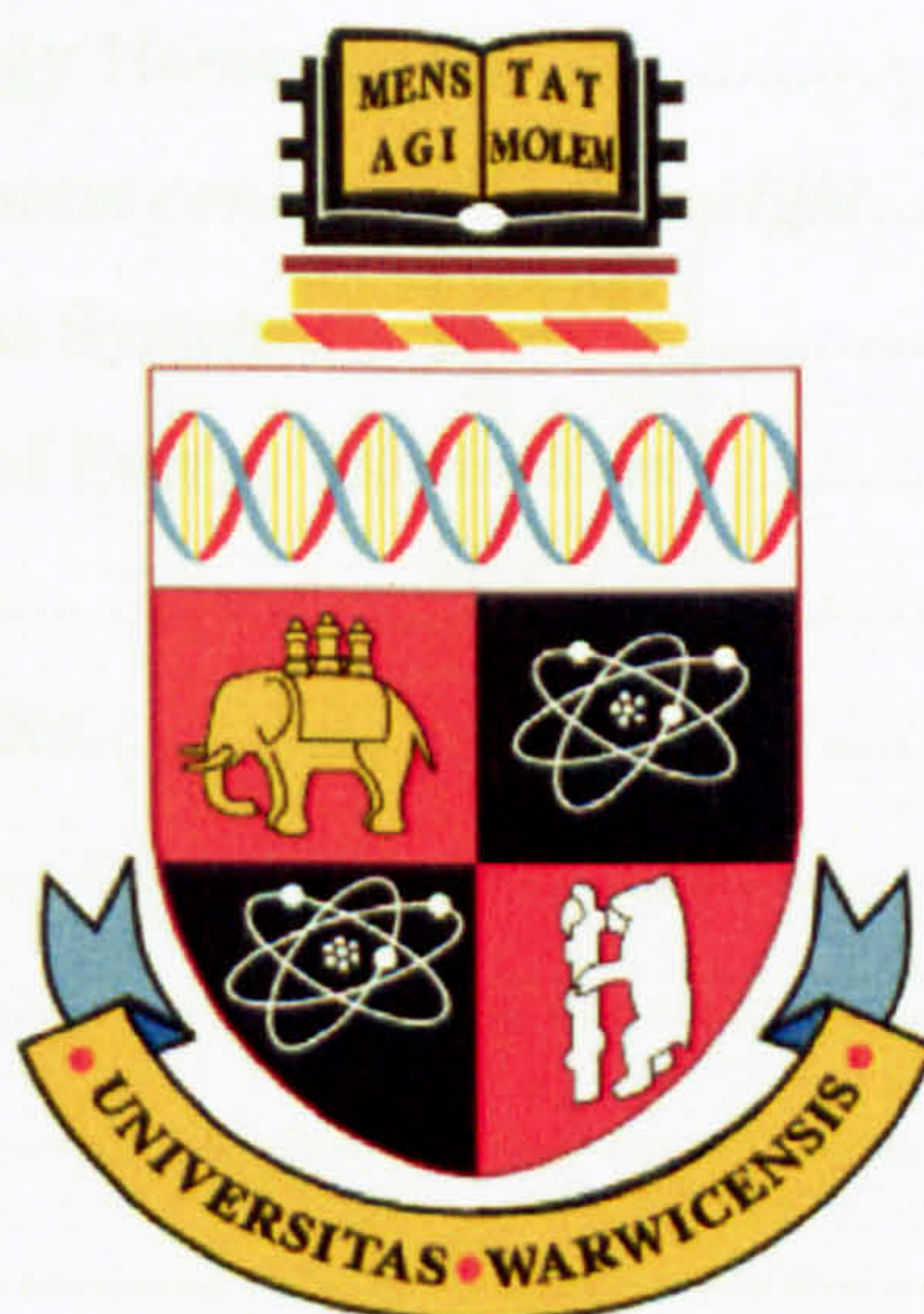
Please refer to the repository record for this item for information to help you to cite it. Our policy information is available from the repository home page.



# **Metabolic and Serotonergic Modulation of Hypothalamic Arcuate Nucleus Neurones *in vitro***

**Louise Saker BSc (Hons)**

*A thesis written in partial fulfilment of the criteria set for the degree of  
Doctor of Philosophy*



THE UNIVERSITY OF  
**WARWICK**

**Clinical Sciences Research Institute  
Warwick Medical School, September 2008**

*Funded by the Biotechnology and Biological Sciences Research Council (BBSRC)*



**BEST COPY**

**AVAILABLE**



---

# Table of Contents

Title Page .....i

Table of Contents .....ii

List of Figures .....vii

List of Tables.....x

Publications .....x

Acknowledgements .....xi

Declaration .....xi

Summary .....xii

Abbreviations ..... xiii

**Chapter 1: General Introduction ..... - 1 -**

1.1 Central Control of Energy Homeostasis ..... - 2 -

*1.1.1 Central nervous system control of body-weight..... - 3 -*

1.2 The Autonomic Nervous System ..... - 4 -

1.3 Hypothalamic Control of Energy Homeostasis..... - 5 -

*1.3.1 Arcuate nucleus..... - 7 -*

1.4 Orexigenic Neuropeptides..... - 11 -

*1.4.1 NPY ..... - 11 -*

*1.4.2 AgRP ..... - 12 -*

*1.4.3 Orexin..... - 12 -*

*1.4.4 MCH..... - 13 -*

1.5 Anorexigenic Neuropeptides..... - 13 -

*1.5.1 POMC ..... - 13 -*

*1.5.2 CART ..... - 14 -*

*1.5.3 CRF ..... - 15 -*

*1.5.4 CCK..... - 15 -*

*1.5.5 Neurotransmitters ..... - 16 -*

1.6 Hormonal and Nutrient Signalling ..... - 16 -

*1.6.1 Leptin ..... - 18 -*

*1.6.2 Insulin..... - 19 -*

*1.6.3 Adipocytokines ..... - 20 -*

*1.6.4 Glucose..... - 20 -*



---

1.6.5 Ghrelin .....	- 23 -
1.6.6 PYY.....	- 24 -
1.7 5-HT .....	- 25 -
1.7.1 5-HT receptors .....	- 26 -
1.7.2 Functional effects mediated by the 5-HT receptors .....	- 29 -
1.7.3 5-HT and control of energy balance .....	- 31 -
1.8 Disorders of Energy Homeostasis.....	- 33 -
1.8.1 Putative drugs for the treatment of obesity.....	- 34 -
1.9 Project Aims.....	- 35 -
<b>Chapter 2: Experimental Procedures.....</b>	<b>- 45 -</b>
2.1 Electrophysiology .....	- 46 -
2.1.1 Slice preparation.....	- 46 -
2.1.2 Electrophysiological recording and data analysis .....	- 47 -
2.1.3 Solutions and drugs.....	- 48 -
2.1.4 Reversal potentials .....	- 50 -
2.2 Immunohistochemistry.....	- 51 -
2.2.1 Immunofluorescence staining of 5-HT receptors.....	- 51 -
2.2.2 Double-immunofluorescence staining for 5-HT receptors and cocaine and amphetamine-regulated transcript (CART) .....	- 52 -
2.2.3 Immunofluorescence staining for CART and Alexa 633 .....	- 53 -
2.3 Molecular Biology .....	- 53 -
2.3.1 Tissue preparation .....	- 53 -
2.3.2 RNA extraction .....	- 54 -
2.3.3 Reverse transcription of mRNA.....	- 55 -
2.3.4 Quantitative real-time PCR.....	- 55 -
2.3.5 Interpretation of real-time PCR data.....	- 56 -
2.4 Statistical Analysis.....	- 57 -



---

<b>Chapter 3: The Effects of Glucose on the Electrophysiological Properties of Rat Arcuate Nucleus Neurones .....</b>	<b>- 62 -</b>
3.1 Introduction .....	- 63 -
3.2 Results .....	- 69 -
3.2.1 <i>Comparison of all neurones recorded in 2 mM and 10 mM glucose-containing aCSF .....</i>	<i>- 70 -</i>
3.2.2 <i>Expression of anomalous inward rectification (Cluster 1 ) .....</i>	<i>- 74 -</i>
3.2.3 <i>Expression of transient outward rectification with <math>I_{an}</math> (Cluster 2) .....</i>	<i>- 76 -</i>
3.2.4 <i>Expression of no obvious subthreshold active conductances (Cluster 3) .....</i>	<i>- 80 -</i>
3.2.5 <i>Expression of time- and voltage-dependent inward rectification (Cluster 4) .....</i>	<i>- 82 -</i>
3.2.6 <i>Expression of T-type conductance and <math>I_h</math> (Cluster 5) .....</i>	<i>- 85 -</i>
3.2.7 <i>Expression of T-type conductance (Cluster 6) .....</i>	<i>- 88 -</i>
3.2.8 <i>Expression of <math>I_{an}</math> and T-type conductances (Cluster 7) .....</i>	<i>- 90 -</i>
3.2.9 <i>Expression of <math>I_{an}</math>, <math>I_h</math> and T-type conductances (Cluster 8) .....</i>	<i>- 93 -</i>
3.2.10 <i>Comparison of percentage of neurones in each cluster recorded in 2 mM and 10 mM glucose-containing aCSF .....</i>	<i>- 98 -</i>
3.2.11 <i>Comparison of percentage of spontaneously active neurones in each cluster recorded in 2 mM and 10 mM glucose-containing aCSF .....</i>	<i>- 98 -</i>
3.3 Discussion .....	- 99 -
3.3.1 <i>Effect of glucose on membrane properties of ARC neurones .....</i>	<i>- 99 -</i>
3.3.2 <i>Electrophysiological characterisation of ARC neurones .....</i>	<i>- 108 -</i>

<b>Chapter 4: The Excitatory Effects of 5-HT on Rat Arcuate Nucleus Neurones .....</b>	<b>- 134 -</b>
4.1 Introduction .....	- 135 -
4.2 Results .....	- 139 -
4.2.1 <i>The excitatory effects of 5-HT on ARC neurones .....</i>	<i>- 140 -</i>
4.2.2 <i>Ionic mechanism underlying the 5-HT-induced depolarisation .....</i>	<i>- 142 -</i>
4.2.3 <i>5-HT-induced membrane potential oscillations .....</i>	<i>- 143 -</i>
4.2.4 <i>5-HT-induced indirect effects on ARC neurones .....</i>	<i>- 143 -</i>
4.2.5 <i>The effects of 5-HT receptor agonists on ARC neurones .....</i>	<i>- 144 -</i>



---

4.2.6 The effects of 5-HT receptor antagonists on 5-HT-induced responses in ARC neurones .....	- 145 -
4.2.7 The effects of ghrelin on ARC neurones.....	- 148 -
4.2.8 5-HT excites CART-expressing neurones .....	- 149 -
4.2.9 5-HT-induced responses in 10 mM and 2 mM glucose-containing aCSF.....	- 150 -
4.2.10 5-HT-induced responses in neurones classified into electrophysiological clusters .....	- 151 -
4.3 Discussion .....	- 153 -

## **Chapter 5: The Inhibitory Effects of 5-HT on Rat Arcuate**

<b>Nucleus Neurones .....</b>	<b>- 191 -</b>
5.1 Introduction .....	- 192 -
5.2 Results.....	- 193 -
5.2.1 The inhibitory effects of 5-HT on ARC neurones .....	- 193 -
5.2.2 Ionic mechanism underlying the 5-HT-induced hyperpolarisation .....	- 194 -
5.2.3 The effects of 5-HT receptor agonists on ARC neurones.....	- 195 -
5.2.4 The effects of 5-HT receptor antagonists on 5-HT-induced responses in ARC neurones.....	- 196 -
5.2.5 The effects of ghrelin on ARC neurones.....	- 198 -
5.2.6 5-HT inhibits orexigenic NPY/AgRP neurones .....	- 199 -
5.2.7 Co-localisation of 5-HT receptors and CART .....	- 200 -
5.3 Discussion .....	- 202 -

## **Chapter 6: The Effects of Feeding Signals on Neuropeptide**

<b>mRNA Expression in the Rat Hypothalamus .....</b>	<b>- 233 -</b>
6.1 Introduction .....	- 234 -
6.2 Results.....	- 238 -
6.2.1 The effects of GABA and AMPA on c-fos mRNA expression .....	- 238 -
6.2.2 The effects of leptin on NPY and POMC mRNA expression .....	- 239 -
6.2.3 The effects of leptin on NPY and POMC mRNA expression in fasted animals .....	- 240 -
6.2.4 The effects of leptin on AgRP mRNA expression .....	- 242 -



---

6.2.5 <i>The effect of changing glucose concentration on NPY and POMC mRNA expression</i> .....	- 243 -
6.3 Discussion .....	- 243 -
<b>Chapter 7: General Discussion</b> .....	<b>- 269 -</b>
7.1 <i>Effect of glucose on electrophysiological properties of ARC neurones</i> ....	- 270 -
7.2 <i>Electrophysiological characterisation of ARC neurones</i> .....	- 274 -
7.3 <i>The differential effects of 5-HT on ARC neurones</i> .....	- 275 -
7.4 <i>Effect of feeding signals on neuropeptide mRNA expression in the hypothalamus</i> .....	- 280 -
7.5 <i>Conclusions and future work</i> .....	- 281 -
<b>Chapter 8: References</b> .....	<b>- 282 -</b>

---

## List of Figures

<b>Figure 1.1</b> The central control of energy homeostasis .....	- 37 -
<b>Figure 1.2</b> Overview of hypothalamic nuclei involved in energy homeostasis ...	- 39 -
<b>Figure 1.3</b> Afferent and efferent connections of the ARC .....	- 41 -
<b>Figure 1.4</b> Anabolic and catabolic pathways controlling energy homeostasis ....	- 43 -
<b>Figure 2.1</b> Diagram showing the location of the ARC within the hypothalamus .....	- 58 -
<b>Figure 2.2</b> Diagram of a rat brain showing the markers used to produce the hypothalamic explant for RT-PCR.....	- 60 -
<b>Figure 3.1</b> Comparison of resting membrane potentials of neurones recorded in 10 mM and 2 mM glucose-containing aCSF .....	- 112 -
<b>Figure 3.2</b> Comparison of input resistances of neurones recorded in 10 mM and 2 mM glucose-containing aCSF .....	- 114 -
<b>Figure 3.3</b> Comparison of membrane time-constants of neurones recorded in 10 mM and 2 mM glucose-containing aCSF .....	- 116 -
<b>Figure 3.4</b> Comparison of spontaneous firing rates of neurones recorded in 10 mM and 2 mM glucose-containing aCSF .....	- 118 -
<b>Figure 3.5</b> Characteristics and analysis of electrical properties of arcuate nucleus neurones .....	- 120 -
<b>Figure 3.6</b> Electrophysiological properties of cluster 1 and 2 neurones .....	- 122 -
<b>Figure 3.7</b> Electrophysiological properties of cluster 3 and 4 neurones .....	- 124 -
<b>Figure 3.8</b> Electrophysiological properties of cluster 5 and 6 neurones .....	- 126 -
<b>Figure 3.9</b> Electrophysiological properties of cluster 7 and 8 neurones .....	- 128 -
<b>Figure 3.10</b> Relative proportion of neurones in each cluster recorded in 10 mM and 2 mM glucose-containing aCSF .....	- 130 -
<b>Figure 3.11</b> Comparison of neurones displaying spontaneous suprathreshold activity in each cluster recorded in 10 mM and 2 mM glucose-containing aCSF .....	- 133 -
<b>Figure 4.1</b> 5-HT differentially regulates ARC neurones.....	- 161 -
<b>Figure 4.2</b> 5-HT directly excites a population of ARC neurones with a concomitant increase in input resistance.....	- 163 -
<b>Figure 4.3</b> 5-HT excites a sub-population of ARC neurones with a concomitant decrease in input resistance .....	- 165 -



---

<b>Figure 4.4</b> 5-HT excites a sub-population of ARC neurones: a response associated with no change in input resistance.....	- 167 -
<b>Figure 4.5</b> 5-HT induces an inward current in ARC neurones.....	- 169 -
<b>Figure 4.6</b> 5-HT induces a burst-like pattern of firing in some ARC neurones. ....	- 171 -
<b>Figure 4.7</b> 5-HT-induced changes in spontaneous synaptic activity.....	- 173 -
<b>Figure 4.8</b> The effects of the 5-HT receptor agonists $\alpha$ -methyl 5-HT and 5-CT on ARC neurones.....	- 175 -
<b>Figure 4.9</b> The effects of the 5-HT receptor agonists 8-OH-DPAT and mCPBG on ARC neurones.....	- 177 -
<b>Figure 4.10</b> The effects of the 5-HT receptor antagonists altanserin and RS102221 on ARC neurones .....	- 179 -
<b>Figure 4.11</b> The effects of the 5-HT receptor antagonists R-96544 and SB 204741 on ARC neurones .....	- 181 -
<b>Figure 4.12</b> The effects of ghrelin on 5-HT-excited ARC neurones.....	- 183 -
<b>Figure 4.13</b> 5-HT excites CART-expressing neurones .....	- 185 -
<b>Figure 4.14</b> A comparison of the effects of 5-HT on ARC neurones under normo- (2 mM glucose) and hyper-glycaemic (10 mM glucose) conditions.....	- 187 -
<b>Figure 4.15</b> Electrophysiological classification of ARC neurones and their responsiveness to 5-HT .....	- 189 -
<b>Figure 5.1</b> 5-HT directly inhibits ARC neurones through activation of a potassium conductance.....	- 207 -
<b>Figure 5.2</b> 5-HT induces an outward current in ARC neurones.....	- 209 -
<b>Figure 5.3</b> The effects of the 5-HT receptor agonists 8-OH-DPAT and 5-CT on ARC neurones .....	- 211 -
<b>Figure 5.4</b> The effects of the 5-HT receptor agonists RU 24969 and CP 93129 on ARC neurones .....	- 213 -
<b>Figure 5.5</b> The effects of the 5-HT receptor antagonists SB 269970 and cyanopindolol on ARC neurones .....	- 215 -
<b>Figure 5.6</b> The effects of the 5-HT receptor antagonists WAY-100635 and SB 224289 on ARC neurones .....	- 217 -
<b>Figure 5.7</b> The effects of the 5-HT receptor antagonists WAY-100635, SB 224289 and SB 269970 in combination on ARC neurones .....	- 219 -

---

<b>Figure 5.8</b> The effects of the 5-HT receptor antagonists MDL7222 and altanserin on ARC neurones.....	- 221 -
<b>Figure 5.9</b> The effects of ghrelin on 5-HT-inhibited neurones .....	- 223 -
<b>Figure 5.10</b> The effects of 5-HT on orexigenic NPY/AgRP neurones .....	- 225 -
<b>Figure 5.11</b> Immunohistochemical detection of a 5-HT <sub>1B</sub> receptor-expressing non-CART positive neurone within the ARC.....	- 227 -
<b>Figure 5.12</b> Immunohistochemical detection of a CART positive neurone within the ARC .....	- 229 -
<b>Figure 5.13</b> Co-localisation of 5-HT <sub>1B</sub> receptor and CART within the ARC....	- 231 -
<b>Figure 6.1</b> The effect of GABA on c-fos gene expression in hypothalamic explants from rats fed <i>ad libitum</i> .....	- 249 -
<b>Figure 6.2</b> The effect of AMPA on c-fos gene expression in hypothalamic explants from rats fed <i>ad libitum</i> .....	- 251 -
<b>Figure 6.3</b> The effect of leptin on NPY and POMC gene expression in hypothalamic explants from rats fed <i>ad libitum</i> .....	- 253 -
<b>Figure 6.4</b> The effect of leptin on NPY and POMC gene expression in individual hypothalamic explants from rats fed <i>ad libitum</i> .....	- 255 -
<b>Figure 6.5</b> The effect of leptin on NPY and POMC gene expression in hypothalamic explants prepared from fasted rats.....	- 257 -
<b>Figure 6.6</b> The effect of leptin on NPY and POMC gene expression in individual hypothalamic explants prepared from fasted rats .....	- 259 -
<b>Figure 6.7</b> The effect of leptin on AgRP gene expression in hypothalamic explants from animals fed <i>ad libitum</i> .....	- 261 -
<b>Figure 6.8</b> The effect of leptin on AgRP gene expression in hypothalamic explants prepared from fasted animals.....	- 263 -
<b>Figure 6.9</b> The effect of changing the glucose concentration on NPY gene expression in hypothalamic explants from rats fed <i>ad libitum</i> .....	- 265 -
<b>Figure 6.10</b> The effect of changing the glucose concentration on POMC gene expression in hypothalamic explants from rats fed <i>ad libitum</i> .....	- 267 -
<b>Figure 7.1</b> 5-HT differentially regulates NPY and POMC neurones within the ARC .....	- 278 -



---

# List of Tables

**Table 1.1** Orexigenic and anorexigenic signalling molecules involved in energy homeostasis ..... - 10 -

**Table 1.2** 5-HT receptors..... - 28 -

**Table 2.1** aCSF ..... - 48 -

**Table 2.2** Intracellular solution..... - 48 -

**Table 2.3** Drugs ..... - 49 -

**Table 2.4** Reversal potentials ..... - 50 -

**Table 2.5** Primary antibodies..... - 52 -

**Table 2.6** Secondary antibodies..... - 53 -

**Table 2.7** PCR primers ..... - 56 -

**Table 3.1** General membrane properties of all neurones..... - 73 -

**Table 3.2** Electrophysiological properties of cluster 1 neurones ..... - 76 -

**Table 3.3** Electrophysiological properties of cluster 2 neurones ..... - 79 -

**Table 3.4** Electrophysiological properties of cluster 3 neurones ..... - 81 -

**Table 3.5** Electrophysiological properties of cluster 4 neurones ..... - 84 -

**Table 3.6** Electrophysiological properties of cluster 5 neurones ..... - 87 -

**Table 3.7** Electrophysiological properties of cluster 6 neurones ..... - 89 -

**Table 3.8** Electrophysiological properties of cluster 7 neurones ..... - 92 -

**Table 3.9** Electrophysiological properties of cluster 8 neurones ..... - 95 -

**Table 3.10** Electrophysiological properties of neurones ..... - 96 -

**Table 3.11** Properties of active conductances ..... - 97 -

**Table 3.12** Comparison of spontaneous activity ..... - 99 -

**Table 5.1** Effects of WAY-100635 on 5-HT-induced hyperpolarisation..... - 197 -

# Publications

**Abstract:**

L. Saker, M. van den Top & D. Spanswick. (2008). 5-HT differentially regulates hypothalamic arcuate nucleus neurones *in vitro*. *Keystone Symposia: Neuronal mechanisms controlling food intake, glucose metabolism and body-weight*: P309

---

## Acknowledgements

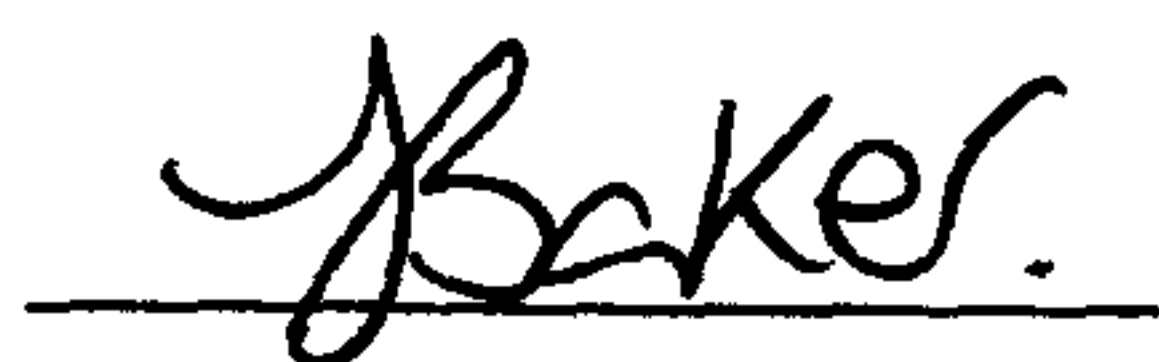
There are many people I wish to thank for their support and encouragement during the course of this PhD. Most importantly I would like to thank Professor David Spanswick for giving me the opportunity to undertake this project, and for his supervision, advice and encouragement throughout the years of my project. I also wish to express particular thanks to Dr. Marco van den Top for his assistance with experiments, for sharing his expertise and for his selfless advice.

I would like to thank all the people who I have had the pleasure of working with over the course of this project, in particular, Dawn Collins, Paul Giles, Ross Jeggo, Dave Lyons, Ratchada Pattaranit, Tony Rush and Andrew Whymant for their support and friendship. Special thanks must go to Jasmeet Virdee for her friendship and for her continuous support.

Finally, I would like to thank my friends and family, especially my parents and Stephen Porter for their endless love and support and for giving me the strength to complete this project.

## Declaration

I hereby declare that this thesis has been composed solely by myself and that it has not been accepted in any previous application for a degree. All work has been done by myself, with the exception of the molecular biology work which was done in collaboration with David Lyons and the immunohistochemistry which was done in collaboration with Marco van den Top. All the sources used have been specifically acknowledged by means of a reference.



Louise Saker



---

## Summary

1. The effects of glucose on the electrophysiological properties of rat hypothalamic arcuate nucleus (ARC) neurones were investigated. Neurones were recorded in 10 mM (hyperglycaemic) and 2 mM (euglycaemic) glucose-containing aCSF. The major findings were that input resistance increased in 10 mM glucose, there was an increase in the activity of neurones in 2 mM glucose and there were a greater percentage of neurones expressing  $I_h$  in 10 mM glucose. Subthreshold active conductances were differentially expressed in ARC neurones including: anomalous inward rectification ( $I_{an}$ ), time- and voltage-dependent inward rectification ( $I_h$ ), A-like transient outward rectification ( $I_A$ ) and T-type calcium-like conductance. Characterisation of the differential expression of these conductances may represent one way of functionally classifying ARC neurones.

2. Whole-cell patch clamp recording techniques were used in isolated hypothalamic brain slice preparations to investigate the effects of 5-HT on ARC neurones. Bath application of 5-HT induced a membrane depolarisation in a sub-population of ARC neurones (30%), a response that persisted in the presence of TTX indicating a direct effect. 5-HT excited ARC neurones through three potential mechanisms: closure of one or more resting potassium conductances; activation of a non-selective cation channel, or a combination of the two; or activation of a pump in the membrane. This response was mediated through the 5-HT<sub>2A</sub>, 5-HT<sub>2B</sub> and/or 5-HT<sub>2C</sub> receptors revealed using a range of 5-HT receptor agonists and antagonists. 5-HT was shown to excite CART-expressing neurones suggesting an anorexigenic role for 5-HT, via 5-HT<sub>2</sub> receptors at the level of the ARC.

3. 5-HT induced a membrane hyperpolarisation in a sub-population of ARC neurones (37%). The 5-HT-induced hyperpolarisation persisted in the presence of TTX indicating a direct effect on ARC neurones. 5-HT inhibited ARC neurones most likely through the activation of one or more potassium conductances, including an inwardly rectifying potassium conductance. Potential roles for 5-HT<sub>1A</sub>, 5-HT<sub>1B</sub> and 5-HT<sub>7</sub> receptors were suggested from studies utilising 5-HT receptor agonists and antagonists. 5-HT inhibited orexigenic NPY/AgRP neurones, identified by their response to ghrelin and by their electrophysiological properties, suggesting an anorexigenic role for 5-HT, acting via 5-HT<sub>1</sub> and 5-HT<sub>7</sub> receptors on NPY/AgRP neurones at the level of the ARC.

4. The effects of feeding-related signals on hypothalamic neuropeptide expression were investigated using real-time-PCR. A new protocol measuring gene expression from hypothalamic explants was developed. Effects of GABA and AMPA on c-fos expression were investigated and subsequent studies showed leptin and glucose modulated the expression of NPY, POMC and AgRP, in fed and fasted animals. Further work is required to validate this novel approach to studying the central control of energy balance.

---

## Abbreviations

5-HT	5-Hydroxytryptamine
aCSF	Artificial cerebrospinal fluid
ACTH	Adrenocorticotropin
ADP	Adenosine monophosphate
AgRP	Agouti-related peptide
AMG	Amygdala
AMPA	Alpha-amino-3-hydroxy-5-methyl-4-isoxazolepropionic acid
AMPK	AMP-activated protein kinase
$\alpha$ -MSH	$\alpha$ -melanocyte stimulating hormone
ANS	Autonomic nervous system
AP5	2-amino-5-phosphonopentanoate
ARC	Arcuate nucleus
ATP	Adenosine triphosphate
BBB	Blood brain barrier
BDNF	Brain derived neurotrophic factor
$\beta$ -MSH	$\beta$ -melanocyte stimulating hormone
BMI	Body mass index
cAMP	Cyclic adenosine-mono-phosphate
CART	Cocaine and amphetamine regulated transcript
CCK	Cholecystokinin
cDNA	Complimentary deoxyribonucleic acid
CNS	Central nervous system
CRF	Corticotrophin releasing factor
CSF	Cerebrospinal fluid
DAT	Digital audio tape
d-fen	D-fenfluramine
DMH	Dorsomedial hypothalamus
DMSO	Dimethylsulphoxide
DNA	Deoxyribonucleic acid
DR	Dorsal raphe
EGTA	Ethylene glycol-bis(2-aminoethylether)-N,N,N',N'-tetraacetic acid
EPSC	Excitatory post-synaptic current



---

EPSP	Excitatory post-synaptic potential
GABA	$\gamma$ -aminobutyric acid
$\gamma$ -MSH	$\gamma$ -melanocyte stimulating hormone
GAD	Glutamic acid decarboxylase
GALP	Galanin-like peptide
GE	Glucose-excited
GH	Growth hormone
GHSR	GH secretagogue receptor
GI	Glucose-inhibited
GI-T	Gastrointestinal tract
GIRK	G-protein coupled inwardly-rectifying potassium channel
GLUT	Glucose transporter
HEPES	4-(2-hydroxyethyl)piperazine-1-ethanesulfonic acid
$I_A$	A-like outward rectifier
$I_{an}$	Anomalous inward rectifier
$I_h$	Hyperpolarisation-activated non-selective cation channel
IPSC	Inhibitory post-synaptic current
IPSP	Inhibitory post-synaptic potential
I-V	Current-voltage relationship
JAK-STAT	Janus-Kinase-Signal transducer and activator of transcription
$K_{ATP}$	ATP-sensitive potassium channel
LC	Locus coeruleus
LH	Lateral hypothalamus
MCH	Melanin concentrating hormone
ME	Median eminence
mRNA	Messenger ribonucleic acid
NBQX	6-nitro-7-sulphamoylbenzo(f)-quinoxaline-2,3-dione
NC-IUPHAR	Nomenclature Committee of the International Union of Pharmacology
NDS	Normal donkey serum
NGF	Nerve growth factor
NGS	Normal goat serum
NMDA	N-methyl-D-aspartate
NPY	Neuropeptide Y

---

NTS	Nucleus of the tractus solitarius
PAG	Periaqueductal gray area
PCR	Polymerase chain reaction
PI3K	Phosphatidylinositol 3-kinase
PLC	Phospholipase C
POA	Preoptic area
POMC	Pre-pro-opiomelanocortin
PVN	Paraventricular nucleus
PYY	Peptide tyrosine tyrosine
RNA	Ribonucleic acid
RT-PCR	Reverse transcriptase polymerase chain reaction
SCN	Suprachiasmatic nucleus
SPN	Sympathetic preganglionic neurones
SUR	Sulphonylurea
TASK	Tandem-pore potassium channel
TBS-T	Tris-buffered saline containing 1% Triton X-100
TGF- $\beta$	Transforming growth factor beta
TTX	Tetrodotoxin
VGAT	Vesicular GABA transporter
VGLUT	Vesicular glutamate transporter
VMN	Ventromedial nucleus
Vp	Vasopressin
WHO	World Health Organisation



# Chapter 1

## *General Introduction*

## 1.1 Central Control of Energy Homeostasis

Energy homeostasis is a complex process involving the integration and co-ordination of multiple metabolic, endocrine and neuronal signals within the body. The central nervous system (CNS) is largely responsible for regulating energy homeostasis. In particular, within the brain the hypothalamus and brainstem are reciprocally connected and play an important role in the central control of energy homeostasis by assessing and integrating the metabolic status of the body and engaging the autonomic nervous system (ANS) to produce efferent responses. Outside the CNS, signals arising from peripheral sites including the liver, the gastrointestinal tract (GI-T), adipose tissue, adrenal glands and pancreas relay the metabolic status of the body to the hypothalamus and the brainstem. The GI-T has direct vagal afferent connections with the brainstem, particularly with the nucleus of the tractus solitarius (NTS), which allows neuronal communication between the GI-T and the brain. Metabolic signals from the GI-T include the satiety signals cholecystokinin (CCK) and peptide tyrosine tyrosine (PYY) and the orexigenic hormone ghrelin, which act upon the brainstem to inform it about the contents of the gut. Adipocytokines from adipose tissue, glucocorticoids from the adrenal glands, insulin from the pancreas and glucose from the liver also all feedback to the hypothalamus and brainstem to provide further information on the energy status of the body. As well as hormonal and neuropeptide signalling, essential nutrients such as proteins, carbohydrates and fatty acids also play an important role in signalling to the CNS the energy status of the body (Schwartz *et al.*, 1999).

As well as being affected by these signals from the periphery, the hypothalamus also receives inputs from within the CNS to control energy homeostasis. These inputs come from higher centres such as the prefrontal cortex,



hippocampus, olfactory systems and the amygdala which add to the multitude of factors regulating energy homeostasis. These higher centres bring in cognitive, motivational and emotional cues, such as the desire for palatable food (Berthoud, 2004) to add further complexity to the regulation of energy homeostasis.

Collectively, these signals and pathways constitute a negative feedback loop, which exists to bring about a co-ordinated response to maintain feeding and energy expenditure (see figure 1.1). For general reviews on the central control of energy homeostasis, see Schwartz *et al.*, 1999, 2000 and Zigman & Elmquist, 2003.

### ***1.1.1 Central nervous system control of body-weight***

Body-weight is controlled by a strict balance between energy intake (i.e. food consumption) and energy expenditure (i.e. exercise). A disruption in this balance will lead to a change in body-weight, which could result in one of two extreme conditions. If energy intake exceeds energy expenditure, i.e. we eat more than we can burn off, then there will be an increase in body-weight, which may eventually result in obesity. If energy expenditure exceeds energy intake, then there will be a decrease in body-weight that could result in the condition anorexia. For the majority of people neither of these conditions will occur because body-weight is strictly regulated by the CNS and small fluctuations in energy balance are controlled within tight limits. However in a few cases, energy homeostasis can become disrupted resulting in an inability to maintain body-weight within these usual limits.

Within the CNS, there are two principal pathways that are responsible for controlling body-weight. These are the anabolic and catabolic pathways, which work as parallel and opposing pathways to maintain body-weight around a defined set point. Stimulation of the anabolic pathway promotes a state of positive energy

balance by increasing food intake and inhibiting energy expenditure, whereas stimulation of the catabolic pathway leads to a decrease in food intake and an increase in energy expenditure. There are many orexigenic and anorexigenic peptides and hormones that are important in controlling these pathways and in regulating energy homeostasis which will be discussed later.

## **1.2 The Autonomic Nervous System**

Homeostasis is defined as the maintenance of the internal environment. The ANS plays a key role in regulating homeostasis. It is predominantly an efferent system of nerves that innervates nearly all tissues and organs within the body, excluding skeletal muscle. The ANS is responsible for controlling visceral functions such as heart rate, blood pressure, body temperature, contraction and relaxation of smooth muscle and secretions from glands. The ANS consists of three divisions, the parasympathetic nervous system, the sympathetic nervous system and the enteric nervous system. The enteric nervous system innervates the gastrointestinal tract, the pancreas and the gall bladder and functions to control gastrointestinal motility and secretions.

The parasympathetic and sympathetic nervous systems are principally responsible for controlling the function of all internal organs, loosely termed 'the viscera' referring to all organs and glands except skeletal muscle. Both systems consist of preganglionic neurones that make synaptic connections with postganglionic neurones, which then make contact with effector organs. Differences between the two systems are reflected in part through the location of preganglionic neurones in the CNS and the neurotransmitter(s) released at the synapses. Parasympathetic preganglionic neurones are located in several nuclei of the



brainstem, and in the sacral segments of the spinal cord, whereas the sympathetic preganglionic neurones arise between the lower cervical and upper lumbar spinal segments of the cord. The principal neurotransmitter released by preganglionic neurones in both systems is acetylcholine whereas it differs for the postganglionic neurones, with the parasympathetic system utilising acetylcholine and the sympathetic system predominantly using noradrenaline with the exception of the sweat glands which use acetylcholine.

In general, the parasympathetic system serves to conserve energy, by reducing blood pressure and heart rate, and facilitating digestion. The sympathetic system has the opposite effect, at its most extreme preparing the body for the classic 'flight or fight' response, by increasing heart rate and blood pressure and diverting blood flow to the skeletal muscle. Although both systems have opposing functions, they function synergistically to maintain homeostasis.

The parasympathetic and sympathetic nervous systems represent the efferent output of the ANS. However the ANS is able to receive afferent signals and one of the most important CNS regions where these signals are integrated is the hypothalamus in the brain. The hypothalamus is therefore a very important centre for regulating ANS activity and essentially for helping to maintain the homeostasis of the body.

### **1.3 Hypothalamic Control of Energy Homeostasis**

The hypothalamus regulates many important homeostatic behaviours including energy balance, thirst, temperature and sexual activity. Within the hypothalamus there are many nuclei that are responsible for controlling particular functions. For example, the suprachiasmatic nucleus (SCN) is responsible for

controlling circadian rhythms, the preoptic area (POA) is important in reproduction and thermoregulation and the lateral hypothalamus (LH) controls sleep and arousal. Energy homeostasis is controlled by several interconnected nuclei including the arcuate nucleus (ARC), LH, ventromedial nucleus (VMN), dorsomedial hypothalamus (DMH) and the paraventricular nucleus (PVN). The various nuclei within the hypothalamus contain reciprocal connections, producing a complex network which functions to coordinate and integrate responses to regulate energy homeostasis (see figure 1.2). Nuclei within the hypothalamus contain populations of neurones that include orexigenic (stimulate feeding) or anorexigenic (inhibit feeding) neurones, which work synergistically to regulate energy homeostasis.

The hypothalamus was first identified as being important in the control of feeding and energy homeostasis through the use of electrical stimulation and lesion studies to ablate regions of the hypothalamus. Hetherington & Ranson (1940) and later Anand & Brobeck (1951) put forward the model of the 'dual-centre' hypothesis, whereby there is a lateral hypothalamic feeding centre and a ventromedial hypothalamic satiety centre. Stimulation of the LH induced obesity whereas lesions in the LH caused decreased food intake and body-weight. The opposite effect was seen in the VMN: stimulation led to a suppression of food intake and lesions of the VMN induced morbid obesity.

Over the years there has been extensive research to try to determine how the body regulates feeding and energy homeostasis. In the 1950s, Kennedy proposed the lipostat hypothesis, where body fat is the principal regulator of energy homeostasis (Kennedy, 1953). This stated that 'humoral signals are generated in proportion to the amount of fat stored and signal to the brain to alter food intake and energy expenditure'. Evidence for this hypothesis was eventually found with the discovery



of leptin, an important adiposity factor (Zhang *et al.*, 1994). A second hypothesis was put forward by Mayer, who believed that glucose was the key regulator of energy homeostasis. This was subsequently termed the 'glucostat hypothesis', whereby the brain is able to sense and respond to carbohydrates to regulate feeding (Mayer, 1953, 1955). Subsequent research has shown that both leptin and glucose are important in the regulation of energy homeostasis; evidence for this will be discussed later.

Of the multiple nuclei within the hypothalamus that control energy homeostasis, the nucleus that has received the most attention and is probably the most important for regulating feeding and body-weight is the ARC.

### ***1.3.1 Arcuate nucleus***

The ARC plays a fundamental role in the control of feeding and energy homeostasis. It is situated adjacent to the third ventricle, immediately above the median eminence and occupies an arc like region, hence its name. It consists of a heterogeneous collection of neurones, which have functions involved in feeding, glucose homeostasis, pain, reproduction, and stress responses to name a few (Chronwall, 1985). It is a major integrative centre within the hypothalamus and receives multiple afferent inputs (Chronwall, 1985). Inputs come from areas within the hypothalamus, including the VMN (Krieger *et al.*, 1979), SCN (Saeb-Parsy *et al.*, 2000) and the LH (Saper *et al.*, 1979), as well as from areas external to the hypothalamus including dorsal raphe neurones (Azmitia & Segal, 1978) and the NTS (Ricardo & Koh, 1978), as well as the amygdala and preoptic area (Anscher *et al.*, 1982; see figure 1.3A).

Neurons from the ARC send projections to multiple brain areas, including other hypothalamic nuclei, to activate second order neurons (Chronwall, 1985; Cone *et al.*, 2001; Williams *et al.*, 2001). Efferent projections from the ARC go to the SCN and preoptic area, the PVN (Harris & Sanghera, 1974; Makara & Hodacs, 1975; Sawchenko & Swanson, 1983; Baker & Herkenham, 1995; Saeb-Parsy *et al.*, 2000), the medial preoptic, anterior periventricular and ventromedial nuclei (Zaborszky & Makara, 1979), LH, DMH and amygdala (Sim & Joseph, 1991). There is also a well-documented projection between the ARC and the median eminence (Rethelyi & Halasz, 1970; Wiegand & Price, 1980). Projections from the ARC also go to the spinal cord (Schwanzel-Fukuda *et al.*, 1984) as well as areas in the brainstem including the periaqueductal gray, dorsal raphe and locus coeruleus (Sim & Joseph, 1991; see figure 1.3B)

Many of the efferent connections from the ARC go to the same areas that send afferent connections to the ARC, indicating reciprocal connections between many areas.

The ARC is ideally situated to co-ordinate feeding and energy homeostasis as it sits just above the circumventricular organ the median eminence, which has a specialised blood-brain-barrier (BBB; Broadwell *et al.*, 1983; Fry *et al.*, 2007). This means that peripheral factors such as hormones can easily access the ARC and it is therefore able to sense and respond to factors that other areas of the brain could not. Further evidence that the ARC is an important site in the regulation of feeding is the fact that it contains a heterogeneous population of neuronal subtypes, which express a diverse array of molecules known to be involved in feeding. These include neuropeptide Y (NPY), pre-pro-opiomelanocortin (POMC), cocaine and amphetamine regulated transcript (CART), agouti-related peptide (AgRP),



neuromedin U and galanin-like peptide (GALP; Chronwall, 1985; Cone *et al.*, 2001). Certain neuronal subtypes within the ARC also express receptors for other substances which are known to be involved in energy homeostasis, for example, leptin, ghrelin, orexin, 5-HT (5-hydroxytryptamine; serotonin) and noradrenaline (Elias *et al.*, 1998b; Broberger, 2005; Elmquist *et al.*, 2005). The ARC is therefore proposed to be the fundamental integrative centre for the control of feeding and energy homeostasis.

Within the hypothalamus there are multiple neuropeptides, hormones and other signalling factors that are involved in the control of energy homeostasis. Orexigenic molecules stimulate the anabolic pathway, by increasing food intake and inhibiting energy expenditure. Anorexigenic molecules stimulate the catabolic pathway, causing a decrease in food intake and an increase in energy expenditure (see table 1.1).

**Table 1.1 Orexigenic and anorexigenic signalling molecules involved in energy homeostasis**

<b>Orexigenic</b>	<b>Anorexigenic</b>
Ghrelin	CCK
NPY	Glucagon-like peptide-1
Orexin A/B	PYY <sub>3-36</sub>
AgRP	Leptin
MCH	Insulin
Endocannabinoids	$\alpha$ -MSH
Noradrenaline	CRF
Galanin	Neuromedin U
GABA	CART
Uncoupling proteins	POMC
Dynorphin	Oxyntomodulin
AMP kinase	Serotonin
	Noradrenaline
	GABA
	Neurotensin
	Obestatin
	Neuromedin S
	Enterostatin
	Pancreatic polypeptide
	Bombesin
	GALP

Within the ARC, there are principally two important neuronal subgroups that control the anabolic and catabolic pathways, those expressing NPY/AgRP and those expressing POMC/CART (see figure 1.4). NPY neurones are expressed in the ventromedial part of the ARC whereas POMC neurones are found more laterally. NPY and POMC are never found expressed in the same neurone (Schwartz *et al.*, 1999; Elmquist *et al.*, 2005). Downstream targets of neurones within the ARC include neurones within the LH and the PVN. Specifically in the LH, there exist two key populations of neurones, orexin and melanin concentrating hormone (MCH), which are innervated by NPY/AgRP and POMC neurones (Elias *et al.*, 1998b), and within the PVN, corticotrophin releasing factor (CRF) neurones are targets of ARC neurones (Baker & Herkenham, 1995). The roles of some of the most important



orexigenic and anorexigenic peptides involved in energy homeostasis will now be discussed in detail.

## **1.4 Orexigenic Neuropeptides**

### **1.4.1 NPY**

NPY is part of the pancreatic polypeptide family that includes peptides such as PYY. It is a 36 amino acid peptide that was discovered in the hypothalamus in 1982 (Tatemoto *et al.*, 1982) and is one of the most abundant peptides in the brain (Adrian *et al.*, 1983), with the highest levels being found in the PVN and the ARC (Chronwall, 1985). Like PYY (Morley *et al.*, 1985), NPY is a potent orexigen as injection into the PVN and cerebral ventricles causes hyperphagia and obesity (Stanley *et al.*, 1986; Zarjevski *et al.*, 1993) and food deprivation increases both NPY and NPY mRNA (Sahu *et al.*, 1988; Sanacora *et al.*, 1990; White *et al.*, 1990; Kalra *et al.*, 1991; Schwartz *et al.*, 1993). NPY neurones have been shown to release the inhibitory neurotransmitter GABA, which exerts a tonic inhibition on neighbouring anorexigenic POMC neurones. This means that when NPY neurones are active, the neighbouring POMC neurones are inhibited, reducing the anorexigenic effects they produce and thereby furthering the orexigenic effects of NPY (Horvath *et al.*, 1997; Cowley *et al.*, 2001). NPY has also been shown to inhibit POMC mRNA expression via the Y<sub>2</sub> receptor (Garcia de Yebenes *et al.*, 1995) and inhibit POMC neuronal activity directly via the Y<sub>1</sub> receptor (Roseberry *et al.*, 2004). Whether NPY or GABA release is the most important signal from NPY neurones remains to be determined but it would appear that both play a role in feeding.

There are 5 types of NPY receptor, Y<sub>1</sub>-Y<sub>5</sub>, although only Y<sub>1</sub>, Y<sub>2</sub> and Y<sub>5</sub> are thought to be involved in feeding (Gerald *et al.*, 1996). They are all G-protein coupled receptors, either to G<sub>i/o</sub> proteins. Predominantly, in the ARC the Y<sub>1</sub> receptor is found on POMC neurones whereas the Y<sub>2</sub> receptor is located on NPY neurones and is thought to act as a presynaptic autoreceptor (Broberger *et al.*, 1997). Mice with deletion of the Y<sub>2</sub> receptor have increased food intake and body-weight (Naveilhan *et al.*, 1999) whereas Y<sub>1</sub> receptor knockout mice show a reduced response to fast-induced re-feeding (Pedrazzini *et al.*, 1998). The Y<sub>5</sub> receptor is involved in the feeding response to centrally administered NPY but it is not a critical feeding receptor (Marsh *et al.*, 1998).

#### **1.4.2 AgRP**

AgRP is an endogenous antagonist for the melanocortin 3 and 4 receptors (MC3-R and MC4-R) and is expressed in the CNS (Ollmann *et al.*, 1997; Shutter *et al.*, 1997). It is an orexigenic peptide that is co-expressed with NPY but not with POMC in the ARC (Hahn *et al.*, 1998) and administration of AgRP leads to an increase in food intake and body-weight (Ollmann *et al.*, 1997). Ablation of AgRP neurones results in acute reduction of feeding showing that they are critical in energy homeostasis (Gropp *et al.*, 2005). AgRP is thought to increase feeding by inhibiting activity at MC-4 receptors thus blocking anorexigenic pathways.

#### **1.4.3 Orexin**

Orexins, (taken from the Greek *orexis* meaning appetite) or hypocretins as they are also known, were discovered as a novel family of neuropeptides that bind to G-protein coupled receptors (de Lecea *et al.*, 1998; Sakurai *et al.*, 1998). They are



abundantly expressed in the LH and are present in two forms, orexin A and orexin B, which are both derived from the precursor prepro-orexin. They bind to two closely related G-protein coupled receptors, orexin receptor 1 and 2. Central injections of orexin stimulate feeding and food restriction leads to an increase in orexin mRNA levels (Sakurai *et al.*, 1998; Dube *et al.*, 1999). The orexigenic effects of orexin may arise due to the inhibition of POMC neurones (Ma *et al.*, 2007) or to the activation of NPY neurones (Yamanaka *et al.*, 2000). Orexins are also strongly implicated in arousal and waking as mutations in the orexin gene or orexin type 2-receptor result in narcolepsy (Lin *et al.*, 1999; Saper *et al.*, 2005).

#### **1.4.4 MCH**

MCH is a 19 amino acid peptide that is expressed exclusively in the LH and zona incerta (Bittencourt *et al.*, 1992). MCH mRNA levels are increased by food deprivation and central injections of MCH increases food intake (Qu *et al.*, 1996; Ludwig *et al.*, 1998). Mice lacking MCH are hypophagic and lean and over-expression of MCH leads to obesity and hyperleptinemia (Shimada *et al.*, 1998). MCH increases the release of both NPY and AgRP, but decreases the release of  $\alpha$ -MSH and CART from hypothalamic explants (Abbott *et al.*, 2003). MCH also acts as an antagonist at the melanocortin receptors (Ludwig *et al.*, 1998).

### **1.5 Anorexigenic Neuropeptides**

#### **1.5.1 POMC**

POMC is the precursor for a family of melanocortin peptides, including  $\alpha$ -melanocyte stimulating hormone ( $\alpha$ -MSH),  $\beta$ -melanocyte stimulating hormone ( $\beta$ -MSH),  $\gamma$ -melanocyte stimulating hormone ( $\gamma$ -MSH), adrenocorticotropin (ACTH)

and  $\beta$ -endorphin. ACTH and  $\alpha$ -MSH both markedly inhibit feeding when injected into the cerebral ventricles (Poggioli *et al.*, 1986). POMC is only expressed at two sites within the brain: the hypothalamus and the NTS in the brainstem (Jacobowitz & O'Donohue, 1978; Watson & Akil, 1979). Ablation of POMC neurones causes obesity (Xu *et al.*, 2005). Within the ARC, POMC neurones are found adjacent to NPY neurones and are believed to principally release  $\alpha$ -MSH (Jegou *et al.*, 1993). Melanocortin peptides bind to five different melanocortin receptors MC1-5-R but only MC3-R and MC4-R are expressed in the brain and are involved in energy homeostasis (Tatro, 1990; Mountjoy *et al.*, 1994; Kishi *et al.*, 2003). The MC4-R is strongly implicated in the control of feeding as knockout of this receptor leads to increased body-weight and obesity (Huszar *et al.*, 1997), and MC4-R agonists cause anorexia while antagonists of this receptor stimulate feeding (Fan *et al.*, 1997). One of the most common monogenic causes of obesity in humans is due to disrupted MC4-R signalling (Yeo *et al.*, 1998). The MC3-R is expressed on POMC neurones, indicating that melanocortins could exert a feedback role onto POMC neurones (Jegou *et al.*, 2000). This is supported by the fact that a MC3-R agonist suppressed hypothalamic POMC expression and stimulated feeding (Lee *et al.*, 2008).

### 1.5.2 CART

CART was first identified as a transcript up-regulated by cocaine and amphetamine in the striatum (Douglass *et al.*, 1995). It is the third most abundant transcript in the rat hypothalamus (Gautvik *et al.*, 1996). CART decreases food intake and fasting reduces CART expression making it an anorexigenic peptide (Kristensen *et al.*, 1998; Lambert *et al.*, 1998). CART is widely expressed in the rat brain and is present in the same neurones as POMC within the ARC (Elias *et al.*,



1998a), but it is not expressed with NPY. It is also co-localised with melanin concentrating hormone (MCH) neurones within the LH (Broberger, 1999). This is unusual as MCH is orexigenic, leading to a neuronal group containing both orexigenic and anorexigenic peptides. In humans however, CART is not expressed on POMC neurones but is instead found on a minority of NPY neurones indicating a possible orexigenic role for CART in the human hypothalamus (Menyhert *et al.*, 2007).

### **1.5.3 CRF**

CRF is a 41 amino acid peptide that is primarily produced in the PVN. It has an important role in controlling hypothalamic-pituitary-adrenal activity but it is also involved in energy balance. It is involved in the catabolic pathway as it leads to a suppression of food intake and an increase in energy expenditure (Arase *et al.*, 1988; Rothwell, 1990).

### **1.5.4 CCK**

CCK is a GI-T peptide, released from the endocrine-I cells in the small intestine, in response to food intake and is known to induce satiety and reduce food intake (Gibbs *et al.*, 1973). It is thought to mediate the short-term control of feeding as repeated administration does not lead to a decrease in body-weight (Cummings & Overduin, 2007). CCK acts via two G-protein coupled receptors, CCK1 and CCK2 (Wank *et al.*, 1992), which are widely expressed in the CNS (Moran *et al.*, 1986), with particularly high levels in the caudate nucleus, cerebral cortex and hypothalamus (Hays *et al.*, 1981). Receptors in the hypothalamus as well as on the

vagus nerve are thought to be responsible for its role in energy homeostasis (Noble *et al.*, 1999).

Alongside hypothalamic peptides, there are also signalling factors that are important in the control of energy homeostasis. These include the neurotransmitters  $\gamma$ -aminobutyric acid (GABA) and glutamate.

### **1.5.5 Neurotransmitters**

The role of fast acting neurotransmitters (GABA and glutamate) in feeding and energy homeostasis has been largely neglected due to the focus on the vast number of neuropeptides thought to be involved. However both GABA and glutamate are thought to play an important role in the regulation of feeding (van den Pol, 2003). A role for GABA is suggested as both glutamic acid decarboxylase (GAD) and the vesicular GABA transporter (VGAT) have been found in NPY neurones (Horvath *et al.*, 1997; Ovesjo *et al.*, 2001) and more recently GAD mRNA was also discovered in a population of POMC neurones (Hentges *et al.*, 2004). A population of POMC neurones however has also been shown to be glutamatergic as the vesicular glutamate transporter (VGLUT2) has been found in POMC neurones (Collin *et al.*, 2003). Therefore orexigenic NPY neurones are proposed to be GABAergic whereas different populations of POMC neurones are either GABAergic or glutamatergic.

## **1.6 Hormonal and Nutrient Signalling**

There are several circulating factors that are thought to impinge on the hypothalamus and contribute to the regulation of energy homeostasis. These include the adiposity factors leptin and insulin, which are proposed to be long-term



regulators of feeding, and glucose and ghrelin, which are thought to be involved on a more short-term basis and help to regulate meal initiation. In addition adipocytokines released from adipose tissue play an important role as do signals from the GI-T including most importantly PYY.

### 1.6.1 Leptin

Leptin (taken from the Greek *leptos* meaning thin) was discovered as the protein product of the *ob* gene and is the long sought after adiposity factor proposed by Kennedy (Zhang *et al.*, 1994; for review, see Friedman & Halaas, 1998). It is produced from adipose tissue in direct proportion to the amount of fat stored and signals this information to the brain. There are at least 6 splice variants of the leptin receptor (Ob-R a-f) but the abundant form in the hypothalamus is the long form of the receptor (Ob-Rb; Tartaglia *et al.*, 1995; Lee *et al.*, 1996). Ob-Rb is expressed in many hypothalamic nuclei involved in energy homeostasis, including the ARC, LH, VMN, and PVN (Hakansson *et al.*, 1998). The leptin receptor is a type I cytokine receptor and activates the JAK2-STAT3 pathway and other pathways downstream including the phosphatidylinositol 3-kinase (PI3K) pathway (Tartaglia *et al.*, 1995; Fruhbeck, 2006).

Mice lacking leptin (*ob/ob*) or the leptin receptor (*db/db*) are obese (Lee *et al.*, 1996). Administration of leptin causes an inhibition of feeding and a decrease in body-weight (Campfield *et al.*, 1995; Halaas *et al.*, 1995; Pelleymounter *et al.*, 1995; Weigle *et al.*, 1995; Schwartz *et al.*, 1996). Leptin can reverse the obesity seen in leptin deficient (*ob/ob*) mice, but not in *db/db* mice. However in some individuals, an increase in leptin has no effect as leptin resistance develops. This may be either

due to impaired leptin receptor signalling or due to lack of leptin access to the brain perhaps due to impaired transport across the BBB.

Direct injection of leptin into the ARC, VMN and LH decreases food intake and body-weight, with the ARC being the primary site of the satiety effect of leptin (Satoh *et al.*, 1997). Leptin acts in the ARC to stimulate POMC/CART neurones and inhibit NPY/AgRP neurones (Stephens *et al.*, 1995; Schwartz *et al.*, 1996, 1997; Thornton *et al.*, 1997; van den Top *et al.*, 2004). Both neuronal subtypes express the leptin receptor (Mercer *et al.*, 1996; Cheung *et al.*, 1997). In *ob/ob* mice, *db/db* mice and *fa/fa* rats, NPY and AgRP mRNA is increased (Beck *et al.*, 1990; Chua *et al.*, 1991; Wilding *et al.*, 1993; Shutter *et al.*, 1997) and POMC and CART mRNA is reduced (Schwartz *et al.*, 1996; Thornton *et al.*, 1997). Repletion of leptin in *ob/ob* mice suppresses this elevated NPY expression and increases POMC expression (Stephens *et al.*, 1995; Schwartz *et al.*, 1996, 1997; Thornton *et al.*, 1997). Knockout of NPY reduces the hyperphagia and obesity seen in *ob/ob* mice indicating that the response to leptin deficiency requires NPY signalling (Erickson *et al.*, 1996).

As well as affecting transcriptional control, leptin can alter the firing properties and electrical activity of ARC neurones. Leptin has been shown to inhibit the firing of a subpopulation of ARC neurones, shown to be glucose-sensing neurones by their sensitivity to changes in extracellular glucose (Spanswick *et al.*, 1997). This occurs through activation of the ATP-sensitive potassium channel ( $K_{ATP}$ ) and subsequent PI3K-dependent signalling (Spanswick *et al.*, 1997; Mirshamsi *et al.*, 2004). Leptin has also been shown to depolarise POMC neurones via activation of a non-selective cation channel, also involving a PI3K-dependent downstream signalling pathway (Hill *et al.*, 2008; Rother *et al.*, 2008).



In addition to regulating NPY/POMC neurones, leptin also targets other hypothalamic neurones, for example, MCH, galanin, GALP, orexin and CRF. Leptin increases the expression of the anorexigenic peptides CRF and GALP (Huang *et al.*, 1998; Kumano *et al.*, 2003) whereas it inhibits the expression of the orexigenic peptides MCH, orexin and galanin (Sahu, 1998; Lopez *et al.*, 2000).

For a review of leptin signalling, see Sahu, 2004 and Myers *et al.*, 2008.

### **1.6.2 Insulin**

Insulin was one of the first signals proposed to regulate energy homeostasis (Porte & Woods, 1981). It is produced from  $\beta$ -cells in the islets of langerhans in the pancreas and circulates in proportion to plasma glucose levels. Insulin receptors are expressed within the brain, including in hypothalamic nuclei (Marks *et al.*, 1990) and both insulin and leptin converge on the same downstream signalling pathway -PI3K. Administration of insulin intracerebroventricularly reduces food intake and body-weight (Brief & Davis, 1984; Ikeda *et al.*, 1986), partly because insulin reduces the levels of the orexigenic peptide NPY (Schwartz *et al.*, 1991, 1992). Genetic models of obese rats with insulin receptor knockouts confirm the role of insulin in energy homeostasis (Bruning *et al.*, 2000). However, obesity does not arise if insulin levels fall, therefore it would appear that leptin is more critical in the regulation of energy homeostasis.

Like leptin, insulin is also able to regulate the firing properties of neurones as it has been shown to hyperpolarise a subset of ARC neurones (Spanswick *et al.*, 2000), including identified POMC neurones (Hill *et al.*, 2008), through activation of the  $K_{ATP}$  channel and subsequent PI3K-dependent signalling pathway (Spanswick *et al.*, 2000; Hill *et al.*, 2008; Rother *et al.*, 2008).

### **1.6.3 Adipocytokines**

Adipose tissue is an endocrine organ that secretes a number of adipocytokines, which play a key role in energy homeostasis. Adipocytokines are factors that are expressed and secreted by adipocytes into the circulation, of which the two most abundant are leptin and adiponectin. Together they act to regulate food intake. Leptin is secreted in direct proportion to the amount of fat stored and is proposed to act as a satiety signal. Opposing leptin's actions, adiponectin is proposed to act as a starvation signal, as it is secreted inversely to the amount of fat stored. Adiponectin has important insulin sensitising effects as a decrease in adiponectin contributes to type 2 diabetes and insulin resistance (Kadowaki *et al.*, 2008). Alongside its anti-diabetic effects, adiponectin is proposed to play a central role in energy homeostasis. The adiponectin receptors, adipoR1 and adipoR2, (Yamauchi *et al.*, 2003) are expressed in the hypothalamus (Kubota *et al.*, 2007), and it has been suggested that adiponectin acts as an orexigenic signal by stimulating AMP-activated protein kinase (AMPK). AMPK acts as an energy sensor in cells as it activates processes that produce energy whilst inhibiting those that consume energy. This leads to an increase in food intake and a decrease in energy expenditure (Minokoshi *et al.*, 2004; Kadowaki *et al.*, 2008).

### **1.6.4 Glucose**

Glucose is the primary energy source of most mammalian cells and therefore it is important that there is a constant supply of glucose within the body. The liver is the principal organ which regulates the production and uptake of glucose and hence maintains glucose homeostasis. Most neurones use glucose as the fuel for their metabolic activity, however there are a specialised group of neurones that are also



able to sense glucose. These neurones monitor and integrate changes in extracellular glucose concentration and are able to regulate their electrical activity in response to these changes. Mayer first postulated over 50 years ago that glucose was sensed by glucoreceptors in the hypothalamus to control food intake (Mayer, 1953) and Anand and Oomura later showed that neurones in the LH and VMN actually used glucose to alter their firing properties (Anand *et al.*, 1964; Oomura *et al.*, 1964). These 'glucose-sensing' neurones have subsequently been found within the ARC and other areas of the hypothalamus (Ashford *et al.*, 1990a; Spanswick *et al.*, 1997).

Glucose-sensing neurons have been divided into glucose-excited neurones (GE), which increase their activity in response to increases in glucose, and glucose-inhibited neurones (GI) that decrease their activity in response to increases in glucose (Levin *et al.*, 1999). The mechanism by which GE neurones sense glucose and alter their activity is via the  $K_{ATP}$  channel (Rowe *et al.*, 1996; Miki *et al.*, 2001). This occurs in an analogous way to the glucose-stimulated insulin release in pancreatic  $\beta$ -cells (Schuit *et al.*, 2001). Briefly, glucose enters the cell via a GLUT transporter and glycolysis occurs via a glucokinase. Glycolysis increases the ATP/ADP ratio, which leads to closure of the  $K_{ATP}$  channel, leading to membrane depolarisation, influx of calcium and generation of an action potential. The GLUT2 transporter, glucokinase and the  $K_{ATP}$  channel have all been shown to be essential components of this process (Dunn-Meynell *et al.*, 2002; Kang *et al.*, 2004; Wang *et al.*, 2004; Bady *et al.*, 2006; Kang *et al.*, 2006; Yang *et al.*, 2007). In particular, the role of the  $K_{ATP}$  channel in the regulation of the electrical activity of glucose sensing neurones in the hypothalamus has been shown in many previous studies (Ashford *et al.*, 1990a, b; Spanswick *et al.*, 1997; Lee *et al.*, 1999; Spanswick *et al.*, 2000; Miki *et al.*, 2001; Zhang *et al.*, 2004). The  $K_{ATP}$  channel is an octameric protein consisting

of 4 pore forming units, the inward rectifier K<sup>+</sup> channel (either Kir 6.1 or Kir 6.2) and 4 sulphonylurea receptors (SUR1 or SUR2). In the ARC, the most probable composition of K<sub>ATP</sub> channels is Kir 6.2 and SUR1, analogous to that found in pancreatic  $\beta$ -cells (Miki *et al.*, 2001; van den Top *et al.*, 2007), although a study of the VMH demonstrated that Kir 6.1 not Kir 6.2 was expressed (Lee *et al.*, 1999). A recent study however found that not all GE neurones detect glucose via the K<sub>ATP</sub> channel but instead sense glucose via a K<sub>ATP</sub>-independent mechanism (Fioramonti *et al.*, 2004). However in this study very high glucose levels were used, between 5 and 20 mM, and hence these neurones were named high-glucose-excited. They hypothesised that these neurones have the ability to sense glucose at a concentration above 5 mM through a K<sub>ATP</sub>-independent mechanism as they found that at 5 mM glucose the K<sub>ATP</sub> channel was mostly closed. Therefore this mechanism may only occur at non-physiological glucose levels.

The mechanism by which glucose inhibits GI neurones is much less clear. Studies indicate that a chloride conductance may be responsible, as activation of chloride channels in the membrane by elevated glucose leads to hyperpolarisation of the cell (Song *et al.*, 2001; Fioramonti *et al.*, 2007). A different mechanism has also been proposed, whereby glucose inhibited orexin neurones in the LH through the involvement of tandem-pore potassium channels (TASK; Burdakov *et al.*, 2006).

Both NPY neurones and POMC neurones within the ARC have been shown to express the K<sub>ATP</sub> channel (van den Top *et al.*, 2007). NPY neurones were found to be GI neurones (Muroya *et al.*, 1999) whereas POMC neurones were found to be GE neurones (Ibrahim *et al.*, 2003), although subsequent studies failed to identify GE neurones as POMC neurones (Wang *et al.*, 2004; Fioramonti *et al.*, 2007). For a



review of glucose-sensing see Levin *et al.*, 2004, 2006 and Mountjoy & Rutter, 2007.

As well as regulating the electrical activity of neurones within the hypothalamus, the  $K_{ATP}$  channel has been shown to play an essential role in the regulation of hepatic glucose homeostasis. Insulin, acting through hypothalamic  $K_{ATP}$  channels, has been shown to inhibit hepatic glucose production (Pocai *et al.*, 2005), and this hypothalamic control by insulin has been shown to be essential in preventing hyperglycaemia (Obici *et al.*, 2002c). In addition, the expression of insulin receptors in the hypothalamus has been shown to be vital for the control of hepatic glucose production by insulin (Obici *et al.*, 2002a). These data provide evidence that hypothalamic control of glucose production by insulin and the  $K_{ATP}$  channel is essential for liver glucose homeostasis.

### 1.6.5 Ghrelin

Ghrelin is a 28 amino acid orexigenic peptide released from the endocrine cells of the stomach, as well as the intestine (Date *et al.*, 2000). The name ghrelin is based on the word root 'ghre' from the Proto-Indo-European languages, meaning grow, as it can stimulate growth hormone (GH) release (Kojima & Kangawa, 2005). It was discovered as the endogenous ligand for the GH secretagogue receptor (GHSR; Kojima *et al.*, 1999) and is modified with an n-octanoyl group at serine 3, a modification essential for its biological activity. The GHSR is found extensively distributed all over the brain and within all areas of the hypothalamus (Guan *et al.*, 1997; Zigman *et al.*, 2006; Harrold *et al.*, 2008). Administration of ghrelin strongly stimulates feeding and suppresses energy expenditure in rats and humans (Tschop *et al.*, 2000; Wren *et al.*, 2001a,b; Lawrence *et al.*, 2002; Wang *et al.*, 2002;

Faulconbridge *et al.*, 2003; Currie *et al.*, 2005) as well as stimulating gastric emptying (Asakawa *et al.*, 2001). Administration of an antagonist to the ghrelin receptor leads to a reduction in body-weight and decrease in feeding (Asakawa *et al.*, 2003). Elevated levels of plasma ghrelin have been associated with a common form of human obesity called Prader-Willi syndrome suggesting that hyperghrelinemia can contribute to obesity (Cummings *et al.*, 2002a). Interventions to lower plasma ghrelin may therefore be useful in the treatment of obesity for sufferers of Prader-Willi syndrome.

Ghrelin is one of the most potent stimulants of short-term feeding, greater than any other known peptide except NPY (Asakawa *et al.*, 2001). It is thought to be involved in the initiation of individual meals, as studies have shown there to be a pre-prandial rise and a postprandial decline in plasma ghrelin levels (Cummings *et al.*, 2001, 2002b). Ghrelin acts in the ARC to stimulate NPY/AgRP neurones as NPY neurons in the ARC express GHSR (Willesen *et al.*, 1999) and ghrelin increases NPY and AGRP mRNA expression in both fed and fasted rats (Kamegai *et al.*, 2000, 2001; Nakazato *et al.*, 2001; Seoane *et al.*, 2003). Further evidence that ghrelin acts via the NPY pathway is that antagonism of NPY receptors attenuates the orexigenic effects of ghrelin (Shintani *et al.*, 2001) and that knockout of NPY and AgRP completely abolishes the orexigenic effect of ghrelin (Chen *et al.*, 2004). For a review of ghrelin signalling see Kojima & Kangawa, 2005.

### **1.6.6 PYY**

There are many peptides and hormones produced in the GI-T that play a key role in the central control of energy homeostasis. GI-T signals principally target the hindbrain, either via vagal afferents from the gut that innervate the NTS or by being



released into the circulation and crossing the BBB. One of the most important GI-T signals is PYY.

PYY is a 36 amino acid peptide belonging to the pancreatic polypeptide family, to which NPY also belongs. It is secreted from L cells in the ileum postprandially and exists in two forms, PYY<sub>1-36</sub> and PYY<sub>3-36</sub>. PYY<sub>1-36</sub>, which binds to the Y<sub>1</sub>, Y<sub>2</sub> and Y<sub>5</sub> receptors, and is cleaved into PYY<sub>3-36</sub> which preferentially binds to the Y<sub>2</sub> receptor (Keire *et al.*, 2000, 2002). Both forms increase food intake when administered centrally but decrease food intake in the periphery. This decrease in feeding is proposed to occur through PYY<sub>3-36</sub> acting at the Y<sub>2</sub> receptor on NPY neurones to reduce NPY expression and dis-inhibit POMC neurones (Morley *et al.*, 1985; Batterham *et al.*, 2002; Batterham & Bloom, 2003; Challis *et al.*, 2003). Further evidence for this comes from a study showing that blockade of the Y<sub>2</sub> receptor with a specific Y<sub>2</sub> antagonist attenuates the anorexigenic effect of peripherally administered PYY (Abbott *et al.*, 2005).

For a review of gastrointestinal regulation of food intake see Cummings & Overduin, 2007 and Mendieta-Zeron *et al.*, 2008.

## 1.7 5-HT

Serotonin was identified in the late 1940s as a 'tonic' substance in the 'serum' that constricts smooth muscle and increases vascular tone (hence the name serotonin; Rapport, 1949). Serotonin (5-hydroxytryptamine; 5-HT) is a neurotransmitter that has been implicated in many different behavioural, psychological and physiological functions and diseases, for example, it is heavily involved in mood disorders such as depression, anxiety and schizophrenia, as well as playing a role in migraine, hypertension and eating disorders. It is associated with

the sleep-wake cycle, reproduction, feeding and energy homeostasis and thermoregulation (Bonate, 1991; Wilkinson & Dourish, 1991; Baldwin & Rudge, 1995; Graeff *et al.*, 1996).

5-HT is synthesised from the amino acid tryptophan in a multistep pathway. Firstly, L-tryptophan is hydroxylated by tryptophan hydroxylase. Hydroxytryptophan is then decarboxylated to produce serotonin. 5-HT is produced in the enterochromaffin cells in the gut and in serotonergic neurones in the raphé nuclei in the brainstem, which send projections all over the brain (Azmitia & Segal, 1978; Steinbusch, 1981). There is a subdivision of 5-HT producing neurones in the brainstem, with those located in the rostral region providing ascending projections to the forebrain whereas those in the caudal region provide descending projections to the spinal cord (Tork, 1990). The dorsal raphé and to a lesser extent the median raphé are the origin of the 5-HT innervation of the hypothalamus (Willoughby & Blessing, 1987) as 5-HT from the periphery and circulation does not cross the BBB, although the precursor tryptophan can.

### **1.7.1 5-HT receptors**

5-HT exerts its effects through at least 14 distinct receptors, which have been arranged into 7 families, making it one of the most complex groups of neurotransmitter receptors. They are all metabotropic receptors, belonging to the G-protein coupled receptor family, except for the 5-HT<sub>3</sub> receptor, which is a ligand-gated ion channel.

The origins of the classification of the 5-HT receptor began in 1957 when Gaddum and Picarelli proposed the M and D receptor, after demonstrating that responses of the guinea pig ileum could be blocked by either morphine (M) or



dibenzylamine (D). Subsequently further research by Peroutka and Snyder (1979) demonstrated that only 5-HT could displace two radioligands from two receptor binding sites, so these sites were labelled 5-HT<sub>1</sub> and 5-HT<sub>2</sub>. The D receptor corresponded to the newly discovered 5-HT<sub>2</sub> binding site. However it was not until 1986 that the 5-HT<sub>3</sub> receptor was discovered which corresponded to the M receptor. With more extensive research and new techniques in molecular biology the 5-HT<sub>4</sub>, 5-HT<sub>5</sub>, 5-HT<sub>6</sub> and 5-HT<sub>7</sub> receptors were subsequently identified, along with multiple subtypes for the 5-HT<sub>1</sub> and 5-HT<sub>2</sub> receptors. The current classification was adopted by the Nomenclature Committee of the International Union of Pharmacology (NC-IUPHAR) in 1994, in which 14 receptors have been split into 7 families (Hoyer *et al.*, 1994). These are shown in table 1.2.

**Table 1.2 5-HT receptors**

<b>Receptor Family</b>	<b>Subgroups</b>	<b>Signalling pathway</b>	<b>Principal distribution within brain</b>
5-HT <sub>1</sub>	1A, 1B 1D, 1E, 1F  (5-HT <sub>1C</sub> was subsequently discovered to be more like the 5-HT <sub>2</sub> group and was renamed 5-HT <sub>2C</sub> )	Gi/o - cAMP	1A: Limbic system, raphe nuclei, hypothalamus 1B: hippocampus, striatum, cerebellum, basal ganglia 1D: caudate-putamen, cortical areas 1E: caudate-putamen, amygdala 1F: raphe nucleus, hippocampus, striatum, thalamus
5-HT <sub>2</sub>	2A, 2B, 2C	Gq - PLC	2A: hippocampus, amygdala, hypothalamus, substantia nigra, cerebral cortex 2B: cerebellum, amygdala, raphe nucleus 2C: choroid plexus, substantia nigra, globus pallidus
5-HT <sub>3</sub>		Ion channels	Amygdala, hippocampus
5-HT <sub>4</sub>		Gs -cAMP	Hypothalamus, amygdala, hippocampus, basal ganglia, substantia nigra
5-HT <sub>5</sub>	5A, 5B	Not yet known	5A: cerebellum, hippocampus, hypothalamus 5B: habenula, dorsal raphe
5-HT <sub>6</sub>		Gs - cAMP	Striatum and nucleus accumbens
5-HT <sub>7</sub>		Gs - cAMP	Thalamus, hypothalamus, hippocampus, amygdala

5-HT<sub>1</sub> receptors couple preferentially to the G-proteins Gi/o to inhibit cyclic adenosine-mono-phosphate (cAMP), whereas 5-HT<sub>2</sub> receptors couple to Gq to modulate the phospholipase C (PLC) pathway. 5-HT<sub>4</sub>, 5-HT<sub>6</sub> and 5-HT<sub>7</sub> receptors couple to Gs to stimulate the cAMP pathway (Hoyer *et al.*, 2002). The 5-HT<sub>5</sub> receptors have not yet been convincingly linked to any signalling pathway.

5-HT<sub>3</sub> receptors are non-selective cation channels and cause a depolarisation of neurones due to the influx of Na<sup>+</sup> and Ca<sup>2+</sup> and the efflux of K<sup>+</sup>.



### 1.7.2 Functional effects mediated by the 5-HT receptors

With the huge diversity of 5-HT receptors comes a diverse range of functions that are controlled by 5-HT. The functions attributed to each receptor will be discussed here. For a full review see Barnes & Sharp (1999).

**5-HT<sub>1</sub>:** The 5-HT<sub>1A</sub> receptor controls thermoregulation (Goodwin *et al.*, 1985; Gudelsky *et al.*, 1986) and sexual behaviour (Ahlenius *et al.*, 1981), as well as having a role in psychiatric disorders. 5-HT<sub>1A</sub> agonists are thought to exert antidepressant effects (Charney *et al.*, 1990). The 5-HT<sub>1B</sub> receptor plays a role in locomotor activity and is important in controlling aggression. 5-HT<sub>1B</sub> receptor knockout mice are more aggressive than wild-type (Saudou *et al.*, 1994). Both the 5-HT<sub>1A</sub> and 5-HT<sub>1B</sub> receptor are also strongly implicated in the control of feeding (see section 1.7.3). No convincing physiological or pathophysiological functions are as yet ascribed to the 5-HT<sub>1D</sub> and 5-HT<sub>1E</sub> receptors due to a lack of selective ligands for these receptors. The functions of the 5-HT<sub>1F</sub> receptor are also not fully known though it is speculated to be involved in visual and cognitive function based upon its location (Barnes & Sharp, 1999).

**5-HT<sub>2</sub>:** It is hard to separate out the functions attributed to the 5-HT<sub>2A/2C</sub> receptor subtypes as there is a high degree of homology between the two and there are relatively few ligands that distinguish between them. However the 5-HT<sub>2A</sub> receptor is thought to play an important role in several psychiatric disorders, such as depression and schizophrenia (Baldwin & Rudge, 1995; Graeff *et al.*, 1996). It is also important in temperature regulation (Gudelsky *et al.*, 1986) as well as neuroendocrine responses (Fuller, 1996). The 5-HT<sub>2C</sub> receptor is widely considered

to be involved in the control of feeding (see section 1.7.3). As it is found in the choroid plexus, it is also thought to regulate the composition and volume of the cerebrospinal fluid (CSF; Pazos *et al.*, 1984). It is also proposed to be important in movement and locomotion and have anxiolytic effects (Kennett *et al.*, 1997b). The functions of the 5-HT<sub>2B</sub> receptor are not well known but agonists for this receptor are also thought to have anxiolytic effects (Duxon *et al.*, 1997b).

**5-HT<sub>3</sub>:** This receptor is thought to control gut motility, as well as having antiemetic effects. It also modulates release of the gut peptide CCK (Paudice & Raiteri, 1991; Grignaschi *et al.*, 1993; Hayes & Covasa, 2005) as well as being implicated in cognitive function (Altman *et al.*, 1987). Within the CNS, it controls neurotransmitter release as well as having roles in anxiety (Hoyer *et al.*, 1994).

**5-HT<sub>4</sub>:** The 5-HT<sub>4</sub> receptor modulates the release of various neurotransmitters, such as acetylcholine and dopamine (Barnes & Sharp, 1999). However it is not proposed to exert any effect on behavioural functions, such as feeding or movement.

**5-HT<sub>5</sub>:** Relatively little is known about the functions of the 5-HT<sub>5A</sub> or 5-HT<sub>5B</sub> receptors.

**5-HT<sub>6</sub>:** The functions of this receptor are also not well known. However because this receptor is localised in extrapyramidal and limbic areas, it has been suggested to be involved in the control of motor function and mood disorders (Gerard *et al.*, 1997). It is also suggested to be involved in mediating the effects of antipsychotic agents as it



has been localised in brain areas that are the sites of action of these drugs (Ward *et al.*, 1995).

**5-HT<sub>7</sub>:** The 5-HT<sub>7</sub> receptor is strongly implicated in the regulation of circadian rhythms as it is localised in the SCN (Gustafson *et al.*, 1996; Neumaier *et al.*, 2001).

### **1.7.3 5-HT and control of energy balance**

The central serotonin system has for many years been associated with the regulation of food intake and body-weight (for review see Blundell, 1977, 1984). Depletion of serotonin using neurotoxins results in hyperphagia and obesity (Breisch *et al.*, 1976; Saller & Stricker, 1976) whereas substances that increase serotonin release, such as d-fenfluramine (d-fen), lead to a reduction in feeding and body-weight (Guy-Grand, 1992). 5-HT levels have been shown to increase in the LH upon feeding (Schwartz *et al.*, 1989) and direct injection of 5-HT into the PVN suppressed food intake (Currie & Coscina, 1996). The specific receptors that mediate the effects of serotonin on energy homeostasis have been extensively studied in the past. The principal receptor subtypes involved are proposed to be 5-HT<sub>1A</sub>, 5-HT<sub>1B</sub> and 5-HT<sub>2C</sub>.

Evidence for the involvement of the 5-HT<sub>1A</sub> receptor comes from the fact that the specific 5-HT<sub>1A</sub> receptor agonist 8-OH-DPAT injected sub-cutaneously elicits feeding and hyperphagia in rats (Dourish *et al.*, 1985, 1986; Hutson *et al.*, 1988) and this receptor has been localised to one of the most important areas involved in energy homeostasis, the ARC (Collin *et al.*, 2002). Alongside its role in stimulating feeding, it has also been shown that the 5-HT<sub>1A</sub> receptor is involved in the control of hypothalamic glucose levels, as 8-OH-DPAT reduced glucose levels in the LH (Voigt *et al.*, 2004).

The 5-HT<sub>1B</sub> receptor has been identified as having a role in feeding and energy homeostasis as agonists for this receptor, including CP-94253, RU 24969 and mCPP injected intraperitoneally (i.p.), promote satiety and hypophagia (Bendotti & Samanin, 1987; Kennett *et al.*, 1987; Kennett & Curzon, 1988; Dryden *et al.*, 1996b; Halford & Blundell, 1996; Lee & Simansky, 1997; Lee *et al.*, 2002). Also the serotonin releaser d-fen (injected via the i.p. route) exerts its inhibitory effects on feeding through the 5-HT<sub>1B</sub> receptor (Neill & Cooper, 1989; Grignaschi & Samanin, 1992; Grignaschi *et al.*, 1995) and 5-HT<sub>1B</sub> knockout mice did not display hypophagia after fenfluramine administration (Lucas *et al.*, 1998). In addition the 5-HT<sub>1B</sub> receptor has been identified within the ARC, placing it in a key position to regulate energy homeostasis (Makarenko *et al.*, 2002; Heisler *et al.*, 2006).

5-HT<sub>2C</sub> receptors are also expressed in the ARC (Wright *et al.*, 1995), on both POMC and non-POMC neurones (Heisler *et al.*, 2002; Lam & Heisler, 2007). The 5-HT<sub>2C</sub> receptor has been implicated in the control of feeding as several studies have shown that 5-HT<sub>2C</sub> agonists promote hypophagia, including d-fen and BVT.X (Heisler *et al.*, 2002; Lam *et al.*, 2008). Also, mice lacking 5-HT<sub>2C</sub> receptors are hypophagic and obese (Tecott *et al.*, 1995). The effects of d-fen are reduced in 5-HT<sub>2C</sub> knockout mice, and the 5-HT<sub>2C</sub> receptor antagonist SB242084 inhibits d-fen-induced hypophagia (Vickers *et al.*, 1999, 2001). The downstream pathways thought to mediate these effects include the melanocortin pathway, specifically via the MC4-R (Lam *et al.*, 2008). 5-HT<sub>2C</sub> receptors have also been shown to have an effect on glucose tolerance independently of food intake and body-weight, suggesting that they might play a role in the treatment of type 2 diabetes as well as obesity (Zhou *et al.*, 2007; Wade *et al.*, 2008). However to date there have been very few drugs which have targeted the 5-HT<sub>2C</sub> receptor as it is very hard to distinguish pharmacologically



between the 5-HT<sub>2</sub> receptors as there is a high degree of homology between them. However, a novel 5-HT<sub>2C</sub> selective agonist, lorcaserin, has recently been identified as a potential drug for the treatment of obesity (Smith *et al.*, 2008).

## **1.8 Disorders of Energy Homeostasis**

When energy homeostasis is disrupted, certain disorders can result of which one of the most widely recognised is obesity. Obesity is an increasingly prevalent global problem, with the World Health Organisation (WHO) currently estimating that there are 1.6 billion adults worldwide who are overweight and 400 million adults that are obese. The prevalence of obesity is increasing not only in adults but also in adolescents and children, leading to a global epidemic. Obesity was originally not well defined, so the WHO designed a specific measure for determining body-weight, the Body Mass Index (BMI). BMI is calculated as the weight of an individual in kg, divided by their height in metres squared:

$$\text{BMI} = \frac{\text{weight in kg}}{(\text{height in m})^2}$$

A normal individual has a BMI between 20 and 24. A BMI over 25 is classified as overweight and a BMI of over 30 is classified as obese. A BMI of fewer than 19 is classified as underweight (World Health Organisation, 2008). Although BMI is recognised as a universal indicator of body-weight, it does have its limitations. It does not give an indication of actual body composition, leading to certain groups of individuals being wrongly classified. For example, bodybuilders who have more muscle mass than fat mass are classified as obese under the BMI system. Studies have also found that the cut-off points are not appropriate for the

universal population as significant ethnic differences have been found in body composition, as well as in different age groups and between genders.

Obesity results when energy intake exceeds energy expenditure, leading to an increase in body-weight. Although many people believe that obesity is caused simply by overeating and a lack of exercise, it is becoming increasingly clear that this is not necessarily the case. Although the increase in high calorific food combined with the more sedentary lifestyle of modern society do contribute, genetic factors also play an important role. These include impaired hormonal signalling, lack of functionally important receptors or impaired neuronal circuits. Obesity is associated with an increased risk of developing secondary diseases such as type II diabetes, certain forms of cancer, and cardiovascular diseases and is therefore a huge financial burden on government health spending (World Health Organisation, 2008). The field of obesity research is rapidly expanding and it is hoped that a better understanding of the areas involved in feeding and energy homeostasis will bring about new treatments and provide hope of controlling the escalating obesity epidemic.

### ***1.8.1 Putative drugs for the treatment of obesity***

The predominant treatment for obesity remains to be a well balanced diet and exercise. However in the majority of cases weight loss is short-lived and weight regain is common, therefore a program of drug treatment is often necessary. There are currently only two approved anti-obesity drugs on the market: sibutramine and orlistat (Rubio *et al.*, 2007).

Sibutramine is a noradrenaline and 5-HT reuptake inhibitor which leads to enhanced satiety and decreased food intake (Luque & Rey, 2002). The use of



sibutramine is accompanied by many side-effects such as nausea, constipation, dry mouth and more severely, an increase in blood pressure (Florentin *et al.*, 2007).

Orlistat is a lipase inhibitor that reduces the intestinal absorption of fat leading to a reduction in calorie intake. However it is accompanied by unpleasant gastrointestinal side-effects.

Other drugs that were approved for use but have since been withdrawn from the market include rimonabant, fenfluramine and dexfenfluramine. Rimonabant was an antagonist for the cannabinoid 1 receptor but was recently withdrawn due to psychiatric complications. Fenfluramine and dexfenfluramine both acted on the serotonergic system leading to weight loss but they were accompanied by a serious side effect on cardiac valves and so they were withdrawn from use in 1997 (Connolly *et al.*, 1997; Mark *et al.*, 1997).

## **1.9 Project Aims**

Obesity is an increasingly prevalent problem. Consequently understanding the mechanisms that underlie the central regulation of feeding and energy homeostasis is fundamental to the future design of novel treatment strategies and therapeutics targeting this debilitating condition. Therefore the aims of the present study were to investigate extrinsic and intrinsic factors involved in the regulation of energy balance at the level of the hypothalamic ARC. In particular the modulation of electrical properties of neurones by glucose, the cellular mechanisms by which 5-HT regulates the excitability of neurones, the detection of 5-HT receptors in the ARC and the ability of feeding signals to alter the gene expression of hypothalamic neuropeptides were studied. Whole-cell patch-clamp recordings, immunohistochemistry and

molecular biology techniques were utilised in order to achieve the specific aims of the project which were:

1. To compare the effects of hyperglycaemic and euglycaemic glucose levels on the electrophysiological properties of ARC neurones and characterise ARC neurones into functional groups based on intrinsic electrophysiological properties (Chapter 3)
2. To investigate the effects of the anorexigenic neurotransmitter 5-HT on the excitability of ARC neurones and to identify receptors and mechanisms of activity by which 5-HT modulates excitability of ARC neurones (Chapters 4 and 5)
3. To investigate the effects of feeding signals on neuropeptide gene expression within the hypothalamus and to determine whether these effects are activity or non-activity dependent (Chapter 6)



**Figure 1.1 The central control of energy homeostasis**

**A:** Peripheral signals such as insulin released from the pancreas, leptin released from adipose tissue, glucose from the liver and peptides released from the gastrointestinal tract such as ghrelin, cholecystokinin (CCK) and peptide tyrosine tyrosine (PYY) all impinge onto the hypothalamus to signal the energy status of the body to the brain. These signals can also exert an influence at the level of the nucleus of the tractus solitarius (NTS) in the brainstem via the vagal nerve. The hypothalamus and brainstem contain reciprocal connections to produce a coordinated response to bring about changes in feeding and energy homeostasis. In addition the hypothalamus and NTS receive inputs from higher centres to further regulate energy homeostasis. In this way there exists a negative feedback loop within the body that regulates energy homeostasis.



Figure 1.1

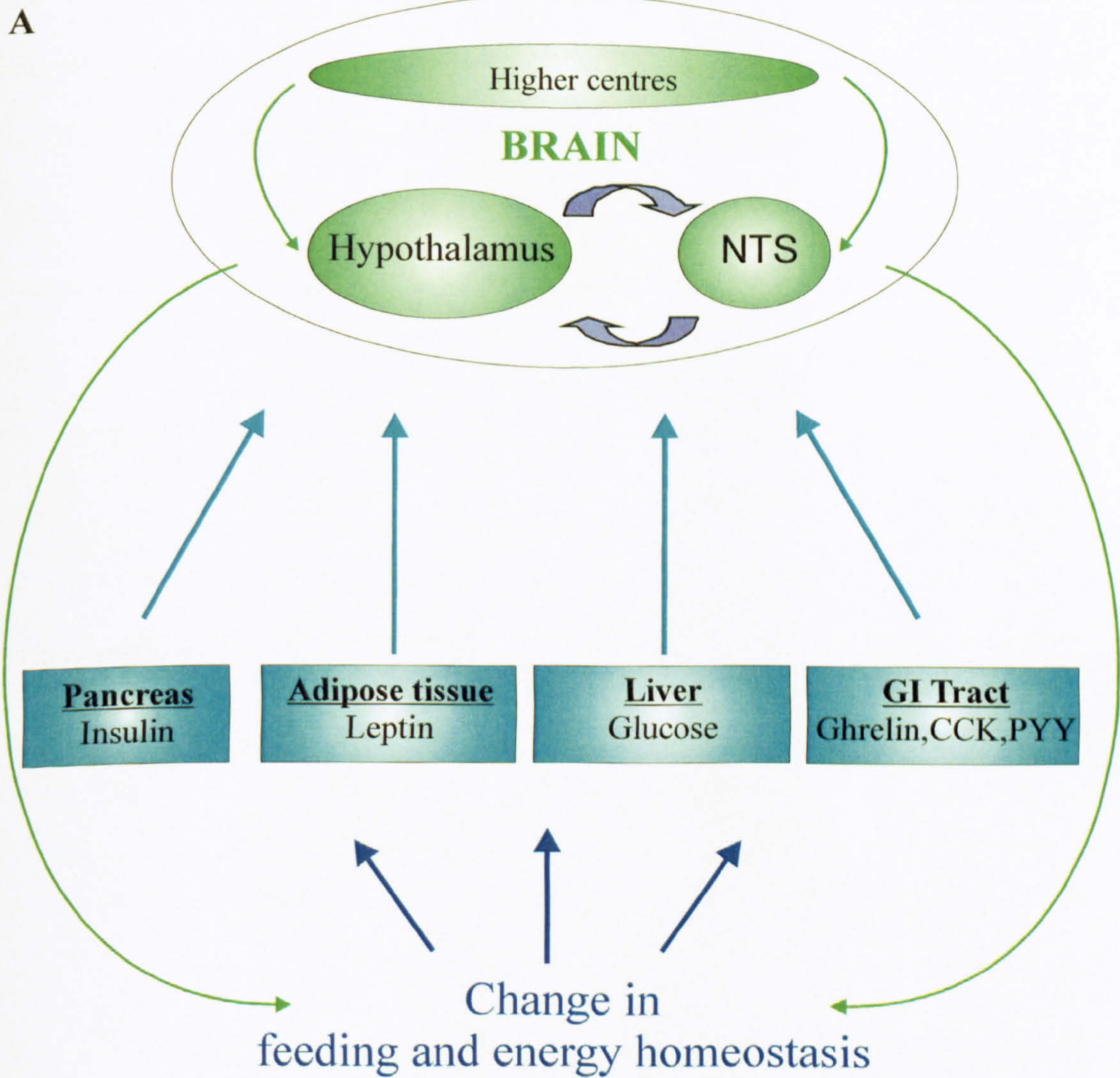




**Figure 1.2 Overview of hypothalamic nuclei involved in energy homeostasis**

**A:** Schematic drawing of the hypothalamus showing the location of the nuclei that are involved in energy homeostasis. These include the arcuate nucleus (ARC), lateral hypothalamus (LH), ventromedial nucleus (VMN), paraventricular nucleus (PVN), and the dorsomedial hypothalamus (DMH). There are reciprocal connections between many of the nuclei that enable them to bring about a coordinated response to energy homeostasis.



Figure 1.2

A

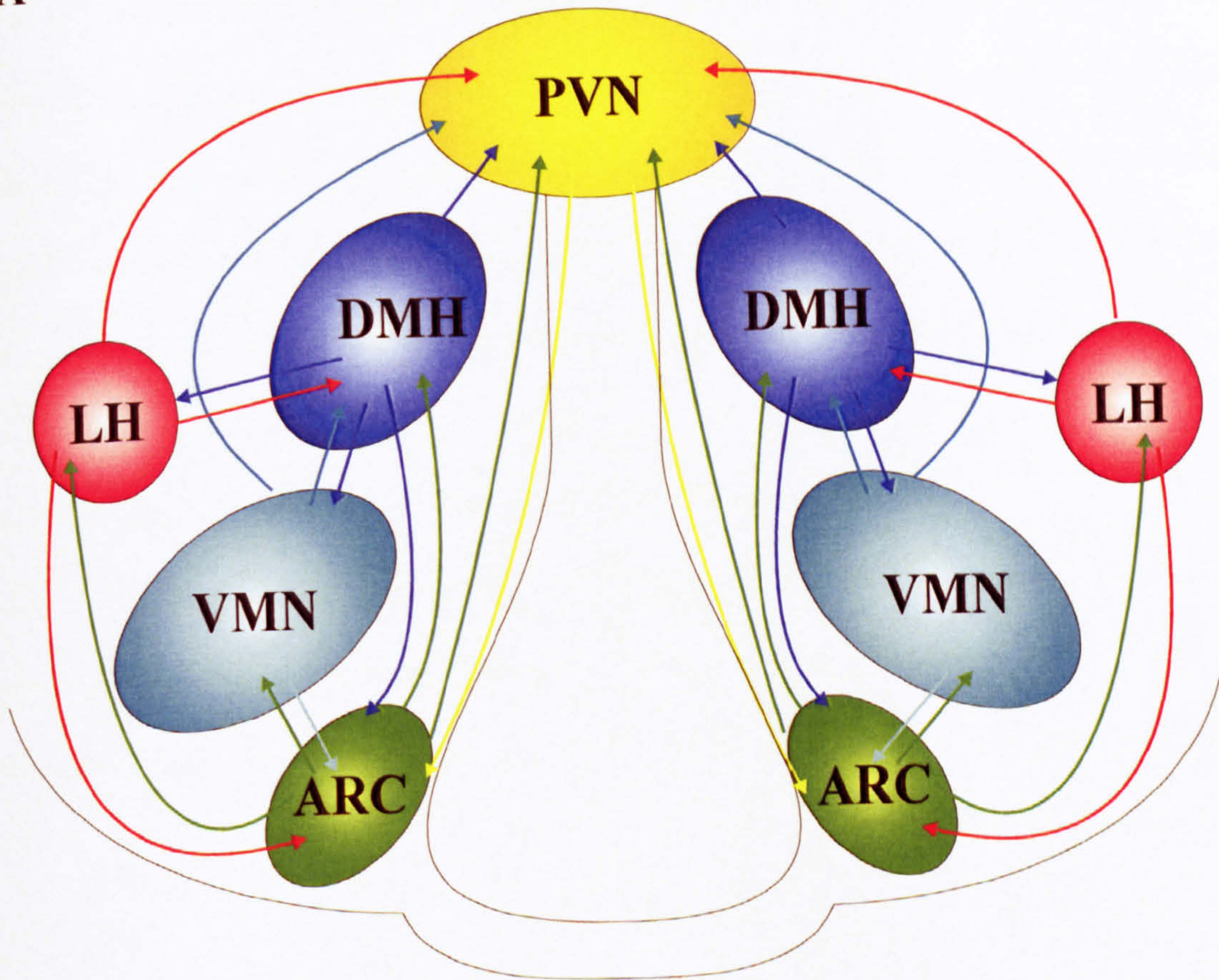




**Figure 1.3 Afferent and efferent connections of the ARC**

**A:** Schematic drawing of a sagittal section of the rat brain showing afferent pathways to the hypothalamic arcuate nucleus (ARC). These inputs come from intrahypothalamic areas such as lateral hypothalamus (LH), ventromedial nucleus (VMN), paraventricular nucleus (PVN), dorsomedial hypothalamus (DMH), suprachiasmatic nucleus (SCN), preoptic area (POA) and the median eminence (ME). Extrahypothalamic inputs include the amygdala (AMG), dorsal raphe (DR), locus coeruleus (LC) and the nucleus of the tractus solitarius (NTS).

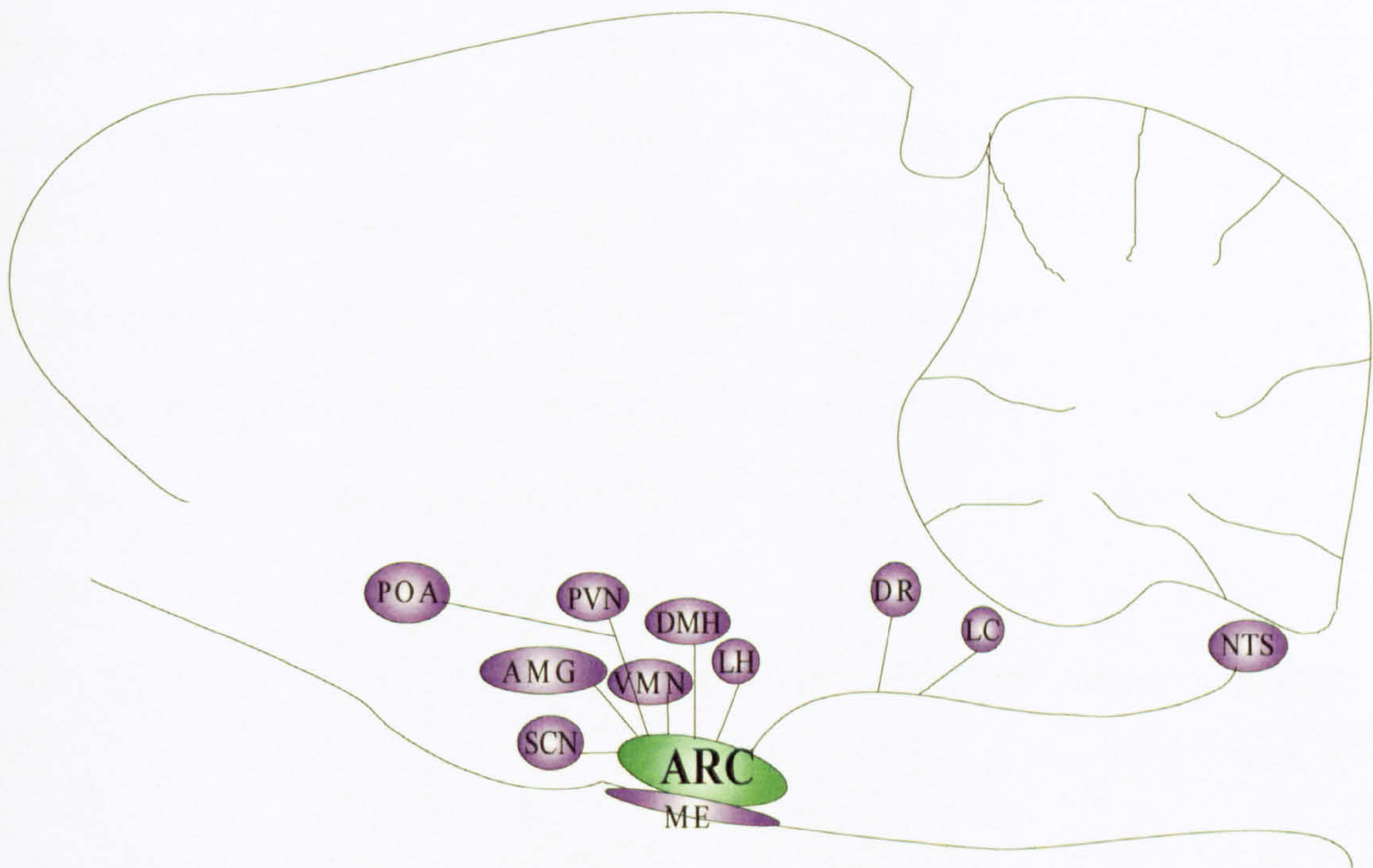
**B:** Schematic drawing of a sagittal section of the rat brain showing efferent pathways from the hypothalamic ARC. Outputs go to intrahypothalamic areas such as LH, VMN, PVN, DMH, SCN, POA, and ME. Extrahypothalamic outputs include the periaqueductal gray area (PAG), AMG, DR, LC and the NTS. There is also an efferent projection to the spinal cord.

(Figures adapted from Yi *et al.*, 2006)

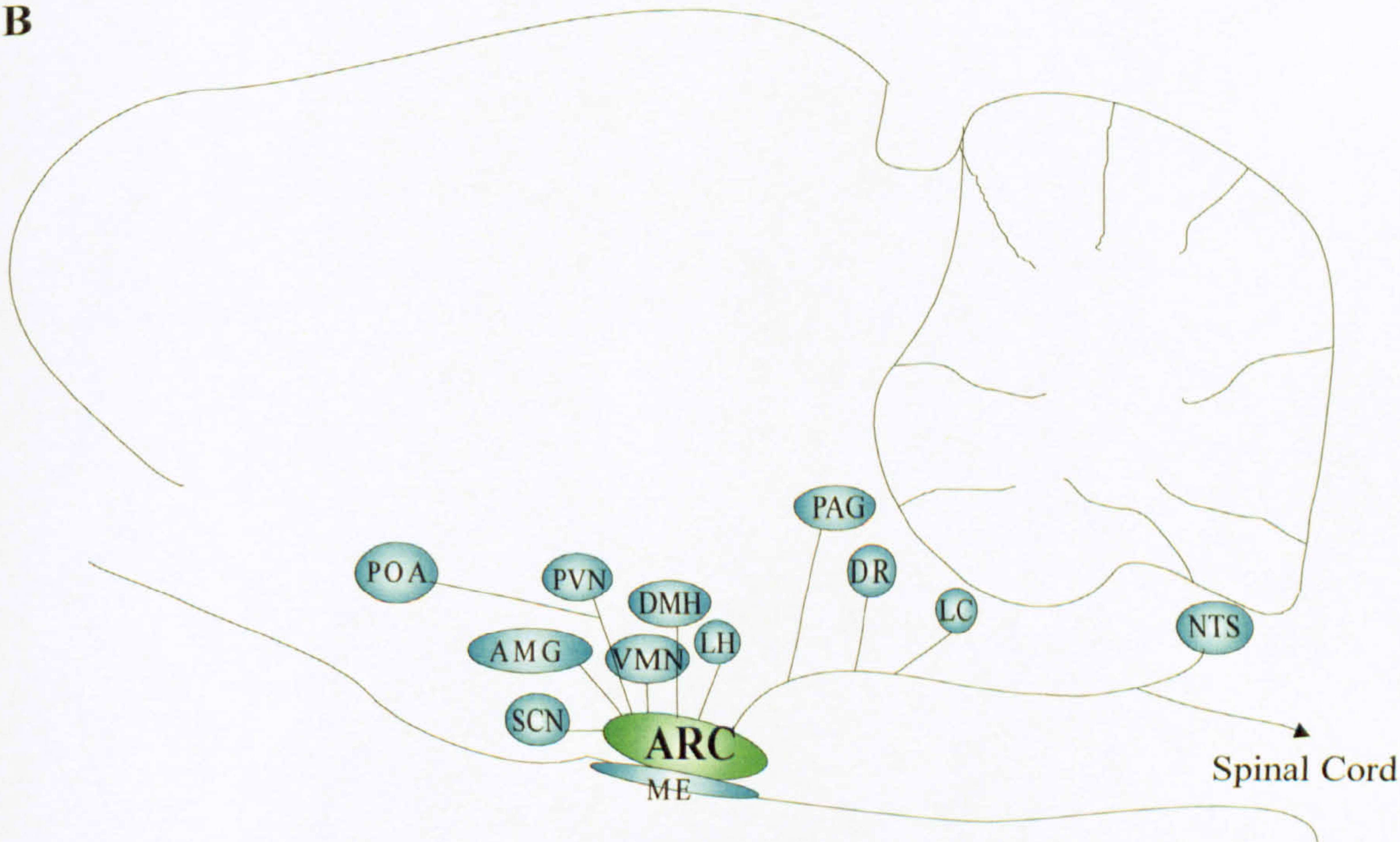


Figure 1.3

A



B





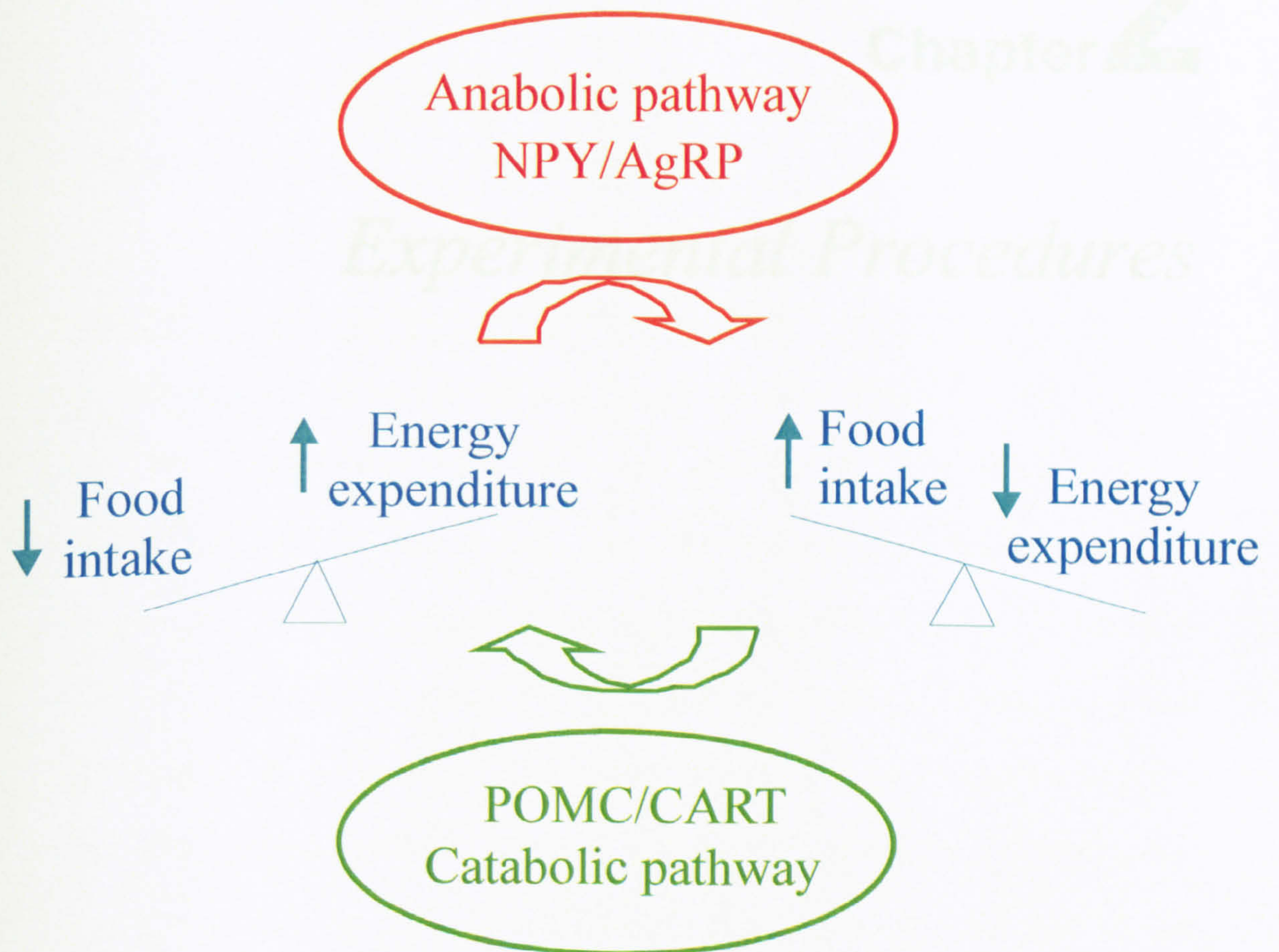
**Figure 1.4 Anabolic and catabolic pathways controlling energy homeostasis**

**A:** Within the CNS, there are two principal pathways that are responsible for controlling bodyweight. These are the anabolic and catabolic pathways, which work as parallel and opposing pathways to maintain bodyweight around a defined set point. Within the ARC, there are principally two important neuronal subgroups that control these pathways, those expressing NPY/AgRP and those expressing POMC/CART. Activation of NPY/AgRP neurones stimulates the anabolic pathway leading to an increase in food intake and inhibition of energy expenditure. Activation of POMC/CART neurones stimulates the catabolic pathway leading to a decrease in food intake and an increase in energy expenditure.



Figure 1.4

A





# Chapter 2

## *Experimental Procedures*

## 2.1 Electrophysiology

### 2.1.1 Slice preparation

Hypothalamic slice preparations were obtained from male Wistar rats between five and ten weeks of age, housed on a 12/12 hour light/dark cycle. All slices were obtained during the light phase of this cycle. Food and water were provided *ad libitum*.

Rats were killed according to a schedule one protocol, either with anaesthesia (isoflurane) followed by decapitation or without anaesthesia and cervical dislocation. All studies were conducted in agreement with UK Animals (Scientific Procedures) Act 1986. Approximately 110 rats were used for the electrophysiology and immunohistochemistry experiments and 150 rats for the molecular biology experiments. The brain was rapidly removed from the cranial cavity and placed in freshly prepared ice-cold, gassed (95 % O<sub>2</sub>, 5 % CO<sub>2</sub>) artificial cerebrospinal fluid (aCSF). aCSF was of the composition shown in table 2.1 with a pH of 7.4 (adjusted using KOH) and an osmolarity of 310-315 mOsm kg<sup>-1</sup> (adjusted using sucrose). For experiments where 2 mM glucose-containing aCSF was used rather than 10 mM glucose-containing aCSF, glucose was replaced in equimolar quantities by D-mannitol to maintain osmolarity.

The brain was trimmed to a block containing the hypothalamus and glued to the plate of a tissue slicer using cryanoacrylate glue. Hypothalamic coronal slices containing the arcuate nucleus (ARC) were cut at a thickness of 300 µm on a vibratome (Intracell series 1000, Royston, UK or Leica VT1000S, Leica Microsystems GmbH, Wetzlar, Germany) and were constantly bathed in ice cold aCSF. The ARC was identified as the area immediately above the median eminence surrounding the third ventricle (see figure 2.1). Slices were transferred to a beaker



containing aCSF, and were left to equilibrate for 1 hour prior to recording, at room temperature. Slices were then transferred to a custom-made recording chamber, held between two grids (the top grid was held on a chloride-coated silver wire which also acted as the bath-earth) and were continuously perfused with oxygenated aCSF at room temperature at a flow rate of 4-8 ml<sup>-1</sup>.

### ***2.1.2 Electrophysiological recording and data analysis***

Whole-cell current-clamp and voltage-clamp recordings were carried out using patch pipettes (4-10 M $\Omega$  when filled with recording solution), made from thin-walled borosilicate glass capillaries (GC150-TF10, Harvard Apparatus LTD, Edenbridge, Kent, UK) pulled on a horizontal electrode puller (P-97, Sutter Instrument Co., Novato, CA, USA). The pipettes were filled with intracellular solution of the composition shown in table 2.2.

Recordings were obtained with an Axopatch 1D amplifier (Axon Instruments, Foster City, CA, USA) and were monitored online on an oscilloscope (Gould 1602, Gould instrument systems) and stored on digital audio tapes (DAT; Biological DTR-1205, Intracel, Royston, UK) or directly on a PC for later offline analysis. Data were filtered at 1-5 kHz (for voltage-clamp studies), digitised at 2-100 kHz (Digidata 1322A, Axon instruments) and stored on PC running pCLAMP 8.2 data acquisition software. Data were analysed using Clampfit 8 software (Axon instruments) on a personal computer.

Resting membrane potentials of silent cells were taken from the trace obtained in Clampex, but in active cells for which this was impossible the low-pass readout of the recording amplifier was used. Membrane potential values were not corrected for off-sets related to the occurrence of liquid junction potentials. Input

resistances were calculated using Ohm's law ( $R=V/I$ ), by injecting small hyperpolarising current pulses (-4 to -40 pA, 0.2 Hz, 800-1000 ms) and measuring the amplitude of the evoked electrotonic potential. Membrane time-constants ( $\tau$ ) were calculated by performing a bi-exponential fit to the first membrane voltage response to a negative current step. Care was taken to perform the fits on steps in the linear portion of the current-voltage relationship.

2.1.3 Solutions and drugs

The ionic composition of the aCSF and intracellular solution were as follows:

Table 2.1: aCSF

	<u>10 mM glucose-containing</u>	<u>2 mM glucose-containing</u>
	<u>aCSF (in mM)</u>	<u>aCSF (in mM)</u>
NaCl	127	127
KH <sub>2</sub> PO <sub>4</sub>	1.2	1.2
KCl	1.9	1.9
NaHCO <sub>3</sub>	26.0	26.0
Glucose	10	2.0
D-Mannitol	0	8.0
CaCl <sub>2</sub>	2.4	2.4
MgCl <sub>2</sub>	1.3	1.3

Table 2.2: Intracellular solution

	<u>mM</u>
K-gluconate	140
KCl	10
HEPES	10
Na <sub>2</sub> ATP	2
EGTA-Na <sub>2</sub>	1
Alexa 633	0.1



Osmolarity was adjusted using sucrose and pH adjusted to 7.4 using KOH. Alexa 633 was only included in the intracellular solution when double-labelling experiments were performed.

Drugs were applied to the slice using 60 ml syringes connected to the main aCSF flow by a series of three-way taps. Drugs were prepared as a stock solution using either distilled water or dimethyl sulfoxide (DMSO; Sigma) as appropriate and diluted to the required concentration in aCSF immediately prior to use. Final DMSO concentrations did not exceed 0.1% and appropriate vehicle controls were performed. All drugs used in this study are listed in table 2.3.

**Table 2.3 Drugs**

<b>Drug</b>	<b>Solvent</b>	<b>Supplier</b>
5-hydroxytryptamine (5-HT)	Distilled water	Sigma-Aldrich, St. Louis, USA
WAY-100635 (maleate salt)	Distilled water	Sigma-Aldrich,
5-Carboxamidotryptamine maleate (5-CT)	Distilled water	Tocris Cookson Ltd., U.K
CP 93129 dihydrochloride	Distilled water	Tocris
8-Hydroxy-DPAT hydrobromide (8-OH-DPAT)	Distilled water	Tocris
RU24969 hemisuccinate	Distilled water	Tocris
Cyanopindolol hemifumarate	DMSO	Tocris
SB224289 hydrochloride	Distilled water	Tocris
$\alpha$ -Methyl-5-hydroxytryptamine	Distilled water	Tocris
Altanserin hydrochloride	DMSO	Tocris
RS 102221 hydrochloride	DMSO	Tocris
<i>m</i> -Chlorophenylbiguanide hydrochloride (mCPBG)	Distilled water	Tocris
MDL 72222	DMSO	Tocris

SB269970 hydrochloride	Distilled water	Tocris
SB 204741	DMSO	Tocris
R-96544 hydrochloride	Distilled water	Tocris
Ghrelin	Distilled water	Bachem, UK
TTX	Distilled water	Alomone Labs, Israel
GABA	Distilled water	Tocris
AMPA	Distilled water	Tocris
Leptin	HCL/NaOH	Calbiochem, San Diego, USA

2.1.4 Reversal potentials

Table 2.4 gives the calculated reversal potentials for ions as determined from the Nernst equation:

$$E_{ion} = \frac{RT}{zF} \ln \frac{[ion]_o}{[ion]_i}$$

(where **E<sub>ion</sub>** = equilibrium potential for permeant ion; **R** = gas constant (8.315 J K<sup>-1</sup> mol<sup>-1</sup>); **T** = absolute temperature (273.16 + T [25 °C]); **F** = faraday’s constant (96,485 C mol<sup>-1</sup>); **Z**= valency of ion; **[Ion]<sub>o</sub>** = extracellular ionic concentration; **[Ion]<sub>i</sub>** = intracellular ionic concentration)

Table 2.4 Reversal potentials

Ion	Extracellular Concentration (mM)	Intracellular Concentration (mM)	Reversal potential (mV)
Na <sup>+</sup>	153	6	81.6
K <sup>+</sup>	3.1	150	-97.7
Ca <sup>2+</sup>	2.4	0.001	196
Cl <sup>-</sup>	136.3	10	-65.8



## 2.2 Immunohistochemistry

### 2.2.1 Immunofluorescence staining of 5-HT receptors

150  $\mu$ m thick hypothalamic slices were prepared using methods similar to those described in section 2.1.1. The tissue was fixed overnight in 4 % paraformaldehyde in 0.1 M phosphate buffer (pH 7.4). The slices were washed in Tris-buffered saline containing 1% Triton X-100 (TBS-T; all washes were 3 x 10 mins). The slices were incubated with either 3 % normal goat serum (NGS; Stratech Scientific Ltd. Suffolk, UK) for the 5-HT<sub>1A/1B</sub> receptors or 5 % NGS for the 5-HT<sub>7</sub> receptor, in TBS-T for 1 hour under agitation on an orbital shaker. The sections were incubated overnight at 4°C under agitation in primary antibody (see table 2.5), in TBS-T containing 1 % NGS. Dilution rates for primary and secondary antibodies were chosen based on previous literature which had utilised these antibodies. After rinsing with TBS-T, slices were incubated for 1-2 hours with secondary antibody (see table 2.6). The secondary antibodies were conjugated to a fluorophore, either Cy2 (absorption peak 492 nm, emission peak 510 nm) or Cy5 (absorption peak 650 nm, emission peak 670 nm). Finally slices were washed in TBS-T before being mounted on microscope slides and covered with Prolong® Antifade (Invitrogen, UK) to prevent fading of immunofluorescence. The sections were examined using a confocal laser microscope (Leica SP2 linked to a Leica DM RE7 upright microscope), using the laser with a wavelength of 488 nm for Cy2 and 633 nm for Cy5. Appropriate controls to test for specificity of each fluorophore were performed by turning off each laser accordingly. All incubations were also conducted in the absence of primary and secondary antibody to act as negative controls for each experiment.

**2.2.2 Double-immunofluorescence staining for 5-HT receptors and cocaine and amphetamine-regulated transcript (CART)**

The protocol was followed as above for 5-HT receptor staining and then the protocol for CART staining was undertaken. After rinsing in TBS-T, the slices were blocked with 4 % NGS in TBS-T for 1 hour under agitation. Sections were incubated overnight under agitation at 4°C in rabbit anti-CART (1:1000) in TBS-T containing 2 % NGS. Slices were rinsed in TBS-T and incubated for 1 hour at room temperature under agitation in Cy2-conjugated goat anti-rabbit secondary antibody (1:200). Slices were washed in TBS-T before being mounted and covered with Prolong® Antifade. The sections were examined using a confocal microscope. All incubations were also conducted in the absence of primary and secondary antibody to act as negative controls for each experiment.

**Table 2.5: Primary antibodies**

Antigen	Antibody	Species	Dilution	Source/Product Code
5-HT <sub>1A</sub>	Anti-serotonin receptor 1A	Guinea Pig	1:1000	Chemicon, USA, AB15350
5-HT <sub>1B</sub>	Anti-serotonin receptor 1B	Guinea Pig	1:1000	Chemicon, USA, AB5410
5-HT <sub>7</sub>	Anti-serotonin receptor 7	Rabbit	1:100	Calbiochem, San Diego, USA, PC249L
CART	Anti-CART	Rabbit	1:1000	Phoenix Pharmaceuticals, Germany, H-003-62



**Table 2.6: Secondary antibodies**

Antigen	Antibody	Species	Dilution	Source/Product Code
5-HT <sub>1A</sub>	Cy5 Goat Anti-guinea pig IgG	Goat	1:50	Stratech 106-175-003
5-HT <sub>1B</sub>	Cy5 Goat Anti-guinea pig IgG	Goat	1:50	Stratech 106-175-003
5-HT <sub>7</sub>	Cy5 Goat Anti- rabbit	Goat	1:200	Stratech 111-175-003
CART	Cy2 Goat Anti- rabbit	Goat	1:200	Stratech 111-225-003

**2.2.3 Immunofluorescence staining for CART and Alexa 633**

Recordings were obtained utilizing an intracellular solution containing the fluorescent dye Alexa 633 hydrazide (100  $\mu$ M; Invitrogen, UK). Post-recording, slices were fixed overnight in a 0.1 M phosphate buffer containing 4 % paraformaldehyde (pH 7.4). Subsequently, slices (300  $\mu$ m thickness) were processed for CART as described in section 2.2.2.

**2.3 Molecular Biology**

**2.3.1 Tissue preparation**

Hypothalamic explants were prepared from age-matched (6 weeks old) male rats. For some experiments, animals were fasted for 24 hours prior to culling. The brain was removed as described in section 2.1.1 and an explant containing the whole hypothalamus was prepared. The approximate markers used to cut the explant are shown in figure 2.2 (figure adapted from Paxinos & Watson, 1998).

The explant was immediately incubated in 2 mM glucose-containing aCSF at 35°C for 60 mins. After this time, the explants were removed and placed into small

vials containing 2 mM glucose-containing aCSF at 35°C. For each experiment, four control animals were used and these four explants were incubated in aCSF for the same time as the challenge time for that experiment. Four explants were used as the test tissues for each experiment and incubated in aCSF containing either leptin (100 nM; Calbiochem), gamma-aminobutyric acid (GABA; 1 µM or 1 mM; Tocris), alpha-amino-3-hydroxy-5-methyl-4-isoxazolepropionic acid (AMPA; 1 µM or 50 µM; Tocris), or a specific concentration of glucose (either 0.2 mM or 5 mM). The challenge time varied depending on the experiment, in order to monitor gene expression over a detailed time scale. Control studies to determine the viability of tissue were not performed. At the end of the incubation time, the explant was removed and placed into an eppendorf and immediately snap-frozen on dry ice. The samples were stored in a -80°C freezer prior to molecular analysis.

### ***2.3.2 RNA extraction***

Total RNA was extracted from the hypothalamic explants using the RNeasy Lipid Tissue Mini Kit (Qiagen, Crawley, UK). Briefly, tissue samples were homogenized in QIAzol lysis reagent using a pellet pestle (Sigma-Aldrich, St. Louis, USA) and then upon addition of chloroform, centrifugation (12,000 x g for 15 min at 4°C) was undertaken to separate the homogenate into aqueous and organic phases. RNA remained in the aqueous phase and was extracted and separated from any protein and DNA. Ethanol was added to the aqueous phase and the sample was then placed through an RNeasy Mini Spin Column, allowing the RNA to bind to the membrane whilst all contaminants were washed away. RNase-free water was used to elute the RNA. 1 µl of RNase inhibitor (Promega, Madison, WI, USA) was added to each sample.



The amount of RNA from each explant was estimated using a Nanodrop ND-1000 Spectrophotometer (Nanodrop Technologies, Wilmington, DE, USA). The RNA was diluted to a final concentration of 150 ng/ $\mu$ l using RNase free water.

### ***2.3.3 Reverse transcription of mRNA***

11  $\mu$ l of RNA was added to a sterile eppendorf containing 1  $\mu$ l of oligo (dt)<sub>20</sub> (Invitrogen, Paisley, UK) and 1  $\mu$ l of 10 mM deoxynucleoside triphosphates (dNTP) mix (Invitrogen). A negative control containing only 13  $\mu$ l of water was also prepared. Samples were mixed and heated at 65°C for 5 mins. After cooling on ice for at least 1 min, 4  $\mu$ l of 5 x First-Strand Synthesis Buffer, 1  $\mu$ l of 0.1M DTT (as supplied with Superscript<sup>TM</sup> III Reverse Transcriptase, Invitrogen), 1  $\mu$ l of RNase inhibitor and 1  $\mu$ l of Superscript III RT were added to each eppendorf. The samples were vortexed and centrifuged and then heated to 50°C for 60 mins. Reactions were stopped by heat inactivating enzyme at 70°C for 15 mins. Each cDNA sample was stored at -20°C until required for real-time PCR.

### ***2.3.4 Quantitative real-time PCR***

A master mix was prepared containing, per reaction: 12.5  $\mu$ l Taqman 2x PCR mastermix (Applied Biosystems), 1.25  $\mu$ l of primer of target gene (see table 2.7; Applied Biosystems), 1.25  $\mu$ l of primer for endogenous control (Human 18s rRNA, Applied Biosystems), 9  $\mu$ l of water and 1  $\mu$ l of cDNA (total volume 25  $\mu$ l). Samples were loaded onto a 96-well plate, in triplicate, along with a negative control where cDNA was replaced with water. The plate was sealed with optical adhesive film and subjected to real-time PCR. All reactions were multiplexed with the house-keeping

gene 18s rRNA as this enabled data to be expressed in relation to an internal reference to allow for differences in reverse transcription efficiency.

Real-time quantitative PCRs were carried out with an ABI Prism 7000 Sequence Detection System. The following PCR conditions were used: one cycle at 50°C for 2 mins and one cycle at 95°C for 10 mins. The amplification was followed by 40 cycles of denaturation at 95°C for 15 s and annealing at 60°C for 1 min.

**Table 2.7: PCR primers**

PRIMER	ACCESSION No.	ASSAY No.
NPY	M15880.1	Rn00561681_m1
POMC	AF510391.1	Rn00595020_m1
c-fos	X06769.1	Rn02396759_m1
AGRP	AF206017.1	Rn01431703_g1

### **2.3.5 Interpretation of real-time PCR data**

Data was obtained as Ct values (the cycle number at which the logarithmic PCR plot crosses a calculated threshold line) according to the manufacturers guidelines, and was used to determine  $\Delta$ Ct values ( $\Delta$ Ct = Ct of target gene - Ct of endogenous control gene (18s)). The  $\Delta$ Ct triplicate values were averaged and any outliers (more than one cycle difference) were discarded. The  $\Delta$ Ct results from the four control animals were averaged to get a single control  $\Delta$ Ct value for each experiment. This  $\Delta$ Ct control value was then subtracted from the four test tissue  $\Delta$ Ct values to give four  $\Delta\Delta$ Ct values for each experiment (n=4). The  $\Delta\Delta$ Ct values were used to calculate the relative levels of expression between control and challenged animals using the formula:



$$\text{Relative expression} = 2^{-\Delta\Delta C_t}$$

This formula gives the control group an arbitrary value of 1 ( $2^0$ ) and the challenged groups a value relative to this arbitrary value. All statistics were performed at the  $\Delta C_t$  stage to avoid potential bias due to averaging data that had been transformed through the equation  $2^{-\Delta\Delta C_t}$ .

## 2.4 Statistical Analysis

Statistical analysis was performed using Excel (Microsoft) and Instat (Graphpad Software Inc., San Diego, USA) with all values given as mean  $\pm$  SEM. Statistical significance was determined using either student's two tailed t-test, paired or unpaired as appropriate, Mann-Whitney test, chi-square test or Kruskal-Wallis test (non-parametric ANOVA).

**Figure 2.1 Diagram showing the location of the ARC within the hypothalamus**

**A:** Diagram showing the location of the ARC within the hypothalamus, indicating the area from which electrophysiological recordings were made. The ARC is identified as the area between the dotted lines on the diagram. It is situated at the base of the hypothalamus, surrounding the third ventricle (3V) and is situated immediately above the median eminence (ME).



**Figure 2.1**

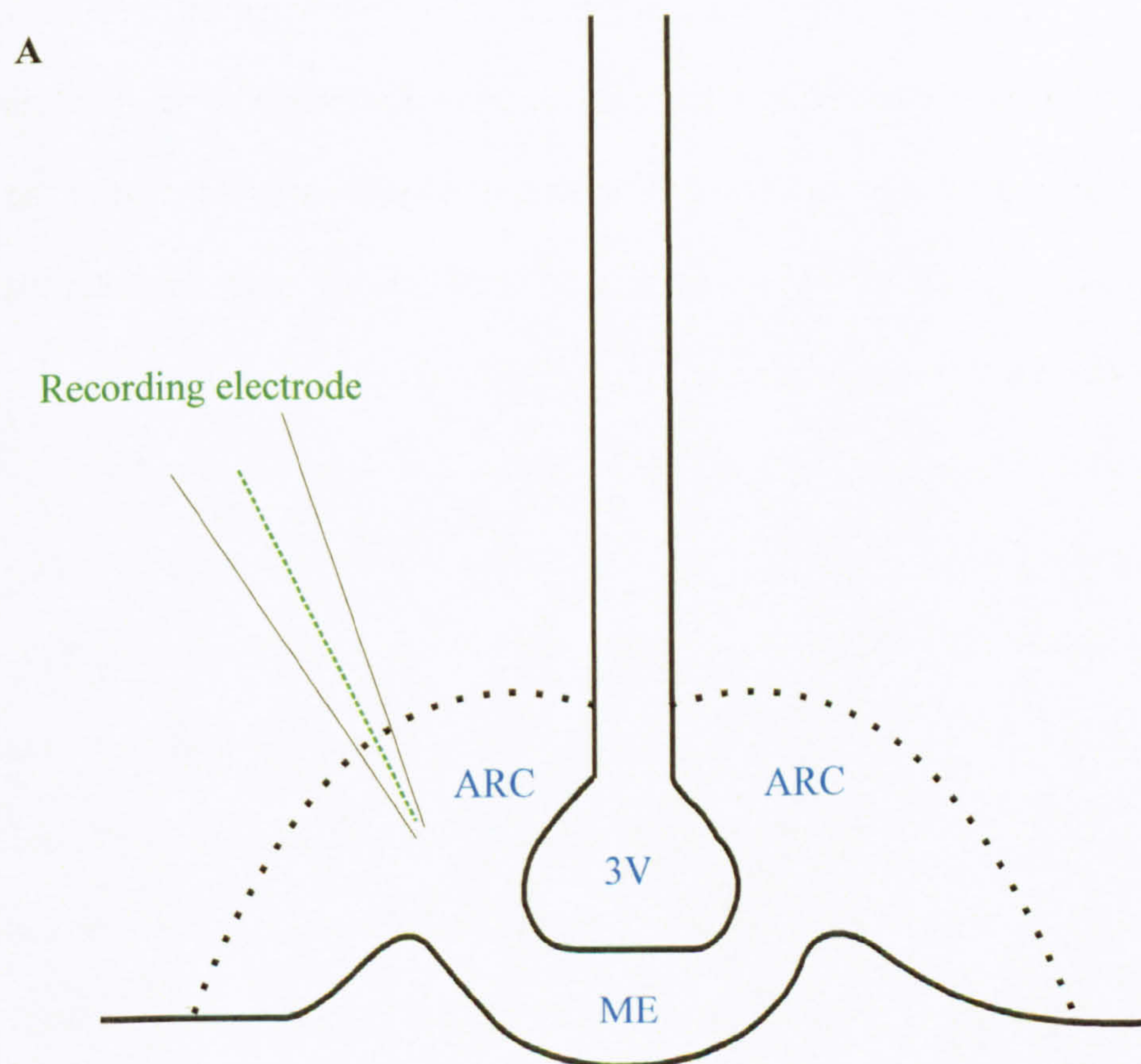


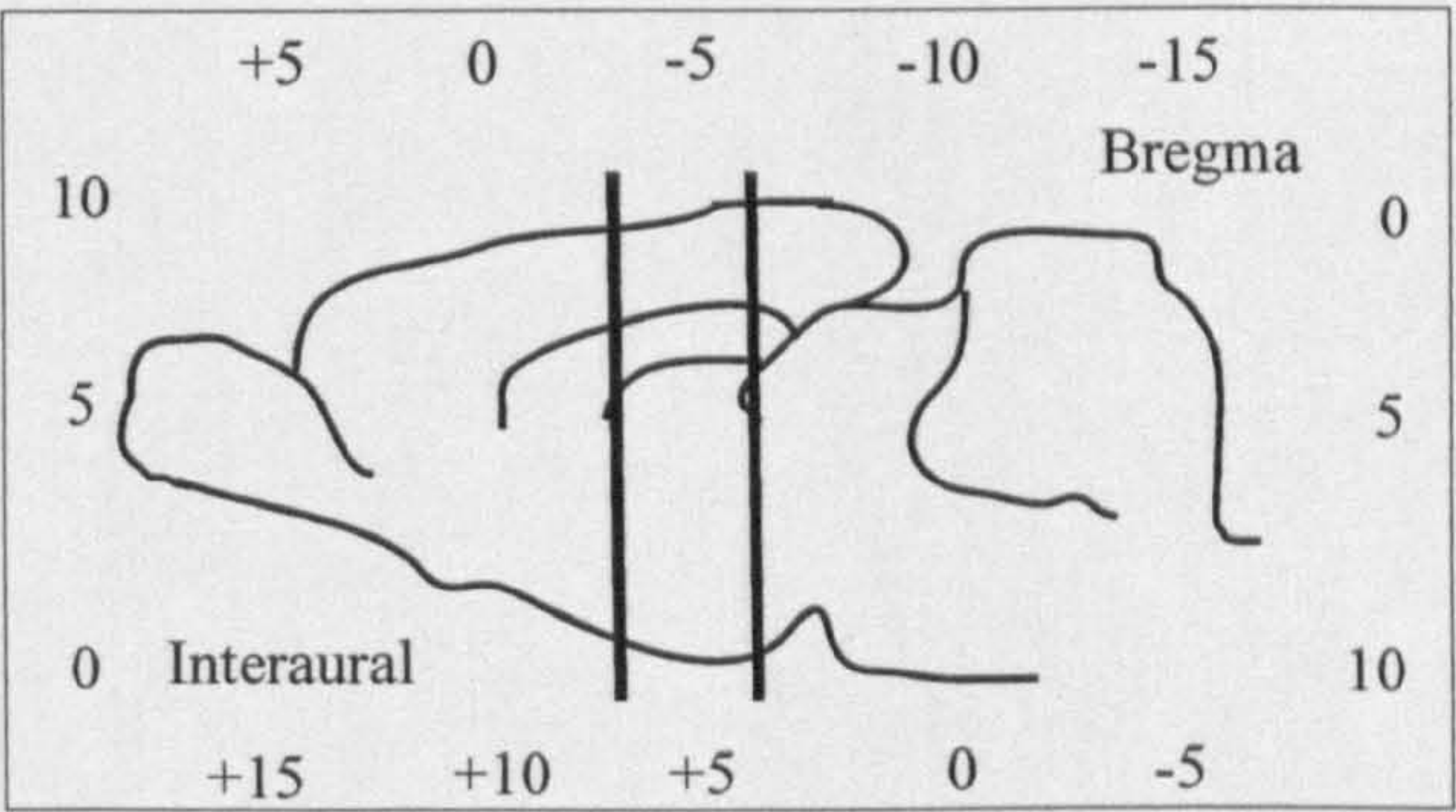
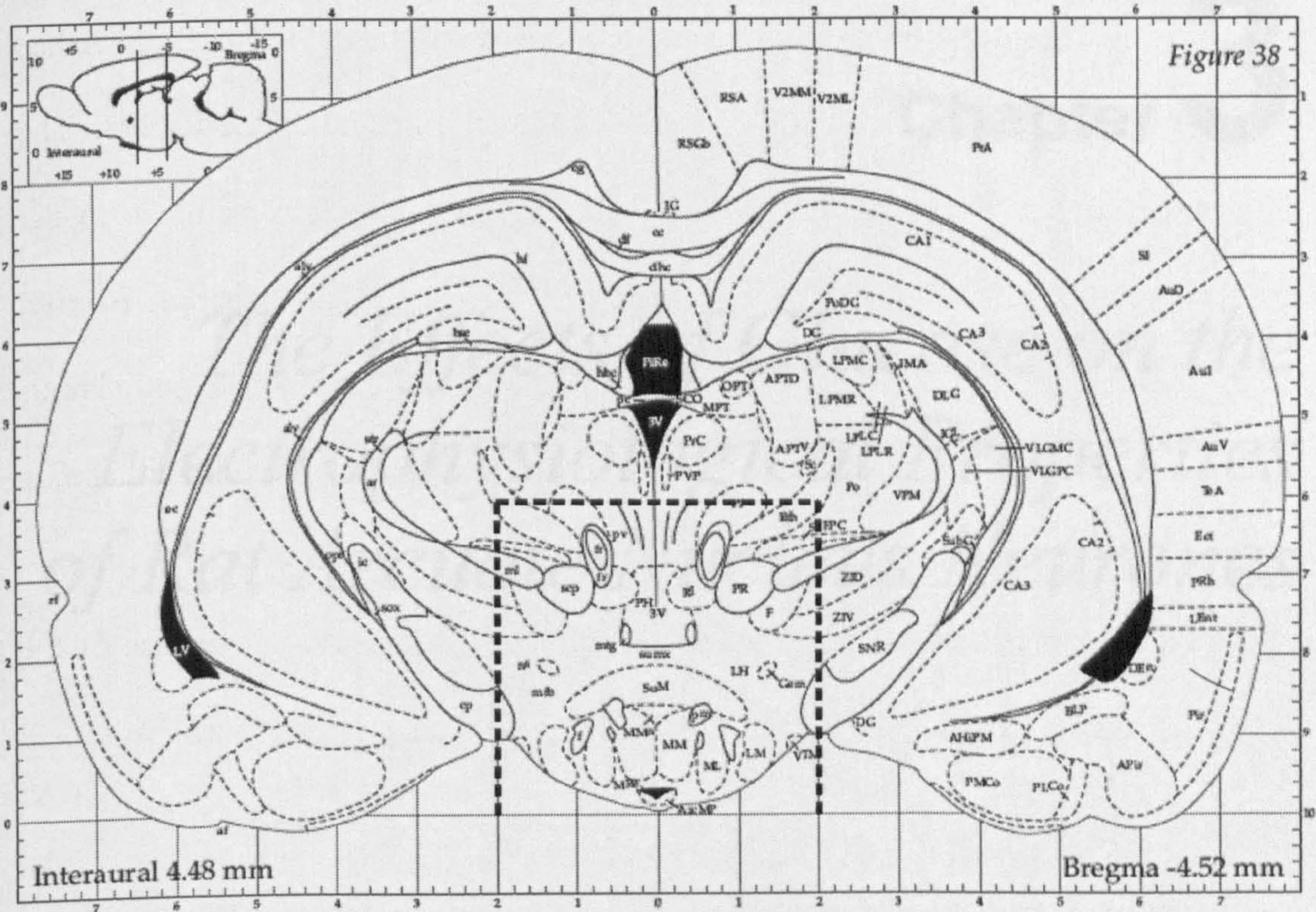
**Figure 2.2 Diagram of a rat brain showing the markers used to produce the hypothalamic explant for RT-PCR**

**A:** Diagram of a coronal section from a rat brain, as taken from the Rat Brain Atlas, Fourth Edition, George Paxinos & Charles Watson, Academic Press 1997. The dotted lines indicate the approximate points at which incisions were made to the coronal section in order to obtain an explant containing the hypothalamus. Briefly, the brain was trimmed until the medial posterior arcuate nucleus of the hypothalamus was visible. Three incisions were then made: an incision was made 2 mm either side of the midline where the central tuberomammillary nucleus meets the cerebral peduncle; the final incision was made 4 mm dorsal from the ventral surface of the hypothalamus just below the precommissural nucleus. The cutting blade was then moved 3 mm rostrally to the level of the optic chiasm and a 4 mm x 4 mm x 3 mm hypothalamic explant was removed. The inset picture in the top left, which has been expanded below, shows a rostro-caudal diagram of the rat brain; the lines show the 3 mm depth of the hypothalamic explant.



Figure 2.2

A





# Chapter 3

## *The Effects of Glucose on the Electrophysiological Properties of Rat Arcuate Nucleus Neurones*



### 3.1 Introduction

Homeostatic mechanisms are dedicated to maintaining the levels of glucose in the blood within tight limits. Aspects of glucose homeostasis are under the control of the brain, specifically the hypothalamus and the brainstem and also the peripheral organs, liver and pancreas. The liver plays a major role in glucose homeostasis by regulating the uptake and storage of glucose via glycogenesis and the release of glucose from glucose stores by glycogenolysis or production of new glucose by gluconeogenesis (Nordlie *et al.*, 1999). The liver is therefore able to produce glucose in times of starvation to ensure that all cells have an adequate supply of glucose for their energy needs. The liver is under the control of hormonal signals including insulin and glucagon which regulate the levels of glucose within the blood. If glucose levels fall outside the tight limits imposed to maintain glucose homeostasis, certain conditions may result, for example, diabetes or hypoglycaemia. Diabetes arises either because of impaired insulin production due to  $\beta$ -cell failure (type 1 diabetes), or insulin resistance (type 2 diabetes). In both type 1 and type 2 diabetes, the failure of insulin to increase glucose uptake into cells or decrease glucose production leads to elevated blood glucose. If left uncontrolled, blood glucose can rise to dangerously high levels and therefore it is imperative that diabetes is treated quickly. The normal level of glucose in the blood (euglycaemia) is considered to be around 4-7 mM, with high blood glucose (hyperglycaemia) considered above about 8 mM. Physiological brain glucose levels still remain unclear but studies indicate that at a plasma glucose level of 5-8 mM, brain glucose levels range between 1 and 2.5 mM (Silver & Erecinska, 1994) and the basal level in the hypothalamus has been suggested to be around 1.4 mM (de Vries *et al.*, 2003; Mayer *et al.*, 2006). Brain glucose levels rarely reach the same level as that in the plasma, only approximately

10-30% of plasma levels (Silver & Erecinska, 1994; de Vries *et al.*, 2003). However, regions with a compromised blood-brain-barrier (BBB), such as the arcuate nucleus (ARC), are suggested to have a glucose concentration close to that found in the plasma, and so ARC neurones are potentially exposed to much higher levels of extracellular glucose, although this has never been directly demonstrated (Routh, 2002; Wang *et al.*, 2004). It seems likely that the level of glucose within the ARC will match more closely that of the brain rather than the plasma, as the contribution of the BBB is unknown. However it is possible that the physiological concentration of glucose within the ARC may lie somewhere between that of the plasma and that of the brain if the BBB does indeed expose the ARC to plasma glucose. Further experiments determining the levels of glucose within the ARC are therefore required.

The brain controls and is critically dependent on glucose levels and it has therefore developed mechanisms to monitor and respond to changes in glucose levels. Over 50 years ago, Mayer proposed the glucostat hypothesis, where hypothalamic 'glucoreceptors' sensed changes in available glucose as a means of regulating food intake (Mayer, 1953, 1955). Anand and Oomura both later demonstrated that there were glucose-sensing neurones in the rat brain which are specialised neurones that change their electrical activity in response to changes in extracellular glucose concentration (Anand *et al.*, 1964; Oomura *et al.*, 1964). They identified neurones in the ventromedial nucleus (VMN) and the lateral hypothalamus (LH) that altered their activity when glucose levels changed. Originally termed glucose-responsive and glucose-sensitive neurones, these neurones have subsequently been re-named glucose-excited and glucose-inhibited neurones, respectively (Levin *et al.*, 1999). These neurones are either inhibited (glucose-



inhibited: GI) or excited (glucose-excited: GE) in response to increases in glucose levels (for review see Levin *et al.*, 2004 and Burdakov *et al.*, 2005).

The mechanism by which GI neurones sense glucose is not well characterised (see general introduction). The mechanism by which GE neurones sense glucose and alter their activity is thought to occur in an analogous way to the glucose-stimulated insulin release in pancreatic  $\beta$ -cells (Schuit *et al.*, 2001 and general introduction). The GLUT2 transporter, glucokinase and the ATP-sensitive potassium channel ( $K_{ATP}$ ) all play an important role in this glucose-sensing mechanism (Spanswick *et al.*, 1997; Dunn-Meynell *et al.*, 2002; Kang *et al.*, 2004; Wang *et al.*, 2004; Bady *et al.*, 2006; Kang *et al.*, 2006; Yang *et al.*, 2007). In particular, the  $K_{ATP}$  channel has been shown to play a key role in the regulation of the electrical activity of glucose-sensing neurones in the hypothalamus. Studies using selective  $K_{ATP}$  channel blockers, such as tolbutamide and glibenclamide, as well as knock-out studies, have shown that the  $K_{ATP}$  channel in neurones is essential for glucose homeostasis and the cellular response to changes in glucose (Ashford *et al.*, 1990a,b; Rowe *et al.*, 1996; Spanswick *et al.*, 1997; Lee *et al.*, 1999; Spanswick *et al.*, 2000; Miki *et al.*, 2001; Zhang *et al.*, 2004). In addition, hypothalamic  $K_{ATP}$  channels have been shown to be important in hepatic glucose production: activation of these channels leading to lower blood glucose levels by inhibiting hepatic gluconeogenesis (Pocai *et al.*, 2005), whereas inhibition of these channels impairs the ability of insulin and fatty acids to inhibit glucose production (Obici *et al.*, 2002b,c). These data suggest that  $K_{ATP}$  channels, as well as being important in glucose-sensing, are essential components in the regulation of glucose production. The  $K_{ATP}$  channel is therefore an important integrator between glucose levels and the excitability of neurones, due

to its ability to couple membrane excitability to cellular metabolism by directly sensing and integrating changes in the concentration of nucleotides.

Glucose-sensing neurones can respond to a wide range of metabolic and hormonal signals making them ideal metabolic sensors to link the control of food intake and energy homeostasis. Within the ARC, orexigenic neuropeptide Y (NPY) neurones were found to be GI neurones (Muroya *et al.*, 1999) and anorexigenic pre-pro-opiomelanocortin (POMC) neurones were found to be GE neurones (Ibrahim *et al.*, 2003). Both NPY and POMC neurones have been shown to express  $K_{ATP}$  channels (van den Top *et al.*, 2007). GE neurones also respond to peripheral hormones such as insulin and leptin (Spanswick *et al.*, 1997, 2000). How the  $K_{ATP}$  channel is proposed to respond selectively to stimuli within the functionally antagonistic NPY and POMC neuronal populations remains to be fully elucidated. One suggestion is that different compositions of the  $K_{ATP}$  channel may induce selective effects, but the subunit composition of ARC  $K_{ATP}$  channels is reported to be the same, ruling out this possibility (van den Top *et al.*, 2007). Therefore it is proposed that the selective response must occur before  $K_{ATP}$  channel activation.

It is important to study neurones in different glucose conditions to see how their properties change in different feeding states, especially as extremes of glucose concentrations can lead to conditions such as diabetes. Understanding further the properties of these neurones will help to lead to better understanding of these conditions. Original studies looking at the activity of neurones under different glucose concentrations utilised extracellular glucose concentrations ranging between 0 and 20 mM (for example see Ashford *et al.*, 1990a). However these concentrations represent non-physiological levels, as the brain would never be bathed in a glucose-free medium and even in extreme hyperglycaemia would never be exposed to



20 mM. Therefore these early glucose-studies do not give any insight into the activity of ARC neurones in physiological glucose levels. Subsequent studies have attempted to address this problem by utilising more likely physiological glucose concentrations (Song *et al.*, 2001; Wang *et al.*, 2004). Therefore in the present study ARC neurones were recorded in either 10 mM glucose-containing aCSF (hyperglycaemic conditions), in order to compare the activity of neurones with classic glucose studies which utilised non-physiological glucose (Ashford *et al.*, 1990a; Spanswick *et al.*, 1997, 2000), or 2 mM glucose-containing aCSF (euglycaemic conditions), similar to more recent studies representing physiological glucose (Song *et al.*, 2001; Wang *et al.*, 2004). Studies outside the ARC, within the brainstem, have also looked at the effects of changing the glucose concentration from 10 mM to 2 mM and 0 mM glucose on activity of neurones (Balfour *et al.*, 2006). The present study will enable us to see whether there were any significant changes in the electrical properties of ARC neurones under these different glucose concentrations.

The hypothalamic ARC surrounds the ventral part of the third ventricle and lies above the median eminence. It is one of several hypothalamic nuclei involved in maintaining energy homeostasis, along with the LH, VMN, paraventricular nucleus (PVN) and dorsomedial hypothalamus (DMH; Williams *et al.*, 2000; Cone *et al.*, 2001; Williams *et al.*, 2001). As it is located immediately above the median eminence, considered a circumventricular organ with a highly compromised BBB (Ganong, 2000), the ARC is in a strategically ideal location to receive and integrate hormonal and nutrient signals related to energy homeostasis and generate appropriate responses. In order to maintain energy homeostasis, the ARC receives afferent inputs from the other hypothalamic nuclei mentioned previously as well as the brainstem

and periphery. Some of the neuropeptides and neurotransmitters contained in these inputs include orexin, serotonin, GABA, glutamate and noradrenaline to name but a few (Chronwall, 1985; Cone *et al.*, 2001; Horvath *et al.*, 2004). The ARC is also exposed to circulating factors like insulin, leptin, ghrelin and glucose, which are all important in the control of energy homeostasis as they signal the peripheral energy status to the central nervous system (Elias *et al.*, 1998b; Schwartz *et al.*, 1999; Cone *et al.*, 2001; Broberger, 2005; Elmquist *et al.*, 2005).

The multiple input pathways and signalling factors that affect the ARC suggests that there is a heterogeneous population of neurones within the ARC. This heterogeneity leads to functional divisions within the ARC with different neurones performing different functions. Several neurones have already been characterised by the neuropeptides they release; for example, neurones which release the orexigenic peptides NPY and agouti-related peptide (AgRP) are distinct from those that release the anorexigenic peptides cocaine and amphetamine-related transcript (CART) and  $\alpha$ -melanocyte stimulating hormone ( $\alpha$ -MSH; Chronwall, 1985; Broberger, 2005). It is therefore important to be able to understand and characterise the cell types within the ARC in order that we can learn more about how it is involved in controlling body-weight. However at present there is still no detailed characterisation of neurones within the ARC. Characterising neurones into groups based on either intrinsic or extrinsic properties may provide one way in which neurones can be functionally classified. In this study a characterisation of neurones in the ARC was carried out based on their electrophysiological properties. This characterisation of neurones builds on previous work done by van den Top (2002). In particular, neurones were classified according to the subthreshold active conductances they expressed. Active conductances are important for shaping the intrinsic properties of



neurones as they contribute to the integration of synaptic inputs and formulate appropriate outputs for neurones (Huguenard, 1996; Pape, 1996; van den Top *et al.*, 2004). They therefore play an important role in determining the functional output of neurones and represent ideal properties on which to classify neurones into functional groups.

The aims of this study were to compare the activity and electrophysiological properties of ARC neurones recorded in 2 mM and 10 mM glucose-containing aCSF and to characterise neurones into potential functional groups based upon their electrophysiological properties.

### 3.2 Results

Whole-cell recordings were obtained from 411 ARC neurones. ARC neurones were identified purely on the basis of their location above the median eminence, on either side of the third ventricle. Recordings were obtained in aCSF containing either 2 mM glucose to determine the activity of neurones in a physiological, euglycaemic glucose concentration, or 10 mM glucose to determine the activity of neurones in a non-physiological hyperglycaemic glucose concentration, which will also enable the activity of neurones to be compared to previous studies that did not use physiological glucose levels. 241 neurones were recorded in 10 mM glucose-containing aCSF and the remaining 170 in 2 mM glucose-containing aCSF in which osmolarity was compensated using D-mannitol. A comparison between the general membrane properties of neurones recorded in 2 mM glucose-containing aCSF and 10 mM glucose-containing aCSF was firstly carried out. A more detailed comparison of the electrical properties of these neurones was then performed and neurones were divided into 8 distinct groups (clusters) based

upon the subthreshold active conductances they expressed. Subthreshold active conductances were looked at in this study, as the intrinsic properties of neurones are important for shaping the activity and output of neurones. Active conductances are therefore ideal properties upon which we can potentially classify neurones into functional groups.

To investigate the active membrane conductances of the neurones, current-voltage (I-V) relationships were generated. Hyperpolarising and depolarising current steps of constant increment (-200 to + 40 pA, 800 ms, 0.1 Hz) were injected into the cell and the membrane responses recorded. Subthreshold active conductances were identified by inspection of the I-V and it was found that some neurones expressed one or more subthreshold active conductances, while others did not express any. In the absence of any subthreshold active conductances, there was a linear relationship between the amount of current injected and the voltage response, indicating a directly proportional relationship between current and voltage. However, the current-voltage relationship in some neurones was non-linear, indicating the expression of one or more active conductances. Statistical significance was determined using a Mann-Whitney test, except when comparing percentage of spontaneously active neurones when a chi-square test was used.

### ***3.2.1 Comparison of all neurones recorded in 10 mM and 2 mM glucose-containing aCSF***

The resting membrane potential, input resistance, membrane time-constant and spontaneous firing rates of all neurones recorded in 10 mM and 2 mM glucose-containing aCSF were calculated, to give an overall comparison between the two different glucose concentrations. Table 3.1 gives an overview of this data.



### ***Resting Membrane Potential***

In 10 mM glucose-containing aCSF, the average resting membrane potential was  $-47.6 \pm 0.5$  mV ( $n=241$ ), whilst it was  $-46.7 \pm 0.5$  mV in 2 mM glucose-containing aCSF ( $n=170$ ). These values were not significantly different ( $P=0.3$ ). The resting membrane potentials of neurones recorded in both 10 mM and 2 mM glucose-containing aCSF are shown in figure 3.1. In 10 mM glucose-containing aCSF, the range containing the highest proportion of neurones was -40 to -44 mV (27 %), although in 2 mM glucose-containing aCSF it was -45 to -49 mV (32 %). The median values were -47 and -46 mV in 10 mM and 2 mM glucose-containing aCSF, respectively.

### ***Input Resistance***

In 10 mM glucose-containing aCSF, the average input resistance was  $1602 \pm 53$  M $\Omega$  ( $n=241$ ) whilst the corresponding value in 2 mM glucose-containing aCSF was  $1387 \pm 53$  M $\Omega$  ( $n=170$ ). The input resistance was significantly lower in 2 mM glucose-containing aCSF ( $P<0.01$ ). 1001-1500 M $\Omega$  was the range containing the largest proportion of neurones in 10 mM glucose-containing aCSF (31 %), and in 2 mM glucose-containing aCSF it was 501-1000 M $\Omega$  (34 %; see figure 3.2). The median values were 1373 and 1255 M $\Omega$  in 10 mM and 2 mM glucose-containing aCSF, respectively. The distribution of input resistances in the 2 mM glucose-containing aCSF plot was skewed to the left compared to the 10 mM glucose-containing aCSF plot, indicating that neurones recorded in the lower glucose concentration generally expressed lower input resistances.

### ***Membrane Time-Constant***

The average membrane time-constant of neurones recorded in 10 mM and 2 mM glucose-containing aCSF was  $39.3 \pm 2.0$  ms ( $n=241$ ) and  $36.6 \pm 1.7$  ms ( $n=170$ ), respectively, a non-significant difference ( $P=0.9$ ). 11-20 ms was the most common membrane time-constant range (20 %) in 10 mM glucose-containing aCSF and 21-30 ms (23 %) in 2 mM glucose-containing aCSF (see figure 3.3). The median value was 31 ms in both cases. There was a very similar distribution pattern in both 10 mM and 2 mM glucose-containing aCSF indicating that we were recording from a population of neurones of similar size in both conditions.

### ***Spontaneous Firing Rate***

234 neurones were recorded in 10 mM glucose-containing aCSF of which 75 (32 %) were spontaneously active at rest and 159 (68 %) were silent (data could not be obtained from 7 neurones as no recording of the trace was made). The average firing frequency of the spontaneously active cells was  $1.1 \pm 0.1$  Hz. 158 neurones were recorded in 2 mM glucose-containing aCSF, 79 (50 %) of which were spontaneously active and 79 (50 %) were silent (data could not be obtained from 12 neurones as no recording of the trace was made). The average firing frequency of these cells was  $1.0 \pm 0.1$  Hz. There was no significant difference between the average firing frequencies of the two populations ( $P=0.9$ ). 0-0.5 Hz was the range with the highest percentage of active neurones in both 2 mM and 10 mM glucose-containing aCSF (see figure 3.4Ai). The median values were 0 and 0.03 Hz in 10 mM and 2 mM glucose-containing aCSF, respectively. There was a significant increase in the percentage of active neurones recorded in 2 mM glucose-containing aCSF (50 %) compared to neurones recorded in 10 mM glucose-containing aCSF



(32 %) and hence an increase in the proportion of spontaneously active cells recorded in 2 mM glucose-containing aCSF ( $P<0.01$ ; see figure 3.4Aii).

**Table 3.1 General membrane properties of all neurones**

	10 mM Glucose	2 mM Glucose	P values
'n' value	241	170	
Resting membrane potential (mV)	$-47.6 \pm 0.5$	$-46.7 \pm 0.5$	0.3
Input resistance ( $M\Omega$ )	$1602 \pm 53$	$1387 \pm 53$	$P<0.01$
Membrane time-constant (ms)	$39.3 \pm 2.0$	$36.6 \pm 1.7$	0.9
Spontaneous activity (%)	32	50	$P<0.01$
Spontaneous firing rate of active neurones (Hz)	$1.1 \pm 0.1$	$1.0 \pm 0.1$	0.9

These data show that the resting membrane potential and membrane time-constant did not significantly change in the two different glucose concentrations. However there was a significant increase in input resistance in 10 mM glucose-containing aCSF and there was a significant increase in the number of spontaneously active neurones in 2 mM glucose-containing aCSF. The expression of subthreshold active conductances was also investigated to see whether expression was altered between euglycaemic and hyperglycaemic conditions. Neurones were grouped into subdivisions based on their differential expression of subthreshold active conductances in an attempt to characterise the neurones into potential functional subgroups. These groups are termed clusters. Properties of action potentials and active conductances were calculated as shown in figure 3.5.

### 3.2.2 Expression of anomalous inward rectification (Cluster 1)

The first group of neurones was identified as having a decrease in input resistance at more negative membrane potentials, indicated by a decrease in the slope in the plot of the I-V (see figure 3.6A and C). This decrease was instantaneous and non-inactivating. This conductance is similar to that described previously in other neurones as an anomalous inward rectifier ( $I_{an}$ ; for example see Constanti & Galvan, 1983; Pickering *et al.*, 1991). Table 3.2 gives an overview of this data.

#### 10 mM glucose-containing aCSF

15 neurones were recorded in 10 mM glucose-containing aCSF that expressed only the anomalous inward rectifier (6 % of the population). Spontaneous activity was recorded in 4 of these neurones (27 %), with an average firing frequency of  $1.6 \pm 0.4$  Hz. These neurones had an average resting membrane potential of  $-50.1 \pm 2.0$  mV (range -40 to -64 mV) and an average input resistance of  $1827 \pm 274$  M $\Omega$  (range 745 to 4664 M $\Omega$ ; n=15). The membrane time-constant was  $48.1 \pm 8.3$  ms (range 13.2 to 139.2 ms). The threshold for spike firing was  $-30.7 \pm 1.1$  mV (n=15), at which point action potentials were generated with an amplitude of  $91.4 \pm 3.6$  mV (range 70 to 111 mV) and a duration at half-height and threshold of  $1.5 \pm 0.1$  ms and  $3.0 \pm 0.2$  ms, respectively. The ratio of the duration (threshold/half-height) was  $2.0 \pm 0.1$ .

$I_{an}$  induced a 35 % reduction in input resistance at a membrane potential of  $-102.6 \pm 0.7$  mV relative to input resistance at rest. The activation threshold calculated from the I-V for  $I_{an}$  was estimated around  $-84.2 \pm 1.7$  mV (n=15).



**2 mM glucose-containing aCSF**

16 neurones were recorded in 2 mM glucose-containing aCSF that expressed only the anomalous inward rectifier (9 % of the population). Spontaneous activity was recorded in 4 out of these 16 neurones (25 %), with an average firing frequency of  $1.4 \pm 0.4$  Hz. These neurones had an average resting membrane potential of  $-50.5 \pm 2.0$  mV (range -35 to -62 mV) and an average input resistance of  $1521 \pm 108$  M $\Omega$  (range 754 to 2350 M $\Omega$ ; n=16). The membrane time-constant was  $41.0 \pm 5.6$  ms (range 13.1 to 86.6 ms). The threshold for spike firing was  $-30.1 \pm 1.3$  mV (n=16), at which point action potentials were generated with an amplitude of  $78.1 \pm 5.8$  mV and a duration at half-height and threshold of  $1.7 \pm 0.1$  ms and  $3.6 \pm 0.3$  ms, respectively. The ratio of the duration (threshold/half-height) was  $2.2 \pm 0.1$ .

$I_{an}$  induced a 44 % reduction in input resistance at a membrane potential of  $-102.2 \pm 0.9$  mV relative to input resistance at rest. The activation threshold calculated from the I-V for  $I_{an}$  was estimated around  $-86.9 \pm 1.0$  mV (n=16).

**Table 3.2 Electrophysiological properties of cluster 1 neurones**

<b>Cluster 1 Properties</b>			
	<b>10 mM Glucose</b>	<b>2 mM Glucose</b>	<b>P values</b>
<b>'n' value</b>	15	16	
<b>Spontaneous activity (%)</b>	27	25	0.9
<b>Spontaneous firing rate (Hz)</b>	$1.6 \pm 0.4$	$1.4 \pm 0.4$	0.8
<b>Membrane potential (mV)</b>	$-50.1 \pm 2.0$	$-50.5 \pm 2.0$	0.9
<b>Input resistance (M<math>\Omega</math>)</b>	$1827 \pm 274$	$1521 \pm 108$	0.7
<b>Membrane time-constant (ms)</b>	$48.1 \pm 8.3$	$41.0 \pm 5.6$	0.6
<b>Threshold for action potential (AP) firing (mV)</b>	$-30.7 \pm 1.1$	$-30.1 \pm 1.3$	0.8
<b>AP amplitude (mV)</b>	$91.4 \pm 3.6$	$78.1 \pm 5.8$	0.1
<b>AP duration half-height (ms)</b>	$1.5 \pm 0.1$	$1.7 \pm 0.1$	0.2
<b>AP duration threshold (ms)</b>	$3.0 \pm 0.2$	$3.6 \pm 0.3$	0.06
<b>Ratio of AP duration: threshold/ half-height</b>	$2.0 \pm 0.1$	$2.2 \pm 0.1$	0.2
<b>Activation threshold <math>I_{an}</math> (mV)</b>	$-84.2 \pm 1.7$	$-86.9 \pm 1.0$	0.2
<b><math>I_{an}</math> induced reduction in input resistance (%)</b>	$35.5 \pm 4.1$	$43.8 \pm 3.4$	0.09

There were no significant differences between any of the membrane properties of cluster 1 neurones recorded in the presence of 10 mM and 2 mM glucose-containing aCSF.

### **3.2.3 Expression of transient outward rectification with $I_{an}$ (Cluster 2)**

The second cluster of neurones identified contained two subthreshold active conductances:  $I_{an}$ , like cluster 1 neurones and a second conductance,  $I_A$ . This second conductance resembled the A-like transient outward rectifier noted in other neurones



(for example see Connor & Stevens, 1971a,b; Miyazaki *et al.*, 1996; see figure 3.6B). This conductance is characterised by a delayed return to resting membrane potential upon termination of injection of negative current. The amplitude of the membrane response was calculated at half-decay time and the average inactivation time of this active conductance was measured from the termination of the negative current injection until the return of the membrane potential to baseline. This cluster of neurones is like the ARC neurones described by van den Top *et al.*, (2004). A characteristic of these neurones is their ability to exhibit burst-like firing patterns of activity. Table 3.3 gives an overview of this data.

### ***10 mM glucose-containing aCSF***

Whole-cell recordings were obtained from 8 neurones in 10 mM glucose-containing aCSF (3 % of the population). 4/8 of these neurones were active at rest (50 %), with an average firing frequency of  $2.2 \pm 0.7$  Hz, one of which exhibited spontaneous burst-like patterns of firing. The average resting membrane potential and input resistance were  $-49.0 \pm 2.1$  mV (range -40 to -56 mV) and  $1782 \pm 458$  M $\Omega$  (range 714 to 4682 M $\Omega$ ) respectively, with a time-constant of  $33.5 \pm 4.9$  ms (range 17.4 to 54.2 ms; n=8). Threshold for action potential firing was  $-30.5 \pm 1.9$  mV, leading to action potentials of amplitude  $85.6 \pm 5.7$  mV. Duration of the action potential at half-height and threshold was  $1.7 \pm 0.2$  ms and  $3.4 \pm 0.5$  ms, respectively, giving a ratio of  $2.0 \pm 0.1$ .

$I_{an}$  induced a 39 % reduction in input resistance at a membrane potential of  $-98.1 \pm 2.1$  mV relative to input resistance at rest. The activation threshold calculated from the I-V for  $I_{an}$  was estimated at  $-82.3 \pm 2.7$  mV (n=8).

The expression of the A-like conductance caused a slow return to baseline after termination of hyperpolarising current pulses. The mean decay-time of the conductance in these neurones was  $1111 \pm 212$  ms (range 507 to 2353 ms) and the amplitude of the response at half-decay time was  $5.1 \pm 0.9$  mV (range 1.4 to 8.5 mV;  $n=8$ ) following negative current injection to an average membrane potential of  $-95.4 \pm 3.0$  mV.

### ***2 mM glucose-containing aCSF***

8 neurones were recorded in 2 mM glucose-containing aCSF that were classified as cluster 2 neurones (5 % of the population). 5/8 of these neurones were spontaneously active (63 %) with an average firing frequency of  $0.2 \pm 0.0$  Hz and 3 of these neurones exhibited a burst-like firing pattern of activity. The average resting membrane potential and input resistance were  $-45.9 \pm 2.3$  mV (range -34 to -58 mV) and  $1243 \pm 206$  M $\Omega$  (range 548 to 2068 M $\Omega$ ) respectively, with a time-constant of  $31.2 \pm 6.4$  ms (range 13.2 to 64.7 ms;  $n=8$ ). Threshold for action potential firing was  $-31.6 \pm 2.4$  mV, leading to action potentials of amplitude  $81.8 \pm 6.8$  mV. Duration of the action potential at half-height and threshold was  $1.7 \pm 0.2$  ms and  $3.5 \pm 0.4$  ms, respectively, giving a ratio of  $2.0 \pm 0.9$ .

$I_{an}$  induced a 35 % reduction in input resistance at a membrane potential of  $-99.6 \pm 0.3$  mV relative to input resistance at rest. The activation threshold calculated from the I-V for  $I_{an}$  was estimated at  $-80.4 \pm 2.9$  mV ( $n=8$ ).

The mean decay time of the A-like conductance was  $838 \pm 174$  ms (range 201 to 1648 ms) and the amplitude of the response at half-decay-time was  $4.7 \pm 0.6$  mV (range 2.6 to 7.7 mV;  $n=8$ ) following negative current injection to an average membrane potential of  $-98.9 \pm 0.5$  mV.



**Table 3.3 Electrophysiological properties of cluster 2 neurones**

<b>Cluster 2 Properties</b>			
	<b>10 mM Glucose</b>	<b>2 mM Glucose</b>	<b>P values</b>
<b>'n' value</b>	8	8	
<b>Spontaneous activity (%)</b>	50	63	0.6
<b>Spontaneous firing rate (Hz)</b>	$2.2 \pm 0.7$	$0.2 \pm 0.0$	$P < 0.05$
<b>Membrane potential (mV)</b>	$-49.0 \pm 2.1$	$-45.9 \pm 2.3$	0.3
<b>Input resistance (M<math>\Omega</math>)</b>	$1782 \pm 458$	$1243 \pm 206$	0.6
<b>Membrane time-constant (ms)</b>	$33.5 \pm 4.9$	$31.2 \pm 6.4$	0.6
<b>Threshold for action potential (AP) firing (mV)</b>	$-30.5 \pm 1.9$	$-31.6 \pm 2.4$	1.0
<b>AP amplitude (mV)</b>	$85.6 \pm 5.7$	$81.8 \pm 6.8$	0.6
<b>AP duration half-height (ms)</b>	$1.7 \pm 0.2$	$1.7 \pm 0.2$	0.9
<b>AP duration threshold (ms)</b>	$3.4 \pm 0.5$	$3.5 \pm 0.4$	0.9
<b>Ratio of AP duration: threshold/ half-height</b>	$2.0 \pm 0.1$	$2.0 \pm 0.9$	0.3
<b>Activation threshold <math>I_{an}</math> (mV)</b>	$-82.3 \pm 2.7$	$-80.4 \pm 2.9$	0.6
<b><math>I_{an}</math> induced reduction in input resistance (%)</b>	$39.3 \pm 7.1$	$35.2 \pm 7.8$	0.9
<b>Decay time <math>I_A</math> (ms)</b>	$1111 \pm 212$	$838 \pm 174$	0.4
<b>Amplitude <math>I_A</math> (mV)</b>	$5.1 \pm 0.9$	$4.7 \pm 0.6$	0.6

There was a significant difference between the spontaneous firing rate of cluster 2 neurones recorded in 2 mM and 10 mM glucose-containing aCSF with an increase in firing in 10 mM glucose ( $P < 0.05$ ). There were no significant differences between any other membrane properties of cluster 2 neurones recorded in 10 mM or 2 mM glucose-containing aCSF. However there appeared to be clear differences in some of the properties which did not reach statistical significance. These include the percentage of spontaneously active neurones (50 % in 10 mM and 63 % in 2 mM),

input resistance and the decay time of the A-like conductance. The reason they may not have reached statistical significance maybe due to the low 'n' numbers.

#### ***3.2.4 Expression of no obvious subthreshold active conductances (Cluster 3)***

Cluster 3 neurones were characterised by the absence of any of the subthreshold active conductances expressed in the other neuronal clusters. The I-Vs of cluster 3 neurones were therefore linear, showing a directly proportional relationship between injected current and membrane response (see figure 3.7A). Table 3.4 gives an overview of this data.

#### ***10 mM glucose-containing aCSF***

23 neurones were recorded in 10 mM glucose-containing aCSF that expressed no obvious subthreshold active conductances (10 % of the population). 6 of these neurones were active at rest (26 %) with an average firing frequency of  $1.4 \pm 0.4$  Hz. The average resting membrane potential and input resistance were  $-49.1 \pm 2.1$  mV (range -30 to -63 mV) and  $1857 \pm 215$  M $\Omega$  (range 490 to 4030 M $\Omega$ ), respectively, with a membrane time-constant of  $37.4 \pm 5.6$  ms (n=23). Spike firing was induced at  $-31.5 \pm 1.9$  mV at which point action potentials were generated of amplitude  $86.0 \pm 2.9$  mV and duration of  $1.6 \pm 0.1$  ms and  $3.2 \pm 0.2$  ms at half-height and threshold, respectively. The ratio between duration at threshold and half-height was  $2.0 \pm 0.0$ .

#### ***2 mM glucose-containing aCSF***

In 2 mM glucose-containing aCSF, 17 neurones that expressed no obvious subthreshold active conductances were obtained (10 % of the population). 8 of these



neurones were active at rest (47 %) with an average firing frequency of  $1.3 \pm 0.5$  Hz. The average resting membrane potential and input resistance were  $-46.4 \pm 2.0$  mV (range -37 to -64 mV) and  $1418 \pm 169$  M $\Omega$  (range 497 to 3038 M $\Omega$ ), respectively, with a membrane time-constant of  $27.0 \pm 4.2$  ms (n=17). Spike firing was induced at  $-29.4 \pm 1.4$  mV at which point action potentials were generated of amplitude  $81.8 \pm 2.2$  mV and a duration of  $1.7 \pm 0.1$  ms and  $3.5 \pm 0.3$  ms at half-height and threshold, respectively. The ratio between duration at threshold and half-height was  $2.1 \pm 0.1$ .

**Table 3.4 Electrophysiological properties of cluster 3 neurones**

<b>Cluster 3 Properties</b>			
	<b>10 mM Glucose</b>	<b>2 mM Glucose</b>	<b>P values</b>
<b>'n' value</b>	23	17	
<b>Spontaneous activity (%)</b>	26	47	0.2
<b>Spontaneous firing rate (Hz)</b>	$1.4 \pm 0.4$	$1.3 \pm 0.5$	0.9
<b>Membrane potential (mV)</b>	$-49.1 \pm 2.1$	$-46.4 \pm 2.0$	0.3
<b>Input resistance (M<math>\Omega</math>)</b>	$1857 \pm 215$	$1418 \pm 169$	0.3
<b>Membrane time-constant (ms)</b>	$37.4 \pm 5.6$	$27.0 \pm 4.2$	0.3
<b>Threshold for action potential (AP) firing (mV)</b>	$-31.5 \pm 1.9$	$-29.4 \pm 1.4$	0.5
<b>AP amplitude (mV)</b>	$86.0 \pm 2.9$	$81.8 \pm 2.2$	0.4
<b>AP duration half-height (ms)</b>	$1.6 \pm 0.1$	$1.7 \pm 0.1$	0.7
<b>AP duration threshold (ms)</b>	$3.2 \pm 0.2$	$3.5 \pm 0.3$	0.5
<b>Ratio of AP duration: threshold/ half-height</b>	$2.0 \pm 0.0$	$2.1 \pm 0.1$	0.8

There were no significant differences between any membrane properties of cluster 3 neurones recorded in 2 mM and 10 mM glucose-containing aCSF.

### 3.2.5 Expression of time- and voltage-dependent inward rectification (Cluster 4)

Another subthreshold active conductance expressed by a subset of ARC neurones was seen as a depolarising ‘sag’ in the membrane response to hyperpolarising current steps at more negative membrane potentials (see figure 3.7B). It is a time- and voltage-dependent inward rectification, which is similar to the hyperpolarisation-activated non-selective cation conductance ( $I_h$ ) reported in other neurones (for example see Halliwell & Adams, 1982; McCormick & Pape, 1990b; Pape, 1996). The threshold for the activation point of  $I_h$  was calculated by averaging the membrane potentials at which  $I_h$  was first visible in the I-V relationship. The change in membrane potential between instantaneous and steady-state was used as a measure of the magnitude of this conductance. Table 3.5 gives an overview of this data.

#### **10 mM glucose-containing aCSF**

23 neurones expressed  $I_h$  in the presence of 10 mM glucose-containing aCSF (10 % of the population) of which 6 were active at rest (26 %) with an average firing frequency of  $1.7 \pm 0.5$  Hz. The average resting membrane potential of these cells was  $-51.5 \pm 1.9$  mV (range -37 to -67 mV), input resistance was  $1134 \pm 128$  M $\Omega$  (range 294 to 2877 M $\Omega$ ) and membrane time-constant was  $26.6 \pm 3.7$  ms (range 6.6 to 88.3ms; n=23). Spike firing was induced at  $-31.4 \pm 1.5$  mV, giving rise to action potentials of amplitude, duration at half-height, and threshold duration of  $79.2 \pm 3.3$  mV,  $1.6 \pm 0.1$  ms and  $3.4 \pm 0.2$  ms, respectively. The ratio between the two durations was  $2.0 \pm 0.1$ .

The average threshold for activation of  $I_h$  was  $-87.2 \pm 1.5$  mV, giving rise to a hyperpolarising sag of amplitude  $6.6 \pm 0.6$  mV at a membrane potential of



-104.8  $\pm$  1.1 mV. This is equivalent to a decrease in input resistance of 12.9 % upon activation of  $I_h$ .

### ***2 mM glucose-containing aCSF***

10 neurones were obtained in the presence of 2 mM glucose-containing aCSF that expressed  $I_h$  (6 % of the population). 6 of these neurones were active at rest (60 %) with an average firing frequency of 1.1  $\pm$  0.3 Hz. The average resting membrane potential of these cells was -49.9  $\pm$  2.4 mV (range -40 to -60 mV), input resistance was 1285  $\pm$  252 M $\Omega$  (range 507 to 2452 M $\Omega$ ) and membrane time-constant was 37.5  $\pm$  7.6 ms (range 5.2 to 93.6 ms; n=10). Spike firing was induced at -32.6  $\pm$  1.7 mV, generating action potentials of amplitude, duration at half-height, and threshold duration of 88.2  $\pm$  4.7 mV, 1.5  $\pm$  0.0 ms and 3.5  $\pm$  0.3 ms, respectively. The ratio between the two durations was 2.3  $\pm$  0.1.

The mean threshold for activation of  $I_h$  was -81.4  $\pm$  2.5 mV, giving rise to a hyperpolarising sag of amplitude 8.8  $\pm$  0.9 mV at a membrane potential of -106.1  $\pm$  2.1 mV. This is equivalent to a decrease in input resistance of 15.7 % upon activation of  $I_h$ .

**Table 3.5 Electrophysiological properties of cluster 4 neurones**

<b>Cluster 4 Properties</b>			
	<b>10 mM Glucose</b>	<b>2 mM Glucose</b>	<b>P values</b>
<b>'n' value</b>	23	10	
<b>Spontaneous activity (%)</b>	26	60	0.06
<b>Spontaneous firing rate (Hz)</b>	$1.7 \pm 0.5$	$1.1 \pm 0.3$	0.5
<b>Membrane potential (mV)</b>	$-51.5 \pm 1.9$	$-49.9 \pm 2.4$	0.6
<b>Input resistance (M<math>\Omega</math>)</b>	$1134 \pm 128$	$1285 \pm 252$	1.0
<b>Membrane time-constant (ms)</b>	$26.6 \pm 3.7$	$37.5 \pm 7.6$	0.1
<b>Threshold for action potential (AP) firing (mV)</b>	$-31.4 \pm 1.5$	$-32.6 \pm 1.7$	0.4
<b>AP amplitude (mV)</b>	$79.2 \pm 3.3$	$88.2 \pm 4.7$	0.06
<b>AP duration half-height (ms)</b>	$1.6 \pm 0.1$	$1.5 \pm 0.0$	0.1
<b>AP duration threshold (ms)</b>	$3.4 \pm 0.2$	$3.5 \pm 0.3$	0.9
<b>Ratio of AP duration: threshold/ half-height</b>	$2.0 \pm 0.1$	$2.3 \pm 0.1$	0.2
<b>Activation threshold <math>I_h</math> (mV)</b>	$-87.2 \pm 1.5$	$-81.4 \pm 2.5$	0.1
<b><math>I_h</math> induced reduction in input resistance (%)</b>	$12.9 \pm 1.2$	$15.7 \pm 1.0$	0.2

There were no significant differences between neurones recorded in the presence of 2 mM and 10 mM glucose-containing aCSF. However, it is important to note that the number of cluster 4 neurones recorded in both conditions was quite different and therefore this may have affected the significance values of these results. It is again apparent that there is a clear difference in the spontaneous activity of neurones recorded under both conditions (26 % in 10 mM and 60 % in 2 mM).



### 3.2.6 Expression of T-type conductance and $I_h$ (Cluster 5)

Cluster 5 neurones were characterised by expression of two subthreshold active conductances:  $I_h$  as seen in cluster 4 neurones and a conductance resembling the T-type calcium conductance (see figure 3.8A). This conductance is characterised by a rebound depolarisation upon termination of negative current injection. This rebound depolarisation is similar to that described before in cells mediated by T-type calcium channels (for example see Llinas & Yarom, 1981). In order to be able to quantify the T-type conductance, the amplitude of the rebound depolarisation was calculated as the difference between the rebound plateau and the resting membrane potential. This value is only an estimate of the amplitude of the T-type conductance as there may be a contribution from  $I_h$  towards the rebound depolarisation. Table 3.6 gives an overview of this data.

#### **10 mM glucose-containing aCSF**

41 neurones were characterised as having  $I_h$  and a T-type calcium conductance in 10 mM glucose-containing aCSF (17 % of the population). 14 neurones were spontaneously active at rest (31 %) with an average firing frequency of  $0.4 \pm 0.1$  Hz. The average resting membrane potential of these neurones was  $-48.7 \pm 1.1$  mV (range -30 to -60 mV) and they had an input resistance of  $1606 \pm 124$  M $\Omega$  (range 498 to 3582 M $\Omega$ ). The membrane time-constant was  $43.6 \pm 4.9$  ms (n=41). The threshold for spike firing was  $-29.3 \pm 0.9$  mV and the amplitude of the generated action potentials were  $78.6 \pm 2.4$  mV, with duration at half-height of  $1.6 \pm 0.1$  ms and at threshold of  $3.4 \pm 0.1$  ms.  $2.1 \pm 0.0$  was the ratio between the two durations.

The mean threshold for activation of  $I_h$  was  $-86.5 \pm 1.4$  mV, giving rise to a hyperpolarising sag of amplitude  $11.6 \pm 4.8$  mV at a membrane potential of  $-105 \pm 0.9$  mV. This is equivalent to a decrease in input resistance of 21.2 % upon activation of  $I_h$ .

Activation of the T-type calcium conductance gave an average membrane depolarisation of  $11.9 \pm 1.1$  mV from a membrane potential of  $-48.5 \pm 1.2$  mV ( $n=38$ ).

### ***2 mM glucose-containing aCSF***

25 neurones were characterised as having  $I_h$  and a T-type calcium conductance when recorded in 2 mM glucose-containing aCSF (15 % of the population), of which 12 were spontaneously firing at rest (48 %) with an average firing frequency of  $1.0 \pm 0.2$  Hz.. The average resting membrane potential of these neurones was  $-49.3 \pm 1.1$  mV (range -42 to -64 mV) and they had a mean input resistance of  $1213 \pm 106$  M $\Omega$  (range 572 to 2868 M $\Omega$ ). The membrane time-constant was  $33.0 \pm 2.6$  ms ( $n=25$ ). The threshold for spike firing was  $-31.7 \pm 0.8$  mV and the amplitude of the generated action potentials were  $83.8 \pm 2.4$  mV, with duration at half-height of  $1.4 \pm 0.0$  ms and at threshold of  $2.9 \pm 0.1$  ms.  $2.0 \pm 0.1$  was the ratio between the two durations.

The mean threshold for activation of  $I_h$  was  $-82.7 \pm 7.1$  mV, giving rise to a hyperpolarising sag of amplitude  $8.1 \pm 0.8$  mV at a membrane potential of  $-106.2 \pm 0.9$  mV. This is equivalent to a decrease in input resistance of 15 % upon activation of  $I_h$ .



Activation of the T-type calcium conductance gave an average membrane depolarisation of  $13.8 \pm 1.9$  mV from a membrane potential of  $-51.2 \pm 1.7$  mV ( $n=14$ ).

**Table 3.6 Electrophysiological properties of cluster 5 neurones**

Cluster 5 Properties			
	10 mM Glucose	2 mM Glucose	P values
'n' value	41	25	
Spontaneous activity (%)	31	48	0.3
Spontaneous firing rate (Hz)	$0.4 \pm 0.1$	$1.0 \pm 0.2$	0.08
Membrane potential (mV)	$-48.7 \pm 1.1$	$-49.3 \pm 1.1$	0.8
Input resistance ( $M\Omega$ )	$1606 \pm 124$	$1213 \pm 106$	$P<0.05$
Membrane time-constant (ms)	$43.6 \pm 4.9$	$33.0 \pm 2.6$	0.6
Threshold for action potential (AP) firing (mV)	$-29.3 \pm 0.9$	$-31.7 \pm 0.8$	$P<0.05$
AP amplitude (mV)	$78.6 \pm 2.4$	$83.8 \pm 2.4$	0.09
AP duration half-height (ms)	$1.6 \pm 0.1$	$1.4 \pm 0.0$	$P<0.05$
AP duration threshold (ms)	$3.4 \pm 0.1$	$2.9 \pm 0.1$	$P<0.01$
Ratio of AP duration: threshold/ half-height	$2.1 \pm 0.0$	$2.0 \pm 0.1$	0.2
Activation threshold $I_h$ (mV)	$-86.5 \pm 1.4$	$-82.7 \pm 7.1$	0.3
$I_h$ induced reduction in input resistance (%)	$21.2 \pm 9.0$	$15.0 \pm 1.8$	0.2
T-type amplitude (mV)	$11.9 \pm 1.1$	$13.8 \pm 1.9$	0.3

There were significant differences between the input resistance (greater in 10 mM glucose-containing aCSF;  $P<0.05$ ), threshold for action potential firing ( $P<0.05$ ) and both spike durations (longer in 10 mM glucose-containing aCSF;  $P<0.05$  and  $P<0.01$ ) of cluster 5 neurones recorded in 2 mM and 10 mM glucose-containing aCSF. Again it must be noted that there is a large difference in the

number of cluster 5 neurones recorded under both conditions which may have affected the significance of these results.

### ***3.2.7 Expression of T-type conductance (Cluster 6)***

Cluster 6 neurones expressed only the T-type calcium conductance (see figure 3.8B). Table 3.7 gives an overview of this data.

#### ***10 mM glucose-containing aCSF***

69 neurons were obtained in 10 mM glucose-containing aCSF that expressed a T-type calcium conductance (29 % of the population), of which 20 were active at rest (29 %) with an average firing frequency of  $1.2 \pm 0.3$  Hz. The average resting membrane potential, input resistance and membrane time-constant were  $-44.7 \pm 0.8$  mV (range -33 to -64 mV),  $1466 \pm 78$  M $\Omega$  (range 508 to 3228 M $\Omega$ ) and  $30.4 \pm 3.1$  ms (range 2.4 to 126.9 ms), respectively (n=69). Spike firing threshold was  $-27.2 \pm 0.6$  mV, generating action potentials of amplitude  $77.7 \pm 1.7$  mV and duration at half-height and threshold of  $1.7 \pm 0.1$  ms and  $3.5 \pm 0.1$  ms, respectively. This gave a ratio between the durations of  $2.1 \pm 0.0$ .

Activation of the T-type calcium conductance gave an average membrane depolarisation of  $9.1 \pm 0.8$  mV from a membrane potential of  $-45.7 \pm 0.9$  mV (n=60).

#### ***2 mM glucose-containing aCSF***

56 neurons were obtained in 2 mM glucose-containing aCSF that expressed a T-type calcium conductance (33 % of the population), of which 31 were active at rest (55 %) with an average firing frequency of  $0.7 \pm 0.2$  Hz. The average resting membrane potential, input resistance and membrane time-constant were



$-45.1 \pm 0.9$  mV (range -30 to -61 mV),  $1427 \pm 111$  M $\Omega$  (range 355 to 4050 M $\Omega$ ) and  $34.0 \pm 3.1$  ms (range 9.8 to 130.1 ms), respectively (n=56). Spike firing threshold was  $-29.5 \pm 0.8$  mV, generating action potentials of amplitude  $79.9 \pm 1.8$  mV and duration at half-height and threshold of  $1.7 \pm 0.1$  ms and  $3.4 \pm 0.1$  ms, respectively. This gave a ratio between the durations of  $2.0 \pm 0.0$ .

Activation of the T-type calcium conductance gave an average membrane depolarisation of  $9.6 \pm 0.9$  mV from a membrane potential of  $-46.8 \pm 1.1$  mV (n=37).

**Table 3.7 Electrophysiological properties of cluster 6 neurones**

Cluster 6 Properties			
	10 mM Glucose	2 mM Glucose	P values
'n' value	69	56	
Spontaneous activity (%)	29	55	$P < 0.01$
Spontaneous firing rate (Hz)	$1.2 \pm 0.3$	$0.7 \pm 0.2$	0.9
Membrane potential (mV)	$-44.7 \pm 0.8$	$-45.1 \pm 0.9$	0.3
Input resistance (M $\Omega$ )	$1466 \pm 78$	$1427 \pm 111$	0.3
Membrane time-constant (ms)	$30.4 \pm 3.1$	$34.0 \pm 3.1$	0.09
Threshold for action potential (AP) firing (mV)	$-27.2 \pm 0.6$	$-29.5 \pm 0.8$	0.06
AP amplitude (mV)	$77.7 \pm 1.7$	$79.9 \pm 1.8$	0.2
AP duration half-height (ms)	$1.7 \pm 0.1$	$1.7 \pm 0.1$	1.0
AP duration threshold (ms)	$3.5 \pm 0.1$	$3.4 \pm 0.1$	0.9
Ratio of AP duration: threshold/ half-height	$2.1 \pm 0.0$	$2.0 \pm 0.0$	0.7
T-type amplitude (mV)	$9.1 \pm 0.8$	$9.6 \pm 0.9$	0.4

There was a significant increase in the level of spontaneous activity of neurones recorded in 2 mM compared to 10 mM glucose-containing aCSF (29 % in 10 mM and 55 % in 2 mM). There were no significant differences between any of

the other membrane properties of cluster 6 neurones obtained in 2 mM and 10 mM glucose-containing aCSF.

### ***3.2.8 Expression of $I_{an}$ and T-type conductances (Cluster 7)***

Cluster 7 neurones were characterised as having an anomalous inward rectifier, as seen in cluster 1 neurones and a T-type calcium conductance as seen in clusters 5 and 6 (see figure 3.9A). Table 3.8 gives an overview of this data.

#### ***10 mM glucose-containing aCSF***

37 neurones were recorded in 10 mM glucose-containing aCSF that expressed both  $I_{an}$  and a T-type calcium conductance (15 % of the population). 16 of these were active at rest (43 %) with an average firing frequency of  $1.1 \pm 0.3$  Hz.  $-46.7 \pm 1.1$  mV (range -34 to -64mV) was the average resting membrane potential of these neurones, and the input resistance and time-constant were  $1741 \pm 131$  M $\Omega$  (range 574 to 3406 M $\Omega$ ) and  $42.1 \pm 4.4$  ms (range 8.6 to 132.6 ms), respectively (n=37). The threshold for spike firing was  $-30.2 \pm 1.0$  mV at which point action potentials of amplitude  $88.3 \pm 1.9$  mV and duration at half-height and threshold of  $1.5 \pm 0.0$  ms and  $3.2 \pm 0.1$  ms, respectively were recorded. This gave a ratio of  $2.1 \pm 0.0$ .

$I_{an}$  activation accounted for a 25 % reduction in input resistance at a membrane potential of  $-99.7 \pm 0.7$  mV relative to input resistance at rest. The activation threshold calculated from the I-V for  $I_{an}$  was estimated around  $-87.0 \pm 1.3$  mV (n=37).

Activation of the T-type calcium conductance gave an average membrane depolarisation of  $8.7 \pm 1.0$  mV from a membrane potential of  $-47.6 \pm 1.2$  mV (n=30).



**2 mM glucose-containing aCSF**

26 neurones were recorded in 2 mM glucose-containing aCSF that expressed both  $I_{an}$  and a T-type calcium conductance (15 % of the population). 18 of these were active at rest (69 %) with an average firing frequency of  $1.8 \pm 0.3$  Hz.  $-44.8 \pm 1.3$  mV (range -34 to -60 mV) was the average resting membrane potential of these neurones, and the input resistance and time-constant were  $1471 \pm 133$  M $\Omega$  (range 495 to 2974 M $\Omega$ ) and  $42.4 \pm 5.2$  ms (range 12 to 92.3 ms), respectively (n=26). The threshold for spike firing was  $-30.1 \pm 1.2$  mV at which point action potentials of amplitude  $85.2 \pm 2.3$  mV and duration at half-height and threshold of  $1.6 \pm 0.1$  ms and  $3.5 \pm 0.2$  ms, respectively, were recorded. This gave a ratio of  $2.1 \pm 0.1$ .

$I_{an}$  induced a 34 % reduction in input resistance at a membrane potential of  $-104.3 \pm 3.9$  mV relative to input resistance at rest. The activation threshold calculated from the I-V for  $I_{an}$  was estimated around  $-83.6 \pm 1.0$  mV (n=26).

Activation of the T-type calcium conductance gave an average membrane depolarisation of  $8.7 \pm 1.5$  mV from a membrane potential of  $-46.6 \pm 2.1$  mV (n=15).

**Table 3.8 Electrophysiological properties of cluster 7 neurones**

<b>Cluster 7 Properties</b>			
	<b>10 mM Glucose</b>	<b>2 mM Glucose</b>	<b>P values</b>
<b>'n' values</b>	37	26	
<b>Spontaneous activity (%)</b>	43	69	$P<0.05$
<b>Spontaneous firing rate (Hz)</b>	$1.1 \pm 0.3$	$1.8 \pm 0.3$	$P<0.05$
<b>Membrane potential (mV)</b>	$-46.7 \pm 1.1$	$-44.8 \pm 1.3$	0.3
<b>Input resistance (M<math>\Omega</math>)</b>	$1741 \pm 131$	$1471 \pm 133$	0.3
<b>Membrane time-constant (ms)</b>	$42.1 \pm 4.4$	$42.4 \pm 5.2$	0.9
<b>Threshold for action potential (AP) firing (mV)</b>	$-30.2 \pm 1.0$	$-30.1 \pm 1.2$	1.0
<b>AP amplitude (mV)</b>	$88.3 \pm 1.9$	$85.2 \pm 2.3$	0.5
<b>AP duration half-height (ms)</b>	$1.5 \pm 0.0$	$1.6 \pm 0.1$	0.7
<b>AP duration threshold (ms)</b>	$3.2 \pm 0.1$	$3.5 \pm 0.2$	0.8
<b>Ratio of AP duration: threshold/ half-height</b>	$2.1 \pm 0.0$	$2.1 \pm 0.1$	1.0
<b>Activation threshold <math>I_{an}</math> (mV)</b>	$-87.0 \pm 1.3$	$-83.6 \pm 1.0$	$P<0.05$
<b><math>I_{an}</math> induced reduction in input resistance (%)</b>	$24.8 \pm 2.6$	$34.1 \pm 3.1$	$P<0.05$
<b>T-type amplitude (mV)</b>	$8.7 \pm 1.0$	$8.7 \pm 1.5$	0.9

The significant differences between the two glucose concentrations were the percentage reduction in input resistance upon activation of  $I_{an}$ , with a larger reduction in 2 mM glucose-containing aCSF ( $P<0.05$ ), the activation threshold for  $I_{an}$  ( $P<0.05$ ), the increase in spontaneous firing rate in 2 mM glucose ( $P<0.05$ ) and the increase in the spontaneous activity of neurones recorded in 2 mM glucose-containing aCSF (43 % in 10 mM and 69 % in 2 mM;  $P<0.05$ ).



### 3.2.9 Expression of $I_{an}$ , $I_h$ , and T-type conductances (Cluster 8)

The final group of neurones was characterised as having  $I_{an}$ , like clusters 1 and 7,  $I_h$ , like clusters 4 and 5, and a T-type conductance, like clusters 6 and 7 (see figure 3.9B). It is important to note that because there are multiple subthreshold active conductances expressed in these neurones, values for properties of each specific each conductance can only be estimated without fully knowing the contribution made by other conductances. Table 3.9 gives an overview of this data.

#### *10 mM glucose-containing aCSF*

In 10 mM glucose-containing aCSF, 25 neurones were recorded which expressed  $I_{an}$ ,  $I_h$  and T-type conductances (10 % of the population). 12 of these neurones were active at rest (48 %) with an average firing frequency of  $1.3 \pm 0.5$  Hz. The average resting membrane potential, input resistance and membrane time-constant were  $-48.6 \pm 1.3$  mV (range -34 to -60 mV),  $1771 \pm 165$  M $\Omega$  (range 500 to 4272 M $\Omega$ ) and  $61.9 \pm 8.9$  ms (range 8.2 to 198.4 ms), respectively (n=25). Spike firing was induced at  $-29.4 \pm 0.9$  mV at which point action potentials were generated of amplitude, duration at half-height and threshold of  $88.0 \pm 2.3$  mV,  $1.5 \pm 0.1$  ms and  $3.2 \pm 0.1$  ms, respectively, giving a ratio of  $2.2 \pm 0.1$ .

$I_{an}$  induced a 29 % reduction in input resistance at a membrane potential of  $-103.5 \pm 1.1$  mV relative to input resistance at rest. The activation threshold calculated from the I-V for  $I_{an}$  was estimated around  $-85.7 \pm 1.3$  mV (n=25).

Activation of the T-type calcium conductance gave an average membrane depolarisation of  $9.5 \pm 1.6$  mV from a membrane potential of  $-49.9 \pm 1.6$  mV (n=19).

The mean threshold for activation of  $I_h$  was  $-86.1 \pm 1.5$  mV, giving rise to a hyperpolarising sag of amplitude  $4.2 \pm 0.5$  mV at a membrane potential of

-103.4  $\pm$  1.0 mV. This is equivalent to a decrease in input resistance of 8 % upon activation of  $I_h$ .

### ***2 mM glucose-containing aCSF***

In 2 mM glucose-containing aCSF, 12 neurones were recorded which expressed  $I_{an}$ ,  $I_h$  and T-type conductances (7 % of the population). 7 of these were active at rest (58 %) with an average firing frequency of 0.4  $\pm$  0.1 Hz. The average resting membrane potential, input resistance and membrane time-constant were -46.3  $\pm$  1.8 mV (range -37 to -55 mV), 1341  $\pm$  200 M $\Omega$  (range 644 to 3183 M $\Omega$ ) and 53.7  $\pm$  7.4 ms (range 24.9 to 107 ms), respectively (n=12). Spike firing was induced at -28.9  $\pm$  1.9 mV at which point action potentials were generated of amplitude, duration at half-height and threshold of 91.6  $\pm$  3.3 mV, 1.4  $\pm$  0.1 ms and 2.9  $\pm$  0.2 ms, respectively, giving a ratio of 2.0  $\pm$  0.1.

$I_{an}$  induced a 28 % reduction in input resistance at a membrane potential of -97.2  $\pm$  5.3 mV relative to input resistance at rest. The activation threshold calculated from the I-V for  $I_{an}$  was estimated around -85.3  $\pm$  2.1 mV (n=12).

Activation of the T-type calcium conductance gave an average membrane depolarisation of 9.5  $\pm$  2.8 mV from a membrane potential of -49.9  $\pm$  2.8 mV (n=5).

The mean threshold for activation of  $I_h$  was -87.7  $\pm$  2.0 mV, giving rise to a hyperpolarising sag of amplitude 5.8  $\pm$  0.5 mV at a membrane potential of -102.5  $\pm$  0.9 mV. This is equivalent to a decrease in input resistance of 10 % upon activation of  $I_h$ .



**Table 3.9 Electrophysiological properties of cluster 8 neurones**

<b>Cluster 8 Properties</b>			
	<b>10 mM Glucose</b>	<b>2 mM Glucose</b>	<b>P values</b>
<b>'n' value</b>	25	12	
<b>Spontaneous activity (%)</b>	48	58	0.6
<b>Spontaneous firing rate (Hz)</b>	$1.3 \pm 0.5$	$0.4 \pm 0.1$	0.2
<b>Membrane potential (mV)</b>	$-48.6 \pm 1.3$	$-46.3 \pm 1.8$	0.3
<b>Input resistance (M<math>\Omega</math>)</b>	$1771 \pm 165$	$1341 \pm 200$	0.1
<b>Membrane time-constant (ms)</b>	$61.9 \pm 8.9$	$53.7 \pm 7.4$	0.8
<b>Threshold for action potential (AP) firing (mV)</b>	$-29.4 \pm 0.9$	$-28.9 \pm 1.9$	0.7
<b>AP amplitude (mV)</b>	$88.0 \pm 2.3$	$91.6 \pm 3.3$	0.4
<b>AP duration half-height (ms)</b>	$1.5 \pm 0.1$	$1.4 \pm 0.1$	0.8
<b>AP duration threshold (ms)</b>	$3.2 \pm 0.1$	$2.9 \pm 0.2$	0.5
<b>Ratio of AP duration: threshold/ half-height</b>	$2.2 \pm 0.1$	$2.0 \pm 0.1$	0.4
<b>Activation threshold <math>I_{an}</math> (mV)</b>	$-85.7 \pm 1.3$	$-85.3 \pm 2.1$	0.8
<b><math>I_{an}</math> induced reduction in input resistance (%)</b>	$29.3 \pm 2.8$	$28.1 \pm 3.3$	0.5
<b>Activation threshold <math>I_h</math> (mV)</b>	$-86.1 \pm 1.5$	$-87.7 \pm 2.0$	0.5
<b><math>I_h</math> induced reduction in input resistance (%)</b>	$8.0 \pm 1.0$	$10.5 \pm 0.8$	$P < 0.05$
<b>T-type amplitude (mV)</b>	$9.5 \pm 1.6$	$9.5 \pm 2.8$	0.9

The only significant difference between cluster 8 neurones recorded in 2 mM and 10 mM glucose-containing aCSF was the reduction in input resistance induced by  $I_h$  (greater in 2mM;  $P < 0.05$ ).

Tables 3.10 and 3.11 show a summary of the electrophysiological properties and properties of the active conductances of each cluster.

Table 3.10 Electrophysiological properties of neurones

Cluster	Glucose concentration (mM)	Membrane potential (mV)	Input resistance (MΩ)	Membrane time-constant (ms)	Threshold action potential (AP) firing (mV)	AP amplitude (mV)	AP duration half-height (ms)	AP duration threshold (ms)	Ratio of AP duration: threshold/ half-height
1	10	-50.1 ± 2.0	1827 ± 274	48.1 ± 8.3	-30.7 ± 1.1	91.4 ± 3.6	1.5 ± 0.1	3.0 ± 0.2	2.0 ± 0.1
	2	-50.5 ± 2.0	1521 ± 108	41.0 ± 5.6	-30.1 ± 1.3	78.1 ± 5.8	1.7 ± 0.1	3.6 ± 0.3	2.2 ± 0.1
2	10	<b>-49.0 ± 2.1</b>	1782 ± 458	33.5 ± 4.9	30.5 ± 1.9	85.6 ± 5.7	1.7 ± 0.2	3.4 ± 0.5	2.0 ± 0.1
	2	<b>-45.9 ± 2.3**</b>	1243 ± 206	31.2 ± 6.4	-31.6 ± 2.4	81.8 ± 6.8	1.7 ± 0.2	3.5 ± 0.4	2.0 ± 0.9
3	10	-49.1 ± 2.1	1857 ± 215	37.4 ± 5.6	-31.5 ± 1.9	86.0 ± 2.9	1.6 ± 0.1	3.2 ± 0.2	2.0 ± 0.0
	2	-46.4 ± 2.0	1418 ± 169	27.0 ± 4.2	-29.4 ± 1.4	81.8 ± 2.2	1.7 ± 0.1	3.5 ± 0.3	2.1 ± 0.1
4	10	-51.5 ± 1.9	1134 ± 128	26.6 ± 3.7	-31.4 ± 1.5	79.2 ± 3.3	1.6 ± 0.1	3.4 ± 0.2	2.0 ± 0.1
	2	-49.9 ± 2.4	1285 ± 252	37.5 ± 7.6	-32.6 ± 1.7	88.2 ± 4.7	1.5 ± 0.0	3.5 ± 0.3	2.3 ± 0.1
5	10	-48.7 ± 1.1	<b>1606 ± 124</b>	43.6 ± 4.9	-29.3 ± 0.9	78.6 ± 2.4	<b>1.6 ± 0.1</b>	<b>3.4 ± 0.1</b>	2.1 ± 0.0
	2	-49.3 ± 1.1	<b>1213 ± 106*</b>	33.0 ± 2.6	-31.7 ± 0.8	83.8 ± 2.4	<b>1.4 ± 0.0**</b>	<b>2.9 ± 0.1**</b>	2.0 ± 0.1
6	10	-44.7 ± 0.8	1466 ± 78	30.4 ± 3.1	-27.2 ± 0.6	77.7 ± 1.7	1.7 ± 0.1	3.5 ± 0.1	2.1 ± 0.0
	2	-45.1 ± 0.9	1427 ± 111	34.0 ± 3.1	-29.5 ± 0.8	79.9 ± 1.8	1.7 ± 0.1	3.4 ± 0.1	2.0 ± 0.0
7	10	-46.7 ± 1.1	1741 ± 131	42.1 ± 4.4	-30.2 ± 1.0	88.3 ± 1.9	1.5 ± 0.0	3.2 ± 0.1	2.1 ± 0.0
	2	-44.8 ± 1.3	1471 ± 133	42.4 ± 5.2	-30.1 ± 1.2	85.2 ± 2.3	1.6 ± 0.1	3.5 ± 0.2	2.1 ± 0.1
8	10	-48.6 ± 1.3	1771 ± 165	61.9 ± 8.9	-29.4 ± 0.9	88.0 ± 2.3	1.5 ± 0.1	3.2 ± 0.1	2.2 ± 0.1
	2	-46.3 ± 1.8	1341 ± 200	53.7 ± 7.4	-28.9 ± 1.9	91.6 ± 3.3	1.4 ± 0.1	2.9 ± 0.2	2.0 ± 0.1

Bold values indicate a significant difference: \*  $P < 0.05$ , \*\*  $P < 0.01$



Table 3.11 Properties of active conductances

Cluster	Glucose Concentration (mM)	Activation threshold $I_{an}$ (mV)	$I_{an}$ induced Reduction in input resistance(%)	Decay time $I_A$ (ms)	Amplitude $I_A$ (mV)	Activation threshold $I_h$ (mV)	$I_h$ induced reduction in input resistance (%)	T-type amplitude (mV)
1	10	-84.2 $\pm$ 1.7	35					
	2	-86.9 $\pm$ 1.0	44					
2	10	-82.3 $\pm$ 2.7	31	1111 $\pm$ 212	5.1 $\pm$ 0.9			
	2	-80.4 $\pm$ 2.9	35	838 $\pm$ 174	4.7 $\pm$ 0.6			
4	10							
	2							
5	10					-87.2 $\pm$ 1.5	13	
	2					-81.4 $\pm$ 2.5*	16	
6	10					-86.5 $\pm$ 1.4	21	11.9 $\pm$ 1.1
	2					-82.7 $\pm$ 7.1	15	13.8 $\pm$ 1.9
7	10							9.1 $\pm$ 0.8
	2							9.6 $\pm$ 0.9
8	10	-87.0 $\pm$ 1.3	<b>25</b>					8.7 $\pm$ 1.0
	2	-83.6 $\pm$ 1.0	<b>34*</b>					8.7 $\pm$ 1.5
8	10	-85.7 $\pm$ 1.3	29			-86.1 $\pm$ 1.5	8	9.5 $\pm$ 1.6
	2	-85.3 $\pm$ 2.1	28			-87.7 $\pm$ 2.0	10	9.5 $\pm$ 2.8

Bold values indicate a significant difference: \*  $P < 0.05$



### ***3.2.10 Comparison of percentage of neurones in each cluster recorded in 2 mM and 10 mM glucose-containing aCSF***

The percentage of neurones in each cluster did not vary considerably between neurones recorded in 2 mM and 10 mM glucose-containing aCSF (see figure 3.10). There were a higher percentage of neurones that fell into the clusters 1, 2 and 6 in 2 mM glucose-containing aCSF than in 10 mM glucose-containing aCSF (ranging between 2-4 % higher). There were a higher percentage of neurones that fell into the clusters 4, 5 and 8, in 10 mM glucose-containing aCSF compared to 2 mM glucose-containing aCSF (2-4 % difference). Clusters 3 and 7 expressed the same percentage of neurones in both glucose concentrations. There were no significant differences between the proportion of neurones in each cluster (chi square test: cluster 1:  $P=0.2$ ; cluster 2:  $P=0.5$ ; cluster 3:  $P=0.9$ ; cluster 4:  $P=0.2$ ; cluster 5:  $P=0.5$ ; cluster 6:  $P=0.3$ ; cluster 7:  $P=1.0$ ; cluster 8:  $P=0.2$ ).

### ***3.2.11 Comparison of percentage of spontaneously active neurones in each cluster recorded in 2 mM and 10 mM glucose-containing aCSF***

There was a distinct difference in the spontaneous activity of neurones in each cluster recorded in 2 mM and 10 mM glucose-containing aCSF (see table 3.12 and figure 3.11). In every cluster except cluster 1, there was an increase in the spontaneous firing of neurones recorded in 2 mM glucose-containing aCSF compared to 10 mM glucose-containing aCSF. However significance was only reached in clusters 6 and 7 (chi square test:  $P<0.01$  and  $P<0.05$ , respectively).



Table 3.12 Comparison of spontaneous activity

Spontaneous Activity (%)			
Cluster	10 mM Glucose	2 mM Glucose	P values
1	27	25	0.9
2	50	63	0.6
3	26	47	0.2
4	26	60	0.06
5	31	48	0.3
6	29	55	$P<0.01$
7	43	69	$P<0.05$
8	48	58	0.6

3.3 Discussion

In this study electrophysiological properties of ARC neurones were compared between neurones recorded in the presence of two different extracellular glucose concentrations; 2 mM and 10 mM. The aim of the present study was to investigate the effects of hyperglycaemic and euglycaemic glucose levels on ARC neurones by observing how their electrophysiological properties change under these respective recording conditions. In particular, the expression of subthreshold active conductances was investigated and also used as the basis upon which to classify neurones into groups.

3.3.1 Effect of glucose on membrane properties of ARC neurones

As well as being dependent on glucose for energy, the brain also contains glucose-sensing neurones that can alter their electrical properties in response to

changes in glucose levels (Anand *et al.*, 1964; Oomura *et al.*, 1964). The ARC has been shown to contain these glucose-sensing neurones (Spanswick *et al.*, 1997; Muroya *et al.*, 1999; Spanswick *et al.*, 2000; Ibrahim *et al.*, 2003). It is important that the levels of glucose within the brain and body are maintained around set limits otherwise conditions such as diabetes arise. Thus, as for many other nutrients and physiological processes, complex and often multiple interacting homeostatic systems are in place and organised to maintain for example, glucose within tight limits. Diabetes arises due to problems with insulin production or insulin resistance leading to high blood sugar levels. Euglycaemia is around 4-6 mM in the plasma whereas the physiological level of glucose in the brain is unclear, although it is reported to be between 1 and 2.5 mM (Silver & Erecinska, 1994). Classical electrophysiological studies which looked at glucose-sensing neurones in the hypothalamus used glucose at concentrations between 0 and 20 mM (for example see Ashford *et al.*, 1990a; Spanswick *et al.*, 1997) but recent studies have suggested that this level is too high and that neurones within the ARC are never exposed to such high levels. This study therefore aimed to compare the effects of both hyperglycaemic (10 mM) and euglycaemic (2 mM) glucose levels on the electrophysiological properties of ARC neurones. In this study, properties used to compare the effects of 10 mM and 2 mM glucose-containing aCSF on ARC neurones centred on the resting membrane potential, input resistance, membrane time-constant and spontaneous firing rates. A more detailed comparison of other electrophysiological properties such as spike threshold, spike duration and activation points of active conductances were also considered. The proportion of neurones expressing particular active conductances was also looked at and these will all be discussed further now.



The major findings of this study were that there were clear differences between the input resistance, the percentage of active neurones and the expression of the active conductance  $I_h$  in neurones recorded in 2 mM compared to 10 mM glucose-containing aCSF.  $I_{an}$  also appeared stronger in 2 mM glucose-containing aCSF in a population of neurones. Perhaps the most interesting finding is that of the change in the activity of neurones. Although the spontaneous firing rate of active neurones did not show a significant difference between 2 mM and 10 mM glucose-containing aCSF, there was a significant change in the percentage of active versus silent neurones in the two conditions in the overall population. Within individual clusters, there was an increase in the percentage of active neurones recorded in 2 mM glucose-containing aCSF compared to 10 mM glucose-containing aCSF in every cluster except cluster 1, with a significant increase in clusters 6 and 7. This indicates that neurones with similar electrophysiological properties have very different patterns of activity under different extracellular glucose concentrations, with neurones being more active under physiological conditions. Previous studies which were carried out in 10 mM glucose-containing aCSF, which is non-physiological, may therefore have produced very different results if they were carried out in physiological glucose. The expression of receptors, neuropeptides, and transmitters within neurones and their associated networks may also be affected by this change in glucose. These data therefore provide compelling evidence for a change in the activity of ARC neurones under different extracellular glucose concentrations and may force us to re-evaluate previous glucose-sensing studies which were carried out in non-physiological glucose levels. Furthermore, if such changes are paralleled at the signalling level, previous studies undertaken in these glucose and energy status-sensing networks may require a major re-evaluation.

Another important property that changed in the two recording conditions was input resistance. Input resistance showed a significant increase in neurones recorded in 10 mM glucose-containing aCSF compared to 2 mM glucose-containing aCSF, indicating that upon increasing glucose concentrations, ion channels are most likely closing within the membrane. The  $K_{ATP}$  channel is an important ion channel thought to be involved in glucose homeostasis and glucose-sensing (Ashford *et al.*, 1990a,b; Rowe *et al.*, 1996; Spanswick *et al.*, 1997; Lee *et al.*, 1999; Spanswick *et al.*, 2000; Miki *et al.*, 2001; Zhang *et al.*, 2004). In 10 mM glucose-containing aCSF, more  $K_{ATP}$  channels may be closed, whilst in 2 mM glucose-containing aCSF, more may be open. Different glucose concentrations between 0 and 10 mM would need to be tested to see if the resistance continued to change over this range of concentrations. The point where resistance no longer changes would indicate when the  $K_{ATP}$  channels are likely to be fully closed. This point regarding  $K_{ATP}$  may be relevant to the observed increase in neuronal input resistance. However it is unlikely to account for the decrease in activity observed here in 10 mM glucose-containing aCSF.

The other major finding of this study was the difference in expression of the active conductance  $I_h$ .  $I_h$  is a time- and voltage-dependent inward rectification, as seen in other neurones (Halliwell & Adams, 1982; Pape, 1996) and is characterised by a 'sag' in the membrane response during negative current injection.  $I_h$  was expressed in 33 % of neurones in this study. There were a greater percentage of neurones expressing  $I_h$  (neurones in clusters 4, 5 and 8) in 10 mM glucose-containing aCSF compared to 2 mM glucose-containing aCSF although this did not reach significance. These data imply that there was greater expression of ion channels mediating the  $I_h$  conductance in 10 mM glucose. This is important as  $I_h$  can contribute to the patterning of activity of neurones (Pape, 1996). In particular, it has



been shown to contribute to burst-like patterns of firing (van Welie *et al.*, 2006) therefore  $I_h$  could contribute to pacemaker activity. It is also thought to contribute to the resting membrane potential of neurones as it prevents neurones from becoming too hyperpolarised. In addition the role of  $I_h$  in thalamic burst firing can be modulated by extrinsic factors including 5-HT and noradrenaline (Pape & McCormick, 1989; McCormick & Pape, 1990a).  $I_h$  could therefore potentially act as a switch to alter the functional output of these neurones under different glucose conditions and in response to extrinsic factors. It would be interesting for future studies to look more closely at the expression of  $I_h$  under different recording conditions to see how it affects the activity of these neurones. An important point to note is that if the expression of active conductances is altered by different glucose concentrations, neurones may be able to switch between clusters, for example a cluster 7 neurone could become a cluster 8 neurone if  $I_h$  becomes activated. The proportion of neurones in each cluster in 2 mM and 10 mM glucose may therefore change, although in this study no significant difference was found.

The fact that electrophysiological properties of neurones have changed under these different recording conditions indicates that 10 mM and 2 mM glucose represent quite different physiological and/or pathophysiological states. 2 mM is thought to be more like the physiological concentration of glucose in the ARC and under these conditions there was an increase in the activity of neurones. This may be the resting activity of neurones in a normal euglycaemic state. 10 mM glucose may represent a hyperglycaemic state and therefore the properties of neurones in this level of glucose may represent those which more likely reflect a diabetic state. Previous studies which were carried out in 10 mM glucose or higher may therefore have been carried out in too high a glucose level and the results from these studies

must be considered in light of this fact.  $I_h$  was observed to be altered in 10 mM glucose indicating that the expression of ion channels or their biophysical properties may change in different physiological states and it may be that many other factors, such as receptors and peptides, may also change their expression in high glucose levels.

Aside from these properties that did change in neurones recorded in the two different glucose concentrations, there were also properties which did not show a significant change. Overall the resting membrane potential of neurones recorded in 10 mM and 2 mM glucose-containing aCSF did not significantly change. These results are in accordance with a previous study that looked at the activity of neurones in 10 mM and 2 mM glucose-containing aCSF. In this study, membrane potential did not alter when reducing glucose concentration from 10 mM to 2 mM (Claret *et al.*, 2007). Cluster 2 neurones are the only neurones that have been functionally identified, as orexigenic NPY neurones (van den Top *et al.*, 2004). Some NPY neurones within the ARC have been identified as GI neurones, although not all NPY neurones are believed to function in this way (Muroya *et al.*, 1999). If these orexigenic cluster 2 neurones form part of the glucose-sensing population then they may be expected to be more active in lower glucose conditions, as was observed here. Cluster 2 neurones had a more depolarised membrane potential in 2 mM as opposed to 10 mM glucose-containing aCSF indicating that they are likely to be glucose-sensing neurones. None of the other clusters were identified as either orexigenic or anorexigenic and as we know that both GE and GI neurones are present within the ARC (Muroya *et al.*, 1999; Ibrahim *et al.*, 2003), there may have been an equal proportion of neurones which were hyperpolarised or depolarised by glucose. Alternatively, it might be possible that some of the neurones in other



clusters are not glucose-sensing at all and so did not detect any changes in glucose and alter their membrane properties.

A further point to consider is that many of the cells we recorded from had a membrane potential very close to or at the threshold for action potential firing and the membrane potential rarely becomes more depolarised than this threshold value. There may not appear to be a significant difference between the membrane potentials of the two populations, as the difference between the threshold values and values just beneath threshold are very small, but the activity of the neurones may be very different which has been shown in this study.

The membrane time-constant gives an indication of the size of the neurone being recorded from, which would not be expected to change in 10 mM or 2 mM glucose-containing aCSF. The results indicate this to be the case as there was no significant change in membrane time-constant between the two different glucose concentrations. This indicates that we were recording from a similar population of neurones.

Overall there were few significant differences between the other electrophysiological properties investigated in this study. The possible reason for this could simply be that the ARC neurones from which we were recording were not glucose-sensing and so did not alter their membrane properties as they were not detecting these changes in glucose. Alternatively, if they were glucose-sensing neurones it may be that they were not sensing this change in glucose due to the fact that it was not significant enough to bring about any changes. One property which did appear different but did not reach statistical significance, probably due to low 'n' numbers, was the decay time of the A-current in cluster 2 neurones. The A-like transient outward rectifier was expressed by 4 % of ARC neurones. This

conductance is characterised by a delayed return to resting membrane potential upon termination of injection of negative current and resembles the activation of A-like potassium conductances (Connor & Stevens, 1971a,b). The decay time of the A-current was smaller in 2 mM glucose-containing aCSF. A-currents are thought to be involved in the regulation of repetitive firing (Rogawski, 1985) therefore any change in the properties of the A-current may lead to differences in the firing properties of neurones. Indeed, in this study the proportion of cells which exhibited burst-like firing patterns was different between the two recording conditions and has also been shown to be different in fasted animals (personal communication, D.Spanswick) indicating that glucose levels are important for controlling firing patterns. It has been shown that firing patterns are important for the release of neuropeptides from neurones; for example, the release of vasopressin from magnocellular neurones in the posterior pituitary depends on burst-like patterns of action potentials (Dutton & Dyball, 1979). A recent study showed that ARC neurones expressing an A-like current produced membrane potential oscillations in the presence of orexigens and were hence termed conditional pacemaker neurones. These neurones were sensitive to orexin and ghrelin and were NPY/AgRP containing neurones (van den Top *et al.*, 2004). The size of the A-current is important for burst-firing: a shorter A-current leads to an increase in the frequency of bursts and may function to signal an increase in neuropeptide release, as would be expected in lower glucose conditions and fasted conditions. Conversely, a longer A-current decreases the frequency of bursts and may signal to reduce neuropeptide release, as expected in high glucose conditions. Cluster 2 neurones in this study might therefore be important in the generation of pacemaker activity in the ARC, which may lead to the



release of specific orexigenic neuropeptides and this pacemaker activity is likely to be different depending on the extracellular glucose concentration.

Another active conductance investigated in this study was  $I_{an}$ .  $I_{an}$ , similar to the anomalous inward rectifier conductance described in other neurones (Constanti & Galvan, 1983), was expressed by 36 % of neurones in this study.  $I_{an}$  is characterised by a decrease in input resistance at more negative membrane potentials. In this study there was a greater decrease in input resistance associated with  $I_{an}$  in 2 mM glucose-containing aCSF compared to 10 mM glucose-containing aCSF although these values did not reach significance in most cases, probably reflecting the low 'n' numbers. There were also a greater number of neurones in clusters 1 and 2, which both express  $I_{an}$ , in 2 mM compared to 10 mM glucose-containing aCSF, although this did not reach significance. These results indicate that the expression of  $I_{an}$  may be greater in physiological glucose. These data add to the evidence that the expression of ion channels is altered under different glucose concentrations. The function of  $I_{an}$  within neurones is unclear though it could help to maintain the membrane potential of neurones within a functional range (van den Top & Spanswick, 2006). However its role within the ARC and elsewhere still remains to be fully elucidated. Potentially the  $K_{ATP}$  channel may be responsible for the increase in  $I_{an}$  in 2 mM glucose as this channel is an inward rectifier. Therefore it may contribute to  $I_{an}$  but further studies utilising blockers of this channel (such as tolbutamide) are needed to clarify this.

The final subthreshold active conductance investigated in this study was the T-type calcium like conductance, which was expressed by 71 % of neurones making it the most abundant conductance in ARC neurones. This conductance is characterised by a rebound depolarisation upon termination of negative current

injection. This rebound depolarisation is similar to that described before in cells activated by T-type calcium channels (Llinas & Yarom, 1981). T-type conductance is a low-voltage activated and rapidly inactivating current. In this study, this conductance was not seen to change between the two recording conditions. T-type conductances are involved in the generation of burst like firing patterns in the CNS, alongside  $I_h$  (Huguenard, 1996) and have also been shown to be involved in the generation of pacemaker activity in the ARC (van den Top *et al.*, 2004). In particular the T-type conductance has been identified as an essential component of thalamic oscillations (Suzuki & Rogawski, 1989; Huguenard & Prince, 1994). Recently, T-type channels have also been shown to be important in the vesicular release of neurotransmitters from neurones (Pan *et al.*, 2001; Carbone *et al.*, 2006). Neurones in this study expressing the T-type conductance may therefore be important in generating specific patterns of activity in neurones and in generating the release of neuropeptides within the ARC.

In addition to comparing the electrophysiological properties of ARC neurones, this study also classified neurones into groups or clusters based upon the subthreshold active conductances they expressed.

### ***3.3.2 Electrophysiological characterisation of ARC neurones***

The ARC within the hypothalamus plays an important role in the control of energy homeostasis (Williams *et al.*, 2000; Cone *et al.*, 2001; Williams *et al.*, 2001). As it is located above the median eminence which is lacking a complete BBB (Ganong, 2000), it is able to receive information from circulating metabolites which signal the energy status of the body and produce an appropriate response. The ARC



receives information from a diverse range of signals and itself contains a diverse population of neurones. Within the ARC there is a complex network of neurones that differ in their intrinsic properties, neuronal inputs and outputs. However, how these neuronal networks function to integrate and produce appropriate responses is still largely unknown. An electrophysiological classification of ARC neurones could help to provide an understanding of their functional roles, as neurones with different properties such as the differential expression of active conductances could indicate a functional heterogeneity between ARC neurones. This classification is important as it means in the future the function of neurones could be identified just by looking at the electrophysiological properties of the neurone and any future experiments could then be placed into a functional context. The classification of ARC neurones in this study is based upon previous work carried out by van den Top (2002), who classified ARC neurones into 6 clusters. This classification has in recent years been extended and now comprises 8 neuronal clusters (unpublished data). The characterisation of neurones in this study builds upon this classification.

A total of 411 ARC neurones were recorded from and these neurones were divided into 8 groups or clusters based upon subthreshold active membrane conductances expressed. These included  $I_{an}$ ,  $I_h$ , the A-like transient outward rectifier and the T-type calcium conductance. Active conductances are important for shaping the electrophysiological properties of individual neurones as they integrate synaptic inputs and help to control the output of neurones by altering their patterns of activity (Huguenard, 1996; Pape, 1996; van den Top *et al.*, 2004). Dividing neurones into groups that contain different active conductances might help to functionally separate ARC neurones, as neurones with different electrophysiological properties could also have different functions within the ARC. These active conductances have previously

been identified in neurones as described before and are easily identifiable from the I-V relationship.

Cluster 1 neurones were identified by the expression of  $I_{an}$ ; cluster 2 neurones expressed  $I_{an}$  and  $I_A$ ; cluster 3 neurones were identified on the basis that they did not express any of the subthreshold active conductances used to characterise the other neurones; cluster 4 neurones expressed  $I_h$ ; cluster 5 neurones expressed  $I_h$  and T-type; cluster 6 neurones expressed T-type; cluster 7 neurones expressed  $I_{an}$  and T-type and cluster 8 neurones expressed  $I_{an}$ ,  $I_h$  and T-type.

Characterising ARC neurones based upon subthreshold active conductances represents one way in which to classify ARC neurones into potential functional groups. However this is by no means a definitive classification and there are many ways in which this classification can be built upon. For example, this classification only looks at subthreshold conductances but there are important suprathreshold conductances, such as the action potential and afterhyperpolarisation which could be used to classify the neurones further into groups. In addition to these intrinsic factors, responses to extrinsic factors such as neuropeptides and hormones could be used to classify neurones into potential functional groups. There are also many ways in which this classification could be improved, for example, determining what receptors or transmitters are expressed within the neurone and determining the inputs to and outputs from the neurones could help to further subdivide ARC neurones into functional groups. As the classification is extended it may become a more useful tool in which to identify functional groups within the ARC based upon their electrophysiological properties. Further studies are therefore needed to extend the classification and divide neurones into even more specific functional groups. Electrophysiological studies need to be combined with studies identifying the



chemical phenotype, the projections, membrane receptors and synaptic physiology and pharmacology in order to fully identify functional groups within the ARC.

In conclusion, recording from neurones in physiological and non-physiological glucose produced several notable differences in the electrophysiological properties of ARC neurones. In particular there was an increase in activity, a decrease in input resistance and a change in the expression of some subthreshold active conductances in neurones recorded in physiological compared to non-physiological glucose. These results are important in showing that neurones under different physiological or pathophysiological states, such as diabetes, have very different properties. In addition, ARC neurones were subdivided into groups based upon the subthreshold active conductances they expressed. These clusters may represent different functional groups within the ARC, as the electrical properties of neurones may represent one way of separating neurones into functional groups, and so have helped us to further understand and characterise ARC neurones.

**Figure 3.1 Comparison of resting membrane potentials of neurones recorded in 10 mM and 2 mM glucose-containing aCSF**

**A:** Bar-chart comparing the membrane potentials of neurones recorded in 10 mM glucose-containing aCSF and 2 mM glucose-containing aCSF. A total of 241 neurones were recorded in 10 mM glucose-containing aCSF and a total of 170 neurones were recorded in 2 mM glucose-containing aCSF. The numbers of neurones in each 5 mV bin were plotted as a percentage of these totals.



**Figure 3.1**

**A**

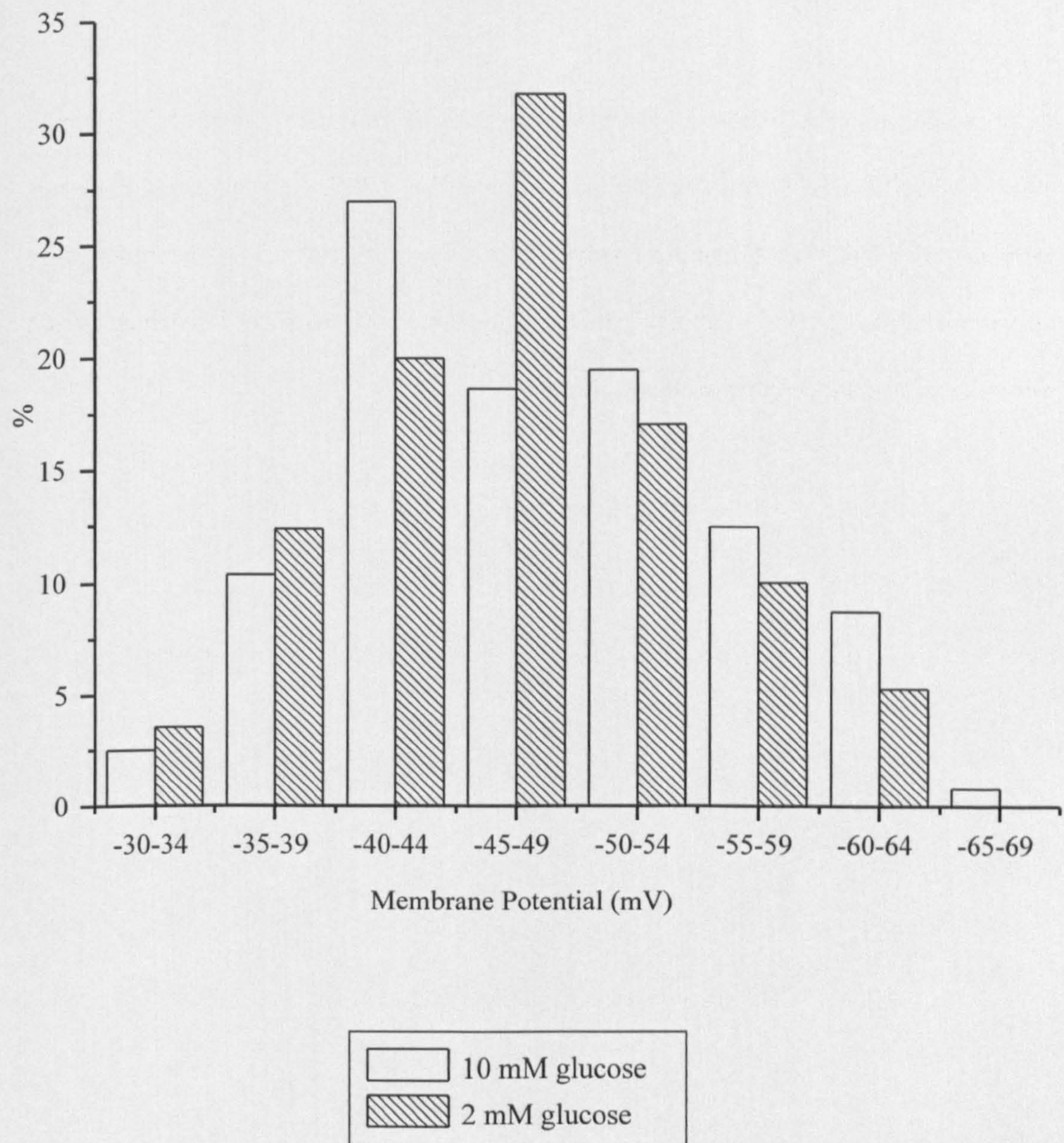




**Figure 3.2 Comparison of input resistances of neurones recorded in 10 mM and 2 mM glucose-containing aCSF**

**A:** Bar-chart comparing the input resistances of neurones recorded in 10 mM glucose-containing aCSF and 2 mM glucose-containing aCSF. A total of 241 neurones were recorded in 10 mM glucose-containing aCSF, and a total of 170 neurones were recorded in 2 mM glucose-containing aCSF. The numbers of neurones in each 500 M $\Omega$  bin were plotted as a percentage of these totals.



**Figure 3.2**

**A**

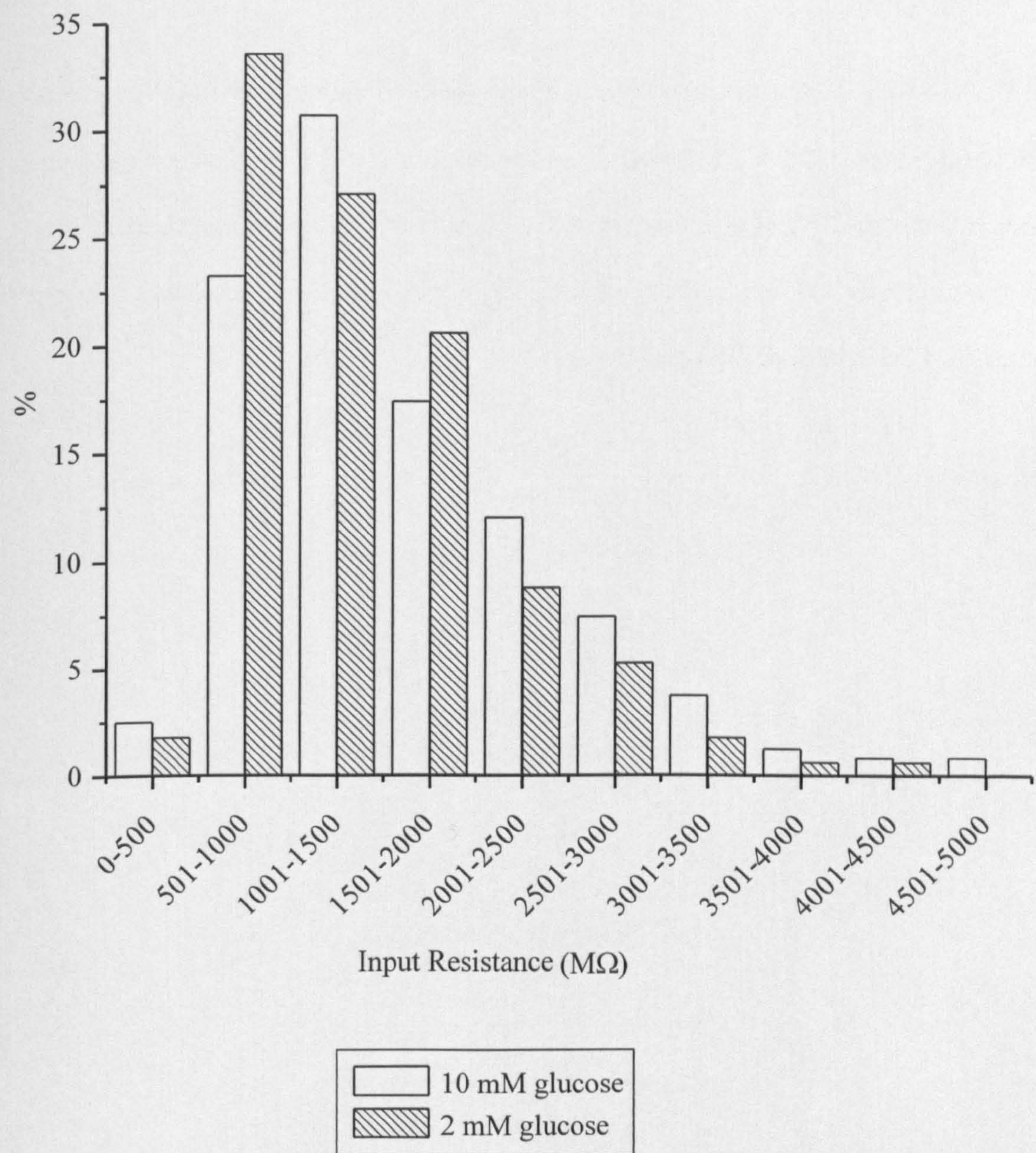




**Figure 3.3 Comparison of membrane time-constants of neurones recorded in 10 mM and 2 mM glucose-containing aCSF**

**A:** Bar-chart comparing the membrane time-constants of neurones recorded in 10 mM glucose-containing aCSF and 2 mM glucose-containing aCSF. A total of 241 neurones were recorded in 10 mM glucose-containing aCSF, and a total of 170 neurones were recorded in 2 mM glucose-containing aCSF. The numbers of neurones in each 10 ms bin were plotted as a percentage of these totals.



**Figure 3.3**

**A**

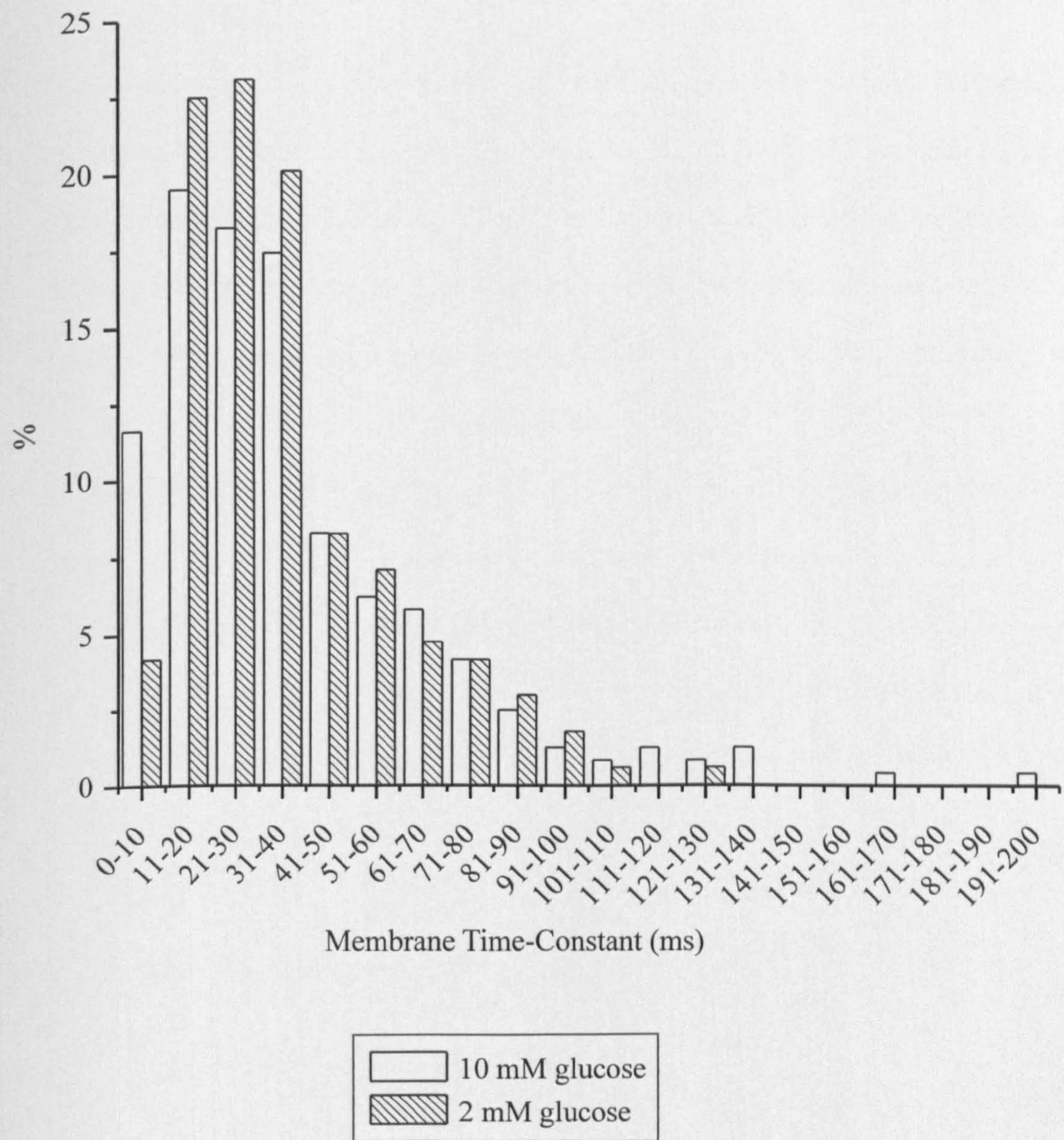




**Figure 3.4 Comparison of spontaneous firing rates of neurones recorded in 10 mM and 2 mM glucose-containing aCSF**

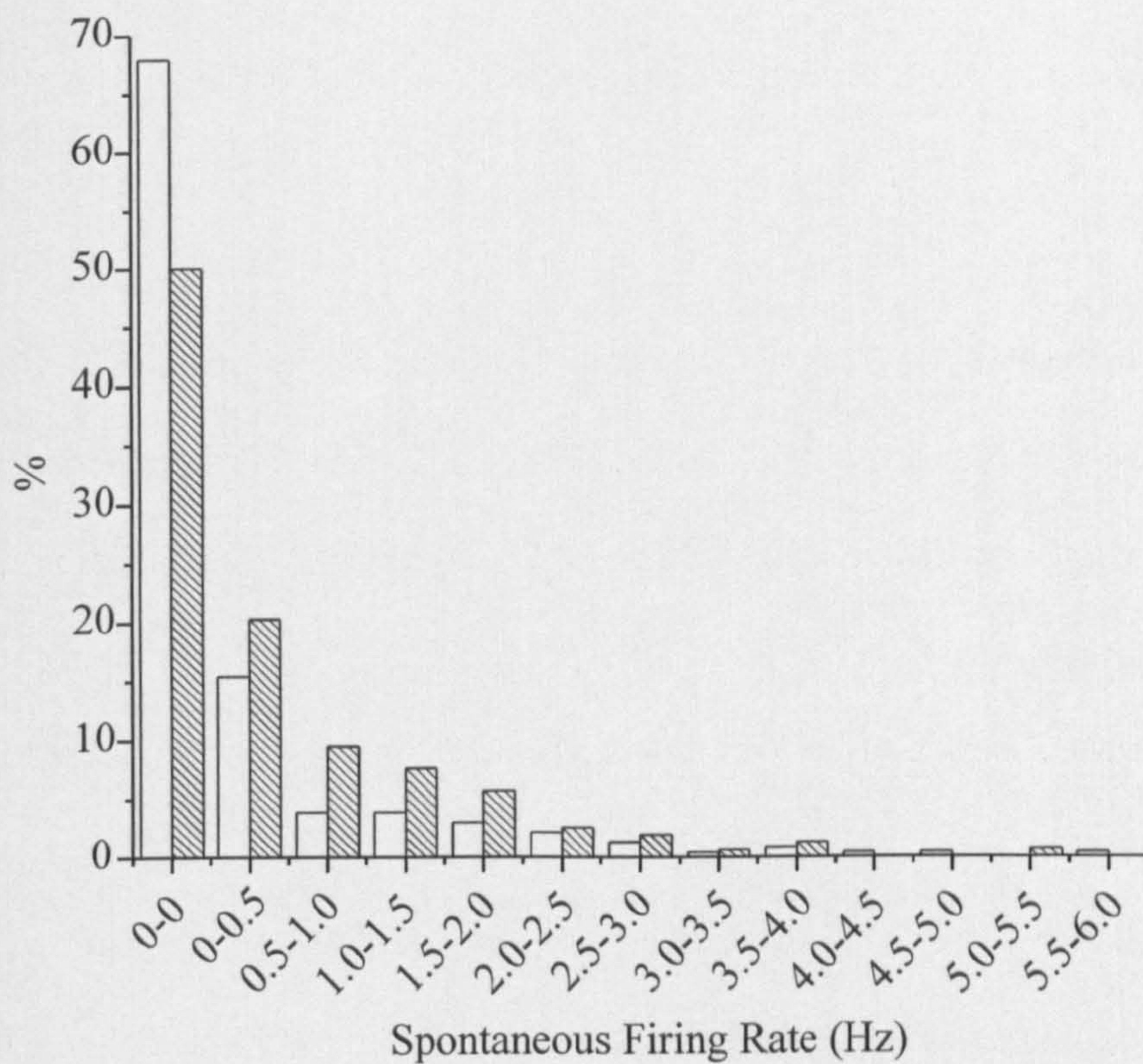
**Ai:** Bar-chart comparing the spontaneous firing rates of neurones recorded in 10 mM glucose-containing aCSF and 2 mM glucose-containing aCSF. Data is included from 234 neurones (75 active cells and 159 silent cells) in 10 mM glucose-containing aCSF and 158 neurones (79 active cells and 79 silent cells) in 2 mM glucose-containing aCSF. The numbers of neurones in each 0.5 Hz bin were plotted as a percentage of these totals.

**Aii:** Bar-chart comparing the proportion of active and silent neurones recorded in 10 mM glucose-containing aCSF and 2 mM glucose-containing aCSF. Note the increase in the proportion of spontaneously active cells from 10 mM glucose-containing aCSF to 2 mM glucose-containing aCSF.



**Figure 3.4**

**Ai**



**Aii**

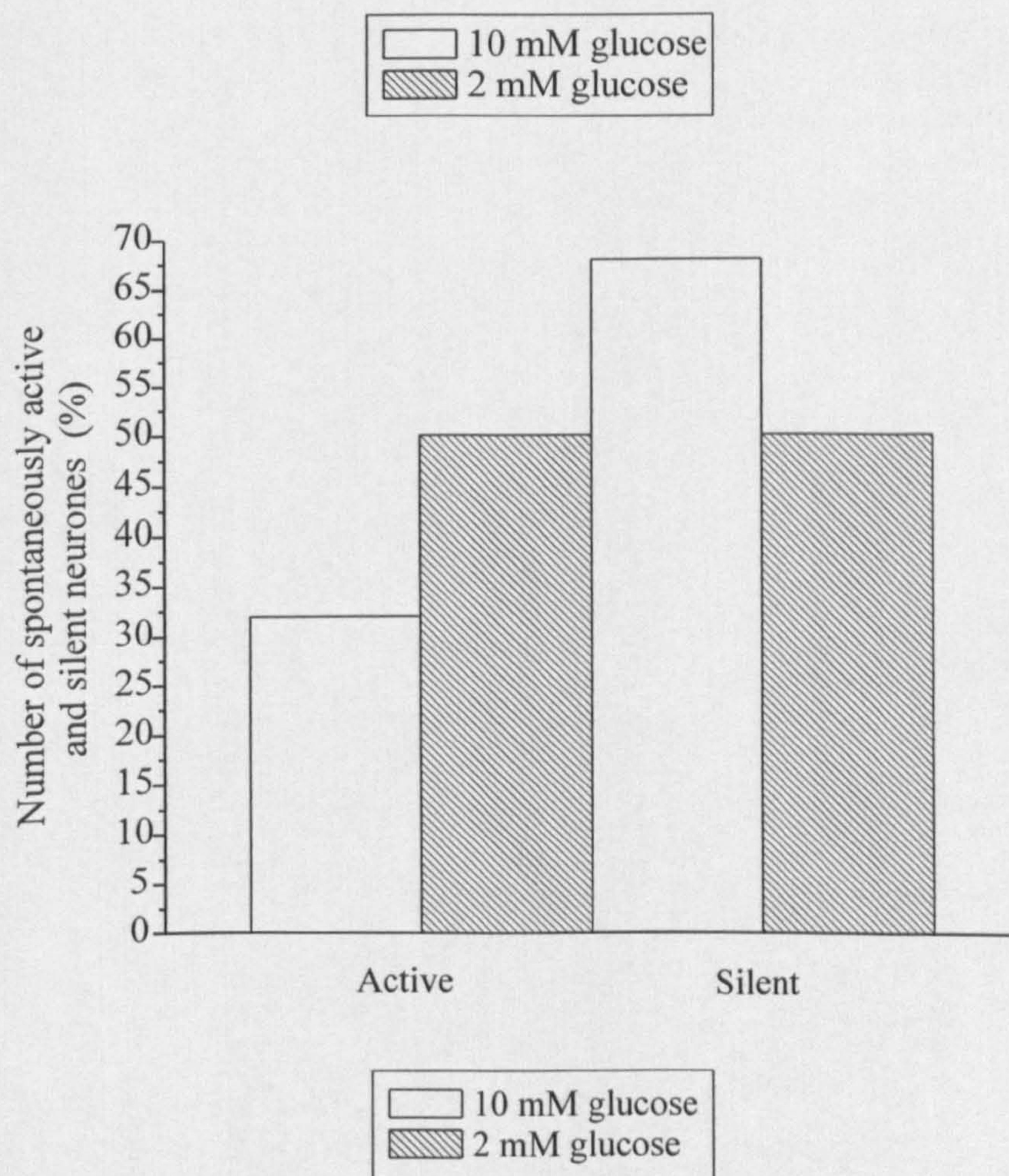




**Figure 3.5 Characteristics and analysis of electrical properties of arcuate nucleus neurones**

**A:** Example of an action potential of an arcuate nucleus (ARC) neurone recorded in current clamp and shown on an expanded time-scale. The amplitude of the spike was calculated as the difference between the membrane potential at the peak of the action potential (upper dashed line) and the membrane potential at the threshold of spike firing (lower dashed line). The duration at half-height was calculated as the difference in time between the rising and falling phase of the action potential at the point of half-amplitude of the action potential (arrow 1). The duration at threshold was calculated as the difference in time between the rising and falling phase of the action potential at the point of threshold (arrow 2).

**Bi:** Activation of the anomalous inward rectifier ( $I_{an}$ ) leads to a decrease in input resistance at more negative membrane potentials. The arrows indicate the decreased membrane response at more hyperpolarised membrane potentials (downward arrow) relative to membrane potential responses close to rest (upward arrow) as a result of the activation of  $I_{an}$ . Note the fast activation and the lack of inactivation of this conductance.

**Bii:** Activation of an A-like conductance resulted in a delayed return to baseline following negative current injection. In the absence of the A-like conductance, the membrane would be expected to discharge at the same rate as it was charged at the beginning of the negative current injection. The duration of the activation of the A-like conductance was measured as the time between the end of current injection (marked by the first vertical dotted line) and the return of the membrane potential to the level prior to the current injection (marked by the second vertical dotted line). The amplitude of the current was measured at half-duration (line marked \*).

**Biii:** The hyperpolarisation-activated non-selective cation conductance ( $I_h$ ) is characterized by a time- and voltage-dependent sag in the membrane response to negative current injection. At negative membrane potentials, there was no inactivation of  $I_h$ . The amplitude of  $I_h$  was measured by subtracting the membrane potential at the end of the negative current injection (upper dotted line) from the membrane potential following steady-state charging of the cellular membrane (lower dotted line).

**Biv:** The activation of the T-type calcium conductance close to the resting membrane potential resulted in a rebound depolarisation at the break of the response to negative current injection. Generally one or more action potentials were generated during the membrane depolarisation. The lower dotted line marks the resting membrane potential and the upper dotted line marks the peak of the rebound depolarisation as observed as a plateau following the action potential. To quantify the amplitude of the T-type conductance, the difference in membrane potential between resting membrane potential and the peak of the membrane depolarisation was taken. Cells in which the plateau was masked due to prolonged action potential firing were not used for analysis.



**Figure 3.5**

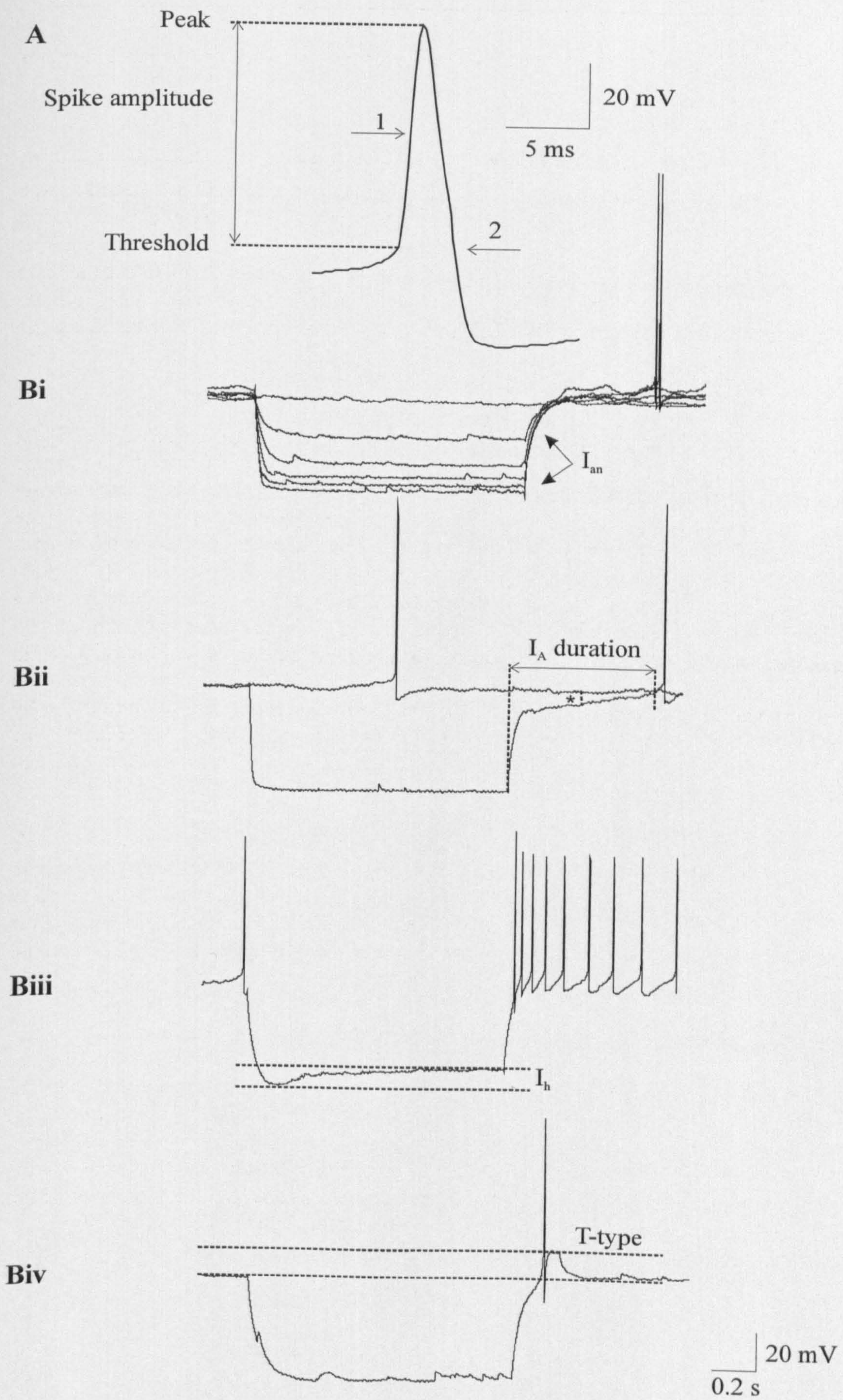




**Figure 3.6 Electrophysiological properties of cluster 1 and 2 neurones**

**A:** Superimposed traces from a continuous whole-cell current clamp recording of a cluster 1 neurone, showing membrane responses to a range of hyperpolarising and depolarising rectangular-wave current steps of constant increment (illustrated beneath). The membrane potential of the neurone is shown to the left in all figures. Anomalous inward rectification ( $I_{an}$ ) can be seen as a relative reduction in the increase of the membrane voltage responses to the linearly increased hyperpolarising current pulses, as indicated by the arrows.

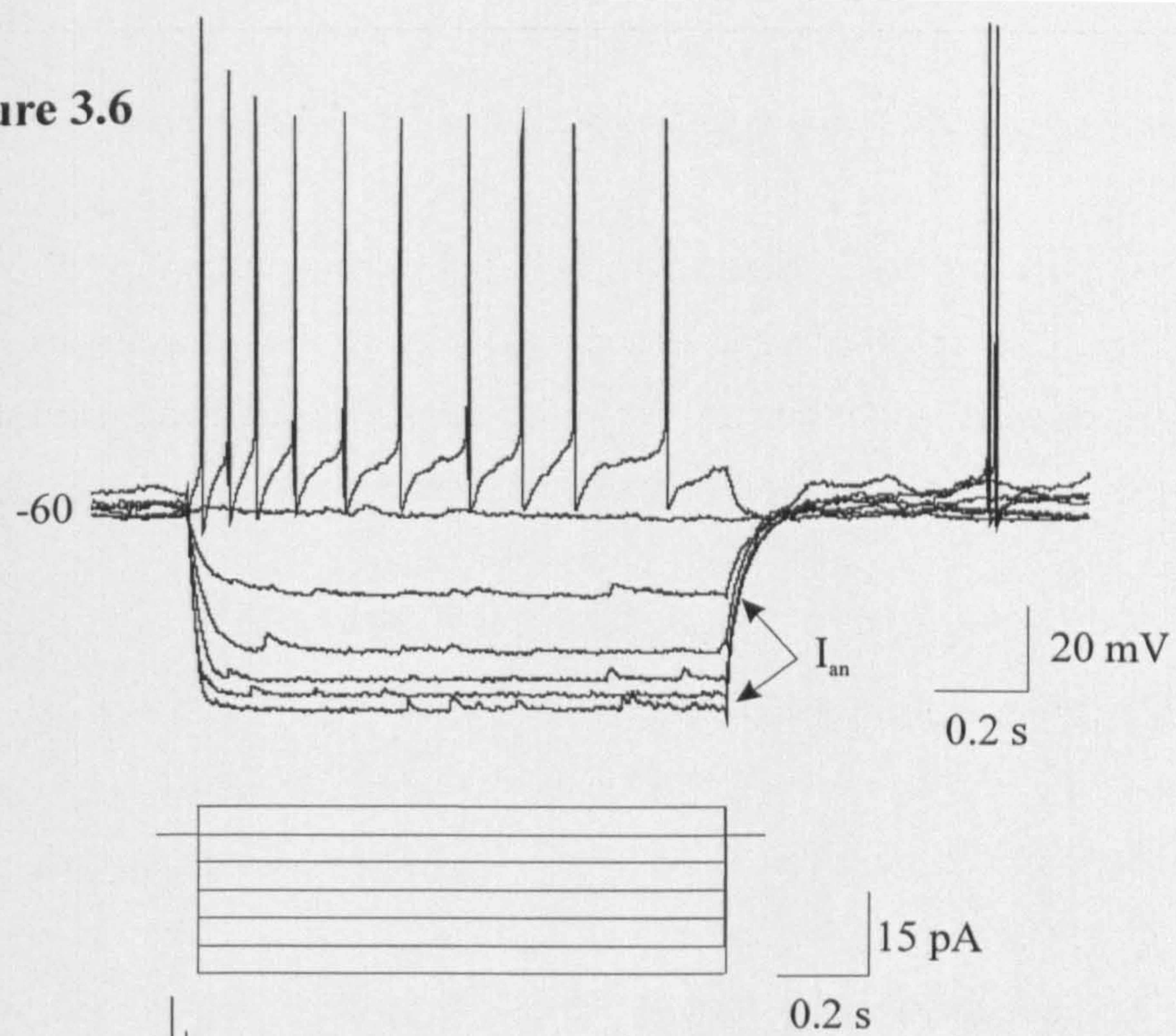
**B:** Superimposed traces from a continuous whole-cell current clamp recording of a cluster 2 neurone, showing membrane responses to a range of hyperpolarising and depolarising rectangular-wave current steps of constant increment (illustrated beneath). Anomalous inward rectification ( $I_{an}$ ) can be seen as a relative reduction in the increase of the membrane voltage responses to the linearly increased hyperpolarising current pulses, as indicated by the arrows. The second arrow indicates the delayed return to baseline following negative current injection as a result of the activation of an A-like conductance.

**C:** Plot of the current-voltage relationship (I-V) of the neurone shown in B as obtained by plotting the current injected into the cell (X-axis) against the resulting membrane potential (Y-axis). Note the reduction in the slope of the plot towards more negative membrane potentials as a result of the activation of  $I_{an}$ . The arrow shows the point in the I-V at which the slope of the plot decreased and the mean activation threshold for  $I_{an}$  was estimated by averaging the membrane potential of this point in the I-V plots of cluster 1 or cluster 2 neurones.

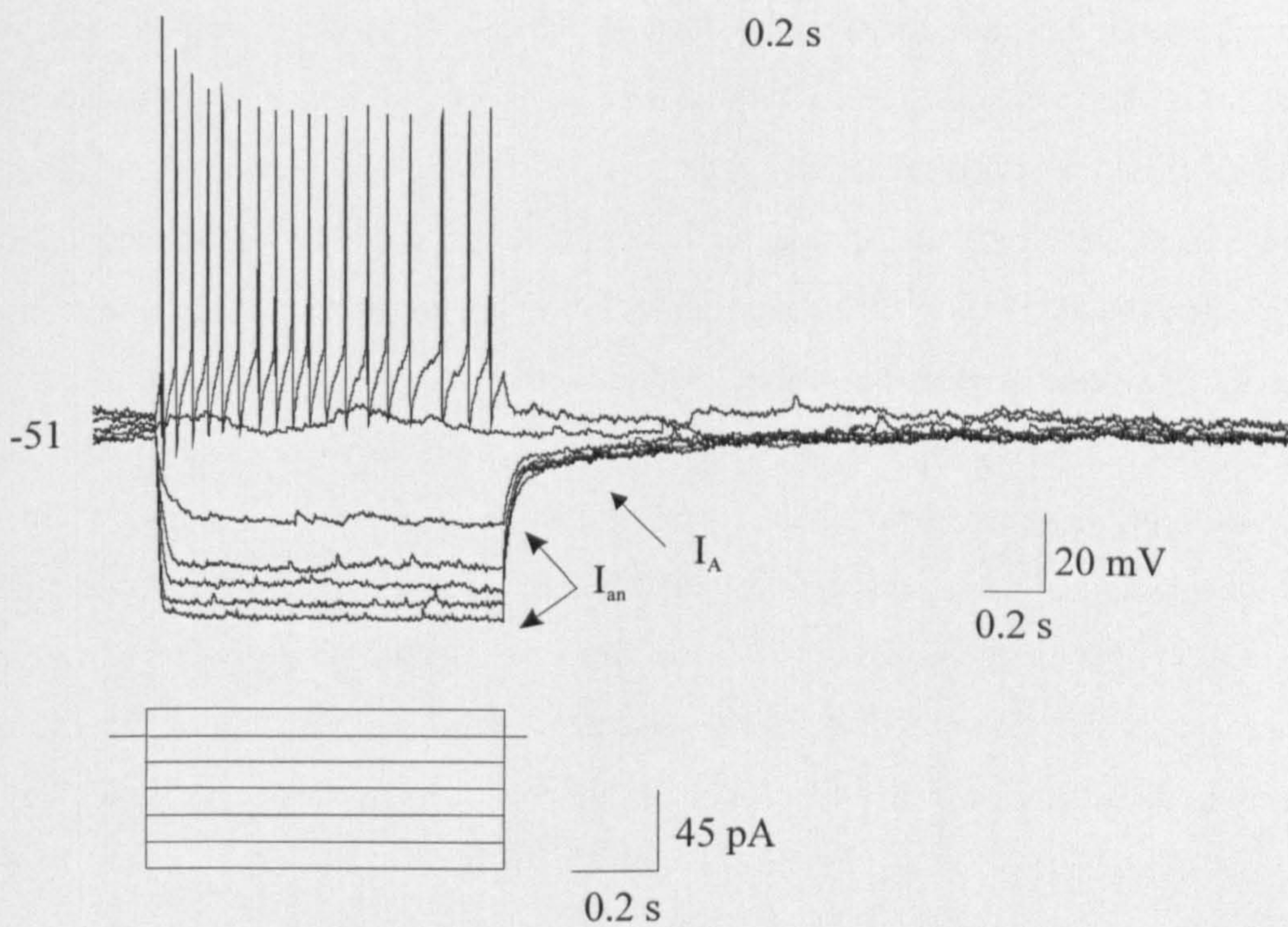


**Figure 3.6**

**A**



**B**



**C**

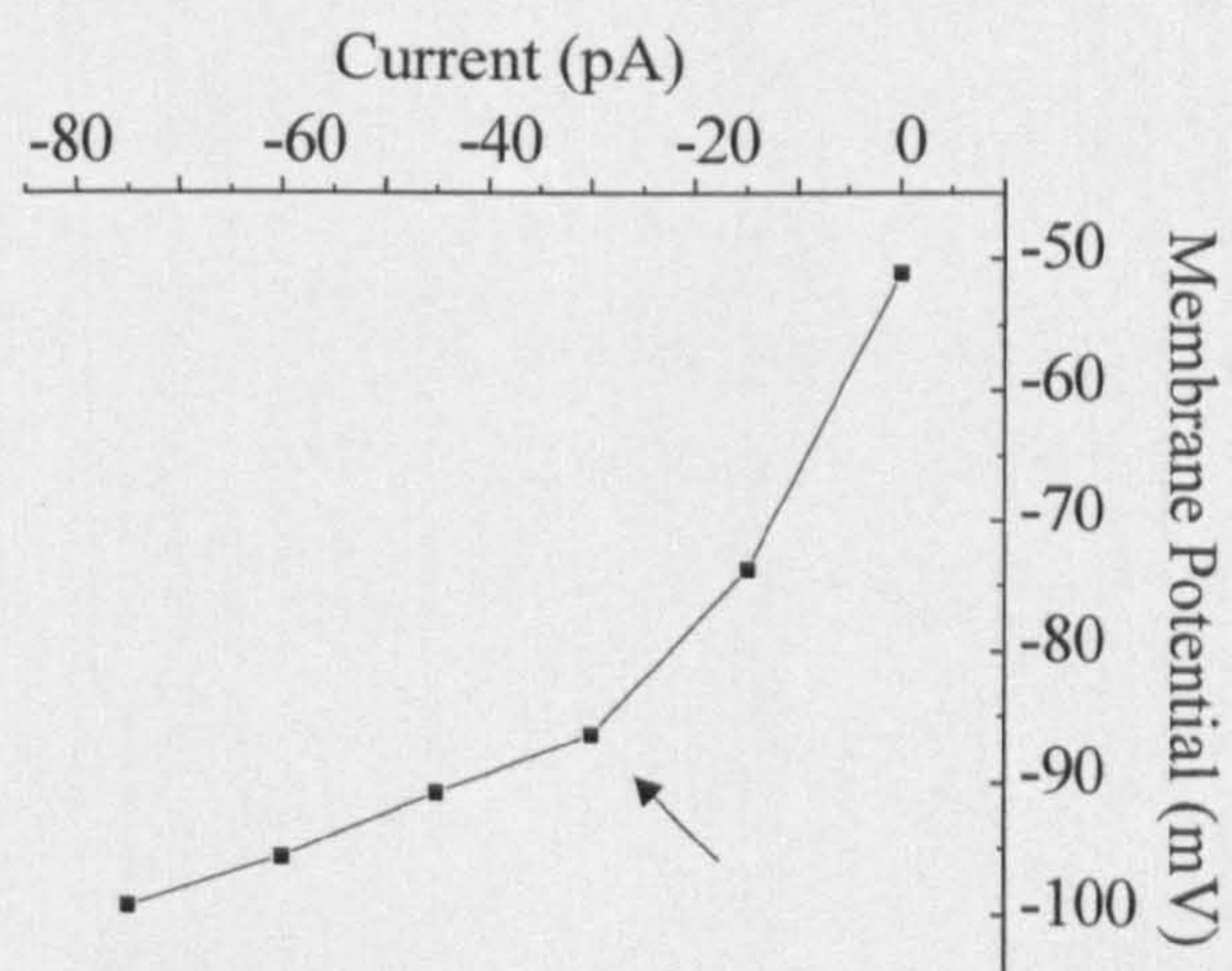




**Figure 3.7 Electrophysiological properties of cluster 3 and 4 neurones**

**Ai:** Superimposed traces from a continuous whole-cell current clamp recording of a cluster 3 neurone, showing membrane responses to a range of hyperpolarising and depolarising rectangular-wave current steps of constant increment (illustrated beneath). Note the lack of any distinctive subthreshold active membrane conductances.

**Aii:** Plot of the current-voltage relationship of the neurone shown in Ai. Note the constant slope of the plot as a result of the constant membrane resistance over the range of membrane potentials tested.

**Bi:** Superimposed traces from a continuous whole-cell current clamp recording of a cluster 4 neurone, showing membrane responses to a range of hyperpolarising and depolarising rectangular-wave current steps of constant increment (illustrated beneath). Note the sag in the membrane response during negative current injection as a result of the activation of  $I_h$ . The amplitude of the  $I_h$  conductance was measured as the difference in membrane potential between the two dotted lines. The arrow heads inserted in the I-V plot mark the activation of  $I_h$  at different membrane potentials as the kinetics of activation are different at different holding potentials. Note the decrease in activation latency (time difference between the two arrowheads) and increased amplitude of the sag at more negative membrane potentials. Square and circle mark the position of the traces used to measure the instantaneous and steady-state membrane responses, respectively (see Bii).

**Bii:** Plot of the instantaneous (square) and steady-state (circle) membrane responses of the neurone shown in Bi. The difference between the lines is indicative of the activation of  $I_h$ , which decreases the steady-state membrane response at negative holding potentials resulting in a non-linear current-voltage relationship. The arrow marks the point used to estimate the activation threshold of  $I_h$  in ARC neurones, which in the neurone shown amounts to approximately  $-88$  mV.



**Figure 3.7**

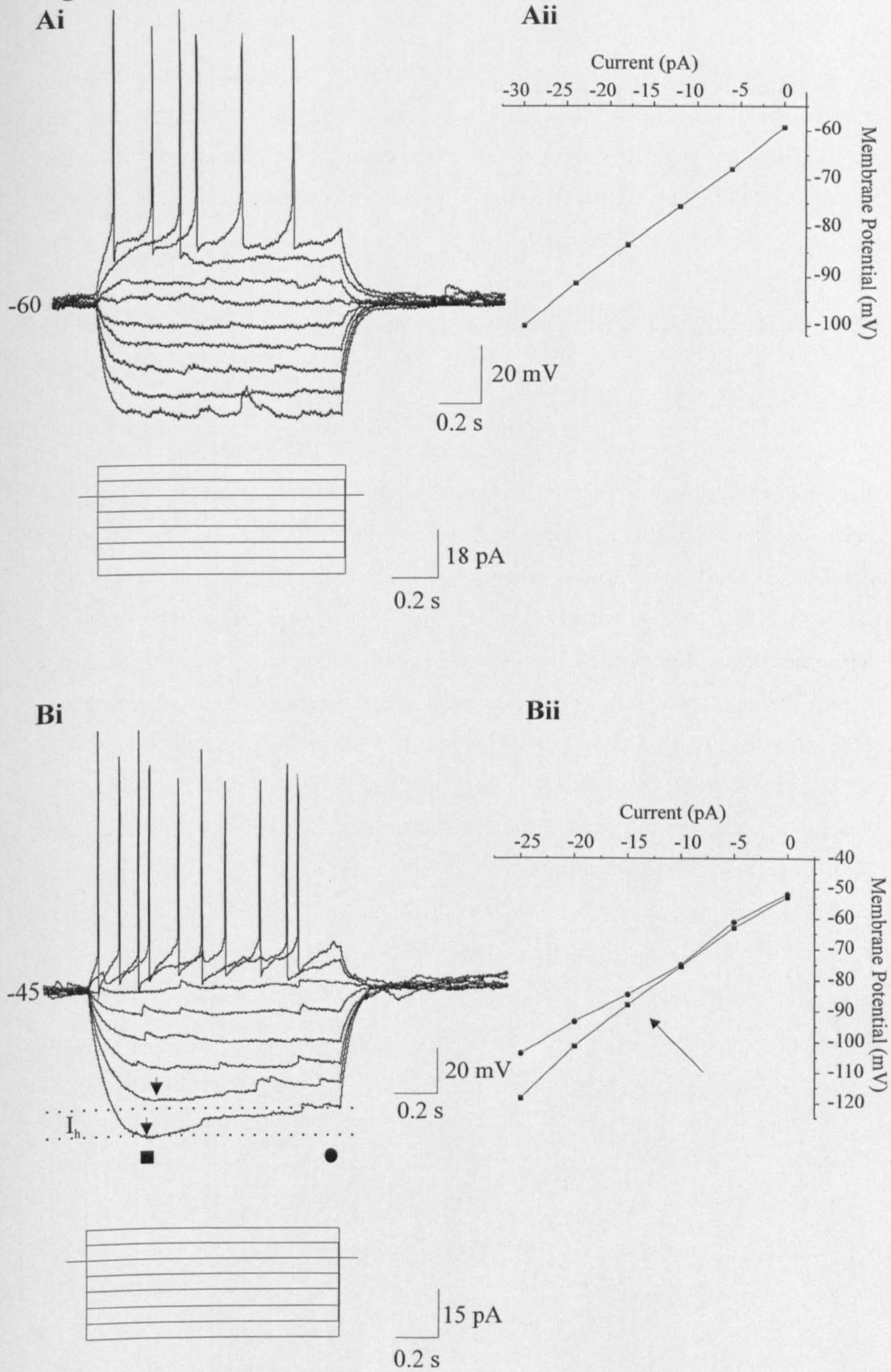




**Figure 3.8 Electrophysiological properties of cluster 5 and 6 neurones**

**Ai:** Superimposed traces from a continuous whole-cell current clamp recording of a cluster 5 neurone, showing membrane responses to a range of hyperpolarising and depolarising rectangular-wave current steps of constant increment (illustrated beneath). Note the sag in the membrane response during negative current injection as a result of the activation of  $I_h$ . Note also the rebound depolarisation upon release of the holding current due to the activation of a T-type calcium conductance (arrow 1), although there may also be some contribution from  $I_h$ .

**Aii:** Plot of the instantaneous (square) and steady-state (circle) membrane responses of the neurone shown in Ai. Note the decrease in the steady-state membrane response at negative holding potentials as a result of the activation of  $I_h$ . Arrow 2 marks the point used to estimate the activation threshold of  $I_h$  in ARC neurones, which in the neurone shown amounts to approximately  $-91$  mV.

**Bi:** Superimposed traces from a continuous whole-cell current clamp recording of a cluster 6 neurone, showing membrane responses to a range of hyperpolarising and depolarising rectangular-wave current steps of constant increment (illustrated beneath). Note the rebound depolarisation upon release of the holding current due to the activation of a T-type calcium conductance (arrow 3) and the absence of any other subthreshold active conductances.

**Bii:** Plot of the current-voltage relationship of the neurone shown in Bi. Note the linear relationship between injected current and the resulting membrane response.



**Figure 3.8**

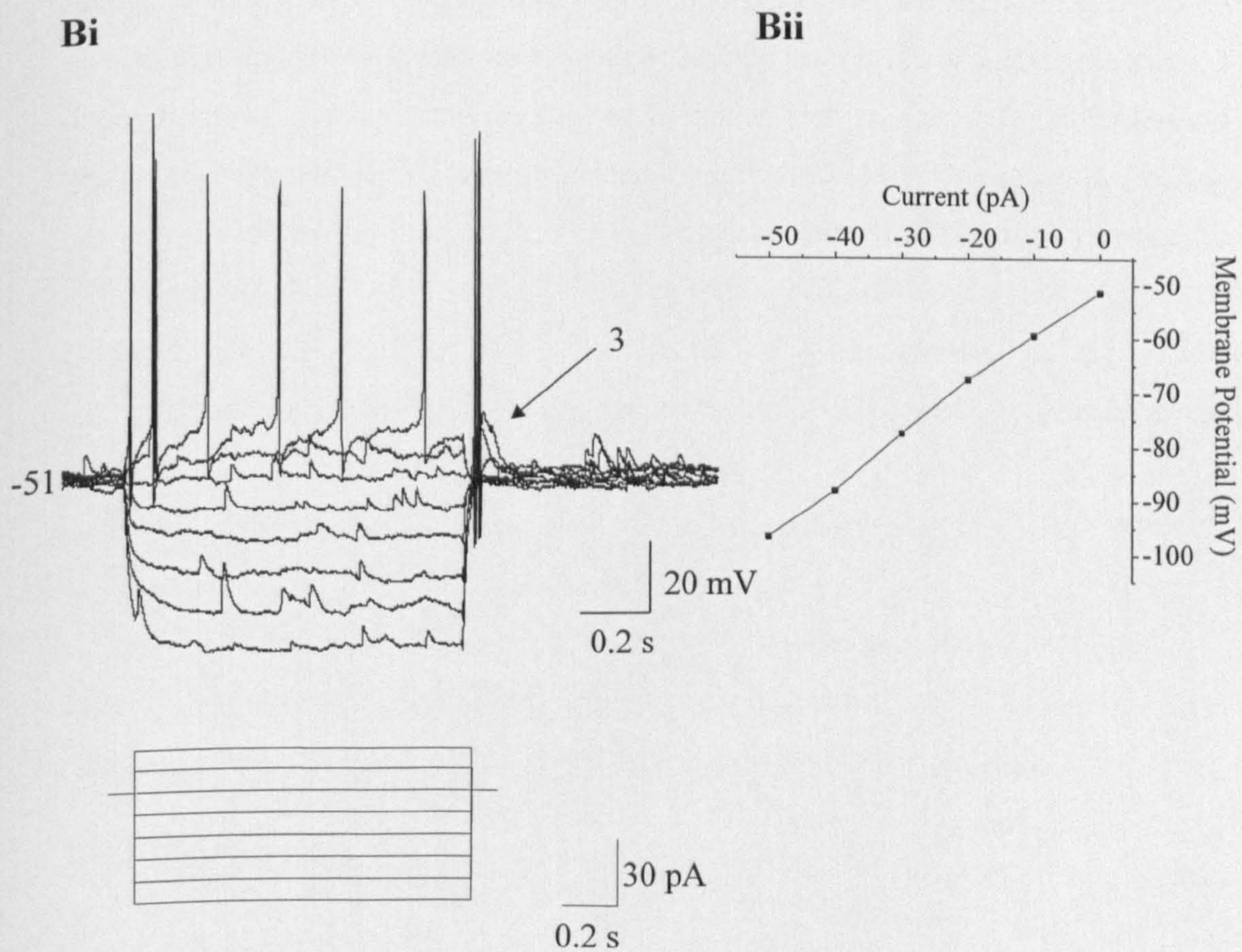
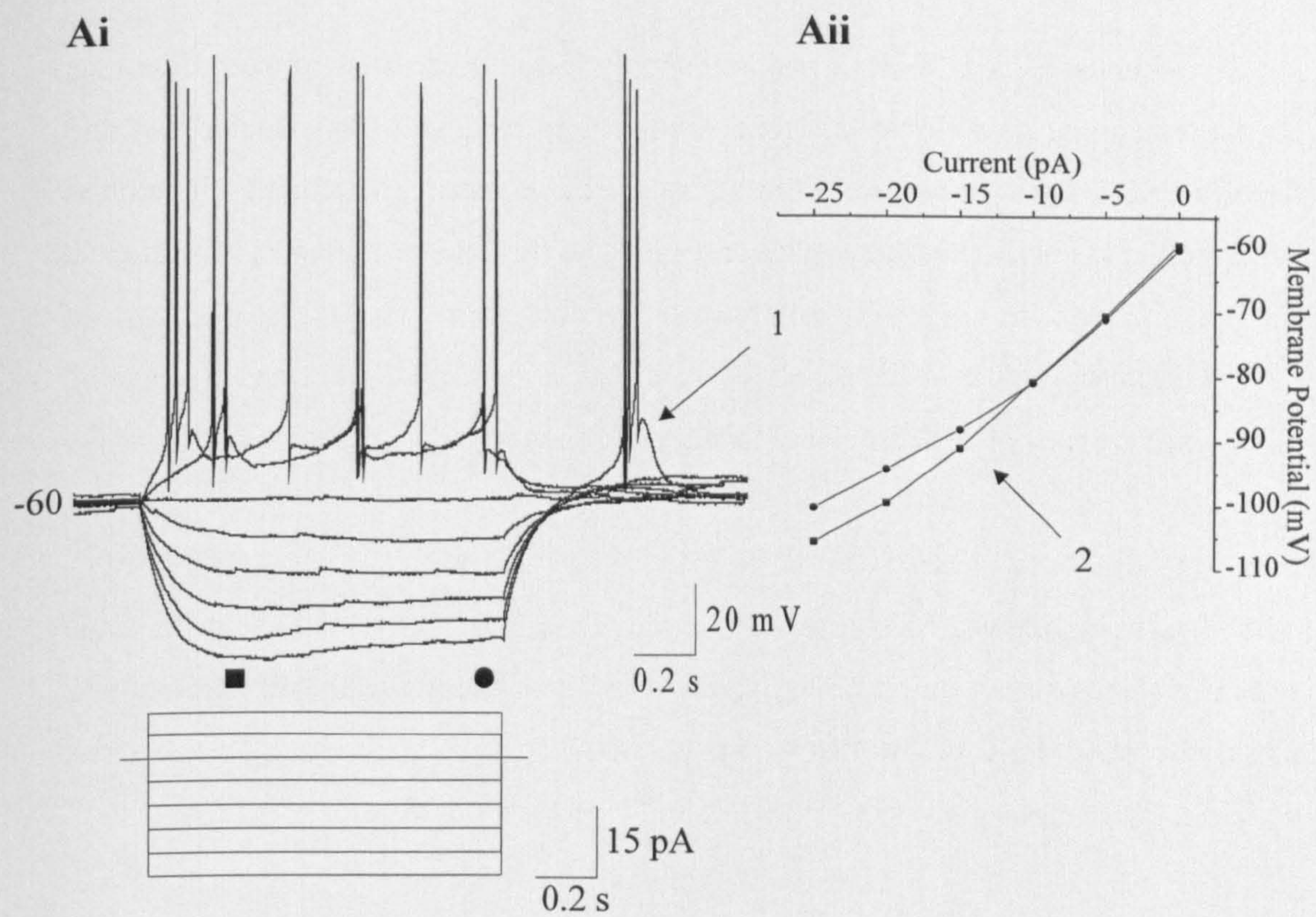




**Figure 3.9 Electrophysiological properties of cluster 7 and 8 neurones**

**Ai:** Superimposed traces from a continuous whole-cell current clamp recording of a cluster 7 neurone, showing membrane responses to a range of hyperpolarising and depolarising rectangular-wave current steps of constant increment (illustrated beneath). Anomalous inward rectification ( $I_{an}$ ) can be seen as a relative reduction in the increase of the membrane voltage responses to the linearly increased hyperpolarising current pulses, as indicated by the arrows. Note also the rebound depolarisation upon release of the holding current due to the activation of a T-type calcium conductance (arrow 1).

**Aii:** Plot of the current-voltage relationship (I-V) of the neurone shown in Ai. Note the reduction in the slope of the plot towards more negative membrane potentials as a result of the activation of  $I_{an}$  (arrow 2).

**Bi:** Superimposed traces from a continuous whole-cell current clamp recording of a cluster 8 neurone, showing membrane responses to a range of hyperpolarising and depolarising rectangular-wave current steps of constant increment (illustrated beneath). Note the sag in the membrane response during negative current injection as a result of the activation of  $I_h$ . Anomalous inward rectification ( $I_{an}$ ) can be seen as a relative reduction in the increase of the membrane voltage responses to the linearly increased hyperpolarising current pulses, as indicated by the arrows. Note the rebound depolarisation upon release of the holding current due to the activation of a T-type calcium conductance (arrow 3). Note also that the active conductances may be contributing towards each other therefore values can only be estimated.

**Bii:** Plot of the instantaneous (square) and steady-state (circle) membrane responses of the neurone shown in Bi. Note the decrease in the steady-state membrane response at negative holding potentials as a result of the activation of  $I_h$ . Note also the reduction in the slope of the instantaneous plot towards more negative membrane potentials as a result of the activation of  $I_{an}$ . Arrow 4 marks both the activation point of  $I_h$  and  $I_{an}$  in this case, at about -93 mV.



**Figure 3.9**

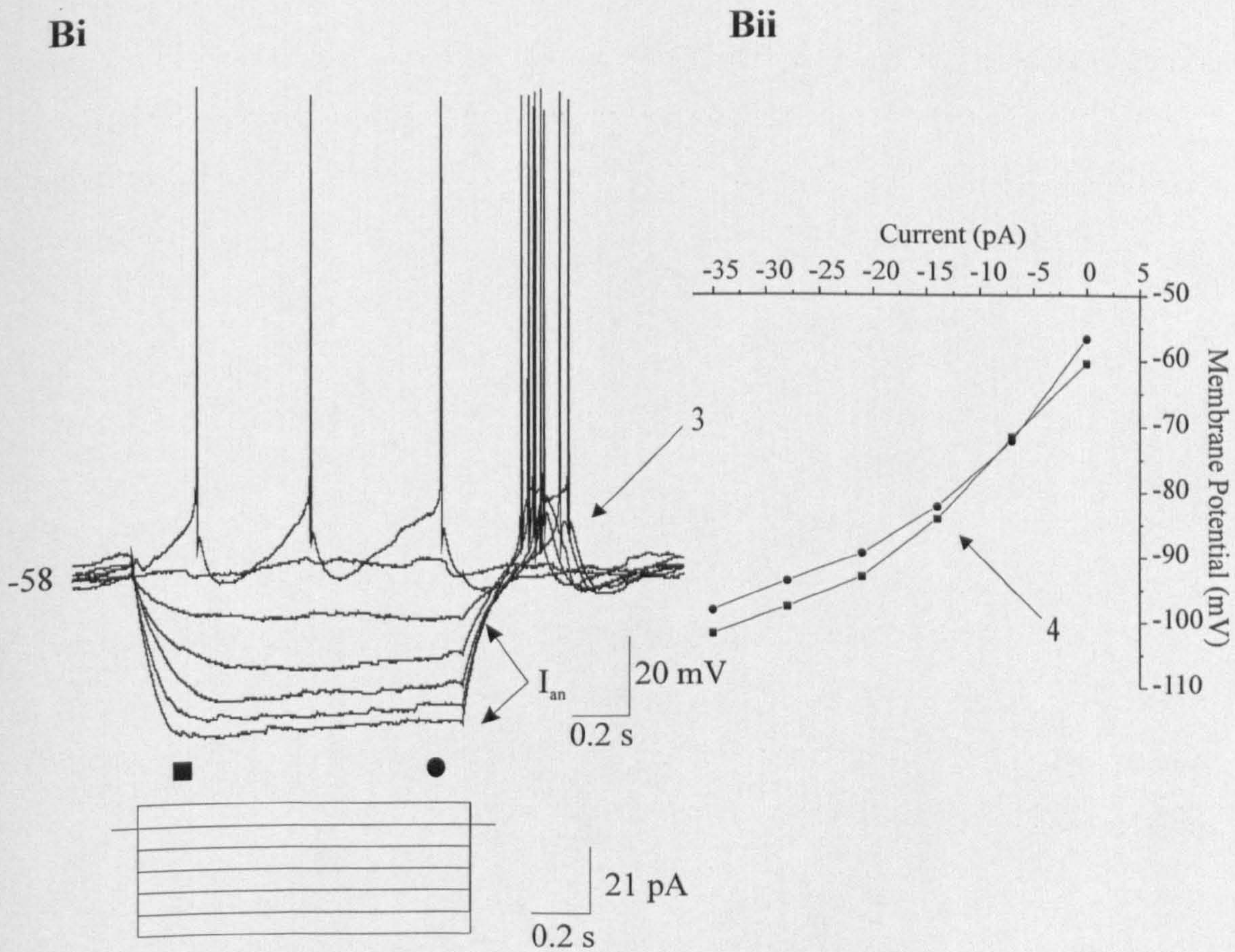
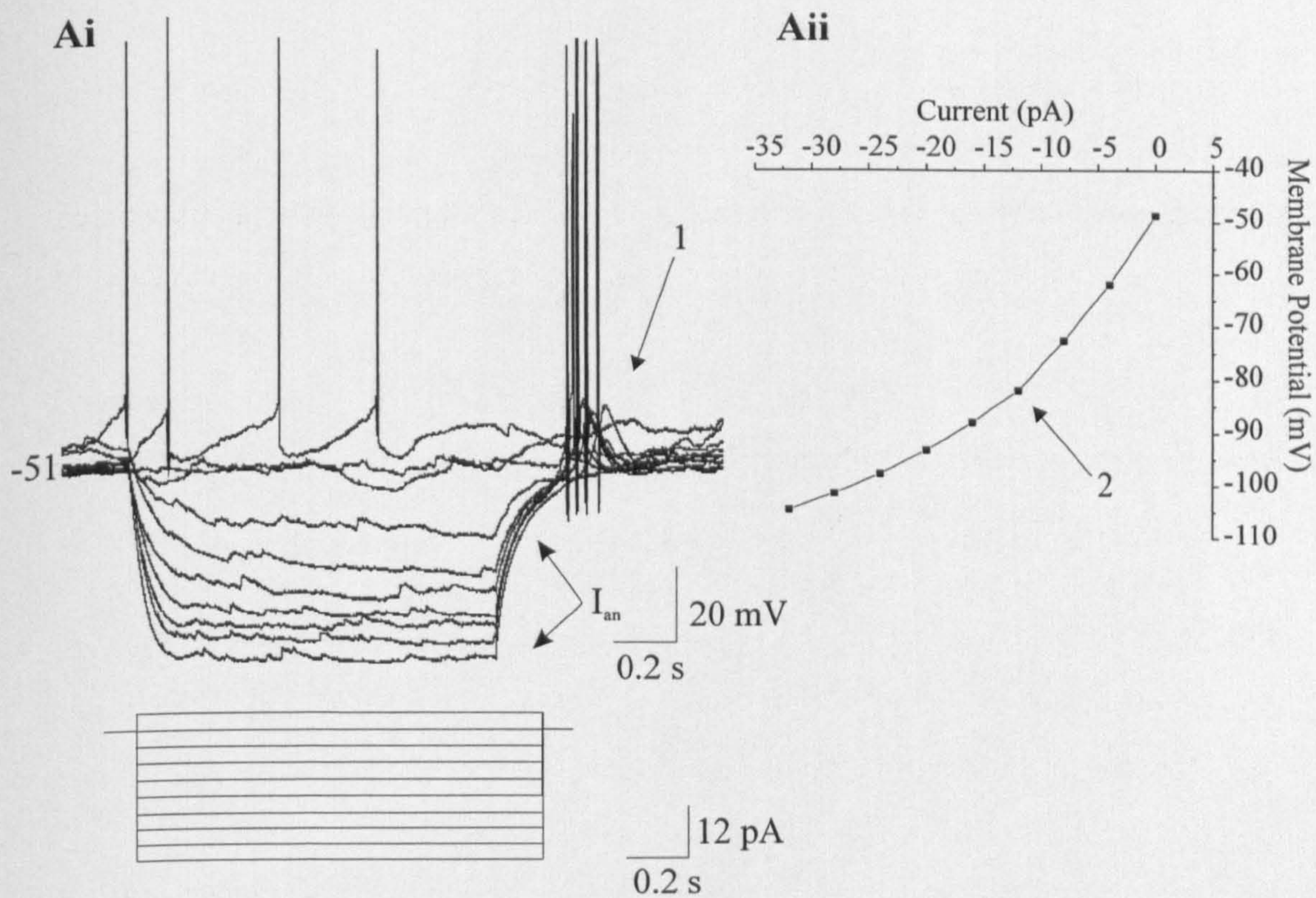




**Figure 3.10 Relative proportion of neurones in each cluster recorded in 10 mM and 2 mM glucose-containing aCSF**

**A:** Bar-chart showing the percentage of neurones classified into each cluster recorded in 10 mM and 2 mM glucose-containing aCSF. Note the percentage of neurones in clusters 1, 2 and 6 is higher in 2 mM glucose-containing aCSF but in clusters 4, 5 and 8, the percentage of neurones is higher in 10 mM glucose-containing aCSF. Clusters 3 and 7 expressed the same percentage of neurones in both glucose concentrations.



**Figure 3.10**

**A**

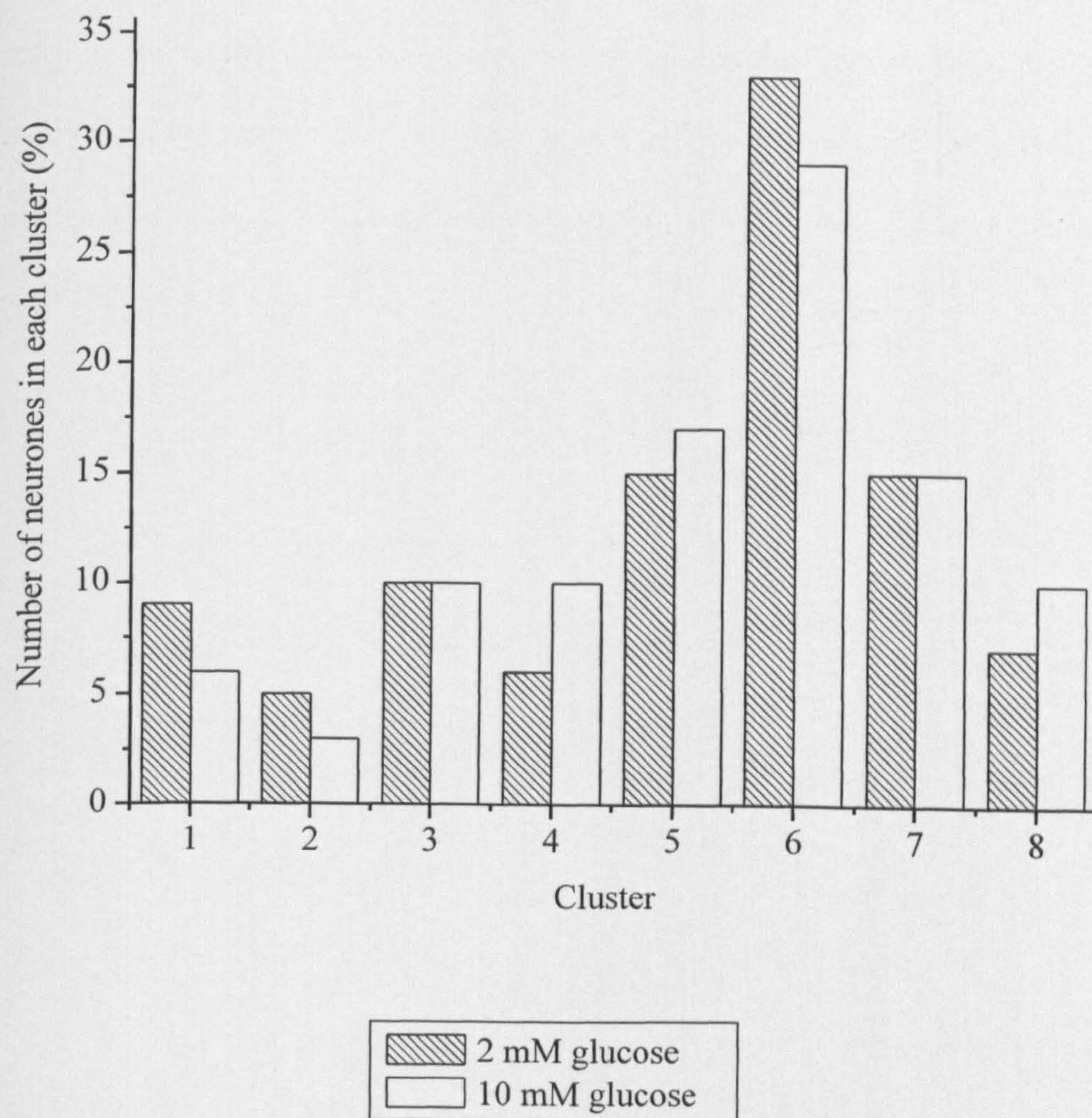




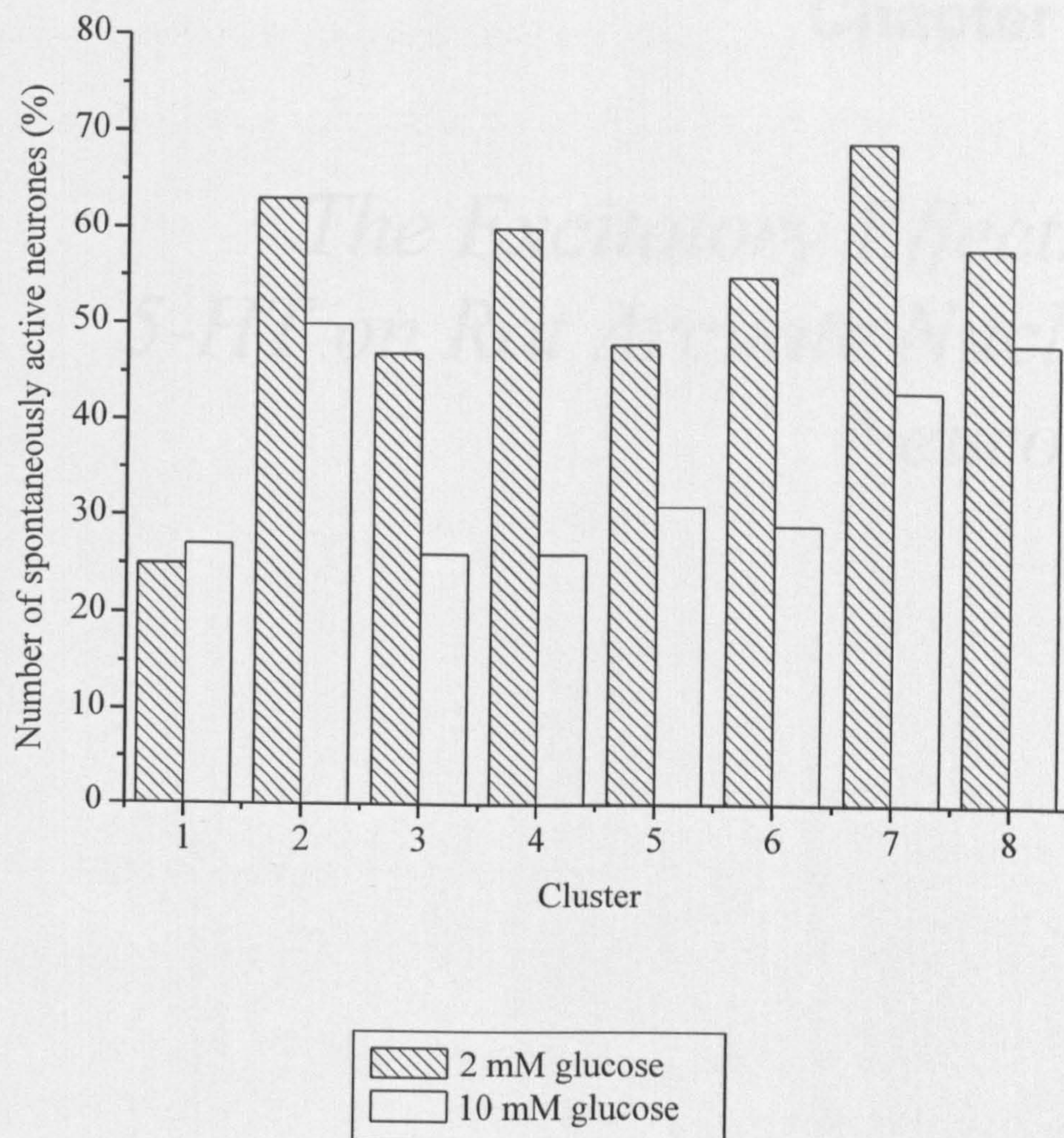
**Figure 3.11 Comparison of neurones displaying spontaneous suprathreshold activity in each cluster recorded in 10 mM and 2 mM glucose-containing aCSF**

**A:** Bar-chart showing the percentage of spontaneously active neurones in each cluster recorded in 10 mM and 2 mM glucose-containing aCSF. Note the percentage of active neurones is higher in all clusters, except cluster 1, in 2 mM glucose compared to 10 mM glucose.



**Figure 3.11**

**A**





# Chapter 4

## *The Excitatory Effects of 5-HT on Rat Arcuate Nucleus Neurones*



## 4.1 Introduction

The arcuate nucleus (ARC) of the hypothalamus is involved in the regulation of feeding and energy homeostasis. It contains two principal neuronal subtypes involved in this process: orexigenic NPY/AgRP neurones and anorexigenic POMC/CART neurones (Cone, 2005). In addition the ARC expresses a variety of other neuronal subtypes including neuromedin U, neurotensin, somatostatin, dopamine and galanin-like peptide (GALP; Chronwall, 1985; Cone *et al.*, 2001). The neurotransmitter 5-HT has been extensively implicated in the control of feeding and energy homeostasis, alongside its regulation of many biological, behavioural and physiological processes such as thermoregulation, stress responses, reproductive behaviour and circadian rhythms (Blundell, 1977; Bonate, 1991; Wilkinson & Dourish, 1991; Lowry, 2002). It is also associated with psychiatric disorders such as depression and anxiety (Baldwin & Rudge, 1995; Graeff *et al.*, 1996), as well as neurodegenerative conditions including Alzheimer's and Parkinson's disease (Cross, 1990). 5-HT is synthesised from tryptophan by tryptophan hydroxylase (Fuller, 1980). It is predominantly produced in the gut but it is also produced in the brain, primarily from the raphe nuclei in the brainstem (Azmitia & Segal, 1978; Sawchenko *et al.*, 1983). 5-HT exerts its actions through multiple receptor subtypes, which have been pharmacologically classified into seven families: 5-HT<sub>1-7</sub> (Hoyer *et al.*, 1994; Barnes & Sharp, 1999). The 5-HT<sub>3</sub> receptor is a ligand-gated ion channel but all the other receptors are G-protein coupled (for review of 5-HT signalling, see general introduction and Raymond *et al.*, 2001 and Adayev *et al.*, 2005).

In the control of feeding specifically, 5-HT acts to suppress food intake whereas depletion of 5-HT increases food intake (Blundell, 1977, 1984; Curzon, 1990; Leibowitz *et al.*, 1990; Curzon, 1991; Samanin & Grignaschi, 1996;

Simansky, 1996). 5-HT levels have been shown to increase in the lateral hypothalamus upon feeding (Schwartz *et al.*, 1989) and direct injection of 5-HT into the PVN suppresses food intake (Currie & Coscina, 1996). As it is a strong candidate for the inhibition of feeding, several serotonergic agents have been used in the pharmacological treatment of obesity. These include d-fenfluramine (d-fen), a serotonin releaser and re-uptake inhibitor (Guy-Grand, 1992) and sibutramine, a combined noradrenaline and serotonin reuptake inhibitor (Luque & Rey, 2002). Both agents have been shown to reduce feeding upon application. d-Fen however was withdrawn from use due to severe cardiopulmonary side-effects (valvular heart disease and pulmonary hypertension; Connolly *et al.*, 1997; Mark *et al.*, 1997).

Studies to-date indicate that the 5-HT receptors likely to be involved in the regulation of feeding are either the 5-HT<sub>1</sub> or 5-HT<sub>2</sub> subtypes (De Vry & Schreiber, 2000). Metergoline, a non-selective 5-HT<sub>1/2</sub> receptor antagonist blocked the inhibitory effect of 5-HT on feeding when injected into the paraventricular nucleus (PVN; Currie & Coscina, 1996) and the 5-HT<sub>1B/2C</sub> agonist mCPP decreased food intake in rats (Dryden *et al.*, 1996b) suggesting evidence of an interaction between the 5-HT<sub>1</sub> and 5-HT<sub>2</sub> receptors in the control of feeding.

More specific evidence for the involvement of the 5-HT<sub>1</sub> receptor is that d-fen has been suggested to exert its inhibitory effects on feeding through the 5-HT<sub>1</sub> receptor, particularly the 5-HT<sub>1B</sub> subtype (Neill & Cooper, 1989; Grignaschi & Samanin, 1992; Grignaschi *et al.*, 1995) but not the 5-HT<sub>1A</sub> subtype (Vickers *et al.*, 1996). Further evidence for a role for the 5-HT<sub>1B</sub> receptor in feeding is shown by the fact that 5-HT<sub>1B</sub> knockout mice did not display hypophagia after fenfluramine administration (Lucas *et al.*, 1998); the 5-HT<sub>1B/2C</sub> agonist mCPP decreased food intake when injected into rats (Dryden *et al.*, 1996b) and the 5-HT<sub>1B</sub> agonists



RU24969, TFMPP and mCPP all induced a dose-dependent reduction in food intake which was blocked by 5-HT<sub>1B</sub> antagonists (Bendotti & Samanin, 1987; Kennett *et al.*, 1987; Kennett & Curzon, 1988). Furthermore, a more selective 5-HT<sub>1B</sub> agonist, CP94253 also induced hypophagia (Halford & Blundell, 1996; Lee & Simansky, 1997; Lee *et al.*, 2002). The 5-HT<sub>1B</sub> receptor is widely expressed throughout the hypothalamus, with particularly strong expression in the magnocellular nuclei, the supraoptic nucleus, and the PVN (Makarenko *et al.*, 2002). Studies have shown 5-HT neurones to interact with neuropeptide Y (NPY) neurones (Guy *et al.*, 1988) and that 5-HT inhibits feeding partly by blocking NPY release in the PVN, as the 5-HT synthesis inhibitor, p-chlorophenylalanine was able to increase the level of NPY available for release (Dryden *et al.*, 1996c). The 5-HT<sub>1B</sub> receptor is expressed on NPY neurones and 5-HT induces a hyperpolarisation in these neurones (Heisler *et al.*, 2006). Collectively these data indicate a key role for the 5-HT<sub>1B</sub> receptor in the control of energy homeostasis.

In contrast to the inhibitory effects of 5-HT on feeding, the 5-HT<sub>1A</sub> receptor agonist flesinoxan increased feeding (Dryden *et al.*, 1996a). Studies showed that the 5-HT<sub>1A/7</sub> agonist 8-OH-DPAT elicited feeding in rats (Dourish *et al.*, 1985, 1986) and later showed that 8-OH-DPAT induced hyperphagia through the 5-HT<sub>1A</sub> receptor (Hutson *et al.*, 1988). In contrast to its usual hypophagic effects, this 5-HT agonist causes hyperphagia due to the fact that the 5-HT<sub>1A</sub> receptor is an auto-receptor and so 5-HT and its agonists act upon presynaptic 5-HT<sub>1A</sub> receptors to inhibit 5-HT release and hence increase feeding. *In situ* hybridisation techniques have been used to show the expression of 5-HT<sub>1A</sub> receptors all over the brain, including within the hypothalamus, particularly the ventromedial nucleus (VMN) and dorsomedial hypothalamus (DMH; Chalmers & Watson, 1991; Pompeiano *et al.*,

1992; Wright *et al.*, 1995), as have studies using immunohistochemistry which showed expression of 5-HT<sub>1A</sub> receptors over a large proportion of the brain, including the hypothalamus (Aznar *et al.*, 2003).

Evidence for the role of the 5-HT<sub>2</sub> receptor in feeding is suggested by the observation that 5-HT affects the activity of POMC neurones through the 5-HT<sub>2C</sub> receptor, as they are expressed on POMC neurones (Heisler *et al.*, 2002). Further evidence for a role for this receptor in the control of feeding was shown by Tecott who demonstrated that 5-HT<sub>2C</sub> knockout mice develop hyperphagia (Tecott *et al.*, 1995), whilst mice with a mutated form of the 5-HT<sub>2C</sub> receptor also showed signs of hyperphagia (Nonogaki *et al.*, 1998). Vickers reported that the effects of d-fen were reduced in 5-HT<sub>2C</sub> knockout mice, and that the 5-HT<sub>2C</sub> receptor antagonist SB242084 inhibited d-fen-induced hypophagia (Vickers *et al.*, 1999, 2001). The non-specific 5-HT<sub>2</sub> receptor antagonist ketanserin also inhibited d-fen-induced hypophagia (Hewson *et al.*, 1988), adding to the evidence indicating that this receptor plays an important role in mediating the effects of the appetite suppressant d-fen. 5-HT<sub>2C</sub> receptors have been localised within the ARC, PVN, and DMH (Wright *et al.*, 1995). Further studies utilised *in situ* hybridisation to show the expression of 5-HT<sub>2C</sub> receptors within the hypothalamus, particularly, in the DMH, lateral hypothalamus (LH) and PVN (Hoffman & Mezey, 1989; Molineaux *et al.*, 1989).

Although most of the literature leans towards a role for the 5-HT<sub>2C</sub> receptor subtype in the control of feeding, some studies have looked at the 5-HT<sub>2A</sub> and 5-HT<sub>2B</sub> receptor subtypes. 5-HT has been shown to reduce hyperphagia in mice over-expressing NPY by acting at 5-HT<sub>2A</sub> receptors (Hsiao *et al.*, 2005). A 5-HT<sub>2A</sub> receptor antagonist was able to block the action of NPY in the PVN, indicating an



interaction between NPY and 5-HT<sub>2A</sub> receptors (Currie *et al.*, 2002). The 5-HT<sub>2B</sub> receptor agonist BW 723C86 induced hyperphagia, in contrast to the effect of other 5-HT<sub>2</sub> agonists (Kennett *et al.*, 1997a). 5-HT<sub>2B</sub> receptors have been reported within the hypothalamus, particularly in the DMH (Duxon *et al.*, 1997a). 5-HT<sub>2A</sub> receptors have not been widely found in the hypothalamus, but are instead predominantly expressed in the amygdala, hippocampus and cortex (Xu & Pandey, 2000). However, there was a study which did find 5-HT<sub>2A</sub> receptors in the PVN using immunohistochemistry (Zhang *et al.*, 2002).

Despite this extensive literature supporting a role for 5-HT receptors in controlling energy balance, the receptors and cellular mechanisms underlying the effects of 5-HT at the level of the ARC are still not completely known. Therefore, the aims of this study, shown in this chapter and the next, were to investigate the cellular mechanisms by which 5-HT regulates key hypothalamic neurones in the ARC involved in regulating energy homeostasis and to elucidate which 5-HT receptor subtypes were mediating these effects by using a range of selective agonists and antagonists. In addition, the phenotype of neurones that are regulated by 5-HT will be investigated using markers for orexigenic (ghrelin) and anorexigenic (CART) neurones.

## 4.2 Results

In this study, 5-HT (50  $\mu$ M) was applied to 122 ARC neurones obtained with the whole-cell patch clamp technique. This concentration of 5-HT was chosen to ensure there was an adequate supply of 5-HT at the synapse to produce a response, as 5-HT is subject to re-uptake. 5-HT was bath applied to the slice by superfusion

for between 45-75 seconds. Results were obtained in 2 mM glucose-containing aCSF unless otherwise stated. These neurones responded to 5-HT either with a depolarisation of the membrane (30 %), a hyperpolarisation of the membrane (37 %) or did not respond (33 %; see figure 4.1). This chapter will describe the excitatory effects of 5-HT on rat ARC neurones whilst the inhibitory effects will be shown in the following chapter. Statistical significance in these chapters was determined using student's two tailed t-test, paired or unpaired as appropriate or chi-square test where stated.

#### ***4.2.1 The excitatory effects of 5-HT on ARC neurones***

Bath application of 5-HT (50  $\mu$ M) to the slice by superfusion for 45-75 s induced a membrane depolarisation in 37 ARC neurones. The depolarisation of the membrane was slow in onset and could reach threshold for action potential firing, resulting in an increase in the activity of these neurones. This response was characterised by depolarisation of the membrane from a mean resting membrane potential of  $-50.2 \pm 1.1$  mV to  $-43.8 \pm 0.9$  mV, a mean peak membrane depolarisation of  $6.4 \pm 0.7$  mV ( $n=37$ ; see figure 4.1C). The response partially recovered upon washout of 5-HT from the bath, returning the mean membrane potential to  $-48.8 \pm 1.5$  mV ( $n=25$ ). The 5-HT-induced depolarisation was maintained in the presence of 500 nM tetrodotoxin (TTX), indicating a direct effect on ARC neurones ( $n=6$ ; see figure 4.2Ai).

The depolarisation induced by 5-HT was associated with either an increase in input resistance, a decrease in input resistance or no measurable change.

*Increase in Input Resistance:* 5-HT-induced depolarisation in a sub-population of neurones was associated with a significant  $33.1 \pm 4.2$  % increase in



neuronal input resistance from a mean of  $939 \pm 140 \text{ M}\Omega$  at rest to  $1225 \pm 160 \text{ M}\Omega$  in the presence of 5-HT, an increase of  $286 \pm 40 \text{ M}\Omega$  ( $P < 0.01$ ;  $n=9$ ; see figure 4.2).

*Decrease in Input Resistance:* The 5-HT-induced membrane depolarisation was also associated with a significant  $25.8 \pm 2.7 \%$  decrease in neuronal input resistance in a sub-population of neurones, from a mean of  $1669 \pm 212 \text{ M}\Omega$  at rest to  $1235 \pm 165 \text{ M}\Omega$  in the presence of 5-HT, a decrease of  $434 \pm 86 \text{ M}\Omega$  ( $P < 0.01$ ;  $n=15$ ; see figure 4.3).

*No change in Input resistance:* In a further subset of neurones, the 5-HT-induced membrane depolarisation was associated with a non-significant  $1.0 \pm 2.1 \%$  change in neuronal input resistance from a mean of  $1413 \pm 161 \text{ M}\Omega$  at rest to  $1424 \pm 162 \text{ M}\Omega$  in the presence of 5-HT, a change of  $11 \pm 34 \text{ M}\Omega$ . (No change in resistance was considered to be a value of 10 % or less;  $P=0.8$ ;  $n=13$ ; see figure 4.4).

In a sub-population of neurones, to confirm that the change in resistance was due to 5-HT and not due to an indirect effect through voltage-dependent conductances being engaged, a period of constant negative current injection was applied during the 5-HT response to eliminate any voltage-dependent effects (for example see figure 4.2Ai).

The effect of 5-HT on ARC neurones was also studied in voltage-clamp. 5-HT induced an inward current (see figure 4.5A), with a mean peak current of  $23.2 \pm 6.6 \text{ pA}$  at a holding potential of  $-40 \text{ mV}$  ( $n=6$ ) and a mean peak current of  $16.6 \pm 5.0 \text{ pA}$  at a holding potential of  $-50 \text{ mV}$  ( $n=6$ ). The current was fast in onset with a slow gradual decay after reaching its peak.

#### ***4.2.2 Ionic mechanism underlying the 5-HT-induced depolarisation***

The 5-HT-induced depolarisation was associated with an increase, a decrease or no change in input resistance. Current-voltage relationships were obtained in control conditions and at the peak of the 5-HT-induced depolarisation to further investigate the underlying ionic mechanism. In neurones which responded to 5-HT with an increase in input resistance, there was an average reversal potential of  $-91.5 \pm 3.0$  mV ( $n=4$ ; see figure 4.2Aiii). This is close to the reversal potential for potassium ions under our recording conditions. In neurones which responded to 5-HT with a decrease in input resistance, extrapolation of the I-V resulted in an average reversal potential of  $-39.5 \pm 0.8$  mV ( $n=6$ ; see figure 4.3Aiii), indicating activation of a non-selective cation conductance. In neurones that responded to 5-HT with no change in resistance, the plots showed a parallel shift ( $n=7$ ; see figure 4.4Aiii) indicating either the activation of an electrogenic pump in the membrane or the concurrent activation/inhibition of more than one conductance. The reversal potential was taken from the point at which the plots of the two current-voltage relations intersected.

Voltage-clamp ramps were also performed in the presence of TTX to identify the ionic mechanism underlying the 5-HT-induced inward current (see figure 4.5B). The currents were obtained from ramp protocols that drove the holding potential from -130 mV to -30 mV, at a rate of 10 mV per second. The current responses in the presence and absence of 5-HT showed a parallel shift indicating no change in input resistance ( $n=2$ ).



### ***4.2.3 5-HT-induced membrane potential oscillations***

In three of the neurones exposed to 5-HT, regular bursts of action potentials were generated, corresponding with underlying membrane potential oscillations (see figure 4.6). These oscillations consisted of a biphasic waveform, with a slow depolarising phase followed by a rapid hyperpolarising component. The mean amplitude of the membrane potential oscillations, measured from the peak of the hyperpolarising to the peak of the depolarising phase, amounted to  $17.1 \pm 2.9$  mV (n=3). The depolarisation of the membrane reached threshold for action potential firing leading to the generation of bursts of action potentials. The average number of action potentials generated per-burst superimposed upon these membrane potential oscillations was  $17.0 \pm 4.6$  and the peak frequency amounted to  $2.3 \pm 0.7$  Hz.

### ***4.2.4. 5-HT-induced indirect effects on ARC neurones***

As well as inducing a direct membrane depolarisation, 5-HT exerted indirect effects on ARC neurones by inducing a change in synaptic activity, either increasing or decreasing the number of spontaneous excitatory post-synaptic potentials (EPSPs) or inhibitory post-synaptic potentials (IPSPs). EPSPs increased in frequency from  $0.9 \pm 0.2$  Hz to  $1.7 \pm 0.3$  Hz in the presence of 5-HT (n=3). IPSPs increased in frequency from  $0.4 \pm 0.1$  Hz to  $1.1 \pm 0.4$  Hz in the presence of 5-HT (n=2; see figure 4.7A). 5-HT also caused a decrease in the number of spontaneous EPSPs or IPSPs in some neurones from a mean frequency of  $1.4 \pm 0.4$  Hz to  $0.3 \pm 0.3$  Hz in the presence of 5-HT (n=2; see figure 4.7B).

To identify which 5-HT receptor subtypes are involved in the 5-HT-induced depolarisation, a range of 5-HT agonists and antagonists were used.

#### 4.2.5 The effects of 5-HT receptor agonists on ARC neurones

To determine the nature of the 5-HT receptor subtypes that mediate the depolarisation induced by 5-HT, the effects of selective agonists were first investigated. All agonists were bath applied to the slice by superfusion for 60-120 s.  $\alpha$ -methyl 5-HT (25  $\mu$ M), a 5-HT<sub>2</sub> receptor preferential agonist depolarised ARC neurones, from a membrane potential of  $-46.8 \pm 1.8$  mV to  $-41.0 \pm 2.1$  mV, a mean peak depolarisation of  $6.0 \pm 0.8$  mV ( $n=17$ ; see figure 4.8A).  $\alpha$ -methyl 5-HT induced depolarisation of neurones to threshold, inducing action potential firing and increasing excitability. Input resistance decreased by  $21.3 \pm 5.0$  % in a sub-population of these neurones, from  $1102 \pm 173$  M $\Omega$  to  $842 \pm 129$  M $\Omega$  in the presence of  $\alpha$ -methyl 5-HT. Input resistance increased by  $22.8 \pm 4.2$  % in a further subset of neurones, from  $1263 \pm 266$  M $\Omega$  to  $1552 \pm 326$  M $\Omega$  in the presence of  $\alpha$ -methyl 5-HT.  $\alpha$ -methyl 5-HT also induced a burst-like pattern of firing in a sub-population of ARC neurones, similar to that observed with 5-HT ( $n=2$ ).

Agonists for the 5-HT<sub>1</sub> receptor were next tested for their ability to mimic the 5-HT-induced depolarisation. The 5-HT<sub>1/5/7</sub> receptor agonist 5-CT (10  $\mu$ M) induced a membrane depolarisation, which reached threshold for action potential firing, from a membrane potential of  $-42.9 \pm 3.3$  mV to  $-37.7 \pm 4.3$  mV, with an associated  $4.2 \pm 6.2$  % increase in membrane resistance from  $961 \pm 8$  M $\Omega$  to  $1002 \pm 63$  M $\Omega$  ( $n=3$ ; see figure 4.8B).

However, the 5-HT<sub>1A/7</sub> receptor agonist 8-OH-DPAT (10  $\mu$ M;  $n=3$ ) and the 5-HT<sub>3</sub> receptor agonist mCPBG (10  $\mu$ M;  $n=3$ ) did not mimic the 5-HT-induced excitation (see figure 4.9) and had no effect on the membrane potential or input resistance of neurones that had responded to 5-HT with depolarisation.



Collectively these data suggest that there may be different receptors mediating the 5-HT-induced depolarisation, through different mechanisms. It may be that different subtypes of the 5-HT<sub>2</sub> receptor may mediate the increase and decrease in input resistance associated with the 5-HT-induced depolarisation and also the 5-HT<sub>1/5</sub> receptors may be partly responsible for mediating the 5-HT-induced depolarisation associated with either no change or a small increase in input resistance.

#### ***4.2.6 The effects of 5-HT receptor antagonists on 5-HT-induced responses in ARC neurones***

To clarify further the potential role of 5-HT<sub>2</sub> receptors in the 5-HT-induced depolarisation, the effects of a selective 5-HT<sub>2</sub> receptor antagonist were tested. All antagonists were bath applied to the slice by superfusion for approximately 5 minutes, this time of application ensuring saturation of the bath at the required concentration. The 5-HT<sub>2</sub> receptor antagonist altanserin inhibited the 5-HT-induced depolarisation in a concentration-dependent manner (see figure 4.10Aiii). Application of the antagonist alone had no effect on the recorded neurones. 200 nM altanserin partially reduced the 5-HT-induced depolarisation with a  $21.4\% \pm 24.1\%$  reduction in mean peak depolarisation compared to control in the absence of antagonist (n=3). 400 nM altanserin partially suppressed the 5-HT-induced depolarisation with a  $30.5 \pm 16.6\%$  reduction in mean peak depolarisation (n=3). 800 nM altanserin further inhibited the depolarisation with a  $58.1 \pm 23.3\%$  reduction in mean peak depolarisation (n=2). In the presence of 1  $\mu$ M altanserin the 5-HT-induced mean peak depolarisation was reduced from  $6.2 \pm 0.7$  mV to  $2.2 \pm 1.3$  mV, a  $57.6 \pm 12.4\%$  reduction (n=5; see figure 4.10A). 1  $\mu$ M altanserin partially reduced

the decrease in input resistance seen in the presence of 5-HT, from a mean peak decrease of  $213 \pm 50 \text{ M}\Omega$  in 5-HT alone to  $125 \pm 180 \text{ M}\Omega$  in the presence of the antagonist.

In order to more specifically identify which subtypes of the 5-HT<sub>2</sub> receptor were mediating the depolarisation, subtype-specific antagonists were tested. Firstly, the 5-HT<sub>2C</sub> receptor antagonist RS102221 was shown to partially suppress the 5-HT-induced depolarisation. In the presence of  $1 \text{ }\mu\text{M}$  RS102221, the mean peak membrane depolarisation induced by 5-HT was reduced from  $7.4 \pm 1.7 \text{ mV}$  to  $4.8 \pm 2.0 \text{ mV}$  in the presence of the antagonist, a  $36.2 \pm 21.5\%$  reduction ( $n=4$ ; see figure 4.10B) whilst mean peak decrease in membrane resistance induced by 5-HT was reduced from  $273 \pm 185 \text{ M}\Omega$  to  $96 \pm 92 \text{ M}\Omega$ . In the presence of  $2 \text{ }\mu\text{M}$  RS102221, mean peak membrane depolarisation induced by 5-HT was reduced by  $37.9 \pm 21.6 \%$  in the presence of the antagonist ( $n=3$ ). At  $3 \text{ }\mu\text{M}$ , RS10221 only partially inhibited the 5-HT-induced depolarisation, as the mean peak depolarisation reduced by  $6.8 \pm 15.6 \%$  ( $n=3$ ). The antagonist alone had no effect on membrane potential or input resistance.

Next, in order to investigate the involvement of the 5-HT<sub>2A</sub> receptor subtype, a selective 5-HT<sub>2A</sub> antagonist was tested. The 5-HT<sub>2A</sub> receptor antagonist R-96544 had no effect on the 5-HT-induced depolarisation at  $1 \text{ }\mu\text{M}$  ( $n=6$ ). However in the presence of  $10 \text{ }\mu\text{M}$  R-96544, there was a reduction in the peak membrane depolarisation induced by 5-HT from  $13.8 \pm 2.8 \text{ mV}$  to  $7.0 \pm 2.3 \text{ mV}$  in the presence of the antagonist, a  $53.1 \pm 6.7 \%$  reduction and a reduction in the 5-HT-induced increase in neuronal input resistance from  $249 \pm 26 \text{ M}\Omega$  in 5-HT alone to



106  $\pm$  110 M $\Omega$  in the presence of the antagonist (n=4; see figure 4.11A). This antagonist alone had no effect on activity of neurones.

Finally, the role of the 5-HT<sub>2B</sub> receptor subtype was investigated. The 5-HT<sub>2B</sub> receptor antagonist SB 204741 partially suppressed the 5-HT-induced depolarisation at 1  $\mu$ M (n=3; see figure 4.11B), with a reduction in mean peak depolarisation of 85.0  $\pm$  32.5 % compared to control in the absence of the antagonist. SB 204741 induced a slight depolarisation of the membrane when applied alone suggesting that this antagonist acted in part as an agonist.

To clarify whether the 5-HT<sub>1</sub> receptor is involved in mediating part of the 5-HT-induced depolarisation, the 5-HT<sub>1</sub> receptor antagonist cyanopindolol was tested on ARC neurones. This antagonist had no effect on activity of neurones by itself and had no effect on the 5-HT-induced depolarisation (10  $\mu$ M; n=3) suggesting that this receptor is not involved in the 5-HT-induced depolarisation.

These data suggest that the principal receptor subtypes involved in mediating the 5-HT-induced depolarisation are the 5-HT<sub>2A</sub>, 5-HT<sub>2B</sub> and 5-HT<sub>2C</sub> receptors.

These results suggest that 5-HT is able to excite a population of ARC neurones but the identity of ARC neurones that are excited by 5-HT remains unknown. In order to try to identify the types of ARC neurones that were excited by 5-HT, two methods were used. Firstly ghrelin, a marker of orexigenic neurones, was applied to neurones that had been exposed to 5-HT and responded with reversible depolarisation. Secondly, a double-labelling protocol was performed with CART, a marker for anorexigenic POMC neurones with which it co-localises (Elias *et al.*, 1998a).

#### 4.2.7 The effects of ghrelin on ARC neurones

Ghrelin is a 28 amino acid peptide, first identified as the endogenous ligand for the growth hormone secretagogue receptor (GHS-R; Kojima *et al.*, 1999). It is an orexigenic hormone that is released from the stomach, and both central and peripheral injections of ghrelin cause an increase in food intake and body-weight in rats and humans (Tschop *et al.*, 2000; Wren *et al.*, 2001a,b; Wang *et al.*, 2002; Faulconbridge *et al.*, 2003; Currie *et al.*, 2005). Ghrelin is reported to exert its effects in the arcuate nucleus via NPY/AgRP neurones, as NPY neurones in the ARC express the GHS-R (Willesen *et al.*, 1999) and ghrelin increases NPY and AgRP mRNA expression (Kamegai *et al.*, 2000, 2001). Antibodies and antagonists of NPY and AgRP abolish the orexigenic effects of ghrelin (Nakazato *et al.*, 2001). A population of hypothalamic neurones that express ghrelin and project to NPY neurones have also been discovered (Cowley *et al.*, 2003; Mondal *et al.*, 2005). Thus, in this study, ghrelin was used as a marker to identify orexigenic neurones as it is known to selectively target orexigenic neurones.

All ghrelin and associated 5-HT-induced responses were obtained in 10 mM glucose. Ghrelin (100-200 nM) was applied to 24 ARC neurones that responded to 5-HT with depolarisation. 58 % of these neurones did not respond to ghrelin. 42 % of these neurones responded with a depolarisation of the membrane upon ghrelin application, from a mean membrane potential of  $-50.5 \pm 2.4$  mV to  $-45.2 \pm 2.6$ , a mean peak depolarisation of  $5.3 \pm 0.9$  mV ( $n=10$ ; see figure 4.12). The ghrelin-induced depolarisation was slow in onset and caused an increase in the activity of these neurones. In a sub-population of neurones ghrelin was able to induce a burst-like pattern of firing (see figure 4.12Aii). Input resistance did not change in the presence of ghrelin, from  $1000 \pm 177$  M $\Omega$  to  $990 \pm 191$  M $\Omega$ , a reduction of



10  $\pm$  70 M $\Omega$ . These data suggest that 5-HT is able to excite a sub-population of both orexigenic neurones and other un-identified neurones.

#### 4.2.8 5-HT excites CART-expressing neurones

CART is a neuropeptide that has been shown to be involved in the regulation of feeding and energy homeostasis. CART was first identified as a mRNA that increased in the rat striatum after acute administration of cocaine or amphetamine (Douglass *et al.*, 1995). The administration of CART peptide fragments into the cerebral ventricles inhibits feeding whereas administration of CART antiserum increases feeding (Kristensen *et al.*, 1998; Lambert *et al.*, 1998). However injection of CART into the hypothalamic nuclei directly increases food intake (Abbott *et al.*, 2001). CART neurones have been shown to express the long form of the leptin receptor (Elias *et al.*, 2001) and in leptin deficient obese mice (*ob/ob*), there is a reduction in CART mRNA and upon repletion of leptin, CART expression is stimulated (Kristensen *et al.*, 1998). Taken together, these data suggest a key role at the level of the ARC for CART signalling in pathways regulating food intake and energy balance.

CART is expressed within the ARC in the hypothalamus (Douglass *et al.*, 1995; Koylu *et al.*, 1998; Elias *et al.*, 2001) and is co-localised in anorexigenic POMC neurones within the ARC (Elias *et al.*, 1998a). Therefore in this study, CART was used as a marker of anorexigenic neurones.

Alexa 633 (50  $\mu$ M) was added to the intracellular recording solution in order to be able to identify the neurones from which we recorded. 5-HT was applied to these neurones and then slices were subsequently stained for CART to identify if these neurones were CART-expressing or non-CART-expressing neurones. 5-HT

excited CART-expressing neurones (n=7; see figure 4.13A), or gave no response (n=1).

Non-CART positive neurones (see figure 4.13B) were excited by 5-HT (n=11), inhibited by 5-HT (n=10) or did not respond (n=6).

These data suggest that 5-HT is able to excite a population of CART-expressing neurones and hence excites anorexigenic neurones.

As well as being the primary metabolic fuel for neurones, a population of neurones within the ARC are able to sense glucose and alter their activity accordingly (Levin *et al.*, 2004). How such a key substrate affects the ability of ARC neurones to integrate extrinsic inputs and formulate responses was explored in this study. Neurones were recorded in both 10 mM and 2 mM glucose-containing aCSF and the response to 5-HT was recorded.

#### ***4.2.9 5-HT-induced responses in 10 mM and 2 mM glucose-containing aCSF***

Neurones were recorded in both 10 mM and 2 mM glucose-containing aCSF. 5-HT induced a depolarisation in 39 % (32/82) of neurones in 10 mM glucose-containing aCSF and 30 % (37/122) of neurones to which it was applied in 2 mM glucose-containing aCSF, a non-significant difference (chi-square test:  $P=0.2$ ). In 10 mM glucose-containing aCSF, 5-HT induced a peak membrane depolarisation of  $8.9 \pm 0.7$  mV (from a mean of  $-49.3 \pm 1.3$  mV to  $-40.4 \pm 1.3$  mV) and in 2 mM glucose-containing aCSF, 5-HT induced a peak membrane depolarisation of  $6.4 \pm 0.7$  mV, (from a mean of  $-50.2 \pm 1.1$  mV to  $-43.8 \pm 0.9$  mV), a significant difference between the two conditions ( $P<0.05$ ). Peak change in input resistance did



not significantly differ between both recording conditions (from  $1401 \pm 116 \text{ M}\Omega$  to  $1299 \pm 95 \text{ M}\Omega$  in 2 mM glucose and from  $1384 \pm 90 \text{ M}\Omega$  to  $1365 \pm 103 \text{ M}\Omega$  in 10 mM glucose;  $P=0.4$ ).

5-HT induced a hyperpolarisation in 17 % (14/82) of neurones to which it was applied in 10 mM glucose-containing aCSF and 37 % (45/122) in 2 mM glucose-containing aCSF, a significant difference between the two conditions (chi-square test:  $P<0.01$ ). In 10 mM glucose-containing aCSF, 5-HT induced a peak membrane hyperpolarisation of  $14.8 \pm 1.7 \text{ mV}$  (from an average of  $-44.2 \pm 2.4 \text{ mV}$  to  $-59.0 \pm 2.5 \text{ mV}$ ) and in 2 mM glucose-containing aCSF, 5-HT induced a peak membrane hyperpolarisation of  $12.7 \pm 0.9 \text{ mV}$  (from an average of  $-49.0 \pm 1.0 \text{ mV}$  to  $-61.6 \pm 1.2 \text{ mV}$ ), a non-significant difference between the two conditions ( $P=0.2$ ). The peak change in input resistance induced by 5-HT did not significantly alter between the two recording conditions (from an average of  $1608 \pm 264 \text{ M}\Omega$  to  $836 \pm 90 \text{ M}\Omega$  in 10 mM glucose and from  $1438 \pm 76 \text{ M}\Omega$  to  $915 \pm 67 \text{ M}\Omega$  in 2 mM glucose;  $P=0.1$ ).

5-HT induced no response in 44 % (36/82) of neurones to which it was applied in 10 mM glucose-containing aCSF and 33 % (40/122) in 2 mM glucose-containing aCSF, a non-significant difference (chi-square test:  $P=0.1$ ; see figure 4.14).

#### ***4.2.10 5-HT-induced responses in neurones classified into electrophysiological clusters***

In chapter three of this thesis, eight neuronal clusters were identified within the ARC based upon their electrophysiological properties. These clusters are

proposed to represent different functional groups within the ARC. The response to 5-HT would thus be expected to produce differential effects across these functional groups. Figure 4.15 shows a histogram showing the responsiveness of each cluster to 5-HT.

Cluster 1 neurones responded to 5-HT with inhibition in 54 % of neurones, excitation in 15 % of neurones and no response in 31 % of neurones (n=13).

Cluster 2 neurones responded to 5-HT with inhibition in all neurones tested (n=4). As these neurones have previously been characterised as NPY/AgRP neurones (van den Top *et al.*, 2004), this suggests that 5-HT is acting as an anorexigenic signal at the level of the ARC.

Neurones in cluster 3 responded to 5-HT with inhibition in 15 % of neurones, excitation in 46 % of neurones and did not respond in 39 % of neurones (n=13).

Cluster 4 neurones responded to 5-HT with inhibition in 42 % of neurones, excitation in 29 % of neurones and no response in 29 % of neurones (n=7).

Neurones classified as cluster 5 responded to 5-HT with inhibition in 20 % of neurones, excitation in 45 % of neurones and no response in 35 % of neurones (n=20).

Cluster 6 neurones responded to 5-HT with inhibition in 24 % of neurones, excitation in 37 % of neurones and no response in 39 % of neurones (n=41).

Neurones in cluster 7 responded to 5-HT with inhibition in 56 % of neurones, excitation in 6 % of neurones and no response in 38 % of neurones (n=16).

Cluster 8 neurones responded to 5-HT with inhibition in 75 % of neurones and excitation in 25 % of neurones (n=8). No neurones in this cluster failed to respond to 5-HT.



### 4.3 Discussion

In the present study, the effects of 5-HT on ARC neurones were investigated using the whole-cell patch-clamp technique. ARC neurones responded to 5-HT either with a depolarisation of the membrane, a hyperpolarisation of the membrane or they did not respond. This chapter focused on the excitatory effects of 5-HT.

5-HT produced an excitatory effect in 37 % of the ARC neurones it was applied to, resulting in a depolarisation of the membrane with either a concomitant increase, decrease or no change in input resistance. The 5-HT-induced depolarisation persisted in the presence of TTX, indicating a direct effect of 5-HT on the recorded neurone. In addition, 5-HT produced indirect effects on ARC neurones by altering synaptic activity.

24 % of neurones that were excited by 5-HT responded with an increase in neuronal input resistance. Current-voltage relationships showed a reversal potential around -91.5 mV indicating that the ionic mechanism most likely involves the closure of one or more resting potassium conductances. 41 % neurones responded with a decrease in input resistance with a reversal potential indicated around -39.5 mV, suggesting activation of a non-selective cation conductance mediating part of the 5-HT-induced depolarisation. 35 % neurones had no change in resistance associated with the 5-HT-induced excitation, with the current-voltage relationship showing a parallel shift indicating activation of an electrogenic pump in the membrane or activation/inhibition of a combination of potassium and non-selective cation conductances. This mechanism was also confirmed by performing voltage-clamp ramps, whereby a parallel shift was obtained. A previous study has reported that 5-HT excites tuberomammillary neurones via a  $\text{Na}^+/\text{Ca}^{2+}$  exchanger and therefore it is possible that this exchanger may be mediating the effects seen here

(Eriksson *et al.*, 2001). This would need further investigation using specific blockers for this pump. Overall, these data suggest that multiple conductances and mechanisms are responsible for mediating the 5-HT-induced depolarisation. This is in agreement with a study in subthalamic neurones which showed that a combination of conductances are involved in the 5-HT-induced excitation (Shen *et al.*, 2007).

As well as inducing a membrane depolarisation, 5-HT was also able to induce membrane potential oscillations in a sub-population of ARC neurones, which were associated with a pattern of bursts of action potential firing. The significance of these membrane potential oscillations and burst-like pattern of firing is unclear but maybe related to the release of neuropeptides from ARC neurones. This is suggested by previous studies that have shown that the pattern of action potential discharge is an important factor for the rate of neuropeptide release from neurones. Studies have shown that burst-like patterns of action potential discharge facilitate the release of vasopressin from nerve terminals of magnocellular neurones located in the posterior pituitary (Dutton & Dyball, 1979; Bicknell & Leng, 1981). Therefore if this also applies to neurones within the ARC, burst-like firing patterns induced by 5-HT may be important for the release of neuropeptides. Within the ARC, a burst-like pattern of firing has been shown in orexigenic NPY neurones (van den Top *et al.*, 2004). Therefore 5-HT may facilitate the release of peptides related to energy homeostasis, for example  $\alpha$ -MSH.

In order to determine which receptors were mediating the 5-HT-induced depolarisation of the membrane, a range of agonists and antagonists for 5-HT receptors were used. The 5-HT-induced depolarisation was mimicked by the 5-HT<sub>2</sub> preferential receptor agonist  $\alpha$ -methyl 5-HT, suggesting that the 5-HT<sub>2</sub> receptor is involved in the excitatory effects of 5-HT on ARC neurones. The  $\alpha$ -methyl 5-HT-



induced depolarisation was associated with both an increase and decrease in input resistance. The 5-HT<sub>1/5/7</sub> receptor agonist 5-CT also mimicked the depolarisation with a minimal increase in input resistance, yet the 5-HT<sub>1A/7</sub> receptor agonist 8-OH-DPAT and the 5-HT<sub>3</sub> receptor agonist mCPBG did not mimic the 5-HT-induced excitation. These results indicate that the 5-HT-induced depolarisation may be mediated by several receptors through different mechanisms. Different subtypes of the 5-HT<sub>2</sub> receptor may be responsible for at least two different mechanisms; one may be responsible for an increase in input resistance and another may be responsible for a decrease in input resistance. The 5-HT<sub>1/5</sub> receptors may be responsible for the 5-HT-induced depolarisation associated with either no change or a small increase in input resistance. Further work looking at the mechanisms underlying the agonist responses and 5-HT responses in the presence of antagonists would help clarify this.

A range of antagonists were then tested to determine further which receptors were involved in the 5-HT-induced depolarisation. The 5-HT<sub>2</sub> receptor antagonist altanserin attenuated the 5-HT-induced depolarisation in a concentration-dependent manner, providing further evidence for a 5-HT<sub>2</sub> receptor mediating this response. In order to clarify further the subtypes involved, specific antagonists for the 5-HT<sub>2A/B/C</sub> subtypes were then tested. The 5-HT<sub>2C</sub> receptor antagonist RS102221 partially inhibited the 5-HT-induced depolarisation, as did the 5-HT<sub>2A</sub> receptor antagonist R-96544 and the 5-HT<sub>2B</sub> receptor antagonist SB 204741. The 5-HT<sub>2A</sub> receptor antagonist R-96544 also reduced the 5-HT-induced increase in neuronal input resistance and the 5-HT<sub>2C</sub> receptor antagonist RS102221 reduced the 5-HT-induced decrease in neuronal input resistance. Further studies need to be carried out to

elucidate if the specific subtypes are specifically associated with either an increase or decrease in input resistance and are hence responsible for different mechanisms.

These results indicate that the 5-HT<sub>2A/2B/2C</sub> receptors all play an important role in mediating the 5-HT-induced depolarisation and are in accordance with previous studies that have suggested the involvement of the 5-HT<sub>2C</sub> receptor in mediating the excitatory effects of 5-HT on ARC neurones (Heisler *et al.*, 2002). The 5-HT<sub>2C</sub> receptor has been shown to play an important role in energy homeostasis as 5-HT<sub>2C</sub> knockout mice develop hyperphagia (Tecott *et al.*, 1995), whilst mice with a mutated form of the 5-HT<sub>2C</sub> receptor also show signs of hyperphagia (Nonogaki *et al.*, 1998). Therefore these data suggest that the excitatory effects of 5-HT through the 5-HT<sub>2</sub> receptor subtypes may play an essential role in controlling energy homeostasis. The 5-HT<sub>1</sub> receptor antagonist cyanopindolol did not block the 5-HT-induced depolarisation, suggesting that the 5-HT<sub>1</sub> receptor is not involved. It has previously been shown that 5-HT hyperpolarises ARC neurones through the 5-HT<sub>1B</sub> receptor and therefore it seems likely that the 5-HT<sub>1</sub> receptor may be responsible for mediating 5-HT-induced hyperpolarisations, not depolarisations (Heisler *et al.*, 2006).

Studies in neurones outside the ARC have also suggested a role for the 5-HT<sub>2</sub> or 5-HT<sub>2C</sub> receptor in mediating 5-HT-induced depolarisations. These include prefrontal cortex neurones (Araneda & Andrade, 1991), sympathetic preganglionic neurones (SPNs; Lewis *et al.*, 1993; Pickering *et al.*, 1994), inferior olivary neurones (Placantonakis *et al.*, 2000), striatal cholinergic interneurones (Blomeley & Bracci, 2005), subthalamic nucleus neurones (Stanford *et al.*, 2005; Xiang *et al.*, 2005; Shen *et al.*, 2007) and PVN neurones (Heisler *et al.*, 2007). However an additional study in the PVN showed that 5-HT-induced depolarisation was not due to 5-HT<sub>2A/2C</sub>



receptors but instead was due to 5-HT<sub>4</sub> and 5-HT<sub>7</sub> receptors (Ho *et al.*, 2007). Results shown here however also provide novel evidence for the involvement of 5-HT<sub>2A</sub> and 5-HT<sub>2B</sub> receptors mediating the 5-HT-induced depolarisation of ARC neurones.

The study then went on to try to identify types of neurones in the ARC that responded to 5-HT with depolarisation. One way in which this was done was by testing the effects of ghrelin. Ghrelin is an orexigenic hormone produced from the stomach and in a small population of neurones within the brain, and is known to potently increase food intake and body-weight in rodents (Kojima *et al.*, 1999; Tschop *et al.*, 2000). Ghrelin was applied to a number of ARC neurones that had been depolarised by 5-HT. Ghrelin caused a depolarisation of the membrane in 42 % of these neurones but 58 % did not respond to ghrelin. As ghrelin is known to selectively activate orexigenic neurones, these results imply that there is a population of orexigenic neurones that are depolarised by 5-HT, with a larger population of non-orexigenic neurones that are depolarised by 5-HT. It has been shown that a small population of POMC neurones do contain the ghrelin receptor, the GHS-R, (Willesen *et al.*, 1999) and so ghrelin appears able to excite a small population of anorexigenic neurones as well as orexigenic neurones. However, it is unlikely that 5-HT depolarises orexigenic neurones as 5-HT functions to inhibit feeding and is therefore more likely to target anorexigenic neurones. This was investigated using immunohistochemistry, by processing alexa-labelled neurones for CART.

CART is an anorexigenic peptide that is co-expressed with POMC neurones (Elias *et al.*, 1998a). 5-HT excited CART-expressing neurones indicating that 5-HT excites anorexigenic neurones. However, 5-HT also excited non-CART expressing neurones, as well as inhibiting or having no effect on them. This indicates that 5-HT

is able to excite both anorexigenic neurones as well as a population of unidentified ARC neurones. These neurones could potentially be orexigenic neurones such as NPY or other unidentified anorexigenic neurones such as neuromedin U or GALP. Alternatively these ARC neurones could have functions unrelated to feeding and energy homeostasis, for example they may be involved in pain responses or reproduction. Further double-labelling experiments would need to be performed in order to characterise the other types of neurones in the ARC that are excited by 5-HT.

As well as being critically dependent on glucose for their fuel, specialised groups of neurones use glucose to alter their activity. Glucose-sensing neurones are specialised neurones that change their electrical activity in response to changes in extracellular glucose concentration (Anand *et al.*, 1964; Oomura *et al.*, 1964; Levin *et al.*, 2004). The ability of ARC neurones to respond to extrinsic factors such as 5-HT may be altered under different glucose concentrations therefore in this study the effects of 5-HT on neurones recorded in 10 mM and 2 mM glucose-containing aCSF was investigated. There was an increase in the percentage of neurones responding with depolarisation or no response in 10 mM compared to 2 mM glucose-containing aCSF although this did not reach statistical significance. In 10 mM glucose-containing aCSF there was also a significant increase in the amplitude of the peak depolarisation. There was a significant reduction in the percentage of neurones responding with hyperpolarisation in 10 mM compared to 2 mM glucose-containing aCSF, although there was no significant difference in the amplitude of the hyperpolarisation. Input resistance did not significantly change in neurones recorded in both conditions.



These data indicate that glucose affects the ability of ARC neurones to respond to extrinsic factors. In this case, under higher glucose conditions, ARC neurones responded to 5-HT with an increased number of depolarisations and a reduction in hyperpolarisations. These results correlate with the glucose-sensing functions of NPY and POMC neurones within the ARC. NPY neurones are inhibited by increases in glucose (Muroya *et al.*, 1999) whereas POMC neurones are excited by increases in glucose (Ibrahim *et al.*, 2003). Therefore in 10 mM glucose, which represents a hyperglycaemic state, NPY neurones should respond with inhibition and POMC neurones should respond with excitation. As 5-HT is known to potently inhibit feeding (Blundell, 1984), one way in which this may occur is through the inhibition of NPY neurones and excitation of POMC neurones. In 10 mM glucose there was a decrease in the percentage of inhibitions and an increase in the percentage of excitations by 5-HT. This could indicate that 5-HT acting at high glucose concentrations has a preferential role of exciting POMC neurones rather than inhibiting NPY neurones.

The ability of ARC neurones to integrate inputs and produce responses is therefore altered under different glucose states. It may be that glucose affects the expression of 5-HT receptors and in different glucose concentrations different levels of 5-HT receptors may be expressed. In higher glucose, more 5-HT<sub>2</sub> receptors may be expressed leading to more depolarisations and in lower glucose more 5-HT<sub>1</sub> receptors, which are thought to mediate the 5-HT-induced hyperpolarisation, may be expressed. Overall these data indicate glucose as a key signalling molecule affecting the ability of ARC neurones to respond to extrinsic factors.

In conclusion, this study has demonstrated that 5-HT directly excites a population of ARC neurones, including identified CART neurones, via 5-HT<sub>2A</sub>, 5-HT<sub>2B</sub> and 5-HT<sub>2C</sub> receptors. Several mechanisms are involved in this depolarisation, namely the activation of a potassium channel, a non-selective cation channel or a mixture of the two, or possibly through activation of an electrogenic pump in the membrane.



**Figure 4.1 5-HT differentially regulates ARC neurones**

**A:** Samples of a continuous whole-cell current-clamp recording from an ARC neurone with a resting membrane potential of  $-45$  mV (shown to the left of the trace in this and subsequent figures). Application of 5-HT ( $50$   $\mu$ M), as indicated by the line above the trace, induced a membrane hyperpolarisation and associated decrease in neuronal input resistance, indicated by the decrease in amplitude of electrotonic potentials (downward deflections of the trace) evoked in response to hyperpolarising rectangular-wave current pulses ( $5$ - $30$  pA,  $1$  s,  $0.2$  Hz; not shown). The large sequential downward and upward deflections in the middle of the response indicate where an I-V was taken.

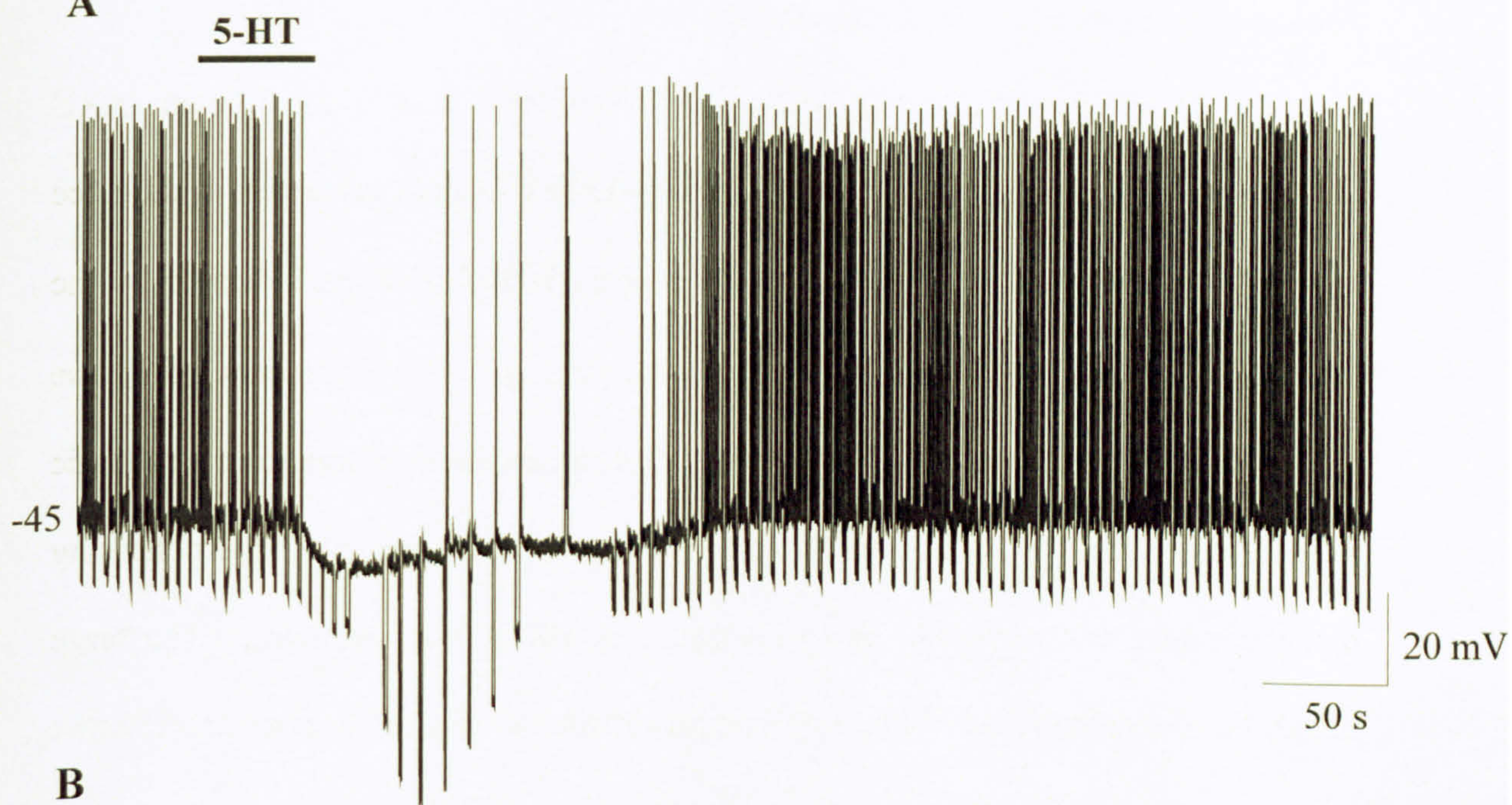
**B:** A pie chart showing the membrane responses of 122 ARC neurones to application of 5-HT. Neurones responded either with a membrane hyperpolarisation ( $45/122$ ; example shown in A), depolarisation ( $37/122$ ; example shown in C), or they did not respond ( $40/122$ ).

**C:** Samples of a continuous whole-cell current-clamp recording from an ARC neurone showing 5-HT-induced depolarisation and an increase in action potential firing.

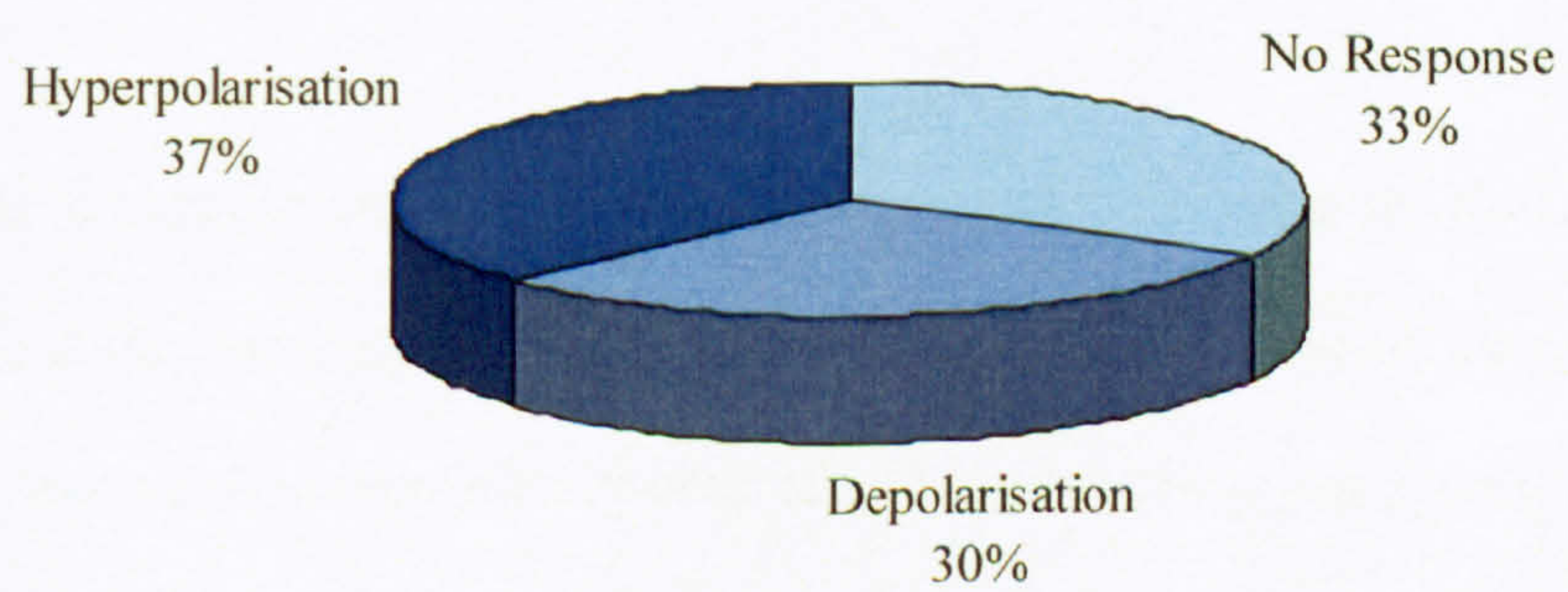


**Figure 4.1**

**A**



**B**



**C**

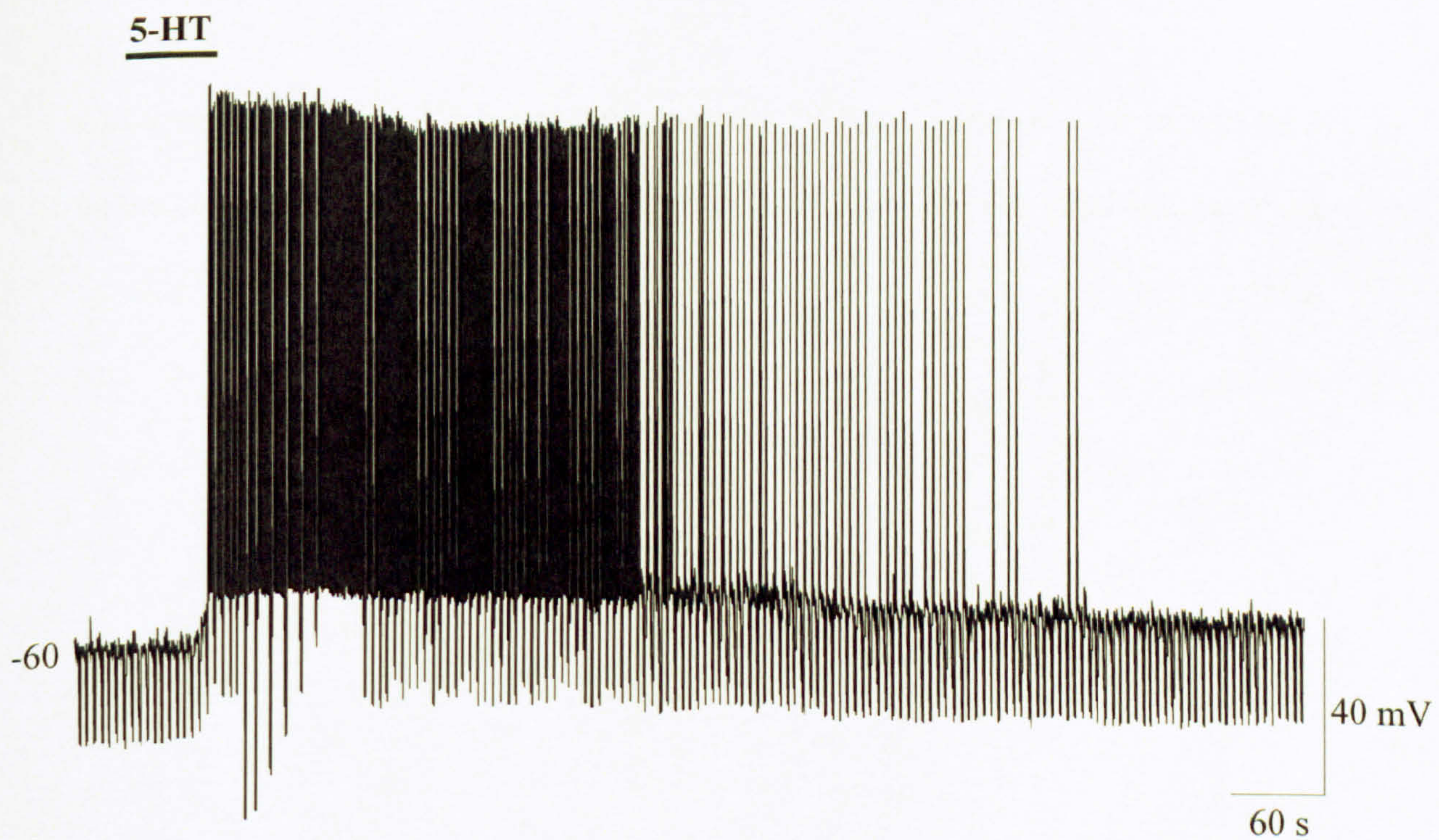




**Figure 4.2 5-HT directly excites a population of ARC neurones with a concomitant increase in input resistance**

**Ai:** Samples of a continuous whole-cell current-clamp recording from an ARC neurone in the presence of TTX (500 nM). Application of 5-HT (50  $\mu$ M) induced a membrane depolarisation and associated increase in neuronal input resistance, indicated by the increase in amplitude of electrotonic potentials (downward deflections of the trace) evoked in response to hyperpolarising rectangular-wave current pulses (not shown), seen during a period of constant negative current injection to eliminate any voltage-dependent effects (as shown by arrows). Note the 5-HT-induced depolarisation persists in the presence of TTX.

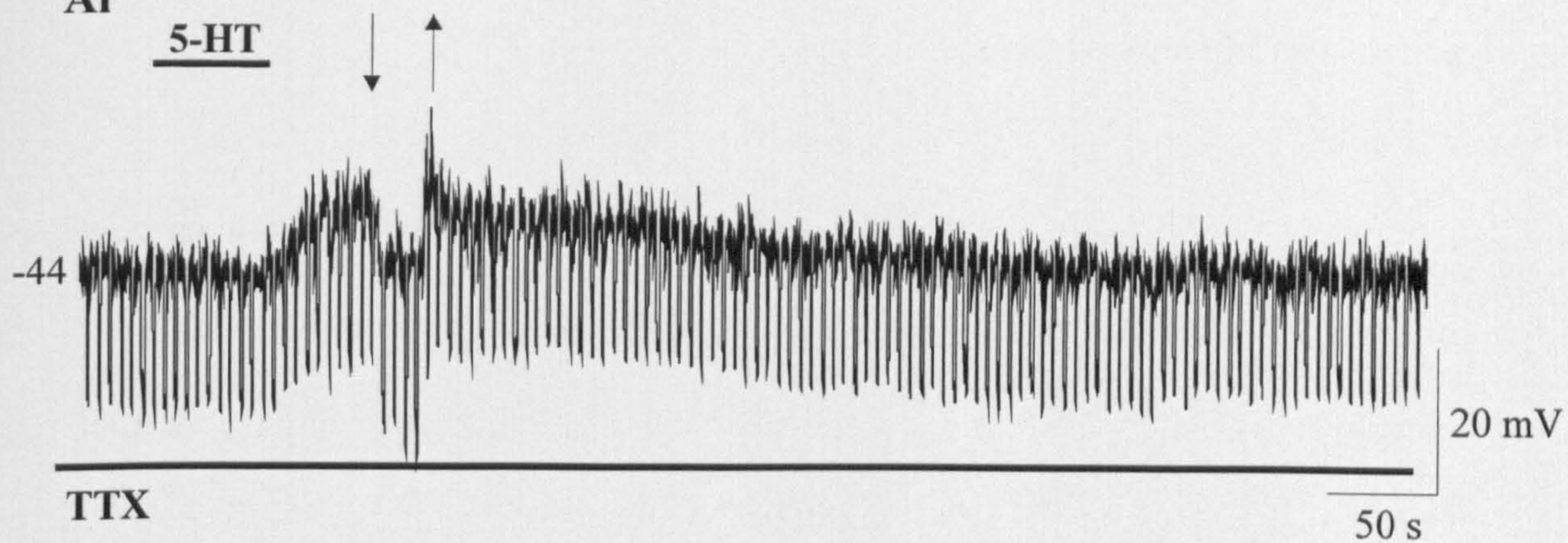
**Aii:** Superimposed samples from a continuous whole-cell current-clamp recording showing membrane potential responses of an ARC neurone to a series of depolarising and hyperpolarising rectangular-wave current pulses of constant increment (-35 to +35 pA, 1 s, 0.1 Hz) before and in the presence of 5-HT.

**Aiii:** Plot of the current-voltage (I-V) relationships before ( $\circ$ ) and in the presence of 5-HT ( $\bullet$ ), shown in Aii. Note the increase in the slope of the I-V in the presence of 5-HT indicating an increase in neuronal resistance, with a reversal potential around -88 mV.



**Figure 4.2**

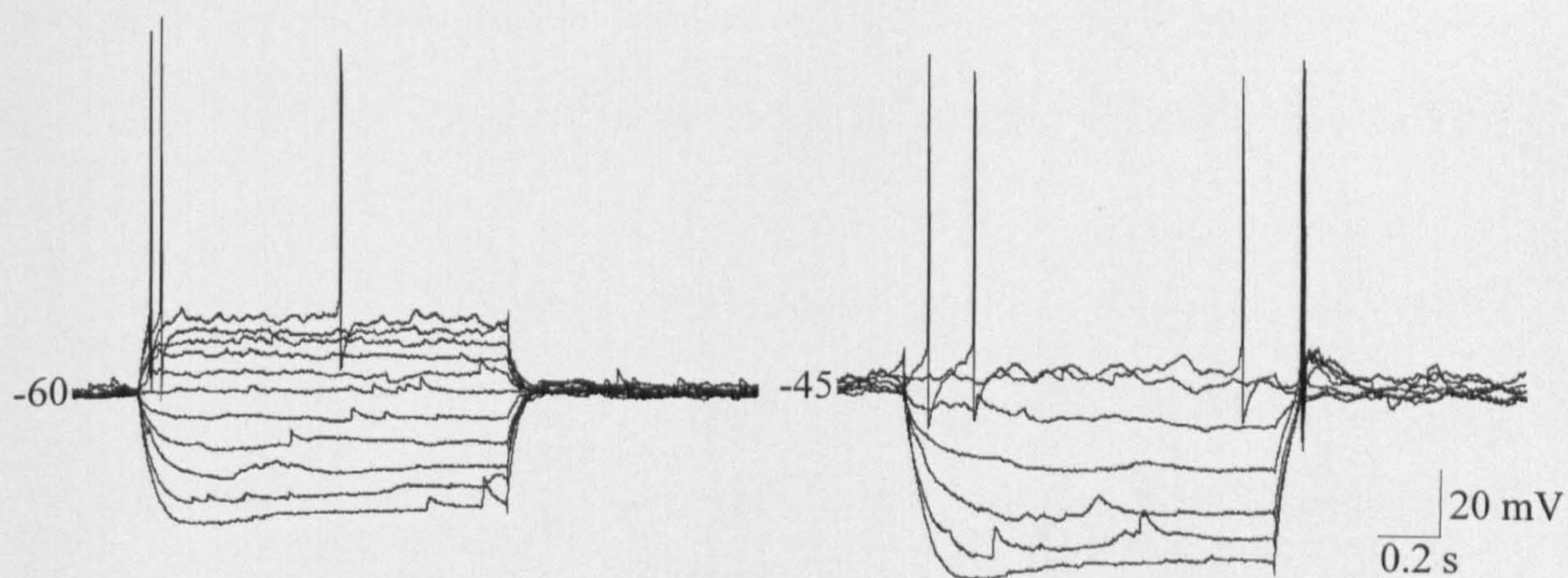
**Ai**



**Aii**

**Control**

**5-HT**



**Aiii**

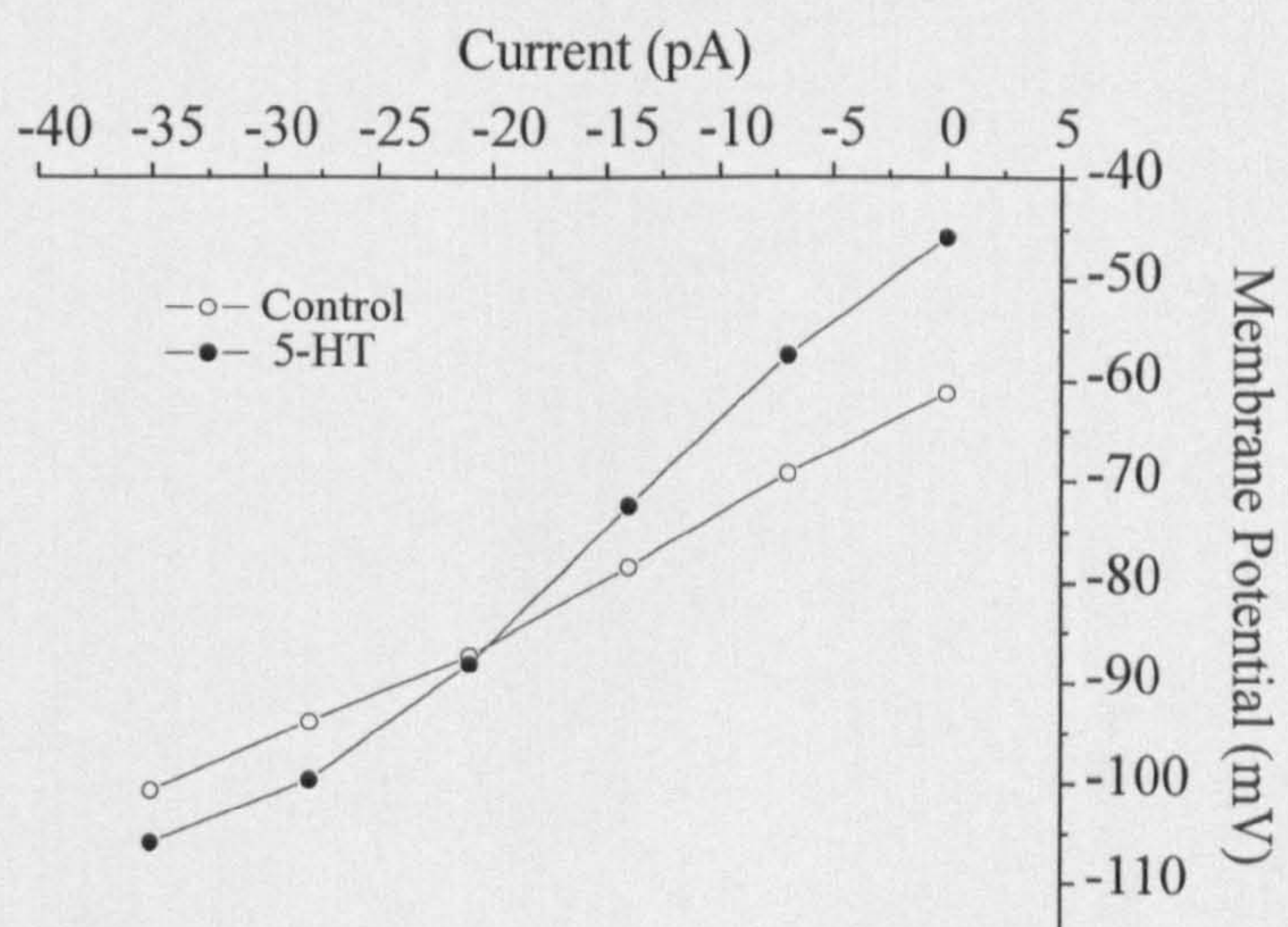




**Figure 4.3 5-HT excites a sub-population of ARC neurones with a concomitant decrease in input resistance**

**Ai:** Samples of a continuous whole-cell current-clamp recording from an ARC neurone showing 5-HT-induced (50  $\mu$ M) depolarisation and increase in firing frequency.

**Aii:** Superimposed samples of a continuous whole-cell current-clamp recording showing membrane potential responses of the ARC neurone shown in Ai to a series of depolarising and hyperpolarising rectangular-wave current pulses, before (-80 to +16 pA, 1 s, 0.1 Hz) and in the presence of 5-HT (-100 to +20 pA, 1 s, 0.1 Hz).

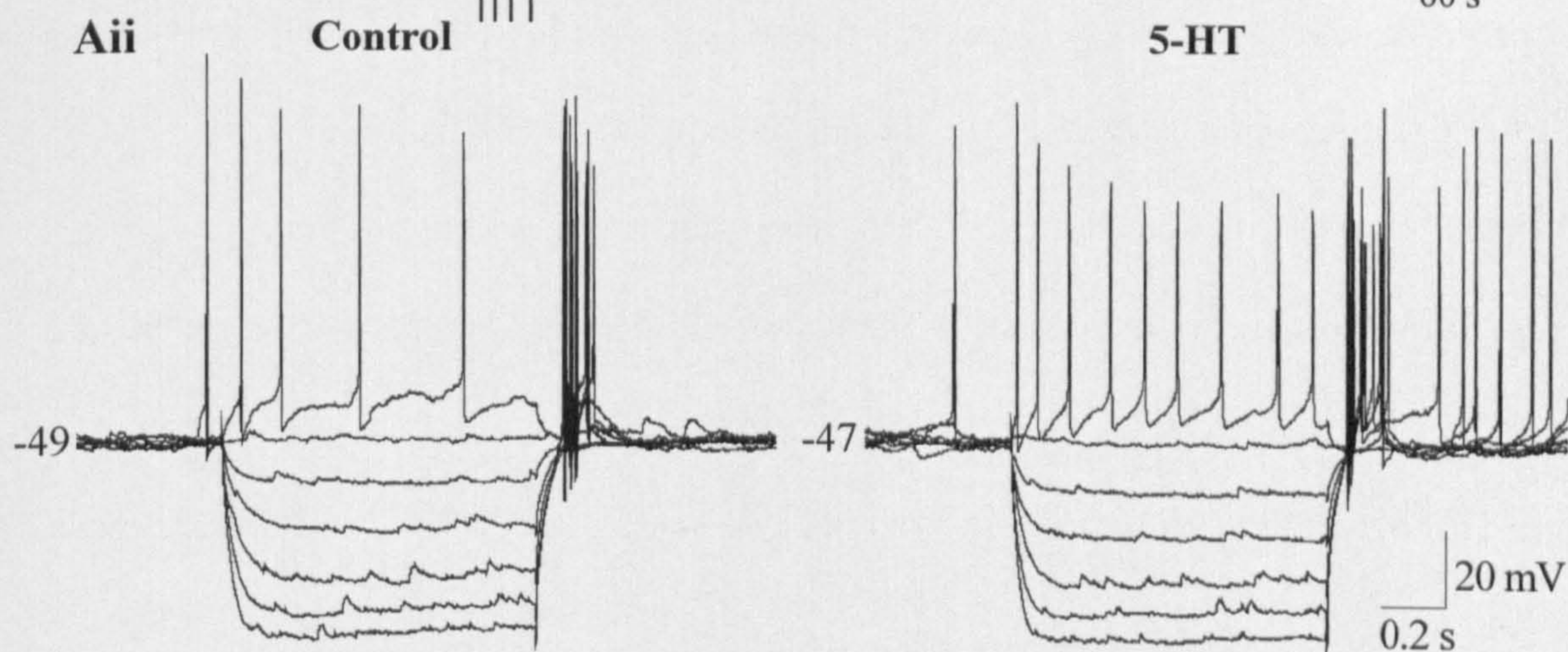
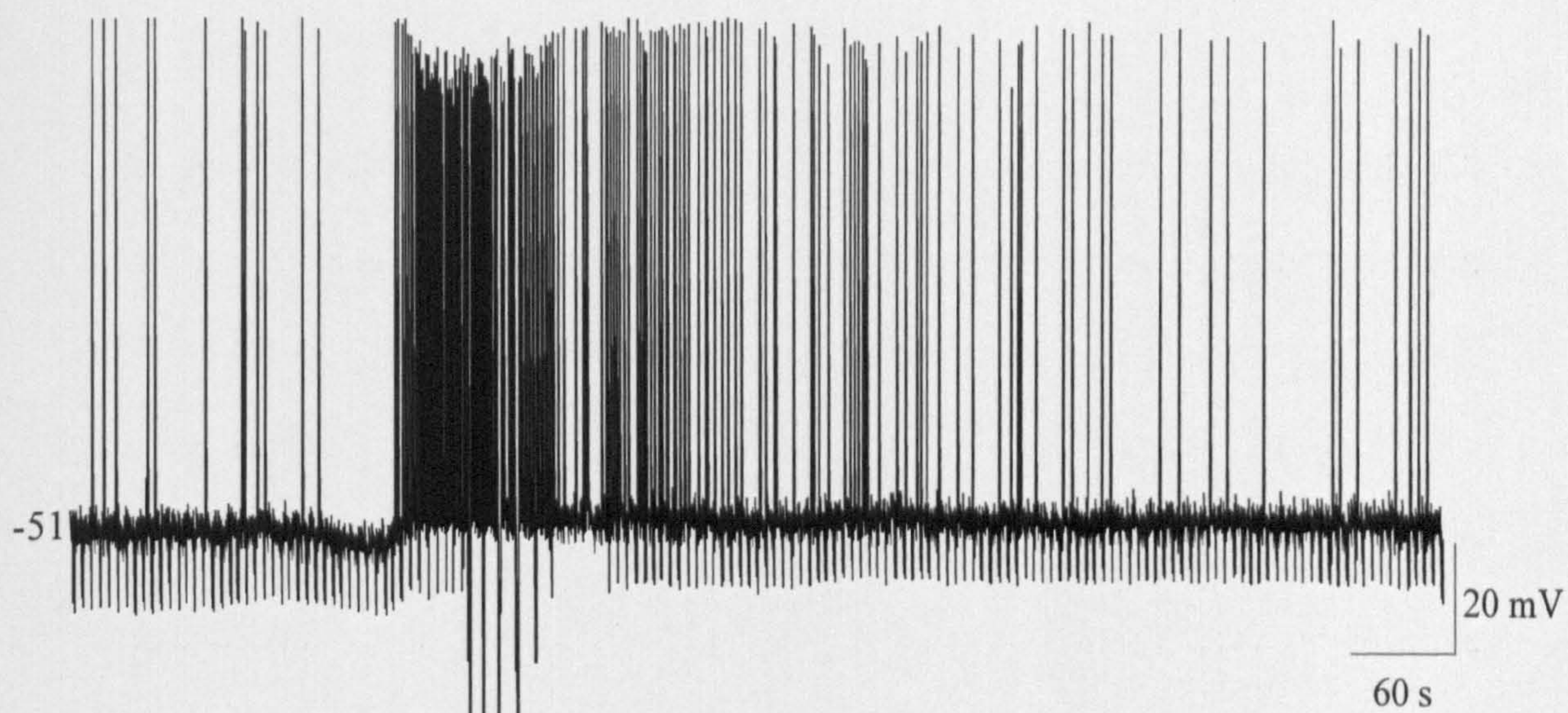
**Aiii:** Plot of the current-voltage (I-V) relationships before ( $\circ$ ) and in the presence of 5-HT ( $\bullet$ ), shown in Aii. Note the decrease in the slope of the I-V in the presence of 5-HT indicating a decrease in neuronal resistance, tending towards a reversal potential, when extrapolated, of -42 mV.



**Figure 4.3**

**Ai**

**5-HT**



**Aiii**

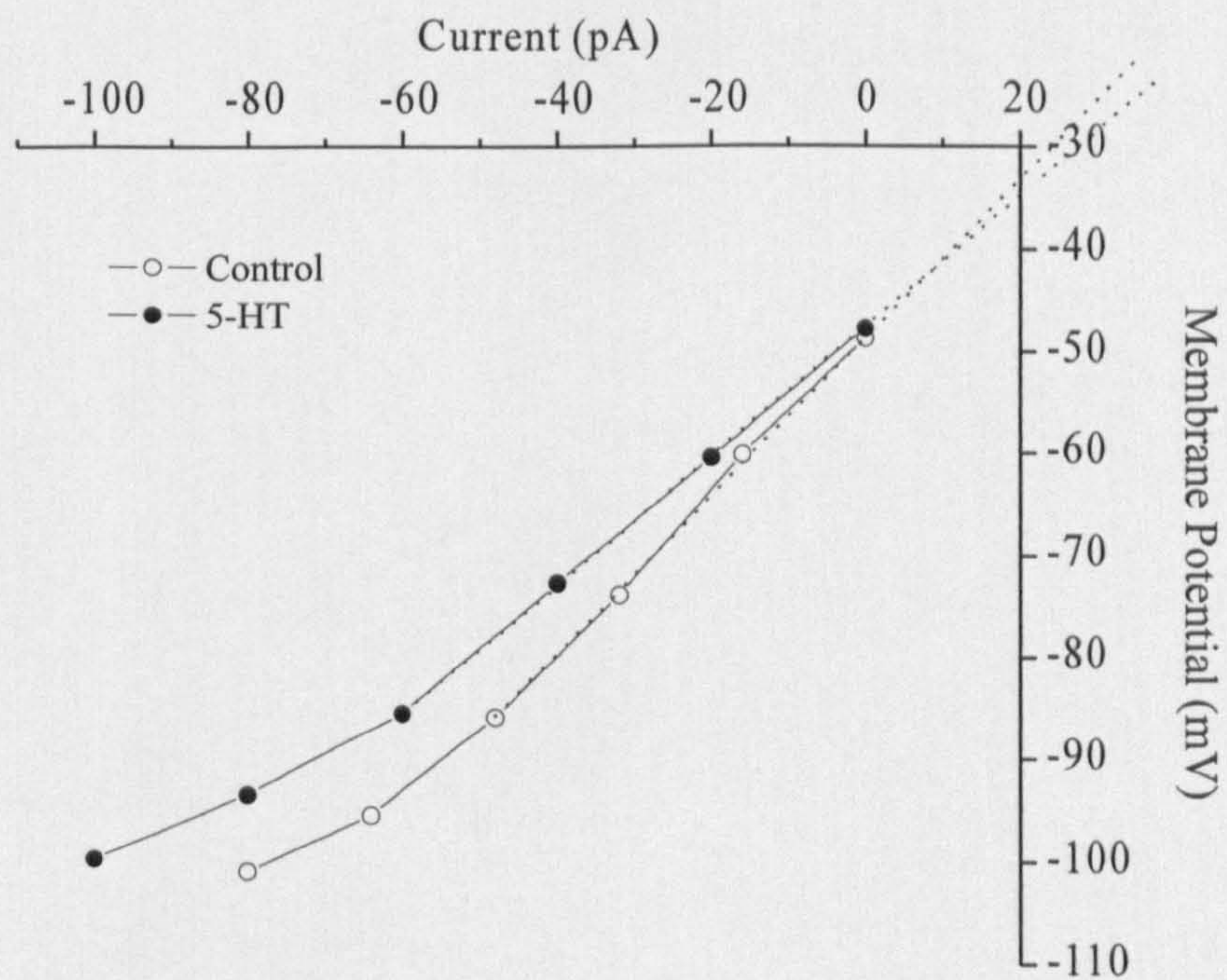




**Figure 4.4 5-HT excites a sub-population of ARC neurones: a response associated with no change in input resistance**

**Ai:** Samples of a continuous whole-cell current-clamp recording from an ARC neurone showing 5-HT-induced depolarisation (50  $\mu$ M).

**Aii:** Superimposed samples from a continuous whole-cell current-clamp recording showing membrane potential responses of the ARC neurone, shown in Ai, to a series of depolarising and hyperpolarising rectangular wave current pulses, before and in the presence of 5-HT (-25 to +10 pA, 1 s, 0.1 Hz).

**Aiii:** Plot of the current-voltage (I-V) relationships before ( $\circ$ ) and in the presence of 5-HT ( $\bullet$ ), shown in Aii. Note the parallel shift between the plots indicating no change in input resistance.



**Figure 4.4**

**5-HT**

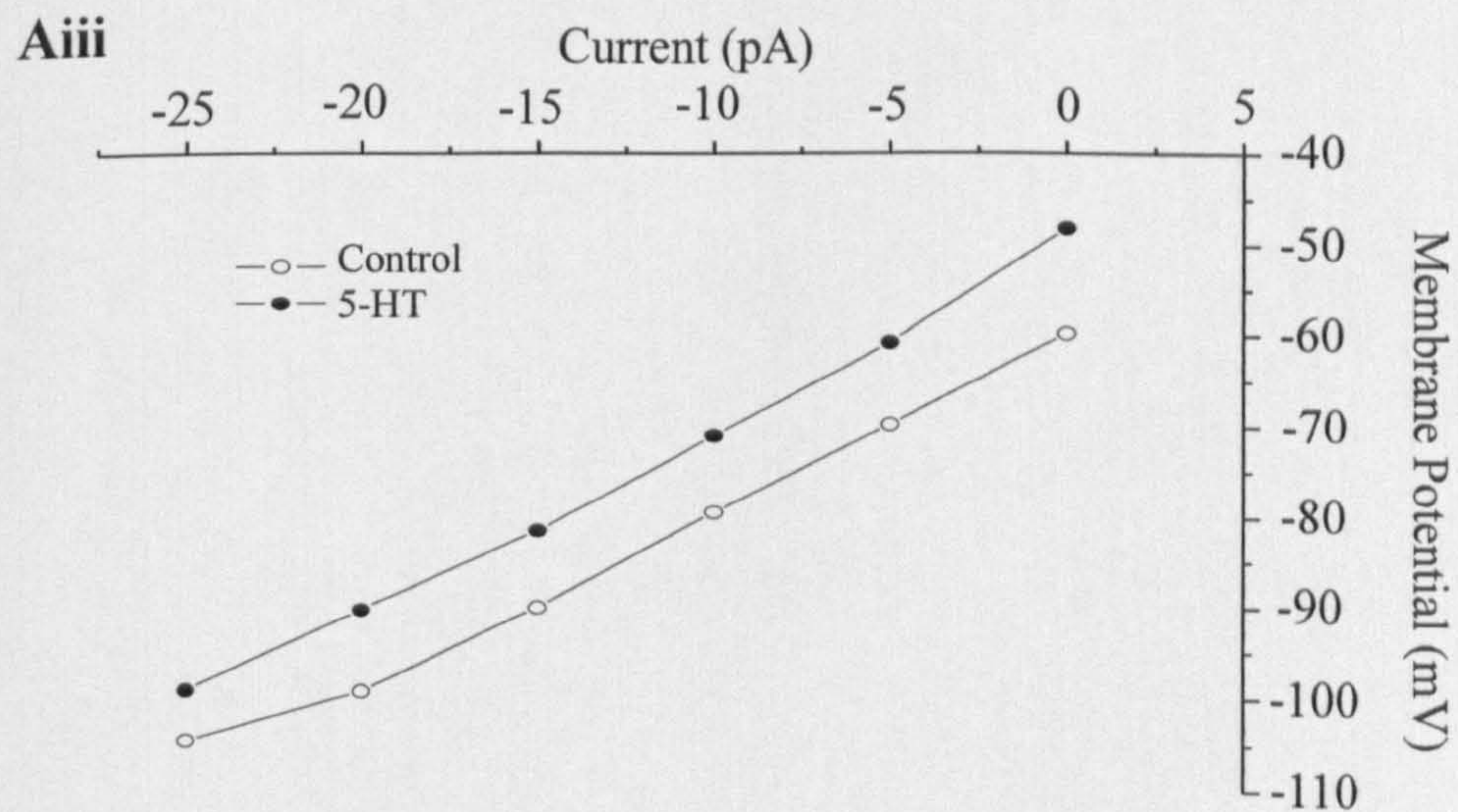
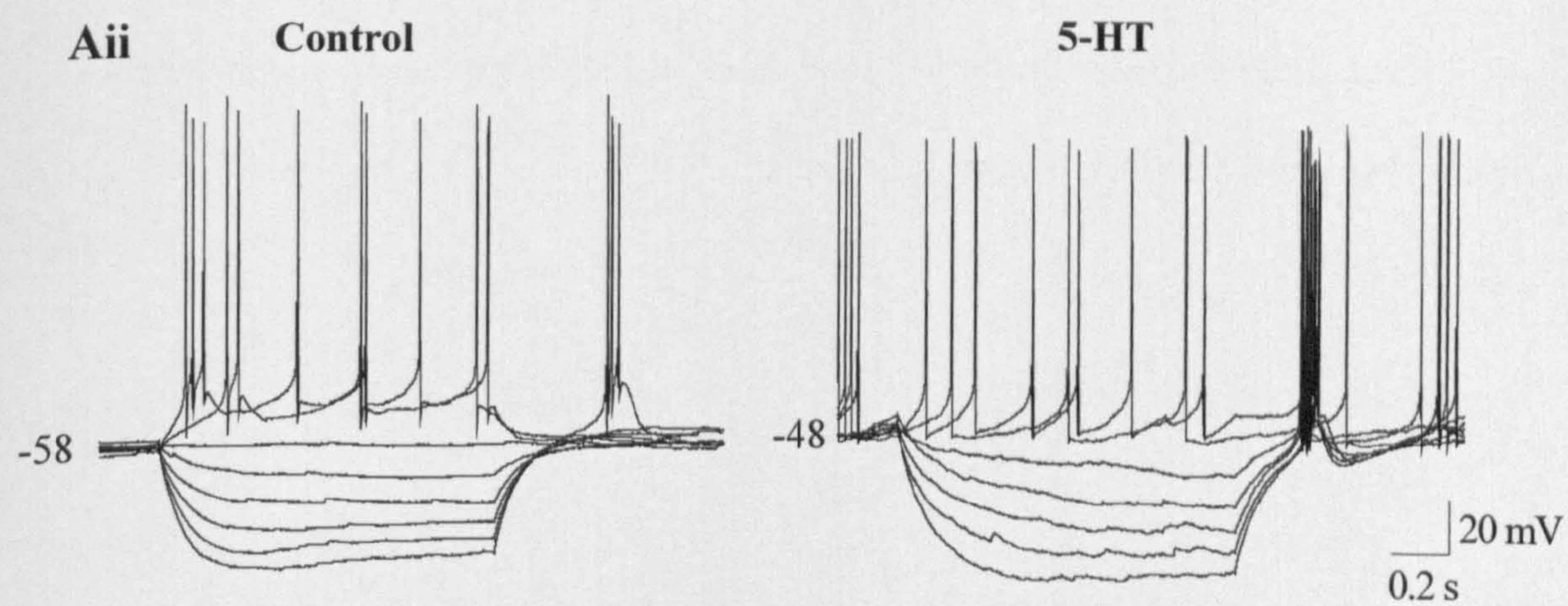
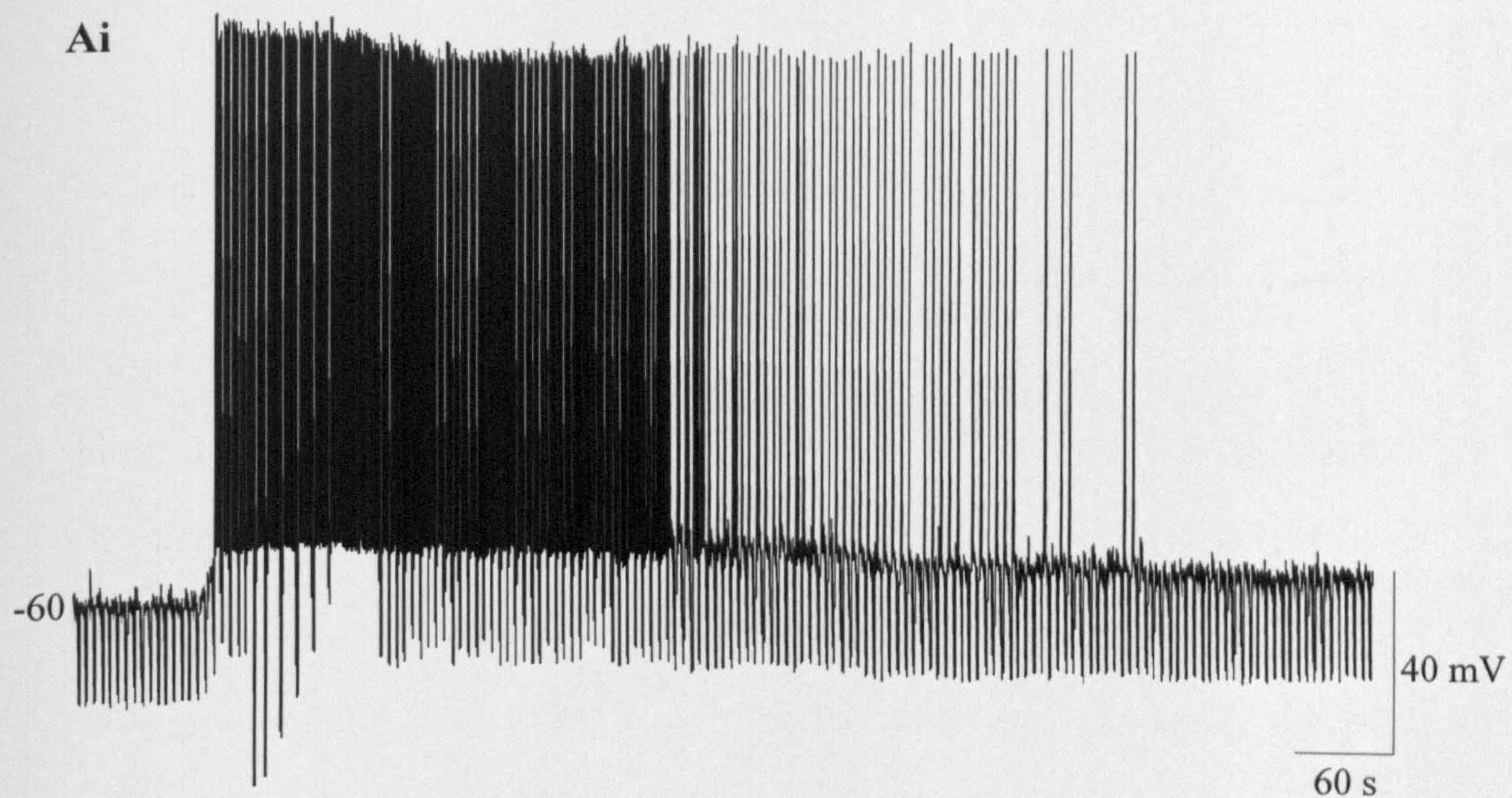




**Figure 4.5 5-HT induces an inward current in ARC neurones**

**A:** Application of 5-HT (50  $\mu$ M) to an ARC neurone clamped at a holding potential of -40 mV (in voltage-clamp mode) induced an inward current and increased the frequency and amplitude of IPSCs (upward deflections) and EPSCs (downward deflections). The IPSCs were reversed in direction by changing the holding potential to -80 mV.

**B:** Current responses obtained in voltage-clamp in the presence (green trace) and absence (black trace) of 5-HT (50  $\mu$ M). The currents were obtained from ramp protocols that drove the holding potential from -130 mV to -30 mV, at a rate of 10 mV per second. These responses are parallel indicating that there was no change in conductance in this neurone.



**Figure 4.5**

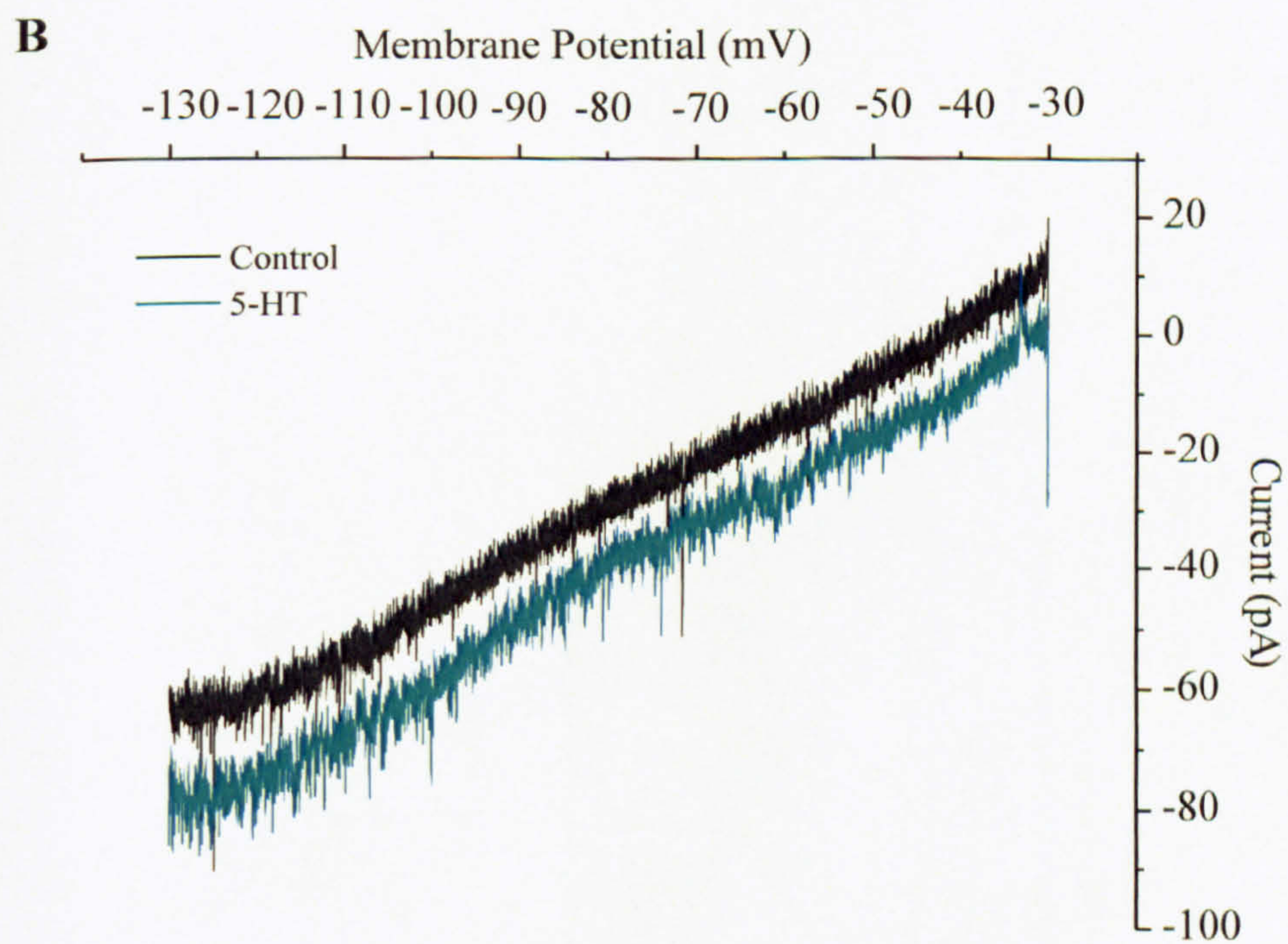
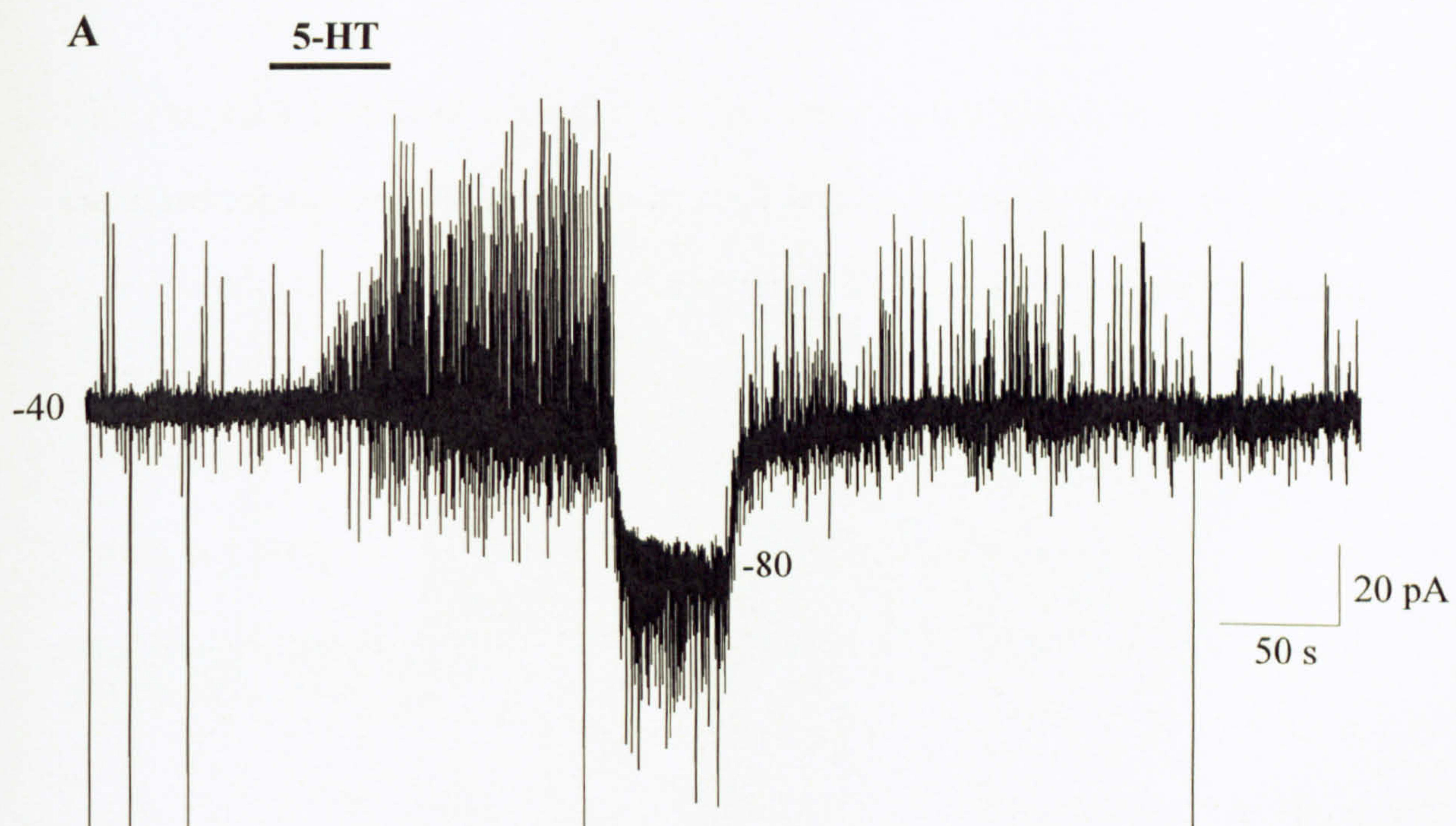




**Figure 4.6 5-HT induces a burst-like pattern of firing in some ARC neurones**

**Ai:** Samples of a continuous whole-cell current-clamp recording from an ARC neurone showing 5-HT-induced (50  $\mu$ M) depolarisation and induction of a burst-like pattern of firing.

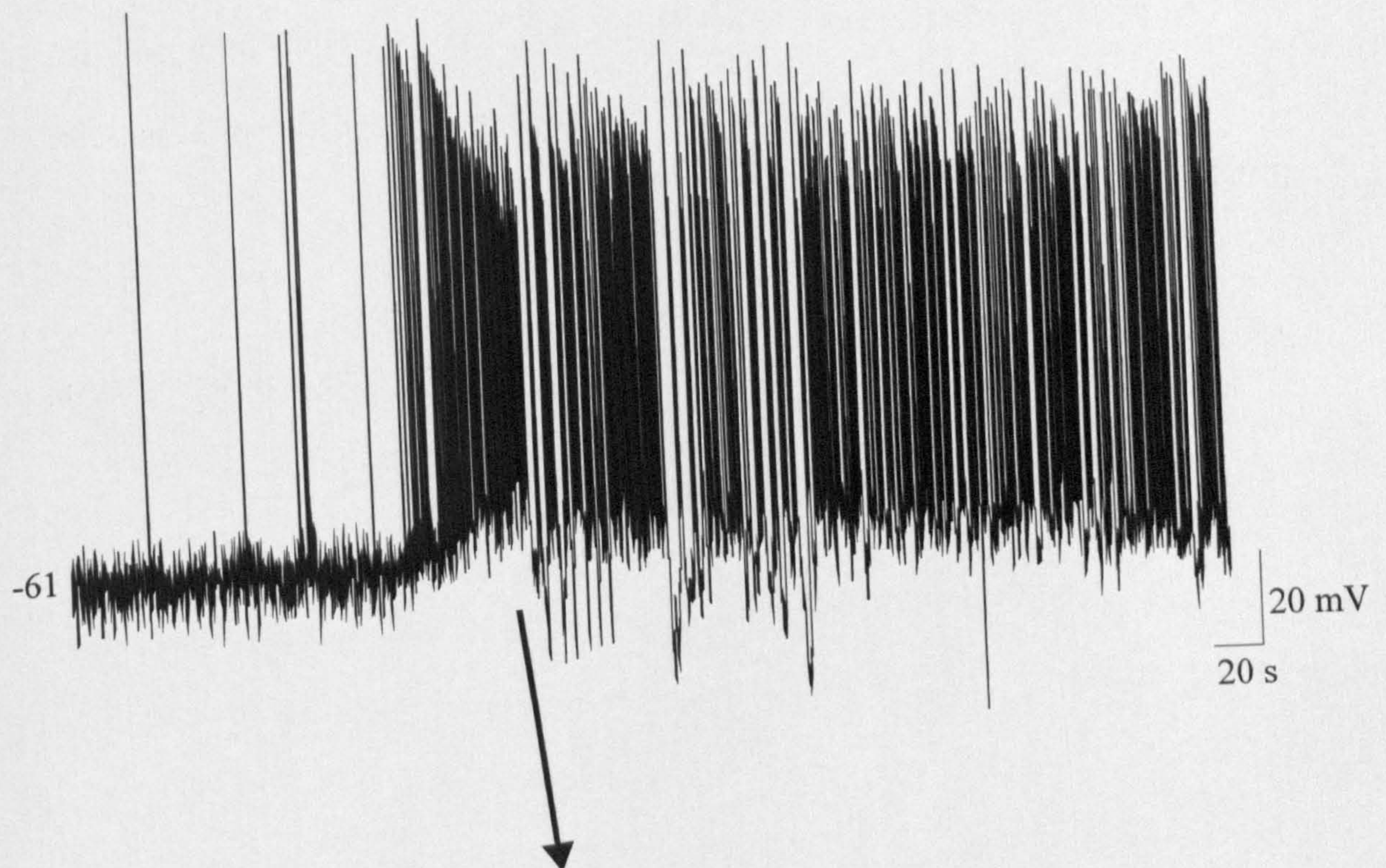
**Aii:** Expanded region, as indicated by the arrow, from the neurone shown in Ai, showing membrane potential oscillations with associated bursts of action potentials.



**Figure 4.6**

**Ai**

**5-HT**



**Aii**

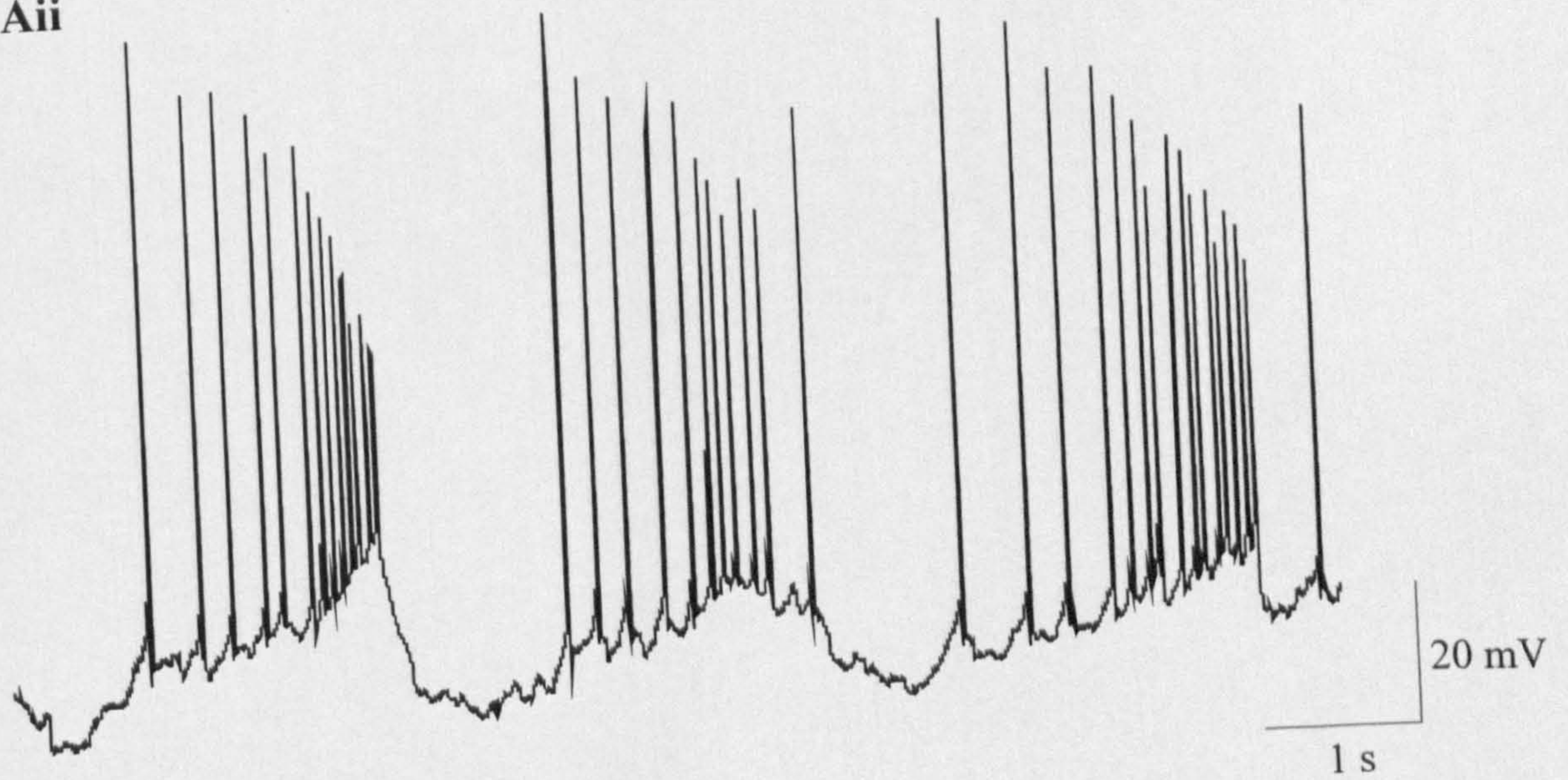




**Figure 4.7 5-HT-induced changes in spontaneous synaptic activity**

**Ai:** Samples of a continuous whole-cell current-clamp recording from an ARC neurone showing 5-HT-induced (50  $\mu$ M) depolarisation and induction of spontaneous IPSPs.

**Aii:** Expanded regions from the neurone shown in Ai, showing few spontaneous IPSPs in the control and upon application of 5-HT, the induction of IPSPs.

**Bi:** Samples of a continuous whole-cell current-clamp recording from an ARC neurone showing 5-HT-induced depolarisation and a reduction in spontaneous EPSPs.

**Bii:** Expanded regions from the neurone shown in Bi, showing spontaneous EPSPs in the control period and their subsequent reduction or loss in the presence of 5-HT.



**Figure 4.7**

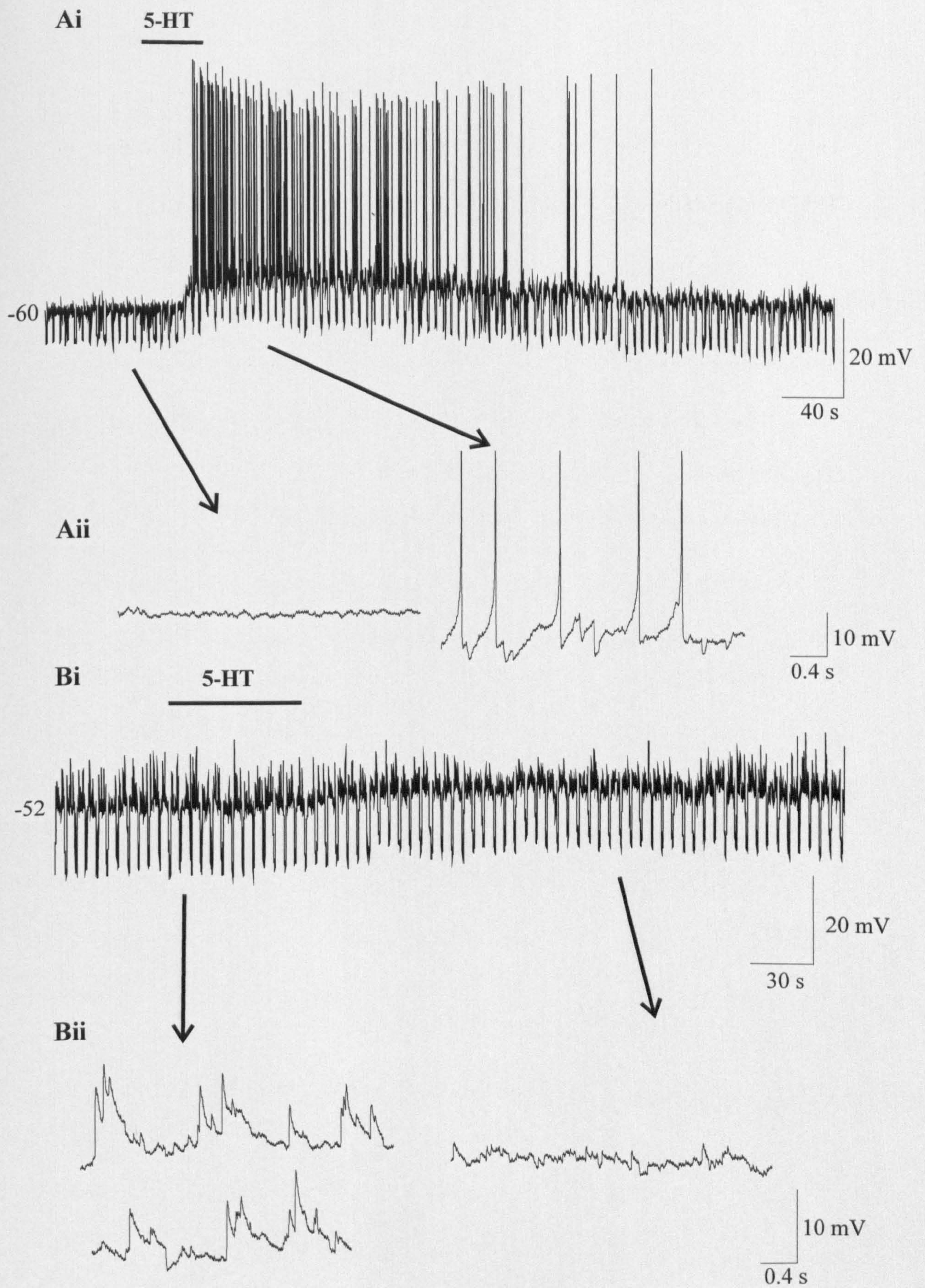




**Figure 4.8 The effects of the 5-HT receptor agonists  $\alpha$ -methyl 5-HT and 5-CT on ARC neurones**

**Ai:** Samples of a continuous whole-cell current-clamp recording from an ARC neurone. Application of 5-HT (50  $\mu$ M) induced membrane depolarisation.

**Aii:** Samples of a continuous whole-cell current-clamp recording from the same ARC neurone as in Ai. Application of the 5-HT<sub>2</sub> receptor agonist  $\alpha$ -methyl 5-HT (25  $\mu$ M) induced membrane depolarisation, mimicking the effect of 5-HT. In this neurone,  $\alpha$ -methyl 5-HT was able to induce a burst-like pattern of firing.

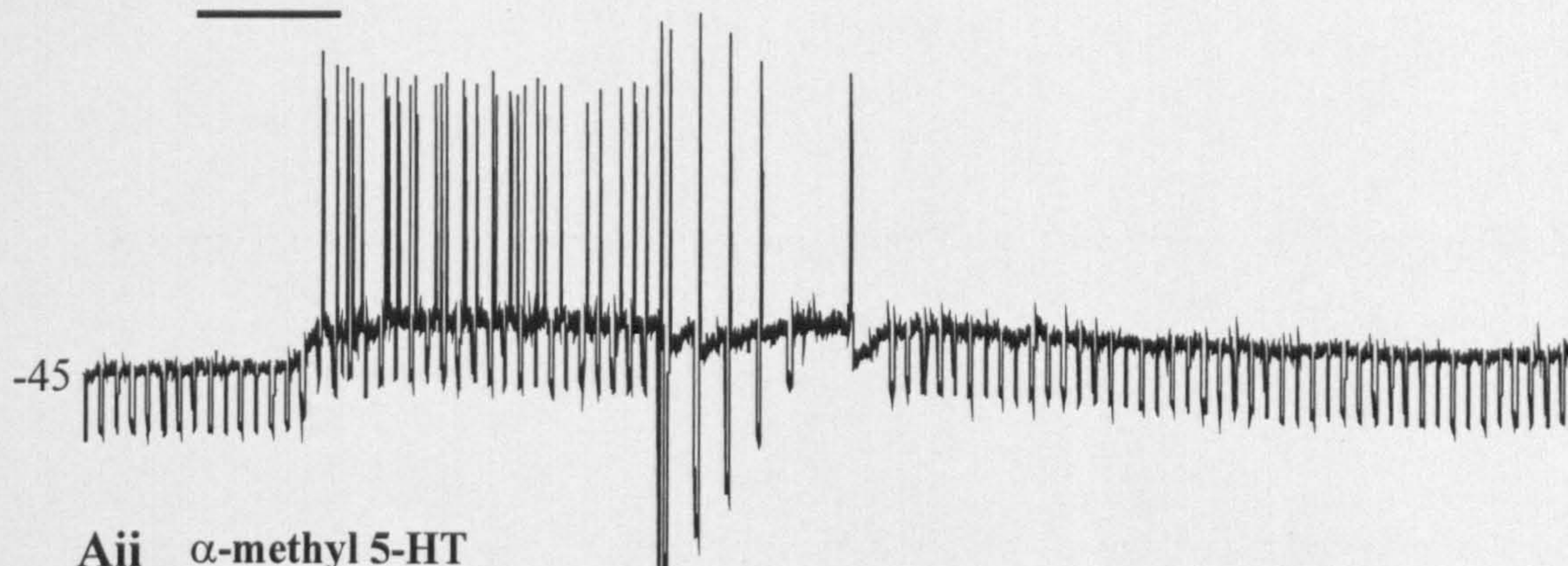
**Bi:** Samples of a continuous whole-cell current-clamp recording from an ARC neurone. Application of 5-HT induced a membrane depolarisation

**Bii:** Samples of a continuous whole-cell current-clamp recording from the same ARC neurone as in Bi. Application of the 5-HT<sub>1/5/7</sub> receptor agonist 5-CT (10  $\mu$ M) induced a membrane depolarisation, partly mimicking the effect of 5-HT.

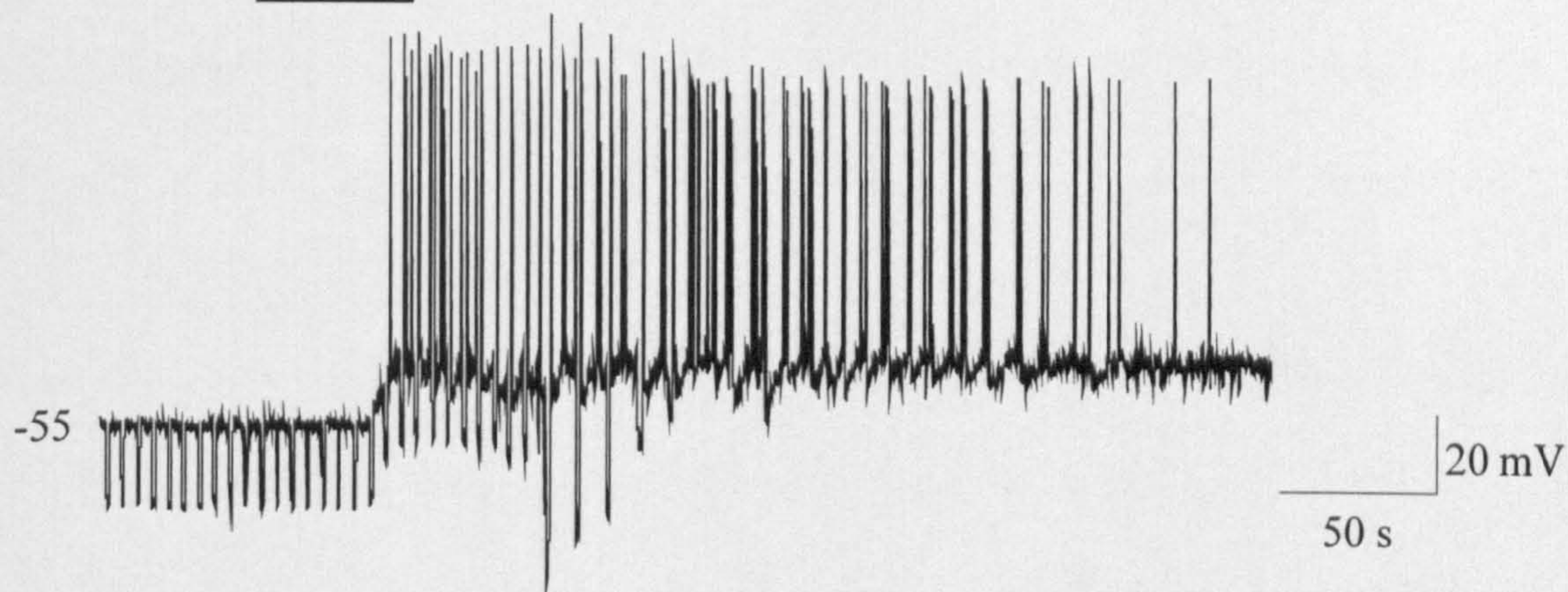


**Figure 4.8**

**Ai**     5-HT

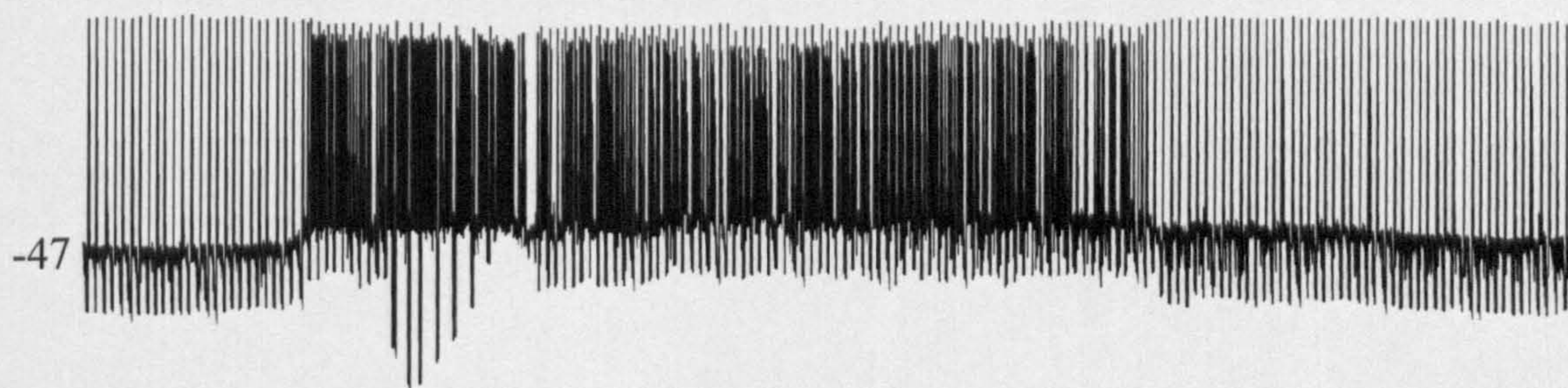


**Aii**      $\alpha$ -methyl 5-HT



**Bi**

5-HT



**Bii**

5-CT

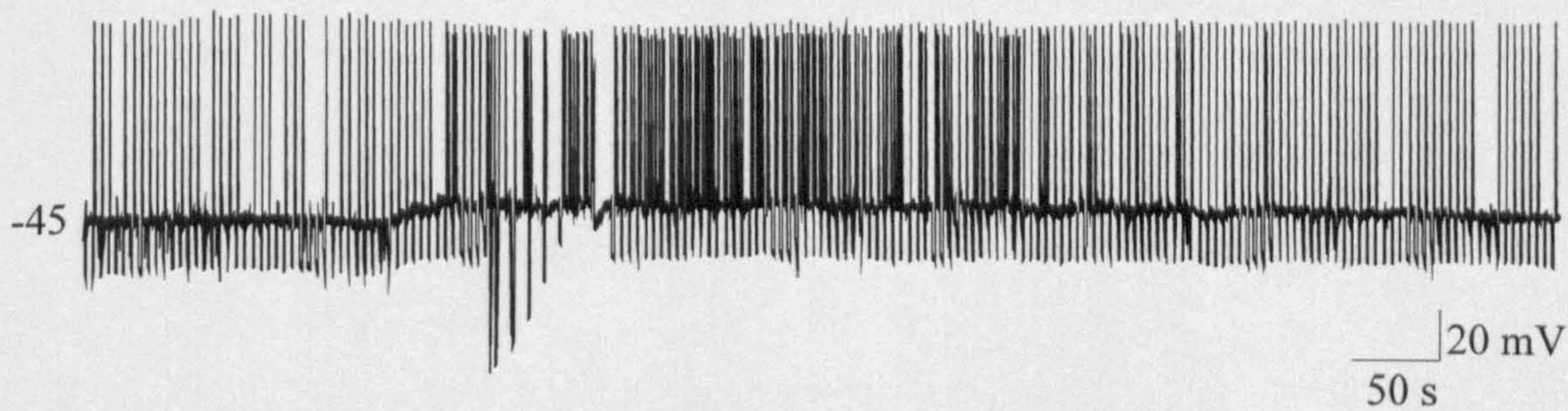




**Figure 4.9 The effects of the 5-HT receptor agonists 8-OH-DPAT and mCPBG on ARC neurones**

**Ai:** Samples of a continuous whole-cell current-clamp recording from an ARC neurone. Application of 5-HT (50  $\mu$ M) induced a membrane depolarisation.

**Aii:** Samples of a continuous whole-cell current-clamp recording from the same ARC neurone as in Ai. Application of the 5-HT<sub>1A/7</sub> receptor agonist 8-OH-DPAT (10  $\mu$ M) had no effect.

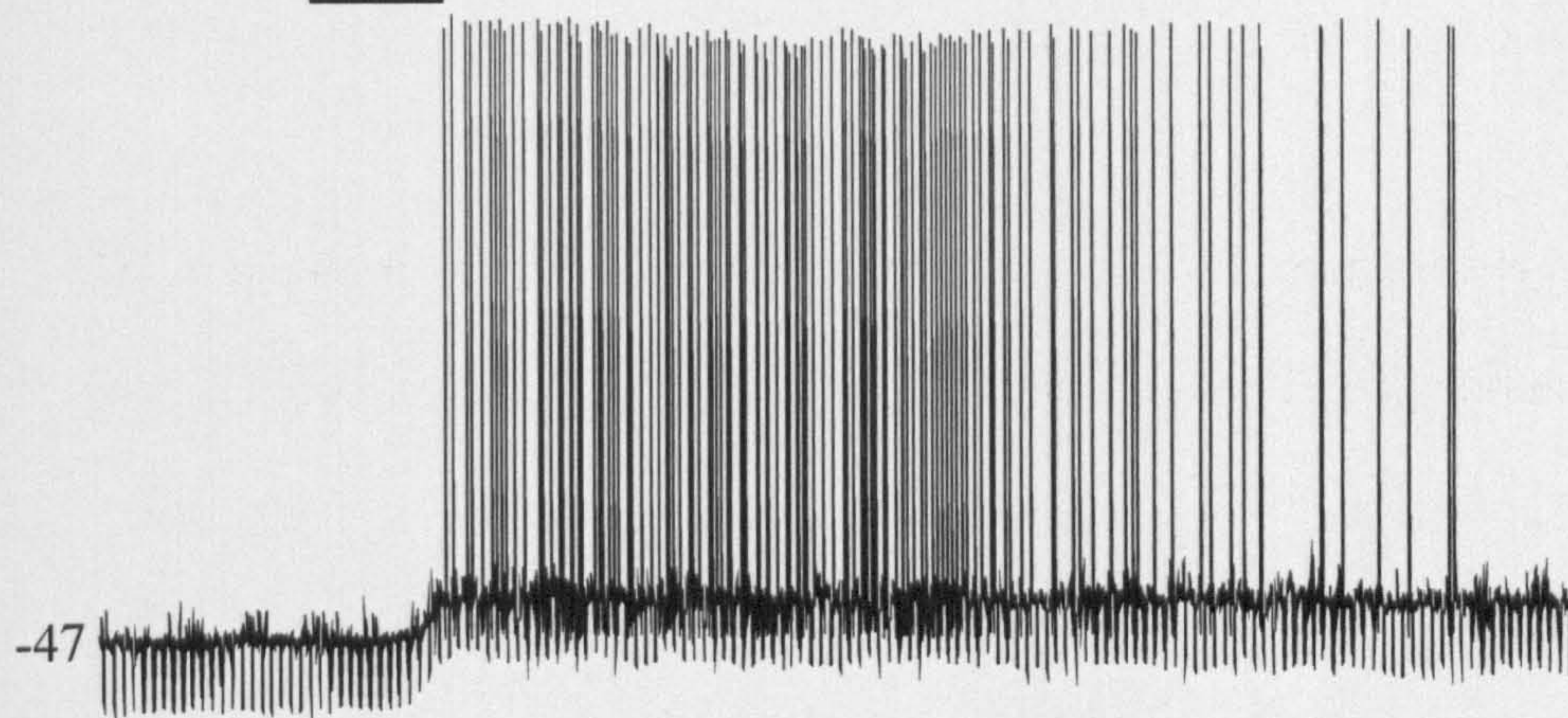
**Bi:** Samples of a continuous whole-cell current-clamp recording from an ARC neurone. Application of 5-HT induced a membrane depolarisation and increase in action potential firing.

**Bii:** Samples of a continuous whole-cell current-clamp recording from the same ARC neurone as in Bi. Application of the 5-HT<sub>3</sub> receptor agonist mCPBG (10  $\mu$ M) had no effect.



**Figure 4.9**

**Ai**      **5-HT**

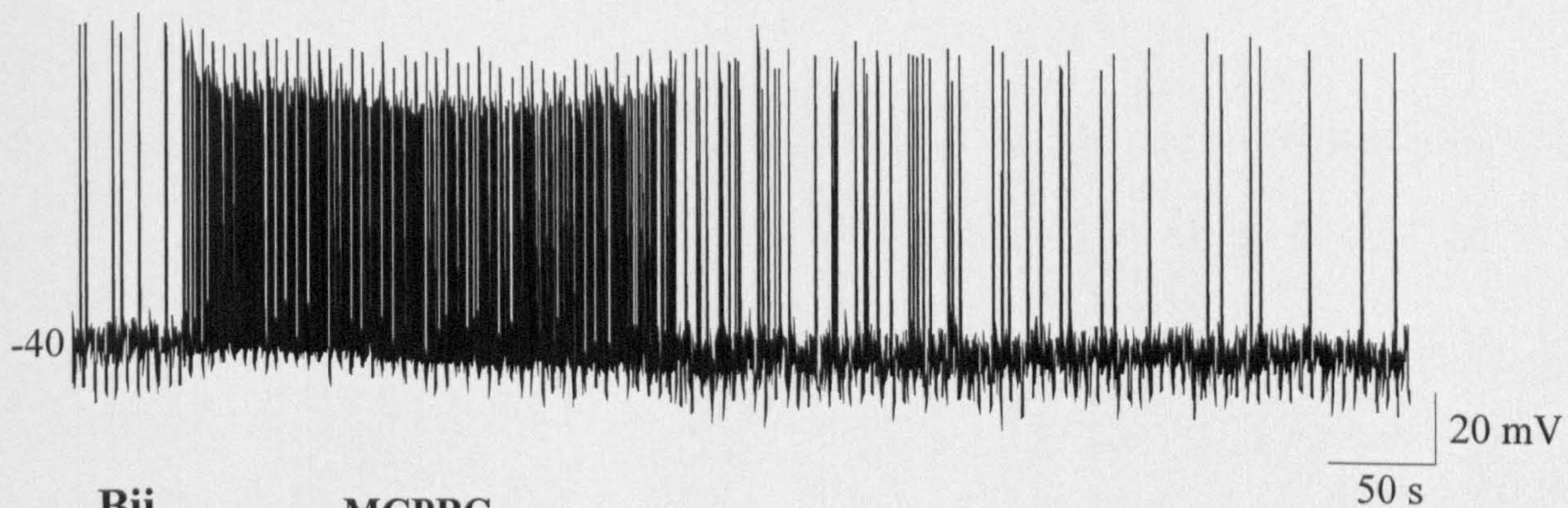


**Aii**      **8-OH-DPAT**



**Bi**

**5-HT**



**Bii**

**MCPBG**

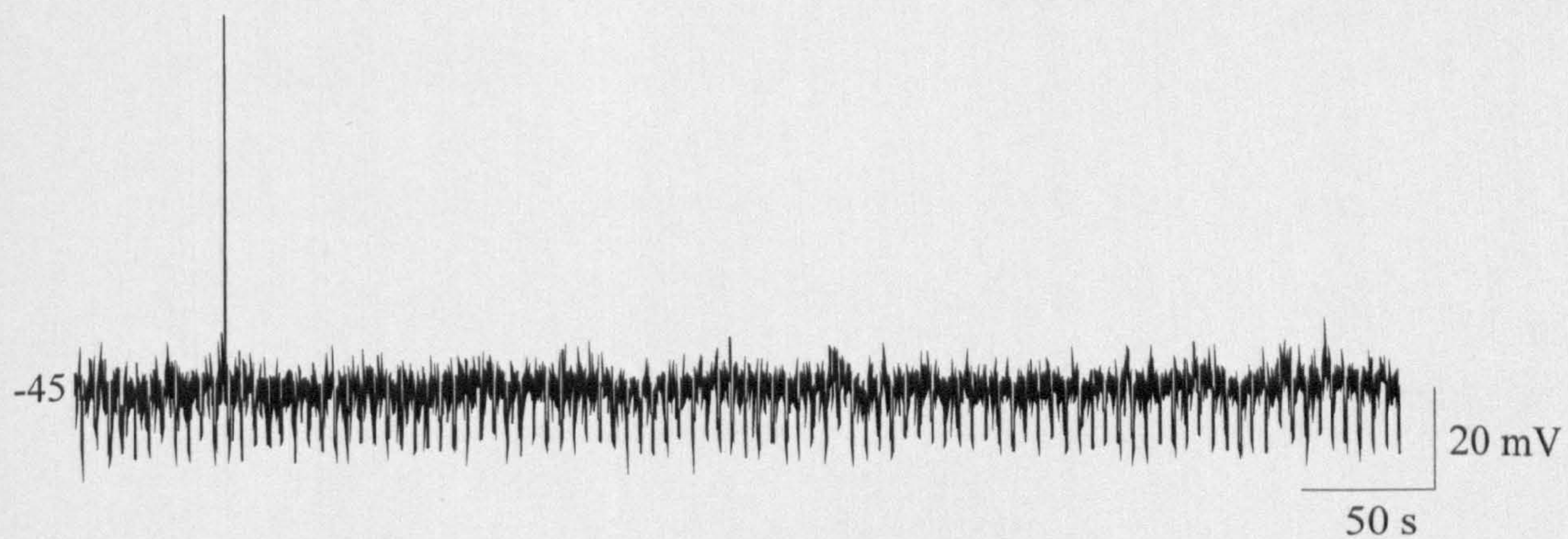




**Figure 4.10 The effects of the 5-HT receptor antagonists altanserin and RS102221 on ARC neurones**

**Ai:** Samples of a continuous whole-cell current-clamp recording from an ARC neurone. Application of 5-HT (50  $\mu$ M) induced a membrane depolarisation. The large downward and upward deflections in the middle of the response indicate where an I-V was taken.

**Aii:** Samples of a continuous whole-cell current-clamp recording from the same ARC neurone as in Ai. Application of the 5-HT<sub>2</sub> receptor antagonist altanserin (1  $\mu$ M) inhibited the 5-HT-induced depolarisation.

**Aiii:** Plot showing the reduction in the amplitude of the 5-HT-induced depolarisation in the presence of increasing concentrations of altanserin. The control response was set as 100% and upon increasing doses of altanserin there was a reduction in the amplitude of the response compared to control.

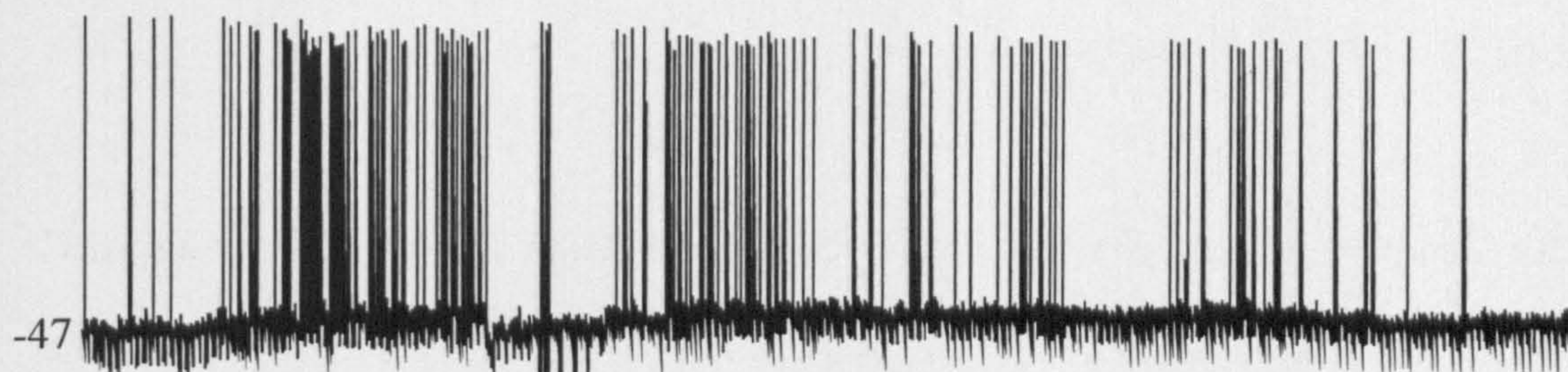
**Bi:** Samples of a continuous whole-cell current-clamp recording from an ARC neurone. Application of 5-HT induced a membrane depolarisation and increase in action potential firing.

**Bii:** Samples of a continuous whole-cell current-clamp recording from the same ARC neurone as in Bi. Application of the 5-HT<sub>2C</sub> receptor antagonist RS102221 (1  $\mu$ M) inhibited the 5-HT-induced depolarisation.

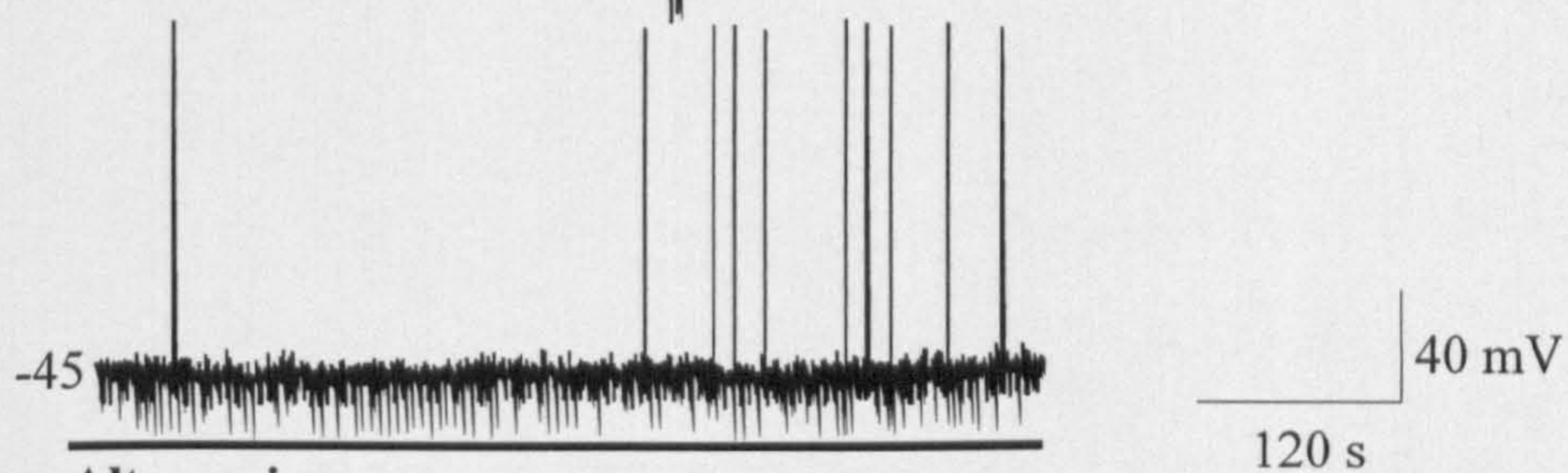


**Figure 4.10**

**Ai**    5-HT

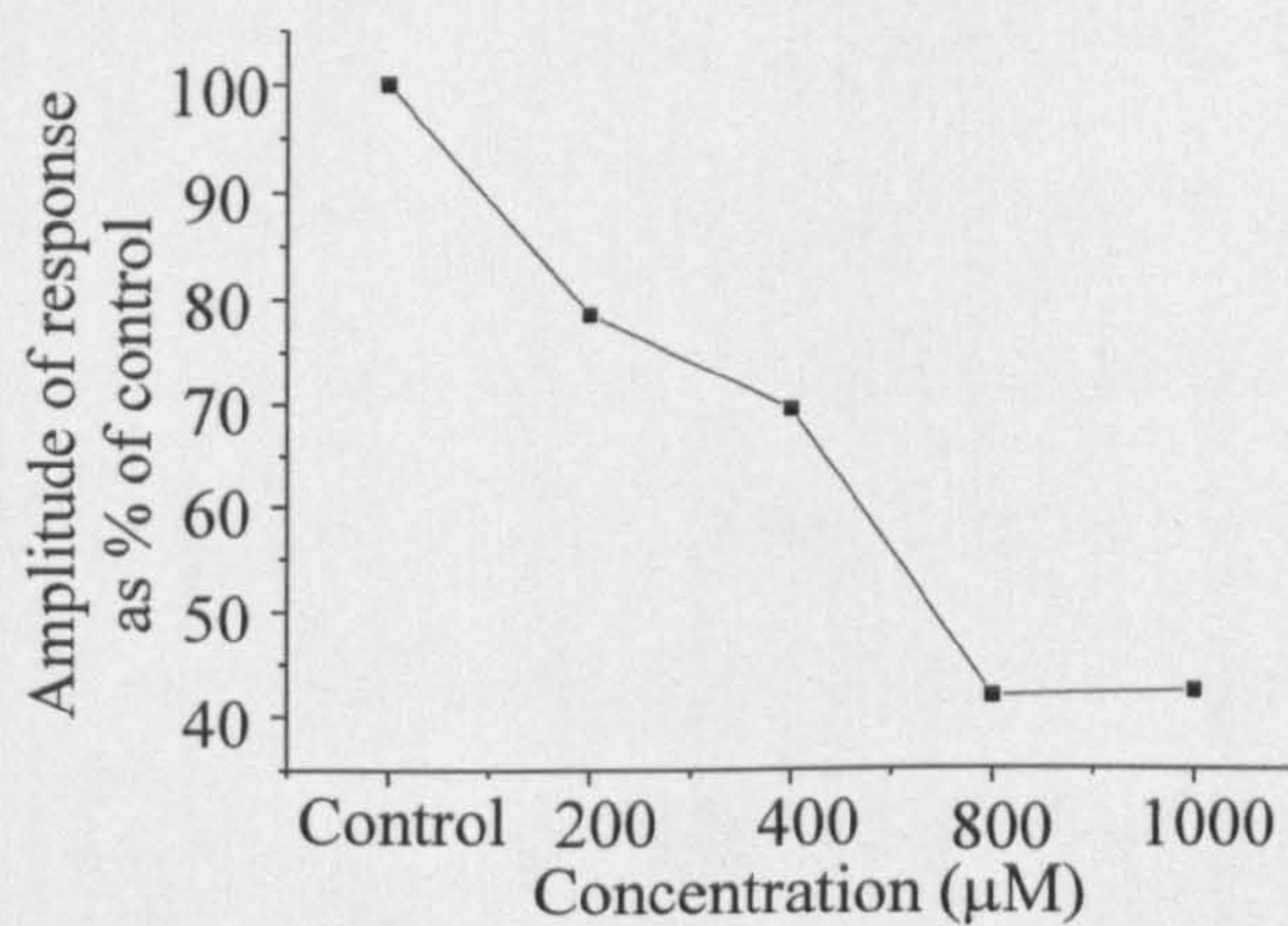


**Aii**    5-HT



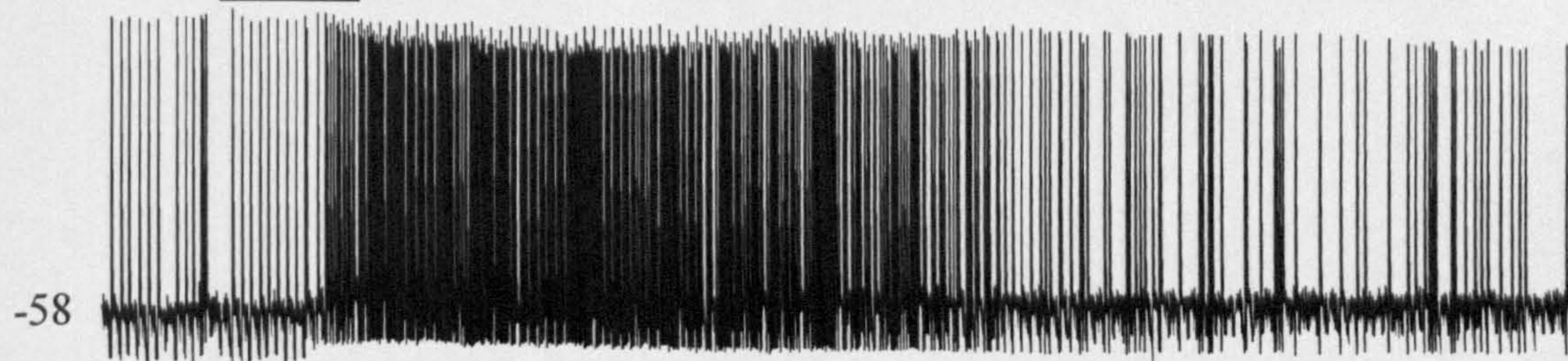
**Altanserin**

**Aiii**

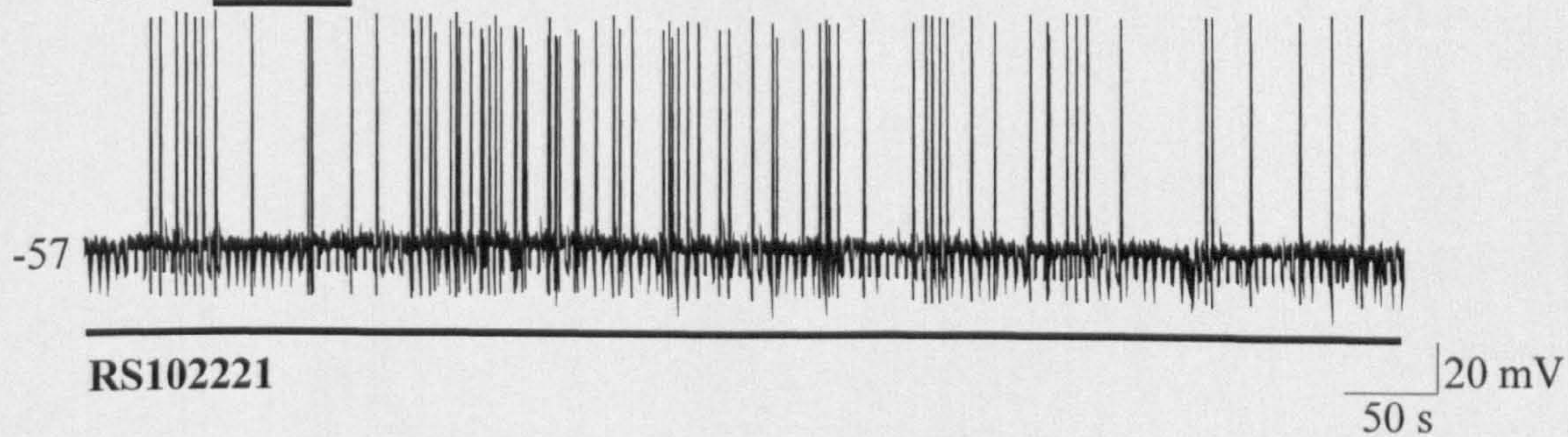


**Bi**

5-HT



**Bii**    5-HT



**RS102221**



**Figure 4.11 The effects of the 5-HT receptor antagonists R-96544 and SB 204741 on ARC neurones**

**Ai:** Samples of a continuous whole-cell current-clamp recording from an ARC neurone. Application of 5-HT (50  $\mu$ M) induced a membrane depolarisation. The dashed lines indicate the time where an I-V was taken.

**Aii:** Samples of a continuous whole-cell current-clamp recording from the same ARC neurone as in Ai. Application of the 5-HT<sub>2A</sub> receptor antagonist R-96544 (10  $\mu$ M) partially reduced the 5-HT-induced depolarisation.

**Bi:** Samples of a continuous whole-cell current-clamp recording from an ARC neurone. Application of 5-HT induced a membrane depolarisation

**Bii:** Samples of a continuous whole-cell current-clamp recording from the same ARC neurone as in Bi. Application of the 5-HT<sub>2B</sub> receptor antagonist SB 204741 (1  $\mu$ M) partially inhibited the 5-HT induced depolarisation.



**Figure 4.11**

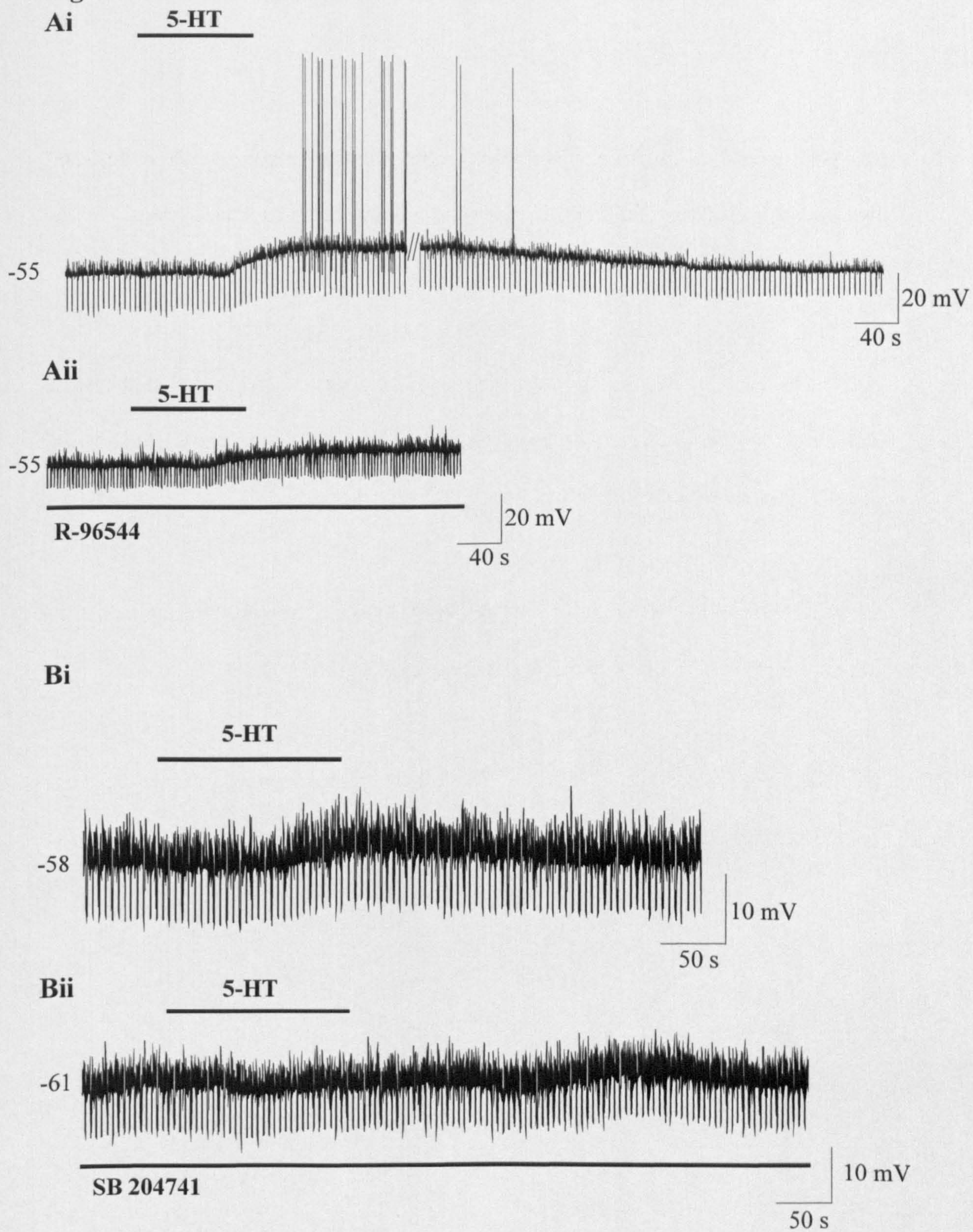




**Figure 4.12 The effects of ghrelin on 5-HT-excited ARC neurones**

**Ai:** Samples of a continuous whole-cell current-clamp recording from an ARC neurone. Application of 5-HT (50  $\mu$ M) induced a membrane depolarisation and subsequent induction of a burst-like pattern of firing.

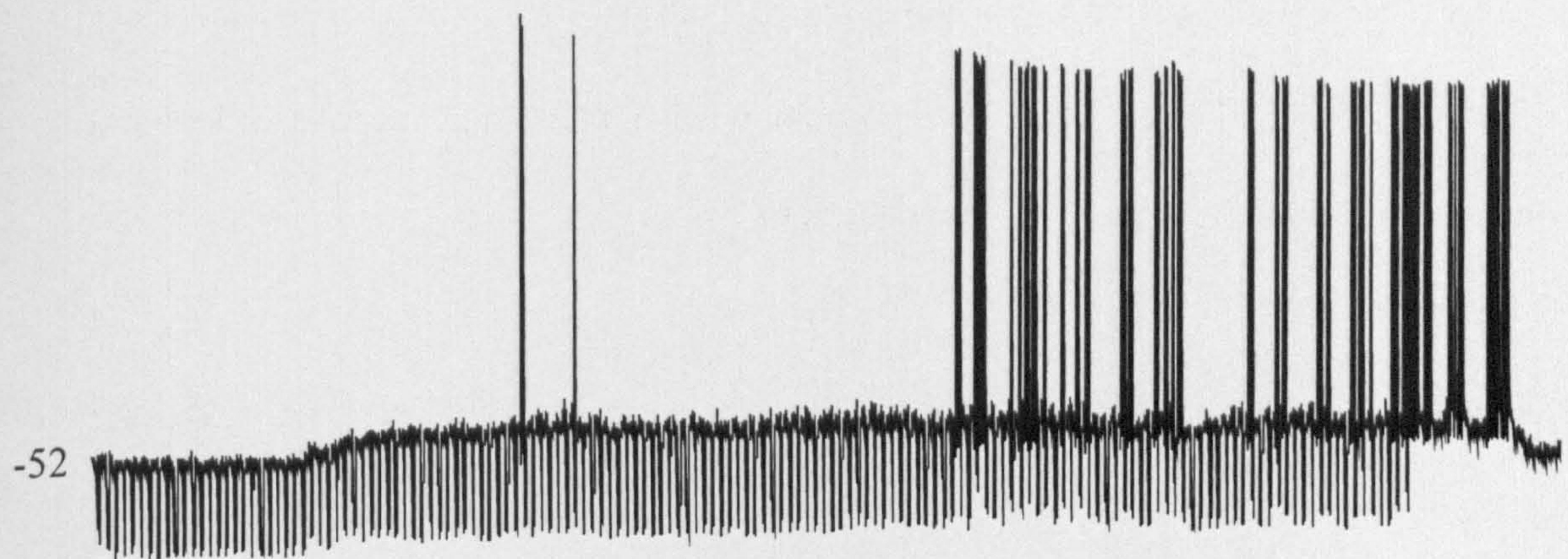
**Aii:** Samples of a continuous whole-cell current-clamp recording from the same ARC neurone in Ai. Application of ghrelin (100 nM) induced a membrane depolarisation and induction of membrane potential oscillations and burst firing pattern of action potential discharge.



**Figure 4.12**

**Ai**

**5-HT**



**Aii**

**Ghrelin**

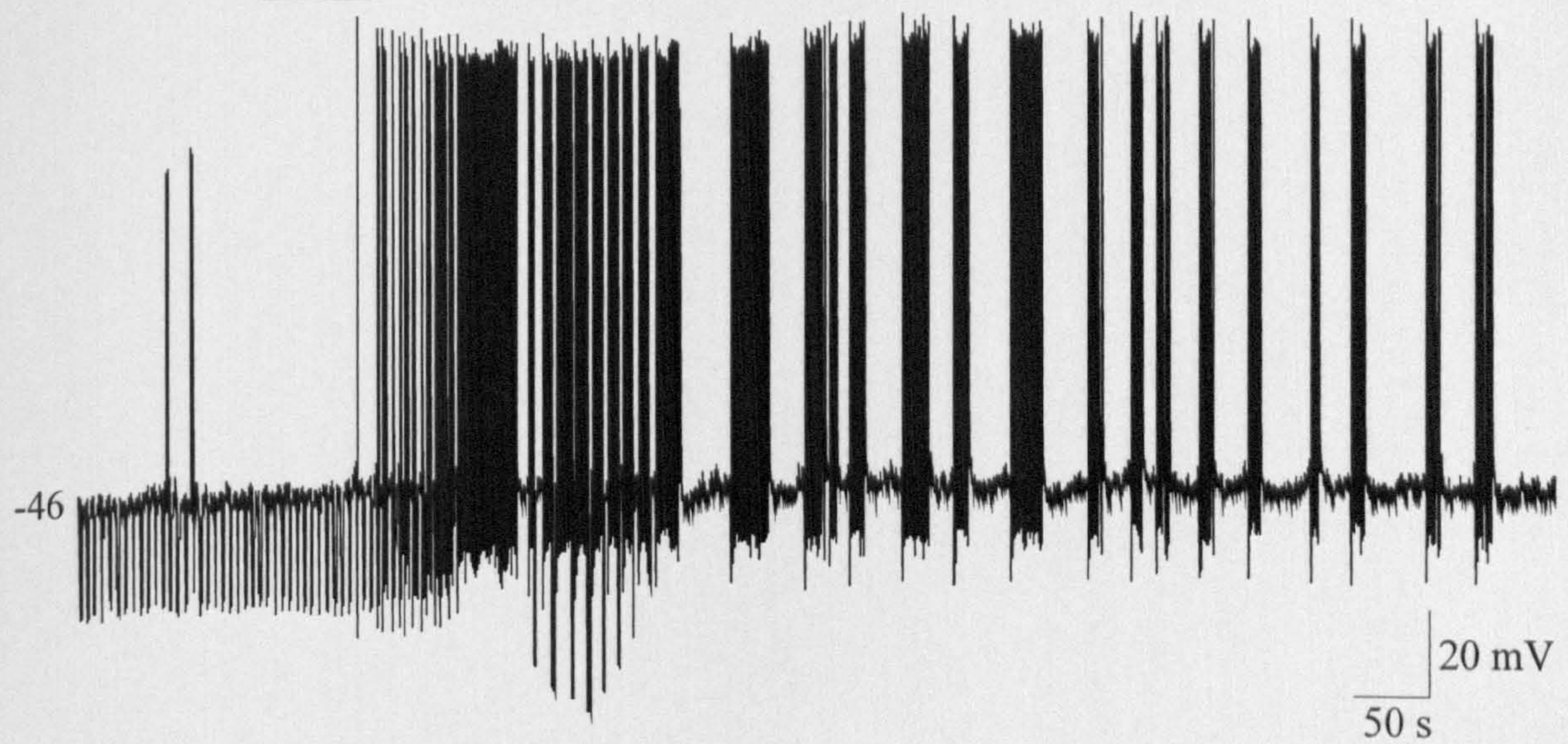




**Figure 4.13 5-HT excites CART-expressing neurones**

**Ai:** Confocal images showing that a single ARC neurone, labelled with Alexa 633 (red) during recording, was CART positive (green, visualised using Cy2). CART positive neurones were either excited by 5-HT or showed no response.

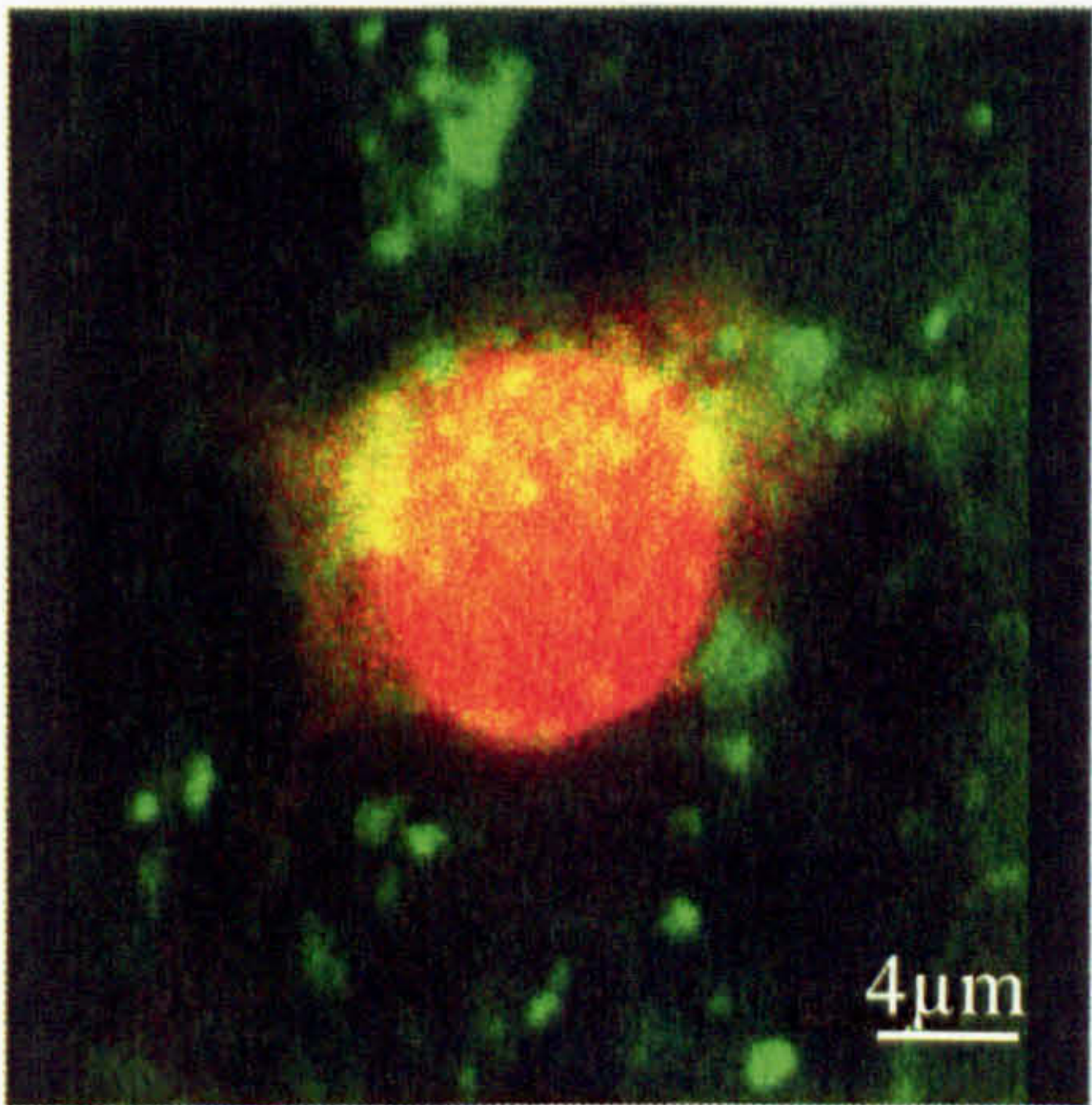
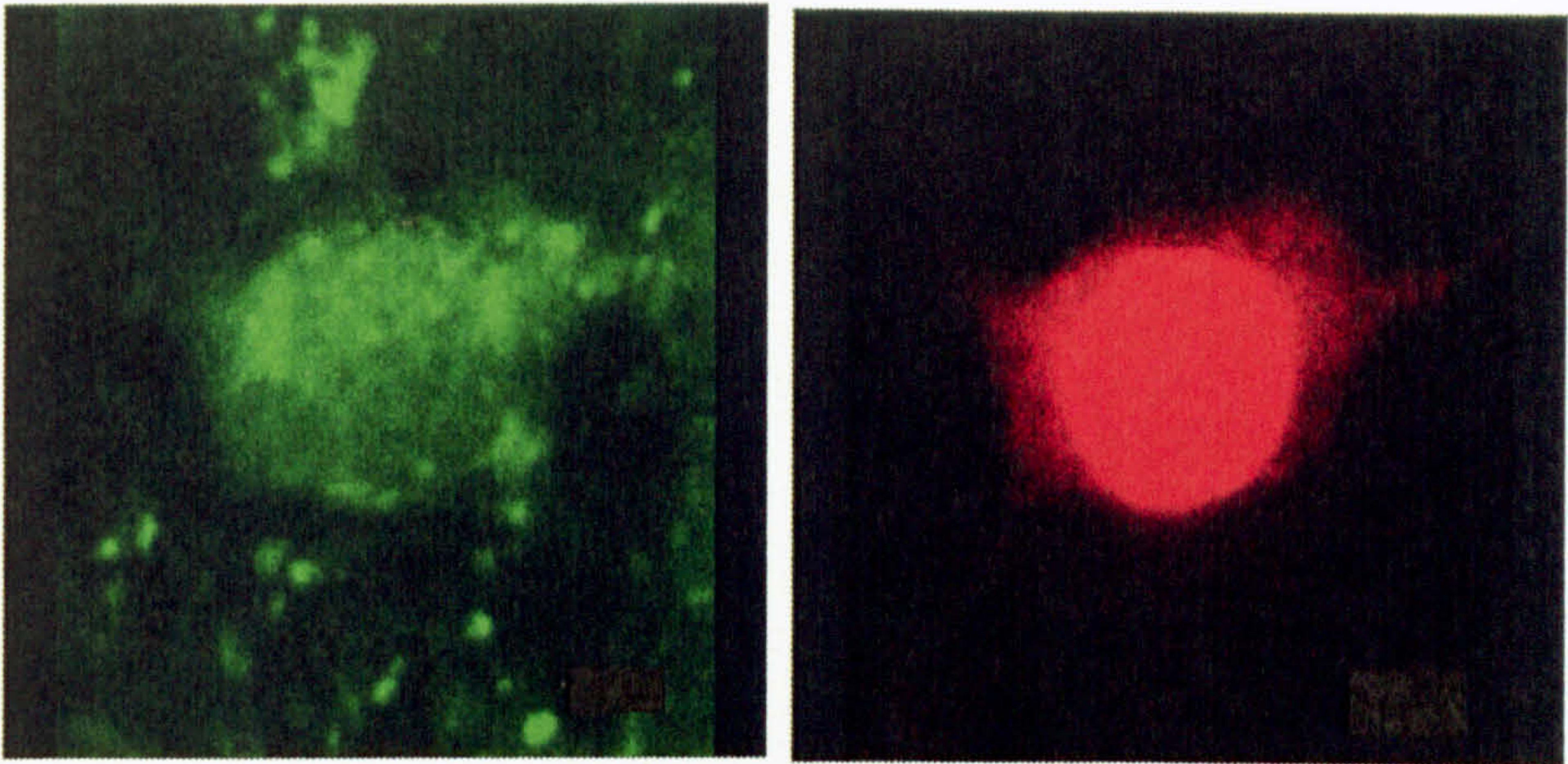
**Aii:** Samples of a continuous whole-cell current-clamp recording from a CART positive ARC neurone showing the 5-HT (50  $\mu$ M) induced excitation in this neurone.

**B:** Confocal images showing that a single ARC neurone labelled with Alexa 633 (red) during recording was not CART positive (green, visualised using Cy2). Non-CART positive neurones were either excited, inhibited or showed no response to 5-HT.



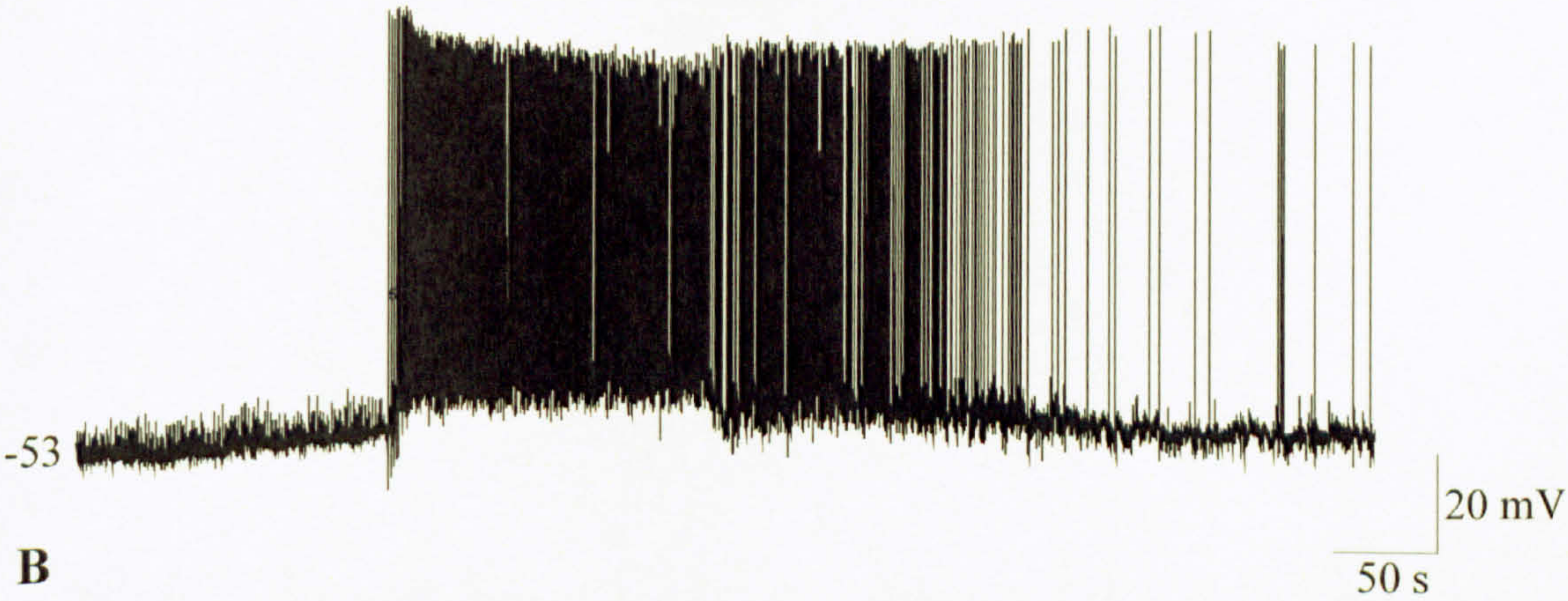
Figure 4.13

Ai



Aii

5-HT



B

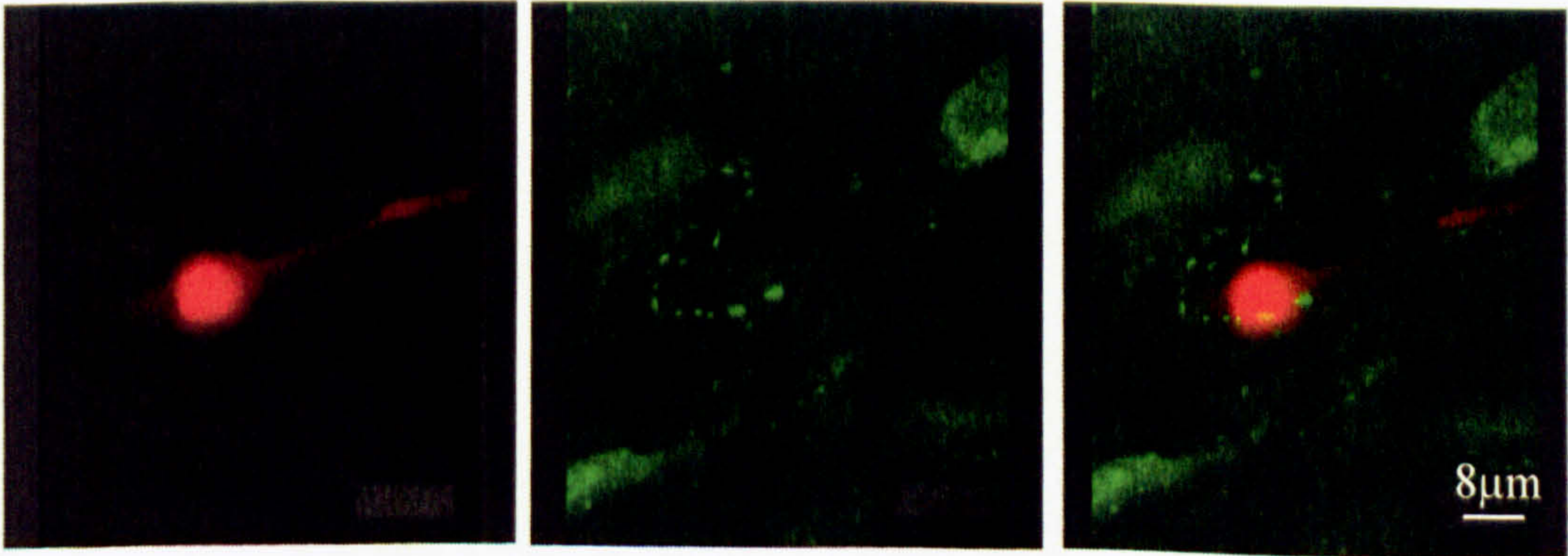




**Figure 4.14 A comparison of the effects of 5-HT on ARC neurones under normo- (2 mM glucose) and hyper-glycaemic (10 mM glucose) conditions**

**A:** Bar-chart comparing the response to 5-HT of ARC neurones recorded in 10 mM and 2 mM glucose-containing aCSF. In 10 mM glucose-containing aCSF, there were a higher proportion of 5-HT-induced excitations and no responses than in 2 mM glucose-containing aCSF, but there were a higher proportion of 5-HT-induced inhibitions in 2 mM compared to 10 mM glucose-containing aCSF.



**Figure 4.14**

**A**

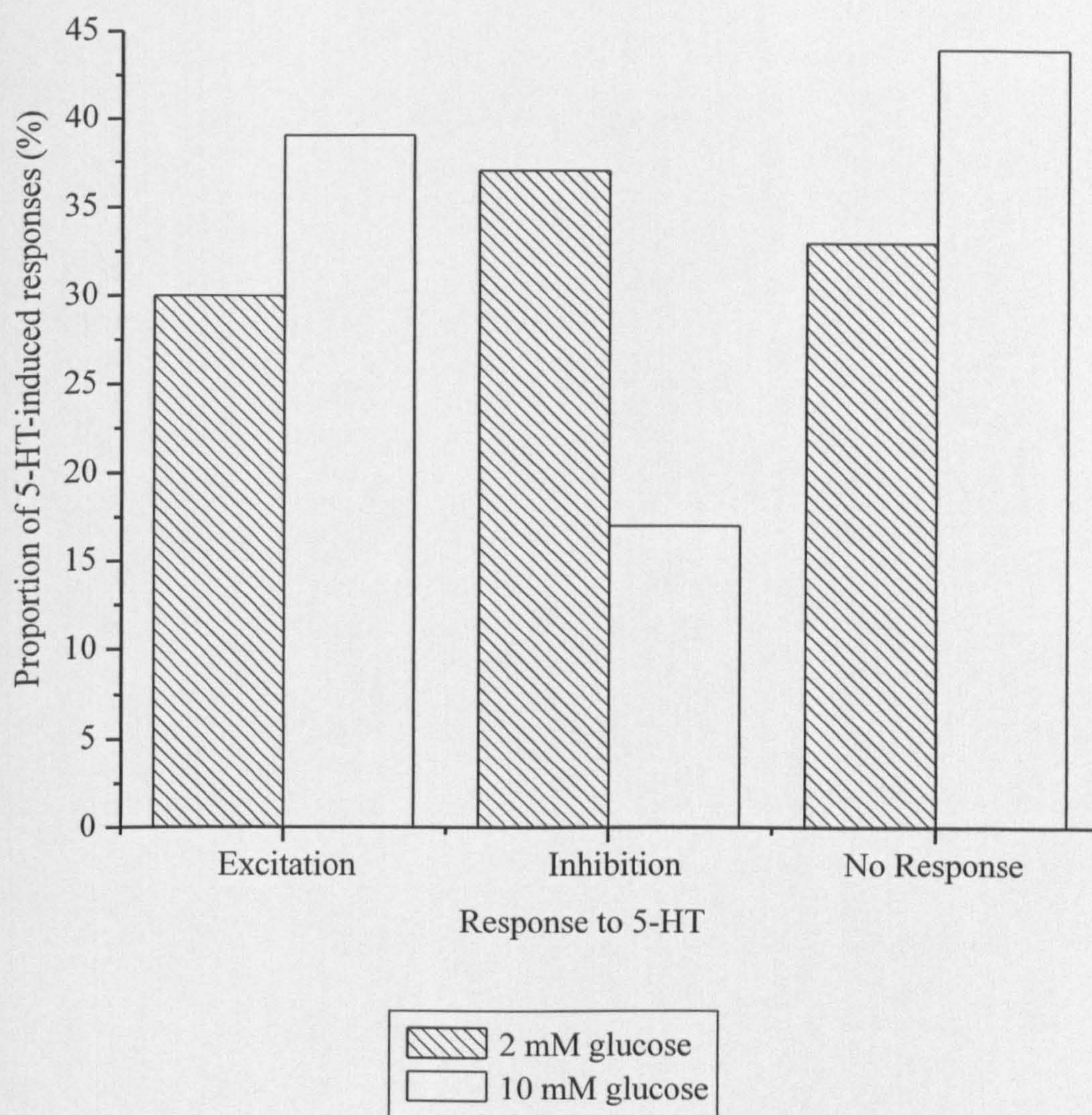


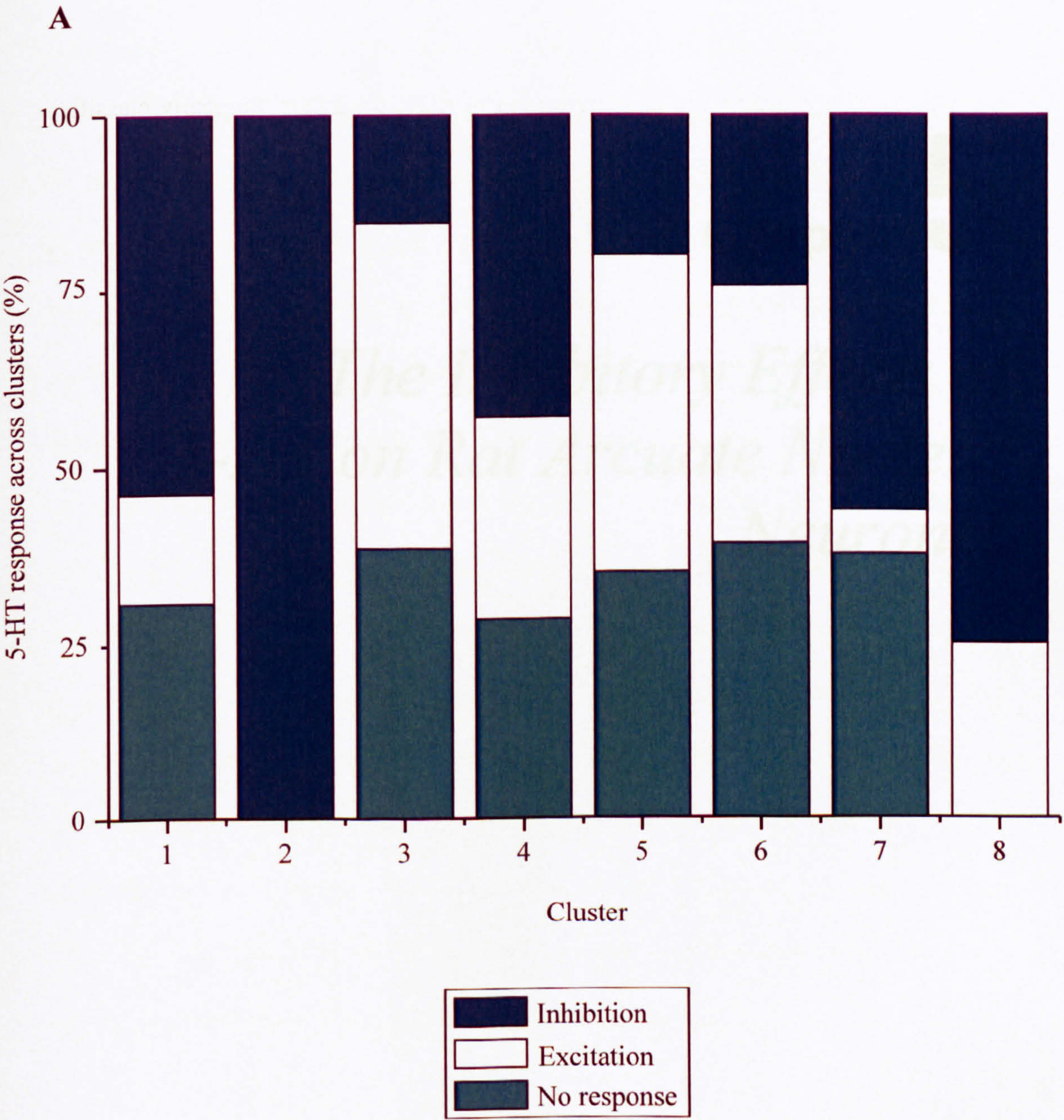


**Figure 4.15 Electrophysiological classification of ARC neurones and their responsiveness to 5-HT**

**A:** A histogram showing the responsiveness of the electrophysiologically classified clusters to 5-HT within the ARC.



**Figure 4.15**





# Chapter 5

## *The Inhibitory Effects of 5-HT on Rat Arcuate Nucleus Neurones*

## 5. 1 Introduction

5-HT is a neurotransmitter that has been implicated in many different behavioural, psychological and physiological functions and diseases. As well as having a role in the control of mood disorders it is also associated with reproduction, feeding and energy homeostasis and thermoregulation (Bonate, 1991; Wilkinson & Dourish, 1991; Baldwin & Rudge, 1995; Graeff *et al.*, 1996). One of the areas of the brain that is responsible for controlling many of these functions is the arcuate nucleus (ARC) of the hypothalamus. In particular, in relation to the control of feeding and energy homeostasis, the 5-HT system and the ARC have been shown to be essential components for the central regulation of energy homeostasis (Blundell, 1977, 1984; Schwartz *et al.*, 1999, 2000). Of the 7 major subgroups of 5-HT receptors, the 5-HT<sub>1</sub> and 5-HT<sub>2</sub> receptors have been predominantly shown to be involved in the control of feeding and energy homeostasis (see chapter 4 and De Vry & Schreiber, 2000). However, the effects of 5-HT acting at the level of the ARC are still poorly understood. In particular the neuronal subtypes of ARC neurones that are modulated by 5-HT are still not fully known. As 5-HT is known to inhibit feeding (Blundell, 1977, 1984), it may be that 5-HT inhibits orexigenic neurones and excites anorexigenic neurones within the ARC to suppress feeding.

Following on from the previous chapter that described the excitatory effects of 5-HT on rat hypothalamic ARC neurones, the aims of this study were to investigate the cellular mechanisms by which 5-HT inhibits ARC neurones and to elucidate which 5-HT receptor subtypes were mediating these effects. In addition, the neuronal subtypes involved in the regulation of energy homeostasis by 5-HT were investigated.



## 5.2 Results

### 5.2.1 *The inhibitory effects of 5-HT on ARC neurones*

Results were obtained in 2 mM glucose-containing aCSF unless otherwise stated. Bath application of 5-HT (50  $\mu$ M) for between 45-75 seconds induced a membrane hyperpolarisation in 45/122 ARC neurones. The hyperpolarisation of the membrane was slow in onset and resulted in the cessation of action potential firing, inhibiting the activity of these neurones. The response was characterised by hyperpolarisation of the membrane from a mean resting membrane potential of  $-49.0 \pm 1.0$  mV to  $-61.6 \pm 1.2$  mV, a mean peak membrane hyperpolarisation of  $12.7 \pm 0.9$  mV ( $n=45$ ; see figure 5.1Ai). The response recovered upon washout of 5-HT from the bath, returning the mean membrane potential to  $-47.9 \pm 1.3$  mV ( $n=37$ ). The membrane hyperpolarisation was associated with a significant  $35.8 \pm 3.2$  % decrease in neuronal input resistance from a mean of  $1438 \pm 76$  M $\Omega$  at rest to  $915 \pm 67$  M $\Omega$  in the presence of 5-HT, a decrease of  $523 \pm 54$  M $\Omega$  ( $P<0.01$ ). To confirm that the change in resistance was due to 5-HT and not due to a change in voltage, a period of constant positive current injection was applied during the 5-HT response to eliminate any voltage-dependent effects in a sub-population of neurones. The 5-HT-induced hyperpolarisation and reduction in input resistance was maintained in the presence of 500 nM TTX, indicating a direct effect on ARC neurones ( $n=4$ ; see figure 5.1Aii).

The effect of 5-HT on ARC neurones was also studied in voltage-clamp. 5-HT induced an outward current ( $n=7$ ; see figure 5.2A), with a mean peak current of  $9.1 \pm 2.1$  pA at a holding potential of -50 mV. The current induced by 5-HT was quick in onset but decayed at a relatively slower rate after reaching its peak.

### ***5.2.2 Ionic mechanism underlying the 5-HT-induced hyperpolarisation***

The 5-HT-induced hyperpolarisation was associated with a decrease in neuronal input resistance (or an increase in conductance). Current-voltage relationships were obtained from 29 cells, in control conditions and at the peak of the 5-HT-induced hyperpolarisation (see figure 5.1B). The 5-HT-induced conductance change had a reversal potential of  $-79.1 \pm 1.8$  mV, approaching the reversal potential for  $K^+$  ions under our recording conditions. In addition, in a sub-population of neurones, 5-HT activated or enhanced an inward rectifier, revealed from the current-voltage relationship in the presence of 5-HT ( $n=4$ ; for example see figure 5.1Bii). Inward rectification is identified as a decrease in input resistance at more negative membrane potentials, indicated by a decrease in the slope in the plot of the I-V.

Voltage-clamp ramps were also performed in the presence of TTX to study the mechanism underlying the 5-HT-induced outward current. The currents were obtained from ramp protocols that drove the holding potential from -130 mV to -30 mV, at a rate of 10 mV per second. Superimposition of currents obtained from ramps before and at the peak of the response revealed an average reversal potential of  $-87.7 \pm 1.2$  mV ( $n=3$ ; figure 5.2B), close to the reversal potential for  $K^+$  ions under our recording conditions.

To identify which 5-HT receptor subtypes are involved in the 5-HT-induced hyperpolarisation, a range of 5-HT agonists and antagonists were used



### 5.2.3 The effects of 5-HT receptor agonists on ARC neurones

To determine the nature of the 5-HT receptor subtypes that mediate the hyperpolarisation induced by 5-HT, the effects of selective agonists were first investigated. Firstly, the 5-HT<sub>1A</sub> agonist 8-OH-DPAT (10  $\mu$ M) was tested, and was shown to hyperpolarise ARC neurones from a membrane potential of  $-45.9 \pm 3.6$  mV to  $-50.3 \pm 4.3$  mV, a mean peak hyperpolarisation of  $4.4 \pm 0.8$  mV, associated with a decrease in input resistance from  $1213 \pm 251$  M $\Omega$  to  $1052 \pm 170$  M $\Omega$  (n=7; see figure 5.3A). The 8-OH-DPAT-induced hyperpolarisation was smaller in amplitude than the 5-HT-induced hyperpolarisation, but still resulted in the cessation of action potential firing and inhibition of these neurones. The 8-OH-DPAT-induced hyperpolarisation did not completely mimic the 5-HT response and did not always wash off.

The next agonist investigated was the 5-HT<sub>1/5/7</sub> agonist 5-CT (10  $\mu$ M). This induced a membrane hyperpolarisation from  $-41.9 \pm 2.9$  mV to  $-55.8 \pm 4.2$  mV, a mean peak hyperpolarisation of  $13.9 \pm 2.9$  mV. There was a concurrent decrease in membrane resistance from  $1223 \pm 179$  M $\Omega$  to  $883 \pm 146$  M $\Omega$  (n=5; see figure 5.3B). The 5-CT-induced hyperpolarisation was of similar magnitude to the 5-HT response and inhibited the activity of neurones but often did not persist as long as the 5-HT-induced hyperpolarisation and was quicker to wash off.

To further clarify the role of the 5-HT<sub>1</sub> receptor in the 5-HT-induced hyperpolarisation, more subtype-specific agonists were tested. Agonists were bath applied for 1-4 mins. The 5-HT<sub>1A/1B</sub> agonist RU24969 (20  $\mu$ M; n=5; see figure 5.4A), and the specific 5-HT<sub>1B</sub> agonist CP93129 at 1  $\mu$ M (n=4; see figure 5.4B) and 10  $\mu$ M (n=3) were without significant effect on neurones in which 5-HT induced a

membrane hyperpolarisation and they did not affect the membrane potential or input resistance of these neurones.

In addition, the 5-HT<sub>3</sub> receptor agonist mCPBG (10  $\mu$ M) did not mimic the 5-HT-induced hyperpolarisation (n=6) and induced no effect on membrane potential or input resistance of neurones to which it was applied.

These data suggest a role for 5-HT<sub>1/7</sub> receptors in the 5-HT-induced hyperpolarisation as agonists at these receptors (8-OH-DPAT and 5-CT) were able to induce a hyperpolarisation of neurones, mimicking the effects of 5-HT.

#### ***5.2.4 The effects of 5-HT receptor antagonists on 5-HT-induced responses in ARC neurones***

To further identify the 5-HT receptors that mediate the 5-HT-induced hyperpolarisation, a range of selective antagonists were tested. Application of all antagonists alone had no effect on the recorded neurones. The 5-HT<sub>7</sub> receptor antagonist SB269970 (10  $\mu$ M) only partially reduced the 5-HT-induced hyperpolarisation (n=8; see figure 5.5A), from a mean peak hyperpolarisation of  $11.7 \pm 2.4$  mV to  $8.7 \pm 2$  mV, a  $27 \pm 7$  % reduction. SB269970 was without effect on 5-HT-induced changes in input resistance as 5-HT induced a mean peak decrease in input resistance of  $493 \pm 134$  M $\Omega$  (from  $1419 \pm 202$  M $\Omega$  to  $864 \pm 139$  M $\Omega$ ) whilst it decreased to  $438 \pm 141$  M $\Omega$  ( $1353 \pm 251$  M $\Omega$  to  $860 \pm 122$  M $\Omega$ ) in the presence of the antagonist.

The role of 5-HT<sub>1</sub> receptors in the 5-HT-induced hyperpolarisation was next investigated. The 5-HT<sub>1A/1B</sub> receptor antagonist cyanopindolol (10  $\mu$ M) reduced the 5-HT-induced hyperpolarisation, from a mean peak of  $6.2 \pm 2.9$  mV to  $1.3 \pm 0.4$  mV in the presence of the antagonist, a  $79.6 \pm 6.8$  % reduction (n=5; see figure 5.5B).



Cyanopindolol reduced the decrease in input resistance induced by 5-HT from  $323 \pm 250$  to  $13 \pm 59 \text{ M}\Omega$  in the presence of the antagonist.

To further differentiate the effects of the 5-HT<sub>1</sub> subtypes mediating the inhibitory response, subtype-specific antagonists were tested. The 5-HT<sub>1A</sub> receptor antagonist WAY-100635 reduced the 5-HT-induced hyperpolarisation in a concentration-dependent manner (see table 5.1 and figure 5.6A).

**Table 5.1: Effects of WAY-100635 on 5-HT-induced hyperpolarisation**

Concentration of WAY- 100635 (nM)	Mean peak hyper-polarisation in 5-HT (mV)	Mean peak hyper-polarisation in 5-HT and antagonist (mV)	% reduction in mean peak hyper-polarisation	Reduction in input resistance in 5-HT ( $\text{M}\Omega$ )	Reduction in input resistance in 5-HT and antagonist ( $\text{M}\Omega$ )
<b>30</b> (n=4)	$11.1 \pm 2.5$	$2.3 \pm 1.3$	$60.3 \pm 14.8$	$346 \pm 140$	$168 \pm 87$
<b>100</b> (n=3)	$9.8 \pm 1.3$	$4.2 \pm 3.4$	$59.8 \pm 29.7$	$99 \pm 40$	$18 \pm 62$
<b>300</b> (n=3)	$9.7 \pm 2.7$	$4.3 \pm 1.0$	$48.3 \pm 18.8$	$361 \pm 252$	$70 \pm 45$
<b>1000</b> (n=3)	$17.4 \pm 3.6$	$3.2 \pm 2.1$	$89.1 \pm 11.6$	$910 \pm 160$	$366 \pm 25$

Next the 5-HT<sub>1B</sub> receptor antagonist SB224289 was tested. At 1  $\mu\text{M}$ , it had no effect on the 5-HT-induced hyperpolarisation, as the mean peak hyperpolarisation induced by 5-HT was  $12.0 \pm 3.5 \text{ mV}$  and  $12.1 \pm 5.8 \text{ mV}$  in the presence of the antagonist (n=3). However at 2  $\mu\text{M}$ , SB224289 suppressed the hyperpolarisation induced by 5-HT from a mean peak of  $12.4 \pm 2.8 \text{ mV}$  to  $4.0 \pm 1.4 \text{ mV}$  in the presence of the antagonist, a  $69.2 \pm 3.3 \%$  reduction (n=4; see figure 5.6B).

As these data imply more than one receptor is involved in the 5-HT-induced hyperpolarisation, a combination of antagonists were tested on the 5-HT-induced response. The 5-HT<sub>1B</sub> antagonist SB224289 (2  $\mu\text{M}$ ) and 5-HT<sub>7</sub> antagonist SB269970

(10  $\mu$ M) in combination only partially reduced the 5-HT-induced hyperpolarisation (n=3; see figure 5.7Aii). However upon addition of the 5-HT<sub>1A</sub> antagonist WAY-100635 (300 nM) there was a reduction in mean peak hyperpolarisation of  $82.3 \pm 14.0$  % (n=5; see figure 5.7Aiii).

Finally, antagonists for other 5-HT receptors were tested to determine their role in the 5-HT-induced hyperpolarisation. The 5-HT<sub>3</sub> receptor antagonist MDL72222 (100 nM) had no effect on the 5-HT-induced hyperpolarisation (n=4; see figure 5.8A), nor did the 5-HT<sub>2</sub> receptor antagonist altanserin (200 nM; n=4; see figure 5.8B).

The results from this study have shown that 5-HT is able to inhibit a population of ARC neurones most likely through 5-HT<sub>1</sub> (predominantly 5-HT<sub>1A</sub>) and 5-HT<sub>7</sub> receptors. However, the identity of these ARC neurones that are inhibited by 5-HT is unknown. In order to try to identify the types of ARC neurones that were inhibited by 5-HT, several methods were used. Firstly ghrelin, a marker of orexigenic neurones, was applied to neurones that had been exposed to 5-HT and responded with a reversible hyperpolarisation. Secondly, the effects of 5-HT on identified neuropeptide Y (NPY) neurones were investigated. Thirdly, immunohistochemistry was used to identify 5-HT receptors and to see if they were co-localised with CART.

### ***5.2.5 The effects of ghrelin on ARC neurones***

Ghrelin is an orexigenic hormone produced from the stomach and in a small population of neurones within the brain, and is known to potently increase food



intake and body-weight in rodents (Kojima *et al.*, 1999; Tschop *et al.*, 2000). It selectively targets orexigenic neurones therefore in this study, ghrelin was used as a marker to identify orexigenic neurones.

All ghrelin and associated 5-HT-induced responses were obtained in 10 mM glucose. Ghrelin (100-200 nM) was applied to 14 ARC neurones that responded to 5-HT with hyperpolarisation. 21 % of these neurones were unaffected by ghrelin. 79 % of these neurones responded with a depolarisation of the membrane upon ghrelin application, from an average membrane potential of  $-49.4 \pm 1.9$  mV to  $-41.1 \pm 1.3$ , a mean peak depolarisation of  $8.3 \pm 1.3$  mV ( $n=11$ ; see figure 5.9). The ghrelin-induced depolarisation was slow in onset and reached threshold for action potential firing, increasing the activity of these neurones. Input resistance increased in the presence of ghrelin, from  $1281 \pm 226$  M $\Omega$  to  $1410 \pm 345$  M $\Omega$  a change of  $130 \pm 141$  M $\Omega$ . These results indicate that 5-HT acts at the level of orexigenic neurones and induced inhibition of these neurones.

#### **5.2.6 5-HT inhibits orexigenic NPY/AgRP neurones**

Some ARC neurones can be identified by their electrophysiological properties. A sub-population of ARC neurones which express the anomalous inward rectifier and an A-like conductance have been identified (cluster 2 neurones described in chapter 3) and these neurones have been shown to express NPY and agouti-related peptide (AgRP; van den Top *et al.*, 2004). NPY and AgRP neurones are both orexigenic peptides and have been shown to co-localise in the ARC (Hahn *et al.*, 1998). These neurones have also been shown to express pacemaker properties as orexigenic peptides such as orexin induce membrane potential oscillations and

burst-like firing patterns. In this study, NPY/AgRP pacemaker neurones in the ARC were inhibited by 5-HT (n=7; see figure 5.10). The response was characterised by hyperpolarisation of the membrane from a mean resting membrane potential of  $-54.0 \pm 6.1$  mV to  $-65.5 \pm 5.3$  mV, a mean peak membrane hyperpolarisation of  $11.5 \pm 2.2$  mV. The membrane hyperpolarisation was associated with a significant  $34.5 \pm 7.6$  % decrease in neuronal input resistance from a mean of  $1564 \pm 250$  M $\Omega$  at rest to  $942 \pm 127$  M $\Omega$  in the presence of 5-HT, a decrease of  $621 \pm 201$  M $\Omega$  ( $P < 0.05$ ). These data provide compelling evidence that 5-HT inhibits identified orexigenic NPY/AgRP neurones.

### 5.2.7 Co-localisation of 5-HT receptors and CART

CART is a neuropeptide that has been shown to be involved in the regulation of feeding and energy homeostasis (see chapter 4 and general introduction). There is a high level of CART expression within the hypothalamus, including in the ARC (Douglass *et al.*, 1995; Koylu *et al.*, 1998; Elias *et al.*, 2001) and CART is co-expressed in POMC neurones within the ARC (Elias *et al.*, 1998a). Therefore if 5-HT receptors are found co-localised with CART in the ARC, this will be strong evidence to suggest a role for 5-HT receptors in catabolic or anorexigenic signalling pathways.

The co-localisation of CART and the 5-HT receptor subtypes: 5-HT<sub>1A</sub>, 1B, and 7 was investigated in this study. Negative controls, in the absence of primary and secondary antibodies, contained no staining in all cases. These results represent preliminary work as further positive and negative controls need to be performed in order to produce detailed results.



The 5-HT<sub>1B</sub> receptor was expressed in two distinct clusters within the ARC, predominantly in the ventromedial region of the ARC, with a smaller cluster present in the lateral ARC (data not shown, due to initial problems capturing pictures on the confocal microscope. Once these problems had been overcome however, the experiment could not be repeated as the 5-HT<sub>1B</sub> antibody was no longer available.) When the double-labelling protocol was applied, in the majority of cases, neurones were identified that were positive only for the 5-HT<sub>1B</sub> receptor (see figure 5.11) or positive only for CART within the ARC (see figure 5.12), indicating no co-localisation between the two.

A minority of neurones were positive for both CART and the 5-HT<sub>1B</sub> receptor, indicating co-localisation between the two (see figure 5.13). Compared to the number of positive 5-HT<sub>1B</sub> and CART neurones, there were fewer co-localised neurones.

During the course of this study the primary antibody being used for the 5-HT<sub>1B</sub> receptor went out of production. Other commercially available 5-HT<sub>1B</sub> primary antibodies could not be used as the species they were raised in would have led to a cross-reaction with the CART antibody. It was therefore not possible to develop these results further to identify the actual percentage of co-localised neurones in the ARC or to further characterise the expression pattern of this receptor within the ARC.

No positive staining was obtained for the 5-HT<sub>1A</sub> or 5-HT<sub>7</sub> receptor. After the initial negative results, the protocol was altered several times to try to achieve positive staining. These changes included either removing or altering the concentration of the blocking serum, doubling the concentration of the primary antibody, changing the time taken to fix the slices, and removing the anti-fade to see

if this was affecting the results. However none of these changes resulted in any positive staining which indicated that the problem was unlikely to be due to the protocol. Further studies need to be carried out using additional positive and negative controls in order to gain confidence from these results.

### 5.3 Discussion

In the present study, the effects of 5-HT on ARC neurones were investigated using the whole-cell patch clamp recording technique.

5-HT hyperpolarised 45 % of ARC neurones with a concurrent decrease in input resistance. The 5-HT-induced hyperpolarisation still persisted in the presence of TTX indicating a direct effect of 5-HT on ARC neurones. The ionic mechanism by which the 5-HT-induced hyperpolarisation occurred is likely to be due to activation of a potassium conductance, as a reversal potential of -88 mV was obtained in voltage clamp, approaching that of  $K^+$  ions under our recording conditions. Additionally, in this study, an inward rectifier was seen to be activated or enhanced in a population of ARC neurones, as revealed from the current-voltage relationship by the decrease in input resistance at more negative membrane potentials. Therefore it is possible that a G-protein coupled inwardly-rectifying potassium channel (GIRK) was activated by 5-HT in this study; this needs to be tested further using specific blockers for this channel, for example tertiapin Q and clozapine. These results are in accordance with other studies that have implicated a potassium conductance in the 5-HT-induced hyperpolarisation, particularly through a GIRK channel (Bayliss *et al.*, 1997; Muraki *et al.*, 2004; Shen *et al.*, 2007).



To clarify the nature of the 5-HT receptors mediating the hyperpolarisation of the membrane, a range of agonists and antagonists were used. The 5-HT-induced hyperpolarisation was partially mimicked by the 5-HT<sub>1A</sub> agonist 8-OH-DPAT and the 5-HT<sub>1/5/7</sub> agonist 5-CT. However neither the 5-HT<sub>1A/1B</sub> agonist RU24969, the 5-HT<sub>1B</sub> agonist CP93129 nor the 5-HT<sub>3</sub> receptor agonist mCPBG were able to mimic the 5-HT-induced hyperpolarisation. These results indicate that the 5-HT-induced hyperpolarisation involves 5-HT<sub>1</sub> receptors and possibly 5-HT<sub>5/7</sub> receptors.

The 5-HT<sub>7</sub> receptor antagonist SB269970 and the 5-HT<sub>1A/1B</sub> receptor antagonist cyanopindolol partially inhibited the 5-HT-induced hyperpolarisation. The 5-HT<sub>1A</sub> receptor antagonist WAY-100635 attenuated the 5-HT-induced hyperpolarisation in a concentration-dependent manner but the 5-HT<sub>1B</sub> receptor antagonist SB224289 only partially reduced the response. The 5-HT<sub>2</sub> receptor antagonist altanserin and the 5-HT<sub>3</sub> receptor antagonist MDL72222 were without effect on the 5-HT-induced hyperpolarisation. These results indicate that predominantly the 5-HT<sub>1A</sub> receptor, and the 5-HT<sub>1B</sub> and 5-HT<sub>7</sub> subtypes are likely to be involved in mediating the 5-HT-induced hyperpolarisation. These results are in agreement with previous studies which have identified these receptors in 5-HT-induced hyperpolarisations both within the ARC (Heisler *et al.*, 2006) and in other areas of the brain, such as the prefrontal cortex (Araneda & Andrade, 1991), subthalamic nucleus (Stanford *et al.*, 2005; Shen *et al.*, 2007), lateral hypothalamus (LH; Muraki *et al.*, 2004) and caudal raphé nucleus (Bayliss *et al.*, 1997).

The study then went on to try to identify types of neurones in the ARC that were hyperpolarised by 5-HT. Ghrelin is an orexigenic hormone that is released from the stomach, and both central and peripheral injections of ghrelin cause an increase in food intake and body-weight in rats and humans (Tschop *et al.*, 2000; Wren *et al.*,

2001a,b; Wang *et al.*, 2002; Faulconbridge *et al.*, 2003; Currie *et al.*, 2005). In this study, ghrelin was used as a marker to identify orexigenic neurones as is it known to selectively target such neurones. Ghrelin was applied to a number of ARC neurones that had responded to 5-HT with membrane hyperpolarisation. Ghrelin caused a depolarisation in 79 % of these neurones with only 21 % of these neurones not responding to ghrelin. As ghrelin is known to selectively activate orexigenic neurones, these results suggest that the neurones that are hyperpolarised by 5-HT are likely to be orexigenic neurones, such as NPY neurones within the ARC. Further evidence that 5-HT is likely to be inhibiting NPY neurones is shown by the fact that a population of neurones have been identified within the ARC that express NPY and AgRP (van den Top *et al.*, 2004). These neurones express certain active conductances that identify them and are called cluster 2 neurones in this study (see chapter 3). 5-HT hyperpolarised cluster 2 neurones in this study, providing further evidence that 5-HT hyperpolarises orexigenic NPY neurones.

The preliminary results from the immunohistochemistry study indicate that the 5-HT<sub>1B</sub> receptor was predominantly located on neurones in the ventromedial ARC with a smaller subset of neurones in the lateral ARC expressing this receptor. CART is an anorexigenic peptide, co-localised with POMC neurones in the ARC, which is known to be involved in the control of feeding (Elias *et al.*, 1998a; Lambert *et al.*, 1998). In this study, it was used in a double-labelling protocol alongside the 5-HT receptors so that we could determine if any of the 5-HT receptors were on the same neurones as CART and hence found on anorexigenic neurones. In the majority of cases, the 5-HT<sub>1B</sub> receptor was not found co-localised on CART neurones, indicating that the 5-HT<sub>1B</sub> receptor is not usually found on anorexigenic POMC neurones. It would be interesting to see what types of neurones 5-HT<sub>1B</sub> receptors do



co-localise with. One possibility is that they may co-localise with the functionally antagonistic population of orexigenic NPY neurones, which has been shown previously (Heisler *et al.*, 2006), but it is not possible to look for co-localisation with NPY using immunohistochemistry as NPY is rapidly transported out of the cell body. In a small number of cases, the 5-HT<sub>1B</sub> receptor did co-localise with CART and hence there may be a subset of anorexigenic neurones within the ARC that do express the 5-HT<sub>1B</sub> receptor.

These results are in accordance with previous studies that have found the expression of 5-HT<sub>1B</sub> receptors in the hypothalamus (Makarenko *et al.*, 2002; Heisler *et al.*, 2006) and provide novel evidence of the expression of this receptor on a sub-population of anorexigenic CART positive neurones. Previous studies have only shown expression of this receptor on NPY neurones (Heisler *et al.*, 2006) or in close proximity to NPY neurones (Makarenko *et al.*, 2002). This study did find expression of 5-HT<sub>1B</sub> receptors on non-CART positive neurones also, which could have been NPY neurones. It was unfortunate that the results could not be developed further due to the problems obtaining the primary antibody for the 5-HT<sub>1B</sub> receptor. The majority of studies in the literature utilise the *in situ* hybridisation technique in order to locate the 5-HT receptors so this technique, or other techniques such as RT-PCR, will be worth considering for future work (for example see Pompeiano *et al.*, 1992 and Heisler *et al.*, 2002).

In conclusion, 5-HT directly inhibits a population of ARC neurones, including identified orexigenic NPY neurones, via the 5-HT<sub>1A</sub>, 5-HT<sub>1B</sub> and 5-HT<sub>7</sub> receptors, through a mechanism most likely involving a potassium conductance.

As 5-HT is recognised to be important in the regulation of energy homeostasis, the results from these studies (chapters 4 and 5) indicate that 5-HT acting upon NPY and POMC neurones within the ARC may contribute to this regulation of feeding and energy homeostasis. In the control of obesity specifically, drugs acting upon the serotonergic system (sibutramine and d-fen) have been used for the pharmacological treatment of obesity (Guy-Grand, 1992; Luque & Rey, 2002). The data from these studies could offer an explanation as to how these drugs were effective. These drugs may have been acting at the level of the ARC by inhibiting NPY neurones and exciting POMC neurones to reduce feeding and increase energy expenditure. In addition these data provide an insight into how selective agonists at 5-HT receptors might be able to produce a decrease in feeding. For example, the inhibitory actions upon feeding by 5-HT<sub>1B</sub> receptor agonists may have been partially due to 5-HT inhibiting orexigenic NPY neurones in the ARC (Bendotti & Samanin, 1987; Kennett *et al.*, 1987; Kennett & Curzon, 1988; Dryden *et al.*, 1996b). The down-regulation of feeding by 5-HT<sub>2C</sub> receptors might have been due to the excitation of anorexigenic POMC neurones by 5-HT within the ARC (Vickers *et al.*, 1999, 2001).

In conclusion these studies have provided further evidence of the involvement of 5-HT in the central control of energy homeostasis and specifically identified mechanisms by which 5-HT acts to regulate neuronal excitability at the level of the ARC.



**Figure 5.1 5-HT directly inhibits ARC neurones through activation of a potassium conductance**

**Ai:** Samples of a continuous whole-cell current-clamp recording from an ARC neurone with a resting membrane potential of  $-45$  mV (shown to the left of the trace in this and subsequent figures). Application of 5-HT ( $50$   $\mu$ M) for approximately 60 s, as indicated by the line above the trace, induced a membrane hyperpolarisation and associated decrease in neuronal input resistance, indicated by the decrease in amplitude of electrotonic potentials (downward deflections of the trace) evoked in response to hyperpolarising rectangular wave current pulses (5-30 pA, 1 s, 0.2 Hz; not shown).

**Aii:** Samples of a continuous whole-cell current-clamp recording from an ARC neurone in the presence of TTX (500 nM). Application of 5-HT ( $50$   $\mu$ M) for approximately 90 s induced a membrane hyperpolarisation and associated decrease in neuronal input resistance. Note the 5-HT-induced hyperpolarisation persists in the presence of TTX.

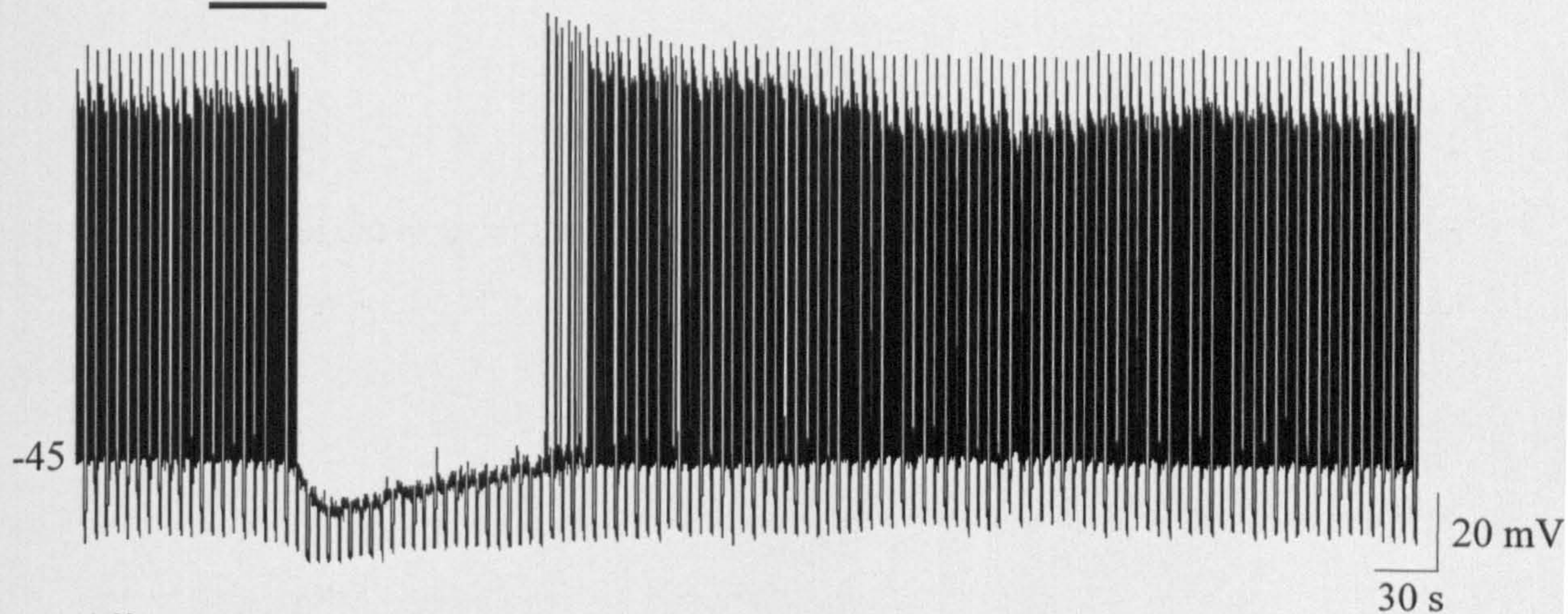
**Bi:** Superimposed samples from a continuous whole-cell current-clamp recording showing membrane potential responses of an ARC neurone to a series of depolarising and hyperpolarising rectangular-wave current pulses of constant increment, before (-130 to +10 pA, 1 s, 0.1 Hz) and in the presence of 5-HT (-150 to 30pA, 1 s, 0.1 Hz).

**Bii:** Plot of the current-voltage (I-V) relationships before ( $\circ$ ) and in the presence of 5-HT ( $\bullet$ ), shown in Bi. Note the decrease in the slope of the I-V in the presence of 5-HT indicating a decrease in neuronal resistance, with a reversal potential around  $-78$  mV, close to that for potassium ions under our recording conditions.

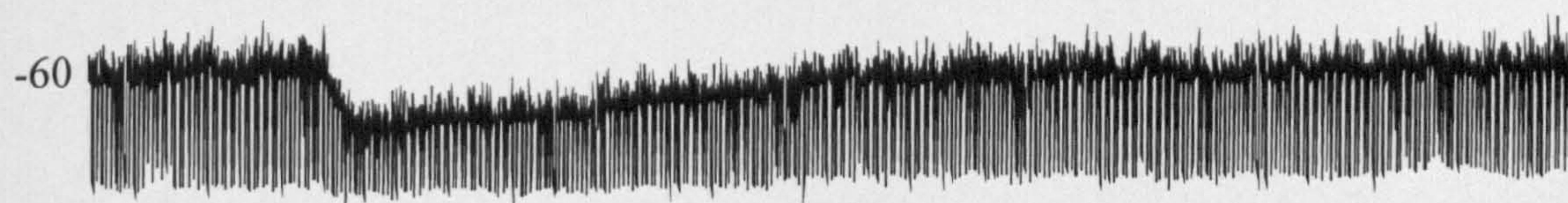


**Figure 5.1**

**Ai**     5-HT

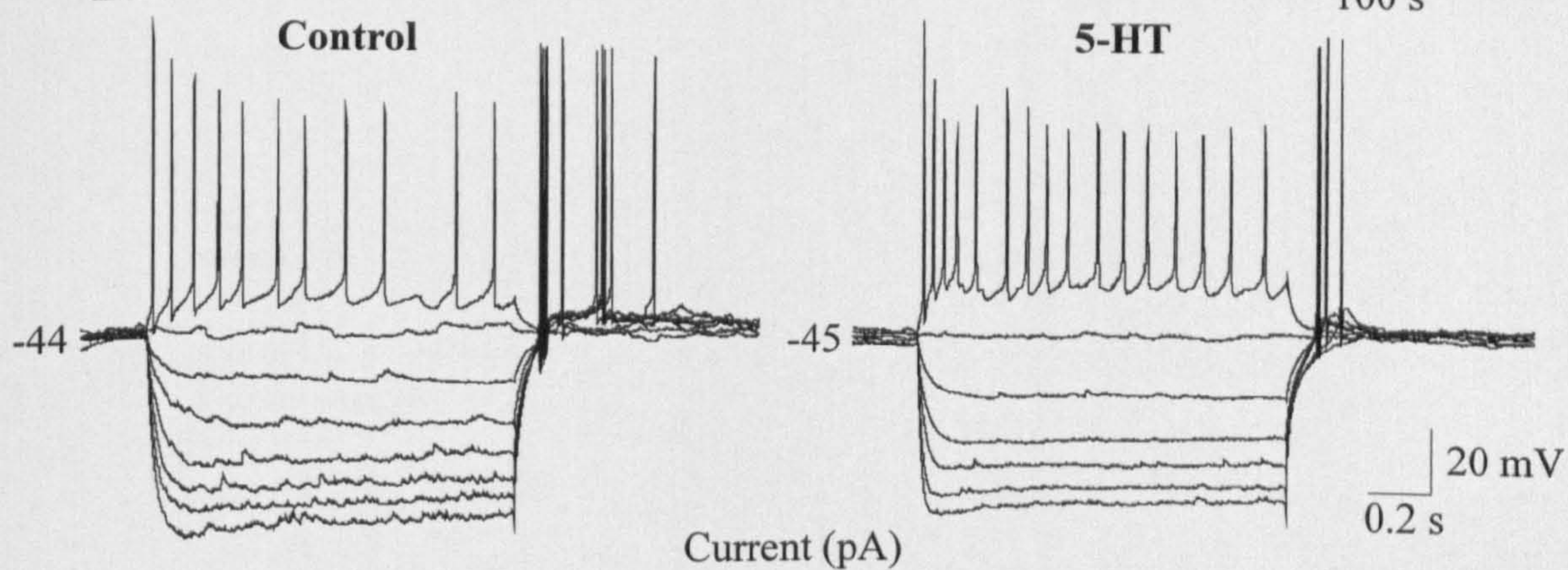


**Aii**     5-HT



**TTX**

**Bi**



**Bii**

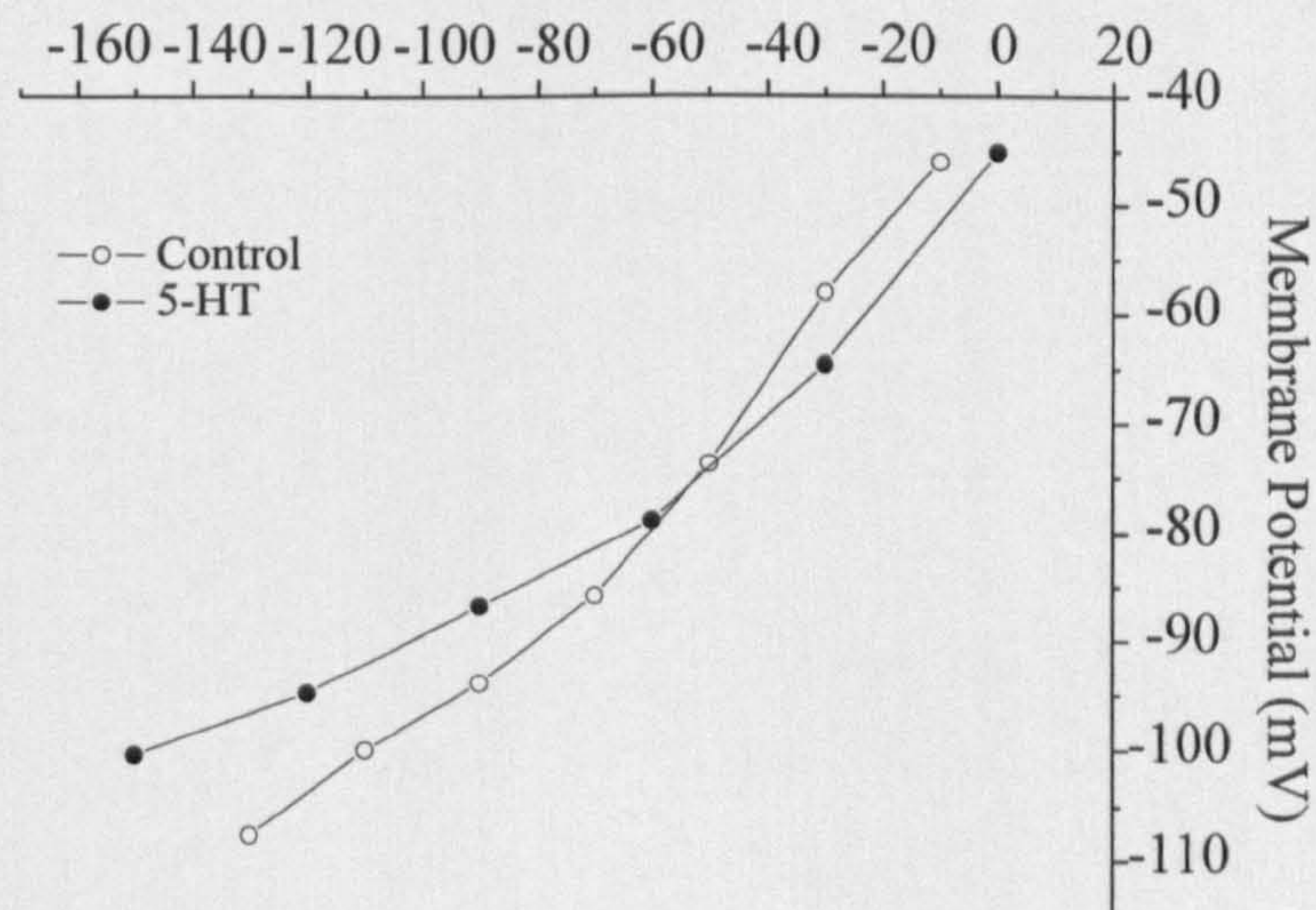




**Figure 5.2 5-HT induces an outward current in ARC neurones**

**A:** Application of 5-HT (50  $\mu$ M) for approximately 60 s, as indicated by the line above the trace, to an ARC neurone voltage-clamped at a holding potential of -40 mV induced an outward current.

**B:** Current responses obtained in voltage-clamp in the presence (green trace) and absence (black trace) of 5-HT. The currents were obtained from ramp protocols that drove the holding potential from -130 mV to -20 mV, at a rate of 10 mV per second. Note the reversal potential of about -84 mV.



**Figure 5.2**

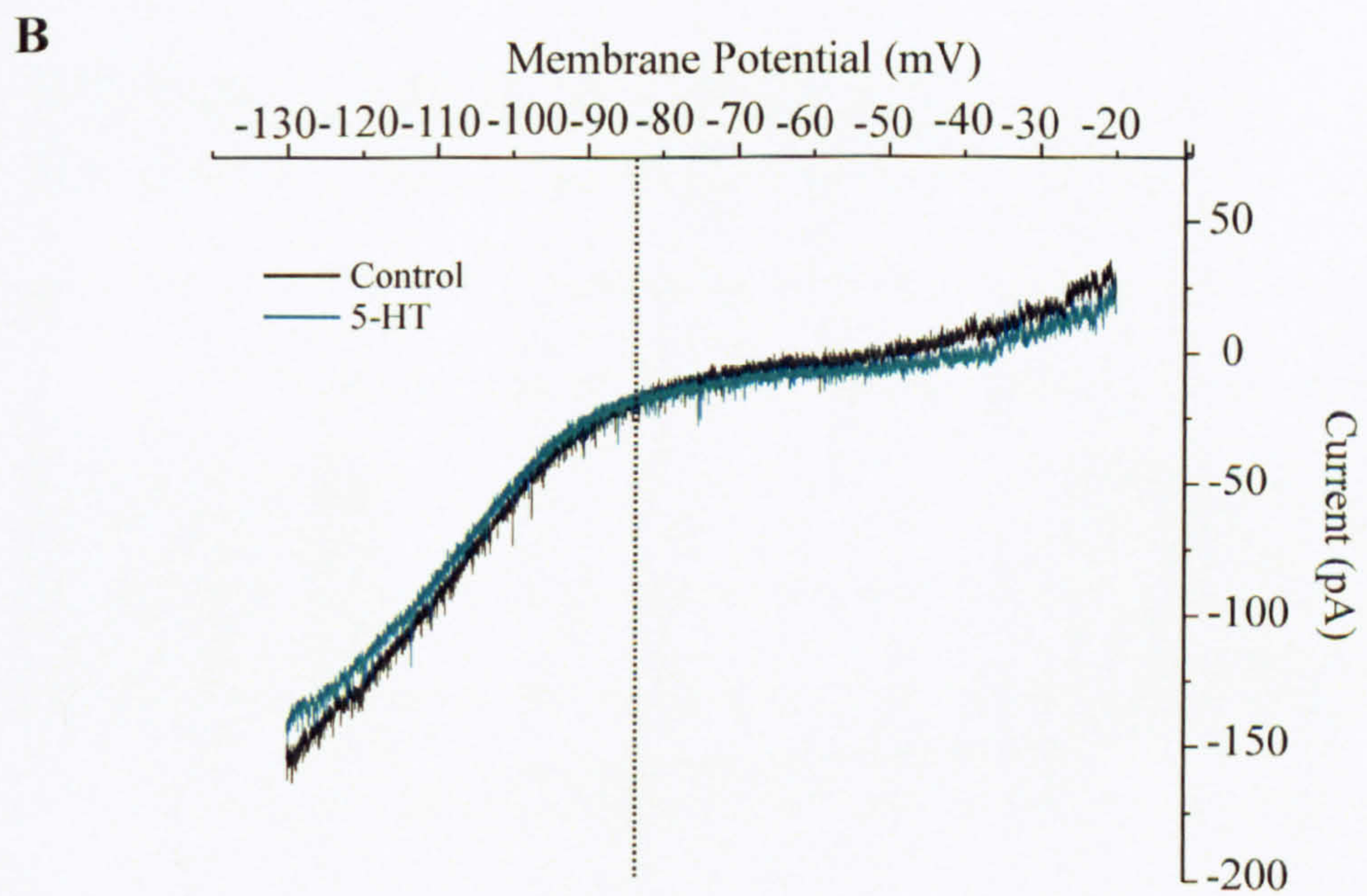
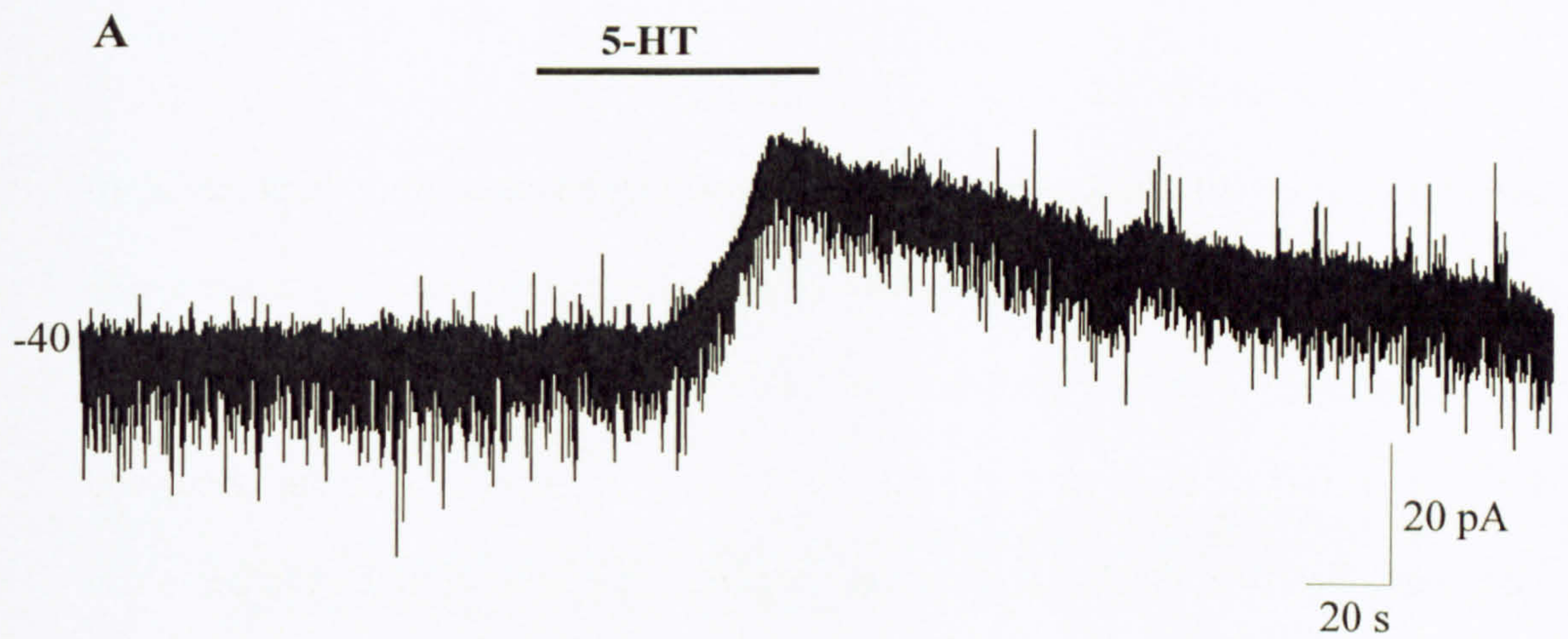




**Figure 5.3 The effects of the 5-HT receptor agonists 8-OH-DPAT and 5-CT on ARC neurones**

**Ai:** Samples of a continuous whole-cell current-clamp recording from an ARC neurone. Application of 5-HT (50  $\mu$ M) for approximately 60 s induced a membrane hyperpolarisation and associated decrease in neuronal input resistance.

**Aii:** Samples of a continuous whole-cell current-clamp recording from the same ARC neurone as in Ai. Application of the 5-HT<sub>1A/7</sub> receptor agonist 8-OH-DPAT (10  $\mu$ M) for approximately 60 s induced a small membrane hyperpolarisation.

**Bi:** Samples of a continuous whole-cell current-clamp recording from an ARC neurone. Application of 5-HT (50  $\mu$ M) for approximately 75 s induced a membrane hyperpolarisation and associated decrease in neuronal input resistance.

**Bii:** Samples of a continuous whole-cell current-clamp recording from the same ARC neurone as in Bi. Application of the 5-HT<sub>1/5/7</sub> receptor agonist 5-CT (10  $\mu$ M) for approximately 75 s induced a membrane hyperpolarisation, mimicking the effect of 5-HT.



**Figure 5.3**

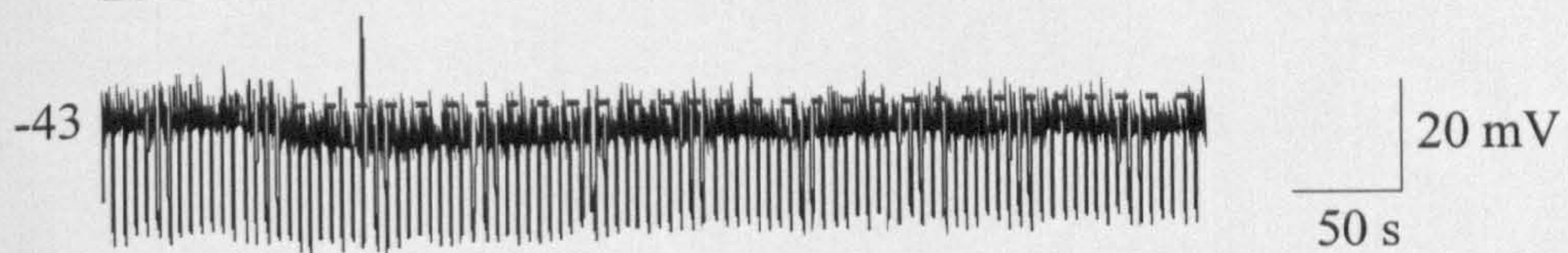
**Ai**

**5-HT**



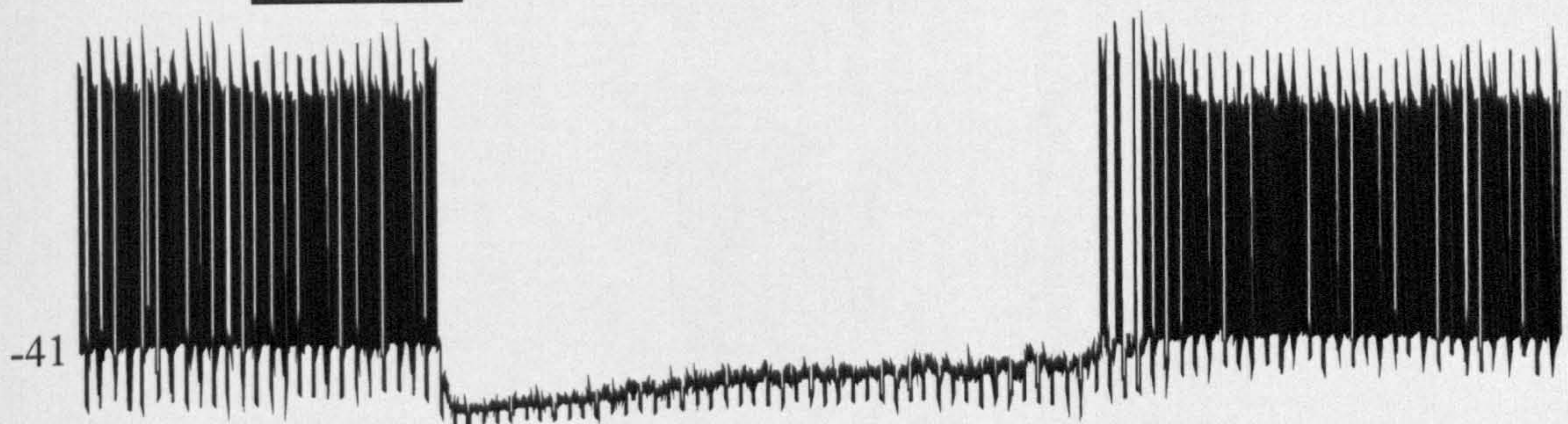
**Aii**

**8-OH-DPAT**



**Bi**

**5-HT**



**Bii**

**5-CT**

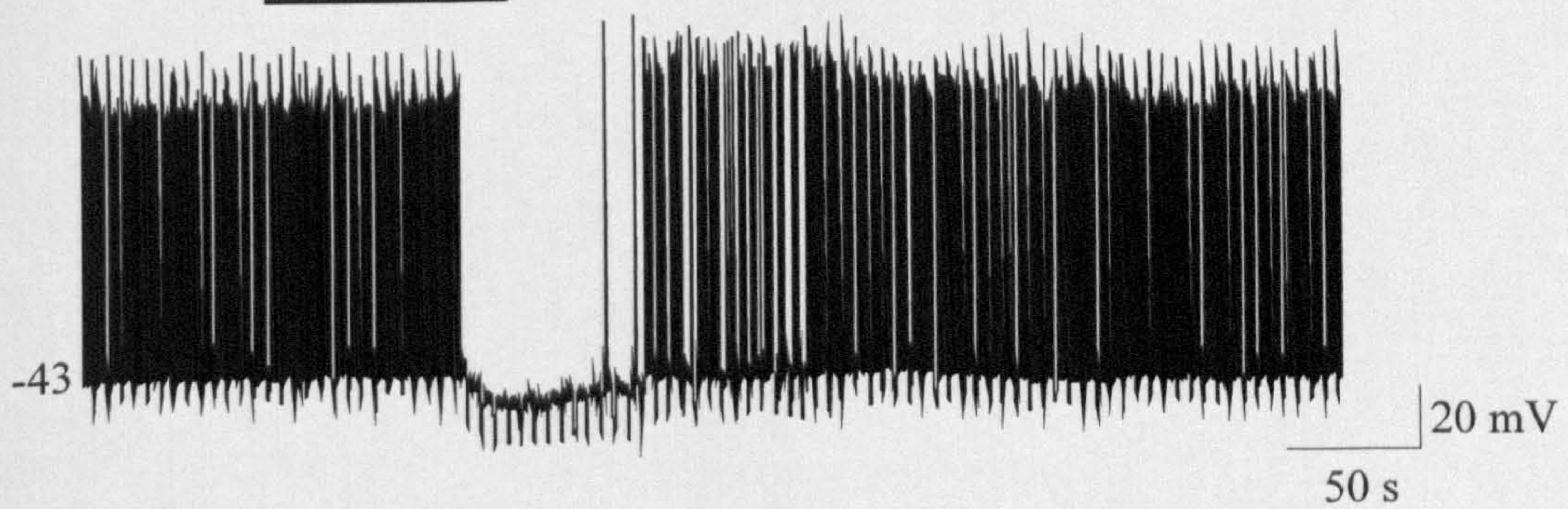




**Figure 5.4 The effects of the 5-HT receptor agonists RU 24969 and CP 93129 on ARC neurones**

**Ai:** Samples of a continuous whole-cell current-clamp recording from an ARC neurone. Application of 5-HT (50  $\mu$ M) for approximately 30 s induced a membrane hyperpolarisation and decrease in neuronal input resistance. The parallel lines indicate a break in the trace during the wash off of 5-HT.

**Aii:** Samples of a continuous whole-cell current-clamp recording from the same ARC neurone as in Ai. Application of the 5-HT<sub>1A/1B</sub> receptor agonist RU 24969 (20  $\mu$ M) had no effect on membrane potential or input resistance.

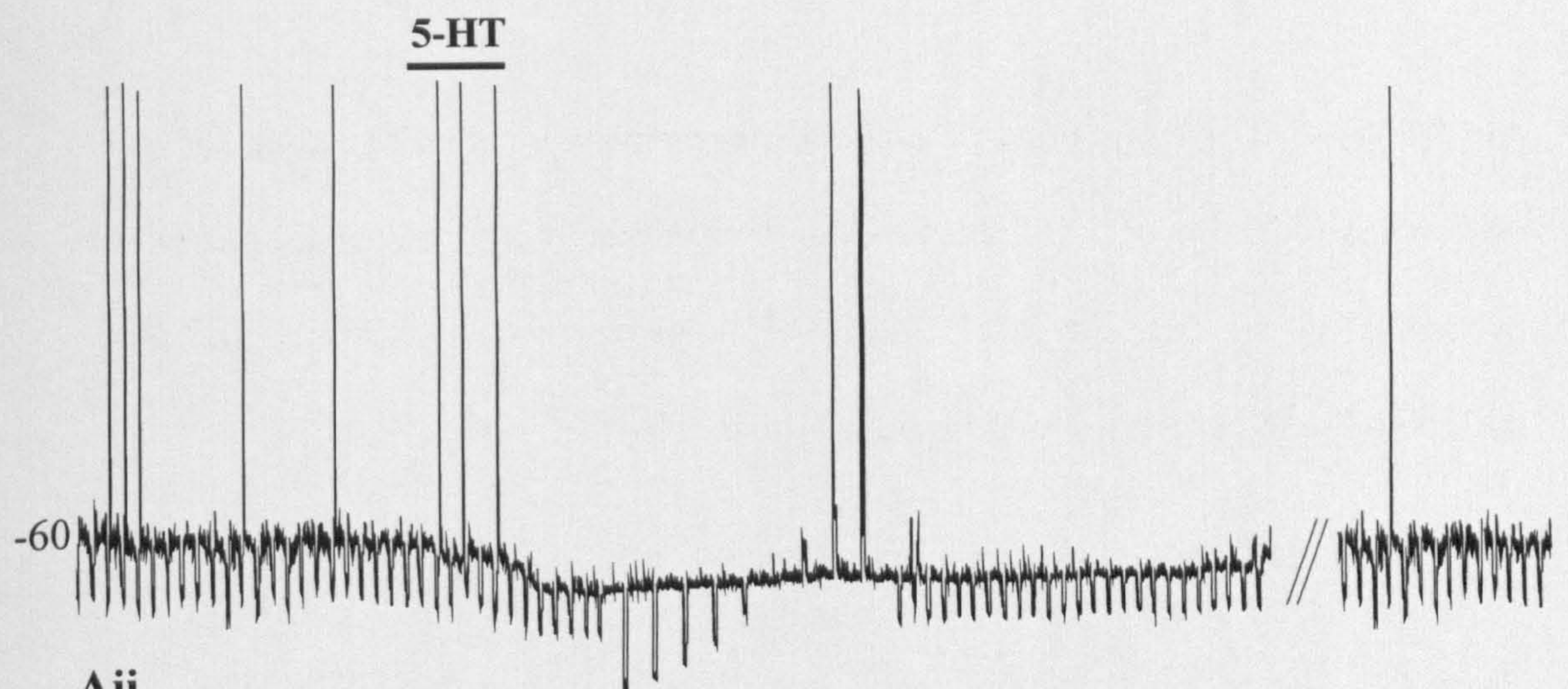
**Bi:** Samples of a continuous whole-cell current-clamp recording from an ARC neurone. Application of 5-HT induced a membrane hyperpolarisation. The parallel lines indicate the time, approximately 60 s, where an I-V was taken.

**Bii:** Samples of a continuous whole-cell current-clamp recording from the same ARC neurone as in Bi. Application of the 5-HT<sub>1B</sub> receptor agonist CP 93129 (1  $\mu$ M) had no effect on membrane potential or input resistance.

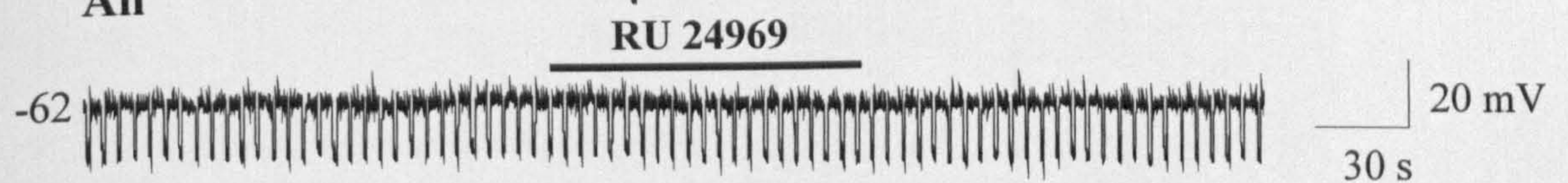


**Figure 5.4**

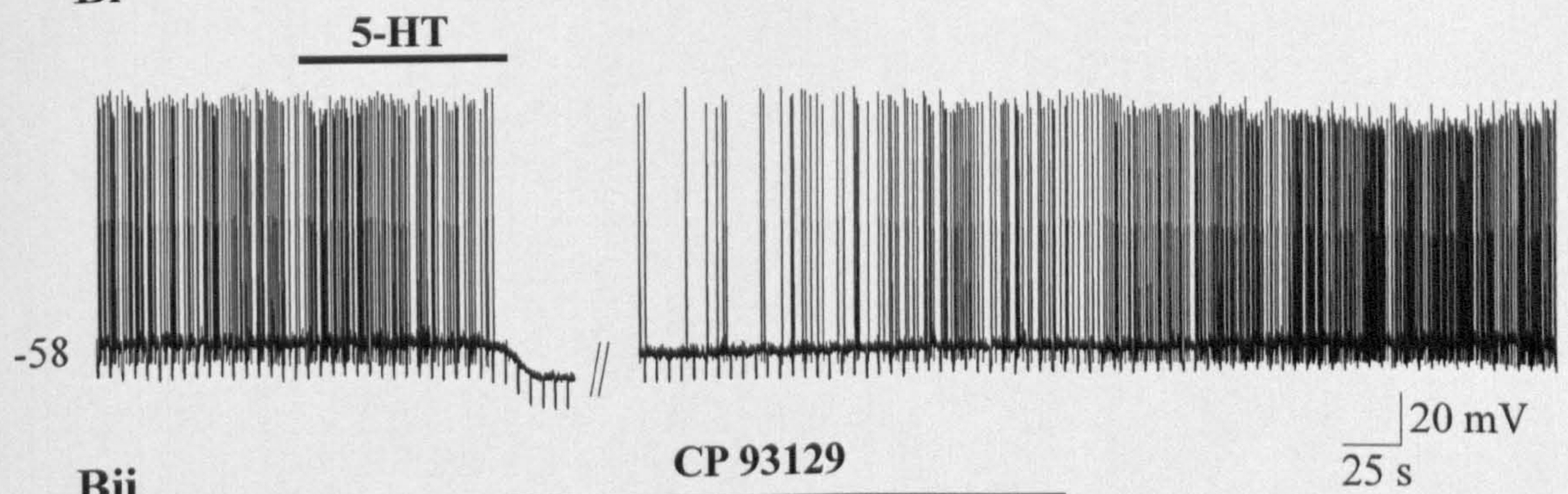
**Ai**



**Aii**



**Bi**



**Bii**

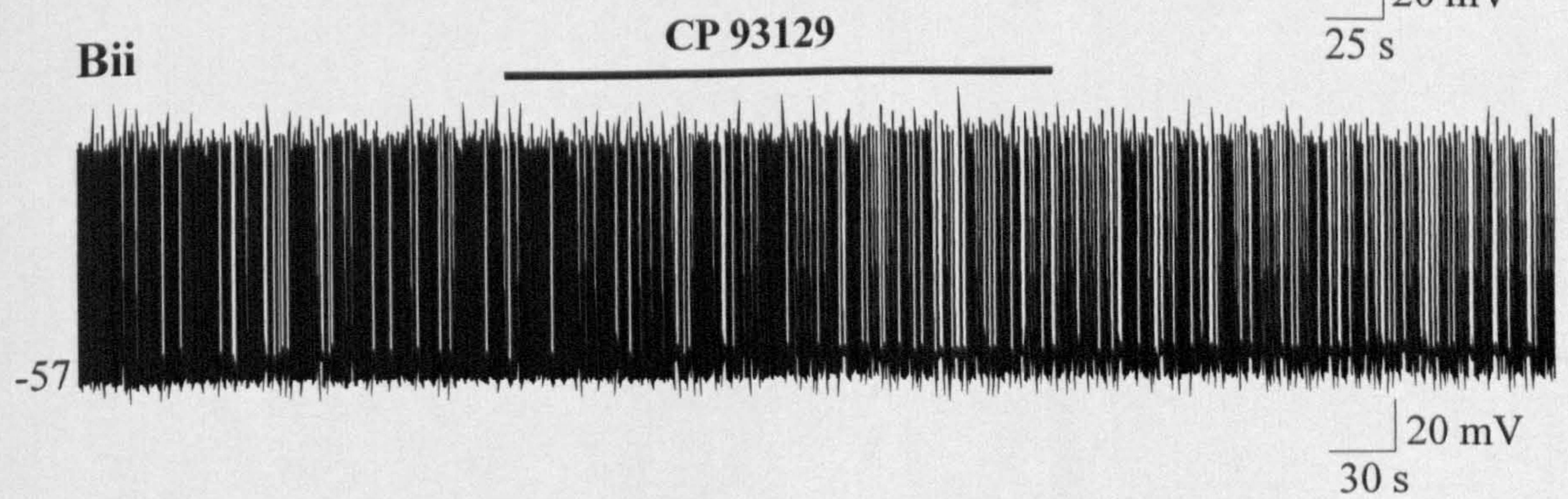




**Figure 5.5 The effects of the 5-HT receptor antagonists SB 269970 and cyanopindolol on ARC neurones**

**Ai:** Samples of a continuous whole-cell current-clamp recording from an ARC neurone. Application of 5-HT (50  $\mu$ M) for approximately 50 s induced a membrane hyperpolarisation and associated decrease in neuronal input resistance. The large deflections at the peak of the response indicate where an I-V was taken.

**Aii:** Samples of a continuous whole-cell current-clamp recording from the same ARC neurone as in Ai. Application of the 5-HT<sub>7</sub> receptor antagonist SB 269970 (10  $\mu$ M), as indicated by the line below the trace, had no effect on the 5-HT-induced hyperpolarisation in this neurone. The large deflections at the peak of the response indicate where an I-V was taken.

**Bi:** Samples of a continuous whole-cell current-clamp recording from an ARC neurone. Application of 5-HT (50  $\mu$ M) for approximately 75 s induced a membrane hyperpolarisation and associated decrease in neuronal input resistance.

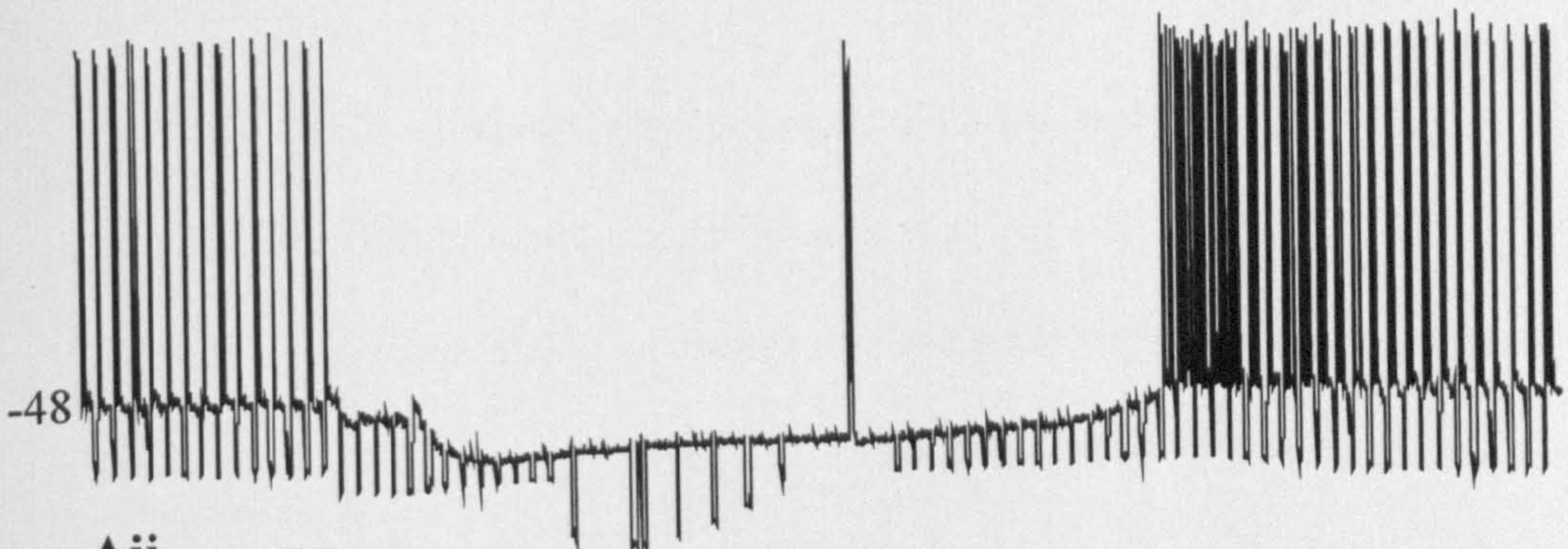
**Bii:** Samples of a continuous whole-cell current-clamp recording from the same ARC neurone as in Bi. Application of the 5-HT<sub>1</sub> receptor agonist cyanopindolol (10  $\mu$ M) significantly attenuated the 5-HT-induced hyperpolarisation.



Figure 5.5

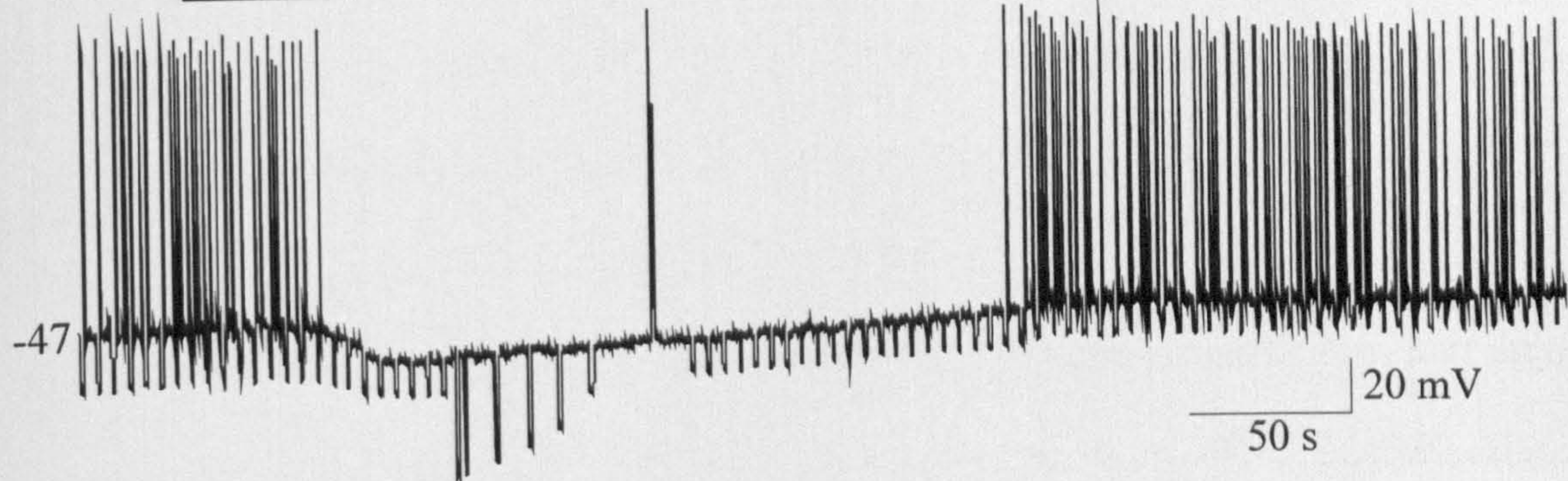
Ai

5-HT



Aii

5-HT

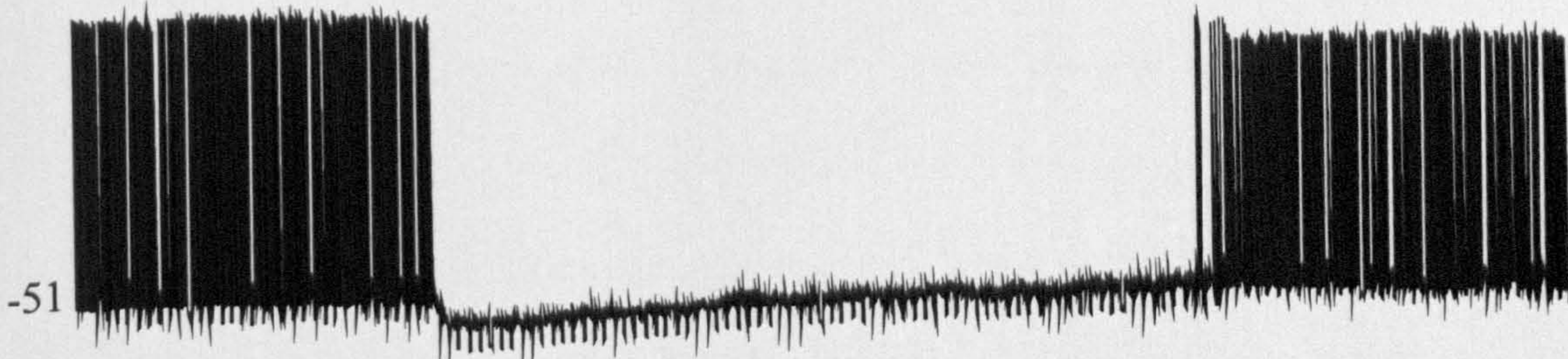


20 mV  
50 s

SB 269970

Bi

5-HT



Bii

5-HT



20 mV  
50 s

Cyanopindolol



**Figure 5.6 The effects of the 5-HT receptor antagonists WAY-100635 and SB 224289 on ARC neurones**

**Ai:** Samples of a continuous whole-cell current-clamp recording from an ARC neurone. Application of 5-HT (50  $\mu$ M) for approximately 30 s induced a membrane hyperpolarisation and associated decrease in neuronal input resistance.

**Aii:** Samples of a continuous whole-cell current-clamp recording from the same ARC neurone as in Ai. Application of the 5-HT<sub>1A</sub> receptor antagonist WAY-100635 (1  $\mu$ M) inhibited the 5-HT-induced hyperpolarisation.

**Aiii:** Plot showing the reduction in the amplitude of the 5-HT-induced depolarisation in the presence of increasing concentrations of WAY-100635. The control response was set as 100% and upon increasing concentrations of WAY-100635 there was a reduction in the amplitude of the response compared to control.

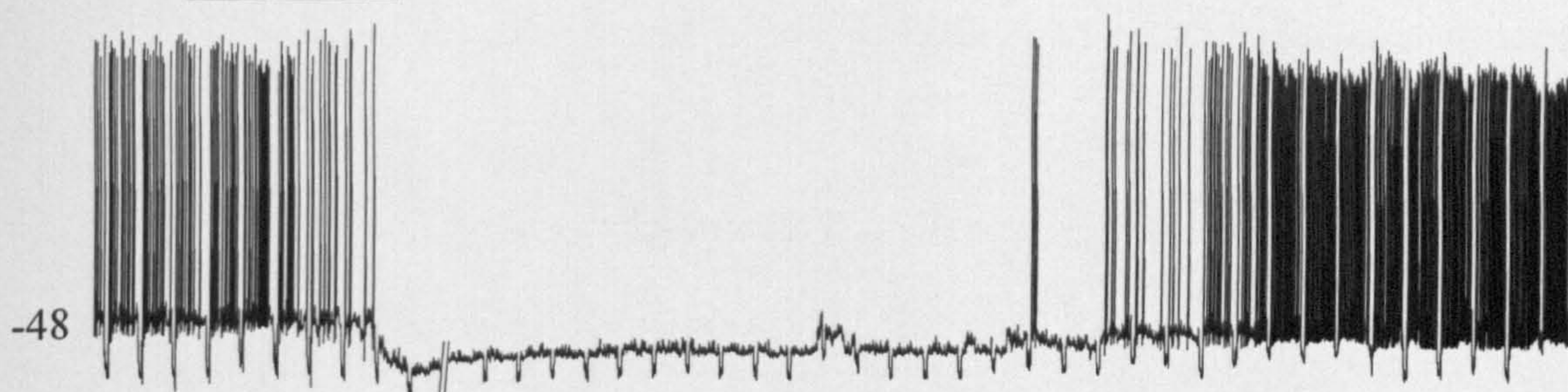
**Bi:** Samples of a continuous whole-cell current-clamp recording from an ARC neurone. Application of 5-HT (50  $\mu$ M) for approximately 40 s induced a membrane hyperpolarisation and associated decrease in neuronal input resistance. The deflections during the response correspond to the point where an I-V was taken.

**Bii:** Samples of a continuous whole-cell current-clamp recording from the same ARC neurone as in Bi. Application of the 5-HT<sub>1B</sub> receptor antagonist SB 224289 (2  $\mu$ M) partially inhibited the 5-HT-induced hyperpolarisation and associated decrease in input resistance.

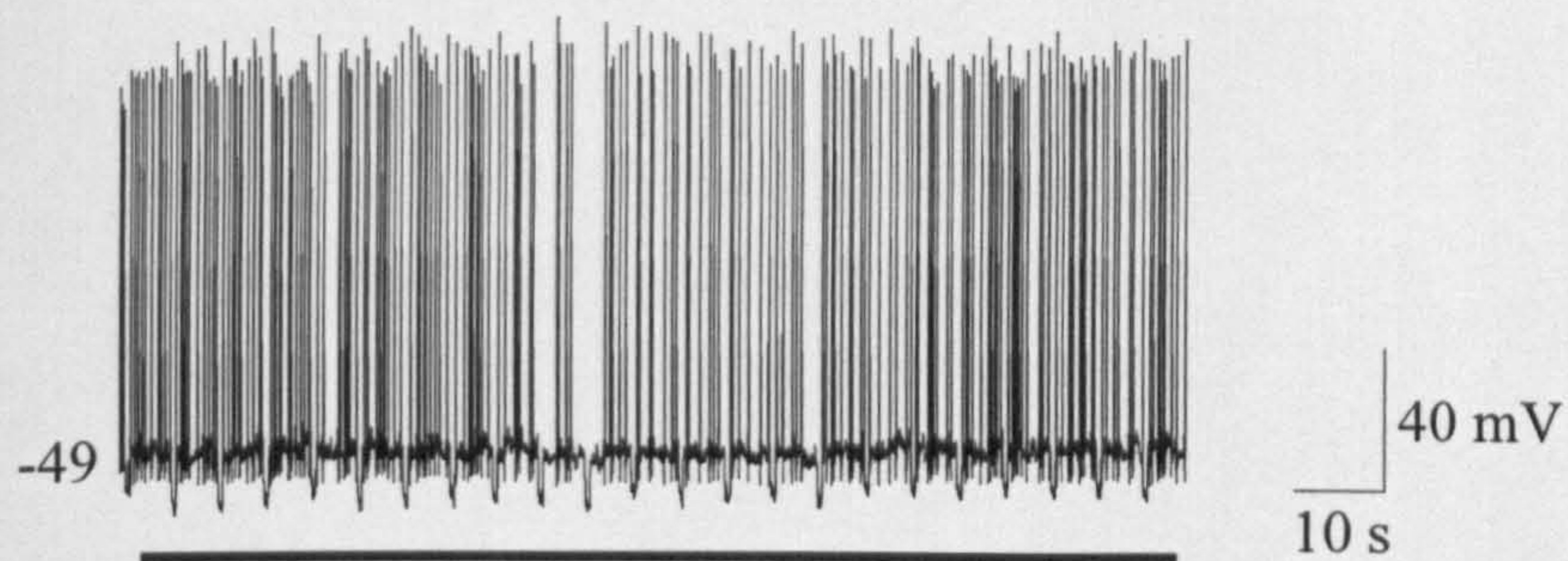


**Figure 5.6**

**Ai**     5-HT

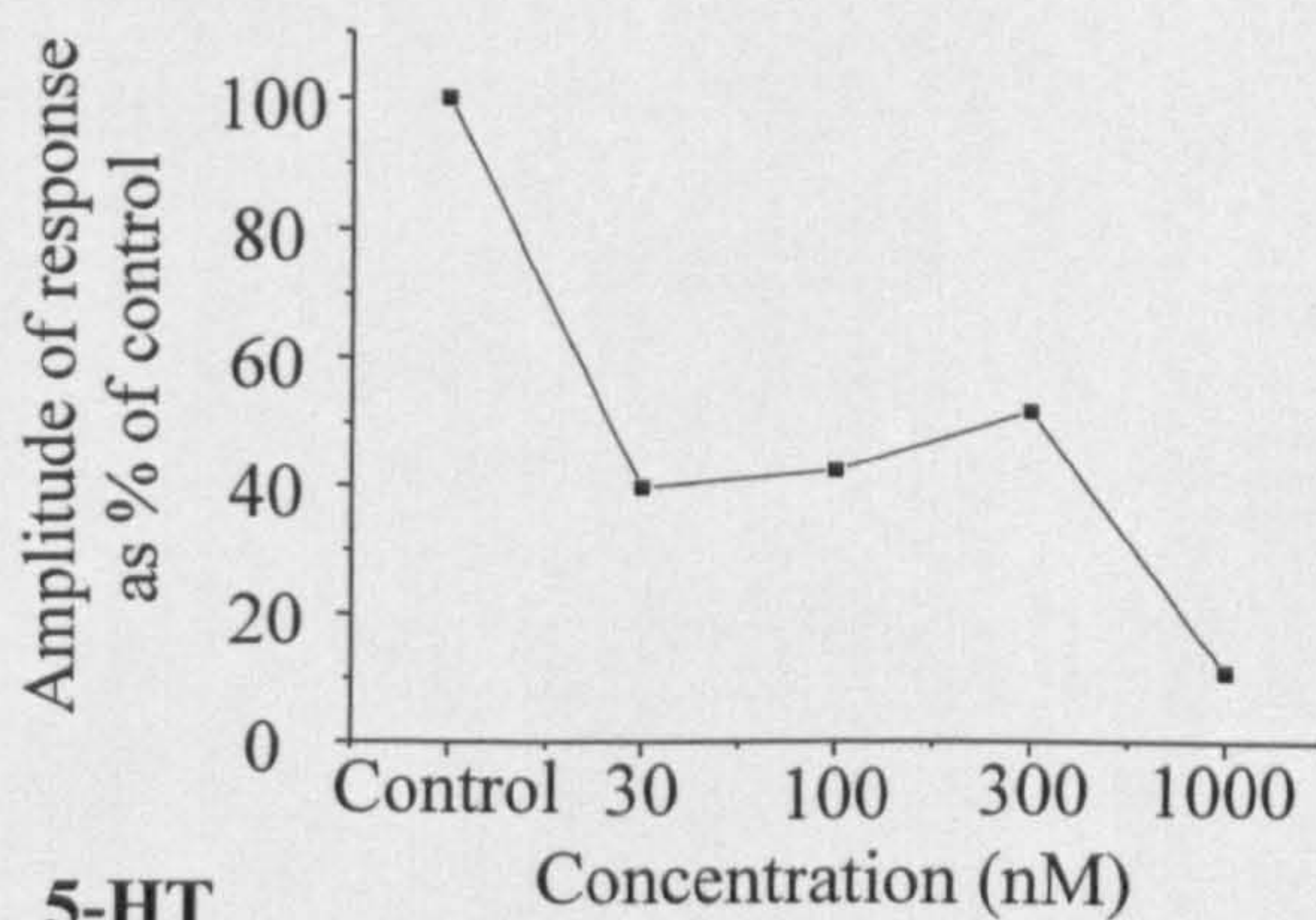


**Aii**     5-HT

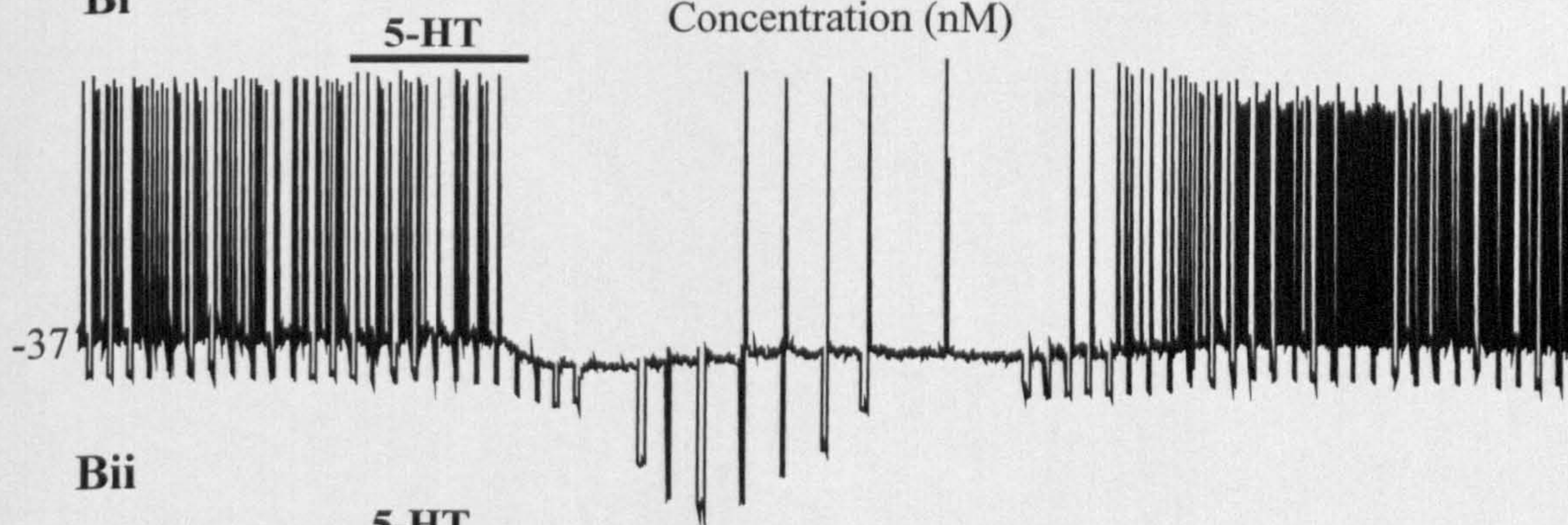


**WAY-100635**

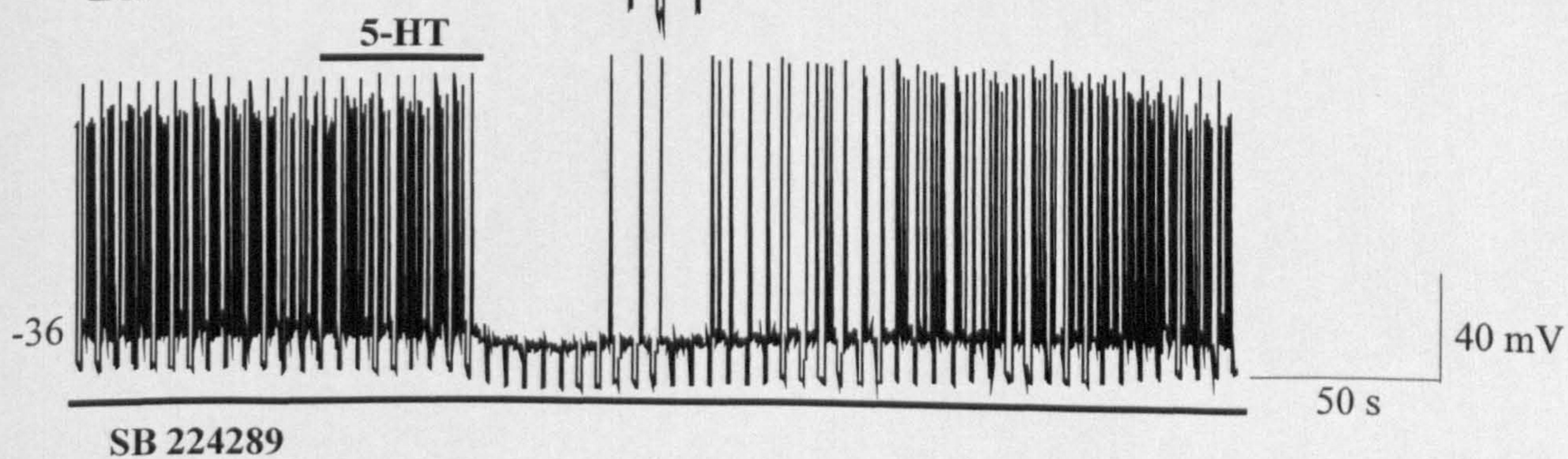
**Aiii**



**Bi**



**Bii**



**SB 224289**



**Figure 5.7 The effects of the 5-HT receptor antagonists WAY-100635, SB 224289 and SB 269970 in combination on ARC neurones**

**Ai:** Samples of a continuous whole-cell current-clamp recording from an ARC neurone. Application of 5-HT (50  $\mu$ M) for approximately 90 s induced a membrane hyperpolarisation and associated decrease in neuronal input resistance. The parallel lines indicate a period of time following washout of the drug.

**Aii:** Samples of a continuous whole-cell current-clamp recording from the same ARC neurone as in Ai. Application of the 5-HT<sub>1B</sub> receptor antagonist SB 224289 (2  $\mu$ M) and the 5-HT<sub>7</sub> receptor antagonist SB 269970 (10  $\mu$ M) partially reduced the 5-HT-induced hyperpolarisation.

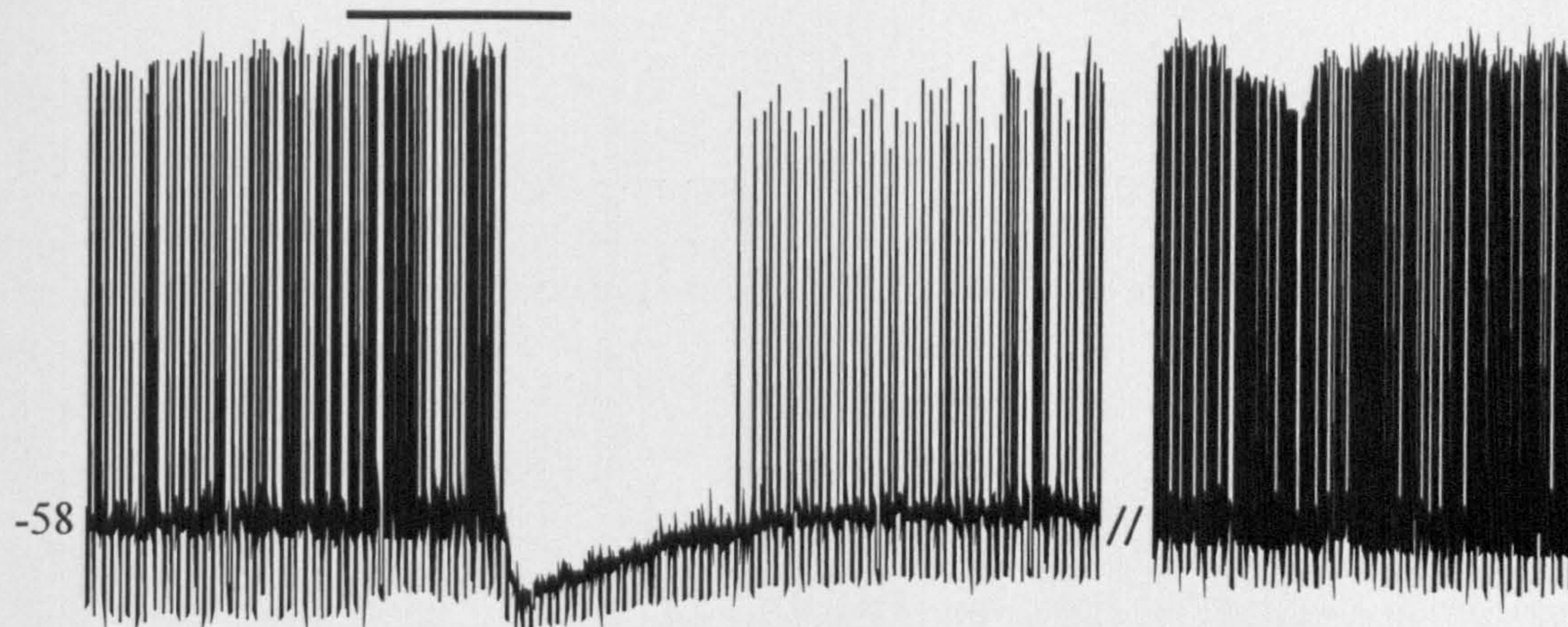
**Aiii:** Samples of a continuous whole-cell current-clamp recording from the same ARC neurone as in Ai. Application of the 5-HT<sub>1A</sub> receptor antagonist WAY-100635 (300 nM), 5-HT<sub>1B</sub> receptor antagonist SB224289 (2  $\mu$ M) and the 5-HT<sub>7</sub> receptor antagonist SB269970 (10  $\mu$ M) suppressed the 5-HT-induced hyperpolarisation.



**Figure 5.7**

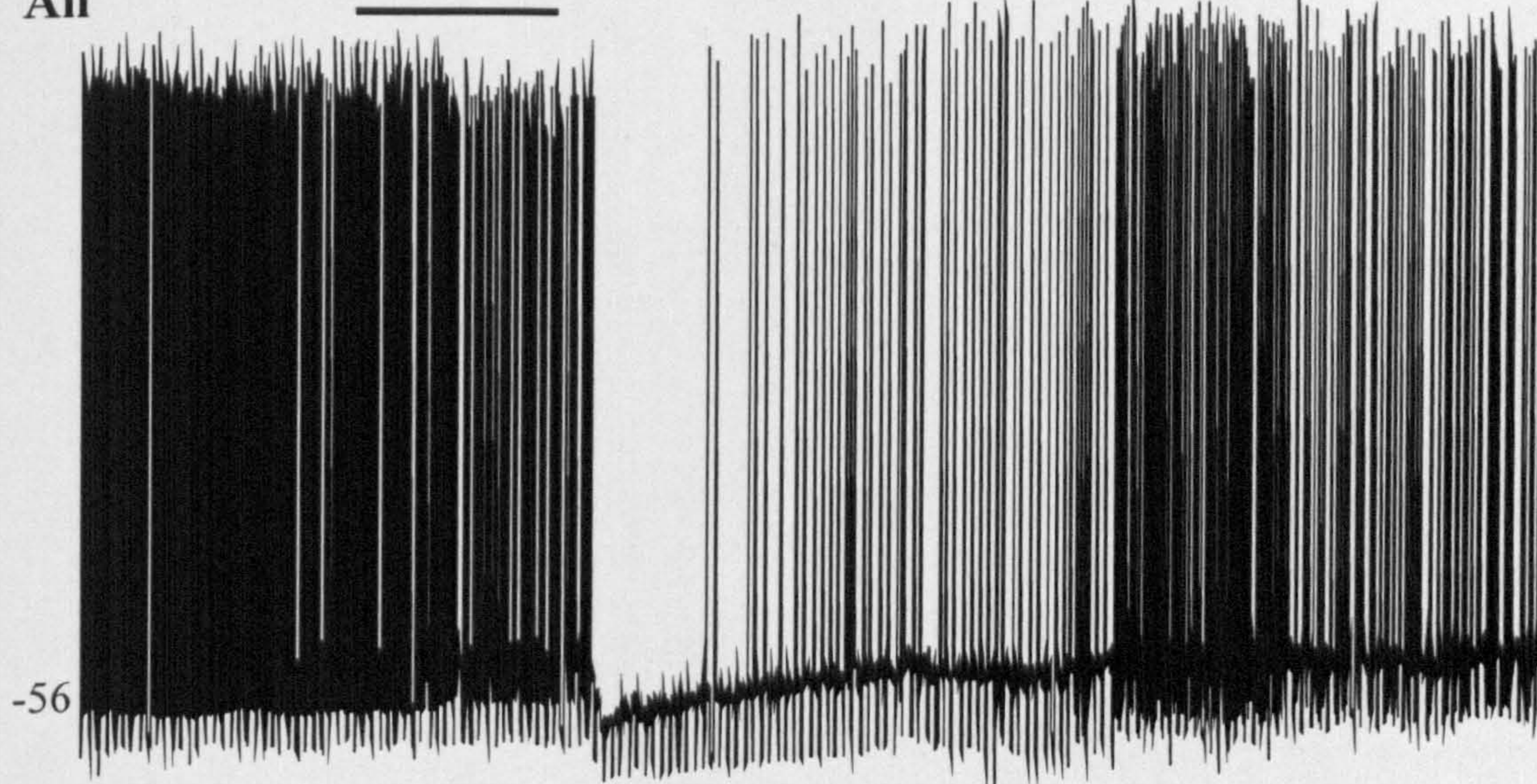
**Ai**

**5-HT**



**Aii**

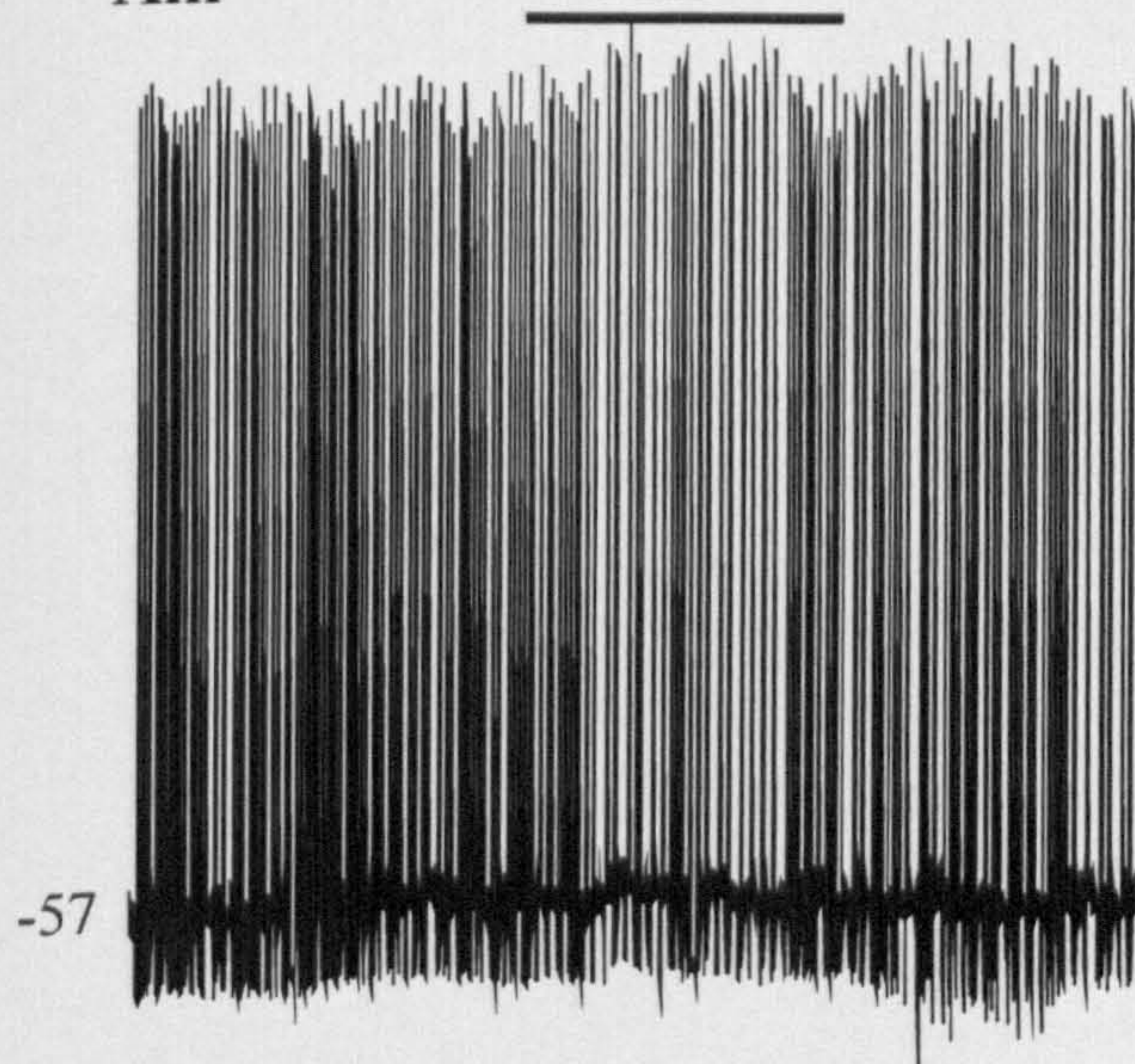
**5-HT**



**SB 224289, SB 269970**

**Aiii**

**5-HT**



**WAY-100635, SB 224289, SB 269970**

20 mV

60 s



**Figure 5.8 The effects of the 5-HT receptor antagonists MDL7222 and altanserin on ARC neurones**

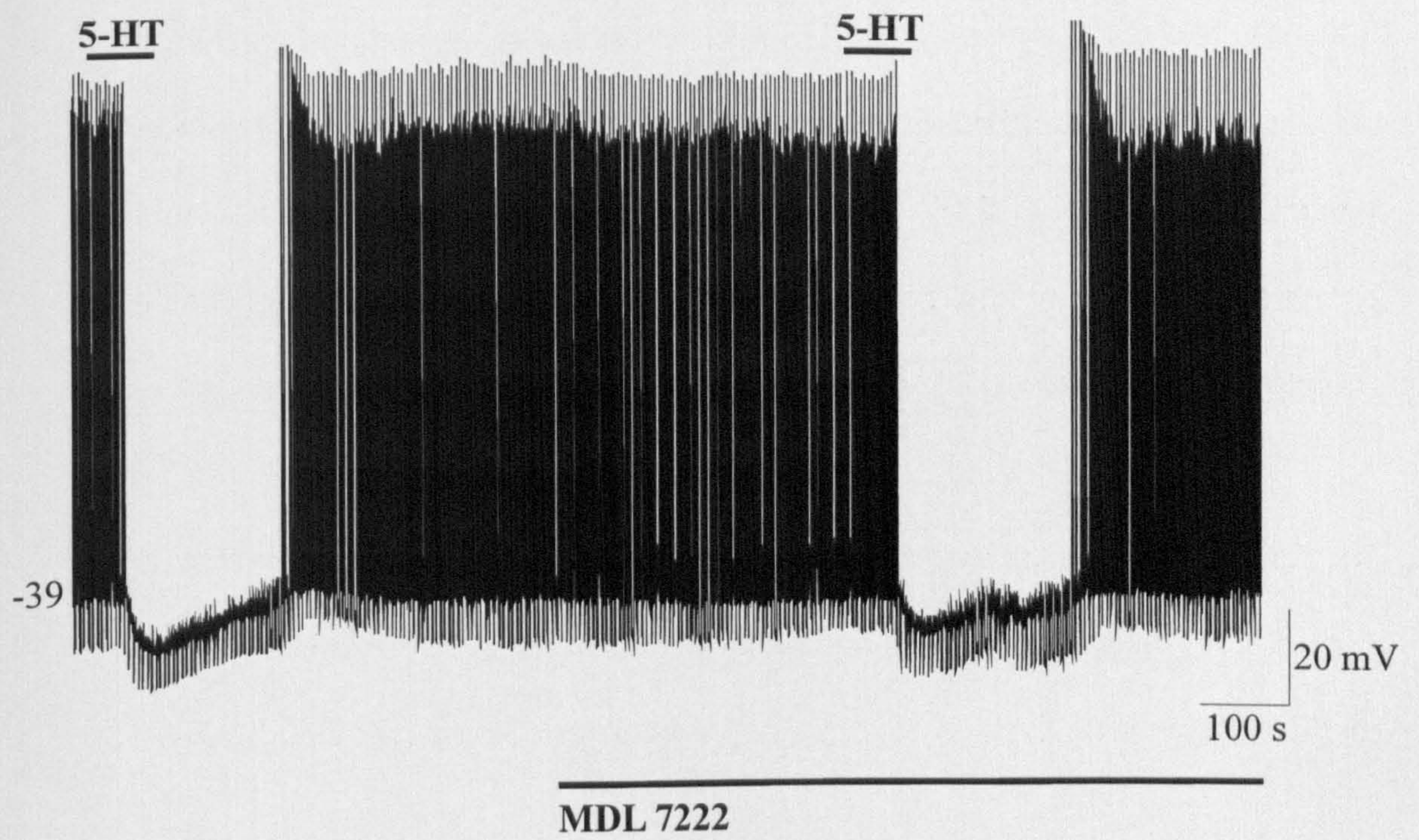
**A:** Samples of a continuous whole-cell current-clamp recording from an ARC neurone. Application of 5-HT (50  $\mu$ M) for approximately 60 s induced a membrane hyperpolarisation; a response unaffected by the subsequent application of the 5-HT<sub>3</sub> receptor antagonist MDL7222 (100 nM).

**B:** Samples of a continuous whole-cell current-clamp recording from an ARC neurone. Application of 5-HT induced a membrane hyperpolarisation; a response unaffected by the application of the 5-HT<sub>2</sub> receptor antagonist altanserin (200 nM).



**Figure 5.8**

**A**



**B**

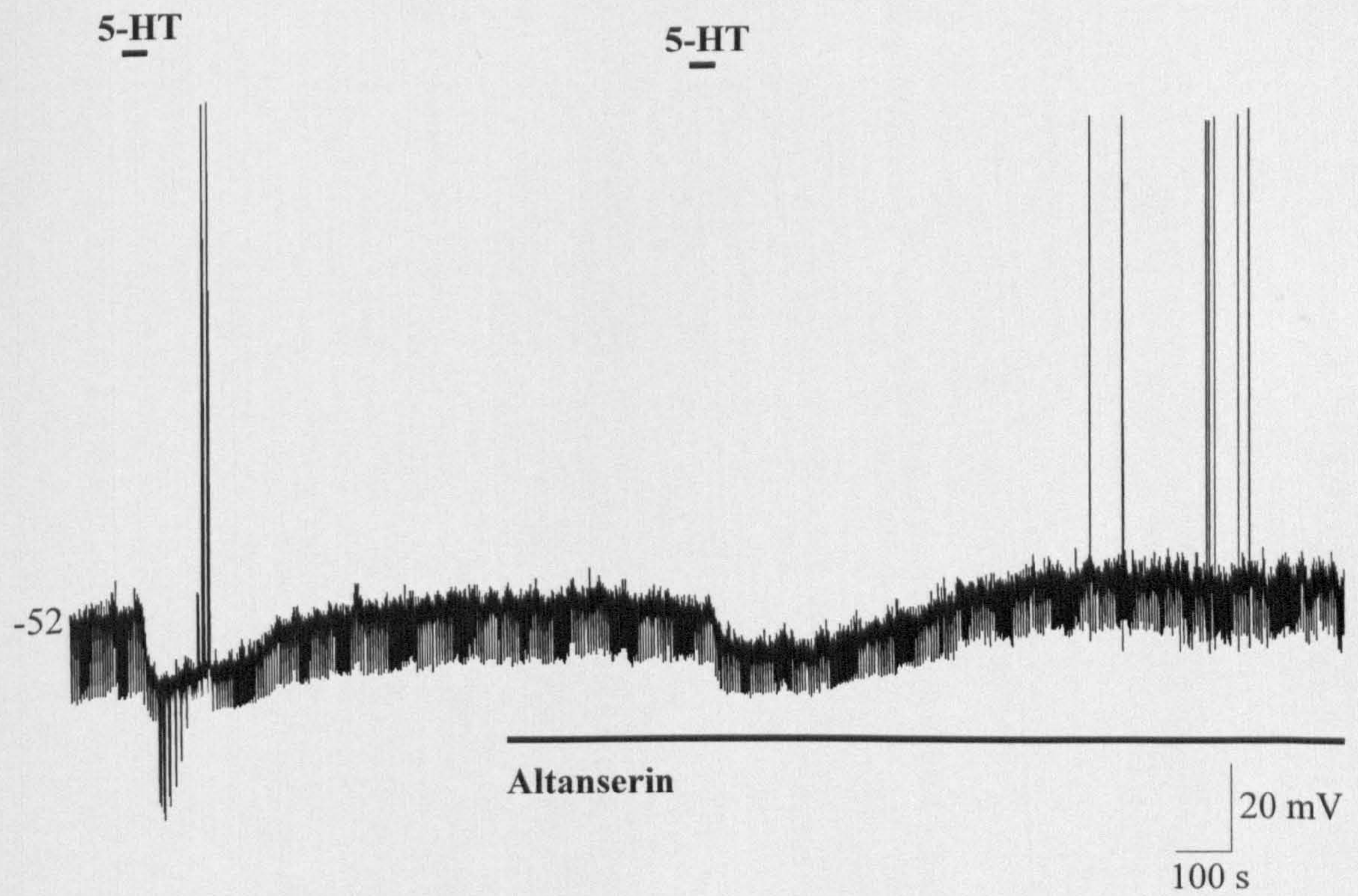




**Figure 5.9 The effects of ghrelin on 5-HT-inhibited neurones**

**Ai:** Samples of a continuous whole-cell current-clamp recording from an ARC neurone. Application of 5-HT (50  $\mu$ M) for approximately 50 s induced a membrane hyperpolarisation.

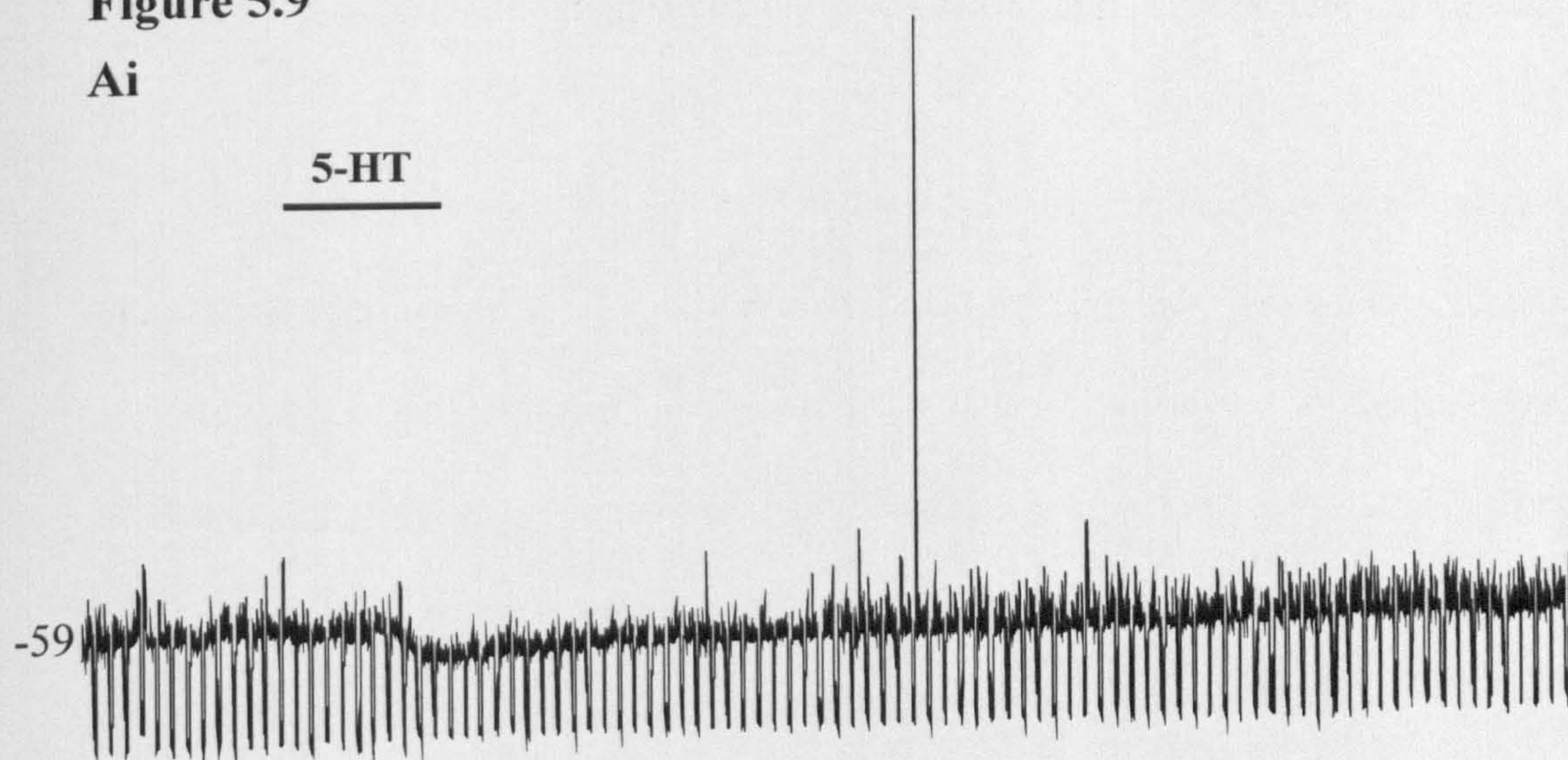
**Aii:** Samples of a continuous whole-cell current-clamp recording from the same ARC neurone in Ai. Application of ghrelin (100 nM) induced a membrane depolarisation and increase in action potential firing.



**Figure 5.9**

**Ai**

5-HT



**Aii**

Ghrelin

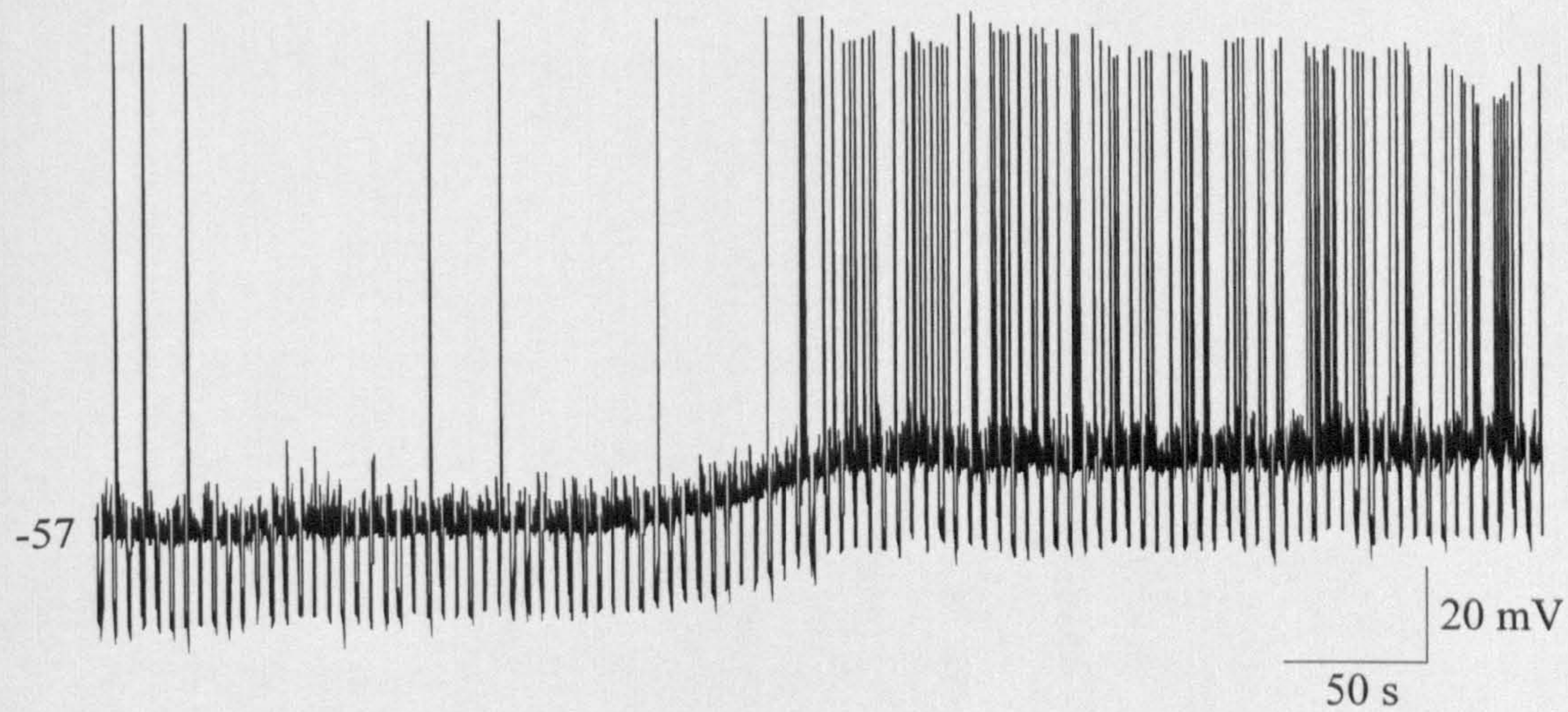




**Figure 5.10 The effects of 5-HT on orexigenic NPY/AgRP neurones**

**A:** Superimposed samples of a continuous whole-cell current-clamp recording showing membrane potential responses to a series of depolarising and hyperpolarising rectangular-wave current pulses of constant increment. This neurone was identified as an orexigenic ARC NPY/AgRP pacemaker neuron, by the presence of an anomalous inward rectifier ( $I_{an}$ ) and an A-like conductance ( $I_A$ ; van den Top *et al.*, 2004).

**Bi:** Samples of a continuous whole-cell current-clamp recording from an orexigenic ARC NPY/AgRP pacemaker neurone, identified based upon its characteristic electrophysiological properties (see A). Application of 5-HT (50  $\mu$ M) induced a membrane hyperpolarisation in these neurones.

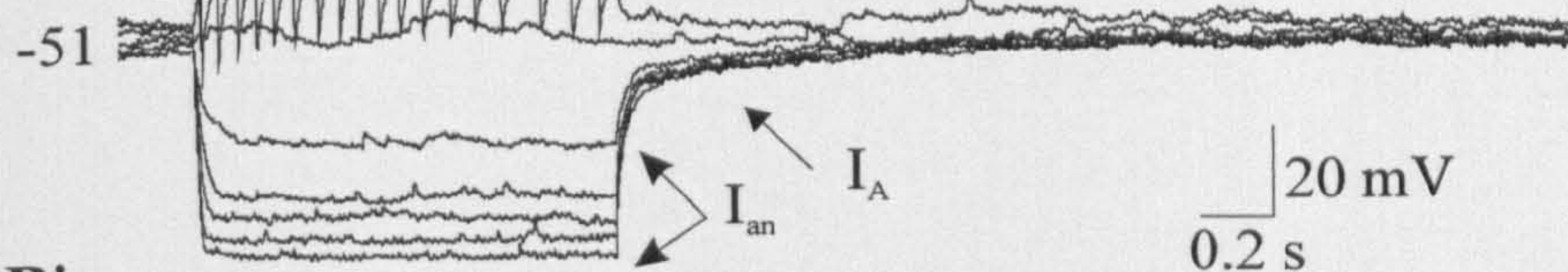
**Bii:** Superimposed samples from a continuous whole-cell current-clamp recording showing membrane potential responses of an orexigenic ARC NPY/AgRP neurone to a series of depolarising and hyperpolarising rectangular-wave current pulses of constant increment, before (-60 to +12 pA, 1 s, 0.1 Hz) and in the presence of 5-HT (-90 to +36 pA, 1 s, 0.1 Hz).

**Biii:** Plot of the current-voltage (I-V) relationships before ( $\circ$ ) and in the presence of 5-HT ( $\bullet$ ), shown in Bii. Note the decrease in the slope of the I-V in the presence of 5-HT indicating a decrease in neuronal resistance, with a reversal potential around -82mV, close to that for potassium ions under our recording conditions.



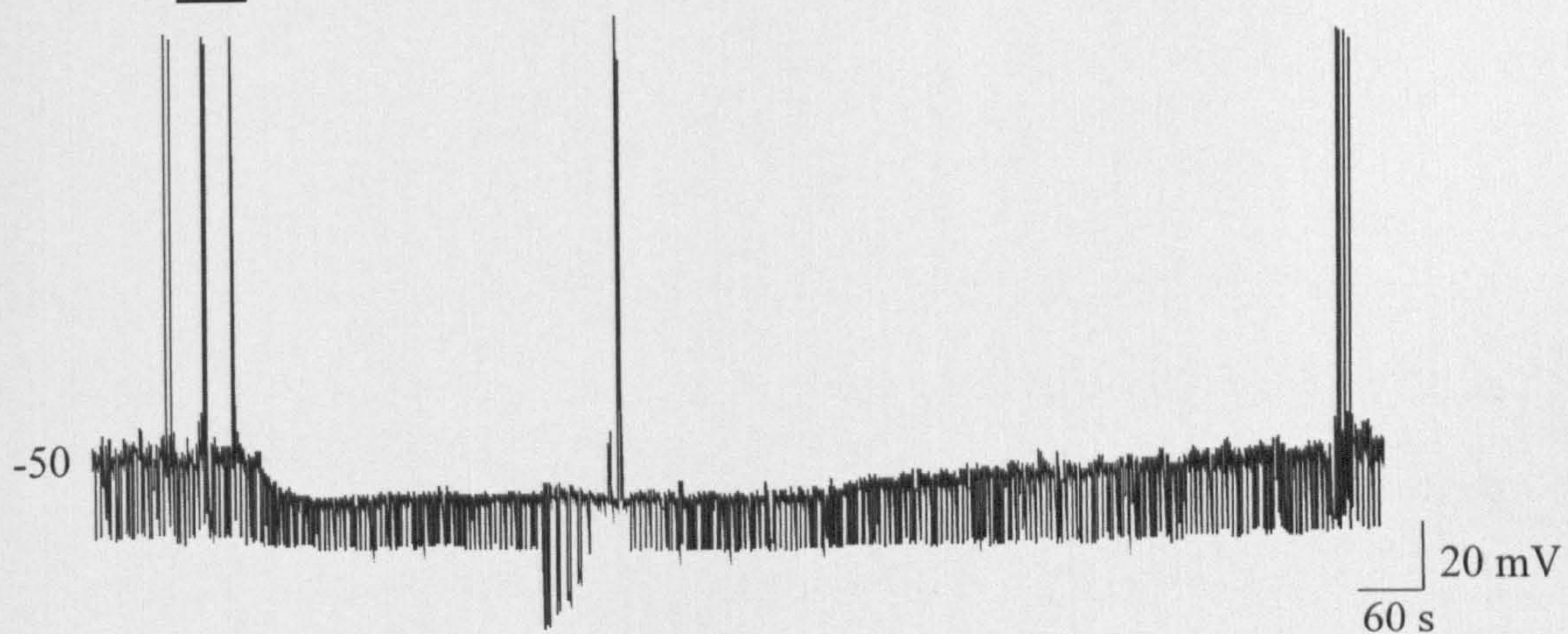
**Figure 5.10**

**A**



**Bi**

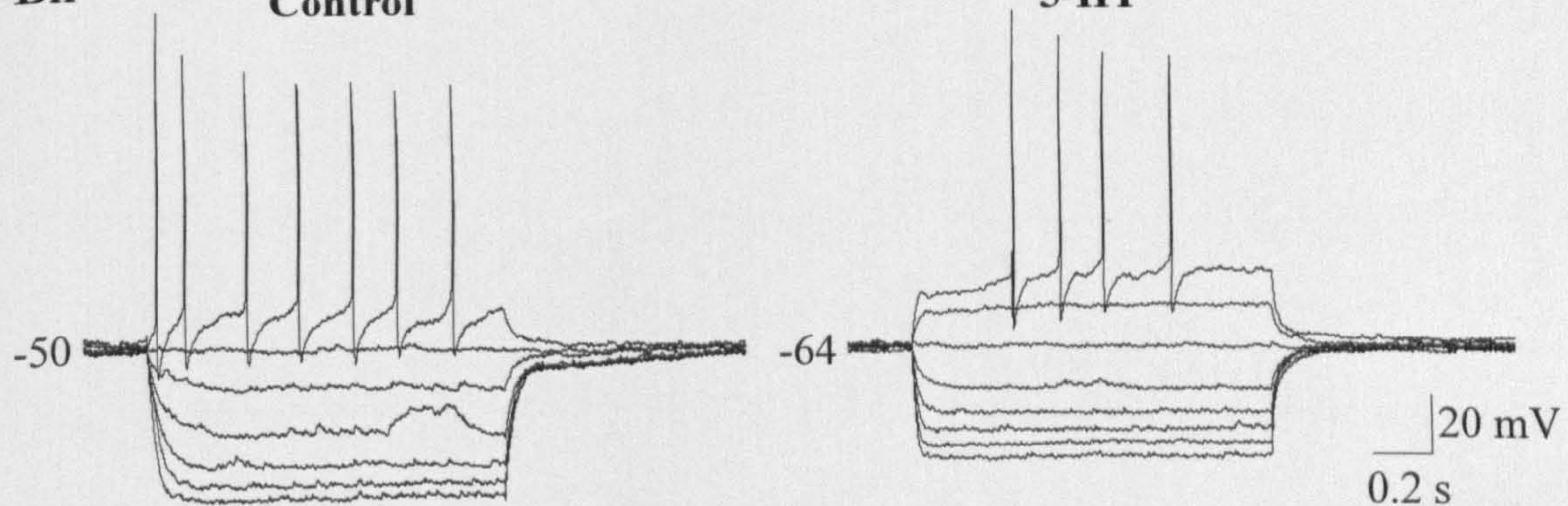
**5-HT**



**Bii**

**Control**

**5-HT**



**Bii**

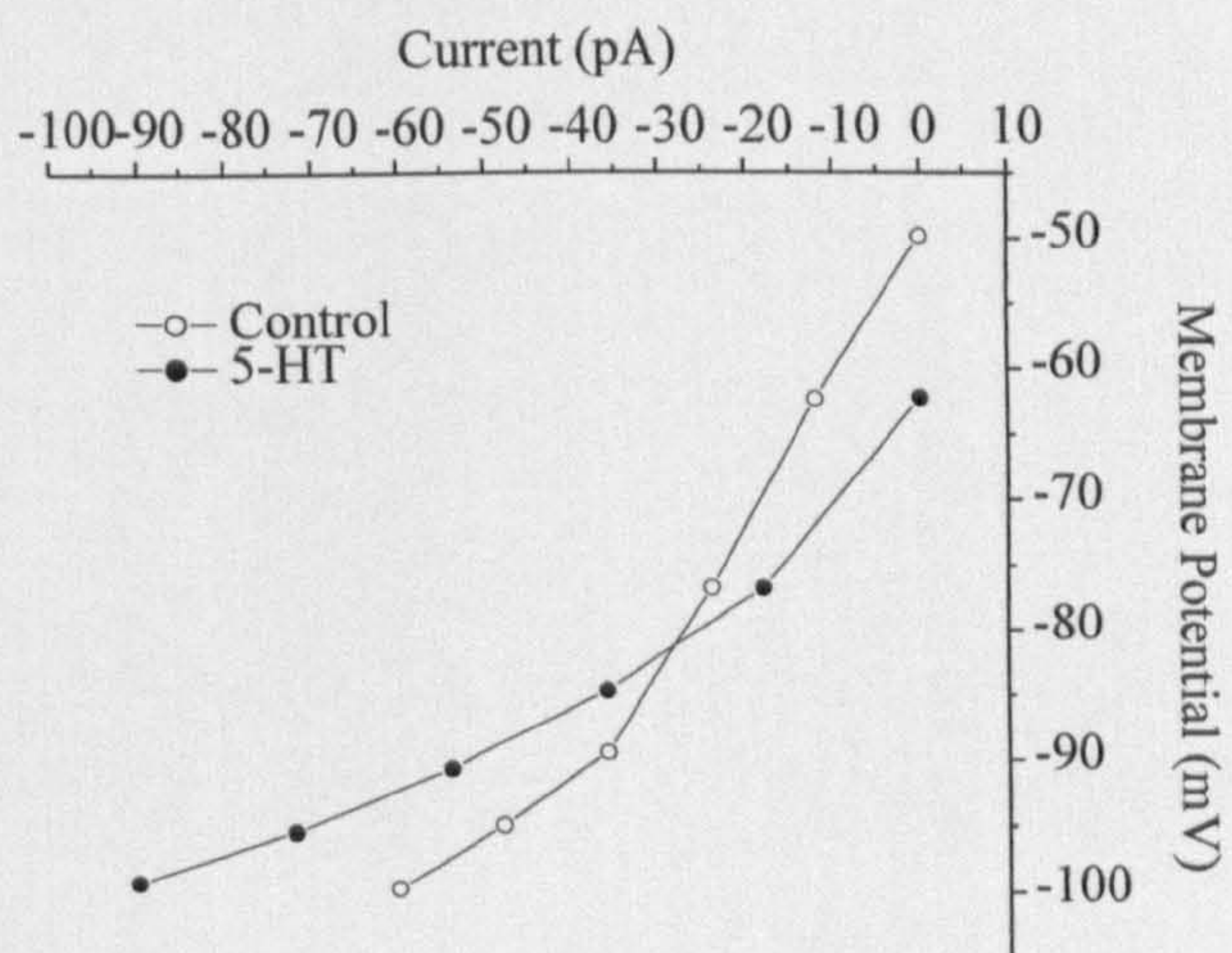




**Figure 5.11 Immunohistochemical detection of a 5-HT<sub>1B</sub> receptor-expressing non-CART positive neurone within the ARC**

**Ai:** Confocal image of a single ARC neurone showing expression of the 5-HT<sub>1B</sub> receptor visualised using Cy5 (red).

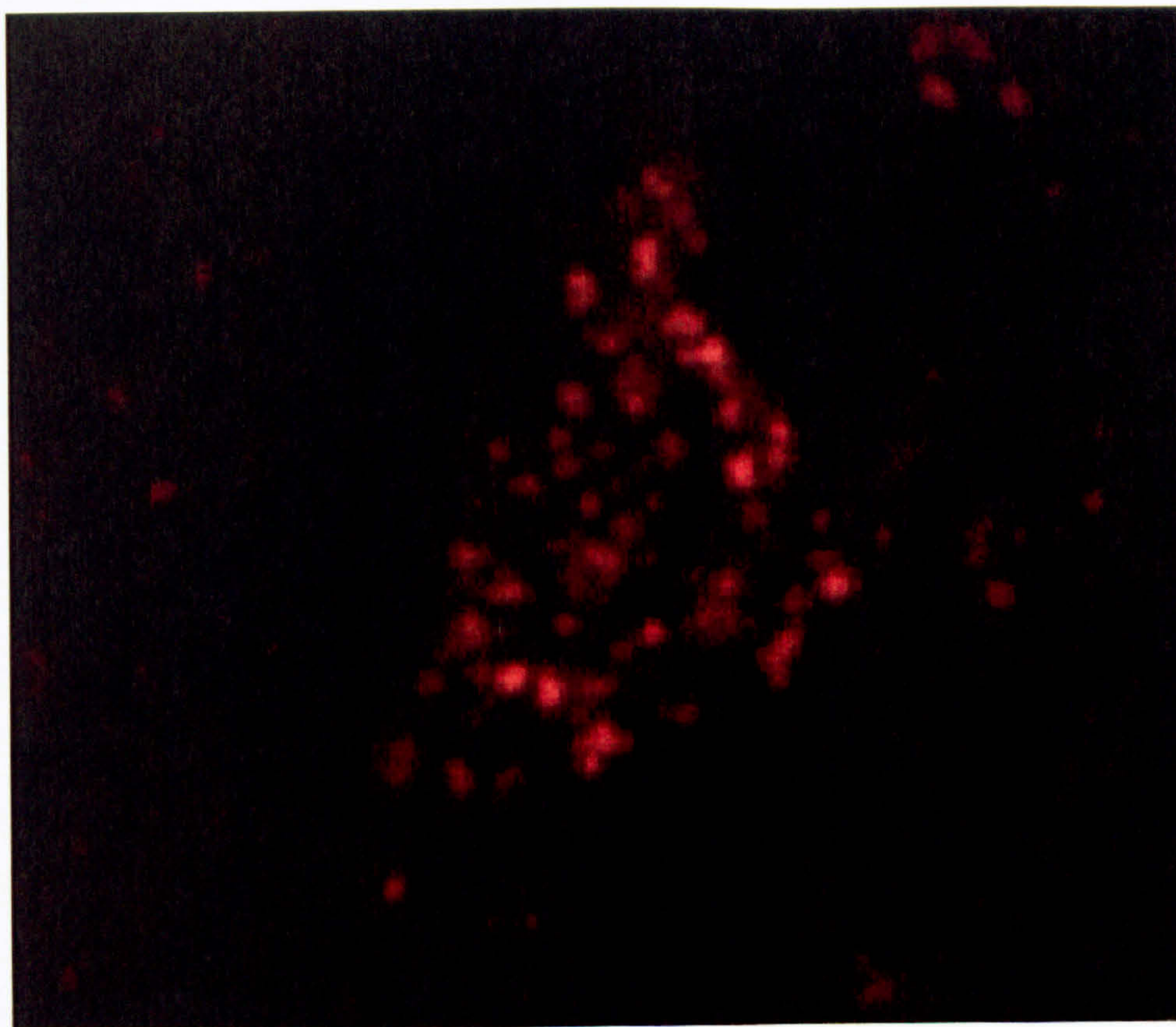
**Aii:** Confocal image showing that the neurone in Ai does not express CART (green).

Scale bar applies to both Ai and Aii.



**Figure 5.11**

**Ai**



**Aii**

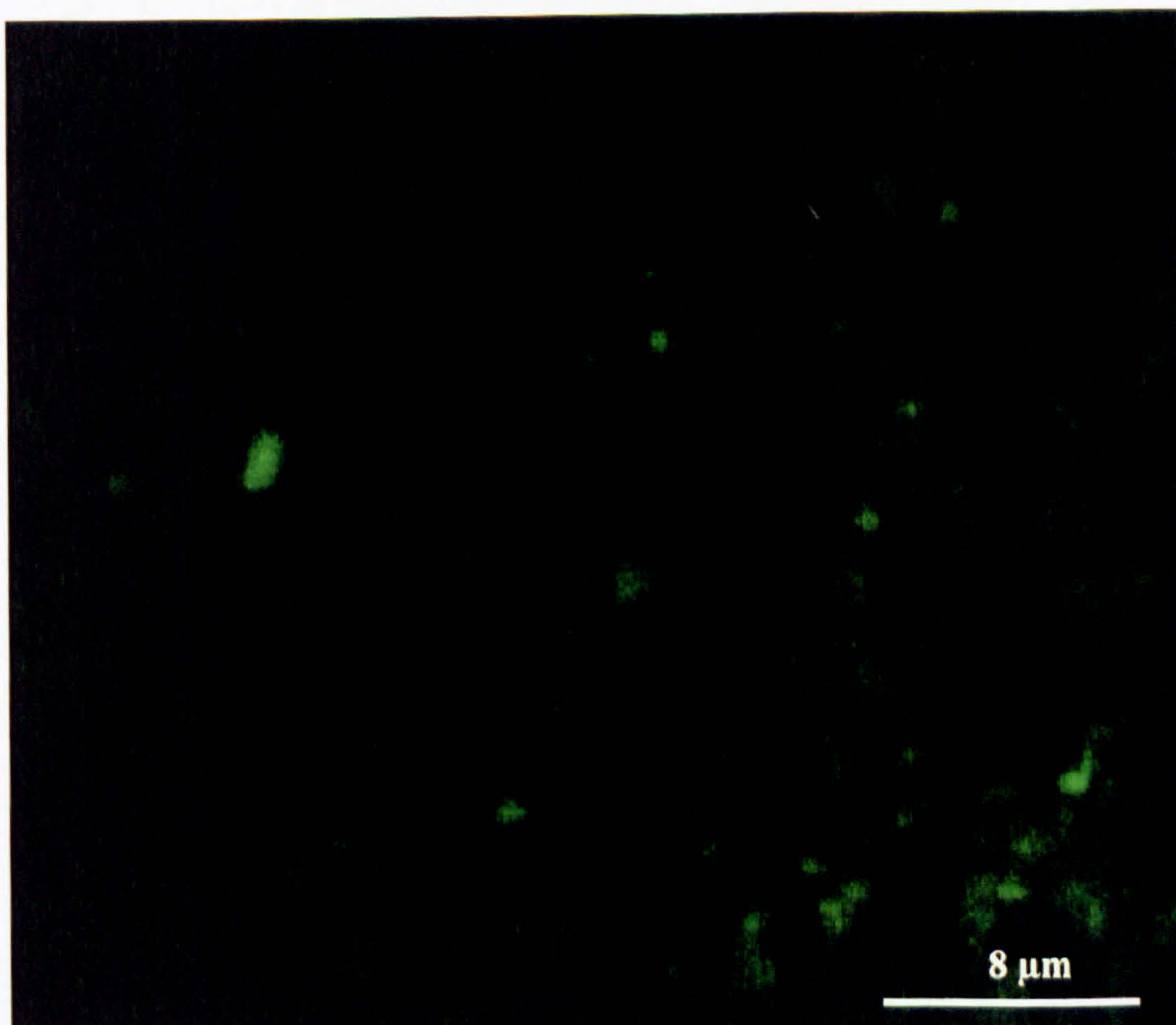




**Figure 5.12 Immunohistochemical detection of a CART positive neurone within the ARC**

**Ai:** Confocal image of a single ARC neurone showing expression of CART visualised using Cy2 (green).

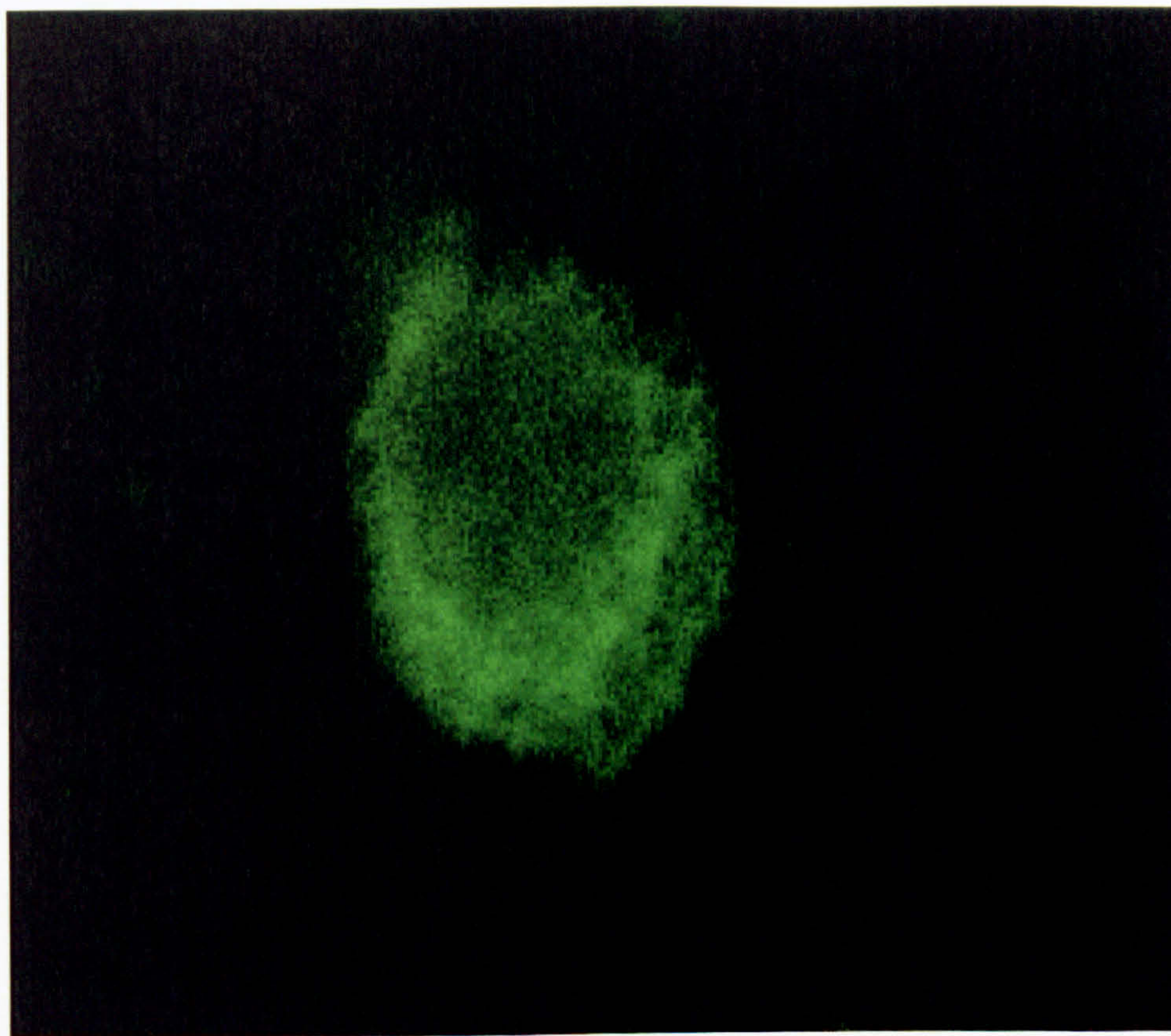
**Aii:** Confocal image showing that the neurone in Ai does not express 5-HT<sub>1B</sub> receptor (red).

Scale bar applies to both Ai and Aii.



**Figure 5.12**

**Ai**



**Aii**

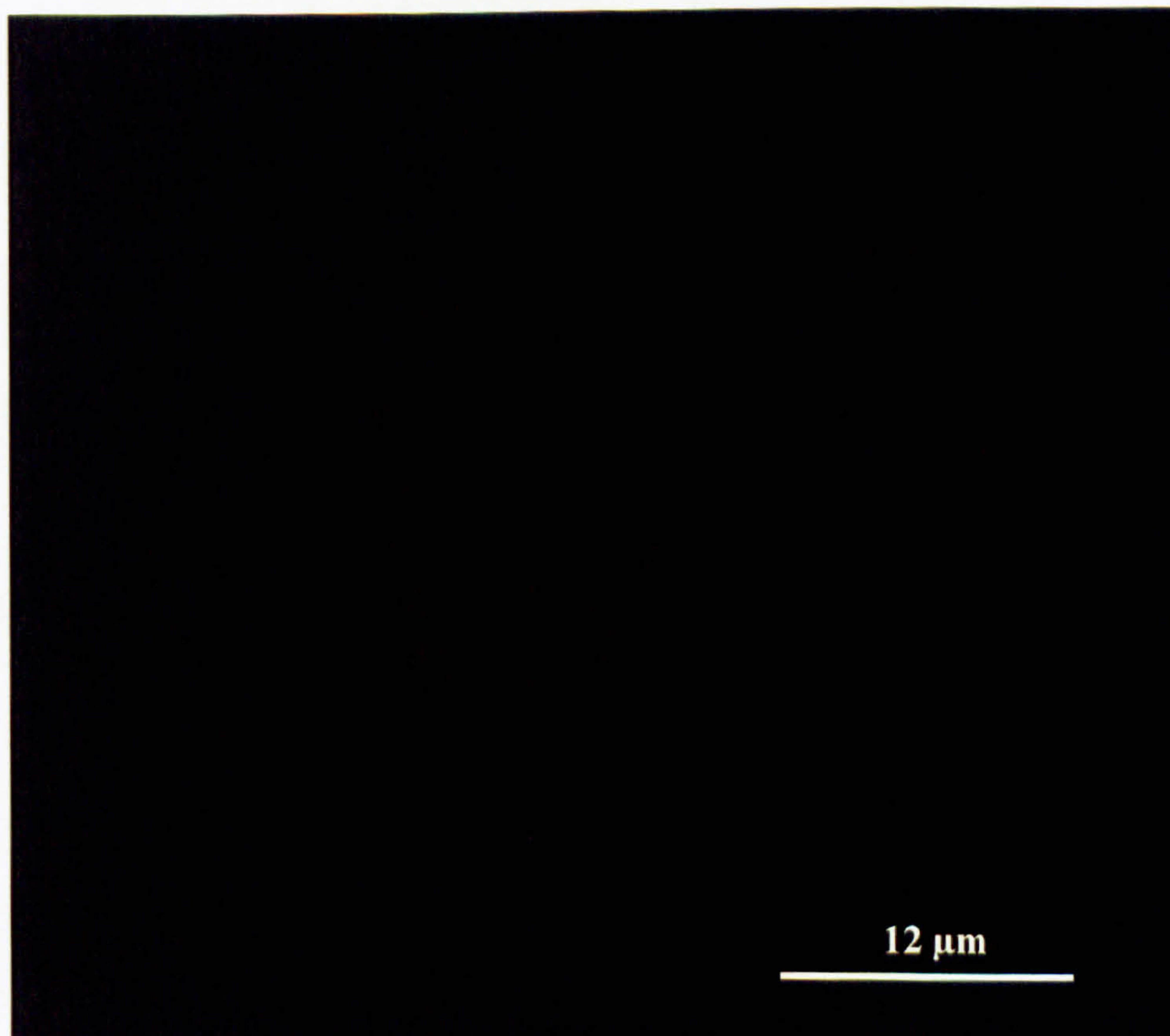




**Figure 5.13 Co-localisation of 5-HT<sub>1B</sub> receptor and CART within the ARC**

**Ai:** Confocal image of a single ARC neurone showing expression of 5-HT<sub>1B</sub> receptor visualised using Cy5 (red).

**Aii:** Confocal image of the same ARC neurone in Ai, showing the expression of CART visualised using Cy2 (green).

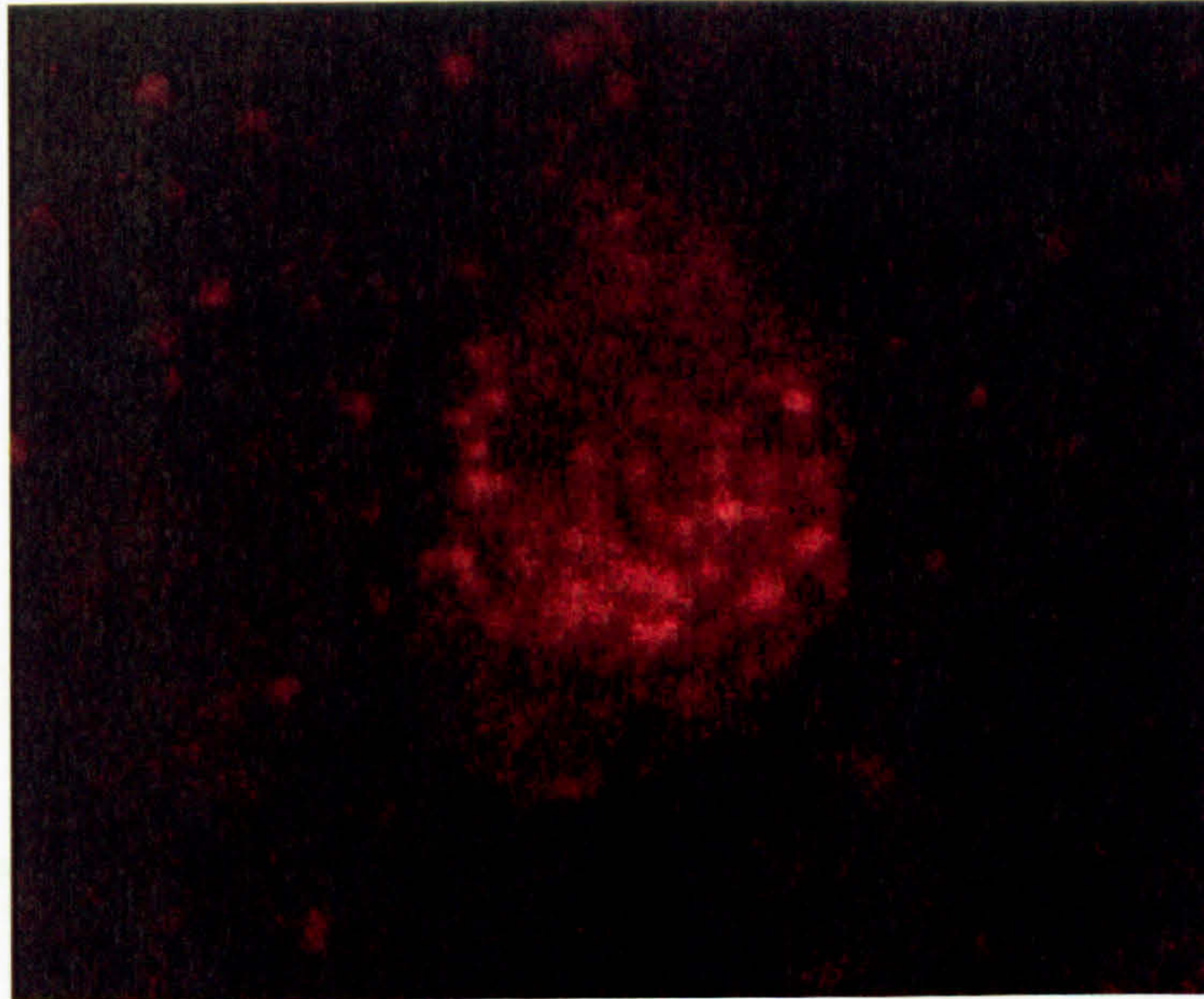
**Aiii:** Superimposed image of Ai and Aii, showing the co-localisation (yellow) of the 5-HT<sub>1B</sub> receptor and CART on a single ARC neurone

Scale bar applies to Ai, Aii and Aiii.

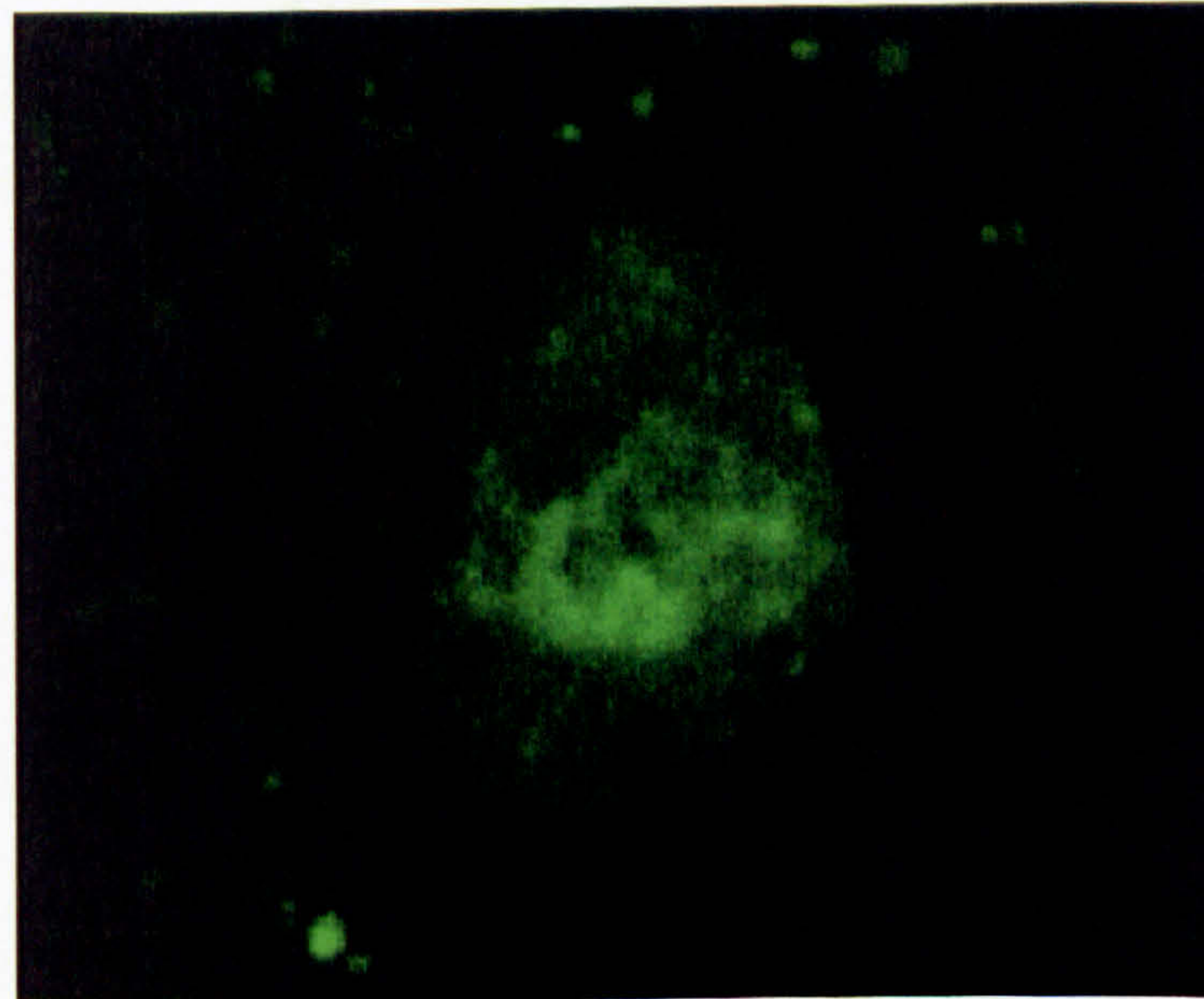


**Figure 5.13**

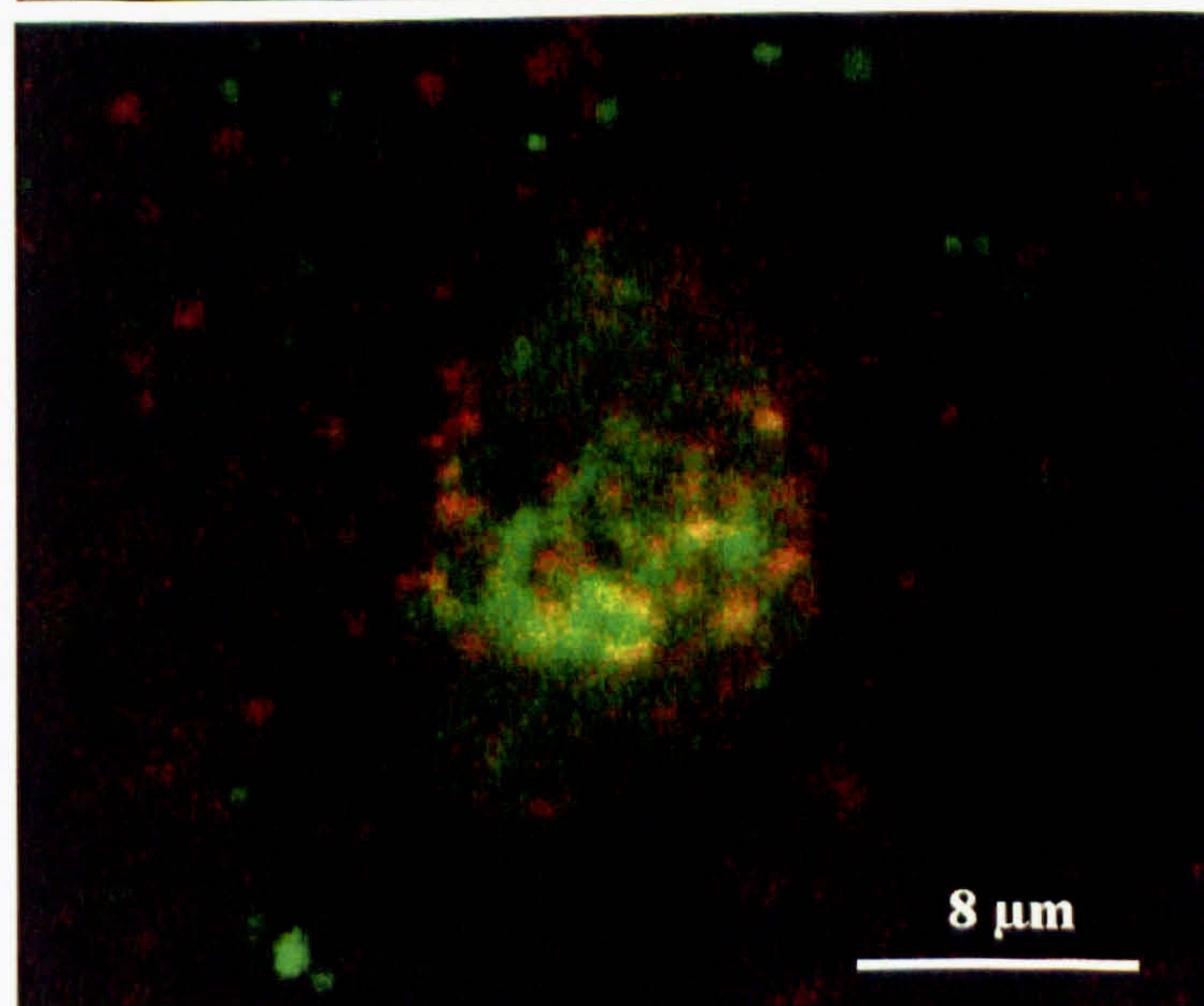
**Ai**



**Aii**



**Aiii**





# Chapter 6

## *The Effects of Feeding Signals on Neuropeptide mRNA Expression in the Rat Hypothalamus*



## 6.1 Introduction

Leptin is the hormonal product of the *ob* gene (Zhang *et al.*, 1994) and acts as an adiposity factor, increasing in proportion to the amount of stored fat in the body and communicating this information to the brain. Leptin deficient mice (*ob/ob*) and leptin resistant mice (*db/db*) and rats (*fa/fa*) have been shown to be hyperphagic and obese (Lee *et al.*, 1996). Administration of leptin causes a decrease in body-weight and food intake in both *ob/ob* and wild-type mice and rats (Campfield *et al.*, 1995; Halaas *et al.*, 1995; Pelleymounter *et al.*, 1995; Weigle *et al.*, 1995; Schwartz *et al.*, 1996). These data therefore support a major role for leptin in regulating body-weight.

Leptin receptors have been found within regions of the brain that are involved in feeding and energy homeostasis, including the arcuate nucleus (ARC), dorsomedial hypothalamus (DMH) and ventromedial nucleus (VMN; Schwartz *et al.*, 1996). There are several splice variants of the leptin receptor (Ob-Ra – Ob-Rf) but the one that is thought to be involved in controlling energy homeostasis is the long form of the leptin receptor (Ob-Rb). Neuropeptide Y (NPY) and pre-pro-opiomelanocortin (POMC) neurones in the ARC have been shown to express this leptin receptor (Mercer *et al.*, 1996; Cheung *et al.*, 1997; Baskin *et al.*, 1999) and to be targets for leptin. Leptin down-regulates the expression of NPY in the ARC (Stephens *et al.*, 1995; Schwartz *et al.*, 1996), and up-regulates the expression of POMC (Schwartz *et al.*, 1997; Thornton *et al.*, 1997). POMC neurones release several melanocortin peptides, including  $\alpha$ -MSH, which bind to and activate melanocortin receptors (Mountjoy *et al.*, 1994). The fact that agonists and antagonists of these receptors inhibit and stimulate feeding respectively (Fan *et al.*, 1997), and MC4-R receptor knockout mice are obese (Huszar *et al.*, 1997), provides compelling evidence that the melanocortin pathway is important in the control of



body-weight. Agouti-related peptide (AgRP) is a peptide that is co-expressed with NPY in the ARC and is an antagonist for MC3-R and MC4-R receptors (Ollmann *et al.*, 1997; Shutter *et al.*, 1997; Hahn *et al.*, 1998). AgRP increases food intake and body-weight and like NPY is down-regulated by leptin (Ebihara *et al.*, 1999). As leptin is able to increase the level of POMC and decrease the level of AgRP, it appears that leptin and the melanocortin pathway are closely linked in the control of feeding.

Several studies have shown that fasting can increase NPY and AgRP and decrease POMC levels, and that leptin is able to reduce NPY and AgRP but increase POMC levels in fasted rats, therefore this study will also look at the effects of leptin on fasted animals. (Baskin *et al.*, 1999; Mizuno & Mobbs, 1999; Korner *et al.*, 2000, 2001; Bi *et al.*, 2003; Perello *et al.*, 2007).

As well as regulating NPY/POMC neurones, leptin also targets other hypothalamic neurones, for example, melanin concentrating hormone (MCH), galanin, galanin-like peptide (GALP), orexin and corticotrophin releasing factor (CRF). Leptin increases the expression of the anorexigenic peptides CRF and GALP (Huang *et al.*, 1998; Kumano *et al.*, 2003) whereas it inhibits the expression of the orexigenic peptides MCH, orexin and galanin (Sahu, 1998; Lopez *et al.*, 2000).

In addition to regulating the expression of hypothalamic neuropeptides, leptin is also able to regulate the electrical excitability of neurones (Spanswick *et al.*, 1997; Cowley *et al.*, 2001). The ability of leptin to alter the activity of neurones is assumed to be independent of its ability to regulate gene expression. However numerous studies have shown activity-dependent gene regulation occurs, particularly in the hippocampus. In neurones, changes in the concentration of intracellular calcium have been shown to mediate important effects on gene expression (Ghosh & Greenberg,



1995). For example, the expression of immediate early genes (genes whose transcription is activated within minutes of stimulation) such as c-fos and c-jun, is associated with an increase in calcium and activation of subsequent second messenger pathways, which leads to the regulation of transcriptional activity of late response genes (Sheng & Greenberg, 1990; Ginty *et al.*, 1992). The increase in calcium responsible for these changes in immediate early gene expression is controlled by activation of two types of calcium channel: the N-methyl-D-aspartate (NMDA) receptor and the voltage gated L-type calcium channel (Cole *et al.*, 1989; Szekely *et al.*, 1989; Murphy *et al.*, 1991). Transcription of c-fos activated by calcium influx through the NMDA receptor and the L-type calcium channel has been studied in the hippocampus and in neuronal cell lines (Bading *et al.*, 1993; Ghosh *et al.*, 1994). Another study has identified the non-NMDA receptor as being important for activity-dependent regulation of brain derived neurotrophic factor (BDNF) and nerve growth factor (NGF) in the hippocampus (Zafra *et al.*, 1990). Activity-dependent release of transforming growth factor beta (TGF- $\beta$ ) has also been demonstrated in the hippocampus (Lacmann *et al.*, 2007).

It is not just activity alone, but the pattern of activity that is important for regulating the expression of genes. For example, specific patterns of action potentials alter the expression of neural cell adhesion molecules (Itoh *et al.*, 1995), neurotransmitters (Hodaie *et al.*, 1995) and immediate early genes (Sheng *et al.*, 1993). These patterns of activity alter the calcium concentration, which leads to changes in gene expression; therefore calcium provides a key link between electrical activity and gene expression.



The aims of this study were to determine the effects of leptin on neuropeptide gene expression within the hypothalamus and to separate activity- versus non-activity-dependent gene regulation. A new technique was developed for this purpose. Hypothalamic explants were prepared from rat brains and were incubated with leptin for various lengths of time. Total RNA was extracted from the explants and quantitative real-time PCR was performed to determine the expression levels of various neuropeptides within the hypothalamus (see section 2.3). Although several studies have used a hypothalamic explant incubation protocol previously, they have not measured the level of gene expression as we do here, but instead measure the release of peptides from the explants (King *et al.*, 1999; Korbonits *et al.*, 1999; Kim *et al.*, 2000; Russell *et al.*, 2001; Dhillon *et al.*, 2002; Breen *et al.*, 2005). This protocol also utilised a more detailed time-course over which to study gene expression that has been absent in previous studies. If our protocol proved effective, then it would be used to determine the effects of leptin on the levels of various peptides and neurotransmitters, such as 5-HT, within the hypothalamus. It would also be used to test whether the effects of leptin on gene regulation are activity- or non-activity-receptor-dependent. The hypothesis is that leptin acts on gene regulation in a non-activity-dependent manner. This would be tested by incubating the explants in antagonists for different ion channels that have been shown to be important in mediating the activity of neurones. These include TTX, which would block sodium channels and remove any action-potential dependent activity; AP5 to block NMDA receptors; NBQX to block non-NMDA receptors and nifedipine to block the L-type calcium channel to block calcium influx. EGTA, a calcium chelator could also be used to block the effects of calcium. If gene expression is affected by any of these



treatments then this would provide insight into the effects of leptin and the role of activity in regulating gene expression.

## 6.2 Results

The initial study aimed to check that our experimental protocols were effective. Briefly, the protocol used was as follows. Hypothalamic explants were prepared from age-matched (6 weeks old) male rats as described in section 2.3.1. The explants were immediately incubated in 2 mM glucose-containing aCSF at 35°C for 60 minutes. After this time, the explants were removed and placed into small vials containing 2 mM glucose-containing aCSF at 35°C. For each experiment, four control animals were used and these four explants were incubated in aCSF for the same time as the challenge time for that experiment. Four explants were used as the test tissues for each experiment and incubated in aCSF containing either leptin, GABA, AMPA, or a specific concentration of glucose. The challenge time varied depending on the experiment. At the end of the incubation time, the explant was removed and placed into an eppendorf and immediately snap-frozen on dry ice. The samples were stored in a -80°C freezer prior to molecular analysis. Statistical significance was determined using Mann Whitney or Kruskal-Wallis tests where stated.

In the first experiment, the regulation of c-fos, a marker of neuronal activity, by the neurotransmitters GABA and AMPA was studied.

### 6.2.1 *The effects of GABA and AMPA on c-fos mRNA expression*

Hypothalamic explants from animals fed *ad libitum* were exposed to either 1  $\mu$ M or 1 mM GABA, or 1  $\mu$ M or 50  $\mu$ M AMPA for 10 mins. Explants were then



snap-frozen after 15 mins. Expression levels of c-fos mRNA were then examined relative to control utilising the real-time PCR protocol as described in chapter 2.

**GABA:** At 1  $\mu$ M, there was an average  $3.1 \pm 10.0$  % change in the level of c-fos mRNA (n=4). At 1 mM, there was an average  $14.5 \pm 32.5$  % change in c-fos mRNA (n=4; see figure 6.1Ai). Neither value was significant. The relative expression of c-fos for each of the 4 individual explants can be seen in figure 6.1Aii.

**AMPA:** At 1  $\mu$ M, there was an average  $18.0 \pm 15.7$  % change in c-fos mRNA expression (n=4) and at 50  $\mu$ M there was an average  $27.0 \pm 30.3$  % change in c-fos mRNA (n=4; see figure 6.2Ai). Neither value was significant. The relative expression of c-fos for each of the 4 individual explants can be seen in figure 6.2Aii.

The next study aimed to determine the effect of leptin on NPY and POMC gene expression in the hypothalamus.

### ***6.2.2 The effects of leptin on NPY and POMC mRNA expression***

Hypothalamic explants from animals fed *ad libitum* were exposed to 100 nM leptin for either 15, 30, 45 or 60 minutes. Expression levels of NPY and POMC mRNA were then examined relative to control.

**NPY:** At 15 mins, leptin caused an average  $16.1 \pm 4.0$  % change in the level of NPY (n=8) and at 30 mins caused an average  $22.1 \pm 7.1$  % change (n=6). At 45 mins, NPY levels changed by  $5.2 \pm 4.4$  % (n=8) and at 60 mins, expression changed by  $3.9 \pm 4.8$  % (n=8). The peak time for leptin regulating NPY levels was 30 mins (see figure 6.3Ai). None of these values were significant. The relative expression of NPY for each of the individual explants can be seen in figure 6.4Ai.



Comparing the expression of NPY mRNA at each time point using the Kruskal-Wallis test indicated no significant difference in expression between any time points.

**POMC:** At 15 mins, the level of POMC changed by an average of  $14.0 \pm 3.1 \%$  (n=8) whilst it changed by  $6.6 \pm 5.6 \%$  at 30 mins (n=6). At 45 mins, POMC expression changed by  $12.7 \pm 5.8 \%$  (n=8) followed by a change at 60 mins of  $0.8 \pm 5.2 \%$  (n=8); see figure 6.3Aii). Again, none of these values were significant. The relative expression of POMC for each of the individual explants can be seen in figure 6.4Aii. Comparing the expression of POMC mRNA at each time point using a Kruskal-Wallis test indicated a significant difference between expression at 15 and 45 mins ( $P < 0.05$ ) and no significant differences in expression between any other time points.

When comparing the regulation of NPY and POMC by leptin, there was a significant difference between the two at 30 mins ( $P < 0.05$ ), but at 15, 45 and 60 mins the expression levels of NPY and POMC were not significantly different (see figure 6.3Aiii).

The next experiment aimed to determine the effect of leptin on NPY and POMC gene expression in the hypothalamus from fasted animals.

### ***6.2.3 The effects of leptin on NPY and POMC mRNA expression in fasted animals***

Hypothalamic explants from animals fasted for 24 hours were exposed to 100 nM leptin for 15, 30, 45, 60, 120 or 240 minutes. Expression levels of NPY and POMC mRNA were then examined relative to control utilising the real-time PCR protocol.



**NPY:** At 15 mins leptin did not change the expression level of NPY, a  $0.4 \pm 8.4\%$  change but at 30 mins there was a significant  $186.8 \pm 96.9\%$  up-regulation ( $P < 0.01$ ). At 45 mins, NPY levels changed by  $0.6 \pm 18.9\%$  and at 60 mins and 120 mins, expression changed by  $3.9 \pm 7.9\%$  and  $3.2 \pm 14.8\%$ , respectively. At 240 mins there was a significant  $49.9 \pm 32.9\%$  up-regulation of NPY ( $P < 0.01$ ;  $n=4$ ; see figure 6.5Ai). The relative expression of NPY for each of the individual explants can be seen in figure 6.6Ai. Comparing the expression of NPY mRNA at each time point using a Kruskal-Wallis test indicated no significant difference in expression between any time points.

**POMC:** At 15 mins, the level of POMC changed by  $5.1 \pm 5.1\%$  whilst at 30 mins there was a significant  $191.8 \pm 98.2\%$  increase ( $P < 0.01$ ). At 45 mins, POMC changed by  $1.7 \pm 11.7\%$  followed by an  $11.8 \pm 6.2\%$  change at 60 mins. At 120 and 240 mins there was a  $21.2 \pm 30.3\%$  and  $20.1 \pm 21.2\%$  change in the level of POMC, respectively ( $n=4$ ). These results indicate that at a peak of 30 mins there was an up-regulation of POMC by leptin (see figure 6.5Aii). The relative expression of POMC for each of the individual explants can be seen in figure 6.6Aii. Comparing the expression of POMC mRNA at each time point using Kruskal-Wallis test indicated no significant difference in expression between any time points.

When comparing the expression of NPY and POMC, there were no significant differences at any time points (see figure 6.5Aiii).

The next study looked at the expression of another hypothalamic peptide, AgRP.



#### 6.2.4 The effects of leptin on AgRP mRNA expression

The effect of 100 nM leptin on the expression of AgRP mRNA in *ad libitum* fed animals was tested over the time-course 15, 30, 45 and 60 mins. At 15 mins there was an average  $7.9 \pm 9.7$  % change in AgRP, at 30 mins and 45 mins there was a significant  $53.6 \pm 1.9$  % and  $31 \pm 6.7$  % down-regulation, respectively ( $P < 0.05$ ), and at 60 mins there was a  $9.5 \pm 6.4$  % change ( $n=3$ ; see figure 6.7Ai). The relative expression of AgRP for each of the individual explants can be seen in figure 6.7Aii. Comparing the expression of AgRP mRNA at each time point using a Kruskal-Wallis test indicated no significant differences in expression between any time points.

The experiment was repeated with fasted animals and the time course was extended to include 120 and 240 mins. At 15 mins, there was an average  $33.3 \pm 2.3$  % increase in AgRP levels. However, there was a  $70.2 \pm 8.5$  % increase in AgRP at 30 mins. At 45, 60 and 120 mins, there was a  $45.4 \pm 5.3$  %,  $3.3 \pm 2.5$  % and  $19.3 \pm 2.4$  % reduction, respectively. At 240 mins there was a  $27.8 \pm 0.3$  % increase in AgRP. At all time points except 60 mins the values were significant ( $P < 0.01$ ;  $n=3$ ; see figure 6.8Ai). The relative expression of AgRP for each of the individual explants can be seen in figure 6.8Aii. Comparing the expression of AgRP mRNA at each time point using Kruskal-Wallis test indicated a significant difference in expression between 30 and 45 mins but no significant differences between any other time points.

We then went on to test whether changing the external glucose concentration could affect the expression of NPY and POMC.



### 6.2.5 The effect of changing glucose concentration on NPY and POMC mRNA expression

Hypothalamic explants from animals fed *ad libitum* were incubated in 2 mM glucose for 60 mins. They were then exposed to either 0.2 mM or 5 mM glucose for 15 mins, and the expression of NPY and POMC mRNA was compared to control animals that had not been exposed to a change in glucose concentration.

**NPY:** From 2 to 0.2 mM, NPY was significantly down-regulated by  $49.5 \pm 15.5 \%$  ( $n=4$ ;  $P<0.01$ ) and from 2 to 5 mM, it was altered by  $32.2 \pm 39.6 \%$  ( $n=4$ ; see figure 6.9Ai). The relative expression of NPY for each of the individual explants can be seen in figure 6.9Aii.

**POMC:** From 2 to 0.2 mM, POMC expression significantly decreased by  $61.3 \pm 3.1 \%$  ( $n=4$ ;  $P<0.01$ ) and from 2 to 5 mM it changed by  $13.4 \pm 19.3 \%$  ( $n=4$ ; see figure 6.10Ai). The relative expression of POMC for each of the individual explants can be seen in figure 6.10Aii.

## 6.3 Discussion

The initial aims of this study were to determine the effects of leptin on neuropeptide gene expression within a whole hypothalamic explant and to identify if these effects on gene expression were dependent on the activity of neurones. In order to achieve these aims a new protocol was developed whereby hypothalamic explants, prepared from rats fed *ad libitum* or fasted, were incubated with leptin and the expression levels of hypothalamic neuropeptide mRNA were subsequently measured over a time-course. Hypothalamic explants were used in this study as this enabled the circuitry within the hypothalamus to remain intact, thereby maintaining all contacts between the multiple nuclei within the hypothalamus in order to mimic the



conditions *in vivo*. However it has the advantage over *in vivo* studies of being able to control and manipulate the external environment and expose the explant only to the factors being studied at that time.

Initially, in order to establish whether our experimental protocols were effective, we measured the level of c-fos gene expression, a marker of neuronal activity, after incubating the explants in different concentrations of GABA and AMPA. Both AMPA, a glutamate receptor agonist and GABA, an inhibitory neurotransmitter had no significant effect on the expression of c-fos mRNA. The incubation time might have been too short to see any significant changes in c-fos mRNA expression and further incubation times should have been investigated to see if significant changes would have occurred over a longer time scale. However due to time constraints these experiments were not performed. As this experiment did not prove that our experimental protocol was effective, a different experiment was performed to try to prove that it was working effectively.

We therefore next decided to study the effect of leptin on hypothalamic neuropeptide gene expression. Leptin is produced from adipose tissue in proportion to the amount of fat stored and is the product of the *ob* gene (Zhang *et al.*, 1994). It plays a highly significant role in the control of feeding and body-weight regulation, as it has been shown to inhibit food intake and body-weight (Campfield *et al.*, 1995; Halaas *et al.*, 1995; Pelleymounter *et al.*, 1995; Weigle *et al.*, 1995). Leptin inhibits the expression of orexigenic peptides such as NPY and stimulates expression of anorexigenic peptides, such as POMC, in the ARC (Stephens *et al.*, 1995; Schwartz *et al.*, 1996, 1997; Thornton *et al.*, 1997).

The first experiment looked at the effect of leptin on NPY and POMC expression in hypothalamic explants prepared from rats fed *ad libitum*. Expression



levels of either NPY or POMC were not affected by leptin in a significant way at any time point. In some instances, significance may have been reached with higher 'n' values. At both 30 mins, leptin significantly differentially regulated NPY and POMC mRNA levels. These results indicate that leptin is able to differentially regulate the level of both NPY and POMC in the hypothalamus. Leptin signalling is a complex process whereby leptin first binds to the Ob-Rb receptor, which is a type 1 cytokine receptor. Binding of leptin activates a JAK (Janus Kinase), which phosphorylates the intracellular region of the receptor. This then serves as a binding site to which a member of the STAT (Signal Transducer and Activator of Transcription) family can bind. Once STAT is activated it moves to the nucleus, where it stimulates transcription of genes (Good, 2000). There is very little published data looking at the actual time-course of leptin's effects on transcription and gene expression. The few studies that have investigated the effect of leptin on neuropeptide expression do not look at expression over such a detailed and immediate time-scale as is done here; instead they look at expression starting from 1 hour up to periods of weeks (Schwartz *et al.*, 1997; Thornton *et al.*, 1997; Sahu, 1998; Ahima *et al.*, 1999; Korner *et al.*, 2001; Swart *et al.*, 2002). The time-course used here therefore provides new information on the regulation of the neuropeptides NPY and POMC by leptin over a detailed time-scale.

The first experiment was repeated using fasted animals. The results showed that leptin significantly up-regulated both NPY and POMC at 30 mins, with relatively minor changes at all other time points. In this study the whole of the hypothalamus was used which is in contrast to previous studies that have focused predominantly on the ARC. Whereas previous studies have shown that leptin down-regulates NPY in the ARC, (Stephens *et al.*, 1995; Schwartz *et al.*, 1996), the results



from this study showing an up-regulation must be considered in light of the fact that other areas of the hypothalamus are also being looked at alongside the ARC. In other areas of the hypothalamus, such as the DMH, it has been shown that both leptin and diet-induced obesity lead to a differential regulation of NPY gene expression compared to the ARC (Guan *et al.*, 1998; Bi *et al.*, 2003; Bi, 2007), leading to a different level of expression of NPY across the whole hypothalamus compared to just the ARC. The POMC data are in accordance with previous studies showing an up-regulation of POMC by leptin (Schwartz *et al.*, 1997; Thornton *et al.*, 1997). However, it must be considered that these data are influenced by three outliers and therefore this experiment may not be very conclusive.

AgRP was subsequently investigated. AgRP is only found in the ARC and is co-expressed with NPY neurones (Hahn *et al.*, 1998). Like NPY, AgRP is down-regulated by leptin (Ebihara *et al.*, 1999). The results from the fed animals showed that leptin significantly down-regulated AgRP expression, with peak down-regulation occurring at 30 mins. The fasted data were slightly ambiguous as there was a significant down regulation of AgRP at 15, 45 and 120 mins but there was a significant up-regulation of AgRP at 30 and 240 minutes.

Finally we decided to see if a change in glucose concentration would affect the gene expression of NPY and POMC. Explants were subjected to both hyperglycaemic (2 to 5 mM) and hypoglycaemic (2 to 0.2 mM) conditions. Inducing hypoglycaemia induced a down-regulation of both POMC and NPY levels. Inducing hyperglycaemia did not significantly change NPY and POMC levels. NPY and POMC neurones within the hypothalamus have been shown to be glucose-sensing neurones (Spanswick *et al.*, 1997; Muroya *et al.*, 1999; Ibrahim *et al.*, 2003). These neurones can detect changes in glucose concentration and alter their activity and



subsequent neuropeptide expression, which explains why NPY and POMC expression were affected by a change in glucose. Several features of hypothalamic circuitry may help to explain why POMC and NPY levels were regulated in the same way under hypoglycaemic conditions. Neurones in particular areas of the hypothalamus, for example orexin neurones in the lateral hypothalamus (LH), have reciprocal connections with neurones in other areas of the hypothalamus, for example NPY neurones in the ARC (Broberger *et al.*, 1998; Elias *et al.*, 1998b, 1999). Orexin neurones may have detected a decrease in glucose and subsequently altered the activity of NPY neurones in the ARC. POMC neurones may have detected the decrease in glucose and altered their own activity if they were glucose-sensing, or alternatively may have been inhibited by neurones in other hypothalamic nuclei, for example MCH neurones in the LH. The reciprocal connections between the hypothalamic nuclei, which are maintained in the hypothalamic explants, are therefore important when considering the effects of glucose.

There are several technical issues that need to be discussed concerning the development of this new experimental protocol. Several stages of the technique may need to be refined. Firstly great care must be taken to ensure the hypothalamic explants are handled carefully as any damage to them may result in abnormal results. The process of incubating the explants in leptin may not provide enough penetration to the tissue; therefore it may be more beneficial to use hypothalamic slices rather than a single explant containing the whole hypothalamus, in order to increase access of leptin to the tissue. The time course that was chosen may have missed the crucial points in the expression of the genes as we were only looking every 15 minutes. It may be necessary to include more time points in order to fully determine the gene



expression profile. Alternatively we may not have incubated the explants for long enough, perhaps more than an hour is needed to observe further changes.

In the fasted experiments, the animals were only fasted for 24 hours. This may not be long enough to fully detect changes due to fasting as many experiments in the literature use a 48 hour fast. Therefore we may not be seeing the full benefit of the fasting protocol. In future a license may need to be obtained for a 48 hour fast.

The processes of RNA extraction through to quantitative real-time PCR are very sensitive and require a great deal of care. It is possible that during these processes errors may occur, for example, due to human error, problems with solutions, contamination of RNA or solutions or errors in the processes themselves, particularly reverse transcription.

This was an initial pilot study that aimed to compare activity versus non-activity-dependent gene regulation and to look at the effects of leptin on regulation of gene expression of hypothalamic neurotransmitters and neuropeptides. Due to time constraints the original aims were not completely fulfilled but the study was successful in providing novel evidence of the specific time-course over which leptin regulates NPY and POMC gene expression in a whole hypothalamic explant. Future work needs to be done to compare the activity versus non-activity-dependent gene regulation by leptin using selective antagonists for sodium channels and calcium channels as described earlier. Also, the hypothalamic explants in this study contained all regions of the hypothalamus whereas previous studies have isolated single areas of the hypothalamus and only study expression levels in each discrete area. It may be interesting in future to try to dissect out particular areas of the hypothalamus in order to isolate those areas and measure gene expression more region specifically.



**Figure 6.1 The effect of GABA on c-fos gene expression in hypothalamic explants from rats fed *ad libitum***

**Ai:** A bar-chart to show the effects of GABA on the expression of c-fos mRNA in fed animals. Hypothalamic explants were exposed to either 1  $\mu$ M or 1 mM GABA for 10 minutes and the expression of c-fos mRNA was compared to control explants that had not been exposed to GABA. In this chart and all subsequent bar-charts control explants have an expression level of 1.0. GABA down-regulated expression of c-fos at 1  $\mu$ M but up-regulated expression of c-fos at 1 mM, although not significantly. Error bars represent S.E.M in this and all subsequent figures.

**Aii:** A scatter graph to show the effects of GABA on the expression of c-fos mRNA in each of the four individual hypothalamic explants from Ai, at 1  $\mu$ M and 1 mM.



**Figure 6.1**

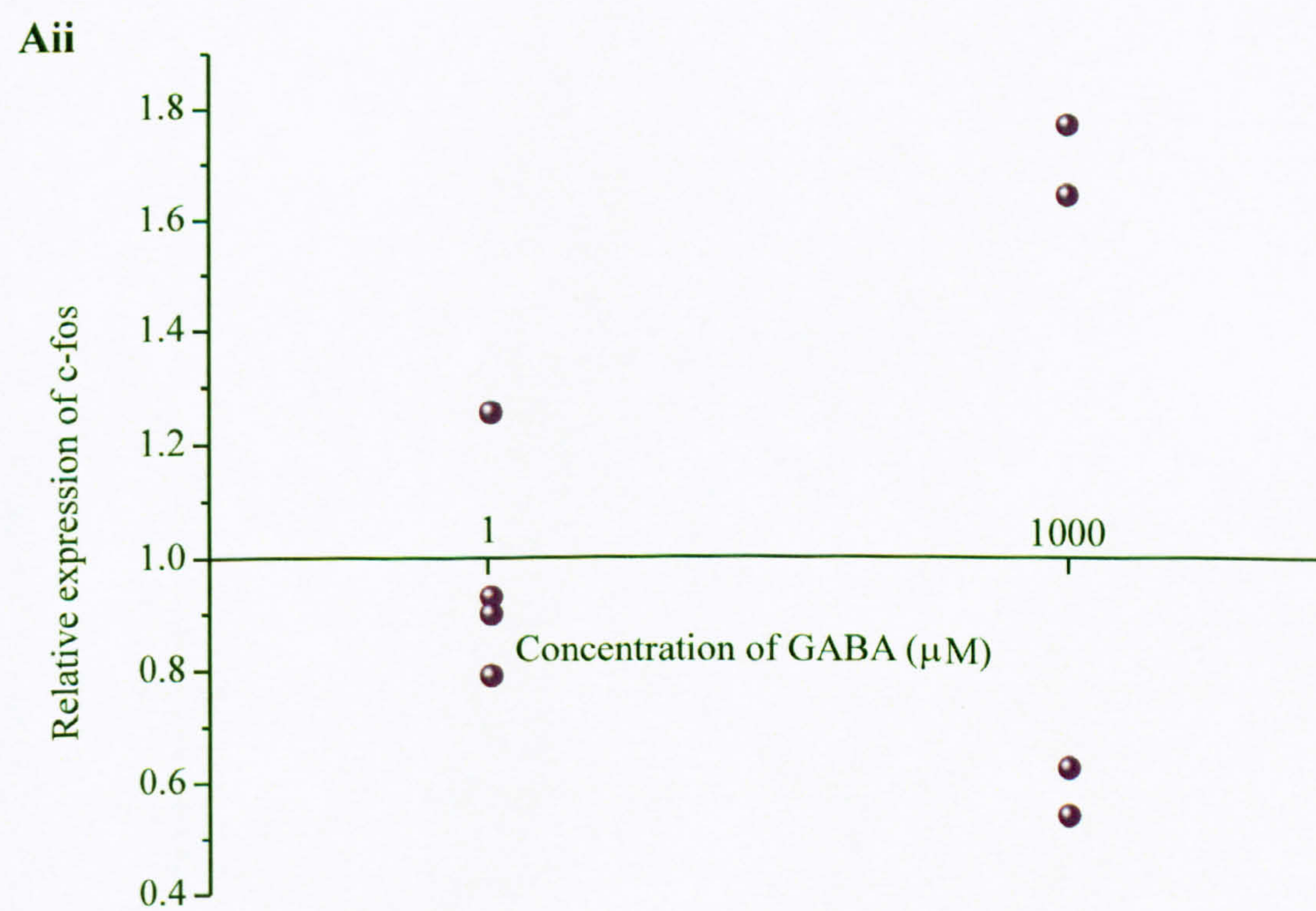
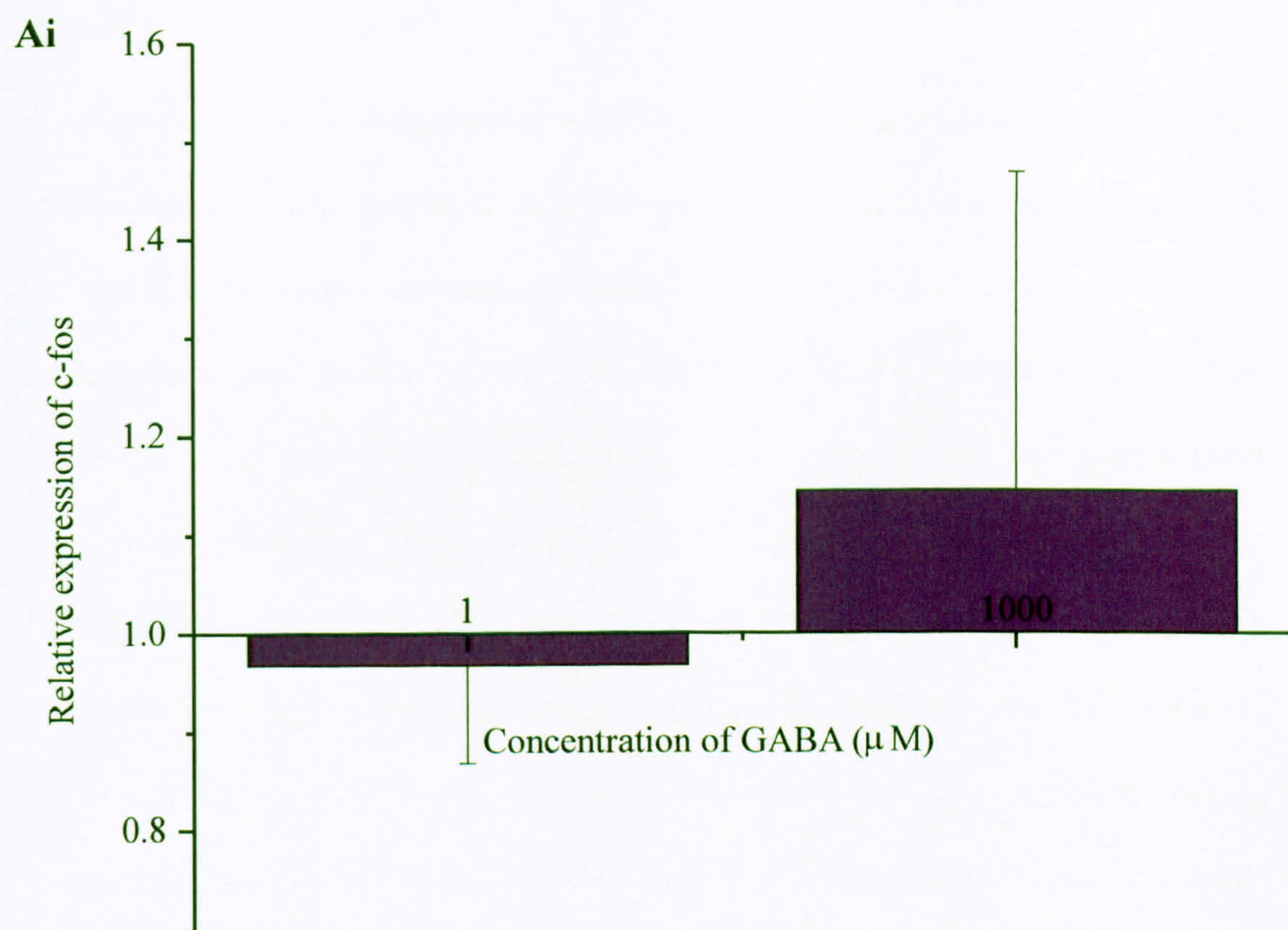




**Figure 6.2 The effect of AMPA on c-fos gene expression in hypothalamic explants from rats fed *ad libitum***

**Ai:** A bar-chart to show the effects of AMPA on the expression of c-fos mRNA in fed animals. Hypothalamic explants were exposed to either 1  $\mu$ M or 50  $\mu$ M AMPA for 10 minutes and the expression of c-fos was compared to control explants that had not been exposed to AMPA. AMPA non-significantly up-regulated expression of c-fos at 1  $\mu$ M and 50  $\mu$ M.

**Aii:** A scatter graph to show the effects of AMPA on the expression of c-fos mRNA in each of the four individual hypothalamic explants from Ai, at 1  $\mu$ M and 50  $\mu$ M.



**Figure 6.2**

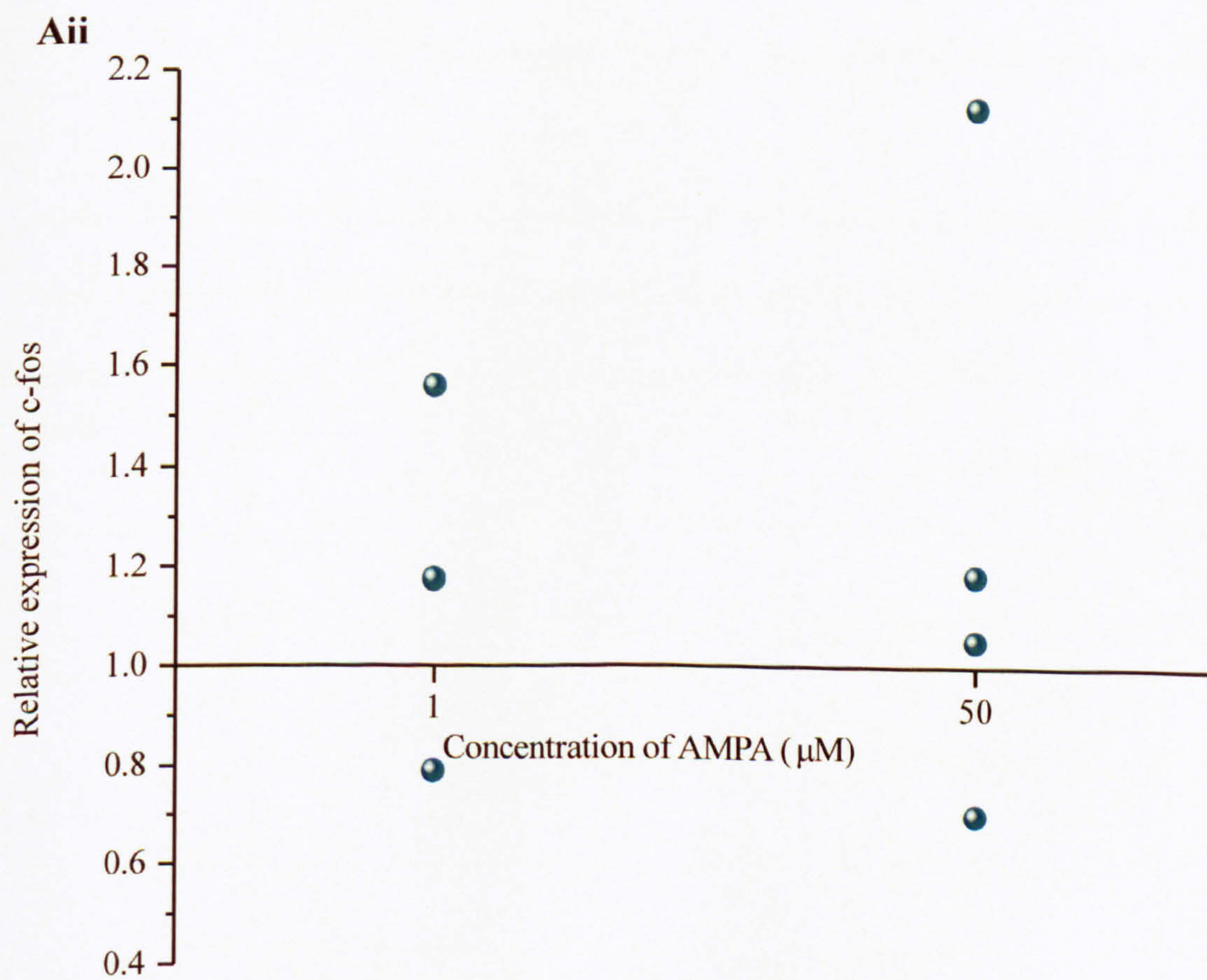
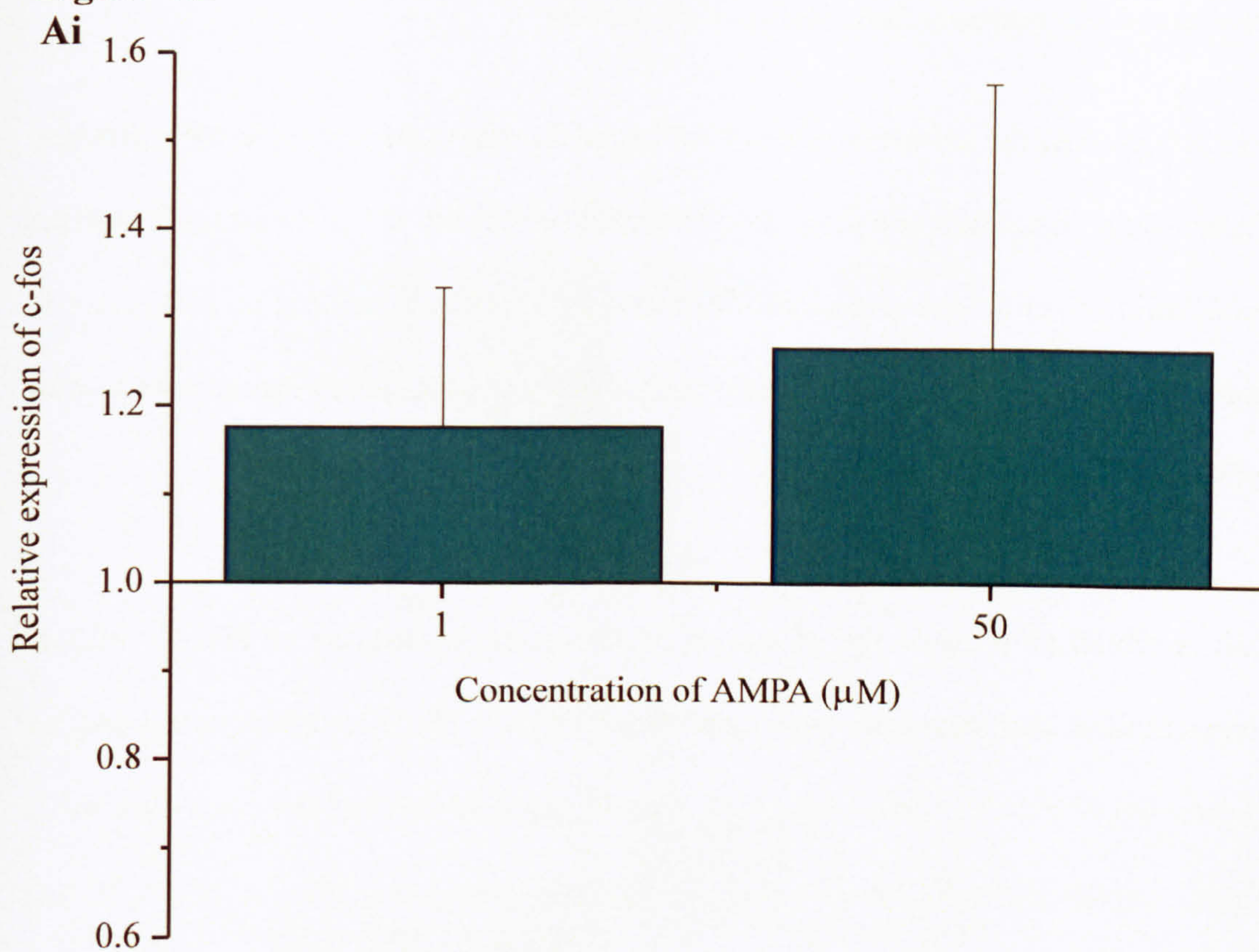




**Figure 6.3 The effect of leptin on NPY and POMC gene expression in hypothalamic explants from rats fed *ad libitum***

**Ai:** A bar-chart to show the effects of leptin on the expression of NPY mRNA. Hypothalamic explants were exposed to leptin for 15, 30, 45 or 60 minutes, and the expression of NPY was compared to control explants that had not been exposed to leptin. Leptin non-significantly down-regulated expression of NPY at all time points, with a peak decrease at 30 mins.

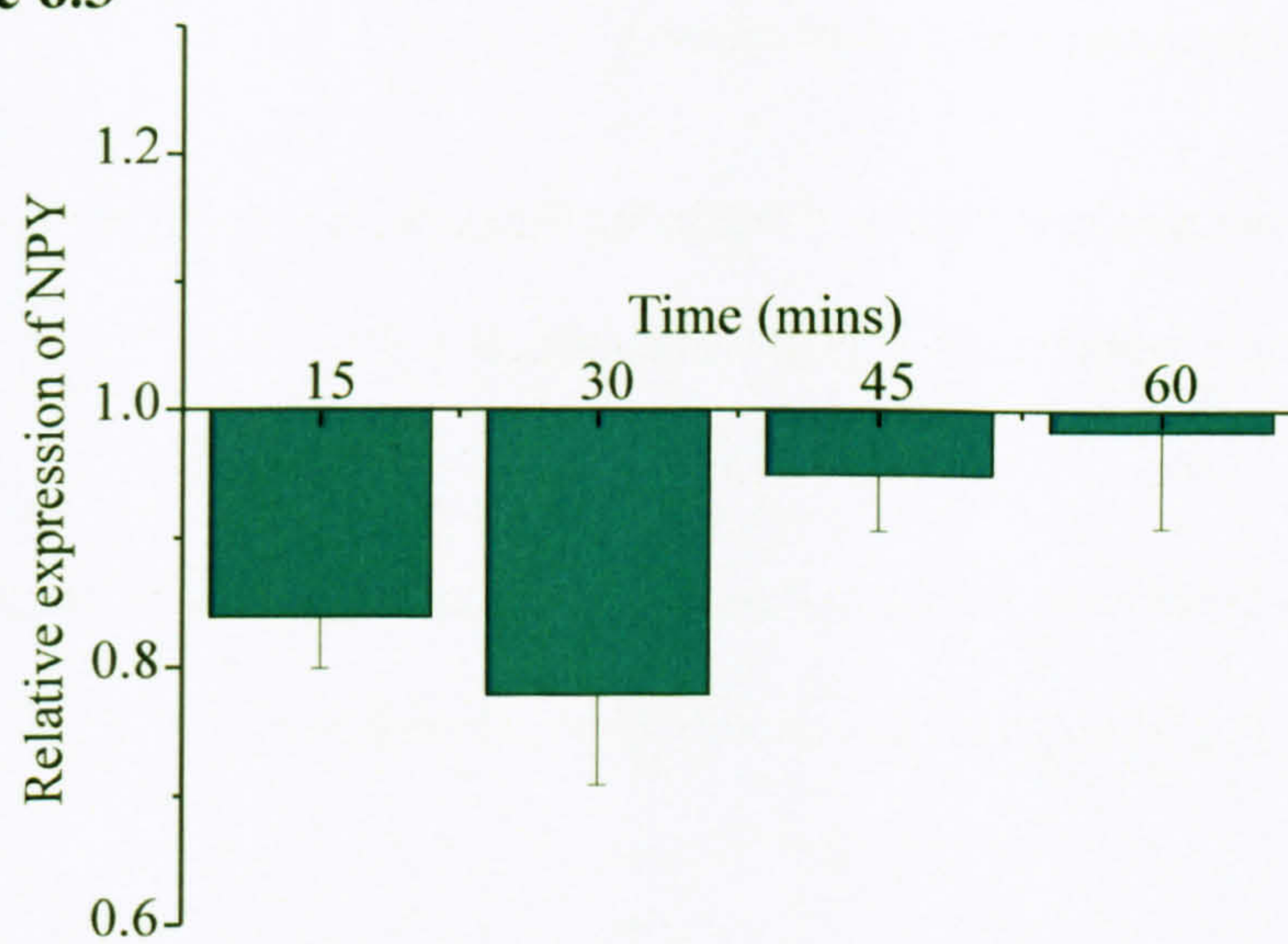
**Aii:** A bar-chart to show the effects of leptin on the expression of POMC mRNA. Hypothalamic explants were exposed to leptin for 15, 30, 45 or 60 minutes, and the expression of POMC was compared to control explants that had not been exposed to leptin. Leptin non-significantly down-regulated expression of POMC at 15, 30 and 60 mins but up-regulated POMC at 45 mins. There was a significant difference in expression between 30 and 45 mins ( $P<0.05$ , indicated by \*).

**Aiii:** A line graph to compare the differential regulation of NPY and POMC gene expression by leptin. The dashed line indicates the level of control expression. There was a significant difference in the regulation of NPY and POMC by leptin at 30 mins ( $P<0.05$ , indicated by \*).

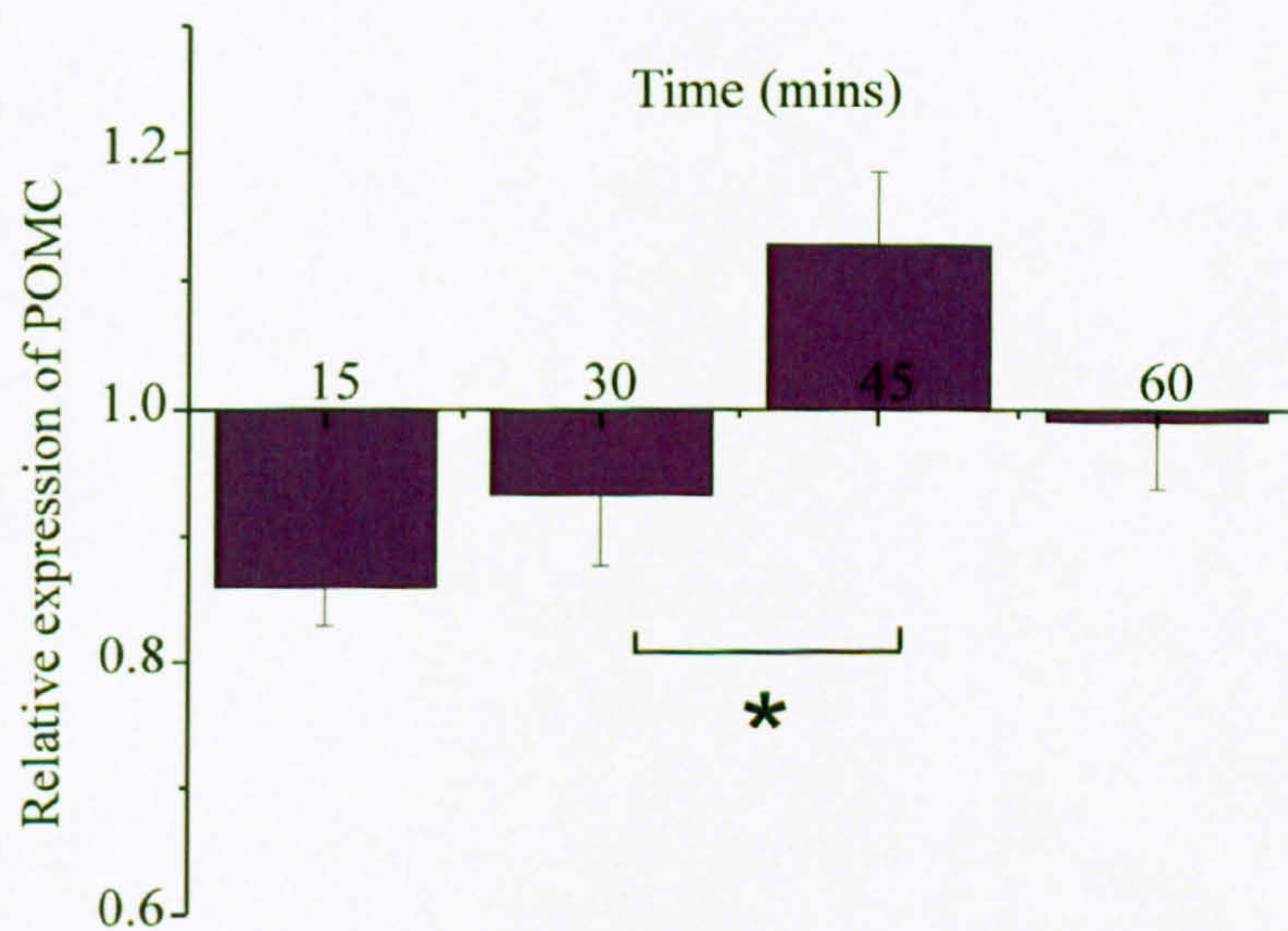


**Figure 6.3**

**Ai**



**Aii**



**Aiii**

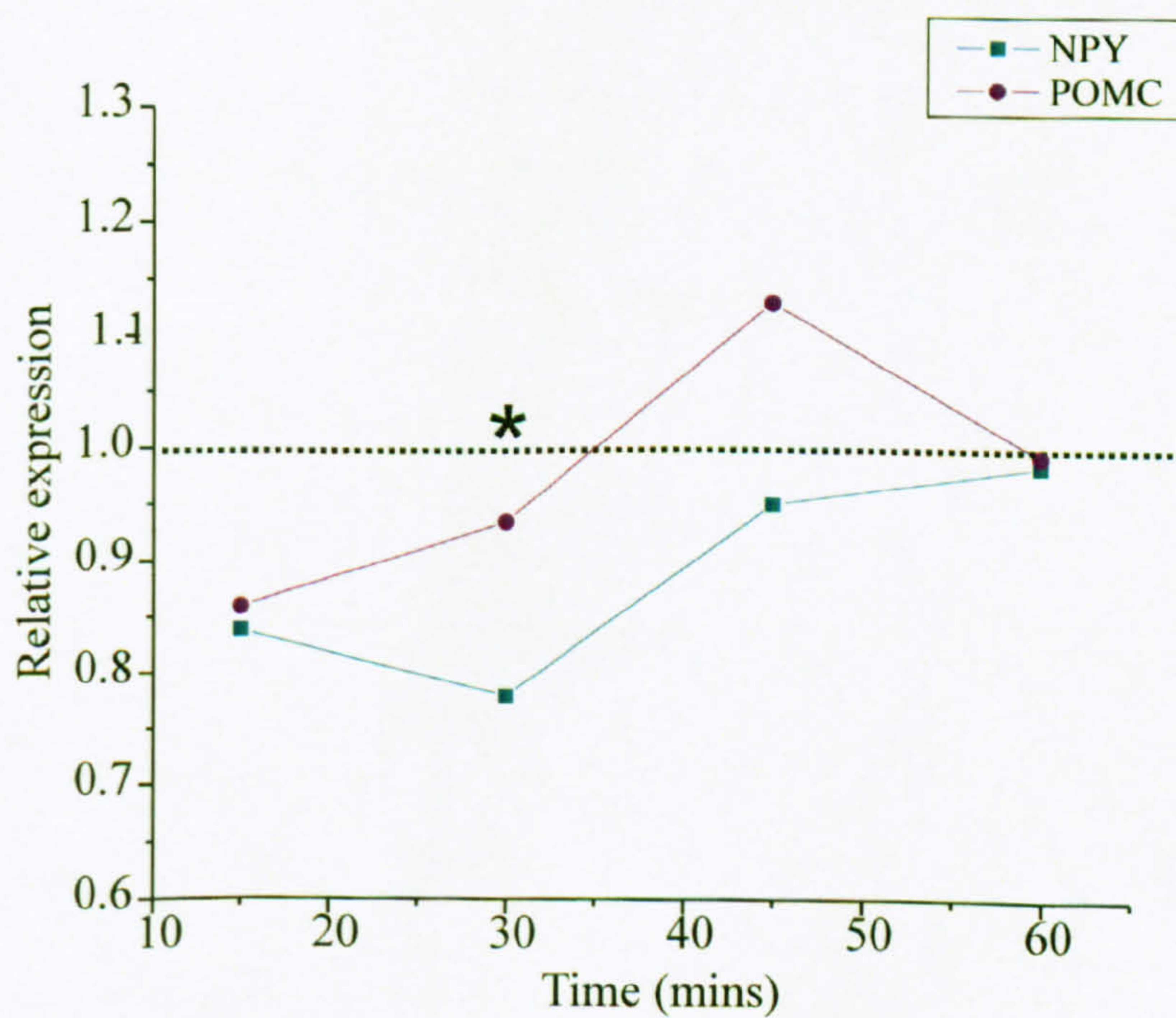




**Figure 6.4 The effect of leptin on NPY and POMC gene expression in individual hypothalamic explants from rats fed *ad libitum***

**Ai:** A scatter graph to show the effects of leptin on the expression of NPY mRNA in each of the individual hypothalamic explants from figure 6.3Ai.

**Aii:** A scatter graph to show the effects of leptin on the expression of POMC mRNA in each of the individual hypothalamic explants from figure 6.3Aii.



**Figure 6.4**

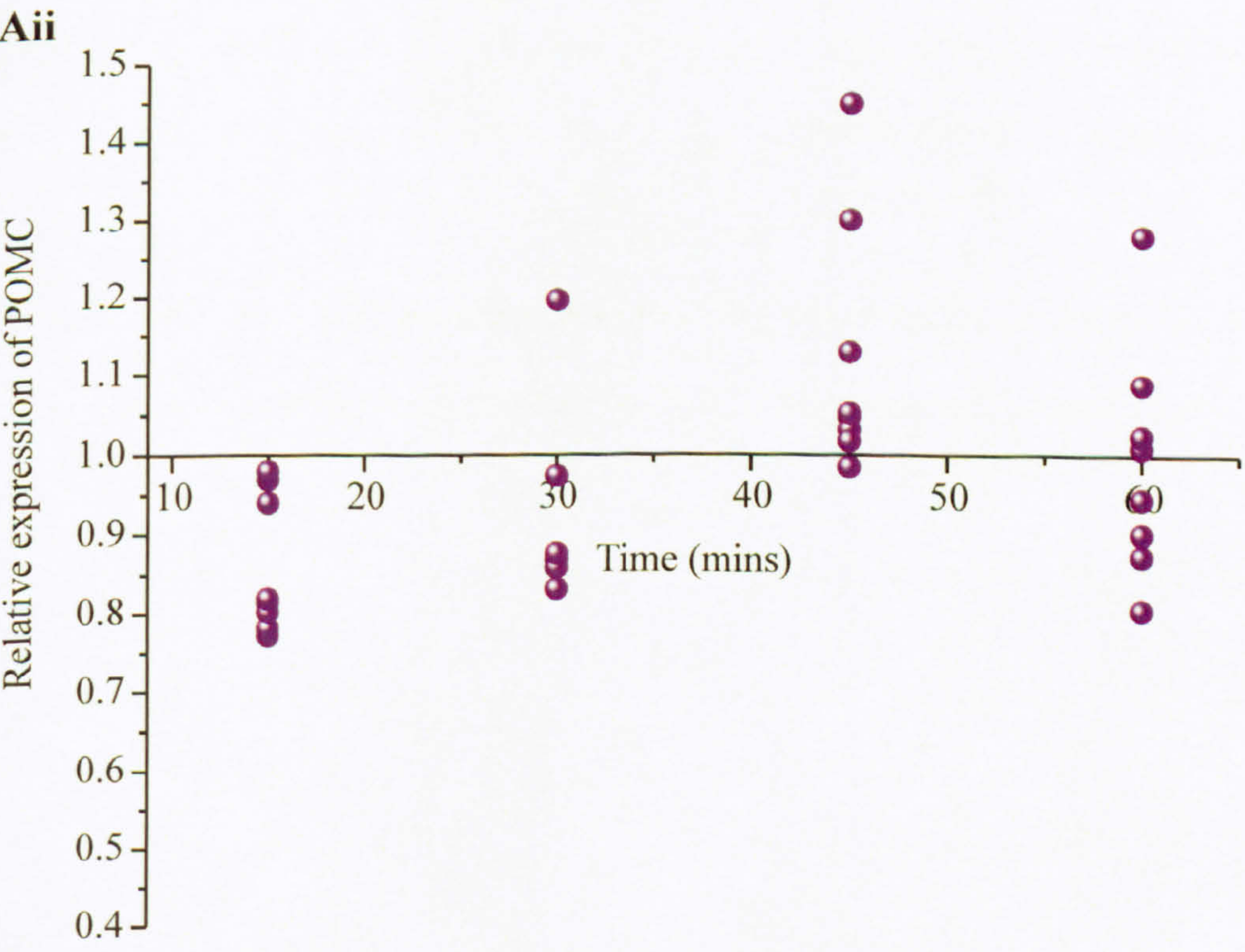
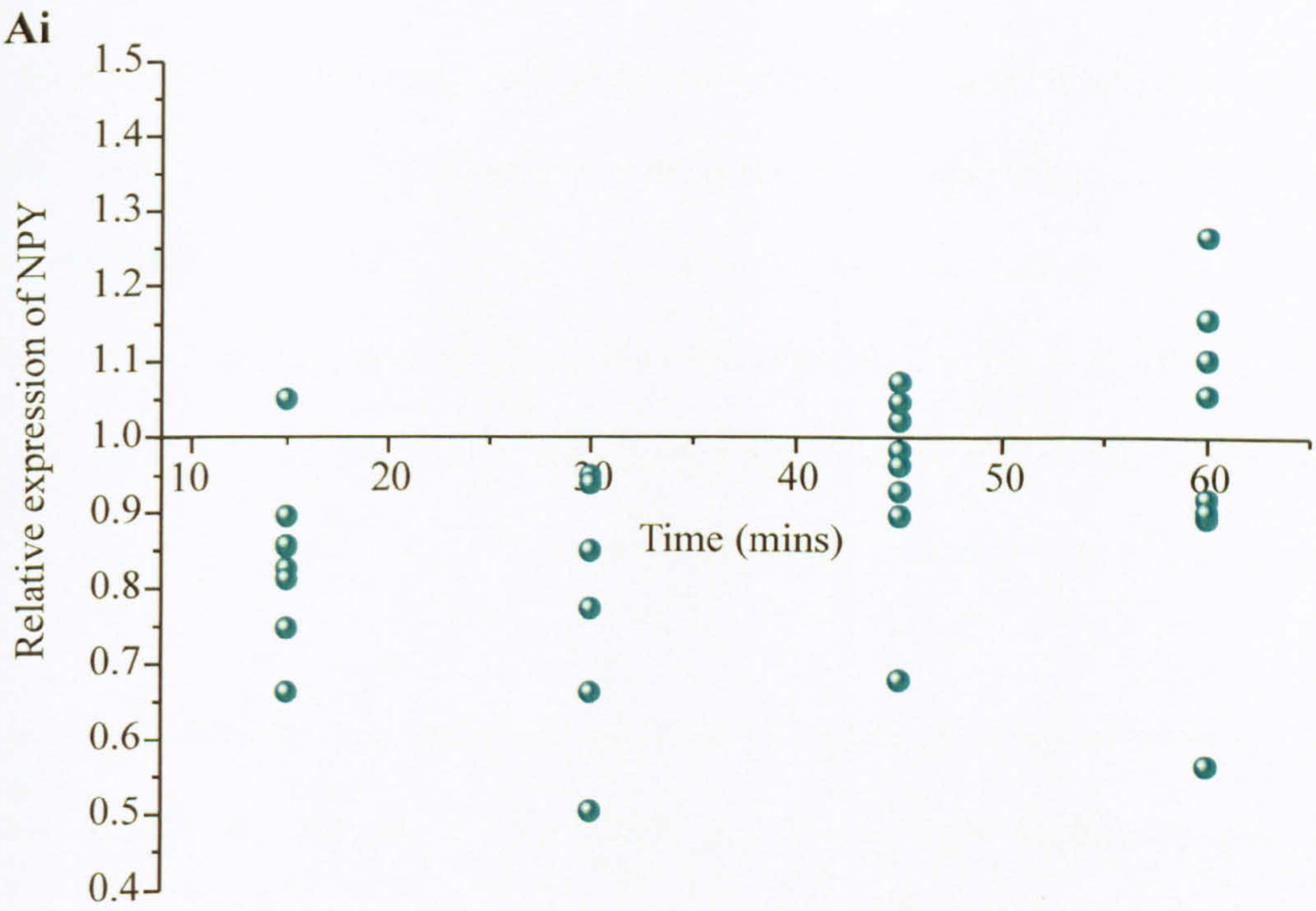




**Figure 6.5 The effect of leptin on NPY and POMC gene expression in hypothalamic explants prepared from fasted rats**

**Ai:** A bar-chart to show the effects of leptin on the expression of NPY mRNA. Hypothalamic explants were exposed to leptin for 15, 30, 45, 60, 120 or 240 minutes, and the expression of NPY was compared to control explants which had not been exposed to leptin. Leptin significantly up-regulated expression of NPY at 30 and 240 mins, with a peak increase at 30 mins ( $P < 0.01$  indicated by \*\*). At all other time points, NPY levels did not significantly change.

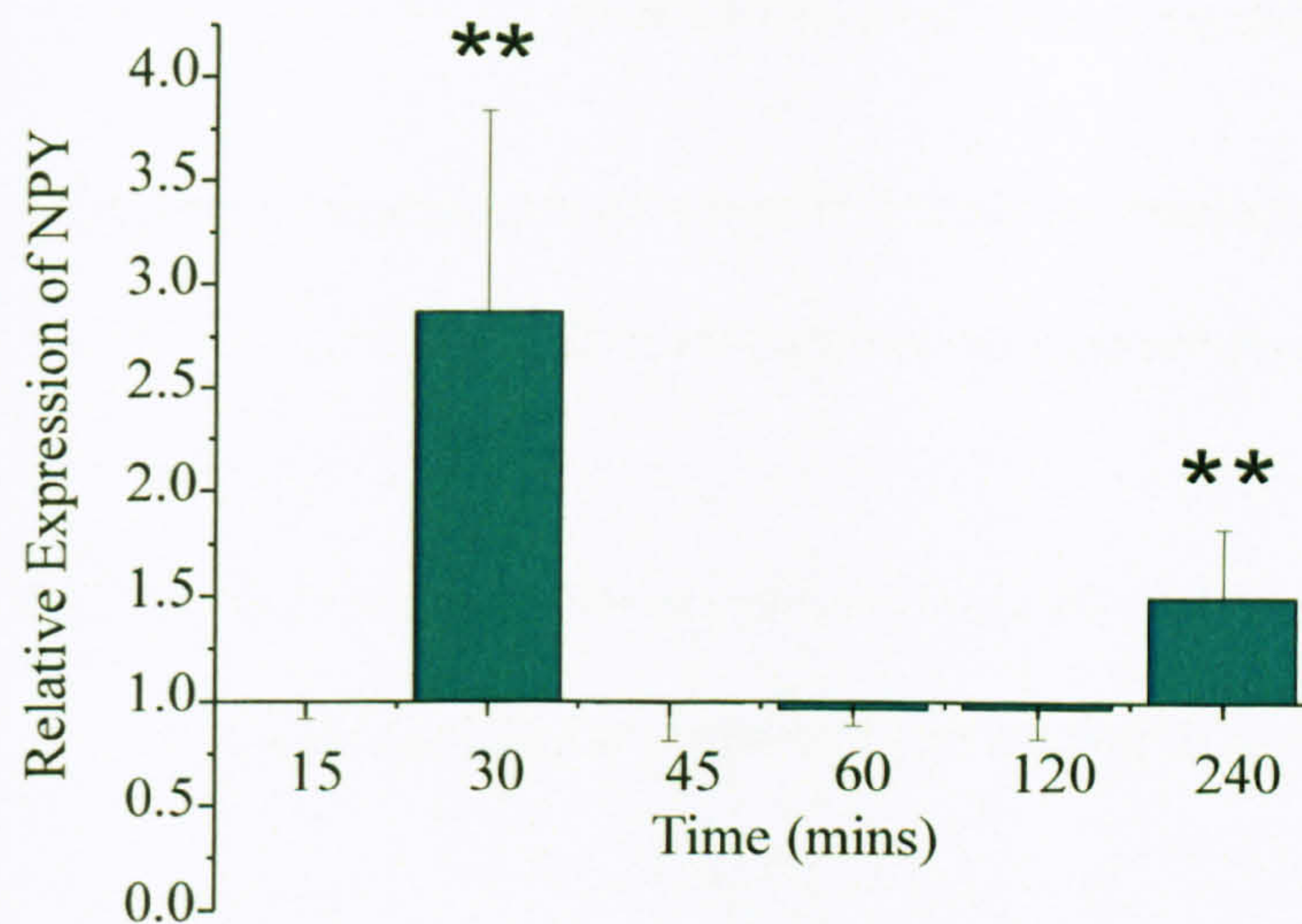
**Aii:** A bar-chart to show the effects of leptin on the expression of POMC mRNA. Hypothalamic explants were exposed to leptin for 15, 30, 45, 60, 120 or 240 minutes, and the expression of POMC was compared to control explants which had not been exposed to leptin. Leptin significantly up-regulated expression of POMC at 30 mins ( $P < 0.01$  indicated by \*\*) but at all other time points, POMC levels were similar to control.

**Aiii:** A line graph to compare the differential regulation of NPY and POMC gene expression by leptin. There were no significant differences at any time points.

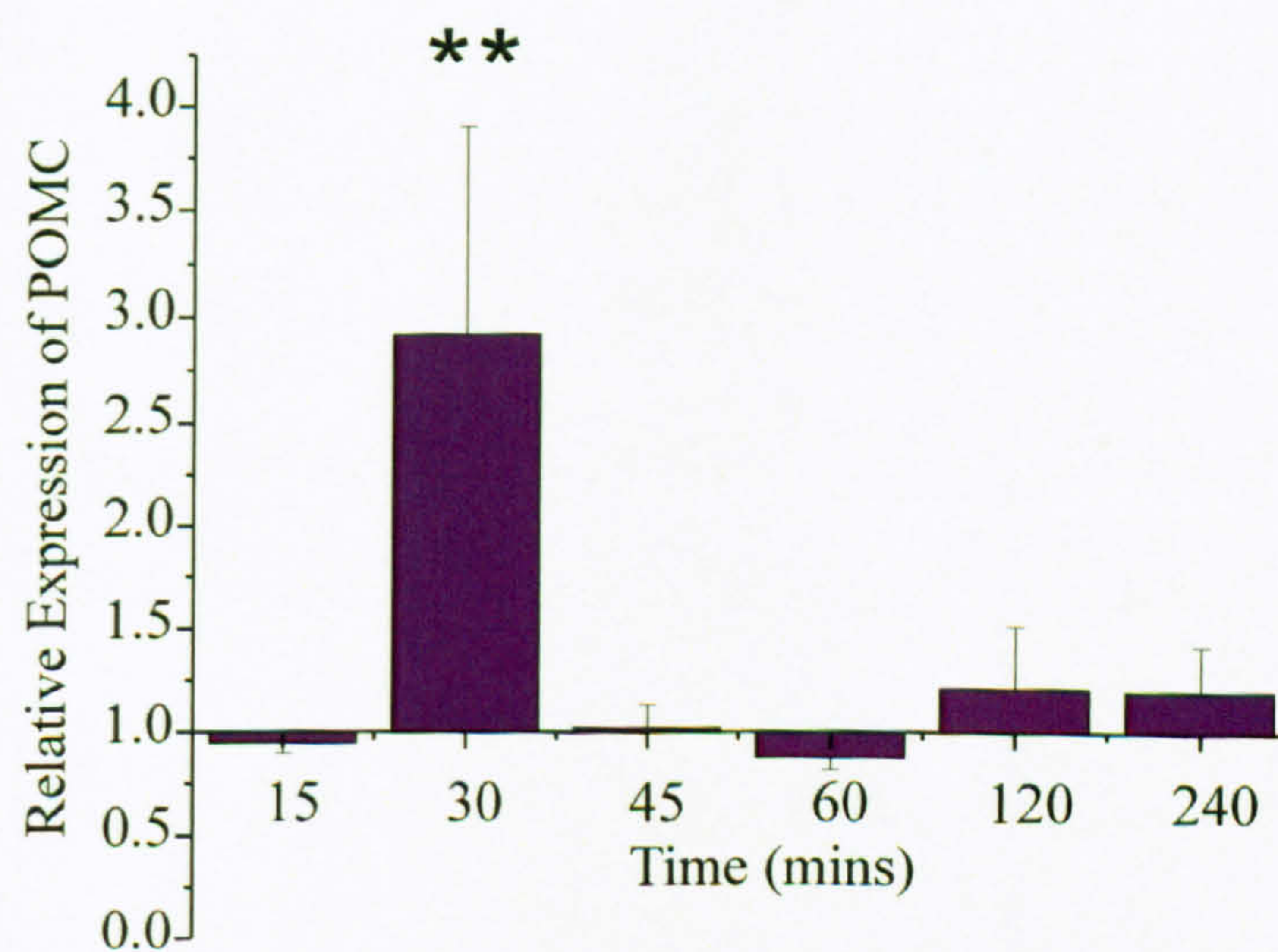


**Figure 6.5**

**Ai**



**Aii**



**Aiii**

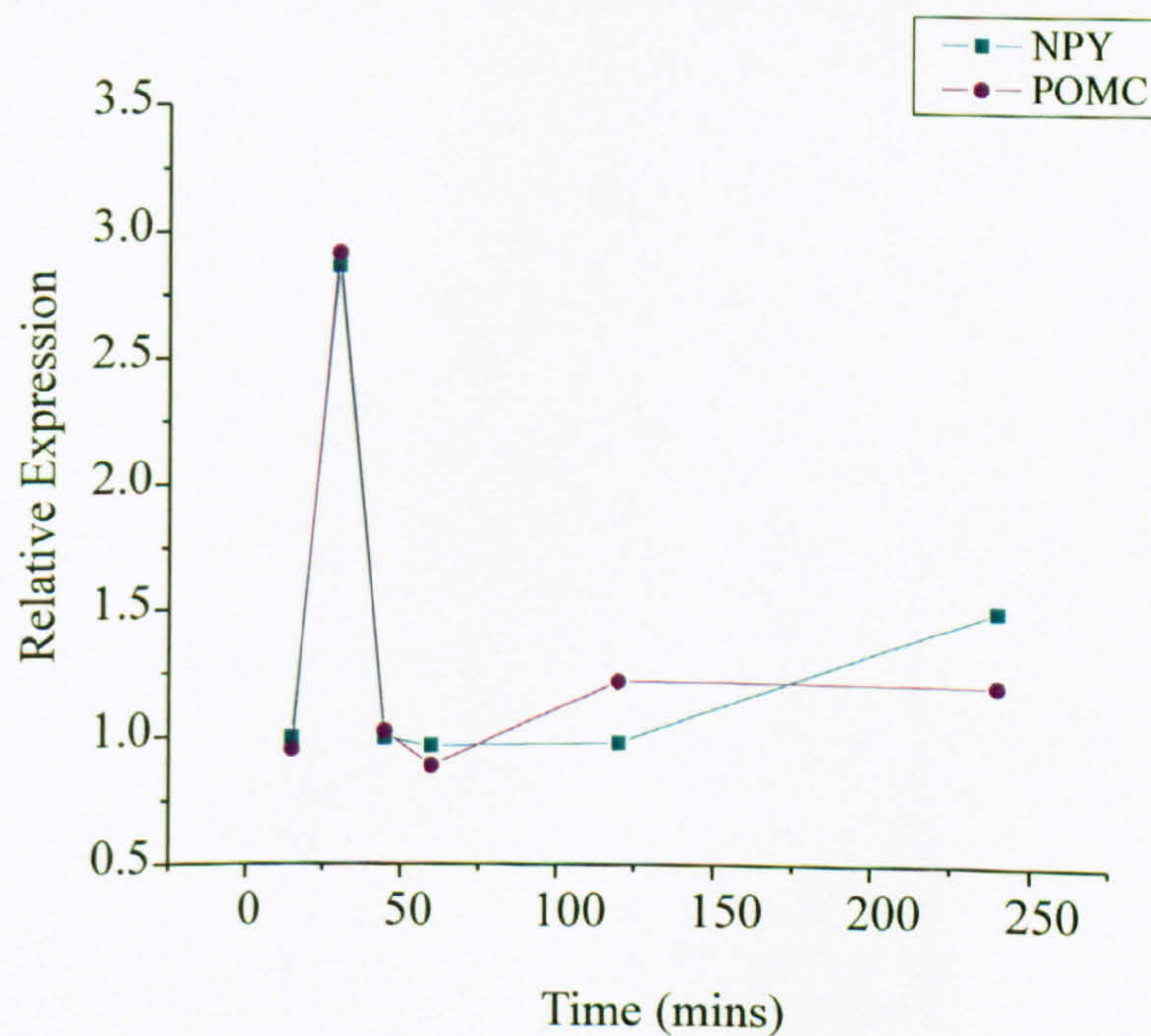




**Figure 6.6 The effect of leptin on NPY and POMC gene expression in individual hypothalamic explants prepared from fasted rats**

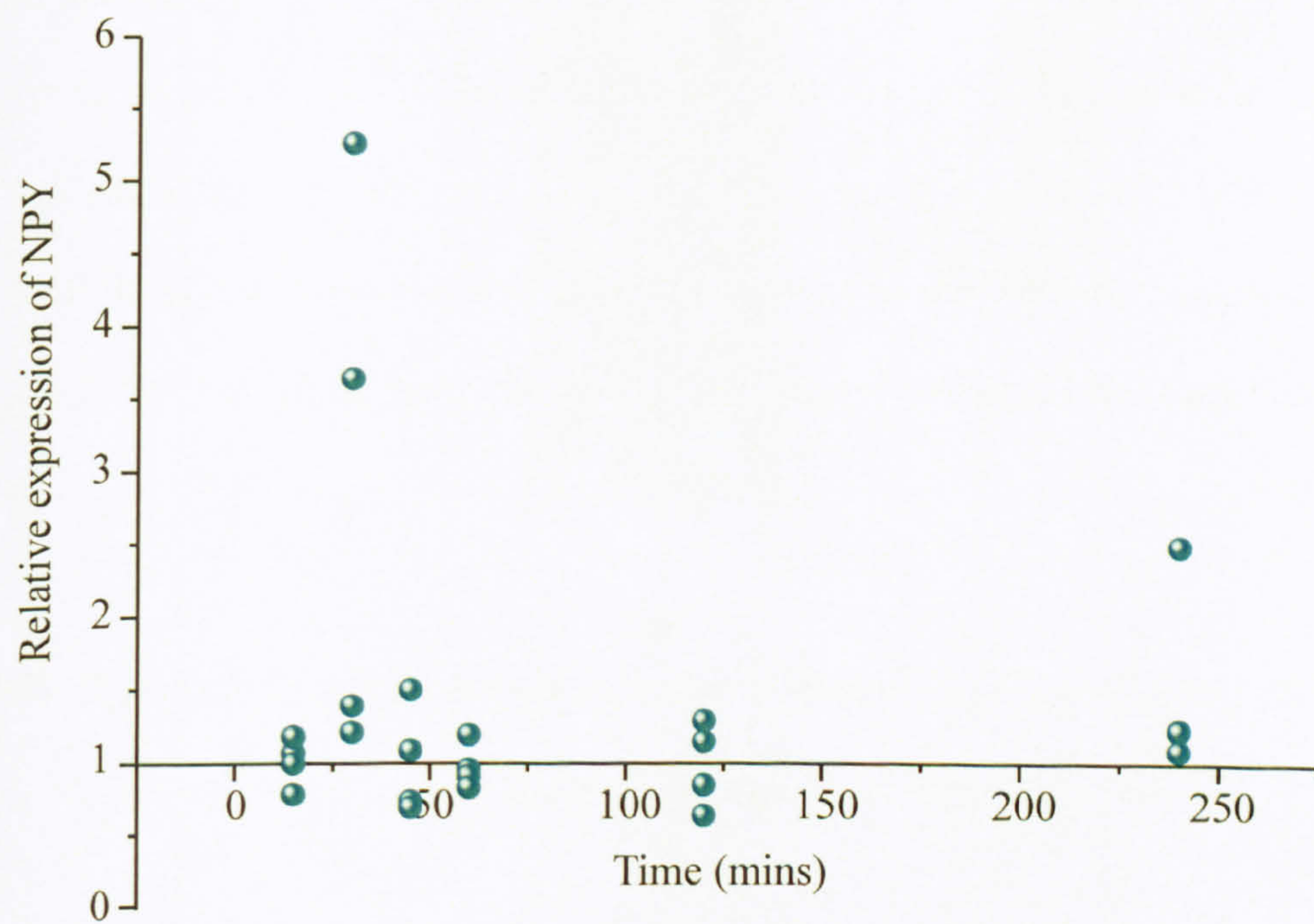
**Ai:** A scatter graph to show the effects of leptin on the expression of NPY mRNA in each of the individual hypothalamic explants from figure 6.5Ai.

**Aii:** A scatter graph to show the effects of leptin on the expression of POMC mRNA in each of the individual hypothalamic explants from figure 6.5Aii.



**Figure 6.6**

**Ai**



**Aii**

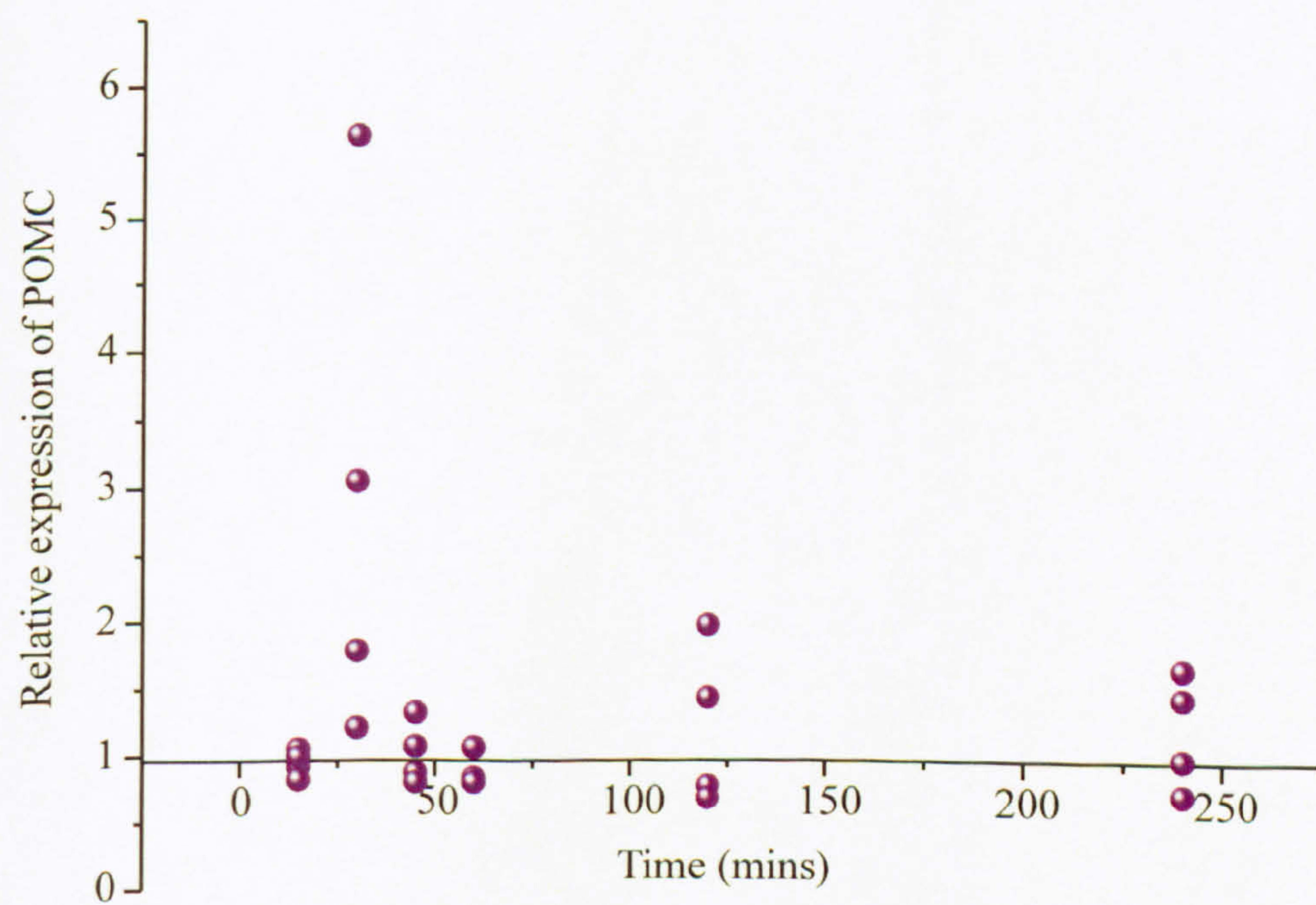




**Figure 6.7 The effect of leptin on AgRP gene expression in hypothalamic explants from animals fed *ad libitum***

**Ai:** A bar-chart to show the effects of leptin on the expression of AgRP mRNA in fed animals. Hypothalamic explants were exposed to leptin for 15, 30, 45 or 60 minutes, and the expression of AgRP was compared to control explants which had not been exposed to leptin. Leptin down-regulated expression of AgRP at all time points, significantly at 30 and 45 mins, with a peak decrease at 30 mins ( $P < 0.05$ , indicated by \*).

**Aii:** A scatter graph to show the effects of leptin on the expression of AgRP mRNA in each of the individual hypothalamic explants from Ai.



**Figure 6.7**

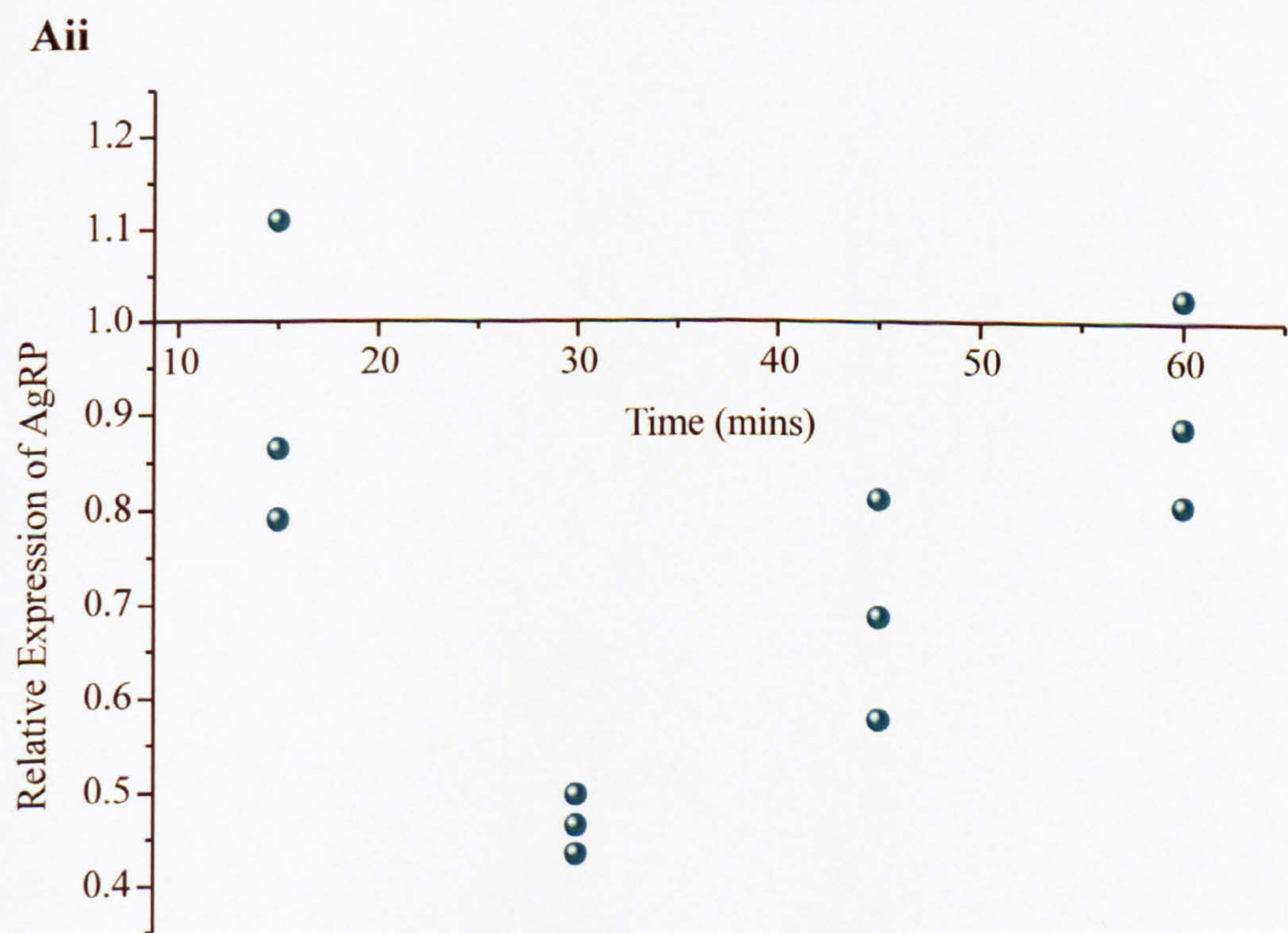
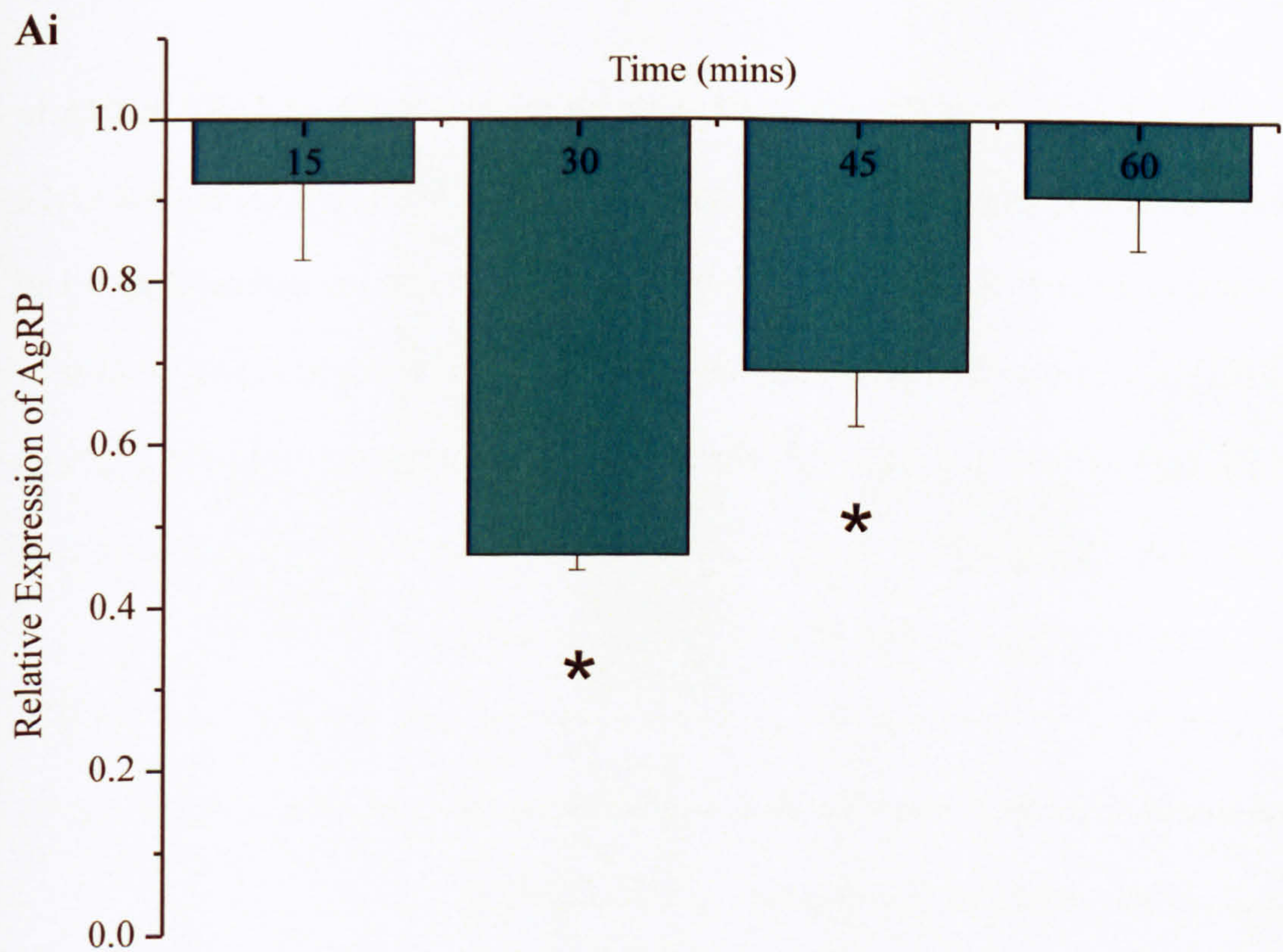




**Figure 6.8 The effect of leptin on AgRP gene expression in hypothalamic explants prepared from fasted animals**

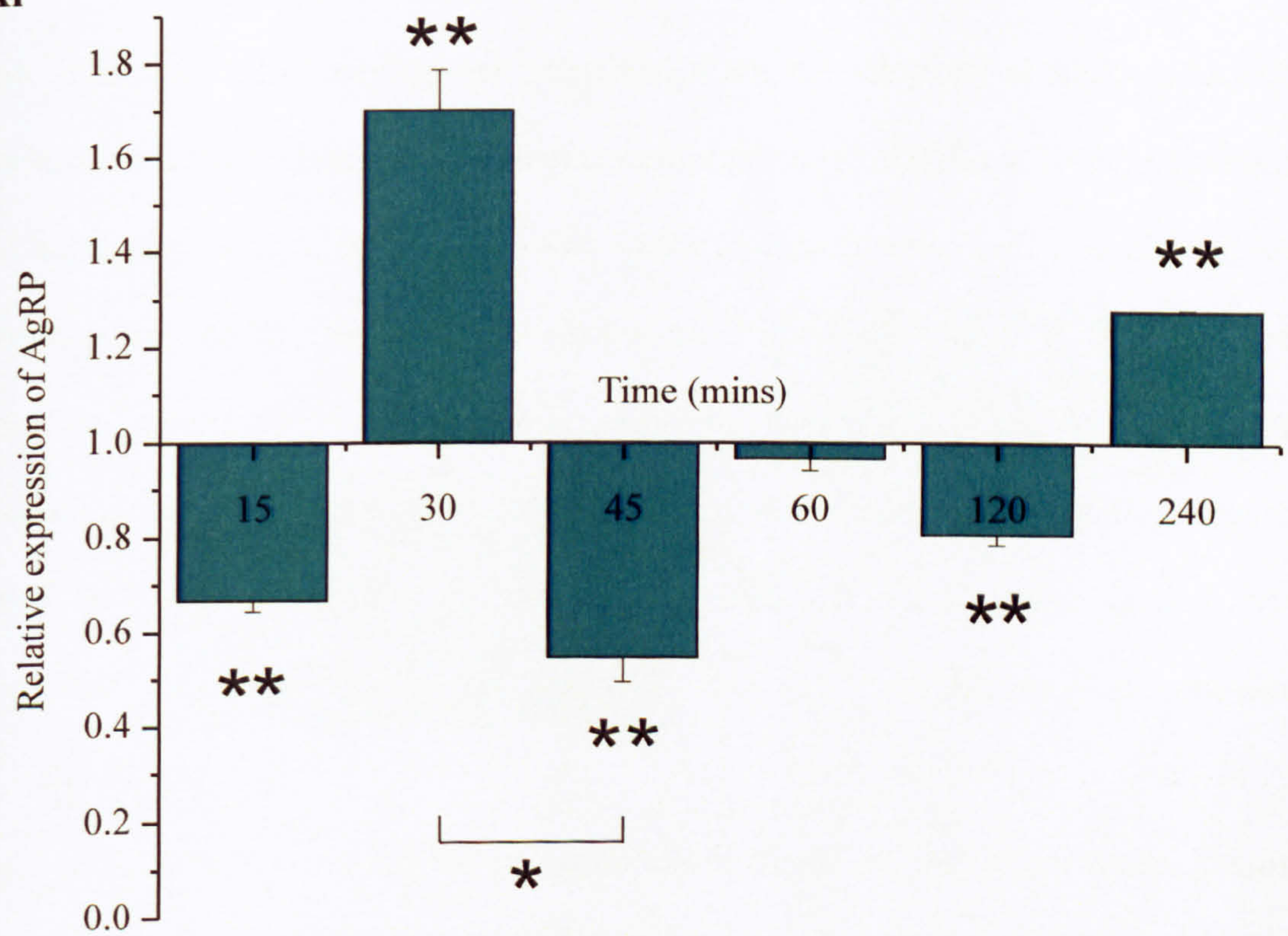
**Ai:** A bar-chart to show the effects of leptin on the expression of AgRP mRNA in fasted animals. Hypothalamic explants were exposed to leptin for 15, 30, 45, 60, 120 or 240 minutes, and the expression of AgRP was compared to control explants which had not been exposed to leptin. Leptin significantly down-regulated expression of AgRP at 15, 45 and 120 mins and significantly up-regulated expression of AgRP at 30 and 240 mins ( $P < 0.01$ , indicated by \*\*). There was a significant difference in expression between 30 and 45 mins ( $P < 0.05$ , indicated by \*).

**Aii:** A scatter graph to show the effects of leptin on the expression of AgRP mRNA in each of the individual hypothalamic explants from Ai.



**Figure 6.8**

**Ai**



**Aii**

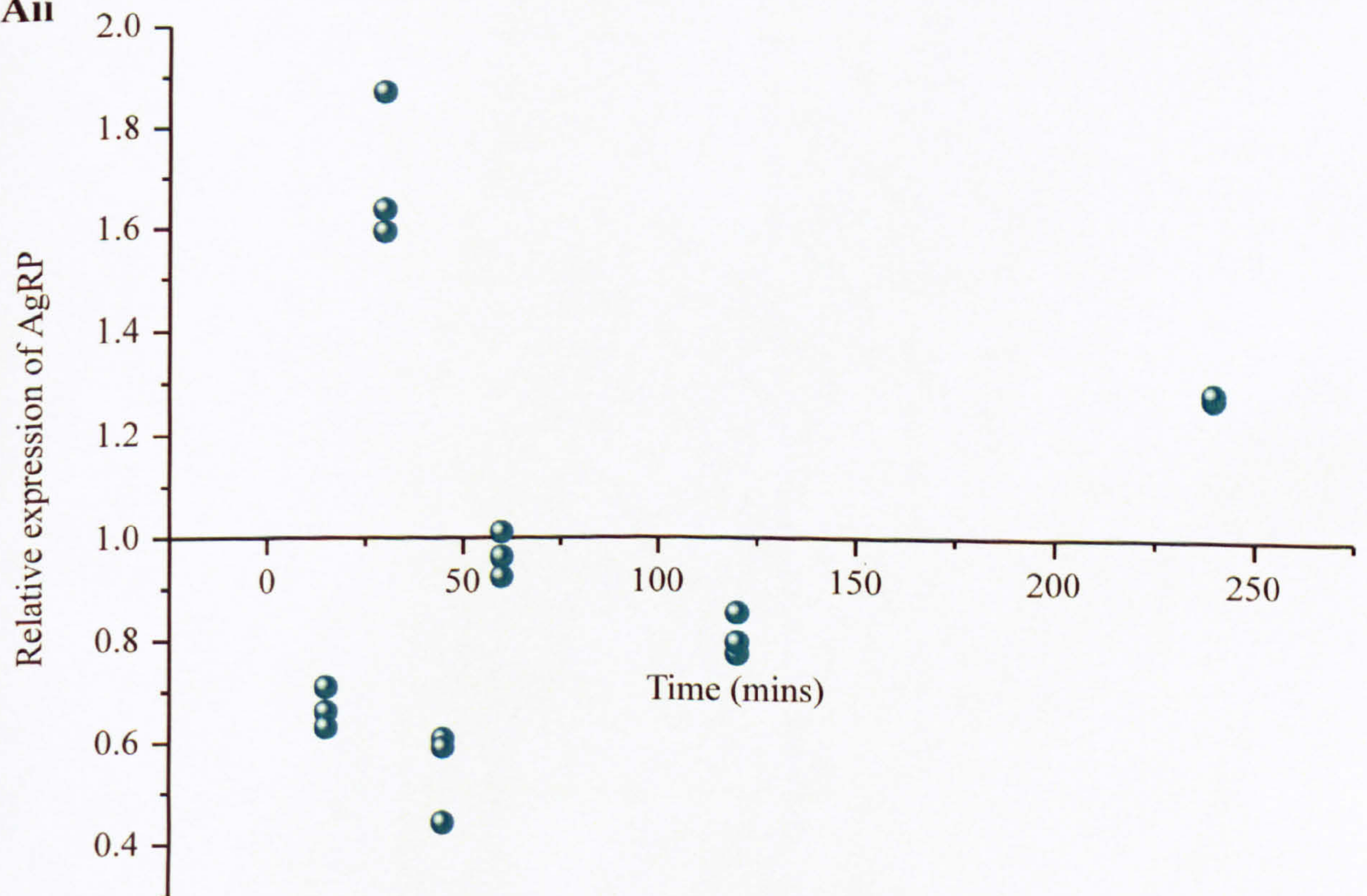




**Figure 6.9 The effect of changing the glucose concentration on NPY gene expression in hypothalamic explants from rats fed *ad libitum***

**Ai:** A bar-chart to show the effects of changing the glucose concentration on the expression of NPY mRNA. Hypothalamic explants were incubated in 2 mM glucose for 60 minutes. They were then exposed to either 0.2 mM or 5 mM glucose for 15 minutes, and the expression of NPY was compared to control explants that had not been exposed to a change in glucose concentration. NPY expression was significantly down-regulated in the explants that were subjected to 0.2 mM glucose ( $P<0.01$ , as indicated by \*\*) and was up-regulated in explants that had been subjected to 5 mM glucose.

**Aii:** A scatter graph to show the effects of changing the glucose concentration on the expression of NPY mRNA in each of the individual hypothalamic explants from Ai.



**Figure 6.9**

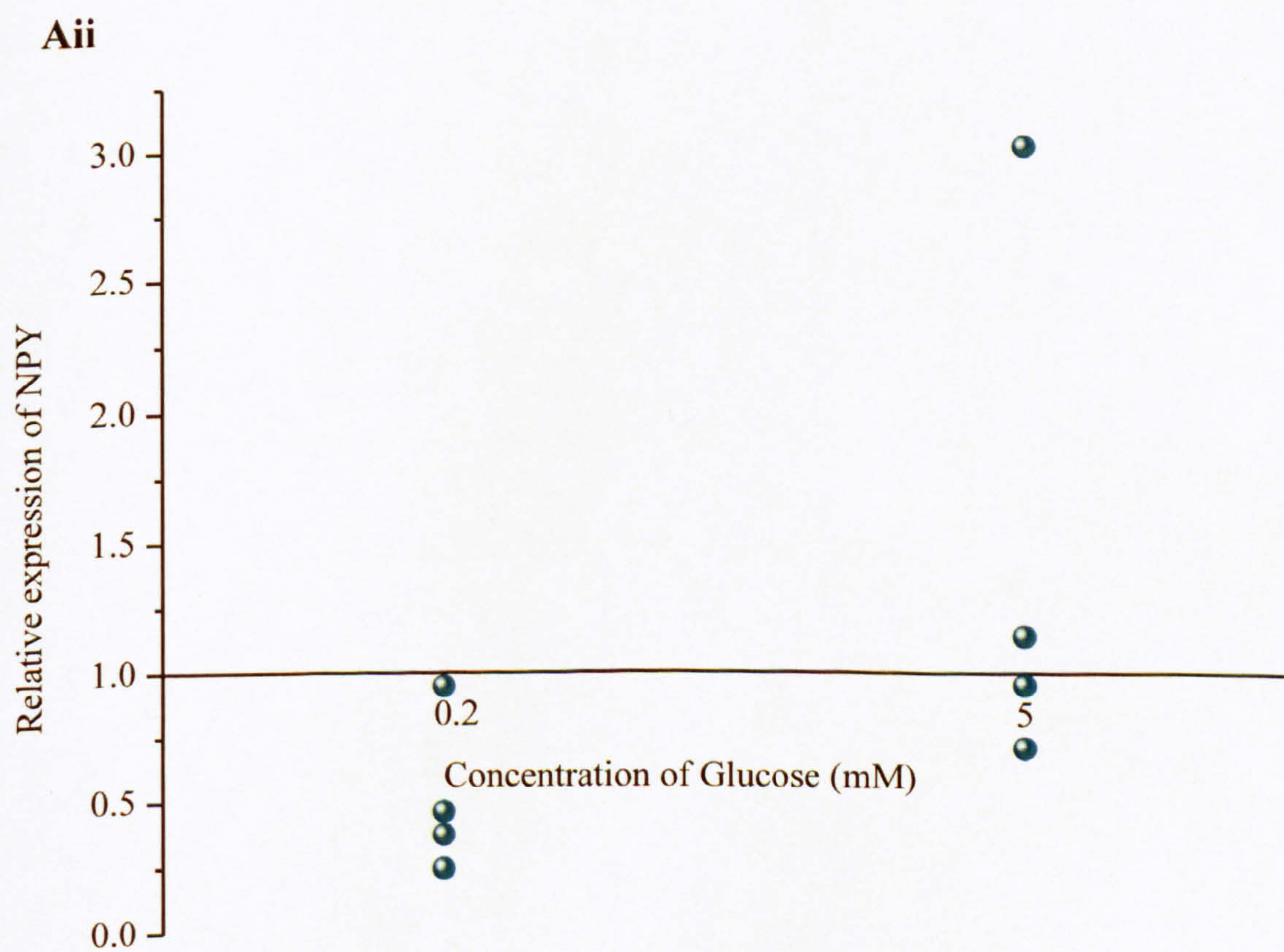
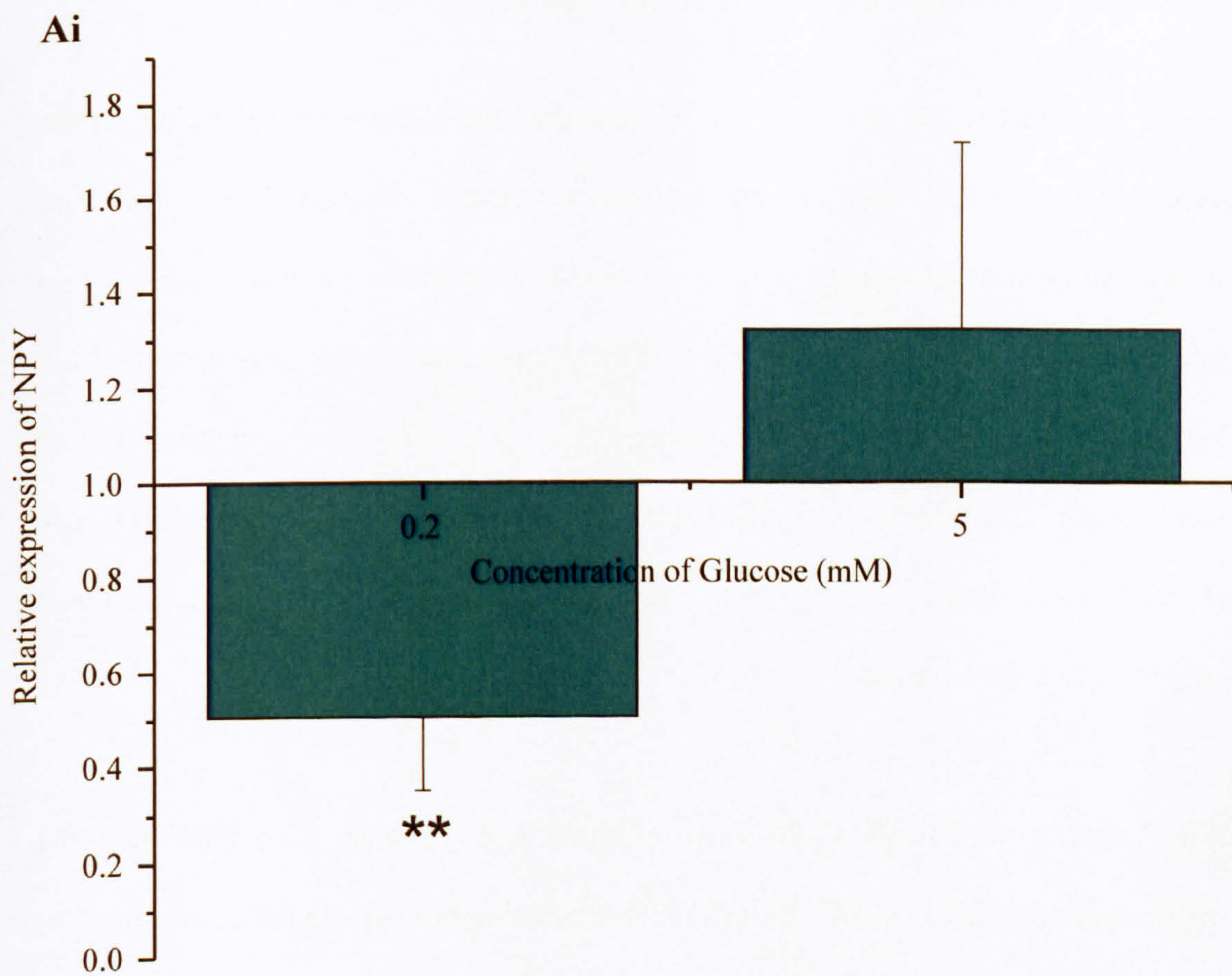




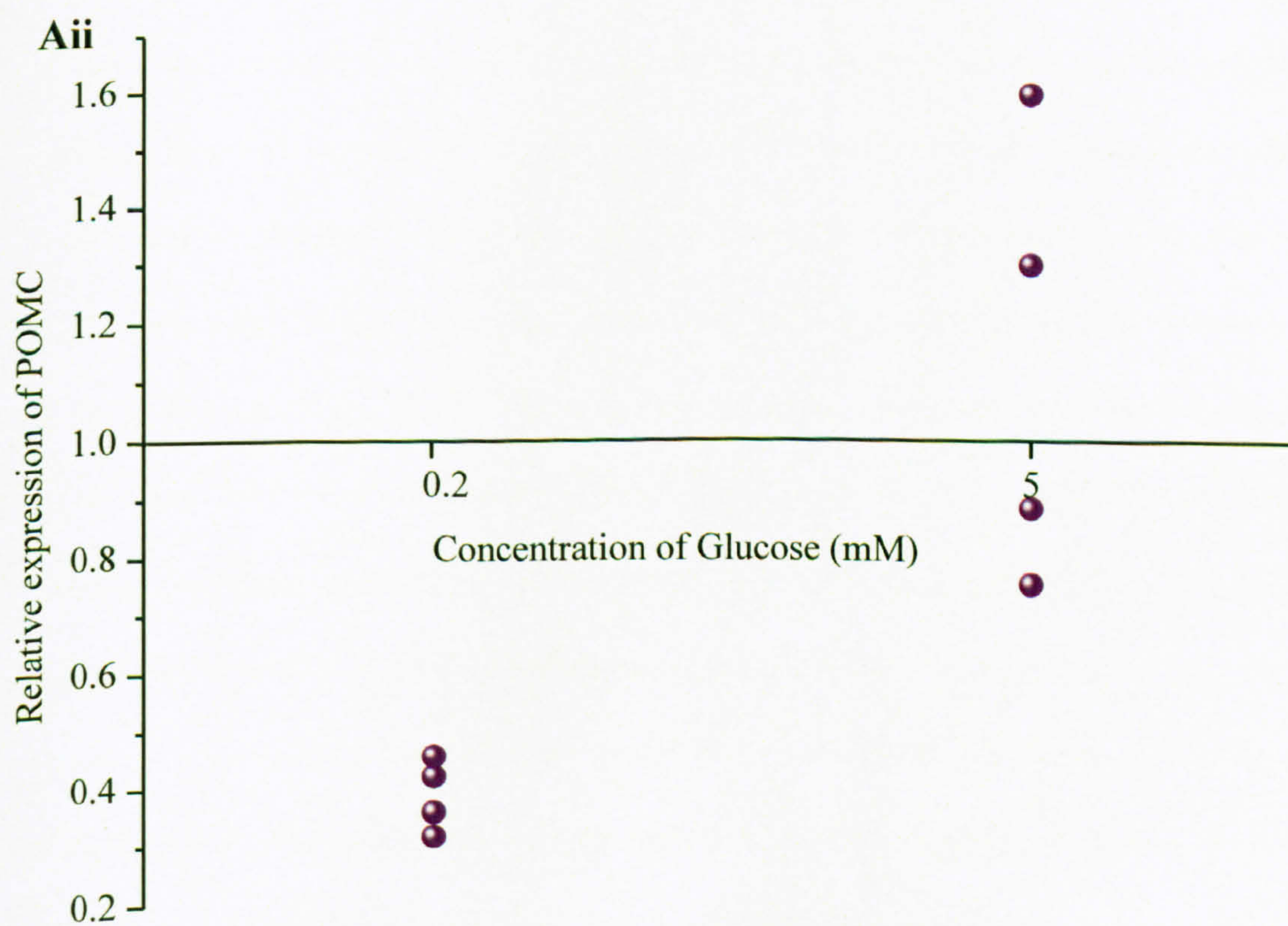
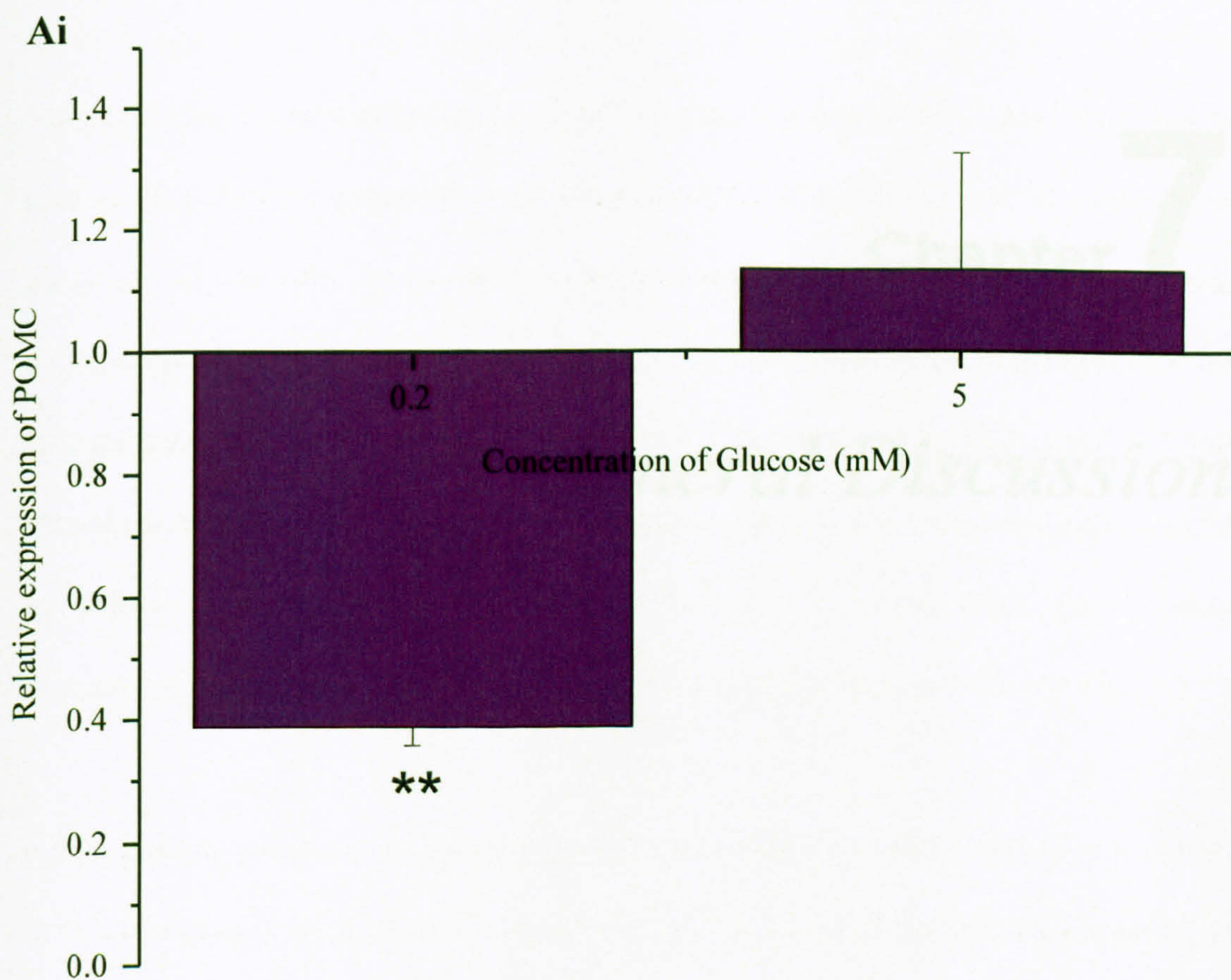
**Figure 6.10 The effect of changing the glucose concentration on POMC gene expression in hypothalamic explants from rats fed *ad libitum***

**Ai:** A bar-chart to show the effects of changing the glucose concentration on the expression of POMC mRNA. Hypothalamic explants were incubated in 2 mM glucose for 60 minutes. They were then exposed to either 0.2 mM or 5 mM glucose for 15 minutes, and the expression of POMC was compared to control explants that had not been exposed to a change in glucose concentration. POMC expression was significantly down-regulated in the explants that were subjected to 0.2 mM glucose ( $P<0.01$ , as indicated by \*\*) and was up-regulated in explants that had been subjected to 5 mM glucose.

**Aii:** A scatter graph to show the effects of changing the glucose concentration on the expression of POMC mRNA in each of the individual hypothalamic explants from Ai.



**Figure 6.10**





# Chapter 7

## *General Discussion*



The central control of energy homeostasis is a complex process involving multiple aspects of the central nervous system and periphery. The arcuate nucleus (ARC) within the hypothalamus is a key integrative centre for the control of energy homeostasis. It is exposed to circulating hormones and nutrients enabling it to monitor the energy status of the body and produce appropriate responses. Understanding the neural pathways and mechanisms underlying the regulation of energy homeostasis is essential to further understand this complex process. Therefore in the present study, the effects of extrinsic and intrinsic factors involved in energy homeostasis at the level of the ARC were investigated using electrophysiology, immunohistochemistry and molecular biology techniques.

### ***7.1 Effect of glucose on electrophysiological properties of ARC neurones***

Glucose is an important metabolic factor involved in energy homeostasis, as not only is it utilised as the primary source of energy for most cells, but it is also able to alter the activity of a population of neurones. These neurones, called glucose-sensing neurones, are able to monitor changes in extracellular glucose and alter their membrane excitability accordingly. Subdivided into two populations, GE neurones are excited by increases in glucose whereas GI neurones are inhibited by increases in glucose (Levin *et al.*, 1999). These glucose-sensing neurones have been localised within the ARC (Ashford *et al.*, 1990a; Spanswick *et al.*, 1997). The levels of glucose to which hypothalamic neurones are exposed is still unclear but is thought to be around 1.4 mM under normal physiological conditions (de Vries *et al.*, 2003; Mayer *et al.*, 2006) but could range between 0 and 8 mM under non-physiological conditions. In this study, the activity and electrophysiological properties of ARC neurones were investigated under two different glucose concentrations, 2 mM



glucose representing a euglycaemic condition and 10 mM representing a hyperglycaemic condition. Previous electrophysiological studies which looked at glucose-sensing neurones in the hypothalamus used glucose at concentrations between 0 and 20 mM but levels above 10 mM are thought to be too high, therefore the present study would also provide useful comparisons with these previous studies.

The major findings of this study were that there were clear differences between the input resistance, the percentage of active neurones and the expression of the active conductance  $I_h$  in neurones recorded in 2 mM compared to 10 mM glucose-containing aCSF. In terms of activity, neurones were more active under physiological conditions (2 mM glucose) compared to hyperglycaemic conditions (10 mM glucose). These data provide strong evidence that under different extracellular glucose concentrations there is a clear change in the activity of ARC neurones. These data may force us to re-evaluate previous glucose-sensing studies which were carried out in non-physiological glucose levels.

Input resistance showed a significant increase in neurones recorded in 10 mM glucose-containing aCSF compared to 2 mM glucose-containing aCSF. As the  $K_{ATP}$  channel has been shown to be important in glucose homeostasis (Ashford *et al.*, 1990a,b; Rowe *et al.*, 1996; Spanswick *et al.*, 1997; Lee *et al.*, 1999; Spanswick *et al.*, 2000; Miki *et al.*, 2001; Zhang *et al.*, 2004), it may be that closure of  $K_{ATP}$  channels may be responsible for the observed increase in input resistance in higher glucose conditions.

The other major finding of this study was the difference in expression of the active conductance  $I_h$  (time- and voltage-dependent inward rectification; Halliwell & Adams, 1982; Pape, 1996). There were a greater percentage of neurones expressing  $I_h$  in 10 mM glucose-containing aCSF compared to 2 mM glucose-containing aCSF.



As  $I_h$  can contribute to the activity of neurones, including by influencing burst-firing (van Welie *et al.*, 2006), it could potentially alter the functional output of neurones. Therefore under different glucose conditions  $I_h$  could be contributing to the activity of neurones.

The active conductance anomalous inward rectifier ( $I_{an}$ ) did not significantly change in this study but there did appear to be a 'stronger' or more active  $I_{an}$  in physiological conditions (2 mM glucose) compared to hyperglycaemic conditions (10 mM glucose). These results indicate that the expression of  $I_{an}$  may be greater in physiological glucose providing further evidence that the expression of ion channels is altered under different glucose concentrations. In addition the expression of the A-like transient outward rectifier ( $I_A$ ), also appeared to change in this study. The decay time of the A-current was smaller in 2 mM glucose-containing aCSF. As A-currents are thought to be involved in the regulation of repetitive firing (Rogawski, 1985) this change in the size of the A-current may lead to differences in the firing properties of neurones. In turn, this could lead to altered release of neuropeptides as firing patterns have been shown to be important for the release of neuropeptides from neurones (Dutton & Dyball, 1979).

As these results indicate that the electrophysiological properties of neurones are able to change under different glucose conditions, it can be concluded that 10 mM and 2 mM glucose represent quite different physiological and/or pathophysiological states. Therefore previous studies undertaken in these glucose and energy status-sensing networks which were carried out in high glucose concentrations may require a major re-evaluation.

Further work which could be done to build upon this study could include the investigation of other electrophysiological properties in 10 mM and 2 mM glucose,



for example the expression of other subthreshold active conductances, or suprathreshold conductances. As the activity of neurones was shown to change, it would be interesting to identify the specific neuronal subgroups within the ARC and see how their individual activity changes. Other glucose concentrations could be tested to investigate the properties of neurones over a range of glucose levels. Ultimately it would be advantageous to determine what the physiological level of glucose is within the hypothalamus in order to identify the properties of neurones in a physiological state.

In addition the expression of ion channels, peptides and receptors could be studied to see if these change under different extracellular glucose levels. In relation to receptor expression, potential differences in the responsiveness of ARC neurones to the extrinsic factor 5-HT were investigated. There was an increase in the number of 5-HT-induced excitations and non-responders in 10 mM glucose while there was an increase in 5-HT-induced inhibitions in 2 mM glucose. The ability of ARC neurones to respond to extrinsic factors and produce responses is therefore altered under different glucose states. It may be that in different glucose concentrations different levels of 5-HT receptors may be expressed. For example, in 10 mM glucose, where there were more excitations, more 5-HT<sub>2</sub> receptors which mediate the 5-HT-induced excitation may be expressed. Conversely, the reduced number of inhibitions in 10 mM glucose may have been due to reduced expression of the 5-HT<sub>1</sub> and 5-HT<sub>7</sub> receptors that mediate the 5-HT-induced inhibition. Overall these data indicate glucose as a key signalling molecule affecting the ability of ARC neurones to respond to extrinsic factors.



## 7.2 Electrophysiological characterisation of ARC neurones

The ARC contains a complex network of neurones, with a diverse array of neuronal subtypes and multiple neuronal inputs and outputs. How these networks function together to integrate and generate responses is still largely unknown; therefore in the present study an electrophysiological classification was performed in an attempt to functionally classify ARC neurones. The classification in this study was designed to be a framework upon which to build a functional classification of ARC neurones. This study was based upon the expression of subthreshold active conductances, as these active conductances have been shown to be important for shaping the electrophysiological properties of individual neurones by integrating synaptic inputs and controlling the output of neurones by altering their patterns of activity (Huguenard, 1996; Pape, 1996; van den Top *et al.*, 2004). Dividing neurones into groups that contain different active conductances might therefore help to functionally separate ARC neurones, as neurones with different electrophysiological properties could also have different functions within the ARC. The subthreshold active conductances utilised in this study to classify neurones were  $I_{an}$ ,  $I_h$ , the A-like transient outward rectifier and the T-type calcium conductance. Neurones were divided into 8 neuronal groups, termed clusters.

Future studies which build upon this classification now need to be undertaken. These electrophysiological studies need to be combined with other techniques which identify the phenotype of the neurones, the inputs to and projections from the neurones, the membrane receptors that are expressed and the synaptic physiology and pharmacology of neurones. Studies have already identified the pharmacology of ARC neurones in relation to 5-HT (see next section). In



combination these techniques will aid in producing a more detailed classification of ARC neurones and will identify, in more detail, functional groups within the ARC.

### ***7.3 The differential effects of 5-HT on ARC neurones***

The monoaminergic neurotransmitter 5-HT controls many biological, behavioural and physiological processes. It exerts its effects through 14 subtypes of receptor, split into seven families (Hoyer *et al.*, 1994). 5-HT has been implicated in the control of feeding and energy homeostasis (Blundell, 1977), and several serotonergic agents have been utilised in the pharmacological treatment of obesity (Luque & Rey, 2002). However despite the evidence implicating 5-HT in the control of energy homeostasis, the receptors and cellular mechanisms underlying the effects of 5-HT in the ARC are still not completely known. Therefore this study investigated the cellular mechanisms by which 5-HT regulates key hypothalamic neurones in the ARC involved in regulating energy homeostasis and elucidated which 5-HT receptor subtypes were mediating these effects.

ARC neurones responded to 5-HT either with a depolarisation of the membrane, a hyperpolarisation of the membrane or they did not respond. The effect of 5-HT persisted in the presence of TTX indicating that it was a direct effect on ARC neurones.

The 5-HT-induced depolarisation was accompanied with a concomitant increase, decrease or no change in input resistance, leading to identification of three possible mechanisms responsible for the 5-HT-induced excitation. The increase in neuronal input resistance is thought to be due to the closure of one or more resting potassium conductances whereas the decrease in input resistance is most likely due to activation of a non-selective cation conductance. The mechanism by which cells



responded with no change in resistance upon 5-HT application was likely due to the activation of an electrogenic pump in the membrane or to activation of a combination of ion channels. Overall, these data suggest that multiple conductances are responsible for mediating the 5-HT-induced depolarisation.

The 5-HT-induced hyperpolarisation was associated with a concurrent decrease in input resistance, likely to be due to activation of a potassium conductance. Current-voltage relationships also revealed the enhancement of an inward rectifier by 5-HT. Further studies need to be carried out to investigate whether a GIRK channel is involved in mediating the 5-HT-induced hyperpolarisation, utilising specific blockers for this channel.

Pharmacological studies identified the receptors mediating the 5-HT-induced depolarisation to be 5-HT<sub>2A</sub>, 5-HT<sub>2B</sub> and 5-HT<sub>2C</sub> receptors and mediating the 5-HT-induced hyperpolarisation to be predominantly 5-HT<sub>1A</sub> receptors, as well as 5-HT<sub>1B</sub> and 5-HT<sub>7</sub> receptors. Further work needs to be done to clarify the mechanisms responsible for the agonist responses and in the presence of the antagonists to identify if a specific subtype of receptor is associated with a particular mechanism. In addition, the downstream signalling pathways at these receptors need to be investigated.

A population of neurones excited by 5-HT were subsequently identified immunohistochemically as CART neurones. CART is an anorexigenic peptide that is co-expressed with POMC neurones (Elias *et al.*, 1998a), which suggests that 5-HT is able to excite anorexigenic neurones. However 5-HT was also able to excite orexigenic neurones as identified by their response to ghrelin, a marker of orexigenic neurones. Therefore 5-HT may be exciting both anorexigenic CART neurones and other un-identified neurones.



Neurones inhibited by 5-HT were identified as orexigenic by their response to ghrelin and due to the fact that 5-HT inhibited identified NPY/AgRP neurones (van den Top *et al.*, 2004) providing evidence that 5-HT hyperpolarises orexigenic NPY neurones. 5-HT<sub>1B</sub> receptors were subsequently identified on non-CART-positive neurones, which could potentially be orexigenic neurones but this needs further investigation. 5-HT<sub>1B</sub> receptors were also found co-localised in CART neurones indicating that these receptors are also localised to a subset of anorexigenic neurones. Further work needs to be done utilising immunohistochemistry, *in situ* hybridisation and single-cell RT-PCR to elucidate other neuronal subtypes that are excited or inhibited by 5-HT.

Overall these data provide compelling evidence for the anorexigenic role of 5-HT acting at the level of the ARC. The present study has identified the mechanisms by which 5-HT acts at the level of the ARC to control the excitability of ARC neurones. 5-HT excites identified anorexigenic CART neurones via the 5-HT<sub>2A</sub>, 5-HT<sub>2B</sub> and 5-HT<sub>2C</sub> receptors. 5-HT inhibits identified orexigenic NPY neurones via the 5-HT<sub>1A</sub>, 5-HT<sub>1B</sub> and 5-HT<sub>7</sub> receptors. A schematic of the effects of 5-HT in the ARC can be seen in figure 7.1. These studies have provided further evidence for the involvement of 5-HT in the central control of energy homeostasis.



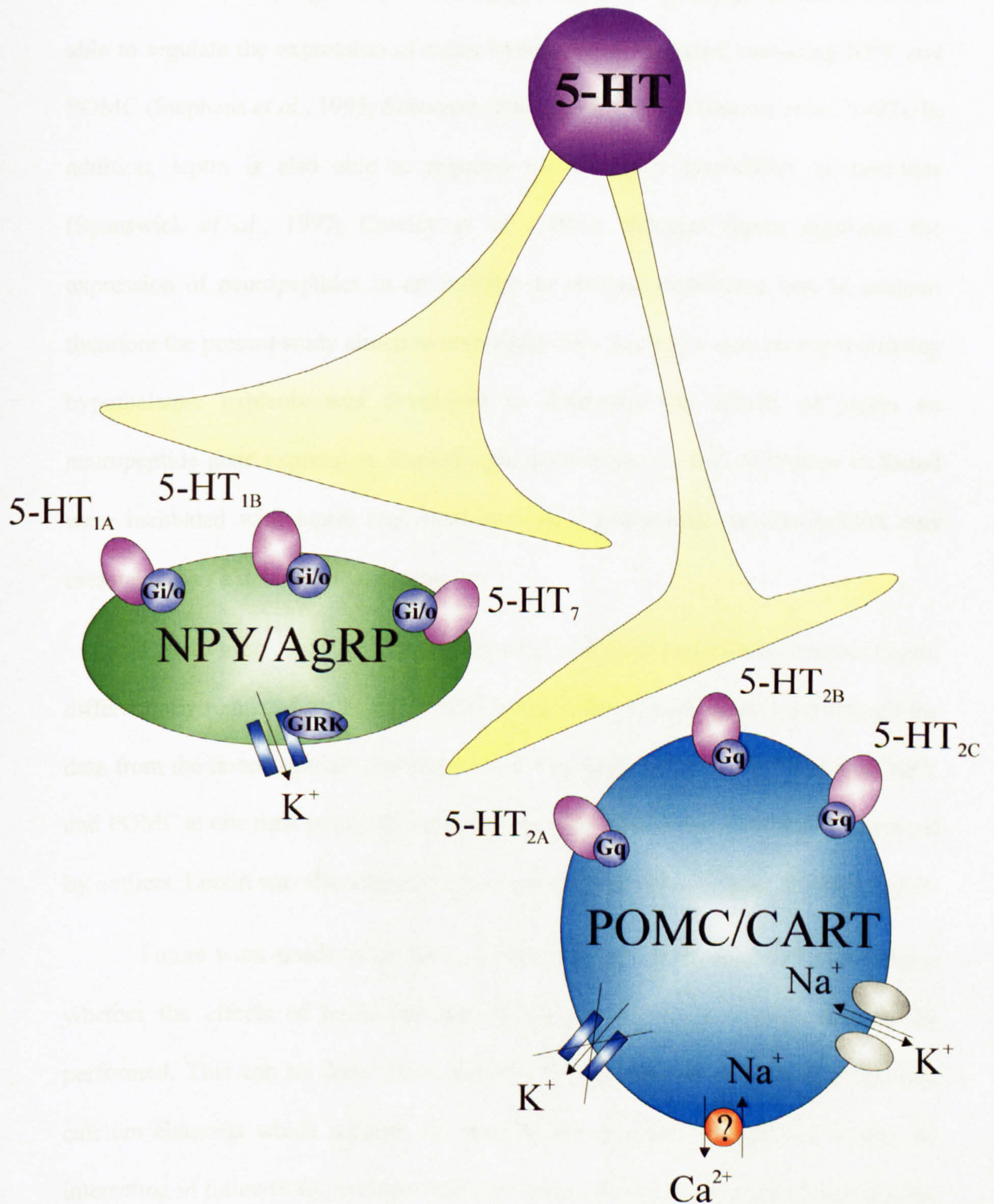
**Figure 7.1 5-HT differentially regulates NPY and POMC neurones within the ARC**

**A:** NPY and POMC neurones within the ARC receive inputs from serotonergic neurones. 5-HT acts directly upon NPY/AgRP neurones, inducing an inhibition in these neurones via 5-HT<sub>1A</sub>, 5-HT<sub>1B</sub> and/or 5-HT<sub>7</sub> receptors, which are coupled to Gi/o proteins. The mechanism responsible for the 5-HT-induced inhibition is likely due to activation of one or more potassium conductances, thought to be G-protein coupled inwardly-rectifying potassium channels (GIRK). 5-HT also acts directly upon POMC/CART neurones, inducing an excitation in these neurones via 5-HT<sub>2A</sub>, 5-HT<sub>2B</sub> and/or 5-HT<sub>2C</sub> receptors, which are coupled to Gq proteins. The mechanism responsible for the 5-HT-induced excitation is likely due to activation of a non-selective cation conductance, block of a potassium conductance or combination of the two, or due to activation of an unidentified pump in the membrane.



**Figure 7.1**

**A**





#### 7.4 Effect of feeding signals on neuropeptide mRNA expression in the hypothalamus

The adiposity signal leptin is an important factor in energy homeostasis. It is able to regulate the expression of many hypothalamic peptides, including NPY and POMC (Stephens *et al.*, 1995; Schwartz *et al.*, 1996, 1997; Thornton *et al.*, 1997). In addition, leptin is also able to regulate the electrical excitability of neurones (Spanswick *et al.*, 1997; Cowley *et al.*, 2001). Whether leptin regulates the expression of neuropeptides in an activity- or receptor-dependent way is unclear; therefore the present study aimed to investigate this. Initially a new protocol utilising hypothalamic explants was developed to determine the effects of leptin on neuropeptide gene expression. Explants prepared from rats fed *ad libitum* or fasted were incubated with leptin and expression of hypothalamic peptide mRNA was measured over a detailed time-course.

Due to time constraints, this study only produced preliminary results. Leptin differentially regulated NPY and POMC levels in fed animals at 30 mins though the data from the fasted animals showed that leptin significantly up-regulated both NPY and POMC at one time point, 30 mins, although this result may have been influenced by outliers. Leptin was also able to down-regulate another orexigenic peptide, AgRP.

Future work needs to be done to extend these results. Studies to investigate whether the effects of leptin are activity or non-activity-dependent need to be performed. This can be done using selective antagonists for sodium channels and calcium channels which regulate the activity of neurones. In addition, it may be interesting in future to try to dissect out particular areas of the hypothalamus in order to isolate those areas and measure gene expression more region specifically.



### ***7.5 Conclusions and future work***

The major findings of this study show that differential levels of extracellular glucose, representing physiological and pathophysiological states, have an effect on the electrophysiological properties of ARC neurones, particularly the activity of these neurones. As properties of neurones are altered under different states, a major re-evaluation of previous studies undertaken in glucose and energy status-sensing networks which were carried out in pathophysiological glucose concentrations may be needed. Studies need to be carried out to determine the physiological concentration of glucose in the ARC; subsequent studies looking at additional electrophysiological properties, the expression of ion channels, peptides and receptors can then be investigated at this physiological concentration.

The major findings from the 5-HT studies are that the cellular mechanisms by which 5-HT acts at specific neuronal subtypes within the ARC have been identified. 5-HT is able to differentially regulate ARC neurones, by inhibiting orexigenic NPY/AgRP neurones and exciting anorexigenic CART/POMC neurones. 5-HT-induced inhibition is mediated through the 5-HT<sub>1A</sub>, 5-HT<sub>1B</sub> and 5-HT<sub>7</sub> receptors via activation of a potassium conductance. 5-HT-induced excitation is mediated through 5-HT<sub>2A</sub>, 5-HT<sub>2B</sub> and 5-HT<sub>2C</sub> receptors via three cellular mechanisms: activation of a non-selective cation conductance, closure of a potassium conductance or a combination of the two, or activation of an electrogenic pump in the membrane. Further studies need to be done to identify whether a specific subtype of receptor is associated with a particular mechanism for 5-HT-induced excitations. Additional techniques, such as single-cell RT-PCR, need to be used to determine other neuronal subtypes within the ARC that are excited or inhibited by 5-HT.



# Chapter 8

## *References*



- Abbott CR, Rossi M, Wren AM, Murphy KG, Kennedy AR, Stanley SA, Zollner AN, Morgan DG, Morgan I, Ghatel MA, Small CJ & Bloom SR.** (2001). Evidence of an orexigenic role for cocaine- and amphetamine-regulated transcript after administration into discrete hypothalamic nuclei. *Endocrinology* **142**, 3457-3463.
- Abbott CR, Kennedy AR, Wren AM, Rossi M, Murphy KG, Seal LJ, Todd JF, Ghatel MA, Small CJ & Bloom SR.** (2003). Identification of hypothalamic nuclei involved in the orexigenic effect of melanin-concentrating hormone. *Endocrinology* **144**, 3943-3949.
- Abbott CR, Small CJ, Kennedy AR, Neary NM, Sajedi A, Ghatel MA & Bloom SR.** (2005). Blockade of the neuropeptide Y Y2 receptor with the specific antagonist BIIE0246 attenuates the effect of endogenous and exogenous peptide YY(3-36) on food intake. *Brain Res* **1043**, 139-144.
- Adayev T, Ranasinghe B & Banerjee P.** (2005). Transmembrane signaling in the brain by serotonin, a key regulator of physiology and emotion. *Biosci Rep* **25**, 363-385.
- Adrian TE, Allen JM, Bloom SR, Ghatel MA, Rossor MN, Roberts GW, Crow TJ, Tatemoto K & Polak JM.** (1983). Neuropeptide Y distribution in human brain. *Nature* **306**, 584-586.
- Ahima RS, Kelly J, Elmquist JK & Flier JS.** (1999). Distinct physiologic and neuronal responses to decreased leptin and mild hyperleptinemia. *Endocrinology* **140**, 4923-4931.
- Ahlenius S, Larsson K, Svensson L, Hjorth S, Carlsson A, Lindberg P, Wikstrom H, Sanchez D, Arvidsson LE, Hacksell U & Nilsson JL.** (1981). Effects of a new type of 5-HT receptor agonist on male rat sexual behavior. *Pharmacol Biochem Behav* **15**, 785-792.
- Altman HJ, Stone WS & Ogren SO.** (1987). Evidence for a possible functional interaction between serotonergic and cholinergic mechanisms in memory retrieval. *Behav Neural Biol* **48**, 49-62.
- Anand BK & Brobeck JR.** (1951). Localization of a "feeding center" in the hypothalamus of the rat. *Proc Soc Exp Biol Med* **77**, 323-324.
- Anand BK, Chhina GS, Sharma KN, Dua S & Singh B.** (1964). Activity of Single Neurons in the Hypothalamic Feeding Centers: Effect of Glucose. *Am J Physiol* **207**, 1146-1154.
- Anschel S, Alexander M & Perachio AA.** (1982). Multiple connections of medial hypothalamic neurons in the rat. *Exp Brain Res* **46**, 383-392.
- Araneda R & Andrade R.** (1991). 5-Hydroxytryptamine<sub>2</sub> and 5-hydroxytryptamine<sub>1A</sub> receptors mediate opposing responses on membrane excitability in rat association cortex. *Neuroscience* **40**, 399-412.



- Arase K, York DA, Shimizu H, Shargill N & Bray GA.** (1988). Effects of corticotropin-releasing factor on food intake and brown adipose tissue thermogenesis in rats. *Am J Physiol* **255**, E255-259.
- Asakawa A, Inui A, Kaga T, Katsuura G, Fujimiya M, Fujino MA & Kasuga M.** (2003). Antagonism of ghrelin receptor reduces food intake and body weight gain in mice. *Gut* **52**, 947-952.
- Asakawa A, Inui A, Kaga T, Yuzuriha H, Nagata T, Ueno N, Makino S, Fujimiya M, Niijima A, Fujino MA & Kasuga M.** (2001). Ghrelin is an appetite-stimulatory signal from stomach with structural resemblance to motilin. *Gastroenterology* **120**, 337-345.
- Ashford ML, Boden PR & Treherne JM.** (1990a). Glucose-induced excitation of hypothalamic neurones is mediated by ATP-sensitive K<sup>+</sup> channels. *Pflugers Arch* **415**, 479-483.
- Ashford ML, Boden PR & Treherne JM.** (1990b). Tolbutamide excites rat glucoreceptive ventromedial hypothalamic neurones by indirect inhibition of ATP-K<sup>+</sup> channels. *Br J Pharmacol* **101**, 531-540.
- Azmitia EC & Segal M.** (1978). An autoradiographic analysis of the differential ascending projections of the dorsal and median raphe nuclei in the rat. *J Comp Neurol* **179**, 641-667.
- Aznar S, Qian Z, Shah R, Rahbek B & Knudsen GM.** (2003). The 5-HT<sub>1A</sub> serotonin receptor is located on calbindin- and parvalbumin-containing neurons in the rat brain. *Brain Res* **959**, 58-67.
- Bading H, Ginty DD & Greenberg ME.** (1993). Regulation of gene expression in hippocampal neurons by distinct calcium signaling pathways. *Science* **260**, 181-186.
- Bady I, Marty N, Dallaporta M, Emery M, Gyger J, Tarussio D, Foretz M & Thorens B.** (2006). Evidence from glut2-null mice that glucose is a critical physiological regulator of feeding. *Diabetes* **55**, 988-995.
- Baker RA & Herkenham M.** (1995). Arcuate nucleus neurons that project to the hypothalamic paraventricular nucleus: neuropeptidergic identity and consequences of adrenalectomy on mRNA levels in the rat. *J Comp Neurol* **358**, 518-530.
- Baldwin D & Rudge S.** (1995). The role of serotonin in depression and anxiety. *Int Clin Psychopharmacol* **9 Suppl 4**, 41-45.
- Balfour RH, Hansen AM & Trapp S.** (2006). Neuronal responses to transient hypoglycaemia in the dorsal vagal complex of the rat brainstem. *J Physiol* **570**, 469-484.



- Barnes NM & Sharp T.** (1999). A review of central 5-HT receptors and their function. *Neuropharmacology* **38**, 1083-1152.
- Baskin DG, Breininger JF & Schwartz MW.** (1999). Leptin receptor mRNA identifies a subpopulation of neuropeptide Y neurons activated by fasting in rat hypothalamus. *Diabetes* **48**, 828-833.
- Batterham RL & Bloom SR.** (2003). The gut hormone peptide YY regulates appetite. *Ann N Y Acad Sci* **994**, 162-168.
- Batterham RL, Cowley MA, Small CJ, Herzog H, Cohen MA, Dakin CL, Wren AM, Brynes AE, Low MJ, Ghattei MA, Cone RD & Bloom SR.** (2002). Gut hormone PYY(3-36) physiologically inhibits food intake. *Nature* **418**, 650-654.
- Bayliss DA, Li YW & Talley EM.** (1997). Effects of serotonin on caudal raphe neurons: activation of an inwardly rectifying potassium conductance. *J Neurophysiol* **77**, 1349-1361.
- Beck B, Burlet A, Nicolas JP & Burlet C.** (1990). Hypothalamic neuropeptide Y (NPY) in obese Zucker rats: implications in feeding and sexual behaviors. *Physiol Behav* **47**, 449-453.
- Bendotti C & Samanin R.** (1987). The role of putative 5-HT<sub>1A</sub> and 5-HT<sub>1B</sub> receptors in the control of feeding in rats. *Life Sci* **41**, 635-642.
- Berthoud HR.** (2004). Mind versus metabolism in the control of food intake and energy balance. *Physiol Behav* **81**, 781-793.
- Bi S.** (2007). Role of dorsomedial hypothalamic neuropeptide Y in energy homeostasis. *Peptides* **28**, 352-356.
- Bi S, Robinson BM & Moran TH.** (2003). Acute food deprivation and chronic food restriction differentially affect hypothalamic NPY mRNA expression. *Am J Physiol Regul Integr Comp Physiol* **285**, R1030-1036.
- Bicknell RJ & Leng G.** (1981). Relative efficiency of neural firing patterns for vasopressin release in vitro. *Neuroendocrinology* **33**, 295-299.
- Bittencourt JC, Presse F, Arias C, Peto C, Vaughan J, Nahon JL, Vale W & Sawchenko PE.** (1992). The melanin-concentrating hormone system of the rat brain: an immuno- and hybridization histochemical characterization. *J Comp Neurol* **319**, 218-245.
- Blomeley C & Bracci E.** (2005). Excitatory effects of serotonin on rat striatal cholinergic interneurons. *J Physiol* **569**, 715-721.
- Blundell JE.** (1977). Is there a role for serotonin (5-hydroxytryptamine) in feeding? *Int J Obes* **1**, 15-42.



- Blundell JE.** (1984). Serotonin and appetite. *Neuropharmacology* **23**, 1537-1551.
- Bonate PL.** (1991). Serotonin receptor subtypes: functional, physiological, and clinical correlates. *Clin Neuropharmacol* **14**, 1-16.
- Breen TL, Conwell IM & Wardlaw SL.** (2005). Effects of fasting, leptin, and insulin on AGRP and POMC peptide release in the hypothalamus. *Brain Res* **1032**, 141-148.
- Breisch ST, Zemlan FP & Hoebel BG.** (1976). Hyperphagia and obesity following serotonin depletion by intraventricular p-chlorophenylalanine. *Science* **192**, 382-385.
- Brief DJ & Davis JD.** (1984). Reduction of food intake and body weight by chronic intraventricular insulin infusion. *Brain Res Bull* **12**, 571-575.
- Broadwell RD, Balin BJ, Salcman M & Kaplan RS.** (1983). Brain-blood barrier? Yes and no. *Proc Natl Acad Sci U S A* **80**, 7352-7356.
- Broberger C.** (1999). Hypothalamic cocaine- and amphetamine-regulated transcript (CART) neurons: histochemical relationship to thyrotropin-releasing hormone, melanin-concentrating hormone, orexin/hypocretin and neuropeptide Y. *Brain Res* **848**, 101-113.
- Broberger C.** (2005). Brain regulation of food intake and appetite: molecules and networks. *J Intern Med* **258**, 301-327.
- Broberger C, De Lecea L, Sutcliffe JG & Hokfelt T.** (1998). Hypocretin/orexin- and melanin-concentrating hormone-expressing cells form distinct populations in the rodent lateral hypothalamus: relationship to the neuropeptide Y and agouti gene-related protein systems. *J Comp Neurol* **402**, 460-474.
- Broberger C, Landry M, Wong H, Walsh JN & Hokfelt T.** (1997). Subtypes Y1 and Y2 of the neuropeptide Y receptor are respectively expressed in pro-opiomelanocortin- and neuropeptide-Y-containing neurons of the rat hypothalamic arcuate nucleus. *Neuroendocrinology* **66**, 393-408.
- Bruning JC, Gautam D, Burks DJ, Gillette J, Schubert M, Orban PC, Klein R, Krone W, Muller-Wieland D & Kahn CR.** (2000). Role of brain insulin receptor in control of body weight and reproduction. *Science* **289**, 2122-2125.
- Burdakov D, Jensen LT, Alexopoulos H, Williams RH, Fearon IM, O'Kelly I, Gerasimenko O, Fugger L & Verkhratsky A.** (2006). Tandem-pore K<sup>+</sup> channels mediate inhibition of orexin neurons by glucose. *Neuron* **50**, 711-722.
- Burdakov D, Luckman SM & Verkhratsky A.** (2005). Glucose-sensing neurons of the hypothalamus. *Philos Trans R Soc Lond B Biol Sci* **360**, 2227-2235.



- Campfield LA, Smith FJ, Guisez Y, Devos R & Burn P.** (1995). Recombinant mouse OB protein: evidence for a peripheral signal linking adiposity and central neural networks. *Science* **269**, 546-549.
- Carbone E, Marcantoni A, Gianniccoli A, Guido D & Carabelli V.** (2006). T-type channels-secretion coupling: evidence for a fast low-threshold exocytosis. *Pflügers Arch* **453**, 373-383.
- Challis BG, Pinnock SB, Coll AP, Carter RN, Dickson SL & O'Rahilly S.** (2003). Acute effects of PYY3-36 on food intake and hypothalamic neuropeptide expression in the mouse. *Biochem Biophys Res Commun* **311**, 915-919.
- Chalmers DT & Watson SJ.** (1991). Comparative anatomical distribution of 5-HT1A receptor mRNA and 5-HT1A binding in rat brain--a combined in situ hybridisation/in vitro receptor autoradiographic study. *Brain Res* **561**, 51-60.
- Charney DS, Krystal JH, Delgado PL & Heninger GR.** (1990). Serotonin-specific drugs for anxiety and depressive disorders. *Annu Rev Med* **41**, 437-446.
- Chen HY, Trumbauer ME, Chen AS, Weingarth DT, Adams JR, Frazier EG, Shen Z, Marsh DJ, Feighner SD, Guan XM, Ye Z, Nargund RP, Smith RG, Van der Ploeg LH, Howard AD, MacNeil DJ & Qian S.** (2004). Orexigenic action of peripheral ghrelin is mediated by neuropeptide Y and agouti-related protein. *Endocrinology* **145**, 2607-2612.
- Cheung CC, Clifton DK & Steiner RA.** (1997). Proopiomelanocortin neurons are direct targets for leptin in the hypothalamus. *Endocrinology* **138**, 4489-4492.
- Chronwall BM.** (1985). Anatomy and physiology of the neuroendocrine arcuate nucleus. *Peptides* **6 Suppl 2**, 1-11.
- Chua SC, Jr., Brown AW, Kim J, Hennessey KL, Leibel RL & Hirsch J.** (1991). Food deprivation and hypothalamic neuropeptide gene expression: effects of strain background and the diabetes mutation. *Brain Res Mol Brain Res* **11**, 291-299.
- Claret M, Smith MA, Batterham RL, Selman C, Choudhury AI, Fryer LG, Clements M, Al-Qassab H, Heffron H, Xu AW, Speakman JR, Barsh GS, Viollet B, Vaulont S, Ashford ML, Carling D & Withers DJ.** (2007). AMPK is essential for energy homeostasis regulation and glucose sensing by POMC and AgRP neurons. *J Clin Invest* **117**, 2325-2336.
- Cole AJ, Saffen DW, Baraban JM & Worley PF.** (1989). Rapid increase of an immediate early gene messenger RNA in hippocampal neurons by synaptic NMDA receptor activation. *Nature* **340**, 474-476.
- Collin M, Backberg M, Onnestam K & Meister B.** (2002). 5-HT1A receptor immunoreactivity in hypothalamic neurons involved in body weight control. *Neuroreport* **13**, 945-951.



- Collin M, Backberg M, Ovesjo ML, Fisone G, Edwards RH, Fujiyama F & Meister B.** (2003). Plasma membrane and vesicular glutamate transporter mRNAs/proteins in hypothalamic neurons that regulate body weight. *Eur J Neurosci* **18**, 1265-1278.
- Cone RD.** (2005). Anatomy and regulation of the central melanocortin system. *Nat Neurosci* **8**, 571-578.
- Cone RD, Cowley MA, Butler AA, Fan W, Marks DL & Low MJ.** (2001). The arcuate nucleus as a conduit for diverse signals relevant to energy homeostasis. *Int J Obes Relat Metab Disord* **25 Suppl 5**, S63-67.
- Connolly HM, Crary JL, McGoon MD, Hensrud DD, Edwards BS, Edwards WD & Schaff HV.** (1997). Valvular heart disease associated with fenfluramine-phentermine. *N Engl J Med* **337**, 581-588.
- Connor JA & Stevens CF.** (1971a). Prediction of repetitive firing behaviour from voltage clamp data on an isolated neurone soma. *J Physiol* **213**, 31-53.
- Connor JA & Stevens CF.** (1971b). Voltage clamp studies of a transient outward membrane current in gastropod neural somata. *J Physiol* **213**, 21-30.
- Constanti A & Galvan M.** (1983). Fast inward-rectifying current accounts for anomalous rectification in olfactory cortex neurones. *J Physiol* **335**, 153-178.
- Cowley MA, Smart JL, Rubinstein M, Cerdan MG, Diano S, Horvath TL, Cone RD & Low MJ.** (2001). Leptin activates anorexigenic POMC neurons through a neural network in the arcuate nucleus. *Nature* **411**, 480-484.
- Cowley MA, Smith RG, Diano S, Tschop M, Pronchuk N, Grove KL, Strasburger CJ, Bidlingmaier M, Esterman M, Heiman ML, Garcia-Segura LM, Nillni EA, Mendez P, Low MJ, Sotonyi P, Friedman JM, Liu H, Pinto S, Colmers WF, Cone RD & Horvath TL.** (2003). The distribution and mechanism of action of ghrelin in the CNS demonstrates a novel hypothalamic circuit regulating energy homeostasis. *Neuron* **37**, 649-661.
- Cross AJ.** (1990). Serotonin in Alzheimer-type dementia and other dementing illnesses. *Ann N Y Acad Sci* **600**, 405-415; discussion 415-407.
- Cummings DE, Clement K, Purnell JQ, Vaisse C, Foster KE, Frayo RS, Schwartz MW, Basdevant A & Weigle DS.** (2002a). Elevated plasma ghrelin levels in Prader Willi syndrome. *Nat Med* **8**, 643-644.
- Cummings DE & Overduin J.** (2007). Gastrointestinal regulation of food intake. *J Clin Invest* **117**, 13-23.
- Cummings DE, Purnell JQ, Frayo RS, Schmidova K, Wisse BE & Weigle DS.** (2001). A preprandial rise in plasma ghrelin levels suggests a role in meal initiation in humans. *Diabetes* **50**, 1714-1719.



- Cummings DE, Weigle DS, Frayo RS, Breen PA, Ma MK, Dellinger EP & Purnell JQ. (2002b).** Plasma ghrelin levels after diet-induced weight loss or gastric bypass surgery. *N Engl J Med* **346**, 1623-1630.
- Currie PJ, Coiro CD, Niyomchai T, Lira A & Farahmand F. (2002).** Hypothalamic paraventricular 5-hydroxytryptamine: receptor-specific inhibition of NPY-stimulated eating and energy metabolism. *Pharmacol Biochem Behav* **71**, 709-716.
- Currie PJ & Coscina DV. (1996).** Metergoline potentiates natural feeding and antagonizes the anorectic action of medical hypothalamic 5-hydroxytryptamine. *Pharmacol Biochem Behav* **53**, 1023-1028.
- Currie PJ, Mirza A, Fuld R, Park D & Vasselli JR. (2005).** Ghrelin is an orexigenic and metabolic signaling peptide in the arcuate and paraventricular nuclei. *Am J Physiol Regul Integr Comp Physiol* **289**, R353-R358.
- Curzon G. (1990).** Serotonin and appetite. *Ann N Y Acad Sci* **600**, 521-530; discussion 530-521.
- Curzon G. (1991).** Effects of tryptophan and of 5-hydroxytryptamine receptor subtype agonists on feeding. *Adv Exp Med Biol* **294**, 377-388.
- Date Y, Kojima M, Hosoda H, Sawaguchi A, Mondal MS, Suganuma T, Matsukura S, Kangawa K & Nakazato M. (2000).** Ghrelin, a novel growth hormone-releasing acylated peptide, is synthesized in a distinct endocrine cell type in the gastrointestinal tracts of rats and humans. *Endocrinology* **141**, 4255-4261.
- de Lecea L, Kilduff TS, Peyron C, Gao X, Foye PE, Danielson PE, Fukuhara C, Battenberg EL, Gautvik VT, Bartlett FS, 2nd, Frankel WN, van den Pol AN, Bloom FE, Gautvik KM & Sutcliffe JG. (1998).** The hypocretins: hypothalamus-specific peptides with neuroexcitatory activity. *Proc Natl Acad Sci USA* **95**, 322-327.
- de Vries MG, Arseneau LM, Lawson ME & Beverly JL. (2003).** Extracellular glucose in rat ventromedial hypothalamus during acute and recurrent hypoglycemia. *Diabetes* **52**, 2767-2773.
- De Vry J & Schreiber R. (2000).** Effects of selected serotonin 5-HT(1) and 5-HT(2) receptor agonists on feeding behavior: possible mechanisms of action. *Neurosci Biobehav Rev* **24**, 341-353.
- Dhillon WS, Small CJ, Stanley SA, Jethwa PH, Seal LJ, Murphy KG, Ghatei MA & Bloom SR. (2002).** Hypothalamic interactions between neuropeptide Y, agouti-related protein, cocaine- and amphetamine-regulated transcript and alpha-melanocyte-stimulating hormone in vitro in male rats. *J Neuroendocrinol* **14**, 725-730.



- Douglass J, McKinzie AA & Couceyro P.** (1995). PCR differential display identifies a rat brain mRNA that is transcriptionally regulated by cocaine and amphetamine. *J Neurosci* **15**, 2471-2481.
- Dourish CT, Hutson PH & Curzon G.** (1985). Low doses of the putative serotonin agonist 8-hydroxy-2-(di-n-propylamino) tetralin (8-OH-DPAT) elicit feeding in the rat. *Psychopharmacology (Berl)* **86**, 197-204.
- Dourish CT, Hutson PH, Kennett GA & Curzon G.** (1986). 8-OH-DPAT-induced hyperphagia: its neural basis and possible therapeutic relevance. *Appetite* **7 Suppl**, 127-140.
- Dryden S, Frankish HM, Wang Q, Pickavance L & Williams G.** (1996a). The serotonergic agent fluoxetine reduces neuropeptide Y levels and neuropeptide Y secretion in the hypothalamus of lean and obese rats. *Neuroscience* **72**, 557-566.
- Dryden S, Frankish HM, Wang Q & Williams G.** (1996c). Increased feeding and neuropeptide Y (NPY) but not NPY mRNA levels in the hypothalamus of the rat following central administration of the serotonin synthesis inhibitor p-chlorophenylalanine. *Brain Res* **724**, 232-237.
- Dryden S, Wang Q, Frankish HM & Williams G.** (1996b). Differential effects of the 5-HT 1B/2C receptor agonist mCPP and the 5-HT1A agonist flesinoxan on hypothalamic neuropeptide Y in the rat: evidence that NPY may mediate serotonin's effects on food intake. *Peptides* **17**, 943-949.
- Dube MG, Kalra SP & Kalra PS.** (1999). Food intake elicited by central administration of orexins/hypocretins: identification of hypothalamic sites of action. *Brain Res* **842**, 473-477.
- Dunn-Meynell AA, Routh VH, Kang L, Gaspers L & Levin BE.** (2002). Glucokinase is the likely mediator of glucosensing in both glucose-excited and glucose-inhibited central neurons. *Diabetes* **51**, 2056-2065.
- Dutton A & Dyball RE.** (1979). Phasic firing enhances vasopressin release from the rat neurohypophysis. *J Physiol* **290**, 433-440.
- Duxon MS, Flanigan TP, Reavley AC, Baxter GS, Blackburn TP & Fone KC.** (1997a). Evidence for expression of the 5-hydroxytryptamine-2B receptor protein in the rat central nervous system. *Neuroscience* **76**, 323-329.
- Duxon MS, Kennett GA, Lightowler S, Blackburn TP & Fone KC.** (1997b). Activation of 5-HT2B receptors in the medial amygdala causes anxiolysis in the social interaction test in the rat. *Neuropharmacology* **36**, 601-608.



- Ebihara K, Ogawa Y, Katsuura G, Numata Y, Masuzaki H, Satoh N, Tamaki M, Yoshioka T, Hayase M, Matsuoka N, Aizawa-Abe M, Yoshimasa Y & Nakao K.** (1999). Involvement of agouti-related protein, an endogenous antagonist of hypothalamic melanocortin receptor, in leptin action. *Diabetes* **48**, 2028-2033.
- Elias CF, Aschkenasi C, Lee C, Kelly J, Ahima RS, Bjorbaek C, Flier JS, Saper CB & Elmquist JK.** (1999). Leptin differentially regulates NPY and POMC neurons projecting to the lateral hypothalamic area. *Neuron* **23**, 775-786.
- Elias CF, Lee C, Kelly J, Aschkenasi C, Ahima RS, Couceyro PR, Kuhar MJ, Saper CB & Elmquist JK.** (1998a). Leptin activates hypothalamic CART neurons projecting to the spinal cord. *Neuron* **21**, 1375-1385.
- Elias CF, Lee CE, Kelly JF, Ahima RS, Kuhar M, Saper CB & Elmquist JK.** (2001). Characterization of CART neurons in the rat and human hypothalamus. *J Comp Neurol* **432**, 1-19.
- Elias CF, Saper CB, Maratos-Flier E, Tritos NA, Lee C, Kelly J, Tatro JB, Hoffman GE, Ollmann MM, Barsh GS, Sakurai T, Yanagisawa M & Elmquist JK.** (1998b). Chemically defined projections linking the mediobasal hypothalamus and the lateral hypothalamic area. *J Comp Neurol* **402**, 442-459.
- Elmquist JK, Coppari R, Balthasar N, Ichinose M & Lowell BB.** (2005). Identifying hypothalamic pathways controlling food intake, body weight, and glucose homeostasis. *J Comp Neurol* **493**, 63-71.
- Erickson JC, Hollopeter G & Palmiter RD.** (1996). Attenuation of the obesity syndrome of ob/ob mice by the loss of neuropeptide Y. *Science* **274**, 1704-1707.
- Eriksson KS, Stevens DR & Haas HL.** (2001). Serotonin excites tuberomammillary neurons by activation of Na(+)/Ca(2+)-exchange. *Neuropharmacology* **40**, 345-351.
- Fan W, Boston BA, Kesterson RA, Hruby VJ & Cone RD.** (1997). Role of melanocortinergic neurons in feeding and the agouti obesity syndrome. *Nature* **385**, 165-168.
- Faulconbridge LF, Cummings DE, Kaplan JM & Grill HJ.** (2003). Hyperphagic effects of brainstem ghrelin administration. *Diabetes* **52**, 2260-2265.
- Fioramonti X, Contie S, Song Z, Routh VH, Lorsignol A & Penicaud L.** (2007). Characterization of glucosensing neuron subpopulations in the arcuate nucleus: integration in neuropeptide Y and pro-opio melanocortin networks? *Diabetes* **56**, 1219-1227.



- Fioramonti X, Lorsignol A, Taupignon A & Penicaud L.** (2004). A new ATP-sensitive K<sup>+</sup> channel-independent mechanism is involved in glucose-excited neurons of mouse arcuate nucleus. *Diabetes* **53**, 2767-2775.
- Florentin M, Liberopoulos EN & Elisaf MS.** (2007). Sibutramine-associated adverse effects: a practical guide for its safe use. *Obes Rev.*
- Friedman JM & Halaas JL.** (1998). Leptin and the regulation of body weight in mammals. *Nature* **395**, 763-770.
- Fruhbeck G.** (2006). Intracellular signalling pathways activated by leptin. *Biochem J* **393**, 7-20.
- Fry M, Hoyda TD & Ferguson AV.** (2007). Making sense of it: roles of the sensory circumventricular organs in feeding and regulation of energy homeostasis. *Exp Biol Med (Maywood)* **232**, 14-26.
- Fuller RW.** (1980). Pharmacology of central serotonin neurons. *Annu Rev Pharmacol Toxicol* **20**, 111-127.
- Fuller RW.** (1996). Serotonin receptors involved in regulation of pituitary-adrenocortical function in rats. *Behav Brain Res* **73**, 215-219.
- Gaddum JH & Picarelli ZP.** (1957). Two kinds of tryptamine receptor. *Br J Pharmacol Chemother* **12**, 323-328.
- Ganong WF.** (2000). Circumventricular organs: definition and role in the regulation of endocrine and autonomic function. *Clin Exp Pharmacol Physiol* **27**, 422-427.
- Garcia de Yebenes E, Li S, Fournier A, St-Pierre S & Pelletier G.** (1995). Regulation of proopiomelanocortin gene expression by neuropeptide Y in the rat arcuate nucleus. *Brain Res* **674**, 112-116.
- Gautvik KM, de Lecea L, Gautvik VT, Danielson PE, Tranque P, Dopazo A, Bloom FE & Sutcliffe JG.** (1996). Overview of the most prevalent hypothalamus-specific mRNAs, as identified by directional tag PCR subtraction. *Proc Natl Acad Sci U S A* **93**, 8733-8738.
- Gerald C, Walker MW, Criscione L, Gustafson EL, Batzl-Hartmann C, Smith KE, Vaysse P, Durkin MM, Laz TM, Linemeyer DL, Schaffhauser AO, Whitebread S, Hofbauer KG, Taber RI, Branchek TA & Weinshank RL.** (1996). A receptor subtype involved in neuropeptide-Y-induced food intake. *Nature* **382**, 168-171.
- Gerard C, Martres MP, Lefevre K, Miquel MC, Verge D, Lanfumey L, Doucet E, Hamon M & el Mestikawy S.** (1997). Immuno-localization of serotonin 5-HT<sub>6</sub> receptor-like material in the rat central nervous system. *Brain Res* **746**, 207-219.



- Ghosh A, Ginty DD, Bading H & Greenberg ME.** (1994). Calcium regulation of gene expression in neuronal cells. *J Neurobiol* **25**, 294-303.
- Ghosh A & Greenberg ME.** (1995). Calcium signaling in neurons: molecular mechanisms and cellular consequences. *Science* **268**, 239-247.
- Gibbs J, Young RC & Smith GP.** (1973). Cholecystokinin decreases food intake in rats. *J Comp Physiol Psychol* **84**, 488-495.
- Ginty DD, Bading H & Greenberg ME.** (1992). Trans-synaptic regulation of gene expression. *Curr Opin Neurobiol* **2**, 312-316.
- Good DJ.** (2000). How tight are your genes? Transcriptional and posttranscriptional regulation of the leptin receptor, NPY, and POMC genes. *Horm Behav* **37**, 284-298.
- Goodwin GM, De Souza RJ & Green AR.** (1985). The pharmacology of the hypothermic response in mice to 8-hydroxy-2-(di-n-propylamino)tetralin (8-OH-DPAT). A model of presynaptic 5-HT<sub>1</sub> function. *Neuropharmacology* **24**, 1187-1194.
- Graeff FG, Guimaraes FS, De Andrade TG & Deakin JF.** (1996). Role of 5-HT in stress, anxiety, and depression. *Pharmacol Biochem Behav* **54**, 129-141.
- Grignaschi G, Mantelli B, Fracasso C, Anelli M, Caccia S & Samanin R.** (1993). Reciprocal interaction of 5-hydroxytryptamine and cholecystokinin in the control of feeding patterns in rats. *Br J Pharmacol* **109**, 491-494.
- Grignaschi G & Samanin R.** (1992). Role of 5-HT receptors in the effect of d-fenfluramine on feeding patterns in the rat. *Eur J Pharmacol* **212**, 287-289.
- Grignaschi G, Sironi F & Samanin R.** (1995). The 5-HT<sub>1B</sub> receptor mediates the effect of d-fenfluramine on eating caused by intra-hypothalamic injection of neuropeptide Y. *Eur J Pharmacol* **274**, 221-224.
- Gropp E, Shanabrough M, Borok E, Xu AW, Janoschek R, Buch T, Plum L, Balthasar N, Hampel B, Waisman A, Barsh GS, Horvath TL & Bruning JC.** (2005). Agouti-related peptide-expressing neurons are mandatory for feeding. *Nat Neurosci* **8**, 1289-1291.
- Guan XM, Yu H, Palyha OC, McKee KK, Feighner SD, Sirinathsinghji DJ, Smith RG, Van der Ploeg LH & Howard AD.** (1997). Distribution of mRNA encoding the growth hormone secretagogue receptor in brain and peripheral tissues. *Brain Res Mol Brain Res* **48**, 23-29.
- Guan XM, Yu H, Trumbauer M, Frazier E, Van der Ploeg LH & Chen H.** (1998). Induction of neuropeptide Y expression in dorsomedial hypothalamus of diet-induced obese mice. *Neuroreport* **9**, 3415-3419.



- Gudelsky GA, Koenig JI & Meltzer HY.** (1986). Thermoregulatory responses to serotonin (5-HT) receptor stimulation in the rat. Evidence for opposing roles of 5-HT<sub>2</sub> and 5-HT<sub>1A</sub> receptors. *Neuropharmacology* **25**, 1307-1313.
- Gustafson EL, Durkin MM, Bard JA, Zgombick J & Branchek TA.** (1996). A receptor autoradiographic and in situ hybridization analysis of the distribution of the 5-HT<sub>7</sub> receptor in rat brain. *Br J Pharmacol* **117**, 657-666.
- Guy J, Pelletier G & Bosler O.** (1988). Serotonin innervation of neuropeptide Y-containing neurons in the rat arcuate nucleus. *Neurosci Lett* **85**, 9-13.
- Guy-Grand B.** (1992). Clinical studies with d-fenfluramine. *Am J Clin Nutr* **55**, 173S-176S.
- Hahn TM, Breininger JF, Baskin DG & Schwartz MW.** (1998). Coexpression of AgRP and NPY in fasting-activated hypothalamic neurons. *Nat Neurosci* **1**, 271-272.
- Hakansson ML, Brown H, Ghilardi N, Skoda RC & Meister B.** (1998). Leptin receptor immunoreactivity in chemically defined target neurons of the hypothalamus. *J Neurosci* **18**, 559-572.
- Halaas JL, Gajiwala KS, Maffei M, Cohen SL, Chait BT, Rabinowitz D, Lallone RL, Burley SK & Friedman JM.** (1995). Weight-reducing effects of the plasma protein encoded by the obese gene. *Science* **269**, 543-546.
- Halford JC & Blundell JE.** (1996). The 5-HT<sub>1B</sub> receptor agonist CP-94,253 reduces food intake and preserves the behavioural satiety sequence. *Physiol Behav* **60**, 933-939.
- Halliwel JV & Adams PR.** (1982). Voltage-clamp analysis of muscarinic excitation in hippocampal neurons. *Brain Res* **250**, 71-92.
- Harris MC & Sanghera M.** (1974). Projection of medial basal hypothalamic neurones to the preoptic anterior hypothalamic areas and the paraventricular nucleus in the rat. *Brain Res* **81**, 401-411.
- Harrold JA, Dovey T, Cai XJ, Halford JC & Pinkney J.** (2008). Autoradiographic analysis of ghrelin receptors in the rat hypothalamus. *Brain Res* **1196**, 59-64.
- Hayes MR & Covasa M.** (2005). CCK and 5-HT act synergistically to suppress food intake through simultaneous activation of CCK-1 and 5-HT<sub>3</sub> receptors. *Peptides* **26**, 2322-2330.
- Hays SE, Goodwin FK & Paul SM.** (1981). Cholecystokinin receptors in brain: effects of obesity, drug treatment, and lesions. *Peptides* **2 Suppl 1**, 21-26.



- Heisler LK, Cowley MA, Tecott LH, Fan W, Low MJ, Smart JL, Rubinstein M, Tatro JB, Marcus JN, Holstege H, Lee CE, Cone RD & Elmquist JK.** (2002). Activation of central melanocortin pathways by fenfluramine. *Science* **297**, 609-611.
- Heisler LK, Jobst EE, Sutton GM, Zhou L, Borok E, Thornton-Jones Z, Liu HY, Zigman JM, Balthasar N, Kishi T, Lee CE, Aschkenasi CJ, Zhang CY, Yu J, Boss O, Mountjoy KG, Clifton PG, Lowell BB, Friedman JM, Horvath T, Butler AA, Elmquist JK & Cowley MA.** (2006). Serotonin reciprocally regulates melanocortin neurons to modulate food intake. *Neuron* **51**, 239-249.
- Heisler LK, Pronchuk N, Nonogaki K, Zhou L, Raber J, Tung L, Yeo GS, O'Rahilly S, Colmers WF, Elmquist JK & Tecott LH.** (2007). Serotonin activates the hypothalamic-pituitary-adrenal axis via serotonin 2C receptor stimulation. *J Neurosci* **27**, 6956-6964.
- Hentges ST, Nishiyama M, Overstreet LS, Stenzel-Poore M, Williams JT & Low MJ.** (2004). GABA release from proopiomelanocortin neurons. *J Neurosci* **24**, 1578-1583.
- Hetherington A & Ranson SW.** (1940). Hypothalamic lesions and adiposity in the rat. *The Anatomical Record* **78**, 149-172.
- Hewson G, Leighton GE, Hill RG & Hughes J.** (1988). Ketanserin antagonises the anorectic effect of DL-fenfluramine in the rat. *Eur J Pharmacol* **145**, 227-230.
- Hill JW, Williams KW, Ye C, Luo J, Balthasar N, Coppari R, Cowley MA, Cantley LC, Lowell BB & Elmquist JK.** (2008). Acute effects of leptin require PI3K signaling in hypothalamic proopiomelanocortin neurons in mice. *J Clin Invest* **118**, 1796-1805.
- Ho SS, Chow BK & Yung WH.** (2007). Serotonin increases the excitability of the hypothalamic paraventricular nucleus magnocellular neurons. *Eur J Neurosci* **25**, 2991-3000.
- Hodaie M, Jeevaratnam P, Salter MW & Roach A.** (1995). Regulation of intracellular calcium and preprotachykinin neurotransmitter precursor gene expression by patterned electrical stimulation in rat sympathetic neurons. *Neurosci Lett* **185**, 195-198.
- Hoffman BJ & Mezey E.** (1989). Distribution of serotonin 5-HT<sub>1C</sub> receptor mRNA in adult rat brain. *FEBS Lett* **247**, 453-462.
- Horvath TL, Bechmann I, Naftolin F, Kalra SP & Leranth C.** (1997). Heterogeneity in the neuropeptide Y-containing neurons of the rat arcuate nucleus: GABAergic and non-GABAergic subpopulations. *Brain Res* **756**, 283-286.



- Horvath TL, Diano S & Tschop M.** (2004). Brain circuits regulating energy homeostasis. *Neuroscientist* **10**, 235-246.
- Hoyer D, Clarke DE, Fozard JR, Hartig PR, Martin GR, Mylecharane EJ, Saxena PR & Humphrey PP.** (1994). International Union of Pharmacology classification of receptors for 5-hydroxytryptamine (Serotonin). *Pharmacol Rev* **46**, 157-203.
- Hoyer D, Hannon JP & Martin GR.** (2002). Molecular, pharmacological and functional diversity of 5-HT receptors. *Pharmacol Biochem Behav* **71**, 533-554.
- Hsiao SH, Chung HH, Inui A, Tong YC & Cheng JT.** (2005). Inhibitory effect of 5-hydroxytryptamine on hyperphagia in mice with genetic overexpression of neuropeptide Y. *Neurosci Lett*.
- Huang Q, Rivest R & Richard D.** (1998). Effects of leptin on corticotropin-releasing factor (CRF) synthesis and CRF neuron activation in the paraventricular hypothalamic nucleus of obese (ob/ob) mice. *Endocrinology* **139**, 1524-1532.
- Huguenard JR.** (1996). Low-threshold calcium currents in central nervous system neurons. *Annu Rev Physiol* **58**, 329-348.
- Huguenard JR & Prince DA.** (1994). Intrathalamic rhythmicity studied in vitro: nominal T-current modulation causes robust antioscillatory effects. *J Neurosci* **14**, 5485-5502.
- Huszar D, Lynch CA, Fairchild-Huntress V, Dunmore JH, Fang Q, Berkemeier LR, Gu W, Kesterson RA, Boston BA, Cone RD, Smith FJ, Campfield LA, Burn P & Lee F.** (1997). Targeted disruption of the melanocortin-4 receptor results in obesity in mice. *Cell* **88**, 131-141.
- Hutson PH, Dourish CT & Curzon G.** (1988). Evidence that the hyperphagic response to 8-OH-DPAT is mediated by 5-HT<sub>1A</sub> receptors. *Eur J Pharmacol* **150**, 361-366.
- Ibrahim N, Bosch MA, Smart JL, Qiu J, Rubinstein M, Ronnekleiv OK, Low MJ & Kelly MJ.** (2003). Hypothalamic proopiomelanocortin neurons are glucose responsive and express K(ATP) channels. *Endocrinology* **144**, 1331-1340.
- Ikeda H, West DB, Pustek JJ, Figlewicz DP, Greenwood MR, Porte D, Jr. & Woods SC.** (1986). Intraventricular insulin reduces food intake and body weight of lean but not obese Zucker rats. *Appetite* **7**, 381-386.
- Itoh K, Stevens B, Schachner M & Fields RD.** (1995). Regulated expression of the neural cell adhesion molecule L1 by specific patterns of neural impulses. *Science* **270**, 1369-1372.



- Jacobowitz DM & O'Donohue TL.** (1978). alpha-Melanocyte stimulating hormone: immunohistochemical identification and mapping in neurons of rat brain. *Proc Natl Acad Sci U S A* **75**, 6300-6304.
- Jegou S, Blasquez C, Delbende C, Bunel DT & Vaudry H.** (1993). Regulation of alpha-melanocyte-stimulating hormone release from hypothalamic neurons. *Ann N Y Acad Sci* **680**, 260-278.
- Jegou S, Boutelet I & Vaudry H.** (2000). Melanocortin-3 receptor mRNA expression in pro-opiomelanocortin neurones of the rat arcuate nucleus. *J Neuroendocrinol* **12**, 501-505.
- Kadowaki T, Yamauchi T & Kubota N.** (2008). The physiological and pathophysiological role of adiponectin and adiponectin receptors in the peripheral tissues and CNS. *FEBS Lett* **582**, 74-80.
- Kalra SP, Dube MG, Sahu A, Phelps CP & Kalra PS.** (1991). Neuropeptide Y secretion increases in the paraventricular nucleus in association with increased appetite for food. *Proc Natl Acad Sci U S A* **88**, 10931-10935.
- Kamegai J, Tamura H, Shimizu T, Ishii S, Sugihara H & Wakabayashi I.** (2000). Central effect of ghrelin, an endogenous growth hormone secretagogue, on hypothalamic peptide gene expression. *Endocrinology* **141**, 4797-4800.
- Kamegai J, Tamura H, Shimizu T, Ishii S, Sugihara H & Wakabayashi I.** (2001). Chronic central infusion of ghrelin increases hypothalamic neuropeptide Y and Agouti-related protein mRNA levels and body weight in rats. *Diabetes* **50**, 2438-2443.
- Kang L, Dunn-Meynell AA, Routh VH, Gaspers LD, Nagata Y, Nishimura T, Eiki J, Zhang BB & Levin BE.** (2006). Glucokinase is a critical regulator of ventromedial hypothalamic neuronal glucosensing. *Diabetes* **55**, 412-420.
- Kang L, Routh VH, Kuzhikandathil EV, Gaspers LD & Levin BE.** (2004). Physiological and molecular characteristics of rat hypothalamic ventromedial nucleus glucosensing neurons. *Diabetes* **53**, 549-559.
- Keire DA, Bowers CW, Solomon TE & Reeve JR, Jr.** (2002). Structure and receptor binding of PYY analogs. *Peptides* **23**, 305-321.
- Keire DA, Mannon P, Kobayashi M, Walsh JH, Solomon TE & Reeve JR, Jr.** (2000). Primary structures of PYY, [Pro(34)]PYY, and PYY-(3-36) confer different conformations and receptor selectivity. *Am J Physiol Gastrointest Liver Physiol* **279**, G126-131.
- Kennedy GC.** (1953). The role of depot fat in the hypothalamic control of food intake in the rat. *Proc R Soc Lond B Biol Sci* **140**, 578-596.



- Kennett GA, Ainsworth K, Trail B & Blackburn TP.** (1997a). BW 723C86, a 5-HT<sub>2B</sub> receptor agonist, causes hyperphagia and reduced grooming in rats. *Neuropharmacology* **36**, 233-239.
- Kennett GA & Curzon G.** (1988). Evidence that hypophagia induced by mCPP and TFMPP requires 5-HT<sub>1C</sub> and 5-HT<sub>1B</sub> receptors; hypophagia induced by RU 24969 only requires 5-HT<sub>1B</sub> receptors. *Psychopharmacology (Berl)* **96**, 93-100.
- Kennett GA, Dourish CT & Curzon G.** (1987). 5-HT<sub>1B</sub> agonists induce anorexia at a postsynaptic site. *Eur J Pharmacol* **141**, 429-435.
- Kennett GA, Wood MD, Bright F, Trail B, Riley G, Holland V, Avenell KY, Stean T, Upton N, Bromidge S, Forbes IT, Brown AM, Middlemiss DN & Blackburn TP.** (1997b). SB 242084, a selective and brain penetrant 5-HT<sub>2C</sub> receptor antagonist. *Neuropharmacology* **36**, 609-620.
- Kim EM, O'Hare E, Grace MK, Welch CC, Billington CJ & Levine AS.** (2000). ARC POMC mRNA and PVN alpha-MSH are lower in obese relative to lean Zucker rats. *Brain Res* **862**, 11-16.
- King PJ, Widdowson PS, Doods HN & Williams G.** (1999). Regulation of neuropeptide Y release by neuropeptide Y receptor ligands and calcium channel antagonists in hypothalamic slices. *J Neurochem* **73**, 641-646.
- Kishi T, Aschkenasi CJ, Lee CE, Mountjoy KG, Saper CB & Elmquist JK.** (2003). Expression of melanocortin 4 receptor mRNA in the central nervous system of the rat. *J Comp Neurol* **457**, 213-235.
- Kojima M, Hosoda H, Date Y, Nakazato M, Matsuo H & Kangawa K.** (1999). Ghrelin is a growth-hormone-releasing acylated peptide from stomach. *Nature* **402**, 656-660.
- Kojima M & Kangawa K.** (2005). Ghrelin: structure and function. *Physiol Rev* **85**, 495-522.
- Korbonits M, Little JA, Forsling ML, Tringali G, Costa A, Navarra P, Trainer PJ & Grossman AB.** (1999). The effect of growth hormone secretagogues and neuropeptide Y on hypothalamic hormone release from acute rat hypothalamic explants. *J Neuroendocrinol* **11**, 521-528.
- Korner J, Savontaus E, Chua SC, Jr., Leibel RL & Wardlaw SL.** (2001). Leptin regulation of Agrp and Npy mRNA in the rat hypothalamus. *J Neuroendocrinol* **13**, 959-966.
- Korner J, Wardlaw SL, Liu SM, Conwell IM, Leibel RL & Chua SC, Jr.** (2000). Effects of leptin receptor mutation on Agrp gene expression in fed and fasted lean and obese (LA/N-faf) rats. *Endocrinology* **141**, 2465-2471.



- Koylu EO, Couceyro PR, Lambert PD & Kuhar MJ.** (1998). Cocaine- and amphetamine-regulated transcript peptide immunohistochemical localization in the rat brain. *J Comp Neurol* **391**, 115-132.
- Krieger MS, Conrad LC & Pfaff DW.** (1979). An autoradiographic study of the efferent connections of the ventromedial nucleus of the hypothalamus. *J Comp Neurol* **183**, 785-815.
- Kristensen P, Judge ME, Thim L, Ribel U, Christjansen KN, Wulff BS, Clausen JT, Jensen PB, Madsen OD, Vrang N, Larsen PJ & Hastrup S.** (1998). Hypothalamic CART is a new anorectic peptide regulated by leptin. *Nature* **393**, 72-76.
- Kubota N, Yano W, Kubota T, Yamauchi T, Itoh S, Kumagai H, Kozono H, Takamoto I, Okamoto S, Shiuchi T, Suzuki R, Satoh H, Tsuchida A, Moroi M, Sugi K, Noda T, Ebinuma H, Ueta Y, Kondo T, Araki E, Ezaki O, Nagai R, Tobe K, Terauchi Y, Ueki K, Minokoshi Y & Kadowaki T.** (2007). Adiponectin stimulates AMP-activated protein kinase in the hypothalamus and increases food intake. *Cell Metab* **6**, 55-68.
- Kumano S, Matsumoto H, Takatsu Y, Noguchi J, Kitada C & Ohtaki T.** (2003). Changes in hypothalamic expression levels of galanin-like peptide in rat and mouse models support that it is a leptin-target peptide. *Endocrinology* **144**, 2634-2643.
- Lacmann A, Hess D, Gohla G, Roussa E & Kriegstein K.** (2007). Activity-dependent release of transforming growth factor-beta in a neuronal network in vitro. *Neuroscience* **150**, 647-657.
- Lam DD & Heisler LK.** (2007). Serotonin and energy balance: molecular mechanisms and implications for type 2 diabetes. *Expert Rev Mol Med* **9**, 1-24.
- Lam DD, Przydzial MJ, Ridley SH, Yeo GS, Rochford JJ, O'Rahilly S & Heisler LK.** (2008). Serotonin 5-HT<sub>2C</sub> receptor agonist promotes hypophagia via downstream activation of melanocortin 4 receptors. *Endocrinology* **149**, 1323-1328.
- Lambert PD, Couceyro PR, McGirr KM, Dall Vechia SE, Smith Y & Kuhar MJ.** (1998). CART peptides in the central control of feeding and interactions with neuropeptide Y. *Synapse* **29**, 293-298.
- Lawrence CB, Snape AC, Baudoin FM & Luckman SM.** (2002). Acute central ghrelin and GH secretagogues induce feeding and activate brain appetite centers. *Endocrinology* **143**, 155-162.
- Lee GH, Proenca R, Montez JM, Carroll KM, Darvishzadeh JG, Lee JI & Friedman JM.** (1996). Abnormal splicing of the leptin receptor in diabetic mice. *Nature* **379**, 632-635.



- Lee K, Dixon AK, Richardson PJ & Pinnock RD.** (1999). Glucose-receptive neurones in the rat ventromedial hypothalamus express KATP channels composed of Kir6.1 and SUR1 subunits. *J Physiol* **515** ( Pt 2), 439-452.
- Lee M, Kim A, Conwell IM, Hruby V, Mayorov A, Cai M & Wardlaw SL.** (2008). Effects of selective modulation of the central melanocortin-3-receptor on food intake and hypothalamic POMC expression. *Peptides* **29**, 440-447.
- Lee MD, Kennett GA, Dourish CT & Clifton PG.** (2002). 5-HT1B receptors modulate components of satiety in the rat: behavioural and pharmacological analyses of the selective serotonin1B agonist CP-94,253. *Psychopharmacology (Berl)* **164**, 49-60.
- Lee MD & Simansky KJ.** (1997). CP-94, 253: a selective serotonin1B (5-HT1B) agonist that promotes satiety. *Psychopharmacology (Berl)* **131**, 264-270.
- Leibowitz SF, Weiss GF & Suh JS.** (1990). Medial hypothalamic nuclei mediate serotonin's inhibitory effect on feeding behavior. *Pharmacol Biochem Behav* **37**, 735-742.
- Levin BE, Dunn-Meynell AA & Routh VH.** (1999). Brain glucose sensing and body energy homeostasis: role in obesity and diabetes. *Am J Physiol* **276**, R1223-1231.
- Levin BE, Routh VH, Kang L, Sanders NM & Dunn-Meynell AA.** (2004). Neuronal glucosensing: what do we know after 50 years? *Diabetes* **53**, 2521-2528.
- Lewis DI, Sermasi E & Coote JH.** (1993). Excitatory and indirect inhibitory actions of 5-hydroxytryptamine on sympathetic preganglionic neurones in the neonate rat spinal cord in vitro. *Brain Res* **610**, 267-275.
- Lin L, Faraco J, Li R, Kadotani H, Rogers W, Lin X, Qiu X, de Jong PJ, Nishino S & Mignot E.** (1999). The sleep disorder canine narcolepsy is caused by a mutation in the hypocretin (orexin) receptor 2 gene. *Cell* **98**, 365-376.
- Llinas R & Yarom Y.** (1981). Electrophysiology of mammalian inferior olivary neurones in vitro. Different types of voltage-dependent ionic conductances. *J Physiol* **315**, 549-567.
- Lopez M, Seoane L, Garcia MC, Lago F, Casanueva FF, Senaris R & Dieguez C.** (2000). Leptin regulation of prepro-orexin and orexin receptor mRNA levels in the hypothalamus. *Biochem Biophys Res Commun* **269**, 41-45.
- Lowry CA.** (2002). Functional subsets of serotonergic neurones: implications for control of the hypothalamic-pituitary-adrenal axis. *J Neuroendocrinol* **14**, 911-923.



- Lucas JJ, Yamamoto A, Searce-Levie K, Saudou F & Hen R.** (1998). Absence of fenfluramine-induced anorexia and reduced c-Fos induction in the hypothalamus and central amygdaloid complex of serotonin 1B receptor knock-out mice. *J Neurosci* **18**, 5537-5544.
- Ludwig DS, Mountjoy KG, Tatro JB, Gillette JA, Frederick RC, Flier JS & Maratos-Flier E.** (1998). Melanin-concentrating hormone: a functional melanocortin antagonist in the hypothalamus. *Am J Physiol* **274**, E627-633.
- Luque CA & Rey JA.** (2002). The discovery and status of sibutramine as an anti-obesity drug. *Eur J Pharmacol* **440**, 119-128.
- Ma X, Zubcevic L, Bruning JC, Ashcroft FM & Burdakov D.** (2007). Electrical inhibition of identified anorexigenic POMC neurons by orexin/hypocretin. *J Neurosci* **27**, 1529-1533.
- Makara GB & Hodacs L.** (1975). Rostral projections from the hypothalamic arcuate nucleus. *Brain Res* **84**, 23-29.
- Makarenko IG, Meguid MM & Ugrumov MV.** (2002). Distribution of serotonin 5-hydroxytryptamine 1B (5-HT(1B)) receptors in the normal rat hypothalamus. *Neurosci Lett* **328**, 155-159.
- Mark EJ, Patalas ED, Chang HT, Evans RJ & Kessler SC.** (1997). Fatal pulmonary hypertension associated with short-term use of fenfluramine and phentermine. *N Engl J Med* **337**, 602-606.
- Marks JL, Porte D, Jr., Stahl WL & Baskin DG.** (1990). Localization of insulin receptor mRNA in rat brain by in situ hybridization. *Endocrinology* **127**, 3234-3236.
- Marsh DJ, Hollopeter G, Kafer KE & Palmiter RD.** (1998). Role of the Y5 neuropeptide Y receptor in feeding and obesity. *Nat Med* **4**, 718-721.
- Mayer CH, Fink H, Rex A & Voigt JP.** (2006). Changes in extracellular hypothalamic glucose in relation to feeding. *Eur J Neurosci* **24**, 1695-1701.
- Mayer J.** (1953). Glucostatic mechanism of regulation of food intake. *N Engl J Med* **249**, 13-16.
- Mayer J.** (1955). Regulation of energy intake and the body weight: the glucostatic theory and the lipostatic hypothesis. *Ann N Y Acad Sci* **63**, 15-43.
- McCormick DA & Pape HC.** (1990a). Noradrenergic and serotonergic modulation of a hyperpolarization-activated cation current in thalamic relay neurones. *J Physiol* **431**, 319-342.
- McCormick DA & Pape HC.** (1990b). Properties of a hyperpolarization-activated cation current and its role in rhythmic oscillation in thalamic relay neurones. *J Physiol* **431**, 291-318.



- Mendieta-Zeron H, Lopez M & Dieguez C.** (2008). Gastrointestinal peptides controlling body weight homeostasis. *Gen Comp Endocrinol* **155**, 481-495.
- Menyhert J, Wittmann G, Lechan RM, Keller E, Liposits Z & Fekete C.** (2007). Cocaine- and amphetamine-regulated transcript (CART) is colocalized with the orexigenic neuropeptide Y and agouti-related protein and absent from the anorexigenic alpha-melanocyte-stimulating hormone neurons in the infundibular nucleus of the human hypothalamus. *Endocrinology* **148**, 4276-4281.
- Mercer JG, Hoggard N, Williams LM, Lawrence CB, Hannah LT, Morgan PJ & Trayhurn P.** (1996). Coexpression of leptin receptor and preproneuropeptide Y mRNA in arcuate nucleus of mouse hypothalamus. *J Neuroendocrinol* **8**, 733-735.
- Miki T, Liss B, Minami K, Shiuchi T, Saraya A, Kashima Y, Horiuchi M, Ashcroft F, Minokoshi Y, Roeper J & Seino S.** (2001). ATP-sensitive K<sup>+</sup> channels in the hypothalamus are essential for the maintenance of glucose homeostasis. *Nat Neurosci* **4**, 507-512.
- Minokoshi Y, Alquier T, Furukawa N, Kim YB, Lee A, Xue B, Mu J, Foufelle F, Ferre P, Birnbaum MJ, Stuck BJ & Kahn BB.** (2004). AMP-kinase regulates food intake by responding to hormonal and nutrient signals in the hypothalamus. *Nature* **428**, 569-574.
- Mirshamsi S, Laidlaw HA, Ning K, Anderson E, Burgess LA, Gray A, Sutherland C & Ashford ML.** (2004). Leptin and insulin stimulation of signalling pathways in arcuate nucleus neurones: PI3K dependent actin reorganization and KATP channel activation. *BMC Neurosci* **5**, 54.
- Miyazaki T, Dun NJ, Kobayashi H & Tosaka T.** (1996). Voltage-dependent potassium currents of sympathetic preganglionic neurons in neonatal rat spinal cord thin slices. *Brain Res* **743**, 1-10.
- Mizuno TM & Mobbs CV.** (1999). Hypothalamic agouti-related protein messenger ribonucleic acid is inhibited by leptin and stimulated by fasting. *Endocrinology* **140**, 814-817.
- Molineaux SM, Jessell TM, Axel R & Julius D.** (1989). 5-HT<sub>1c</sub> receptor is a prominent serotonin receptor subtype in the central nervous system. *Proc Natl Acad Sci U S A* **86**, 6793-6797.
- Mondal MS, Date Y, Yamaguchi H, Toshinai K, Tsuruta T, Kangawa K Nakazato M.** (2005). Identification of ghrelin and its receptor in neurons of the rat arcuate nucleus. *Regul Pept* **126**, 55-59.
- Moran TH, Robinson PH, Goldrich MS & McHugh PR.** (1986). Two brain cholecystinin receptors: implications for behavioral actions. *Brain Res* **362**, 175-179.



- Morley JE, Levine AS, Grace M & Kneip J.** (1985). Peptide YY (PYY), a potent orexigenic agent. *Brain Res* **341**, 200-203.
- Mountjoy KG, Mortrud MT, Low MJ, Simerly RB & Cone RD.** (1994). Localization of the melanocortin-4 receptor (MC4-R) in neuroendocrine and autonomic control circuits in the brain. *Mol Endocrinol* **8**, 1298-1308.
- Mountjoy PD & Rutter GA.** (2007). Glucose sensing by hypothalamic neurones and pancreatic islet cells: AMPle evidence for common mechanisms? *Exp Physiol* **92**, 311-319.
- Muraki Y, Yamanaka A, Tsujino N, Kilduff TS, Goto K & Sakurai T.** (2004). Serotonergic regulation of the orexin/hypocretin neurons through the 5-HT1A receptor. *J Neurosci* **24**, 7159-7166.
- Muroya S, Yada T, Shioda S & Takigawa M.** (1999). Glucose-sensitive neurons in the rat arcuate nucleus contain neuropeptide Y. *Neurosci Lett* **264**, 113-116.
- Murphy TH, Worley PF & Baraban JM.** (1991). L-type voltage-sensitive calcium channels mediate synaptic activation of immediate early genes. *Neuron* **7**, 625-635.
- Myers MG, Cowley MA & Munzberg H.** (2008). Mechanisms of leptin action and leptin resistance. *Annu Rev Physiol* **70**, 537-556.
- Nakazato M, Murakami N, Date Y, Kojima M, Matsuo H, Kangawa K & Matsukura S.** (2001). A role for ghrelin in the central regulation of feeding. *Nature* **409**, 194-198.
- Naveilhan P, Hassani H, Canals JM, Ekstrand AJ, Larefalk A, Chhajlani V, Arenas E, Gedda K, Svensson L, Thoren P & Ernfors P.** (1999). Normal feeding behavior, body weight and leptin response require the neuropeptide Y Y2 receptor. *Nat Med* **5**, 1188-1193.
- Neill JC & Cooper SJ.** (1989). Evidence that d-fenfluramine anorexia is mediated by 5-HT1 receptors. *Psychopharmacology (Berl)* **97**, 213-218.
- Neumaier JF, Sexton TJ, Yracheta J, Diaz AM & Brownfield M.** (2001). Localization of 5-HT(7) receptors in rat brain by immunocytochemistry, in situ hybridization, and agonist stimulated cFos expression. *J Chem Neuroanat* **21**, 63-73.
- Noble F, Wank SA, Crawley JN, Bradwejn J, Seroogy KB, Hamon M & Roques BP.** (1999). International Union of Pharmacology. XXI. Structure, distribution, and functions of cholecystokinin receptors. *Pharmacol Rev* **51**, 745-781.



- Nonogaki K, Strack AM, Dallman MF & Tecott LH.** (1998). Leptin-independent hyperphagia and type 2 diabetes in mice with a mutated serotonin 5-HT<sub>2C</sub> receptor gene. *Nat Med* **4**, 1152-1156.
- Nordlie RC, Foster JD & Lange AJ.** (1999). Regulation of glucose production by the liver. *Annu Rev Nutr* **19**, 379-406.
- Obici S, Feng Z, Karkanias G, Baskin DG & Rossetti L.** (2002a). Decreasing hypothalamic insulin receptors causes hyperphagia and insulin resistance in rats. *Nat Neurosci* **5**, 566-572.
- Obici S, Feng Z, Morgan K, Stein D, Karkanias G & Rossetti L.** (2002b). Central administration of oleic acid inhibits glucose production and food intake. *Diabetes* **51**, 271-275.
- Obici S, Zhang BB, Karkanias G & Rossetti L.** (2002c). Hypothalamic insulin signaling is required for inhibition of glucose production. *Nat Med* **8**, 1376-1382.
- Ollmann MM, Wilson BD, Yang YK, Kerns JA, Chen Y, Gantz I & Barsh GS.** (1997). Antagonism of central melanocortin receptors in vitro and in vivo by agouti-related protein. *Science* **278**, 135-138.
- Oomura Y, Kimura K, Ooyama H, Maeno T, Iki M & Kuniyoshi M.** (1964). Reciprocal Activities of the Ventromedial and Lateral Hypothalamic Areas of Cats. *Science* **143**, 484-485.
- Ovesjo ML, Gamstedt M, Collin M & Meister B.** (2001). GABAergic nature of hypothalamic leptin target neurones in the ventromedial arcuate nucleus. *J Neuroendocrinol* **13**, 505-516.
- Pan ZH, Hu HJ, Perring P & Andrade R.** (2001). T-type Ca<sup>2+</sup> channels mediate neurotransmitter release in retinal bipolar cells. *Neuron* **32**, 89-98.
- Pape HC.** (1996). Queer current and pacemaker: the hyperpolarization-activated cation current in neurons. *Annu Rev Physiol* **58**, 299-327.
- Pape HC & McCormick DA.** (1989). Noradrenaline and serotonin selectively modulate thalamic burst firing by enhancing a hyperpolarization-activated cation current. *Nature* **340**, 715-718.
- Paudice P & Raiteri M.** (1991). Cholecystokinin release mediated by 5-HT<sub>3</sub> receptors in rat cerebral cortex and nucleus accumbens. *Br J Pharmacol* **103**, 1790-1794.
- Paxinos G & Watson C.** (1998). *The rat brain in stereotaxic coordinates*. San Diego Academic Press.



- Pazos A, Hoyer D & Palacios JM.** (1984). The binding of serotonergic ligands to the porcine choroid plexus: characterization of a new type of serotonin recognition site. *Eur J Pharmacol* **106**, 539-546.
- Pedrazzini T, Seydoux J, Kunstner P, Aubert JF, Grouzmann E, Beermann F & Brunner HR.** (1998). Cardiovascular response, feeding behavior and locomotor activity in mice lacking the NPY Y1 receptor. *Nat Med* **4**, 722-726.
- Pelleymounter MA, Cullen MJ, Baker MB, Hecht R, Winters D, Boone T & Collins F.** (1995). Effects of the obese gene product on body weight regulation in ob/ob mice. *Science* **269**, 540-543.
- Perello M, Stuart RC & Nillni EA.** (2007). Differential effects of fasting and leptin on proopiomelanocortin peptides in the arcuate nucleus and in the nucleus of the solitary tract. *Am J Physiol Endocrinol Metab* **292**, E1348-1357.
- Peroutka SJ & Snyder SH.** (1979). Multiple serotonin receptors: differential binding of [3H]5-hydroxytryptamine, [3H]lysergic acid diethylamide and [3H]spiroperidol. *Mol Pharmacol* **16**, 687-699.
- Pickering AE, Spanswick D & Logan SD.** (1991). Whole-cell recordings from sympathetic preganglionic neurons in rat spinal cord slices. *Neurosci Lett* **130**, 237-242.
- Pickering AE, Spanswick D & Logan SD.** (1994). 5-Hydroxytryptamine evokes depolarizations and membrane potential oscillations in rat sympathetic preganglionic neurones. *J Physiol* **480** ( Pt 1), 109-121.
- Placantonakis DG, Schwarz C & Welsh JP.** (2000). Serotonin suppresses subthreshold and suprathreshold oscillatory activity of rat inferior olivary neurones in vitro. *J Physiol* **524** Pt 3, 833-851.
- Pocai A, Lam TK, Gutierrez-Juarez R, Obici S, Schwartz GJ, Bryan J, Aguilar-Bryan L & Rossetti L.** (2005). Hypothalamic K(ATP) channels control hepatic glucose production. *Nature* **434**, 1026-1031.
- Poggioli R, Vergoni AV & Bertolini A.** (1986). ACTH-(1-24) and alpha-MSH antagonize feeding behavior stimulated by kappa opiate agonists. *Peptides* **7**, 843-848.
- Pompeiano M, Palacios JM & Mengod G.** (1992). Distribution and cellular localization of mRNA coding for 5-HT1A receptor in the rat brain: correlation with receptor binding. *J Neurosci* **12**, 440-453.
- Porte D, Jr. & Woods SC.** (1981). Regulation of food intake and body weight in insulin. *Diabetologia* **20** Suppl, 274-280.



- Qu D, Ludwig DS, Gammeltoft S, Piper M, Pellemounter MA, Cullen MJ, Mathes WF, Przypek R, Kanarek R & Maratos-Flier E.** (1996). A role for melanin-concentrating hormone in the central regulation of feeding behaviour. *Nature* **380**, 243-247.
- Rapport MM.** (1949). Serum vasoconstrictor (serotonin) the presence of creatinine in the complex; a proposed structure of the vasoconstrictor principle. *J Biol Chem* **180**, 961-969.
- Raymond JR, Mukhin YV, Gelasco A, Turner J, Collinsworth G, Gettys TW, Grewal JS & Garnovskaya MN.** (2001). Multiplicity of mechanisms of serotonin receptor signal transduction. *Pharmacol Ther* **92**, 179-212.
- Rethelyi M & Halasz B.** (1970). Origin of the nerve endings in the surface zone of the median eminence of the rat hypothalamus. *Exp Brain Res* **11**, 145-158.
- Ricardo JA & Koh ET.** (1978). Anatomical evidence of direct projections from the nucleus of the solitary tract to the hypothalamus, amygdala, and other forebrain structures in the rat. *Brain Res* **153**, 1-26.
- Rogawski MA.** (1985). The A-current: how ubiquitous a feature of excitable cells is it ? . *Trends Neurosci* **8**, 214-219.
- Roseberry AG, Liu H, Jackson AC, Cai X & Friedman JM.** (2004). Neuropeptide Y-mediated inhibition of proopiomelanocortin neurons in the arcuate nucleus shows enhanced desensitization in ob/ob mice. *Neuron* **41**, 711-722.
- Rother E, Konner AC & Bruning JC.** (2008). Neurocircuits integrating hormone and nutrient signaling in control of glucose metabolism. *Am J Physiol Endocrinol Metab* **294**, E810-816.
- Rothwell NJ.** (1990). Central effects of CRF on metabolism and energy balance. *Neurosci Biobehav Rev* **14**, 263-271.
- Routh VH.** (2002). Glucose-sensing neurons: are they physiologically relevant? *Physiol Behav* **76**, 403-413.
- Rowe IC, Treherne JM & Ashford ML.** (1996). Activation by intracellular ATP of a potassium channel in neurones from rat basomedial hypothalamus. *J Physiol* **490** ( Pt 1), 97-113.
- Rubio MA, Gargallo M, Isabel Millan A & Moreno B.** (2007). Drugs in the treatment of obesity: sibutramine, orlistat and rimonabant. *Public Health Nutr* **10**, 1200-1205.
- Russell SH, Small CJ, Dakin CL, Abbott CR, Morgan DG, Ghatei MA & Bloom SR.** (2001). The central effects of orexin-A in the hypothalamic-pituitary-adrenal axis in vivo and in vitro in male rats. *J Neuroendocrinol* **13**, 561-566.



- Saeb-Parsy K, Lombardelli S, Khan FZ, McDowall K, Au-Yong IT & Dyball RE.** (2000). Neural connections of hypothalamic neuroendocrine nuclei in the rat. *J Neuroendocrinol* **12**, 635-648.
- Sahu A.** (1998). Evidence suggesting that galanin (GAL), melanin-concentrating hormone (MCH), neurotensin (NT), proopiomelanocortin (POMC) and neuropeptide Y (NPY) are targets of leptin signaling in the hypothalamus. *Endocrinology* **139**, 795-798.
- Sahu A.** (2004). Minireview: A hypothalamic role in energy balance with special emphasis on leptin. *Endocrinology* **145**, 2613-2620.
- Sahu A, Kalra PS & Kalra SP.** (1988). Food deprivation and ingestion induce reciprocal changes in neuropeptide Y concentrations in the paraventricular nucleus. *Peptides* **9**, 83-86.
- Sakurai T, Amemiya A, Ishii M, Matsuzaki I, Chemelli RM, Tanaka H, Williams SC, Richardson JA, Kozlowski GP, Wilson S, Arch JR, Buckingham RE, Haynes AC, Carr SA, Annan RS, McNulty DE, Liu WS, Terrett JA, Elshourbagy NA, Bergsma DJ & Yanagisawa M.** (1998). Orexins and orexin receptors: a family of hypothalamic neuropeptides and G protein-coupled receptors that regulate feeding behavior. *Cell* **92**, 573-585.
- Saller CF & Stricker EM.** (1976). Hyperphagia and increased growth in rats after intraventricular injection of 5,7-dihydroxytryptamine. *Science* **192**, 385-387.
- Samanin R & Grignaschi S.** (1996). Role of 5-hydroxytryptamine receptor subtypes in satiety and animal models of eating disorders. In *Drug receptor subtypes and ingestive behaviour*, ed. Cooper SJ & Clifton PG, pp. 39-58. Academic Press, London.
- Sanacora G, Kershaw M, Finkelstein JA & White JD.** (1990). Increased hypothalamic content of preproneuropeptide Y messenger ribonucleic acid in genetically obese Zucker rats and its regulation by food deprivation. *Endocrinology* **127**, 730-737.
- Saper CB, Scammell TE & Lu J.** (2005). Hypothalamic regulation of sleep and circadian rhythms. *Nature* **437**, 1257-1263.
- Saper CB, Swanson LW & Cowan WM.** (1979). An autoradiographic study of the efferent connections of the lateral hypothalamic area in the rat. *J Comp Neurol* **183**, 689-706.
- Satoh N, Ogawa Y, Katsuura G, Hayase M, Tsuji T, Imagawa K, Yoshimasa Y, Nishi S, Hosoda K & Nakao K.** (1997). The arcuate nucleus as a primary site of satiety effect of leptin in rats. *Neurosci Lett* **224**, 149-152.
- Saudou F, Amara DA, Dierich A, LeMeur M, Ramboz S, Segu L, Buhot MC & Hen R.** (1994). Enhanced aggressive behavior in mice lacking 5-HT1B receptor. *Science* **265**, 1875-1878.



- Sawchenko PE & Swanson LW.** (1983). The organization of forebrain afferents to the paraventricular and supraoptic nuclei of the rat. *J Comp Neurol* **218**, 121-144.
- Sawchenko PE, Swanson LW, Steinbusch HW & Verhofstad AA.** (1983). The distribution and cells of origin of serotonergic inputs to the paraventricular and supraoptic nuclei of the rat. *Brain Res* **277**, 355-360.
- Schuit FC, Huypens P, Heimberg H & Pipeleers DG.** (2001). Glucose sensing in pancreatic beta-cells: a model for the study of other glucose-regulated cells in gut, pancreas, and hypothalamus. *Diabetes* **50**, 1-11.
- Schwanzel-Fukuda M, Morrell JI & Pfaff DW.** (1984). Localization of forebrain neurons which project directly to the medulla and spinal cord of the rat by retrograde tracing with wheat germ agglutinin. *J Comp Neurol* **226**, 1-20.
- Schwartz DH, McClane S, Hernandez L & Hoebel BG.** (1989). Feeding increases extracellular serotonin in the lateral hypothalamus of the rat as measured by microdialysis. *Brain Res* **479**, 349-354.
- Schwartz MW, Baskin DG, Kaiyala KJ & Woods SC.** (1999). Model for the regulation of energy balance and adiposity by the central nervous system. *Am J Clin Nutr* **69**, 584-596.
- Schwartz MW, Marks JL, Sipols AJ, Baskin DG, Woods SC, Kahn SE & Porte D, Jr.** (1991). Central insulin administration reduces neuropeptide Y mRNA expression in the arcuate nucleus of food-deprived lean (Fa/Fa) but not obese (fa/fa) Zucker rats. *Endocrinology* **128**, 2645-2647.
- Schwartz MW, Seeley RJ, Campfield LA, Burn P & Baskin DG.** (1996). Identification of targets of leptin action in rat hypothalamus. *J Clin Invest* **98**, 1101-1106.
- Schwartz MW, Seeley RJ, Woods SC, Weigle DS, Campfield LA, Burn P & Baskin DG.** (1997). Leptin increases hypothalamic pro-opiomelanocortin mRNA expression in the rostral arcuate nucleus. *Diabetes* **46**, 2119-2123.
- Schwartz MW, Sipols AJ, Grubin CE & Baskin DG.** (1993). Differential effect of fasting on hypothalamic expression of genes encoding neuropeptide Y, galanin, and glutamic acid decarboxylase. *Brain Res Bull* **31**, 361-367.
- Schwartz MW, Sipols AJ, Marks JL, Sanacora G, White JD, Scheurink A, Kahn SE, Baskin DG, Woods SC, Figlewicz DP & et al.** (1992). Inhibition of hypothalamic neuropeptide Y gene expression by insulin. *Endocrinology* **130**, 3608-3616.
- Schwartz MW, Woods SC, Porte D, Jr., Seeley RJ & Baskin DG.** (2000). Central nervous system control of food intake. *Nature* **404**, 661-671.



- Seoane LM, Lopez M, Tovar S, Casanueva FF, Senaris R & Dieguez C.** (2003). Agouti-related peptide, neuropeptide Y, and somatostatin-producing neurons are targets for ghrelin actions in the rat hypothalamus. *Endocrinology* **144**, 544-551.
- Shen KZ, Kozell LB & Johnson SW.** (2007). Multiple conductances are modulated by 5-HT receptor subtypes in rat subthalamic nucleus neurons. *Neuroscience* **148**, 996-1003.
- Sheng HZ, Fields RD & Nelson PG.** (1993). Specific regulation of immediate early genes by patterned neuronal activity. *J Neurosci Res* **35**, 459-467.
- Sheng M & Greenberg ME.** (1990). The regulation and function of c-fos and other immediate early genes in the nervous system. *Neuron* **4**, 477-485.
- Shimada M, Tritos NA, Lowell BB, Flier JS & Maratos-Flier E.** (1998). Mice lacking melanin-concentrating hormone are hypophagic and lean. *Nature* **396**, 670-674.
- Shintani M, Ogawa Y, Ebihara K, Aizawa-Abe M, Miyanaga F, Takaya K, Hayashi T, Inoue G, Hosoda K, Kojima M, Kangawa K & Nakao K.** (2001). Ghrelin, an endogenous growth hormone secretagogue, is a novel orexigenic peptide that antagonizes leptin action through the activation of hypothalamic neuropeptide Y/Y1 receptor pathway. *Diabetes* **50**, 227-232.
- Shutter JR, Graham M, Kinsey AC, Scully S, Luthy R & Stark KL.** (1997). Hypothalamic expression of ART, a novel gene related to agouti, is up-regulated in obese and diabetic mutant mice. *Genes Dev* **11**, 593-602.
- Silver IA & Erecinska M.** (1994). Extracellular glucose concentration in mammalian brain: continuous monitoring of changes during increased neuronal activity and upon limitation in oxygen supply in normo-, hypo-, and hyperglycemic animals. *J Neurosci* **14**, 5068-5076.
- Sim LJ & Joseph SA.** (1991). Arcuate nucleus projections to brainstem regions which modulate nociception. *J Chem Neuroanat* **4**, 97-109.
- Simansky KJ.** (1996). Serotonergic control of the organization of feeding and satiety. *Behav Brain Res* **73**, 37-42.
- Smith BM, Smith JM, Tsai JH, Schultz JA, Gilson CA, Estrada SA, Chen RR, Park DM, Prieto EB, Gallardo CS, Sengupta D, Dosa PI, Covell JA, Ren A, Webb RR, Beeley NR, Martin M, Morgan M, Espitia S, Saldana HR, Bjenning C, Whelan KT, Grottick AJ, Menzaghi F & Thomsen WJ.** (2008). Discovery and structure-activity relationship of (1R)-8-chloro-2,3,4,5-tetrahydro-1-methyl-1H-3-benzazepine (Lorcaserin), a selective serotonin 5-HT<sub>2C</sub> receptor agonist for the treatment of obesity. *J Med Chem* **51**, 305-313.



- Song Z, Levin BE, McArdle JJ, Bakhos N & Routh VH.** (2001). Convergence of pre- and postsynaptic influences on glucosensing neurons in the ventromedial hypothalamic nucleus. *Diabetes* **50**, 2673-2681.
- Spanswick D, Smith MA, Groppi VE, Logan SD & Ashford ML.** (1997). Leptin inhibits hypothalamic neurons by activation of ATP-sensitive potassium channels. *Nature* **390**, 521-525.
- Spanswick D, Smith MA, Mirshamsi S, Routh VH & Ashford ML.** (2000). Insulin activates ATP-sensitive K<sup>+</sup> channels in hypothalamic neurons of lean, but not obese rats. *Nat Neurosci* **3**, 757-758.
- Stanford IM, Kantaria MA, Chahal HS, Loucif KC & Wilson CL.** (2005). 5-Hydroxytryptamine induced excitation and inhibition in the subthalamic nucleus: action at 5-HT(2C), 5-HT(4) and 5-HT(1A) receptors. *Neuropharmacology* **49**, 1228-1234.
- Stanley BG, Kyrkouli SE, Lampert S & Leibowitz SF.** (1986). Neuropeptide Y chronically injected into the hypothalamus: a powerful neurochemical inducer of hyperphagia and obesity. *Peptides* **7**, 1189-1192.
- Steinbusch HW.** (1981). Distribution of serotonin-immunoreactivity in the central nervous system of the rat-cell bodies and terminals. *Neuroscience* **6**, 557-618.
- Stephens TW, Basinski M, Bristow PK, Bue-Valleskey JM, Burgett SG, Craft L, Hale J, Hoffmann J, Hsiung HM, Kriauciunas A & et al.** (1995). The role of neuropeptide Y in the antiobesity action of the obese gene product. *Nature* **377**, 530-532.
- Suzuki S & Rogawski MA.** (1989). T-type calcium channels mediate the transition between tonic and phasic firing in thalamic neurons. *Proc Natl Acad Sci U S A* **86**, 7228-7232.
- Swart I, Jahng JW, Overton JM & Houtp TA.** (2002). Hypothalamic NPY, AGRP, and POMC mRNA responses to leptin and refeeding in mice. *Am J Physiol Regul Integr Comp Physiol* **283**, R1020-1026.
- Szekely AM, Barbaccia ML, Alho H & Costa E.** (1989). In primary cultures of cerebellar granule cells the activation of N-methyl-D-aspartate-sensitive glutamate receptors induces c-fos mRNA expression. *Mol Pharmacol* **35**, 401-408.
- Tartaglia LA, Dembski M, Weng X, Deng N, Culpepper J, Devos R, Richards GJ, Campfield LA, Clark FT, Deeds J, Muir C, Sanker S, Moriarty A, Moore KJ, Smutko JS, Mays GG, Wool EA, Monroe CA & Tepper RI.** (1995). Identification and expression cloning of a leptin receptor, OB-R. *Cell* **83**, 1263-1271.



- Tatemoto K, Carlquist M & Mutt V.** (1982). Neuropeptide Y--a novel brain peptide with structural similarities to peptide YY and pancreatic polypeptide. *Nature* **296**, 659-660.
- Tatro JB.** (1990). Melanotropin receptors in the brain are differentially distributed and recognize both corticotropin and alpha-melanocyte stimulating hormone. *Brain Res* **536**, 124-132.
- Tecott LH, Sun LM, Akana SF, Strack AM, Lowenstein DH, Dallman MF & Julius D.** (1995). Eating disorder and epilepsy in mice lacking 5-HT<sub>2c</sub> serotonin receptors. *Nature* **374**, 542-546.
- Thornton JE, Cheung CC, Clifton DK & Steiner RA.** (1997). Regulation of hypothalamic proopiomelanocortin mRNA by leptin in ob/ob mice. *Endocrinology* **138**, 5063-5066.
- Tork I.** (1990). Anatomy of the serotonergic system. *Ann N Y Acad Sci* **600**, 9-34; discussion 34-35.
- Tschop M, Smiley DL & Heiman ML.** (2000). Ghrelin induces adiposity in rodents. *Nature* **407**, 908-913.
- van den Pol AN.** (2003). Weighing the role of hypothalamic feeding neurotransmitters. *Neuron* **40**, 1059-1061.
- van den Top M.** (2002). Neuropeptide and hormonal signalling in mammalian central autonomic neurones. University of Warwick, Coventry.
- van den Top M, Lee K, Whyment AD, Blanks AM & Spanswick D.** (2004). Orexin-sensitive NPY/AgRP pacemaker neurons in the hypothalamic arcuate nucleus. *Nat Neurosci* **7**, 493-494.
- van den Top M, Lyons DJ, Lee K, Coderre E, Renaud LP & Spanswick D.** (2007). Pharmacological and molecular characterization of ATP-sensitive K(+) conductances in CART and NPY/AgRP expressing neurons of the hypothalamic arcuate nucleus. *Neuroscience* **144**, 815-824.
- van den Top M & Spanswick D.** (2006). Integration of metabolic stimuli in the hypothalamic arcuate nucleus. *Prog Brain Res* **153**, 141-154.
- van Welie I, Remme MW, van Hooft JA & Wadman WJ.** (2006). Different levels of I<sub>h</sub> determine distinct temporal integration in bursting and regular-spiking neurons in rat subiculum. *J Physiol* **576**, 203-214.
- Vickers SP, Clifton PG & Dourish CT.** (1996). Behavioural evidence that d-fenfluramine-induced anorexia in the rat is not mediated by the 5-HT<sub>1A</sub> receptor subtype. *Psychopharmacology (Berl)* **125**, 168-175.



- Vickers SP, Clifton PG, Dourish CT & Tecott LH.** (1999). Reduced satiating effect of d-fenfluramine in serotonin 5-HT(2C) receptor mutant mice. *Psychopharmacology (Berl)* **143**, 309-314.
- Vickers SP, Dourish CT & Kennett GA.** (2001). Evidence that hypophagia induced by d-fenfluramine and d-norfenfluramine in the rat is mediated by 5-HT2C receptors. *Neuropharmacology* **41**, 200-209.
- Voigt JP, Nwaiser B, Rex A, Mayer C & Fink H.** (2004). Effect of 5-HT1A receptor activation on hypothalamic glucose. *Pharmacol Res* **50**, 359-365.
- Wade JM, Juneja P, MacKay AW, Graham J, Havel PJ, Tecott LH & Goulding EH.** (2008). Synergistic impairment of glucose homeostasis in ob/ob mice lacking functional serotonin 2C receptors. *Endocrinology* **149**, 955-961.
- Wang L, Saint-Pierre DH & Tache Y.** (2002). Peripheral ghrelin selectively increases Fos expression in neuropeptide Y - synthesizing neurons in mouse hypothalamic arcuate nucleus. *Neurosci Lett* **325**, 47-51.
- Wang R, Liu X, Hentges ST, Dunn-Meynell AA, Levin BE, Wang W & Routh VH.** (2004). The regulation of glucose-excited neurons in the hypothalamic arcuate nucleus by glucose and feeding-relevant peptides. *Diabetes* **53**, 1959-1965.
- Wank SA, Harkins R, Jensen RT, Shapira H, de Weerth A & Slattery T.** (1992). Purification, molecular cloning, and functional expression of the cholecystokinin receptor from rat pancreas. *Proc Natl Acad Sci U S A* **89**, 3125-3129.
- Ward RP, Hamblin MW, Lachowicz JE, Hoffman BJ, Sibley DR & Dorsa DM.** (1995). Localization of serotonin subtype 6 receptor messenger RNA in the rat brain by in situ hybridization histochemistry. *Neuroscience* **64**, 1105-1111.
- Watson SJ & Akil H.** (1979). The presence of two alpha-MSH positive cell groups in rat hypothalamus. *Eur J Pharmacol* **58**, 101-103.
- Weigle DS, Bukowski TR, Foster DC, Holderman S, Kramer JM, Lasser G, Lofton-Day CE, Prunkard DE, Raymond C & Kuijper JL.** (1995). Recombinant ob protein reduces feeding and body weight in the ob/ob mouse. *J Clin Invest* **96**, 2065-2070.
- White JD, Olchovsky D, Kershaw M & Berelowitz M.** (1990). Increased hypothalamic content of preproneuropeptide-Y messenger ribonucleic acid in streptozotocin-diabetic rats. *Endocrinology* **126**, 765-772.
- World Health Organisation.** Obesity and Overweight, accessed 1 September 2008 <<http://www.who.int/mediacentre/factsheets/fs311/en/index.html>>



- Wiegand SJ & Price JL.** (1980). Cells of origin of the afferent fibers to the median eminence in the rat. *J Comp Neurol* **192**, 1-19.
- Wilding JP, Gilbey SG, Bailey CJ, Batt RA, Williams G, Ghatei MA & Bloom SR.** (1993). Increased neuropeptide-Y messenger ribonucleic acid (mRNA) and decreased neurotensin mRNA in the hypothalamus of the obese (ob/ob) mouse. *Endocrinology* **132**, 1939-1944.
- Wilkinson LO & Dourish CT.** (1991). Serotonin and animal behaviour. In *Serotonin receptor subtypes: basic and clinical aspects*, ed. S.J P, pp. 147-210. Wiley-Liss Inc., New York.
- Willesen MG, Kristensen P & Romer J.** (1999). Co-localization of growth hormone secretagogue receptor and NPY mRNA in the arcuate nucleus of the rat. *Neuroendocrinology* **70**, 306-316.
- Williams G, Bing C, Cai XJ, Harrold JA, King PJ & Liu XH.** (2001). The hypothalamus and the control of energy homeostasis: different circuits, different purposes. *Physiol Behav* **74**, 683-701.
- Williams G, Harrold JA & Cutler DJ.** (2000). The hypothalamus and the regulation of energy homeostasis: lifting the lid on a black box. *Proc Nutr Soc* **59**, 385-396.
- Willoughby JO & Blessing WW.** (1987). Origin of serotonin innervation of the arcuate and ventromedial hypothalamic region. *Brain Res* **418**, 170-173.
- Wren AM, Seal LJ, Cohen MA, Brynes AE, Frost GS, Murphy KG, Dhillon WS, Ghatei MA & Bloom SR.** (2001a). Ghrelin enhances appetite and increases food intake in humans. *J Clin Endocrinol Metab* **86**, 5992.
- Wren AM, Small CJ, Abbott CR, Dhillon WS, Seal LJ, Cohen MA, Batterham RL, Taheri S, Stanley SA, Ghatei MA & Bloom SR.** (2001b). Ghrelin causes hyperphagia and obesity in rats. *Diabetes* **50**, 2540-2547.
- Wright DE, Seroogy KB, Lundgren KH, Davis BM & Jennes L.** (1995). Comparative localization of serotonin1A, 1C, and 2 receptor subtype mRNAs in rat brain. *J Comp Neurol* **351**, 357-373.
- Xiang Z, Wang L & Kitai ST.** (2005). Modulation of spontaneous firing in rat subthalamic neurons by 5-HT receptor subtypes. *J Neurophysiol* **93**, 1145-1157.
- Xu AW, Kaelin CB, Morton GJ, Ogimoto K, Stanhope K, Graham J, Baskin DG, Havel P, Schwartz MW & Barsh GS.** (2005). Effects of hypothalamic neurodegeneration on energy balance. *PLoS Biol* **3**, e415.
- Xu T & Pandey SC.** (2000). Cellular localization of serotonin(2A) (5HT(2A)) receptors in the rat brain. *Brain Res Bull* **51**, 499-505.



- Yamanaka A, Kunii K, Nambu T, Tsujino N, Sakai A, Matsuzaki I, Miwa Y, Goto K & Sakurai T.** (2000). Orexin-induced food intake involves neuropeptide Y pathway. *Brain Res* **859**, 404-409.
- Yamauchi T, Kamon J, Ito Y, Tsuchida A, Yokomizo T, Kita S, Sugiyama T, Miyagishi M, Hara K, Tsunoda M, Murakami K, Ohteki T, Uchida S, Takekawa S, Waki H, Tsuno NH, Shibata Y, Terauchi Y, Froguel P, Tobe K, Koyasu S, Taira K, Kitamura T, Shimizu T, Nagai R & Kadowaki T.** (2003). Cloning of adiponectin receptors that mediate antidiabetic metabolic effects. *Nature* **423**, 762-769.
- Yang XJ, Mastaitis J, Mizuno T & Mobbs CV.** (2007). Glucokinase regulates reproductive function, glucocorticoid secretion, food intake, and hypothalamic gene expression. *Endocrinology* **148**, 1928-1932.
- Yeo GS, Farooqi IS, Aminian S, Halsall DJ, Stanhope RG & O'Rahilly S.** (1998). A frameshift mutation in MC4R associated with dominantly inherited human obesity. *Nat Genet* **20**, 111-112.
- Yi CX, van der Vliet J, Dai J, Yin G, Ru L & Buijs RM.** (2006). Ventromedial arcuate nucleus communicates peripheral metabolic information to the suprachiasmatic nucleus. *Endocrinology* **147**, 283-294.
- Zaborszky L & Makara GB.** (1979). Intrahypothalamic connections: an electron microscopic study in the rat. *Exp Brain Res* **34**, 201-215.
- Zafra F, Hengerer B, Leibrock J, Thoenen H & Lindholm D.** (1990). Activity dependent regulation of BDNF and NGF mRNAs in the rat hippocampus is mediated by non-NMDA glutamate receptors. *Embo J* **9**, 3545-3550.
- Zarjevski N, Cusin I, Vettor R, Rohner-Jeanrenaud F & Jeanrenaud B.** (1993). Chronic intracerebroventricular neuropeptide-Y administration to normal rats mimics hormonal and metabolic changes of obesity. *Endocrinology* **133**, 1753-1758.
- Zhang Y, Damjanoska KJ, Carrasco GA, Dudas B, D'Souza DN, Tetzlaff J, Garcia F, Hanley NR, Scripathirathan K, Petersen BR, Gray TS, Battaglia G, Muma NA & Van de Kar LD.** (2002). Evidence that 5-HT<sub>2A</sub> receptors in the hypothalamic paraventricular nucleus mediate neuroendocrine responses to (-)DOI. *J Neurosci* **22**, 9635-9642.
- Zhang Y, Proenca R, Maffei M, Barone M, Leopold L & Friedman JM.** (1994). Positional cloning of the mouse obese gene and its human homologue. *Nature* **372**, 425-432.
- Zhang Y, Zhou J, Corll C, Porter JR, Martin RJ & Roane DS.** (2004). Evidence for hypothalamic K<sup>+</sup>(ATP) channels in the modulation of glucose homeostasis. *Eur J Pharmacol* **492**, 71-79.



**Zhou L, Sutton GM, Rochford JJ, Semple RK, Lam DD, Oksanen LJ, Thornton-Jones ZD, Clifton PG, Yueh CY, Evans ML, McCrimmon RJ, Elmquist JK, Butler AA & Heisler LK.** (2007). Serotonin 2C receptor agonists improve type 2 diabetes via melanocortin-4 receptor signaling pathways. *Cell Metab* **6**, 398-405.

**Zigman JM & Elmquist JK.** (2003). Minireview: From anorexia to obesity--the yin and yang of body weight control. *Endocrinology* **144**, 3749-3756.

**Zigman JM, Jones JE, Lee CE, Saper CB & Elmquist JK.** (2006). Expression of ghrelin receptor mRNA in the rat and the mouse brain. *J Comp Neurol* **494**, 528-548.